State-of-the-Art Report on Light Water Reactor Accident-Tolerant Fuels

OECD
BETTER POLICIES FOR BETTER LIVES

anniversary 60th

NEA
NUCLEAR ENERGY AGENCY

Nuclear Science

State-of-the-Art Report on Light Water Reactor Accident-Tolerant Fuels

ORGANISATION FOR ECONOMIC CO-OPERATION AND DEVELOPMENT

The OECD is a unique forum where the governments of 36 democracies work together to address the economic, social and environmental challenges of globalisation. The OECD is also at the forefront of efforts to understand and to help governments respond to new developments and concerns, such as corporate governance, the information economy and the challenges of an ageing population. The Organisation provides a setting where governments can compare policy experiences, seek answers to common problems, identify good practice and work to co-ordinate domestic and international policies.

The OECD member countries are: Australia, Austria, Belgium, Canada, Chile, the Czech Republic, Denmark, Estonia, Finland, France, Germany, Greece, Hungary, Iceland, Ireland, Israel, Italy, Japan, Latvia, Lithuania, Luxembourg, Mexico, the Netherlands, New Zealand, Norway, Poland, Portugal, Korea, the Slovak Republic, Slovenia, Spain, Sweden, Switzerland, Turkey, the United Kingdom and the United States. The European Commission takes part in the work of the OECD.

OECD Publishing disseminates widely the results of the Organisation's statistics gathering and research on economic, social and environmental issues, as well as the conventions, guidelines and standards agreed by its members.

This work is published under the responsibility of the Secretary-General of the OECD.
The opinions expressed and arguments employed herein do not necessarily reflect the official
views of the Organisation or of the governments of its member countries.

NUCLEAR ENERGY AGENCY

The OECD Nuclear Energy Agency (NEA) was established on 1 February 1958. Current NEA membership consists of 33 countries: Argentina, Australia, Austria, Belgium, Canada, the Czech Republic, Denmark, Finland, France, Germany, Greece, Hungary, Iceland, Ireland, Italy, Japan, Luxembourg, Mexico, the Netherlands, Norway, Poland, Portugal, Korea, Romania, Russia, the Slovak Republic, Slovenia, Spain, Sweden, Switzerland, Turkey, the United Kingdom and the United States. The European Commission and the International Atomic Energy Agency also take part in the work of the Agency.

The mission of the NEA is:

– to assist its member countries in maintaining and further developing, through international co-operation, the scientific, technological and legal bases required for a safe, environmentally sound and economical use of nuclear energy for peaceful purposes;

– to provide authoritative assessments and to forge common understandings on key issues as input to government decisions on nuclear energy policy and to broader OECD analyses in areas such as energy and the sustainable development of low-carbon economies.

Specific areas of competence of the NEA include the safety and regulation of nuclear activities, radioactive waste management and decommissioning, radiological protection, nuclear science, economic and technical analyses of the nuclear fuel cycle, nuclear law and liability, and public information. The NEA Data Bank provides nuclear data and computer program services for participating countries.

This document, as well as any [statistical] data and map included herein, are without prejudice to the status of or sovereignty over any territory, to the delimitation of international frontiers and boundaries and to the name of any territory, city or area.

Corrigenda to OECD publications may be found online at: *www.oecd.org/publishing/corrigenda*.

Cover photos: Top view of the TREAT core (INL); Segment of SiC/SiC fuel cladding (Sauder, 2014).

Foreword

As part of a broader spectrum of collaborative activities underpinning nuclear materials research – from modelling and simulation, including advanced multiscale and multi-physics methods, to the development of databases for current and advanced nuclear fuels – the Nuclear Energy Agency (NEA) is supporting efforts towards the development of advanced materials, including fuels for partitioning and transmutation purposes and accident-tolerant fuels (ATFs). ATFs cover a broad range of materials potentially envisaged for the core of generation II light water reactors (LWRs) currently in operation, as well as for generation III reactors under construction. ATFs usually imply, for example, materials for the fuel sub-assembly (fuel, cladding, boiling water reactor [BWR] channel box) and for control rods devices. Although R&D on some ATF candidate materials had begun before the 2011 accident at the Fukushima Daiichi nuclear power plant (NPP), the international debate that followed this tragic event identified the development of advanced fuel designs with a substantially enhanced performance under severe accidents as a focal point of progress in the safety of light water reactors. As a result, the expansion of national and international R&D programmes on ATFs began to gather momentum in 2011.

In order to underpin and complement national R&D efforts devoted to ATFs, the NEA Nuclear Science Committee organised two international workshops on ATFs in 2012 and 2013, and subsequently established an expert group in 2014 – the NEA Expert Group on Accident-tolerant Fuels for Light Water Reactors (EGATFL) – under the auspices of the NEA Nuclear Science Committee. This expert group acts primarily as a forum for scientific and technical information exchange on advanced LWR fuels with enhanced accident tolerance. Following the two international workshops, the expert group defined a collaborative programme of work to help advance the scientific knowledge needed to provide the technical groundwork essential for the development of advanced LWR fuels with enhanced accident tolerance, as well as other non-fuel core components with important roles in LWR performance under accident conditions. This state-of-the-art report, authored by 38 experts from 35 organisations, representing 15 NEA member countries, is the result of this collaborative endeavour.

Acknowledgements

Table of contents

List of figures

List of tables

List of abbreviations and acronyms

ABG	Attribute guide
ADELINE	Advanced Device for Experimenting up to Limits Irradiated Nuclear fuel Elements
ADOPT	Advanced Doped Pellet Technology
ADS	Accelerator-driven systems
ANL	Argonne National Laboratory (United States)
ATCR	Accident-tolerant control rods
AOOs	Anticipated operational occurrences
ASN	Autorité de Sûreté Nucléaire (France)
ASTEC	Accident Source Term Evaluation Code
ATCR	Accident-tolerant controls rods
ATF	Accident-tolerant fuel
ATR	Advanced test reactor
BDBAs	Beyond-design-basis accidents
BNL	Brookhaven National Laboratory (United States)
BOL	Beginning of life
BU	Burn-up
BWR	Boiling water reactor
CANDU	Canada Deuterium Uranium (pressurised heavy water reactor)
CA-PVD	Cathode arc physical vapour deposition
CDW	Capacitive discharge welding
CEA	French Alternative Energies and Atomic Energy Commission
CERCER	CERamic-ceramic
CERMET	CERamic METal

CGN   China General Nuclear Power Group

CHF   Critical heat flux

CIP   Cabri International Programme

CMRR   China Mianyang research reactor

CNL   Canadian Nuclear Laboratories

CRs   Control rods

CRIEPI   Central Research Institute of Electric Power Industry (Japan)

CTE   Coefficient of thermal expansion

CVD   Chemical vapour deposition

CVI   Chemical vapour infiltration

DBA   Design-basis accident

DECs   Design extension conditions

DHRS   Decay heat removal system

DLLs   Dynamic link libraries

DNB   Departure from nucleate boiling

DNBR   Departure from nucleate boiling ratio

DOE   Department of Energy (United States)

DSC   Differential scanning calorimetry

EATF   Enhanced accident-tolerant fuel

EB   Electron beam

ECCS   Emergency core cooling system

ECR   Equivalent-cladding reacted

EDF   Electricité de France

EDS   Energy dispersive spectroscopy

EGATFL   Expert Group on Accident-tolerant Fuels for Light Water Reactors (NEA)

EPMA   Electron probe micro-analysis

EPR   European pressurised reactor

EPRI   Electric Power Research Institute (United States)

FB-CVD	Fluidised bed chemical vapour deposition
FBR	Fast breeder reactor
FBTR	Fast breeder test reactor
FCM	Fully ceramic microencapsulated
FE	Finite element
FFA	Fuel flask assembly
FFTF	Fast flux test facility
FG	Fission gas
FGR	Fission gas release
FMEA	Failure modes and effects analysis
FP	Fission product
FR	Fast reactor
FWHM	Full width at half maximum
GG	Green granule
GRS	Global Research for Safety (Germany)
HANARO	High-flux Advanced Neutron Application Reactor (Korea)
HBWR	Halden boiling water reactor (Norway)
HFR	High-flux reactor
HFIR	High-flux isotope reactor
HM	Heavy metal
HPSI	High-pressure safety injection
HRP	Halden Reactor Project (Norway)
HT	High-temperature
HTR	High-temperature reactor
HTGR	High-temperature gas-cooled reactor
HVE	Hot vacuum extraction
HWC	Hydrogen water chemistry
IAEA	International Atomic Energy Agency

ID	Inner diameter
IFE	Institute for Energy Technology (Norway)
IMDP	Inert matrix dispersion pellets
IMAGO	Irradiation of Materials for Accident-tolerant fuels in the Gösgen reactor
INL	Idaho National Laboratory (United States)
INPO	Institute of Nuclear Power Operations (United States)
IRSN	Institut de radioprotection et de sûreté nucléaire (France)
JAEA	Japan Atomic Energy Agency
JHR	Jules Horowitz Reactor (France)
KAERI	Korea Atomic Energy Research Institute
KAIST	Korean Advanced Institute of Science and Technology
KepcoNF	Kepco nuclear fuel (Korea)
KfK	Karlsruhe Nuclear Reseach Centre (Germany)
KIT	Karlsruhe Institute of Technology (Germany)
KTH	Royal Institute of Technology (Sweden)
LB-LOCA	Large-break loss-of-coolant accident
LCAC	Low carbon arc cast
LEU	Low-enriched uranium
LFA	Lead fuel assembly
LFR	Lead fuel rods
LHGR	Linear heat generation rate
LHR	Linear heat rate
LMFBR	Liquid metal cooled fast breeder reactor
LOCA	Loss-of-coolant accident
LORELEI	Light water, One Rod Equipment for LOCA Experimental Investigations
LPS	Liquid phase sintering
LPSI	Low-pressure safety injection
LTA	Lead test assemblies

LTR	Lead test rod
LTO	Long-term operation
LWR	Light water reactor
MAAP	Modular accident analysis program
MADISON	Multi-rod Adaptable Device for Irradiation of experimental fuel Samples Operating in Normal conditions
MCPR	Minimum critical power ratio
METI	Ministry of Economy, Trade and Industry (Japan)
MEXT	Ministry of Education, Culture, Sports, Science and Technology (Japan)
MOOSE	Multi-physics object-oriented simulation environment
MOX	Mixed-oxide fuel
MTR	Materials test reactor
MTS	Methyl trichlorosilane
MUG	MAAP User Group
NASA	National Aeronautics and Space Administration (United States)
NCA	Toshiba Nuclear Critical Assembly (Japan)
NDE	Non-destructive evaluation
NEA	Nuclear Energy Agency
NEAMS	Nuclear energy advanced modelling and simulation
NFD	Nippon Nuclear Fuel Development
NITE	Nano-infiltration and transient eutectic phase
NPP	Nuclear power plant
NPS	Nuclear power station
NRC	Nuclear Regulatory Commission (United States)
NRG	Nuclear Research and Consultancy Group (Netherlands)
NSRR	Nuclear Safety research reactor (Japan)
NTD	Neutron transmutation doping
NWC	Normal water chemistry

OD	Outer diameter
ODS	Oxide dispersion strengthened
OLNC	On-line noble metal chemistry
ORNL	Oak Ridge National Laboratory (United States)
PARCS	Purdue Advanced Reactor Core Simulator (United States)
PBAT	Particle-based accident tolerance
PCI	Pellet-clad interaction
PCMI	Pellet-clad mechanical interaction
PIE	Post-irradiation examination
PM	Powder metallurgy
PNNL	Pacific Northwest National Laboratory (United States)
PQD	Post-Quench ductility
PSF	Poolside facility
PSI	Paul Scherrer Institute (Switzerland)
PUREX	Plutonium and Uranium Refining by EXtraction
PVD	Physical vapour deposition
PWR	Pressurised water reactor
PyC	Pyrolitic carbon
RA	Reduced activation
RCCA	Rod cluster control assembly
RCS	Reactor coolant system
RE	Rare-earth elements
RFEF	Reactor Fuel Examination Facility (JAEA, Japan)
RIA	Reactivity-initiated accident
RPV	Reactor pressure vessel
RT	Room temperature
SA	Severe accident
SAFDLS	Specified acceptable fuel design limits

SAM	Severe accident management
SANS	Small-angle neutron scattering
SB	Slug bisque
SBO	Station blackout
SCC	Stress corrosion cracking
SEM	Scanning electron microscopy
SFR	Sodium fast reactor
SIMS	Secondary ion mass spectrometry
SLCS	Stand-by liquid control system
SOARCAs	State-of-the-Art Reactor Consequence Analyses (NRC, United States)
SPS	Spark plasma sintering
SSM	Swedish Radiation Safety Authority
TD	Theoretical density
TIG	Tungsten inert gas
TREAT	Transient reactor test facility
TRISO	Tri-structural Isotropic
TRLs	Technology readiness levels
TSD	Thermal spray deposition
TSO	Technical support organisation
UF	University of Florida
UIUC	University of Illinois Urbana-Champaign
UTS	Ultimate tensile strength
VHT	Very-high-temperature
VVER	Water-water energetic reactor (Russia)
WDS	Wavelength dispersive spectroscopy
WDX	Wavelength dispersive X-ray spectroscopy
XRD	X-ray diffraction

Executive summary

All light water reactors (LWRs) around the world are currently using fuel systems comprised of uranium oxide (UO_2) encased within a zirconium-based alloy cladding. Some reactors use uranium-plutonium oxide fuels, which are also known as mixed oxide (MOX) fuels. The oxide fuel-zircaloy system has been optimised over many decades and performs very well under normal operations and anticipated transients. However, because of the highly exothermic nature of zirconium-steam reactions, under some low frequency accidents – when core cooling is temporarily lost and part of the core is uncovered – low probability accidents may lead to an excess generation of heat and hydrogen, resulting in undesirable core damage.

After the 2011 Great East Japan Earthquake and Tsunami, and the events that followed at the Fukushima Daiichi power plant, global interest has expanded in exploring fuels with enhanced performance during such rare events, with accident-tolerant fuel development programmes starting in many research institutions and industry teams. While there is broad consensus that a new fuel system alone is insufficient to mitigate accident consequences, fuel in combination with other systems may provide some relief in responding to such rare events, while providing additional benefits during more frequent events and/or normal operations.

The NEA organised two international workshops in 2012 and 2013 to gauge the interest of its member countries in the development of LWR fuels with enhanced accident tolerance. Because of the wide-ranging interest, the Expert Group on Accident-tolerant Fuels for Light Water Reactors (EGATFL) was subsequently established in 2014. A total of 35 institutions from 14 member countries – Belgium, the Czech Republic, France, Germany, Japan, Korea, the Netherlands, Norway, Russia, Spain, Sweden, Switzerland, the United Kingdom and the United States – as well as invited technical experts from China, take part in the activities of the group.

The expert group is divided into three task forces, which address the following issues:

- evaluation metrics and systems assessment;

- cladding and core materials options;

- fuel options.

The task forces, comprised of experts from the participating institutions, worked between 2014 and 2017, with semi-annual integration meetings, to generate the deliverables of the EGATFL. Task Force I was devoted to the preparation of a framework for the evaluation of accident-tolerant fuels (ATFs) by:

- defining the desired properties, behaviours and performances of ATF systems (claddings and fuels);

- introducing appropriate metrics to evaluate ATF performances against the oxide fuel-zircaloy system and to compare the different designs;

- describing standard tests to investigate key features and behaviours of ATFs.

The scope of the work of Task Force I also included:

- the description of illustrative accident scenarios that may be adopted to assess, through severe accident analysis codes, the potential performance enhancement of ATFs relative to the current standard fuel system in accident conditions;

- a definition of the technology readiness levels (TRLs) applicable to ATFs;

- a survey of the available modelling and simulation tools (fuel performance and severe accident analysis codes) and experimental facilities available to support the development of the various ATF concepts.

Task Forces II and III focused on cladding and fuel options, respectively. Their objectives were to review and evaluate the available ATF knowledge and to express a consensual position on the state of the art for the various options in terms of properties, available experimental data, available modelling results and ongoing R&D activities. In addition, an evaluation of the current TRLs for each option was provided based on a consensual assessment of the participating experts.

The efforts of the three task forces were co-ordinated to provide a single deliverable, where the different contributions were jointly compiled with the objective of summarising the existing knowledge on ATFs, including the potential benefits of each concept, and identifying additional development needs for successful commercialisation. The present report reflects the consensus reached by the participating organisations. This consensus will be useful for subsequent decisions in various national and industrial programmes, for example to guide technology choices and development strategies.

The objective of the report is not to prioritise the different technologies or to down select to the most promising technologies. National programmes and industrial stakeholders may use the report to decide on their own set of priorities and choose the most appropriate technology based on their specific strategy, business case and deployment schedules, which vary from state to state, as well as from company to company.

The *State-of-the-Art Report on Light Water Reactor Accident-Tolerant Fuels* is organised in five parts:

- Part I: Evaluation metrics and illustrative scenarios;

- Part II: Cladding and core materials:

    - coated and improved zirconium (Zr) alloys;

    - advanced steels;

    - refractory metals (molybdenum);

    - silicon carbide (SiC) and SiC/SiC composites;

    - accident-tolerant control rods and SiC channel box for boiling water reactors (BWRs).

- Part III: Advanced fuel designs:

    - improved UO_2;

    - high-density fuels;

    - microencapsulated fuel.

- Part IV: Technology readiness level evaluation;

- Part V: Cross-cutting issues between fuel and cladding designs.

The structure of the report reflects the work method of the task groups. For example, based on the evaluation metrics established by Task Force I, relevant attribute guides were defined for each cladding and fuel technology in order to provide a comprehensive evaluation of the different designs by thoroughly covering the following key topics:

- fabrication/manufacturability;

- normal operation and anticipated operation occurrences (AOOs);

- behaviour in accident conditions (design-basis accidents, design extension conditions);

- fuel cycle-related issues (fuel storage, transport, disposal, reprocessing).

Attribute guides were established for each fuel, cladding and non-fuel component candidate concept so as to assess the gap between the present R&D status on ATF designs and the requirements to be met for commercial deployment in LWRs. The completed attribute guides represent the backbone of EGATFL work, and the information collected by the authors.

Using information gathered in the attribute guides, Task Force II provided five chapters containing state-of-the-art knowledge and describing the consensus reached among the different organisations, based on exchanges that took place within the EGATFL framework. Each of the five chapters is devoted to either a cladding candidate design (coated and improved Zr-alloys; advanced steels: FeCrAl; refractory metals: lined Mo-alloy cladding and SiC/SiC-composite cladding) or to non-fuel components (accident-tolerant control rods, SiC-composite for BWR channel box). Task Force III took a similar approach for various candidate fuel designs (doped UO_2, high-thermal conductivity fuel, high-density fuel, encapsulated fuel). Task Force II and Task Force III results are collected in Part II and Part III, respectively.

The Technology readiness level evaluation in Part IV focuses on the TRL evaluation for different fuel-cladding and non-fuel component candidate designs. According to the definition of TRLs provided in this report, coated and improved Zircaloy concepts and advanced steels concepts for ATF cladding accomplished the proof-of-concept stage (up to TRL 3), and the R&D for the proof-of-principle stage (above TRL 3) has begun. The R&D activity to achieve the TRL 3 level is ongoing for refractory metal and SiC-based concepts. The R&D level for the reviewed non-fuel core components achieved TRL 3. As for the fuel design concepts, doped UO_2 are already in the proof-of-performance stage (above TRL 6); although data need to be accumulated for accident conditions. Metallic and BeO additive concepts for high thermal conductivity fuel has achieved the proof-of-concept stage (up to TRL 3). The R&D of other advanced fuel concepts, including advanced additives, high-density fuels and encapsulated fuels, is still in the proof-of-concept stage.

Based on the state-of-the-art information collected in Parts II and III, Part V completes the report by proposing an assessment of the compatibility between fuels and cladding designs with respect to different classes of properties (e.g. chemical, mechanical, neutronics, thermal). This evaluation suggests that, whatever the cladding, data are missing for high-density fuel designs, especially with regard to chemical and mechanical properties. Neutronics is recognised as being a potential issue for FeCrAl and refractory metal cladding, requiring a more challenging design (without compromising the concept itself), except when these claddings are combined with high-density uranium silicide, uranium carbide and metal fuels. Low ductility of SiC/SiC cladding is recognised as being a potential challenge for this cladding concept, whichever the fuel design; more data on the pellet cladding mechanical interaction need to be collected.

The present report attempts to reach out to different audiences through a structure that provides different levels of information adapted to the specific reader's needs.

Part I provides some of the keys that are required to access the technical level through the introduction of the metrics upon which the attribute guides are based. It is also useful for decision makers as it provides a thorough description of the TRL scale, together with a review of the available R&D tools to address scientific and engineering issues related to ATFs (e.g. test facilities, fuel performance codes, system codes, severe accident analysis codes).

Readers who are interested in an overview of the current status of technologies described in the report can refer to Part IV, which contains an assessment of the industrial maturity of each design, without interfering with the assessment of the performance. This part of the report also gives an expert viewpoint on the correct use of the TRL when employed in specific contexts such as irradiation, fabrication, safety for normal operation and anticipated operational occurrences, and safety for off-normal operations and design-basis accidents, as well as design extension conditions.

Based on the information presented in Parts I and IV, stakeholders from both industry and government can acquire insight into the current developmental stages of ATFs and the capability of existing infrastructures to face the challenges that innovative fuels represent for R&D organisations, the nuclear industry and for regulatory bodies. When examined in the context of country-specific perspectives, and completed with technical experts' advice, this material can assist decision makers in sketching out the R&D strategies that would need to be implemented within national programmes to pursue the development of future nuclear fuels.

Parts II and III allow the reader to explore the technical details of ATFs, by providing a consistent and complete – although synthetic – description of the technical details collected in the attribute guides. The information is accessible to readers who are not necessarily specialised in nuclear fuel and cladding design, but who have a scientific background.

Finally, more demanding readers, such as fuel specialists, will be able to access the raw evaluations emerging from this expert group's efforts. These evaluations are presented in Appendices A and B, where the completed attribute guides are provided for the cladding and core materials (Appendix A) and for the advanced fuel designs (Appendix B). The attribute guides explore in detail the ATF concept properties and the features that ATF concepts exhibit in different contexts. They are presented in the form of tables where each of the characteristics is evaluated through the following colour code:

	properties not addressed; colour status not identified because of a lack of knowledge
	data available; results are good; concept is matured
	data available; results not good enough; further optimisation needed
	lack of data; not challenging
	lack of data and potentially challenging
	potential showstopper identified

It is important to emphasise that this report primarily reviews ongoing research, and presents fuel and cladding concepts that are not at the same level of development. Although Parts IV and V (see tables beginning on page 248) are valuable means of presenting a global picture of the current status of the development of advanced fuels and claddings and their compatibility, given the complexity of these issues, the reader is nonetheless invited to refer to the central parts of the report (Parts I, II, and III) for a more extensive discussion on the scientific and technological details.

The present report reflects the situation of ATFs as of the beginning of January 2018 when the EGATFL approved the report during its final meeting.

Part I: Evaluation metrics and illustrative scenarios

1. Introduction

The safe, reliable and economic operation of the world's nuclear power reactor fleet has always been a top priority for the nuclear industry. Continual improvement of technology, including advanced materials and nuclear fuels, remains central to the industry's success. Decades of research combined with continual operation have produced steady advancements in technology and have yielded an extensive base of data, experience and knowledge on light water reactor (LWR) fuel performance under both normal and accident conditions. Enhancing the accident tolerance of LWRs became a topic of serious discussion following the 2011 Great East Japan Earthquake, the resulting tsunami and subsequent damage to the Fukushima Daiichi nuclear power plant complex.

The current nuclear power industry is based on mature technology and has an excellent safety and operational record. The current UO_2 – zirconium alloy fuel system (i.e. fuel rod) meets all performance and safety requirements while keeping nuclear energy an economically competitive clean-energy option. The goal of accident-tolerant fuel (ATF) development is to identify alternative fuel system technologies to further enhance the safety, competitiveness and economics of commercial nuclear power. Any new fuel concept should be evaluated against current design, operational, economic and safety requirements to assess the regulatory safety compliance with operational and economic constraints. Holistic considerations of the potential impact of ATF concepts on the entire fuel cycle should be addressed. For example, reprocessing and disposal considerations in specific countries may drive ATF implementation decisions.

The complex multi-physics behaviour of LWR nuclear fuel makes defining specific material or design improvements difficult. Hence, establishing desirable performance attributes is critical in guiding the design and development of fuels and cladding with enhanced accident tolerance. ATF designs would endure severe accident conditions in the reactor core for a longer period of time[1] than the current fuel system while maintaining or improving fuel performance during normal operations. Key requirements for advanced fuels relate to the nuclear fuel performance, cladding performance and adherence to overall system constraints.

This document defines a proposed set of international metrics, related standardised tests and illustrative severe accident scenarios for the evaluation of ATF concepts that can be applied within all the participating organisations, which operate pressurised water reactors (PWRs), boiling water reactors (BWRs) and water-water energetic reactors (VVERs). The metrics and evaluation approach is derived from a detailed evaluation approach and associated sensitivity studies proposed in the United States (Bragg-Sitton et al., 2013, 2015, 2016), generalised to be more broadly applicable in the international community. The proposed technical evaluation methodology will be applied to assess the ability of each concept to meet performance and safety goals relative to the current UO_2-zirconium alloy system. The development status of fuel performance and severe accident analysis codes to support ATF analysis is also summarised to provide guidance for future code enhancements, and agreed-upon illustrative accident scenarios for analysis of ATF concepts are described.

---

1. Note that the specific time frame achieved by any ATF solution will be strongly dependent on the LWR system in which is it adopted and the specific accident scenario.

References

Bragg-Sitton, S.M. et al. (2016), "Metrics for the technical performance evaluation of LWR accident tolerant fuel", *Nuclear Technology*, Vol. 195(2), pp. 111-123, August 2016.

Bragg-Sitton, S.M. et al. (2015), "Evaluation of enhanced accident tolerant LWR fuels", *Proceedings of Top Fuel 2015*, Zurich.

Bragg-Sitton, S.M. et al. (2013), *Enhanced LWR Accident Tolerant Fuel Performance Metrics*, INL/EXT-13-29957, Idaho National Laboratory, prepared for the US Department of Energy Advanced Fuel Campaign.

2. ATF design constraints and desired attributes

Enhanced accident-tolerant fuels (ATFs) are defined as fuels that can tolerate a severe accident in the reactor core for a longer time period than the current UO_2 zirconium alloy fuel system, while maintaining or improving the fuel performance during normal operations and operational transients. Any new fuel concept should be evaluated against current design, operational, economic and safety requirements to assess the regulatory safety compliance with operational and economic constraints. The constraints associated with commercial nuclear fuel development and deployment that are applied to ATF designs include:

- backward compatibility: compatible with existing fuel handling equipment, fuel rod or assembly geometry and co-resident fuel in existing and future LWRs; concept designs should maintain or increase access to non-intrusive and intrusive examinations and inspections;

- operations: maintains or extends plant operating cycles, reactor power output and reactor control; fuel system concepts seeking regulatory approval will need to demonstrate reliability under normal operations and transients (i.e. anticipated operational occurrences);

- safety: meets or exceeds current fuel system performance under normal, operational transient, design-basis accident (DBA) conditions and design extension conditions (DECs; previously referred to as beyond-design-basis accidents [BDBAs]);

- front end of the nuclear fuel cycle: adheres to regulations and policies, for both the fuel fabrication facility and the operating plant, with respect to technical, regulatory, equipment and fuel performance considerations;[2]

- back end of the nuclear fuel cycle: cannot degrade the transport, storage (wet and dry) or repository performance of the fuel (assuming a once-through fuel cycle); should consider possible use within a closed fuel cycle.

The economics of a proposed ATF concept should be evaluated to determine the potential of the fuel system being adopted by industry. However, that is difficult to assess early in the development of new materials because of significant uncertainty in material and fabrication costs during this development phase and enhanced safety performance is the primary driver for ATFs. Hence, separation of economic evaluation from the technical performance and safety assessment is likely necessary to allow for prioritisation of concepts for further development. The technical performance data will provide more information for future assessment of the overall economics of the proposed fuel system, which may differ in each country as a function of the regional energy markets. It is noted that it is of significant importance to maintain economic viability for new fuel concepts with respect to additional costs (e.g. fabrication) and potential cost reductions realised through improved performance (e.g. additional margins for higher burn-up, extended cycle operation and power upgrades, reduced waste) or increased safety margin. This increased performance and safety margin may, in turn, be utilised to derive an economic

---

2. Note that although the same safety criteria cannot be directly applied to different materials, the same basic considerations and intended outcomes of established regulatory guidelines and safety criteria can and should be followed.

benefit in terms of plant equipment or resource elimination, or risk reclassification, depending on the regulatory landscape of the particular country.

The desired ATF attributes highlight the performance of the fuel system, which includes both the fuel and cladding (but not the fuel assembly structure), under normal and postulated accident conditions. Key attributes for a fuel system demonstrating enhanced accident tolerance include reduced steam reaction kinetics (reaction rate and heat of reaction), lower hydrogen generation rate (or generation of other combustible gases), and reduction of the initial and residual stored energy in the core. The desired behaviours should be accomplished while maintaining or improving cladding and fuel thermo-mechanical properties, fuel rod thermo-hydraulic properties, fuel-clad interactions and fission product behaviour. A set of qualitative guidelines and metrics derived from these desired attributes across all fuel performance regimes (versus specific quantitative targets for each property) will aid in the optimisation and prioritisation of candidate fuel system designs. Note also that the thermo-hydraulic and mechanical performance of the fuel assembly should also be maintained or improved when introducing ATF. This document, however, focuses on fuel rod properties as the most critical performance indicators with respect to accident conditions and does not address the fuel assembly.

The principle of "do no harm" is guiding the development of candidate fuel systems, meaning that, under all operating conditions, it is desirable that the fuel system perform at least as well as or better than the current fuel system. Note, however, that it may not be possible to improve on all performance indicators under all scenarios, but significant improvements in some of the key attributes may outweigh modest performance gains or vulnerabilities in other attributes. As such, a candidate fuel and cladding system should seek to preserve or improve upon:

- burn-up limit/cycle length (while maintaining criticality and fuel performance);

- operational parameters (power distribution, peaking factors, safety margins, etc.);

- reactivity coefficients and control parameters (shutdown margin, rod worths);

- handling, transport and storage (consideration of fuel isotopics, handling dose, mechanical integrity);

- compatibility with existing infrastructure (e.g. core loading, in-core operations, post-irradiation handling and storage, etc.).

To be considered "accident tolerant" the fuel system must additionally provide improved response to some of the scenarios described by anticipated operational occurrences (AOOs), DBAs (e.g. reactivity-initiated accident [RIA], loss-of-coolant accident [LOCA], or station blackout [SBO]) and DEC, noting that the concept may not exhibit improved performance under all scenarios. In short, the expected performance of a particular fuel and cladding should be examined under all postulated normal operation and accident conditions throughout its intended lifetime (e.g. at high burn-up), noting that specific quantitative limits originally set for zirconium alloys may not be applicable to new fuel designs or to the operation of the current fuel system to higher burn-up. Concepts will be evaluated based on their ability to maintain behaviour under normal operation while increasing the "fuel coping time" under design extension conditions, where the fuel coping time is defined as follows.

Fuel coping time

For a given accident scenario, the "fuel coping time" is the time lapse between departure from normal operation and the moment at which significant loss of geometry of the fuel assemblies occurs, such that the reactor core can no longer be cooled or the fuel cannot be removed from the reactor using currently available tools and procedures.

As defined, the magnitude/scope of the "loss of geometry" is not specified, as the specific amount of degradation that defines an uncoolable condition may differ somewhat for each reactor design. In determining the fuel coping time the "minimum unit" may be considered to be the fuel assembly, as a limited number of failed fuel rods is currently acceptable for operating reactors. Inclusion of the specification that assemblies should be removable from the core using currently available tools and procedures ensures that the coping time will be measured up to the point that the asset is still recoverable. Coping time could also be defined as the time during which public protection can be ensured, but the definition provided by the NEA Expert Group on Accident-tolerant Fuels for LWRs (EGATFL) offers a more conservative approach. The latter calculation of a time to reach public impact is much more akin to a reactor system coping time, which would be highly reliant on safety systems that would allow for mitigating actions.

Note that each fuel system concept should have an associated failure modes and effects analysis (FMEA) conducted to determine the onset of failure modes that would lead to unacceptable conditions or performance. Additionally, the appropriate coping time for comparison of fuel systems may correspond to the point at which the condition is not recoverable. This is sometimes referred to as an "escalation point", e.g. a point at which the addition of water to the vessel can no longer provide sufficient cooling to halt the accident progression or could make the situation worse. At this point mitigating actions would not be expected to be effective. For a specific reactor system design and fuel cladding system it would be useful to identify a success criterion that links "fuel coping time" to a quantifiable reactor condition, above which the accident progression would be irreversible. Such conditions or thresholds could be applied to peak cladding temperature, percent oxidation of the cladding, cladding ductility, amount of hydrogen generated, etc. Such limitations are included in the Nuclear Regulatory Commission (NRC) regulations (i.e. 10CFR50.46) for the current UO_2-Zr-alloy fuel system.

3. Definition of evaluation metrics and related testing

"Metrics" describe a set of technical bases by which multiple concepts can be fairly evaluated against a common baseline and against one another. In some cases this may equate to a specific quantitative target value for selected properties or behaviours. "Metrics" can also describe a clear technical methodology for evaluation that can be used to rank concepts. Because of the complex multi-physics behaviour of nuclear fuel rods and the large set of performance requirements that must be met, the latter definition is adopted for the evaluation of candidate accident-tolerant fuel (ATF) designs (Bragg-Sitton et al., 2013, 2015, 2016). The following sections describe specific performance attributes and desired properties, behaviours and performance for ATF cladding, ATF fuel and the combined fuel system.

Cladding materials

Zirconium alloys, which have been optimised over several decades of use, are the current state-of-the-art cladding for light water reactors (LWRs). Several types of cladding are envisioned for ATF applications, ranging from metallic to fully ceramic cladding, each having very different neutronic and/or material properties and behaviours. Nevertheless, these different materials have to be assessed and compared to determine the concept viability and to prioritise resources to obtain the cladding concept with the best compromise in terms of properties and behaviour in both normal and accident conditions.

Desired cladding properties, behaviour and performance

The cladding for a nuclear fuel rod has two major roles:

- confine the fissile material and solid and gaseous fission products within the fuel rod without hindering the nuclear reaction from taking place;

- enable efficient thermal transfer from the fuel to the coolant.

To fulfil these two roles, an ideal cladding material needs to have certain properties and exhibit specific behaviours as follows:

- ease of fabrication:

  – compatibility with large-scale fabrication, including material availability;
  – good welding/sealing behaviour;
  – possibility of quality control.
  – Thermo-mechanical behaviour:
  – high-thermal conductivity;
  – high melting temperature;
  – high strength (up to high temperature);
  – high ductility;
  – leak-tightness (impermeable to fission gas [including tritium] and fission products) throughout the fuel rod lifetime, including plant operation, storage and long-term disposal.

- corrosion behaviour:
    - high corrosion resistance in LWR environments;
    - high corrosion resistance in high-temperature steam;
    - low H_2 or other combustible gas production;
    - low-hydrogen embrittlement, if any.

- chemical compatibility:
    - compatibility with irradiated and non-irradiated fuel;
    - compatibility with coolant;
    - compatibility with other fuel assembly components, with specific attention to potential eutectic formation as temperature increases.

- irradiation behaviour:
    - stable or predictable thermal, mechanical and corrosion behaviour under irradiation;
    - resistance to pellet-clad interaction;
    - dimensional stability (i.e. stable or predictable swelling, creep and growth under irradiation);
    - low irradiation embrittlement;
    - low-thermal neutron absorption cross-section;
    - low activation.

- back-end behaviour:
    - low tritium permeation;
    - transportable;
    - good long-term storage behaviour, including thermal and dose considerations;
    - minimal to no impact on repository design;
    - minimal impact on reprocessing (where applicable).

A realistic cladding material will not exhibit all of these ideal properties and behaviours. Therefore, a baseline for evaluation and assessment of candidate materials has to be established, which corresponds to the metrics described below. These metrics will help researchers make the best selection by evaluating the cladding material exhibiting the best compromise of properties and behaviours.

Definition of the metrics

Cladding metrics are divided into two separate sections: primary material properties inherent to the material, which are described by single quantified values and material behaviour observed through standardised tests or experiments, which are mainly described by material laws used in modelling. Standardised tests are not intended to analyse fully the material behaviour, but to provide decision makers with sufficient information to perform a prioritisation of the various cladding material solutions within a specific fuel rod design. To fully characterise the materials and obtain sufficient data for licensing of the various cladding solutions, complementary tests in addition to those recommended here will be necessary.

Primary material properties for initial evaluation

This section defines the physical properties that are relevant for the comparison of ATF concepts. A "physical property" refers to something that can be summarised in one quantified value inherent to a material, such that it varies little when slight changes are made to the microstructure or the composition. These values can be compared directly between different families of ATF-cladding concepts for general assessment.

Common physical properties for all concepts

The inherent material properties that should be compared between various ATF solutions are primarily thermal and neutronic properties:

- Melting/sublimation temperature, which determines the potential margin gain to core melt. The melting temperature should be as high as possible, if possible above the zirconium melting temperature (around 1 850°C). Any eutectics that could form between the cladding and fuel, cladding and structural materials, or cladding and coating (if present) should be identified and associated eutectic temperatures determined (see Parts II and III of this report).

- Thermal conductivity, which determines the cladding's capacity to transfer the fuel heat efficiently to the coolant and to limit the fuel centreline temperature.

- Specific heat capacity/enthalpy, which determines the capacity of the material to limit the added heat to the fuel rod system and increase the efficiency of the heat transfer to the coolant.

- Thermal expansion coefficient, which should be characterised to ensure dimensional stability of the cladding.

- Thermal neutron absorption cross-section, which determines whether the cladding material will have an impact on the nuclear reaction and the cycle length. The goal is to maintain or increase the cycle length possible with zirconium alloy cladding.

Concept-specific properties for multi-layer cladding

The properties described above are applicable to all potential ATF material solutions. Additional properties are important when investigating coated metallic or multi-layer cladding solutions because of the presence of two materials in contact, primarily to verify good compatibility between the two materials. These complementary properties include:

- Thermal expansion coefficient of each material, where the difference in coefficients between the coating and substrate materials should not be too large. Significant difference in expansion coefficients would correspond to a higher probability of coating delamination as temperature increases. This issue is especially important for ceramic-based coatings because of their intrinsic brittle behaviour. For metallic coatings, one can expect some viscoplastic accommodation capability at high temperature.

- Eutectic temperature, which determines the "superficial melting" temperature of a coated cladding. Additionally, the kinetics of the eutectic formation between the coating and substrate should be investigated to understand the behaviour of the coated solution near the eutectic temperature to determine whether it is viable or not. Because the eutectic may arise from inter-diffusion between the coating material and the substrate by creating an alloy with a lower intrinsic melting temperature, the thickness of the melted materials has to be quantified and compared to the cladding wall thickness.

Standard tests to evaluate key behaviour and performance

Apart from the physical properties inherent to the material described above and defined by specific values, which can be compared easily, the behaviour of the materials has to be assessed through tests conducted using standardised conditions to enable more direct comparison and evaluation of the performance of the various concepts relative to one another. Comparison can only be performed if the same experimental conditions are used to analyse the behaviour of the different ATF concepts. Once assessed, the behaviour is then transcribed into a law that can be used in computational models, rather than being described by a single quantified value like the physical properties.

This section proposes some standardised tests to assess cladding behaviour under normal and accident conditions. The goal of this section is not to give an exhaustive list of all the tests to be performed on ATF samples, but only those necessary to characterise the main behaviours to be assessed. Complementary tests should be performed to properly evaluate the behaviour in more specific conditions and to help quantify the added margins obtained relative to the current fuel system. For each solution, additional concept-specific tests may also be necessary. The initial set of tests performed should provide sufficient information to compare the performance of a proposed ATF concept to the standard fuel system and to rank or prioritise concepts relative to one another.

Manufacturing and handling feasibility

The assessment of cladding performance through standardised tests provides comparative data for the various cladding solutions to determine the most promising options. Additionally, it is essential to confirm the manufacturing feasibility of the cladding solutions, which is necessary for implementation and, therefore, an essential part of the material selection. Furthermore, the manufacturing will have a direct impact on the economics of the solution.

No standardised tests exist to assess manufacturing feasibility because it is highly dependent on the cladding solution. Thus, each cladding manufacturer will need to demonstrate the adequacy of the solution for large-scale industrial production, with a particular focus on the following points:

- cladding tube sealability/weldability;
- development of specific quality control techniques (including but not limited to: diameter, wall thickness, ovality, straightness, weld quality);
- interaction with fuel assembly structure (fuel rod insertion in grids, for example);
- general handling capability, including fuel assembly shipping and receipt inspection.

Normal operation

ATF-cladding materials must first provide adequate performance under normal operating conditions prior to considering accident performance, where "adequate" indicates that the performance is as good as or better than the current state-of-the-art cladding materials for LWRs. Standard tests selected to verify cladding performance under normal operating conditions are defined below.

Corrosion

Standardised corrosion tests are performed to assess the chemical compatibility of the ATF-cladding concepts with the reactor coolant under normal operating conditions. This is a key behaviour to evaluate the potential implementation of the ATF concept, since poor corrosion behaviour under normal LWR conditions will make the concept not viable for use in current LWRs. The goal of this section is to give a few standardised tests based on the Zr-alloys' behaviour that should be performed for direct comparison of the corrosion behaviour. Nevertheless, these tests are not sufficient to complete the development of an

ATF-cladding concept; therefore, complementary tests are also proposed as guidance to evaluate corrosion behaviour in other water chemistry conditions.

Concerning the standardised tests, two primary long-term corrosion tests are proposed in Table 3.1 to evaluate the corrosion behaviour in normal operating conditions. The long-term LWR tests should be performed under representative water chemistry conditions to approximate the in-pile behaviour. Additionally, an acceleration of kinetics is observed for zirconium alloys under irradiation. Therefore, potential acceleration under irradiation must also be investigated for candidate cladding materials. The steam corrosion test helps obtain accelerated kinetics to approach the potentially accelerated in-pile corrosion rates.

The PWR water chemistry contains boric acid (H_3BO_3) for fuel management and lithium hydroxide (LiOH) to adjust the pH between 6.9 and 7.4. BWRs may have several water chemistry conditions, including normal water chemistry (NWC), hydrogen water chemistry (HWC), and online noble metal chemistry (OLNC). The NWC was chosen as a standard test since it corresponds to a common BWR water chemistry. To ensure that the ATF solutions behave as expected in other water chemistries, complementary corrosion tests in the other specific chemistries may also be implemented as a validation of the concept but are not necessary for initial comparison purposes.[3] Concerning water-water energetic reactors (VVERs), the primary difference with PWR nominal conditions is the water chemistry for normal operations: while PWRs use lithium hydroxide (LiOH) for chemistry control, VVERs use potassium hydroxide (KOH). This chemistry leads to slightly different test conditions for normal operation corrosion tests as shown in Table 3.1.

Table 3.1. Standard static cladding corrosion tests for ATF

Test		Conditions	Time
Long-term LWR	PWR	T = 360°C, [Li] = 2-2.2 ppm, [B] = 600-1 000 ppm, Deaerated, no H_2 addition	At least 200 days
	BWR	T = 288°C, [O_2] = 200 ppb, no H_2 addition	At least 200 days
	VVER	T = 360°C, [K] = 15.9 ppm, [B] = 1 050 ppm, [Li] = 1 ppm	At least 200 days
Long-term steam		T = 415°C, steam	At least 200 days

Note: Shorter test duration may be used for initial screening, but longer duration tests are necessary for eventual comparison of viable cladding solutions.

Important data to assess during the recommended static cladding corrosion tests include:

- outer surface visual inspection: observe potential delamination of oxide or coating layer, if present;
- corrosion kinetics through:
  - weight change measurement;

---

3. Typical BWR test conditions: NWC – 200 ppb O_2, <5 ppb H_2; HWC without Pt – 150-200 ppb H_2 only; OLNC without Pt – 40-80 ppb O_2 + 30-40 ppb H_2; reactor soluble Zn – 5-15 ppb.

- oxide thickness measured by cross-sectional metallography (investigate oxygen diffusion within substrate, stability of the oxide-metal interface and susceptibility for localised corrosion);

- evaluation of microstructural changes in the cladding material.

- water chemistry analyses to assess potential dissolution of certain species in the water;

- evaluation of hydrogen pickup;

- evaluation of the potential for Crud production and deposition.

Depending on the concept, post-corrosion mechanical tests may be performed to evaluate the influence of environmental degradation on the mechanical behaviour of the cladding.

To study specific corrosion behaviours, additional complementary tests may also be performed but should not replace the standard tests described above. These complementary tests only serve to evaluate specific cladding behaviour, primarily in degraded water chemistry conditions.

Proposed complementary tests:

- for short-term screening purposes, the ASTM G2 88 standard test condition should be run for up to three days to obtain quick feedback on the corrosion potential of the ATF solution; these results will support concept improvement through multiple iterations;

- for PWR and VVER applications, the following complementary corrosion tests provide additional insight on the corrosion behaviour of the cladding material:

  - long-term exposure to de-ionised water at 360°C;

  - long-term exposure to de-ionised water at 360°C with [Li] = 70 ppm;

  - evaluate stress corrosion cracking behaviour; tests are dependent on failure mode but may include: C-ring U-bend, slow strain rate tests, or tests in an iodine rich environment.

- for BWR applications, a corrosion test at 288°C in water with 2 ppm of O_2 can also be performed to evaluate the stress corrosion cracking behaviour; this will also serve as a bounding test in terms of oxygen content;

- conduct tests to assess localised effects, including coating or multi-layer spallation;

- mechanical performance.

Standard tests to assess cladding mechanical performance are summarised in Table 3.2.

Table 3.2. Standard cladding mechanical tests

Test	Temperatures	Conditions
Tensile	Room temperature (RT) and 400°C	ASTM E8 E21 5 µm/mm/min for strain <0.2% 50 µm/mm/min for strain >0.2%
Internal pressure creep	400°C	130 MPa for at least 240 h
Internal pressure burst	RT and 400°C	140 bar/min at RT 60 bar/min at 400°C

New failure modes could be introduced for some ATF concepts relative to the current fuel system. Because of varied failure modes of the proposed ATF-cladding concepts, complementary mechanical tests may be performed, including:

- leak-tightness: this test (at RT and 400°C, with internal and external overpressure) is especially important for composite cladding, such as SiC/SiC, having a large amount of porosity;

- fatigue: tests at 400°C with internal pressure or thermal cycling depending on the failure mode; pressure or temperature ramp rates are to be defined according to the expected failure mode.

Accident behaviour

After verifying that a selected cladding material exhibits desirable performance under normal operating conditions, the material performance under selected accident conditions should then be assessed. Specific tests selected to determine potential accident performance of candidate cladding materials are summarised below. Additionally, the degradation and failure modes of the different cladding solutions will need to be evaluated for various postulated accident conditions. An "acceptable damage limit" should be defined for cladding exhibiting cumulative damage under irradiation (i.e. ceramic cladding). If new failure modes appear compared to standard zirconium alloy cladding, then complementary tests should be performed to fully understand the failure mechanisms of the candidate ATF-cladding solutions.

- High-temperature oxidation

To evaluate high-temperature (HT) steam oxidation behaviour without creating a new set of regulatory limits, it is suggested to remain at temperatures equivalent to Loss-of-coolant accident (LOCA) conditions, i.e. between 600 and 1 200°C steam followed by a quench.[4] Testing at 1 200°C would be followed by a slow cooling phase down to around 800°C, then a quench. The time that the material is held at elevated temperature could be varied to characterise the enhanced performance of the proposed ATF cladding. At a minimum, the material should be held at elevated temperature conditions for ~600 seconds for one-sided oxidation and for ~150 seconds for two-sided oxidation (these times are typical for 570 µm to 600 µm thick cladding), which corresponds to the "historical" LOCA oxidation criteria for zirconium alloys based on an equivalent-cladding reacted (ECR) value of 17%. The test result should be evaluated through weight gain and metallographic cross-section to reveal the post-quench microstructure. Hydrogen pickup measurements should also be performed, preferably by hot vacuum extraction technique (HVE). Additionally, electron probe micro-analysis (EPMA) and/or micro-hardness measurements could be applied on the residual prior-beta layer to derive its oxygen content, which is one of the main influencing parameters on the residual HT oxidised Zr-alloy based cladding ductility/toughness. Several HT steam exposure times (at temperatures ranging from 600°C to 1 200°C) should be analysed to evaluate the time limit to degradation (to be defined initially depending on the cladding solution investigated) at that temperature, which provides information for a comparison of the accident behaviour of different ATF solutions.

The HT oxidation test should be complemented by post-quench mechanical analysis using an applicable test method, such as ring compression tests – preferentially at 135°C and at RT – to evaluate the post-quench ductility. Structural mechanical tests are conducted to assess cladding strength (see Table 3.2). The various solutions investigated will behave differently under these conditions, such that it may be possible to infer their comparative behaviour at even higher temperatures. Fuel safety under LOCA conditions

---

4. Note that steam oxidisation tests can be run at higher temperatures to determine the ultimate temperature limit, but this would not be considered part of the standard set of tests.

can be evaluated and confirmed by mechanical analysis or laboratory-scale simulated tests. In contrast, performance under reactivity-initiated accident (RIA) conditions is primarily evaluated by in-pile tests in a transient test facility. Since selection of the test method will differ based on the specific cladding material and regulatory requirements in each country, fundamental consideration for the fuel safety performance under LOCA should be taken into account, noting that the evaluation method could differ somewhat based on the cladding material being investigated. Basic considerations for LOCA criteria are summarised in the NEA CSNI Technical Opinion Papers No.13 *LOCA Criteria Basis and Test Methodology* (NEA, 2011). It should be noted that cladding oxidation could have a positive impact for some cladding materials on account of the resultant increase in the melting temperature for the oxidised layer.

▪ Mechanical performance in accident conditions:

The primary mechanical behaviour of interest under accident conditions, apart from the post-quench analysis described above, pertains to ballooning and burst behaviour at elevated temperatures. Consequently, it is suggested that the following tests be performed to simulate various design-basis accident (DBA) and beyond-design-basis accident/design extension condition (BDBA/DEC) conditions:

- Isothermal internal pressure burst tests at multiple temperature set points, such as 600°C, 800°C and 1 000°C, for example [LOCA]. These temperatures are used for Zr-alloy tests. These tests will allow one to determine the time that the cladding can withstand these temperatures relative to the current state-of-the-art cladding material. Higher temperature tests may be appropriate based on cladding type and scenario being evaluated.

- Dynamic internal pressure burst tests with increasing temperature until cladding failure with temperature ramp speeds ranging from 0.1 to 100°C/s and pressures from 10 to 150 bar [LOCA, SBO].

- Rapid burst test with increasing temperature until cladding failure [RIA].

For all these tests, which are summarised in Table 3.3, the important examinations to be performed are:

- measure balloon size in burst tests, e.g. measure circumferential elongation at rupture and a few centimetres away from the rupture opening, width of rupture opening, etc.;

- measure minimum (steady-state) creep rate;

- measure rupture time and temperature;

- ramp tests: determine rupture temperature and time.

Table 3.3. Standard cladding tests for accident conditions

Test	Temperatures	Conditions	Post-test characterisation
HT steam oxidation	From 600°C to 1 200°C	Exposure times for one-sided oxidation: 600s to material limit	RCT Structural mechanical tests
Isothermal HT creep	From 600°C to 1 200°C	Various pressures at each temperature: 10 to 150 bars	Circumferential elongation Rupture and time at rupture
Dynamic HT burst	Thermal ramp speeds: 0.1 to 100°C/s	Various pressures at each temperature: 10 to 150 bars	Circumferential elongation Rupture and time at rupture

Concept-specific performance assessment for multi-layer cladding

A primary concern for the performance of multi-layered/coated cladding is layer adhesion and/or cracking under all conditions; in addition, the initial coating behaviour should be maintained under all conditions (no dissolution, no eutectic at relevant temperatures, etc.). For this purpose, the corrosion and mechanical behaviour tests for normal operating conditions are important to ensure that the coating does not spall-off during corrosion, tensile and internal pressure burst/deformation tests. These tests should be performed on samples with varying coating/layer thicknesses to determine the impact of the coating/layer thickness on adhesion.

Several tests may be used to determine adhesion of the multiple layers of cladding, such as:

- scratch tests; ideal for fabrication control, but difficult to quantify;

- 3- or 4-point bend tests to determine the strain level at which the layers delaminate; this test gives more quantifiable data but may be more used for general performance evaluation;

- selection of mechanical tests (e.g. burst, tensile or creep tests), defined above, to determine the stress at which delamination occurs.

Corrosion and mechanical performance tests should also be performed on a sample that has a damaged outer coating/layer (e.g. full-thickness scratch through the coating layer, intentional cracks in the coating, localised removal of the coating, etc.). The force required to achieve the full-depth scratch will provide valuable information on the overall durability of the coating to withstand handling procedures or fretting. If a eutectic is expected to form below 1 482°C (PWR) or 1 200°C (VVER), then testing should also be performed up to the eutectic temperature. These temperatures represent the limit temperature based on early experimental data on the fuel failure boundary for LOCA-type conditions in a PWR; this limit temperature is 1 200°C for a VVER (IAEA, 2003).

Finally, analysis of the interfaces in multi-layer cladding should include evolution after corrosion testing in both normal operating and accident conditions, with a particular focus on the potential presence or appearance of porosity at the interface. The impact of irradiation on these interfaces and the bonding of the coating to the substrate or multiple layers of the concept will be a key to the development of a coating/multi-layer solution and the ability to license the coated/multi-layer cladding design. However, there is still a need to define normalised tests for evaluating the coating adhesion and susceptibility to cracking before and after irradiation.

Behaviour under irradiation

The goal of material testing under irradiation is to assess and quantify/characterise the following behaviours in order to develop a database of material performance with increasing irradiation:

- evolution of the cladding microstructure under irradiation;

- dimensional stability of the cladding under irradiation:

    – swelling;

    – creep;

    – growth, including differential growth of the two materials in the case of multi-layer cladding.

- evolution of the mechanical behaviour under irradiation through post-irradiation tensile and burst tests, primarily focusing on irradiation embrittlement;

- material corrosion and hydrogen pickup kinetics under fully representative conditions (PWR, BWR, VVER);

- high-temperature oxidation tests, followed by quench.

The cladding behaviour under irradiation can be assessed through unfuelled sample irradiations in research or commercial reactors at different levels of fluence (or dpa) to determine the evolution of the behaviour with irradiation. Nevertheless, the main investigations under irradiation should be performed on fuel rods containing ATF pellets or UO_2 fuel, as described in Parts II and III of this report.

Back-end behaviour

Characterisation of fuel system behaviour at the back-end (end of life) does not contain any specific standardised test because the criteria for transport or short or long-term storage are dependent on the casks or technology used. Nevertheless, certain tests may aid characterisation of candidate materials at end of life conditions:

- Transport: tensile tests at high tensile speeds over a large range of temperatures to serve in the modelling of transport accidents:

  - speed: $1s^{-1}$;

  - temperatures: -40°C, RT and +70°C.

- General behaviour: tritium release or tritium cladding permeation; this is an important behaviour to investigate for utilities since they prefer the cladding to be leak-tight to tritium to limit the on-site dose; if the rod is leak-tight to tritium, the problem will be displaced to the reprocessing plant, so it is viewed here as a back-end issue; tritium release during reactor operation must also be considered in the fuel cladding design, as it affects plant operation.

One should also consider impact of the cladding concept on the repository or reprocessing scenarios, as applicable. The chemical compatibility of the cladding with reprocessing should be evaluated in terms of chemical impact on the fuel dissolution and the waste vitrification process and in terms of mechanical impact for shearing the cladding and compacting the hulls to reduce waste volume.

Fuel materials

The current standard fuel for water-cooled reactors (PWRs, BWRs, VVERs) is UO_2, enriched to approximately 4.0 to 4.95% ^{235}U. Several fuel materials are currently under consideration for ATFs, ranging from slight variations on the current UO_2 technology to more significant departures from the current state of the art that could provide significant enhancement to fission product retention.

Desired performance, properties and behaviour

Fuel performance under normal operating conditions and the potential enhanced accident tolerance of a specific ATF concept can be estimated from the fuel behaviours determined from material properties. Key material properties fall into several categories, including thermal, mechanical, chemical and neutronic properties. The desired trends for these properties to achieve the desired fuel performance are discussed below, considering relative impacts on the fuel performance in the current fuel system and taking the variation in fuel behaviour under irradiation into account. Quantification of target values for the various attributes/properties is extremely challenging because of the complex interrelationship among properties. Hence, it is important to consider the integrated effects of the material properties for each advanced fuel design. The fuel must function in the overall system throughout the intended fuel lifetime, while adhering to the constraints established for use of the fuel in the current LWR fleet.

Consideration should be given to the pellet burn-up structure and fragmentation. The ATF pellets should maintain or enhance the margin to formation of the high burn-up structure, fission gas release, fuel fragmentation and possible dispersal into the coolant during DBAs and BDBAs/DECs. Note that microstructural changes in the fuel that occur during operation could result in detrimental fuel rod behaviour during a transient (e.g. RIA or LOCA).

Fuel thermal properties

The thermal behaviour of LWR fuel is dominated by its thermal properties, which include melting point, thermal conductivity, specific heat capacity and thermal expansion. The variation in density and porosity type also impacts the thermal behaviour. The thermal behaviour of LWR fuel, in turn, greatly impacts the fission product release, fuel swelling and fuel mechanical properties. Minimal, predictable fuel swelling and minimal fission product release are important in fuel rod design. The range of thermal behaviour for candidate fuel materials must fall within allowable limits under normal operating conditions prior to considering accident tolerance. Desired trends for these properties to improve safety performance are indicated below.

- Melting point: Higher melting point is preferred, in general. This property is important for evaluating fuel performance under anticipated operational occurrences (AOOs), RIA and LOCA conditions. The maximum fuel temperature that will be reached depends on the fuel system design, reactor design and the accident scenario. The margin to melt for the fuel concept in normal and accidental conditions, in terms of linear power, depends mainly on the melting point and thermal conductivity parameters. Note that different fuel types may operate at significantly different temperature than the current fuel system (e.g. metallic fuel will operate at lower temperature than ceramic fuel because of higher thermal conductivity). The margin between operating temperature and melt temperature is a more significant parameter than the specific melt temperature alone.

- Thermal conductivity: For identical linear power and gap and cladding thermal barriers, fuels with high-thermal conductivity operate at lower centreline temperature. Operation at lower centreline temperature reduces all diffusion-driven processes (among others, fission gas release). At identical density and heat capacity (see below) the stored thermal energy is lower, yielding lower fuel system temperatures (fuel and cladding) upon coolant failures. This creates additional margin to departure from nucleate boiling (DNB) and generally reduces corrosion and mechanical deformation under accident conditions.

- Specific heat capacity: Lower specific heat is preferred such that less energy is stored in the fuel at the onset of accident conditions, e.g. LOCA or transients with DNB occurrence. Given the relation $\lambda = \alpha\, C_p\, \rho$ between thermal conductivity (λ), thermal diffusivity (α), specific heat (C_p), and density (ρ), optimisation is necessary for the proper fuel design to improve the fuel total performance.

- Pellet density: Density affects the initial stored energy at onset of LOCA and also impacts DNB under loss of flow conditions. The porosity type should be optimised in order to lower fission gas release, lower fuel-water interaction and to optimise other properties.

- Coefficient of thermal expansion (CTE): Lower CTE is preferred. Thermal expansion is a key parameter in pellet-clad interaction (PCI) under over-power conditions.

Fuel mechanical properties

Mechanical stability of the LWR fuel is determined by the mechanical properties, which include yield strength, toughness, creep rate and modulus of elasticity. Fuel should not swell or fragment excessively during reactor operation.

- Yield strength: Lower yield strength is preferred; such that the fuel plastically deforms (creeps) at high temperature. Yield strength is important to the mechanical stability of the fuel under AOO conditions because of the relationship to swelling.

- Toughness: Higher toughness is preferred. Toughness is important for the mechanical stability of the fuel under AOO conditions because of the relationship to swelling. Also, high toughness is desirable to maintain mechanical integrity during LOCA and severe accidents.

- Creep rate: Rapid creep rate is preferred. Creep is important for the mechanical stability of the fuel during normal operation and AOO conditions because of the relationship to swelling, as far as pellet-clad mechanical interaction (PCMI) is concerned. More ductile fuel is less likely to breach cladding during normal operation (PCMI), during power transient AOO (pellet-clad chemical interaction [PCCI]) and RIA. However, brittle fuel behaviour on the fuel pellet exterior also increases the number of the cracks and reduces the stresses on the internal cladding, reducing PCI risk.

- Modulus of elasticity: High elastisticity is preferred. The modulus of elasticity is extremely important for mechanical stability of the fuel during normal operation because of the relationship to structural rigidity and is also important under AOO conditions because of the relationship to swelling.

Fuel chemical properties

Chemical behaviour of the LWR fuel is evaluated based on its chemical properties, which include phase transition, corrosion and fission product chemistry.

- Phase transition: Solid-solid phase transformations, be it chemically driven (corrosion, interaction with fission products) or physically driven (temperature, formation of glassy phases), often result in unwanted swelling or contraction.

- Corrosion: Lower corrosion is preferred. If fuel cladding is breached under normal operations, AOO, DBA or DEC conditions, understanding the chemical interactions between the fuel and water coolant is very important to evaluate the safety. Compatibility with coolant should be considered from the viewpoint of the complete fuel system. Fuel dispersion arising from the interaction between fuel and coolant is also important for safety and should be avoided. Lower corrosion and lower generation of combustible gases generation from fuel-water coolant interaction is preferred to ensure fuel integrity. Fuel cladding chemical interaction is further discussed in Parts II and III of this report.

- Fission product (FP) chemistry: Lower FP release (higher FP retention), particularly gaseous and volatile fission products, is preferred but benefits should be verified using appropriate test conditions. Chemically stable forms of fission products, particularly volatile FPs, are also preferred. Lower temperatures and use of fuel microstructure and barrier additives in the fuel pellet design can aid in the reduction of FP release.

Fuel neutronic properties

Neutronic characteristics of the LWR fuel include fissile density, cross-sections and reactivity feedback.

- Fissile density: Higher fissile density (uranium inventory/assay) is preferred. The current limitation for UO_2 fuel in commercial reactors is < 5 wt%-^{235}U. The fuel enrichment may, however, be increased up to <20 wt%-^{235}U while maintaining the designation of "low-enriched fuel" (LEU), which corresponds to the non-

proliferation limit. Uranium density is important in maximising neutron economy in the fuel, which impacts fabrication and fuel cycle costs.

- Cross-sections: Higher fission cross-section and lower parasitic absorption are preferred. Lower supplementary gas production due to parasitic absorption is also preferred.

- Reactivity feedback: It is desirable to maintain similar magnitude and parametric behaviour of reactivity coefficients relative to the current reference fuel system (UO_2-Zr-alloy), such that the safety and control systems are not significantly impacted when ATF is adopted in the existing LWR fleet.

Fuel characterisation: Standard tests for normal operation and accident conditions

A number of out-of-pile tests can be conducted to determine properties of candidate fuel materials before initiating irradiation tests. If a fuel material appears promising from the out-of-pile characterisation, one can proceed with a series of irradiation tests and post-irradiation examinations (PIEs) at least up to the anticipated burn-up.

Fuel thermal property tests

The thermal conductivity, thermal diffusivity, specific heat and coefficient of thermal expansion, up to or near the fuel melting point, should be measured prior to and following irradiation. Irradiation effects on thermal properties should be taken into account.

- Melting point: The fuel melting point must be determined. The thermal arrest method is proposed to evaluate melting point or solidus/liquidus temperature, although other methods may be available. This test must be conducted using the same atmosphere gas as will be present within the fuel rod (e.g. helium gas for a standard UO_2-Zr-alloy fuel rod).

- Thermal conductivity: Thermal conductivity should be evaluated up to the fuel melting point, including chemical composition, stoichiometry, microstructure and irradiation effects. Thermal conductivity is usually evaluated from thermal diffusivity, specific heat capacity and density for unirradiated homogeneous materials up to approximately 3 000 K (for UO_2 and MOX). Fuel centreline and surface temperature measurement during irradiation is a possible alternative or complementary approach, which yields the integral thermal conductivity from the fuel surface to the centreline if a gap conductance is assumed. If experimental means are available, a power to melt test (thermal conductivity integral measurement) is useful in evaluating higher temperature thermal conductivity up to the fuel melting point. Measurement of thermal diffusivity via a transient method, such as laser flash, is proposed for evaluating thermal conductivity for unirradiated and irradiated homogeneous materials. For heterogeneous materials, thermal diffusivity should be measured using a specimen that is sufficiently thick to obtain homogeneous heat flow.

- Specific heat: Specific heat should ideally be evaluated up to the fuel melting point, but available techniques are generally limited to ~1 500 K. Irradiation effects are expected to be small, with the exception of the radiation damage recovery effect. Differential scanning calorimetry (DSC) or drop calorimetry is proposed to evaluate specific heat. Calculation using Neumann-Kopp's law is also useful.

- Coefficient of thermal expansion: Thermal expansion should be evaluated up to the fuel melting point. Volume change due to melting is also important. Dilatometer measurement is proposed to determine the CTE. Alternatively, high-temperature X-ray diffraction (XRD) may be used.

Fuel mechanical property tests

Fuel mechanical properties of interest include yield stress, creep rate and fracture toughness, ideally measured up to the fuel melting point. However, it may be possible to extrapolate values measured at lower temperatures up to the melt temperature. It should be noted that mechanical properties are affected by fuel microstructure, including porosity, grain size, etc. Since diffusion-controlled behaviours, such as creep, are affected by the fission profile, this irradiation effect should also be taken into account. Note that the atmosphere selected for conducting the mechanical tests shall not change the fuel stoichiometry or phases.

- Yield stress: A compression test with constant strain rate is proposed to evaluate yield stress up to the fuel melting point (or as high as possible). Measured yield stress depends on strain rate, porosity size distribution, grain size, etc.

- Creep rate: Creep rate should be evaluated up to yield stress and melting temperature (or as high as possible), including irradiation effects. It is easier to measure creep rate on unirradiated materials in a stress range from about 5 to 100 MPa, in a temperature range from approximately 1 500 to 1 900 K. In the case that creep behaviour is controlled by cation diffusion, irradiation effects should be taken into account, including radiation-induced diffusion and athermal diffusion. A compression test conducted with constant stress is proposed to evaluate the (steady-state) creep rate up to the fuel melting point (or as high as possible). Irradiation effects may be evaluated from other behaviour controlled by cation diffusion.

- Fracture toughness: Fracture toughness should be evaluated up to the fuel melting point (or as high as possible). The bi-axial flexure technique (Radford, 1979; Oguma, 1982) is proposed to evaluate fracture toughness.

- Elastic moduli: Elastic moduli should be evaluated up to the melting point (or as high as possible). The acoustic velocity method or compression test with constant stress is proposed to evaluate elastic moduli at lower temperature. At higher temperature, a compression test is proposed.

Fuel chemical property tests

- Structural stability: Structural stability should be evaluated, including irradiation effects, both under steady-state and under transient conditions that may arise in scenarios such as AOOs and RIA/LOCA. A temperature ramp test for unirradiated fuel is proposed to evaluate structural stability up to the fuel melting point. Microstructural change may be analysed with ceramography, scanning electron microscopy (SEM), electron dispersive spectroscopy (EDS)/wavelength dispersive spectroscopy (WDS), etc. Post-annealing tests for irradiated fuel is proposed to evaluate the irradiation effect on structural stability. The temperature ramp rate is one of the necessary test parameters.

- Cladding compatibility: Compatibility between the fuel and cladding should be evaluated up to eutectic temperature or melting temperature of the fuel and the cladding. Oxygen potential (gas composition) and contact pressure are key test parameters.

- Corrosion: Corrosion of fuel by the water coolant should be evaluated under conditions similar to those applied for the cladding corrosion tests (see Table 3.1 for coolant chemistry conditions). Autoclave tests are recommended for evaluating the fuel corrosion behaviour with coolant. Testing can begin at the coolant temperatures indicated in Table 3.1, but the degradation mechanism for each fuel type should be considered in determining conditions for testing at elevated temperatures.

- FP chemistry: FP chemistry should be evaluated with regard to FP retention, FP evaporation/migration, fission gas release, etc., up to ~3 000 K or to the fuel melting point (or as high as possible). Assay for irradiated material with EDS or wavelength dispersive X-ray spectroscopy (WDX) is recommended to evaluate FP retention under normal operating conditions. Chemical assay is also a possible option. Post-annealing tests are proposed to evaluate FP behaviour (FP evaporation/migration, fission gas release) from normal operation conditions to accident conditions.

Fuel neutronic property tests

Neutronic properties are calculated using particle transport codes and evaluated nuclear data libraries.5 Fission gas and fuel fragment isotopic analysis should be performed after irradiation to confirm the neutronic calculations for advanced fuel pellets.

Effect of irradiation and predictability of fuel behaviour

Irradiation affects many fuel properties/characteristics, including microstructure, composition, dimensions, thermal/mechanical properties, etc. Measurement techniques for individual effects are described above.

Measured properties and characteristics should be applied to predict fuel behaviour with irradiation. Overall performance should, however, be verified via integrated tests. Fuel irradiation testing with instrumentation is proposed to evaluate the overall performance, including change of thermal/mechanical properties up to high burn-up. Note that fuel fragmentation under RIA and LOCA conditions is one of the leading issues to be resolved to extend the burn-up for the current UO_2 fuel system. Test parameters include linear heat generation rate (LHGR), fuel characteristics and fuel design.

Considerations for the fuel cladding system

Once the fuel and the cladding have been well characterised separately, the complete fuel rod must be evaluated through the analysis of chemical compatibility of the two fuel rod components and the validation of the concept through segmented fuel rod irradiations in normal, transient and accident conditions. In the following section, the primary interaction between the fuel and the cladding investigated through out-of-pile tests is the chemical compatibility since the main mechanical aspects of the fuel rod should have been determined specifically for the cladding (i.e. leak-tightness, internal mandrel test, pressure deformation/burst tests). Some bi-axial mechanical tests are also proposed to determine PCMI conditions. The thermo-mechanical compatibility of the two fuel rod components can be studied through in-pile tests. In-pile transient experiments are mainly used to evaluate safety under conditions that could lead to SCC-PCI failure or PCMI loading to the cladding (e.g. slow power ramp or high strain rate transients, such as RIA) and to a certain extent LOCA conditions. Note that fuel rod compatibility with other reactor system components (e.g. spacer grid) must also be determined in order to evaluate the viability of the proposed ATF concept.

Fuel system chemical interactions

The chemical compatibility between the fuel and cladding materials should be evaluated using diffusion couples at various temperatures ranging from normal operating temperatures (~400°C) up to melting of one of the two components (or melting of a fuel-clad eutectic) for at least 1 000 h. Note that the appropriate temperature may be lower than the individual melt temperature of the fuel or cladding because of the formation of eutectics at lower temperature between the fuel and cladding, cladding and structural materials, or cladding and control rod materials.

---

5. See, for example, www-nds.iaea.org/exfor/endf.htm, www.nndc.bnl.gov/exfor/endf00.jsp, https://tendl.web.psi.ch/home.html.

Important data to assess for these tests are:

- potential eutectic formation and kinetics thereof, including cladding-fuel and cladding-structural material eutectics;

- diffusion length of interacted material at the various temperatures;

- impact of FPs (gas and others) on the cladding.

Some ATF fuel rod concepts may contain a fuel pellet with a lower melting temperature than the cladding; in these cases it is essential to investigate the behaviour of the melted fuel material with the cladding. The compatibility of the FPs with cladding should be investigated, as well as any specific failure mode anticipated for each fuel system concept.

Pellet-cladding system behaviour, including irradiation testing protocol

Validation of the performance of a proposed fuel rod concept is primarily accomplished via irradiation of either segmented or full-length test rods in either a research reactor at representative conditions or in a commercial reactor, with, if possible, on-line fuel temperature, pressure and axial elongation measurements. Post-irradiation examinations (non-destructive and destructive examinations) should be conducted at various burn-ups (e.g. 15, 30, 45 and 60 GWd/t; testing to higher burn-up may be desired as a function of the expected use case) to determine the following:

- fuel rod dimensional measurements:
  - axial growth (elongation);
  - diametric evolution.

- potential defects on the cladding surface, observed visually;

- rod internal pressure using a rod puncture technique and measurement of fission gas release;

- fuel behaviour under irradiation via study of the fuel microstructure (e.g. stability of microcell microstructure), fission gas retention and release, other FP behaviour, fuel swelling (e.g. using metallographic and micro-scale examinations such as SEM, EPMA), etc.;

- fuel cladding chemical and mechanical interaction under irradiation (e.g. via internal cladding observation).

Ramp tests on segmented rods to evaluate the fuel rod behaviour under various transient conditions complement the evaluation of fuel behaviour at normal operating conditions. Primary test parameters include initial power levels (mainly 100 W/cm and 200 W/cm), the ramp rate and the length of time at the maximum power. Various ramp rates may be considered, ranging from 0.1 W/cm/min to 600 W/cm/min as a function of the scenario, for fuel rods that have been irradiated to various burn-up levels (e.g. 15, 30, 45 and 60 GWd/t, or up to a burn-up relative to the expected use case). At a minimum, the following ramp tests are recommended:

- power ramp tests to be performed on selected fuel rods with the following test conditions:
  - initial power levels corresponding to the final in-reactor linear heat rates (LHRs) of the selected fuel rods (typically between 100 and 200 W/cm);
  - burn-ups of 30 GWd/t and 60 GWd/t (with a focus on the burn-up corresponding to a closed pellet-clad gap);
  - for each burn-up, perform the ramp at 0.1, 100, and 600 W/cm/min (with a focus on 100 W/cm/min ramp rate).

Additionally, LOCA and SCC-PCI and RIA-type ramp tests should also be performed on segmented rods (with a focus on intermediate burn-up for SCC-PCI failure mode and high burn-up fuel rodlets for LOCA and RIA). Complementary to the ramp tests, VHT experiments can be performed on irradiated fuel in properly equipped hot laboratories to characterise the fission gas release and to reproduce severe accident conditions in a test facility in which on-line measurements are possible.

References

Bragg-Sitton, S.M. et al. (2016), "Metrics for the technical performance evaluation of LWR accident tolerant fuel", *Nuclear Technology*, Vol. 195(2), pp. 111-123, August 2016.

Bragg-Sitton, S.M. et al. (2015), "Evaluation of enhanced accident tolerant LWR fuels", *Proceedings of Top Fuel 2015*, Zurich.

Bragg-Sitton, S.M. et al. (2013), *Enhanced LWR Accident Tolerant Fuel Performance Metrics,* INL/EXT-13-29957, Idaho National Laboratory, prepared for the US Department of Energy Advanced Fuel Campaign.

IAEA (2003), *Analysis of Differences in Fuel Safety Criteria for WWER and Western PWR Nuclear Power Plants*, IAEA-TECDOC-1381, IAEA, Vienna.

NEA (2011), "CSNI Technical Opinion Papers No.13 LOCA Criteria Basis and Test Methodology"*,* NEA/CSNI/R(2011)7.

Oguma, M. (1982), "Microstructure effects on fracture strength of UO_2 fuel pellets", *Journal of Nuclear Science and Technology*, Vol. 19(12), pp. 1005-1014.

Radford, K.C. (1979), "Effect of fabrication parameters and microstructure on the mechanical strength of UO_2 pellets", *Journal of Nuclear Materials*, Vol. 84(1-2), pp. 222-236.

4. Application of evaluation metrics/paths forward

Evaluation of accident-tolerant fuel (ATF) cladding, fuel and fuel system concepts should encompass all performance regimes for the fuel, including:

- fabrication;

- normal operation and anticipated operational occurrences (AOOs);

- design-basis accidents;

- design extension conditions;

- used fuel storage, transport and disposition.

As discussed in Chapter 3, there are numerous attributes within each performance regime that must be considered in evaluating the fuel system performance. Key attributes for the fuel and cladding were discussed in the section on considerations for the fuel cladding system, along with a summary of standard tests recommended for measuring specific properties and characterising performance under the specified conditions. Note that while it may not be possible to improve on the current state-of-the-art fuel system in all attributes and regimes, significant improvement in some of the key attributes may outweigh modest performance gains – or modest vulnerabilities – in other attributes.

A detailed list of proposed attributes for evaluation is provided (Bragg-Sitton et al., 2013), with additional weighting factors and quantitative assessment approach (Bragg-Sitton et al., 2016). Early in the development of a new fuel system, it may not be possible to apply a detailed, quantitative assessment approach because of the lack of sufficient data to quantitatively determine each of the performance attributes. The attributes summarised in this document and the recommended tests for fuel and cladding, can instead be used as a qualitative guide to assess the performance of candidate materials relative to the current state-of-the-art materials and relative to one another. As more property data and performance characterisation becomes available, a more rigorous quantitative assessment can be applied. Overall properties and behaviours of cladding and fuel solutions that are incorporated into the metrics and concept evaluations and the status of available data for each concept are summarised in the state-of-the-art report produced by Task Forces 2 and 3 of the NEA Expert Group on ATF for LWRs (EGATFL).

References

Bragg-Sitton, S.M. et al. (2016), "Metrics for the technical performance evaluation of LWR accident tolerant fuel", *Nuclear Technology*, Vol. 195(2), pp. 111-123, August 2016.

Bragg-Sitton, S.M. et al. (2013), *Enhanced LWR Accident Tolerant Fuel Performance Metrics*, INL/EXT-13-29957, Idaho National Laboratory, prepared for the US Department of Energy Advanced Fuel Campaign.

5. Technology readiness levels

Technology readiness levels (TRLs) are a means of measuring technology maturity, providing a degree of standardisation and allowing comparison between different technologies. Originally defined by the United States National Aeronautics and Space Administration (NASA [Mankins, 1995; NASA, 2012]), TRLs have been adopted by many industries and governments around the world including the United Kingdom (UK), United States (US) and European Union (EU) governments, who now routinely consider TRLs when evaluating technology investment proposals. The TRL scale traditionally has nine levels. As the technology matures from TRL 1 to TRL 9, it moves from a scientific idea through to a fully developed application that has demonstrated its usefulness by being deployed in operational situations.

Because the deployment of a new nuclear fuel form requires lengthy and expensive research, development and demonstration, application of the TRL concept to advanced fuel development is very useful as a management and tracking tool.

Definition of TRLs relative to nuclear fuel

The language of the NASA TRLs is not an exact match with respect to nuclear power applications including nuclear fuels and claddings; however, its application can be readily visualised. TRL definitions have been used elsewhere in the energy industry, nuclear industry and for nuclear fuels. The majority of these definitions remain reasonably similar to the original NASA definitions, but they are often simplified and made more general with the removal of space-specific terminology. Examples include those from the UK Department of Energy and Climate Change (DECC, 2012), the Japan Atomic Energy Agency (JAEA, 2010; Kurata, 2017) and the US Department of Energy (DOE, 2011; Carmack et al., 2017). Each of these organisations has expanded significantly upon the original NASA definitions by including a greater level of detail that is specific to a selected application, e.g. nuclear fuel. Appendix A of the *State-of-the-Art Report on Innovative Fuels for Advanced Nuclear Systems* produced by the NEA Expert Group on Innovative Fuels, also provides a detailed definition of TRLs specific to transmutation fuel development (OECD, 2014).

A study undertaken by Idaho National Laboratory (INL) in the United States established TRL definitions that are much more specific to nuclear fuel and materials in terms of the established qualification processes (Carmack, 2014; Carmack et al., 2017). These processes include a sequence of steps that progress through out-of-pile studies, the use of test reactors, use of lead rods and assemblies in commercial reactors, full-core reloads and, eventually, widespread usage.

The INL work also identifies the need for clarification between two key components, namely fabrication process maturity and fuel performance maturity, used to evaluate the maturity of a new fuel type in terms of deployment readiness. The present work by the Expert Group on Accident-tolerant Fuels for LWRs (EGATFL) includes an additional component for the maturity of fuel performance codes to support the new fuel system.

- fabrication process maturity, which measures how well the fabrication process is understood and validated;

- fuel performance maturity, which measures how well the in-pile performance of the fuel is understood and validated;

- performance code maturity, which measures the applicability of available fuel performance codes or development and validation of a new fuel performance code for the specific fuel system.

A comprehensive TRL definition should include classification for each of these elements. For example, a mature fabrication process tested at very large scales for novel fuels with large uncertainties in its performance should be differentiated from a mature fabrication process for existing fuels. As shown in Figure 5.1, there are two key attributes that are important in assessing the TRL for the fabrication process and performance maturity evaluation elements.

Figure 5.1. Summary of TRL evaluation elements and attributes
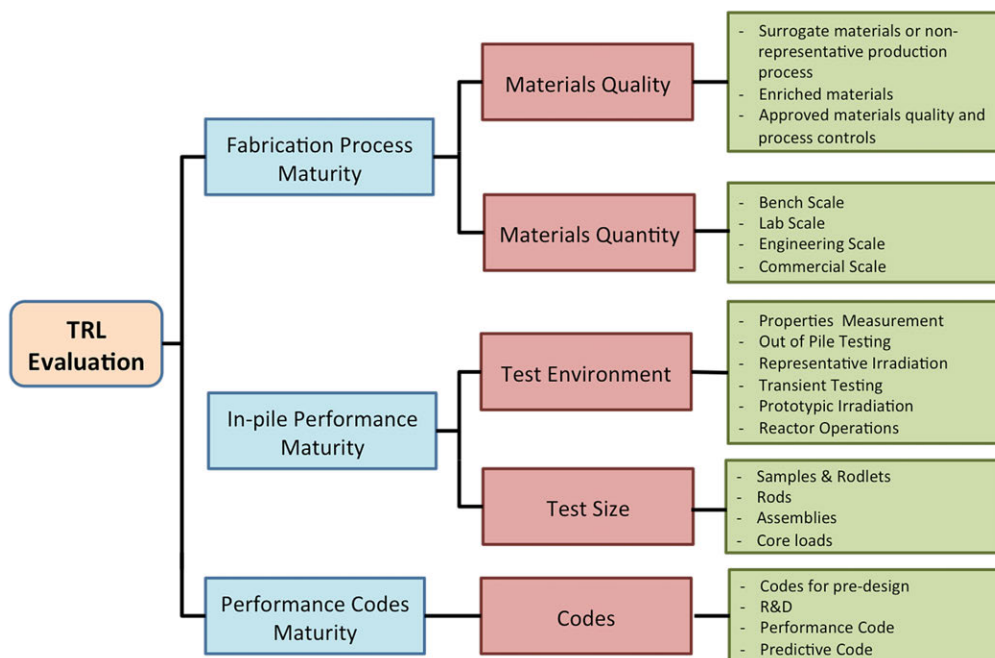
Source: OECD (2014) and Carmack et al. (2017).

Assignment of TRL definitions

As discussed previously, there is little difference between the TRL definitions assigned by the different international studies. The envelope covered by the TRL definitions (one through nine) ranges from fundamental first principles of science to long-term routine commercial operations (full maturity). The intermediate steps correspond to the detailed research and development process. INL researchers have proposed that this pathway can be represented by a diagram of key criteria versus TRL, as summarised in Figure 5.2.

The key performance indicators can then be categorised for the specified development categories (fabrication process maturity and fuel performance maturity), as described in Carmack et al. (2017). This categorisation provides clear direction for identifying the specific technology TRL. Note that fuel performance code maturity has been added in this document as a separate development category necessary in the TRL advancement of new fuel systems, such as those proposed for accident-tolerant fuels (ATFs). It is important to note that the measured TRL requires *all* of the previous TRL

criteria to be achieved; i.e. if elements of TRL 3 are incomplete for *any* of the development categories, but some elements of TRL 4 have been achieved, the TRL is still assigned as 3 until all elements have been achieved. Figures 5.3 and 5.4 establish the requirements against the TRL measures.

Figure 5.2. Key criteria for each TRL
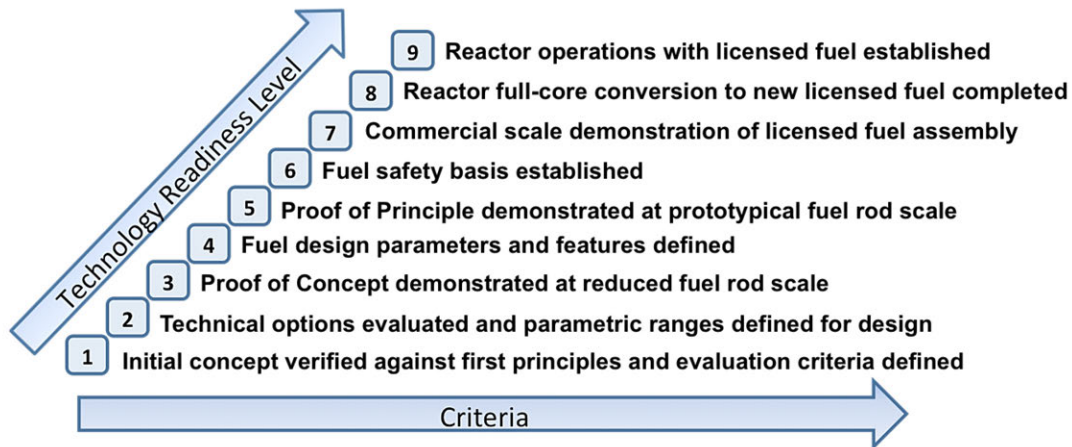
Source: Modified from OECD (2014) and Carmack et al. (2017).

Figure 5.3. TRL classification for fabrication process maturity

Source: Modified from OECD (2014) and Carmack et al. (2017).

From the classifications laid out in Figures 5.3 and 5.4, a table of criteria for each of the TRLs has been established (see Table 5.1). The TRL definitions have been mainly developed from an engineering point of view. Consideration and preparation of safety standards and criteria are required before the implementation of ATF in commercial reactors. Therefore, TRL definitions for licensing also should be considered as a part of the development process. At TRL 4, the appropriate regulator is engaged to ensure that no significant issues exist that could impede a lead use programme in a commercial LWR. At TRL 7, the regulator has issued formal licensing topical reports indicating acceptance of the concept.

**Figure 5.4. Classification of fuel performance maturation,
from out-of-pile tests through irradiation**

	Fundamental property measurements	Out-of-pile testing	In-pile testing representative spectrum	Transient testing	In-pile testing prototypic spectrum	Reactor Operations
Multiple assemblies (core loads)						TRL 8-9
Few assemblies					TRL 7	TRL 8
Rods		TRL 4	TRL 5	TRL 5-6	TRL 6	
Samples & rodlets	TRL 4	TRL 4	TRL 4	TRL 5	TRL 5	

Note that the following nomenclature applies – "Rods" refers to full-length fuel rods, while "Rodlets" refers to partial-length fuel rods.

Source: Modified from OECD (2014) and Carmack et al. (2017).

TRL summary

TRLs provide a helpful means for assessing technology maturity. It should be noted that TRL values are potentially more useful for comparison between technologies than they are when considered individually as absolute values.

It is also important, however, to recognise the limitations of TRL classification. TRLs give no indication of the amount of time, effort or cost required to increase a technology's readiness level. If two technologies currently have the same TRL, then there is no guarantee that these will continue to be developed successfully at the same rate or for similar costs. Indeed, a technology with a lower current TRL may reach deployment sooner than another with a higher current TRL because of increased R&D effort, fewer feasibility issues, etc.

TRLs themselves also provide no indication of the relative benefits of the different technologies if they were fully deployed. This weakness can be overcome to an extent by plotting TRLs against appropriate measures of benefit, such as operating temperature. Application of TRL assessment with the performance attributes and evaluation metrics defined in Chapter 3 will provide an assessment of both the ability of a technology to meet the performance goals established for ATFs and to meet the targeted development timeline.

Limitations of TRLs specific to nuclear fuels and claddings include:

- fuel and cladding TRLs with respect to their use in one reactor type may be different with respect to their use in another reactor type;

- TRLs for fuels and cladding with respect to a particular reactor type may be different with respect to deployment in different countries because of varying regulatory systems, capability, etc.

Sufficient data for licensing of a new fuel system should be available at TRL 7.

Table 5.1. Summary of TRL definitions for advanced nuclear fuels

TRL	Function	Definition
1	Proof of concept	A new concept is proposed. Technical options for the concept are identified and relevant literature data reviewed. Criteria are developed.
2		Technical options are ranked. Performance range and fabrication process parametric ranges are defined based on analysis.
3		Concepts are verified through laboratory-scale experiments and characterisation. Fabrication process is verified using surrogates.
4	Proof of principle	Fabrication of small samples (rodlets) at bench-scale. Irradiation testing of rodlets in a relevant environment. Design parameters and features are established. Basic properties are compiled.
5		Fabrication of full-length rods using prototypic materials at laboratory scale. Rod-scale irradiation testing in a relevant environment (test reactor). Primary performance parameters with representative compositions under normal operating conditions are quantified. Fuel compositions under normal operating conditions are quantified. Fuel behaviour models are developed for use in fuel performance code(s).
6		Fabrication of rods using prototypic materials at laboratory scale and using prototypic fabrication processes. Rod-scale irradiation testing at relevant (test reactor) and prototypic (commercial LWR, referred to as lead test rods) environment (steady-state and transient testing)[a]. Predictive fuel performance code(s) and safety basis are established.
7	Proof of performance	Fabrication of test assemblies using prototypic materials at engineering-scale and using prototypic fabrication processes (also referred to as lead use assemblies). Assembly-scale irradiation testing in prototypic (commercial LWR) environment[b]. Predictive fuel performance code(s) are validated. Safety basis established for full-core operations.
8		Fabrication of a few core-loads of fuel and operation of a commercial reactor with such fuel.
9		Routine commercial-scale operations. Multiple reactors operating.

a)   Initial rods irradiated in a commercial LWR are referred to as "lead fuel rods" (LFRs).

b)   Initial assemblies irradiated in a commercial LWR are referred to as "lead fuel assemblies" (LFAs) or "lead use assemblies" (LUA).

References

Carmack, J. (2014), *Technology Readiness Levels for Advanced Nuclear Fuels and Materials Development*, FCRD-FUEL-2014-000577, INL/EXT-14-31243, Idaho National Laboratory.

Carmack, W.J., et al. (2017), "Technology readiness levels for advanced nuclear fuels and materials development", *Nuclear Engineering and Design*, Vol. 313, pp. 177-184.

DECC (2012), "The Energy Entrepreneurs Fund – First Phase Guidance Notes", Appendix 2 – *TRLs*, UK Department of Energy and Climate Change (DECC), 23 August 2012.

DOE (2011), *Technology Readiness Assessment Guide*, DOE G 413.3-4A, DOE.

JAEA (2010), "Technology readiness levels for partitioning and transmutation of minor actinides in Japan", Presentation, K Minato et al., OECD NEA 11 IEMPT Conference, 1-4 November 2010.

Kurata, M. (2016), "Research and development methodology for practical use of accident tolerant fuel in LWRs", *Nuclear Engineering and Technology*, Vol. 48 (1), pp. 26-32.

Mankins, J.C. (1995), *Technology Readiness Levels*, Advanced Concepts Office, Office of Space Access and Technology, National Aeronautics and Space Administration.

NASA (2012), *Technology Readiness Levels,* available online at www.nasa.gov/directorates/heo/scan/engineering/technology/txt_accordion1.html, accessed 5 April 2017.

NEA (2014), "Appendix A: Definition of TRLs for transmutation fuel development", *State-of-the-Art Report on Innovative Fuels for Advanced Nuclear Systems,* OECD, Paris.

6. Definition of illustrative scenarios for evaluation

Two key illustrative scenarios are proposed for application to general water-cooled reactor concepts to assess potential performance enhancements relative to the current standard fuel system. These scenarios are identified to bound the range of severe accidents and they are not intended to be overly prescriptive or specific to a particular facility design. Modelling of these scenarios should utilise the appropriate initiating event and be allowed to carry through to the point of core failure.

It should be noted that the proposed scenarios assume no operator actions are taken or that the actions taken are unsuccessful. The authors of this report recognise that plants are required to have emergency operating procedures and severe accident mitigation guidelines and, in addition, industry has developed the capability for additional off-site support and equipment via programmes such as FLEX[6] in the United States. These actions have been developed and implemented for the UO_2-Zircaloy fuel system currently employed. For some operator actions, the timing, actuation criteria, limits, flow rates, etc. may vary based on the fuel system employed. Furthermore, when simulating operator actions, assumptions in action, timing, success/failure, flow rates, durations, locations, etc. must be made. These factors confound simulation of operator actions and the comparison between different fuel systems. Therefore, recommended "hands-off" accident scenarios are described herein for initial comparison of candidate accident-tolerant fuel (ATF) concepts to avoid the complications described above and to provide more clear and direct comparison between fuel system options.

The international community has selected two scenarios for ATF evaluation that are applicable to general reactor designs:

- station blackout (SBO): high-pressure scenario; evaluation taken to the point of reactor pressure vessel failure;

- large-break loss-of-coolant accident (LB-LOCA): low-pressure scenario (high decay heat at loss-of-coolant).

Simulation of these scenarios should be conducted using a pressurised water reactor (PWR), boiling water reactor (BWR), or water-water energetic reactor (VVER) model, as appropriate to the country conducting the evaluation. Illustrative scenarios should be considered standard, baseline scenarios for the comparison of a candidate ATF concept to the standard UO_2-Zr-alloy fuel system that is currently employed (using the appropriate alloys, enrichment, etc. for the reactor type being simulated) and for comparison of multiple ATF concepts to one another.

As noted above, the proposed scenarios are intended to provide bounding cases for fuel performance. It is expected that each country or development team will utilise fuel performance and system analysis codes that are accepted within the associated organisation to conduct these evaluations. See for example the US Nuclear Regulatory Commission website for additional information on the State-of-the-Art Reactor Consequence Analyses (SOARCA) Project, which provides additional information on

---

6. See http://safetyfirst.nei.org/industry-actions/flex-the-industry-strategy-to-enhance-safety, accessed 5 April 2017.

accident scenario definition and accident analysis.[7] All ATF evaluations under the selected accident conditions should be allowed to progress to the point of core failure in the analysis. This allows one to estimate the potential increase in coping time that might be offered by candidate ATF concepts and to assess potential outcomes should failure occur (e.g. if the fuel fails, how does it fail?). Pressure is a significant parameter in the accident progression, as reflected by the selection of both a high-pressure and low-pressure scenario. Following completion of bounding analyses, it is recommended that researchers perform parametric studies for these illustrative scenarios to develop a better understanding of the impact of additional variables. Such parametric studies could include variation of the point in the operating cycle when the accident occurs (e.g. how much burn-up has been accumulated in the fuel?) and the time after reactor scram that core cooling is lost. Additionally, one should note that while analysing scenarios with "no mitigating action" simplifies the analyses and likely provides a bounding result, it must be recognised that the performance of specific ATF concepts may depend on the mitigating actions available and the degree of reliance on their performance during specific accidents. Hence, once a leading ATF candidate is selected, utilities planning to adopt the new fuel type must apply all standard accident analyses for the specific plants that will use the fuel, with available mitigating actions applied.

Each section below provides suggested input parameters that should be applied for the selected illustrative scenarios. Key output variables that should be calculated when evaluating the performance of a selected fuel system include primary vessel pressure, cladding temperature, fuel temperature and combustible gas production.

High-pressure scenario: Station blackout

A station blackout (SBO) scenario describes a condition in which the nuclear plant loses all sources of AC supply (off-site power and on-site AC power, including all diesels). All DC power is also assumed lost at the initiation of the accident. This scenario assumes that feedwater supply to steam generators is unavailable for PWRs. The primary system is isolated and the system pressure increases. When the pressure limit is exceeded, the quick-acting pressure reducing system is designed to open automatically.

Characteristics of the SBO scenario

- primary circuit pressure at the initial stage of the accident is high;

- primary circuit pressure is high at the moment of reactor pressure vessel (RPV) failure.

Assumptions

- plant loses all sources of AC supply (including all diesels);

- plant is operating at its nominal full power rating when failure occurs;

- the reactor automatically scrams at the point AC power fails.

Several studies have been conducted for the occurrence of an SBO for specific reactor designs. See, for example, NUREG-1935 (NRC, 2012a) and NUREG-7110, Volumes 1 and 2 (NRC, 2013a, 2013b). In many cases it is assumed that the reactor operator takes some mitigating action during the course of the accident. However, it is recommended that no mitigating action be assumed for evaluation of ATF performance under this scenario to ensure that the potential performance enhancements for multiple ATF concepts can be adequately compared and the estimated "fuel coping time" for these fuel systems can be

---

7. See www.nrc.gov/about-nrc/regulatory/research/soar.html, accessed 26 May 2017, last updated March 2015.

calculated. It is also recommended that sensitivity analyses be performed to assess the impact of varying input parameters and other assumptions. For instance, it may be appropriate to vary the time of onset of accident conditions relative to the point in the cycle (the time that the reactor has been operating and, hence, fuel burn-up and decay heat).

Low-pressure scenario: Large-break loss-of-coolant accident

The initiating event for a large-break loss-of-coolant accident (LB-LOCA) is guillotine rupture of a large coolant pipe. For PWRs, the cold leg of the main circulation pipeline near the reactor inlet (two-way primary coolant leakage) is assumed to fail. For generation II and III BWRs the piping on the suction side of the recirculation pump is assumed to fail. The LB-LOCA is assumed to occur with a concurrent station blackout of all AC power (including all diesels). The passive decay heat removal system (DHRS) and systems relying on DC power, such as some systems in the emergency core cooling system (ECCS), are assumed to operate according to their design characteristics (i.e. the ECCS will operate until the available water volume or DC power is exhausted). Total operation time of these systems is approximately 24 h from the accident start.

Characteristics of the LB-LOCA scenario

- The primary circuit pressure drops as a result of the break. Temporary core dry-out and fuel assembly heat-up occur at the initial stage of the accident.

- Core heat-up occurs at a later time following initiation of accident conditions relative to the SBO scenario. Operation of the passive DHRS and ECCS supports maintenance of the core water level for 24 hours.

- A large mass of combustible gases will be generated for zirconium alloy cladding because of significant cladding oxidation.

Assumptions

- guillotine rupture of a large coolant pipe (i.e. the main circulation pipeline cold leg near the reactor inlet for PWRs);

- loss of all sources of AC supply (including all diesels); DC power remains available;

- the reactor scrams immediately upon initiation of accident conditions;

- water injection is provided by the ECCS (high-pressure and low-pressure coolant injection systems that do not rely on AC power);

- the passive DHRS is operational.

Several studies have been conducted for the occurrence of a LB-LOCA for specific reactor designs. See, for example, NUREG/IA-0067 (NRC, 1992), NUREG-1935 (NRC, 2012a) and NUREG-7110, Volumes 1 and 2 (NRC, 2013a, 2013b). In many cases it is assumed that the reactor operator takes some mitigating action during the course of the accident. However, it is recommended that no mitigating action be assumed for evaluation of ATF performance under this scenario to ensure that the potential performance enhancements for multiple ATF concepts can be adequately compared and the estimated "grace time" for these fuel systems can be calculated. It is also recommended that sensitivity analyses be performed to assess the impact of varying input parameters and other assumptions (e.g. 2 sigma power and 2 sigma decay heat are considered to address measurement uncertainties). For instance, sensitivity analyses might include variation in the time of onset of accident conditions relative to the point in the cycle (the time that the reactor has been operating and, hence, fuel burn-up and decay heat), variation in the size of the break and its location for a specific reactor type, and/or failure of the initial scram signal to the reactor.

References

NEA (2011), "CSNI Technical Opinion Papers No.13 LOCA Criteria Basis and Test Methodology", NEA/CSNI/R(2011)7.

NEA (2009), *Nuclear Fuel Behaviour in Loss-of-coolant Accident (LOCA) Conditions,* NEA No. 6846, OECD, Paris, www.oecd-nea.org/nsd/docs/2009/csni-r2009-15.pdf.

NRC (2015), *State-of-the-Art Reactor Consequence Analyses (SOARCA),* www.nrc.gov/about-nrc/regulatory/research/soar.html, accessed 20 April 2017.

NRC (2013a), *State-of-the-Art Reactor Consequence Analyses (SOARCA) Project*, Volume 1: Peach Bottom Integrated Analysis, NUREG/CR-7110, Vol. 1, Rev. 1, U.S. NRC Office of Nuclear Regulatory Research, May 2013.

NRC (2013b), *State-of-the-Art Reactor Consequence Analyses (SOARCA) Project*, Volume 2: Surry Integrated Analysis, NUREG/CR-7110, Vol. 2, Rev. 1, U.S. NRC Office of Nuclear Regulatory Research, August 2013.

NRC (2012a), *State-of-the-Art Reactor Consequence Analyses (SOARCA) Report,* NUREG-1935, US NRC Office of Nuclear Regulatory Research, November 2012, www.nrc.gov/reading-rm/doc-collections/nuregs/staff/sr1935/index.html.

NRC (2012b), *Modeling Potential Reactor Accident Consequences*, NUREG/BR-0359 Rev. 1, US NRC Office of Nuclear Regulatory Research, December 2012, www.nrc.gov/reading-rm/doc-collections/nuregs/brochures/br0359.

NRC (1992), *Recirculation Suction Large Break LOCA Analysis of the Santa Maria De Garoia Nuclear Power Plant Using TRAC-BF1 (G1J1),* NUREG/IA-0067, ICSP-BA-LOCA-T, International Agreement Report, published by US NRC Office of Nuclear Regulatory Research.

7. Applicable multi-physics codes for fuel performance evaluation and system impact

Fuel performance and system codes that can be used to evaluate accident-tolerant fuel (ATF) performance, can be modified to evaluate ATF concepts, or are under development are briefly summarised in this chapter (see Tables 7.1 to 7.4 for a summary of the codes used for screening, fuel performance and severe accident analyses). Current limitations of the identified codes, data required to run these codes and availability of the identified codes to other organisations or countries are included. For a summary of the codes used by the US Nuclear Regulatory Commission (NRC), refer to www.nrc.gov/about-nrc/regulatory/research/safetycodes.html.

Standard evaluation of ATF concepts include fuel performance analysis (neutronic, thermal-hydraulic) and detailed systems analyses. A standard suite of tools is typically used for initial screening analyses, including infinite lattice calculations to estimate basic concept feasibility and three-dimensional core analysis to assess thermal-hydraulics, temperature feedback, etc. Work is currently being conducted in France, Japan, Korea, Switzerland and the United States, to develop advanced modelling and simulation tools and to incorporate ATF properties and behavioural characteristics. Additionally, existing severe accident analysis tools are being modified to incorporate ATF characteristics. Although some of the tools are limited in fidelity, particularly with regard to ATF concepts for which little property and behavioural data is available, they do provide initial, sometimes qualitative, estimates of performance for these concepts.

Discussion among the Expert Group on Accident-tolerant Fuels for LWRs (EGATFL) members has identified additional codes that are being utilised for ATF analysis. Many of these tools are limited in their application to ATF concepts at present, but additional data that will be made available from ongoing research programmes will significantly enhance these capabilities (see Parts II and III of this report). In many cases, companies and organisations select their own internal tools to conduct fuel performance, system and severe accident analyses. The overall trends observed for materials using these different codes should be studied; the EGATFL Task Force activities will not attempt to benchmark codes against one another.

Standard screening analyses for ATF concepts

Design of an advanced fuel system demonstrating enhanced performance and safety relative to the current fuel system first requires understanding the current state-of-the-art fuel system performance under the various system operating regimes (normal operation through severe accident scenarios). An assessment of the potential beneficial impact or unintended negative consequences of candidate ATF concepts must address "fuel specific" characteristics of the concept and how implementation of the concept will affect reactor performance and safety characteristics. Assessment must include neutronics and thermal-hydraulics analyses to ensure that the reactor will operate as intended with the candidate fuel system. Coupled thermal-hydraulic-neutronic analysis of candidate ATF concepts is essential in understanding the synergistic impact of the thermal properties and reactivity feedback.

Standard evaluation of ATF concepts includes neutronics, thermal-hydraulic analyses, fuel performance and detailed systems analyses. Each of these analyses is briefly described below. Additional details on the code set employed in screening analysis in the United States for fuel and cladding concepts are described in Todosow et al. (2015). As noted in Bragg-Sitton et al. (2013, 2016), the analysis fidelity and level of detail depend on the development stage of the modelled concept. During the initial "screening" stage, analyses have limited detail, based on the current state of knowledge for the concept. The level of detail may range from literature reviews and expert judgment through limited experiments and computational analyses. In evaluating the potential performance of an ATF concept, the goal is to have sufficient confidence in the assessment, given a reasonable investment of time and resources, which identified that the changes relative to the reference fuel system (UO_2-Zr-alloy) are known well enough to proceed with continued development, or to conclude that the concept should be modified or abandoned.

Researchers at Brookhaven National Laboratory (BNL) working within the US DOE Advanced Fuels Campaign have developed and benchmarked a method for screening the reactor performance and safety characteristics of proposed advanced concepts (Todosow et al., 2015). Similar methods are used in other organisations responsible for evaluating ATF concepts. Key elements in the methodology include initial screening, three-dimensional core analysis and transient analysis. Initial screening analysis entails infinite lattice calculations at the fuel assembly level to estimate ATF impact on cycle length/burn-up, reactivity and control coefficients as a function of selected fuel enrichment. Subsequent three-dimensioal core analyses include thermal-hydraulic and temperature feedback, providing a platform for fuel cycle analysis and time-dependent accident analysis. Analysis of selected transients is then conducted to provide an estimate of "coping time" under the modelled conditions. Screening analyses must indicate a reasonable increase in the coping time for candidate ATF concepts relative to the reference fuel system (e.g. on the order of hours) to be considered "accident tolerant."

Many LWR fuel concepts have been analysed using the described screening analyses (Todosow et al., 2015; Carmack et al., 2006; Brown et al., 2013a, 2013b, 2014, 2015). These screening analyses provide information on the potential impact of fuel and cladding materials on reactor performance and safety characteristics. In addition, the screening analyses can help identify limitations in state-of-the-art modelling tools that may impact the ability to accurately model all aspects of some concepts.

The constraint of "backward compatibility" for ATF means that a candidate fuel should be able to replace the current reference fuel without significantly impacting handling operations, core thermal-hydraulics, emergency systems, etc. This requirement also places reasonable limitations on the possible enrichment of proposed fuels, recognising that the current limit on fuel enrichment for commercial reactor applications is <5 w/o ^{235}U. Maintaining the backward capability constraint could restrict opportunities for performance optimisation, but also reduces issues with licensing the fuel and implementing it in the current LWR fleet. Initial screening analyses can evaluate the ability of concepts to adhere to this constraint.

Nuclear data requirements

Measured nuclear data necessary to evaluate performance include cross-sections, decay chains, radioactive emissions, etc. This data requires processing to generate pointwise and/or multi-group data files in the appropriate formats for use in-reactor design codes. Common processing codes include NJOY and AMPX. Pre-processed libraries of nuclear data are based on ENDF, JEFF, JENDL and TENDL. In general, basic nuclear data are available for the elements/isotopes of interest for ATF; however, some data may have high uncertainties if they have not commonly been used in nuclear systems.

Initial neutronic screening analyses

Initial analyses are often performed at the fuel assembly level (especially for PWRs) using the linear reactivity model (or an appropriate enhancement; Driscoll, Downar and Pilat, 1990). This model is used to estimate the cycle length and discharge burn-up as a function of the number of batches in the fuel management scheme, power peaking and to estimate reactivity and control coefficients relative to the reference UO_2 configuration. Codes selected to conduct these analyses in the United States (at BNL) for candidate ATF include deterministic codes such as TRITON/NEWT (ORNL, 2011), POLARIS, HELIOS and CASMO, or Monte Carlo codes such as MCNP (LANL, 2005) and Serpent (Leppänen et al., 2015). The Monte Carlo codes provide results that are essentially benchmark quality and are constrained only by the available nuclear data and the geometric detail and statistics employed in the modelling.

The example reactor assembly nuclear design codes are sufficiently "general" with respect to geometry, materials, temperatures and modelling of neutron transport that different ATF concepts can be adequately modelled via input by a knowledgeable user. Use of codes and/or data that have been tuned to improve agreement in calculations for existing reactors should be used with caution for ATF concepts that employ significantly different fuel and/or cladding from traditional UO_2-Zr.

Three-dimensional core analyses

Ultimately, core-level analyses are required to assess the potential benefits, as well as any negative aspects, associated with the implementation of a specific concept. The assembly-level lattice analyses described above provide the nuclear data (e.g. neutron cross-sections, etc.) for subsequent full-core, three-dimensional analyses that include thermal-hydraulic and temperature feedback. These calculations can be used for fuel cycle analyses and some time-dependent accident analyses. For the ATF concepts both the thermal properties and the reactivity coefficients will change relative to the reference UO_2-Zr-alloy system. BNL researchers have selected the deterministic Purdue Advanced Reactor Core Simulator (PARCS) nodal code for this analysis step (Downar et al., 2012). Thermal-hydraulic analyses can be performed at the assembly or core-level for steady-state estimates of the Departure from nucleate boiling ratio (DNBR) or minimum critical power ratio (MCPR). Codes that can be used for thermal-hydraulic analyses include VIPRE and COBRA. Coupled thermal-hydraulic–neutronic analysis of candidate ATFs is essential in understanding the synergistic impact of the thermal properties and reactivity feedback.

As noted for the reactor assembly design codes, the example three-dimensional design codes are sufficiently "general" with respect to geometry, materials, temperatures and modelling of neutron transport that different ATF concepts can be adequately modelled via input by a knowledgeable user. The thermal feedback requires properties such as thermal conductivity, heat capacity, heat transfer coefficients (e.g. gas-gap conductance), which may not be well known for some ATF concepts. Hence, estimated values must be used initially, introducing uncertainty in estimated performance. Sensitivity analyses can provide insight on what parameters may have the greatest impact on performance estimates, providing guidance in prioritising property measurements.

Transient analyses

As noted previously, ATF concepts must be evaluated over the full spectrum of AOOs, DBAs and BDBAs to estimate potential safety enhancements in addition to evaluating the potential performance enhancements under normal operating conditions. The full spectrum of accidents can be found in Chapter 15 of a standard Safety Analysis Report for Nuclear Power Plants. Thermal-hydraulic transients are typically modelled in the TRACE code, but PARCS (standalone) or PARCS-TRACE is used to study reactivity transients where three-dimensional kinetics effects are important. While this analysis is again limited by the available data on the proposed fuel system, it can provide a preliminary estimate of "coping time".

One important caveat is that the screening analyses frequently require assumptions for the properties of candidate materials. The best available material properties are used in these analyses, but it is noted that material properties of candidate fuel and cladding materials depend on radiation damage, fraction of cold working, temperature and other conditions. These dependencies may be unknown or have significant uncertainty for proposed novel candidate fuel or cladding materials, resulting in significant uncertainty in the predicted performance.

Fuel performance codes

In the last decade, efforts have been made to simulate accidents such as LOCA with coupled thermohydraulics and thermomechanics codes, such as TRACE and FRAPCON (Raynaud et al., 2014) or Falcon (Cozzo et al., 2016). Provided the implementation of a validated model to represent the material behaviour, this type of methodology can also be used. The coping time, as defined within this document, does not require the code to be able to handle advanced behaviour such as core melt. The fuel performance code FRAPTRAN is being developed for application to ATF analysis in several countries, including the Czech Republic (to allow evaluation of SiC/SiC-cladding) and Korea. Likewise, the Electric Power Research Institute (EPRI) previously implemented a few models of Duplex SiC/SiC-cladding in Falcon. PSI is now continuing the development of Falcon to model SiC/SiC-cladding.

Advanced fuel performance modelling tools

Detailed measurement of material properties and characteristics is necessary to perform a fuel performance calculation. Behavioural models will include concept-specific material properties, which must be derived from validated models, experimental data, or assumptions. In some cases, the proposed fuel and cladding concept may be similar to the current fuel system, such that existing behavioural models can be applied with limited modification. However, cases in which the concepts deviate significantly from the current system will require development of material-specific behavioural models. Such models should be developed as the concept is matured and tested (see Chapter 5 on *Technology Readiness Levels*). If the developed models are sufficient to support fuel performance analysis, then work can proceed using the available analysis tools with the correct behavioural models inserted.

MOOSE/BISON/MARMOT

The US DOE Nuclear Energy Advanced Modelling and Simulation (NEAMS) programme is developing an advanced modelling and simulation toolset for application in a wide array of problems. Several NEAMS tools function within the Multi-physics Object-Oriented Simulation Environment (MOOSE; Gaston et al., 2009) framework. MOOSE provides a high-level interface to sophisticated non-linear solver technology and it provides the framework upon which other analysis tools are created. The associated fuel performance code, BISON, is a finite element-based code applicable to a wide variety of fuel forms. It solves the fully-coupled equations of thermomechanics and species diffusion, for either one-dimensional spherical, two-dimensional axisymmetric, or three-dimensional geometries. MARMOT is a lower-length-scale code that interacts with BISON to predict the effect of radiation damage on microstructure evolution, including void nucleation and growth, bubble growth, grain boundary migration and gas diffusion and segregation. In addition, MARMOT calculates the effect of the microstructure evolution on various bulk material properties, including thermal conductivity and porosity. When complete, the MOOSE/BISON/MARMOT tool set will be capable of evaluating detailed irradiation damage effects in materials, which may speed deployment of ATF by partially reducing the need for as much test reactor irradiation and PIE data.

In the absence of specific data on the properties and behaviours of many of the candidate fuel and cladding materials, specific fuel performance modelling within BISON is limited. Parts II and III of this report will support the completion of specific behavioural models for fuel performance modelling. The US NEAMS programme is focused on expanding the existing BISON/MARMOT fuel performance modelling and simulation capability to enable evaluation of some leading ATF concepts. Efforts are under way to expand the BISON fuel performance code to perform a representative assessment of accident tolerance for selected concepts. Concept-specific material and behavioural models are expected to require experimental data generated by R&D activities and it will also rely on lower-length-scale models developed under the NEAMS programme (i.e. MARMOT). Note that confidence in predictive results from fuel performance analysis will depend on the availability of all the needed property data for the simulations.

A preliminary sensitivity study was conducted at INL in 2014 to identify trends and to determine the overall impact of the variation of multiple thermo-physical parameters on fuel performance (Smith et al., 2014). Using a simplified loss-of-coolant accident (LOCA) scenario, the impact of thermal conductivity, specific heat capacity, Young's Modulus and thermal expansion coefficient on the maximum creep strain, peak cladding temperature, maximum principle stress and maximum von Mises stress was calculated. Note that although creep is the primary non-linear deformation mechanism for most cladding materials, this parameter does not lend itself to a simple parametric study. A specific creep model must be adopted in future studies of specific ATF candidates. This simplified study was essentially a proof-of-concept in using BISON to investigate ATF performance under a postulated accident condition. Despite the simplified approach, the work points to a few key conclusions. Under LOCA conditions, it was found that creep strain is most sensitive to thermal conductivity and specific heat. Hence, new cladding materials with low-thermal conductivity and low specific heat will have the least creep strain.

Falcon

In the late 1990s, the Electric Power Research Institute (EPRI) developed Falcon (EPRI Product ID 3002009086) to perform a best estimate analysis of fuel performance. This mechanical-based finite element analysis code combines thermal and other nuclear fuel rod specific physics models to perform a broad range of two-dimensional thermal/mechanical LWR fuel rod performance modelling analyses. This different approach to fuel performance analysis delivers a code validated to high-burn-up, approaching 80 GWd/t_U, for evaluating LWR UO$_2$-Zr fuel rods under steady-state operation and transient events. The steady-state time scale is used to place a fuel rod in a valuable burn-up state where transients associated with postulated accidents can be applied to test acceptance criteria.

EPRI has modified Falcon (Falcon is the newer version of Falcon which includes graphical interface) to rudimentarily investigate silicon carbide cladding behaviour (EPRI Product ID 1022907). This investigation provides an opportunity to test more advanced silicon carbide cladding behaviour models with Falcon as experimental data becomes available to develop such models. Falcon uses dynamic link libraries (DLLs), written in FORTRAN, to allow users to introduce different cladding models for 12 material properties. Source code modification is generally required to increase fuel thermal and mechanical models to support additive fuel concepts. This is also the case for cladding model modifications that go beyond those available by DLL. The Paul Scherrer Institute (PSI) is currently continuing the development of Falcon to model SiC/SiC-cladding.

The finite element model construction is tied to two-dimensional LWR configurations in R-Z and R-theta space. The finite element solver is also optimised for this geometry. Falcon can accommodate cladding composed of two different materials, specifically for modelling BWR liner fuel rod cladding. Code modifications could be made to allow Falcon to properly model an exterior coating over a base metal.

TRANSURANUS

The TRANSURANUS fuel performance code is a simulation tool for the thermal and mechanical analysis of cylindrical fuel rods for nuclear reactors, hence a key instrument for fuel performance modelling that is used by various research centres, universities, nuclear safety authorities and industrial partners. The code has a materials data bank for oxide, mixed-oxide, carbide and nitride fuels, zircaloy and steel claddings and different coolants. The scope of the covered phenomena and the numerical solution methods enables the code to simulate both long fuel cycles and hypothetical accidents. Options for probabilistic analysis are also involved in order to provide the possibility of a statistics-based evaluation such as Monte Carlo simulations. Since its inception in the 1970s, the development as well as the verification of the code is carried out following rigorous quality procedures and is organised in three steps. The first step consists of verifying the mechanical–mathematical framework. To this end, the models in the code are compared with exact solutions, which are available in many special cases (analytical verification) and several solution techniques are tested, which are applied in order to optimise the numerical analysis. During the second step, extensive verification of separate models incorporated in the fuel performance code is performed on the basis of separate-effect data. Finally, in the third and last step the verification is completed by code-to-code evaluations with experimental data from the International Fuel Performance Experimental database of the NEA, as well as comparison with experiments in the frame of international benchmarks organised by the IAEA and the NEA.

PLEIADES/ALCYONE

The simulation platform PLEIADES (Michel et al., 2013), which is co-developed by the French Alternative Energies and Atomic Energy Commission (CEA), the French utility Electricité de France (EDF) and AREVA, is dedicated to the simulation of nuclear fuel behaviour. Its architecture provides generic tools for multi-physics algorithms, data exchange based on SALOME software and links with fuel databases. It includes tools for pre-processing and post-processing with user-friendly interfaces. The PLEIADES platform also provides a physical components library for fuel simulation embedded in C++ classes in a unified software environment. The computational algorithm is built with the architecture and the physical component library, with a user interface dedicated to each fuel concept. Some of the fuel performance codes in the PLEIADES platform are dedicated to specific fuel concept studies (ALCYONE for PWR, GERMINAL for Sodium Fast Reactor (SFR), MAIA for materials test reactor [MTR], etc.). PLEIADES also includes the VER application which is devoted to simulation at the volume element scale for generic fuel microstructure analyses and the LICOS application, which is used for preliminary fuel design studies on non-standard geometry.

ALCYONE (Marelle et al., 2016) is a multi-dimensional fuel performance code. It is dedicated to the simulation of the in-reactor behaviour of PWR fuel rods during normal (base irradiation) and off-normal (power ramps and accidental situations) operating conditions with three calculation schemes. A one-dimensional reference scheme, based on a one-dimensional axi-symmetric description of the fuel element associated with a discrete axial decomposition of the fuel rod in stacked independent fuel slices, is used to study the behaviour of the complete fuel rod. A two-dimensional scheme that describes PCI at the mid-pellet plane of a pellet fragment is available to precisely assess stress concentration in the cladding near a pellet crack tip (Sercombe, Masson and Helfer, 2013). A three-dimensional model of the complete pellet fragment and overlying cladding is also of interest when detailed studies of pellet-clad interaction (PCI) at pellet-pellet interfaces are required (Michel et al., 2008). The different schemes use the finite element (FE) code Cast3M to solve the thermo-mechanical problem and share the same physical material models at each node or integration points of the FE mesh. Moreover, two advanced schemes can be used in one dimension. MARGARET (Noirot 2011) is an advanced gas model that more precisely describes gas diffusion and gas release in the

fuel and RACHEL is a model dedicated to helium release in MOX fuels. Finally, accidental schemes (e.g. LOCA, RIA) are used to simulate accidental situations with the activation of specific models and constitutive laws. From now on, LOCA studies have been performed using a one and one-half-dimensional scheme. For LOCA transient analysis, ALCYONE is not able to calculate the cladding temperature evolution with time, so this information must be provided as input data. Nevertheless, the coupling of ALCYONE with the system code CATHARE will be available in the near future.

ALCYONE has been extensively validated on more than 350 rods representing various irradiation conditions (base irradiation up to high burn-up, power ramp tests performed in MTR or accidental situations such as LOCA and RIA) and various fuels (UO_2 and MOX fuels) and claddings (Zy-4 and M5). These objects are simulated with different modelling schemes (one-dimensional, two-dimensional and three-dimensional) and using different kinds of gas models. Calculated results are compared to experimental values at different scales, from overall measurements on the whole rod such as overall fission gas release or geometric changes to the local measurements on the fuel pellet by SIMS and EPMA. Moreover, fuel temperature calculations are validated specifically on MTR experiments that present a thermocouple in the fuel centre.

Considering its calculation schemes, models and functionalities, the PLEIADES/ALCYONE code can be used to assess various ATF concepts.

FEMAXI

The FEMAXI fuel performance code is a simulation tool for the variation of the thermal, mechanical and chemical status and the interactions of fuel pellet, cladding and inner gas under the normal and the transient operation conditions of LWR fuels, by two-dimensional (R-Z) FE method, which was developed by JAEA. FEMAXI was developed in three steps. In the first step, FEMAXI-I was developed as a base analytical system for the two-dimensional elasticity-plasticity PCMI analysis and then improved as FEMAXI-III under collaboration with fuel vendors and universities in Japan, which was opened to the NEA Data Bank in 1984. In the second step, improvement for the analysis of high burn-up fuel performance was included by introducing mechanistic models. The FEMAXI-6 code was opened to the NEA Data Bank.

In the third step, kinetic models for FP-gas release was implemented and the ability for the analysis of high burn-up fuel performance was further improved. FEMAXI-7 was then opened to the NEA Data Bank. The improvement of FEMAXI-7 has continued by establishing the optimised input conditions, based on analysis using irradiation test results from the Halden reactor and other reactors. Furthermore, analytical functions are being improved not only for the conventional combinations of oxide fuel (UO_2, MOX, UO_2-Gd_2O_3), zircaloy-cladding and water coolant, but also for the other advanced combinations of nitride fuel, stainless steel cladding, SiC-based cladding, Na coolant and Pb-Bi coolant. Some of these advanced system analyses have already commenced. Regarding SiC-based cladding, fundamental equations for properties were already implemented and the interaction models for three-layer cladding structure were improved, in which monolithic-SiC (inner), SiC/SiC-composite (intermediate) and monolithic-SiC (outer) can be analysed. By using the improved models, functions for identifying cladding failure conditions for SiC-based cladding was implemented in FEMAXI.

JAEA is also developing a link between FEMAXI and RANNS or FURBEL for analysis of accidental conditions. RANNS and FURBEL are RIA-analysis and LOCA-analysis codes, respectively.

MACROS

Since 2003, SCK•CEN started developing the MACROS code to perform full-scale analysis of urania, plutonia and thoria based mixed-oxide fuel pins with minor actinides in the thermal and fast reactor conditions. This code combines multi-group neutronic models,

thermal-mechanical properties and physical models for specific phenomena to perform two-dimensional analysis of in-reactor behaviour of LWR and fast reactor (FR) fuel pins. Participation in a number of European Framework Programmes, such as OMICO, FAIRFUELS and PELGRIMM supported verification and validation work for the MACROS code, including ATF prototypes with SiC as a cladding material and SiC as an inert matrix in addition to other inert matrices (MgO and Mo-based). Capabilities of the MACROS code recently have been extended to perform analysis of fuel fragmentation and dispersion under LOCA and RIA conditions.

SCANAIR/DRACCAR

The IRSN has developed two specific codes over many years: SCANAIR for the simulation of PWR fuel rods in RIA conditions and DRACCAR for the simulation of PWR assemblies in LOCA conditions.

SCANAIR models a PWR rod subjected to a reactivity insertion accident and the phenomena specifically related to irradiated fuel. It is comprised of three main modules which are strongly coupled: a heat module that calculates radial conduction in the fuel and cladding, as well as heat transfers with the coolant; a module that calculates the swelling of fission gas bubbles, grain boundary failure in the fuel and gas flows into the free volumes; a mechanical module that calculates the different types of fuel deformation (thermal, elastic and plastic related to cracks and swelling caused by fission gases) leading to cladding deformation or failure by taking into account the corroded state of the cladding. The mechanical properties of cladding have been determined thanks to an analytical test programme. Heat exchanges between the cladding and the coolant have been validated through separate-effects tests under PWR conditions and tests from the NSRR programme. The SCANAIR software is systematically validated during Cabri-REP-Na programme tests.

DRACCAR is a three-dimensional multi-rod software package capable of modelling a fuel rod assembly to determine the blockage rate due to deformed rods and the impact on cooling, while taking into account mechanical and thermal interactions between rods. DRACCAR models the following physical phenomena: thermal conduction in the fuel and cladding in three-dimensional conditions; heat exchanges between the fuel rods and the coolant; cladding deformation due to creep and failure of the fuel rods; relocation of fuel in the deformed areas of the rods; oxidation and hydriding of the fuel rod cladding due to steam; mechanical interactions between the deformed fuel rods and feedback due to fuel rod deformation on the coolant flow areas.

Analysis of severe accident behaviour

Scoping simulations performed using a severe accident analysis code can be applied to investigate the influence of advanced materials on BDBA progression and to identify any existing code limitations.

MELCOR

MELCOR is a systems-level severe accident analysis code that is being developed and maintained at Sandia National Laboratories in New Mexico (SNL/NM) for the NRC to support licensing activities. MELCOR includes the major phenomena of the system thermal-hydraulics, fuel heat-up, cladding oxidation, radionuclide release and transport, fuel melting and relocation, etc.

MELCOR is designed for current LWR core material configurations. As such, the code contains material property definitions for UO_2, zircaloy, ZrO_2, steel, steel oxide and Inconel for the fuel, cladding, spacer grids, support plates and channel boxes. However, an effort to extend the MELCOR capability to include candidate accident-tolerant cladding materials was undertaken beginning in fiscal year (FY) 2012. To date, INL researchers have added properties and behaviours for silicon carbide (SiC) and FeCrAl to the MELCOR reactor core

oxidation and material properties routines (Merrill, Bragg-Sitton and Humrickhouse, 2014, 2017). These code versions also decouple material composition assignments, such that changes can be made to the composition of one component (e.g. the cladding) without affecting other core structures. These alternate materials may be selected as the sole cladding material or as a coating (or sleeve) on a standard metallic cladding (e.g. SiC sleeve over metallic cladding, such as a Zr-alloy; FeCrAl coating on Zr-alloy). Modifications to include additional fuel materials (beyond UO_2) have not yet been addressed.

Scoping evaluations for candidate materials can be performed using the revised MELCOR models if sufficient data is known from characterisation activities. The manner in which a candidate cladding material oxidises will determine which code version should be used (e.g. SiC or FeCrAl versions). The FeCrAl version of the code should be selected for candidate cladding materials that demonstrate parabolic oxidation behaviour (similar to FeCrAl and other metals); in this case, the FeCrAl properties could be overwritten by the user to assess performance of an alternate candidate material. For materials that exhibit both parabolic oxidation and linear volatilisation, similar to SiC, the SiC version should be employed, with material-specific properties entered as appropriate. Key material properties and behaviours necessary for MELCOR simulation include:

- properties of the base material (e.g. SiC) and its oxide (e.g. SiO_2), as a function of temperature and irradiation:
  - melting temperature of the base material, oxide and any eutectics that may form;
  - thermal conductivity;
  - specific heat;
  - density;
  - emissivity.
- oxidation reactions, including oxidation rate, heat of reaction, reaction products, etc.;
- Arrhenius relationship for parabolic oxidation rate behaviour.

In the absence of specific property and behaviour data or significant uncertainty in the available data for selected materials, MELCOR can be employed to perform parametric studies. Key parameters, such as the oxidation rate or the material thermal conductivity, can be varied over a reasonable range to determine the overall impact on behaviours of interest, such as peak cladding temperature. In this manner, the properties that most impact the accident performance of the fuel system can be identified.

The INL-modified version of MELCOR has been applied in the analysis of a pressurised water reactor accident (specifically Three Mile Island Unit 2 [TMI-2] and the associated [LOCA] sequence) to determine potential safety enhancements that could be realised with SiC or FeCrAl cladding materials (Merrill, Bragg-Sitton and Humrickhouse 2014, 2017). Analysis of the impact of FeCrAl replacement of all zirconium alloy components in a BWR (specifically, Peach Bottom) station blackout scenario (as occurred at Fukushima Daiichi) has been conducted by Oak Ridge National Laboratory (ORNL; Ott, Robb and Wang 2014).

MAAP

EPRI's Modular Accident Analysis Programme, or MAAP, enables users to analyse actual and simulated nuclear plant accident scenarios. The software predicts plant responses to upset events up to and including accidents involving severe core damage by evaluating the condition of the plant, including the core, reactor vessel and the containment. It also tracks the transport of energy and mass, accounting for inventories of water, hydrogen,

aerosols and radioactive species. MAAP has been under development at EPRI for more than 20 years. A software user group, the MAAP User Group (MUG), has been established and provides guidance on new software features, as well as ongoing training and user support for the MAAP software.

MAAP can calculate the time to and extent of fuel cladding failure, time to core melt and the extent of core degradation. Accordingly, MAAP has been identified as a useful tool for evaluating the relative benefit of various ATF designs in terms of increased time to onset of core damage and reduction in hydrogen production from in-core oxidation. EPRI is developing a new version of the MAAP5 code to help evaluate the potential benefits of introducing alternative nuclear fuel and cladding materials into LWRs relative to zircaloy and to each other.

The MAAPv5.05 code has recently been modified to allow user-input of different cladding materials, a different cladding material for B_4C control blades and new fuel material. In general, the modifications cover four major areas: i) property calculation, ii) reaction calculation for new materials and H_2O, iii) potential change in fuel and fuel cladding failure criteria and iv) fission product (FP) release rate from fuel materials.

The following properties and kinetic equations are needed to model new cladding and fuel materials:

- density as a function of temperature;

- specific heat and specific internal energy as a function of temperature;

- thermal conductivity;

- melting temperature;

- latent heat of fusion;

- viscosity;

- surface tension;

- emissivity;

- molecular weights of new cladding materials and oxide materials;

- kinetic equation for oxidation with steam and reaction energy.

ATF modifications for MAAP

Several modifications to the MAAP code have recently been implemented and are currently being tested as MAAPv5.05 Beta version. Modifications include:

- a new user-input flag is provided to model ATF cladding and fuel materials;

- material properties: subroutines PSOLID and USOLID have been modified to calculate properties of new cladding and fuel materials;

- for the new materials:

  – new user-input lookup tables have been provided for density, specific heat, specific internal energy and thermal conductivity;

  – new user-input have been provided for the melting temperature, latent heat of fusion, viscosity, surface tension and emissivity;

  – new oxide material (produced as a result of reaction with steam/water) properties have been provided as new user inputs.

With respect to kinetic equations:

- A flag has been provided that allows the user to turn off oxidation completely.

- A parameter has been provided that allows the user to define a fraction of hydrogen generated (a fraction compared to Zr) and a fraction of reaction power.

- New input-driven general reaction equations have been provided.

- User inputs have been created to specify reaction kinetic equations as a function of temperature.

- New inputs are defined for up to three temperature ranges.

- Options are provided to allow for user-specified selection of material for cladding, fuel, fuel can and control blades. For the control blades, the steel sheath with B_4C can be replaced with the ATF material with B_4C.

- The user is able to select the following materials:

  – cladding: zircaloy or steel, or any arbitrary ATF cladding specified by the user;

  – fuel: UO_2 or any uranium-based ATF fuel material;

  – control rod/water rod: zircaloy guide tube or ATF-cladding material;

  – fuel can: zircaloy or ATF material;

  – control blade: steel or ATF material with B_4C.

- A user option is provided to have ATF material in fuel cladding and Zr guide tubes for control rods (limited amount of Zr in the core).

- Temperature calculation: Routines calculating cladding, fuel, control rods, fuel can and control blade temperatures have been modified to handle different materials. The logic in the temperature calculation routines has been changed to handle general "user-input melting temperature".

- Fuel cladding rupture criterion (TCLRUP) for FP release, initiation of molten fuel relocation (TCLMAX) and fuel collapse logic (LMCOL0 to LMCOL3) have been reviewed and proper user inputs provided for general use.

- FP release correlation: CORSOR-O and ORNL-BOOTH models have been reviewed/modified to add user-input parameters to control the FP release rates from new ATF fuel materials.

- Core and Reactor Coolant System (RCS) energy balance routines have been updated for the ATF materials.

MAAP limitations

The ATF modifications for MAAPv5.05 do NOT include the following:

- Eutectic formation of cladding materials with other core materials will not be explicitly modelled in detail at this time, i.e.:

  – no eutectic formation with UO_2 for new ATF-cladding materials;

  – no eutectic formation with Zr, B_4C, or Steel-B_4C.

- Relocation of new ATF materials into the lower plenum region and subsequent relocation into the containment will not be modelled. All simulations will be stopped at the time of core material relocation into the lower plenum.

ASTEC

The ASTEC code (Accident Source Term Evaluation Code, Chatelard et al., 2016), jointly developed over several years by IRSN and GRS and now developed only by IRSN, aims at simulating an entire severe accident (SA) sequence in a water-cooled nuclear reactor

from the initiating event through the release of radioactive elements out of the containment, including the behaviour of engineered safety systems and procedures used in severe accident management (SAM). The main applications are source term determination studies, probabilistic safety assessment level 2 (PSA-2) studies including the determination of uncertainties, accident management studies and physical analyses of experiments to improve the understanding of the phenomenology and to support the development of new models.

As to the in-vessel degradation phenomena, ASTEC describes both early and late degradation phases, up to vessel failure, including the behaviour of fuel rods and control rods, channel boxes (for BWR), fuel assemblies with spacer grids, in-core two-dimensional thermal-hydraulic fluid with channels possibly blocked with molten/frozen mixtures, corium molten pool with crusts, debris beds as well as peripheral and lower/upper core structures (horizontal plates, vertical surrounding walls such as barrels or shrouds).

Focusing on the fuel modelling, ASTEC V2.1 notably allows simulation of fuel rod heat-up, clad ballooning and burst, clad oxidation, fuel rod embrittlement or melting, subsequent molten mixture candling and relocation.

The main models that can be activated in the frame of ASTEC applications are:

- heat transfers: axial and radial conduction between two wall nodes, gap exchanges between pellets and clad, convection between fluid and wall as well as radiation. For the latter, a general in-core heat transfer model (based on an equivalent radiative conductivity approach) allows one to deal with radiative exchanges in a reactor core regardless of the degradation level (intact rods, moderately degraded rods, severely damaged core, large cavities, etc.), thus managing in a continuous way the heat transfers throughout the evolution of the core geometry degradation;

- power: either nuclear power generated by FPs or generated in a given material, or electric power generated in some out-of-pile experiments:

  – rod mechanics: ballooning, creep and burst of zircaloy fuel rod cladding (including both Zry-4 and Zr1%Nb alloys), creep of control rod stainless steel cladding, embrittlement and loss of integrity of fuel rods (per user criteria);

  – oxidation of Zr by steam, oxidation of stainless steel by steam, dissolution of UO_2 by solid and liquid Zr, dissolution of Zr by liquid silver-indium-cadmium alloy, dissolution of Zr by solid steel, oxidation and degradation of B_4C control rods, zircaloy oxidation under air atmosphere, including a preliminary treatment of nitriding processes that could occur under oxygen starvation conditions;

  – release of FPs and structural materials from both intact or degraded core.

To define all the material properties, an external material data bank called MDB is used by ASTEC. This library groups together all material properties under a unique simple readable format. This includes:

- all simple materials of a water-cooled reactor (solid, liquid and gas) and associated usual properties (enthalpy, conductivity, density, etc.);

- ideal chemistry (equilibrium reactions).

The MDB library includes all the recent research on nuclear material properties performed in international projects: for FP, CIT and ENTHALPY FP4 projects and for corium OECD, RASPLAV and MASCA projects. The evaluation of corium properties is based on the NUCLEA/MEPHISTA databases for corium thermo-chemistry. It also benefits from a continuous validation at IRSN of the database contents. Specific modelling work could be done on some ternary thermodynamic systems identified as very important for ATF to complete the NUCLEA/MEPHISTA database for practical applications.

The MDB library allows overwriting of existing properties to test new materials and to perform sensitivity analyses. Properties are in readable format and can be changed easily. It is also possible to create new materials, adding them in the MDB index. Users can also define new complex laws that may need programming without code compiling. This programming must use the ASTEC/MDB external language analyser. Because data are in a readable format, it is possible to overwrite existing properties in MDB to test new materials and to perform sensitivity analyses. These types of studies with the ASTEC code have previously been performed for iodine containment chemistry (Chevalier-Jabet et al., 2011).

SOCRAT

SOCRAT is a systems-level SA analysis code that was jointly developed by several Russian organisations: IBRAE RAS, VNIIEF, SPbAEP, NRC "Kurchatov Institute" and others. This software package allows realistic analysis of VVER reactor facilities in cases of severe LOCAs by simulating physical processes throughout all the accident development stages, with account of VVER design-specific features. Physical and mathematical models, as well as improved-precision computational modules, allow a co-ordinated description of a variety of thermal-hydraulic, physical, chemical and thermo-mechanical phenomena. SOCRAT verifications performed on the basis of data obtained from Russian and foreign experimental studies of individual phenomena and from integral experiments confirm this code's capability to properly describe the totality of processes and phenomena associated with design extension conditions (also referred to as BDBAs) in VVER reactor facilities.

The SOCRAT code solves the following basic tasks:

- realistic assessment of steam and hydrogen sources to assure fire and explosion safety of the reactor containment;

- realistic assessment of the reactor status, analysis of reactor response to possible accident-control measures;

- realistic assessment of mass and energy of corium to be released from the RPV in case the RPV floor is destroyed.

The code enables appropriate mathematical simulation of the following thermo-physical, physical and chemical processes, which have the strongest impact on the SA course:

- zirconium oxidation, suppression of oxidation reactions in steam-starvation conditions;

- oxidation of steel components of the core and in-vessel devices;

- rupture of fuel cladding, with possible start of cladding oxidation on both sides;

- oxidation of absorber rod material;

- melting of steel structures in the core, protective tubing and baffle;

- eutectic interactions;

- melting of fuel cladding material;

- heat-up of lower areas by down-flowing molten core and in-vessel structures to temperatures at which intensive oxidation starts;

- possible core re-flooding, with hydrogen generation accelerated by corium oxidation and by bare metallic surfaces that no longer have a surface oxide layer;

- failure of fuel assembly tail-pieces leading to corium propagation to fuel assembly supports followed by their collapse and corium penetration into the lower plenum;

- molten material interaction with water, its dispersion and full oxidation, additional steam ingress to the core, and intensified oxidation;

- reheating and remelting of core and in-vessel structures, heat-up and melting of lower plenum structures and formation of corium pool in the lower plenum;

- disintegration of in-vessel barrel bottom with formation of corium pool on the RPV floor;

- development of natural convection processes inside the corium, its stratification, effect of heat flow "focusing" in the metallic layer.

For numerical simulation of all the above physical phenomena and processes, SOCRAT applies the following software modules, which are its basic components:

- RATEG – full-circuit two-fluid thermo-hydraulic and heat transfer in solids;

- SVECHA – in-core physical and chemical processes (up to total core disintegration) taking place in case of severe accident;

- HEFEST – processes in the lower plenum, concrete barrel or core catcher, behaviour of materials in case of core meltdown accidents and RPV melt-through. HEFEST also simulates the processes of corium retention and cooldown in the lower regions of the RPV.

It should be noted here the SOCRAT code was specifically designed for use with current VVER reactor core and material configurations. ATF-related enhancements to the SOCRAT code could include user-defined input parameters for fuel and cladding properties, with default values remaining the standard UO_2-Zr-alloy system. NRC "Kurchatov Institute" is currently working to extend the existing code for ATF materials under SA conditions.

The modified version of SOCRAT has been applied in the analysis of VVER reactor accidents to determine potential safety enhancements that could be realised with ATF materials. Namely, the analysis of the impact of ATF replacement of the standard UO_2-Zr fuel cladding system in VVER-1200 reactor LB-LOCA and SBO scenarios has been conducted by NRC "Kurchatov Institute" (Zvonarev, Melnikov and Kireeva 2017).

The main code limitations associated with potential ATF materials are the following:

- modelling material interactions;

- eutectic formation;

- cladding oxidation kinetics.

Vendor evaluation of ATF concepts

The thermal-mechanical performance of fuel rods is typically evaluated using fuel vendor codes to assure safe operation using criteria established by the US NRC in the early 1970s. Specifically in general design criterion (GDC) 10, within Appendix A to 10 CFR Part 50, "as it relates to assuring that specified acceptable fuel design limits are not exceeded during any condition of normal operation". In the case of fuel rod failure, the specified acceptable fuel design limits are not to be exceeded during postulated accidents as specified for all design criteria in US NRC SRP 4.2. To evaluate these limits, which are associated with internal pressure and fuel rod axial growth, fuel melting, cladding stress, strain, oxidation, hydriding, fatigue, flattening and corrosion, fuel vendors have optimised their codes, methods and procedures for their specific fuel rod products. Modifications to vendor codes may be necessary to accommodate ATF.

Table 7.1. Selection of standard screening analysis tools

Standard screening analysis					
Name	Calculation type	ATF readiness	Country or organisation	External availability	Notes, key reference, etc.
TRITON/ NEWT	Fuel assembly level, neutronics.	Applied in ATF screening calculations.	US, BNL		ORNL, 2011
MCNP	Fuel assembly level, neutronics.	Applied in ATF screening calculations.	US, BNL		LANL, 2005
Serpent	Multipurpose three-dimensional continuous-energy Monte Carlo particle transport code; fuel assembly level.	Applied in ATF screening calculations.	US, BNL		Leppänen et al., 2015 http://montecarlo.vtt.fi
PARCS	Three-dimensional core-level thermal-hydraulic analysis.	Applied in ATF screening calculations.	US		Downer et al., 2012
DeCART2D/ MASTER	Fuel assembly level, neutronics.	Applied for microcell UO_2 pellet (Korea).	Korea, KAERI	Export limited.	KAERI, 2004 KAERI, 2013
VIPRE	Subchannel analysis tool designed for general-purpose thermal-hydraulic analysis under normal operating conditions, operational transients and events of moderate severity.		US, Zachry Nuclear Engineering, Inc.		www.csai.com/vipre

Table 7.2. Selection of transient screening analysis tools

Transient screening analysis					
Name	Calculation type	ATF readiness	Country or organisation	External availability	Notes
TRACE (TRAC/RELAP Advanced Computational Engine)	Three-dimensional thermal-hydraulic analysis.		US NRC; PSI (Switzerland)	No.	Preliminary coping time estimate for spectrum of Ch. 15 accident conditions; Interacts with Falcon in the PSI methodology; SiC models: density, specific heat, thermal conductivity and emissivity, Reference: www.nrc.gov/about-nrc/regulatory/research/safetycodes.html.
PARCS (Purdue Advanced Reactor Core Simulator)	Three-dimensional thermal-hydraulic analysis.	Applied in ATF screening analysis.			Reference: www.nrc.gov/about-nrc/regulatory/research/safetycodes.html.
PARCS-TRACE	Three-dimensional thermal-hydraulic analysis.				Used to study reactivity transients where 3D kinetics effects are important.
CATHARE (Code for Analysis of THermalhydraulics during an Accident of Reactor and safety Evaluation)	System code for PWR safety analysis.		France	Licence agreement required.	www-cathare.cea.fr/.

Table 7.2. Selection of transient screening analysis tools (continued)

Transient screening analysis					
Name	Calculation type	ATF readiness	Country or organisation	External availability	Notes
ALCYONE RIA	ALCYONE is a multi-dimensional (1D, 2D or 3D) fuel performance code dedicated to PWRs; allows for modelling under RIA.		CEA		Marelle et al., 2011, 2016.
SCANAIR	Simulates the thermo-mechanical behaviour of fuel rods during an RIA in a PWR.		IRSN		Moal et al., 2014 www.irsn.fr/EN/Research/ Scientific-tools/Computer-codes/Pages/SCANAIR-computer-code.aspx.
DRACCAR	System code for LOCA analysis in a PWR.		IRSN		www.irsn.fr/EN/Research/ Scientific-tools/Computer-codes/Pages/DRACCAR-software.aspx.
RELAP5 (Reactor Excursion and Leak Analysis)	Thermal-hydraulic analysis.		US NRC		Home page: www.relap.com KAERI is performing the DBA analysis for the conductivity and oxidation rate effects for ATF pellet and cladding.

Table 7.3. Fuel performance modelling tools

Fuel performance modelling tools					
Name	Calculation type	ATF readiness	Country or organisation	External availability	Notes
BISON	Fully-coupled thermomechanics and species diffusion; one-dimensional spherical, two-dimensional axisymmetric, or three-dimensional geometries.	Under development .	US, INL-developed, multiple users.		MOOSE-based https://bison.inl.gov/.
MARMOT	Lower-length-scale code to predict effect of radiation damage on microstructure evolution, including void nucleation and growth, bubble growth, grain boundary migration and gas diffusion and segregation.		US, INL-developed, multiple users.		MOOSE-based, interacts with BISON https://moose.inl.gov/marmot/SitePages/Home.aspx.
FRAPCON/ FRAPTRAN	Steady-state and transient fuel performance analysis.	Under development (Korea).	multiple		frapcon.labworks.org/.
Falcon	Fuel performance and severe accident analysis; coupled with TRACE for LOCA and SBO analyses.	Under development.	US, EPRI-directed collaborative development; PSI.	Limited – requests must be directed to EPRI.	Interacts with TRACE in the PSI methodology. SiC models (EPRI Product ID 1022907): thermal conductivity, specific heat, irradiation swelling, Young's modulus, Yield stress, Ultimate tensile stress and shear modulus. Creep and oxidation are neglected.
FEMAXI	LWR fuel analysis code, normal and transient conditions.	Under development.	Japan.		Suzuki et al., 2013.
Copernic	One and one-half dimensional fuel rod performance code.	Under development.	AREVA NP.		Bernard et al., 1999.

Table 7.3. Fuel performance modelling tools (continued)

Fuel performance modelling tools					
Name	Calculation type	ATF readiness	Country or organisation	External availability	Notes
ALCYONE	Multi-dimensional fuel performance code.	May be applied to ATF.	CEA.		Marelle et al., 2011, 2016.
Cyrano	Fuel rod performance code.		EdF.		
TRANS-URANUS	Steady-state and design-basis accident fuel rod performance analysis.	Fuels: material properties and models for UC and UN fuels included, material properties and models for U_3Si_2 under development Claddings: material properties for standard stainless steels included, preliminary confidential data for SiC/SiCf included, material properties and models for MAX coating, FeCrAl and other steels under development.	Euratom co-ordinated, multiple users and developers.	> 35 licensees across the globe.	https://ec.europa.eu/jrc/en/scientific-tool/transuranus.
MACROS	Steady-state, transient, LOCA and RIA fuel performance analysis.	Verified version for MgO-based CERCER fuels; SiC-based matrices and cladding; Mo-based dispersed MetCer fuels.	Belgium, SCK•CEN.	Preparations for release to NEA Databank.	Fully autonomic fuel performance code with neutronic and hydraulic calculations; radial and axial distributions.

Table 7.4. Severe accident analysis tools

Severe accident analysis					
Name	Calculation type	ATF readiness	Country or organisation	External availability	Notes
MELCOR	Systems-level severe accident analysis.	Some ATF materials implemented (see Merrill et al., 2017).	US (maintained and distributed by Sandia National Laboratories, used by multiple US laboratories).	Limited – requests must be directed to Sandia National Laboratories.	Includes major phenomena of the system thermal-hydraulics, fuel heat-up, cladding oxidation, radionuclide release and transport, fuel melting and relocation, etc.; approved versions for current LWR core materials; experimental version for some ATF-cladding materials.
MAAP	Severe accident analysis; LOCA and non-LOCA transients.	Modifications implemented.	US (EPRI)	EPRI owned and licensed.	www.fauske.com/nuclear/maap-modular-accident-analysis-program.
ASTEC (Accident Source Term Evaluation Code)	Simulates severe accident sequence in water-cooled reactors.		IRSN		www.grs.de/en/astec.
SOCRAT	System-level severe accident analysis.	Under development.	Russia	Limited – request must be directed to Rosenergoatom.	Includes major phenomena of the system thermal-hydraulics, fuel heat-up, cladding oxidation, FP release and transport, fuel melting and relocation, etc.; approved version for current VVER core materials; ATF-related enhancements to the SOCRAT code include user-defined input parameters for fuel and cladding properties.

References

Bernard, L.C., C. Foissaud and E. Van Schel (1999), Copernic: "Framatome fuel rod performance code to address high burnups and advanced claddings", *Proceedings of the 1999 Annual Meeting of Nuclear Technology*, pp. 391-394, Karlsruhe.

Brown, N.R., M. Todosow, A. Cuadra (2015), "Screening of advanced cladding materials and UN-U3Si5 fuel", *Journal of Nuclear Materials*, Vol. 462, pp. 26-42.

Brown, N.R., et al. (2014), "Neutronic performance of uranium nitride composite fuels in a PWR", *Nuclear Engineering and Design*, Vol. 275, pp. 393-407.

Brown, N.R. et al. (2013a), "Neutronic evaluation of a PWR with fully ceramic microencapsulated fuel. Part I: Lattice benchmarking, cycle length, and reactivity coefficients", *Annals of Nuclear Energy*, Vol. 62, pp. 538–547.

Brown, N.R. et al. (2013b), "Neutronic evaluation of a PWR with fully ceramic microencapsulated fuel. Part II: Nodal core calculations and preliminary study of thermal-hydraulic feedback", *Annals of Nuclear Energy*, 62, pp. 548-557.

Carmack, W.J. et al. (2006), "Inert matrix fuel neutronic, thermal-hydraulic, and transient behavior in a LWR", *Journal of Nuclear Materials*, 352, pp. 276–284.

Cozzo, C. et al. (2016), "Full core LOCA analysis for BWR/6 – Methodology and First Results", *Proceedings of Top Fuel 2016*, Boise.

Downar, T.J. et al. (2012), *PARCS v3.0 U.S. NRC Core Neutronics Simulator Theory Manual*, University of Michigan Technical Report.

Driscoll, M.J., T.J. Downar and E.E. Pilat (1990), "The linear reactivity model for nuclear fuel management", *American Nuclear Society*, La Grange Park, Illinois.

Gaston, D. et al. (2009), "MOOSE: A parallel computational framework for coupled systems of non-linear equations", *Nuclear Engineering and Design*, Vol. 239(10), pp. 1768-1778.

KAERI (2013), *DeCART2D v1.0 User's Manual*, KAERI/TR-5116/2013.

KAERI (2004), *MASTER 3.0 User's Manual*, KAERI/UM-8/2004.

LANL (2005), *MCNP-A General Monte Carlo N-Particle Transport Code*, Version 5, Los Alamos National Laboratory, LA-UR-03-1987.

Leppänen, J. et al. (2015), "The Serpent Monte Carlo code: Status, development and applications in 2013", *Annals of Nuclear Energy*, Vol. 82(SI), pp. 142-150.

Marelle, V. et al. (2016), "New developments in ALCYONE 2.0 fuel performance code", *Proceedings of Top Fuel 2016,* Boise.

Marelle, V. et al. (2011), "Thermo-mechanical modeling of PWR fuel with ALCYONE", *Proceedings of Top Fuel 2011*, 11-14 September 2011, paper T2-028, Chengdu.

Merrill, B.J., S.M. Bragg-Sitton and P.W. Humrickhouse (2017), "Modification of MELCOR for severe accident analysis of candidate accident tolerant cladding materials", *Nuclear Engineering and Design*, Vol. 315, pp. 170-178.

Merrill, B.J., S.M. Bragg-Sittona and P.W. Humrickhouse (2014), *Status Report on Advanced Cladding Modeling Work to Assess Cladding Performance Under Accident Conditions*, Idaho National Laboratory, INL/EXT-13-30206 Rev. 1.

Michel, B. et al. (2013), "Simulation of pellet-cladding interaction with the PLEIADES fuel performance software environment", *Nuclear Technology*, Vol. 182, pp. 124-137 (2013).

Michel, B. et al. (2008), "3D Fuel cracking modelling in pellet cladding mechanical interaction", *Engineering Fracture Mechanics*, Vol. 75, pp. 3581-3598.

Moal, A., V. Georgenthum and O. Marchand (2014), "SCANAIR: A transient fuel performance code, Part One: General modeling description", *Nuclear Engineering and Design*, Vol. 280, pp. 150-171.

Noirot, L. (2011), "MARGARET, a comprehensive code for the description of fission gas behaviour", *Nuclear Engineering and Design*, Vol. 241(6), pp. 2099-2118.

Ott, L.J., K.R. Robb and D. Wang (2014), "Preliminary assessment of accident-tolerant fuels on LWR performance during normal operation and under DB and BDB accident conditions", *Journal of Nuclear Materials*, Vol. 448(1-3), pp.520-533.

ORNL (2011), *SCALE: A Comprehensive Modeling and Simulation Suite for Nuclear Safety Analysis and Design*, ORNL, ORNL/TM-2005/39.

Raynaud, P.A.C. et al. (2014), "Predictions of fuel dispersal during a LOCA", *Proceedings of the 2014 Water Reactor Fuel Performance Meeting (WRFPM 2014)*, Sendai.

Smith, C. et al. (2014), *Accident Tolerant Fuel Analysis*, Idaho National Laboratory, INL/EXT-14-33200.

Suzuki, M. et al. (2013), *LWR Fuel Analysis Code FEMAXI-7; Model and Structure, JAEA-Data/Code 2013-005*, http://jolissrch-inter.tokai-sc.jaea.go.jp/pdfdata/JAEA-Data-Code-2013-005.pdf.

Todosow, M. et al. (2015), *Plan for Analyses to be Performed and the Methodology to be Used*, Brookhaven National Laboratory, FCRD-FUEL-2015-000174.

Zvonarev, Yu., I. Melnikov and A. Kireeva (2017), "Numerical analysis of accident tolerant fuel efficiency for VVER-1200", *Proceedings of 10th ISTC «Safety Assurance of NPP with VVER, OKB Gidropress»*, 16-19 May 2017, Podolsk.

8. Irradiation facilities for in-pile testing of ATF materials

Several research reactor facilities around the world are planned for use in irradiation testing of accident-tolerant fuel (ATF) cladding and fuel materials. Applicable facilities for steady-state and transient testing are summarised here. This summary is not intended to be comprehensive of all potential testing facilities, but includes those facilities that are currently operating in the Nuclear Energy Agency (NEA) member and observer countries that are a part of the Expert Group on Accident-tolerant Fuels for LWRs (EGATFL).

Advanced test reactor (ATR) (INL, United States)

The ATR at Idaho National Laboratory in the United States is a pressurised, light water moderated and cooled reactor with a beryllium reflector.[8] It provides high-neutron fluxes while being operated in a radially unbalanced condition while maintaining constant axial power (flux) profile. The serpentine fuel arrangement affords experimental versatility while ensuring maximum efficiency of core reactivity control components.

ATR is equipped with numerous test positions of various volumes. Within ATR are six pressurised water test loops with individual experiment temperature, pressure, flow and chemistry control. The ATR operates in short-duration cycles, with (generally) two to eight weeks between refuelling outages. The ATR is located at the ATR Complex on the INL site and has been operating continuously since 1967. The primary mission of this versatile facility was initially to serve the US Navy in the development and refinement of nuclear propulsion systems; however, in recent years the ATR has been used for a wider variety of government- and privately-sponsored research.

Today, the ATR remains the largest test reactor in the world with a unique serpentine fuel arrangement. The available ATR experimental space is shared by the US Department of Energy, commercial users, other nations, Nuclear Science User Facilities members (see https://nsuf.inl.gov) and the US Navy. ATR is considered the premier resource in the United States for fuels and materials irradiation testing, nuclear safety research and nuclear isotope production. General characteristics are summarised in Table 8.1, flux values are provided in Table 8.2 and primary coolant characteristics are provided in Table 8.3. The cross-sectional layout of ATR is shown in Figure 8.1.

---

8. For more information, see www4vip.inl.gov/research/advanced-test-reactor/ and the ATR User's Guide, https://nsuf.inl.gov/File/ATRUsersGuide.pdf.

Table 8.1. ATR general characteristics

Reactor	
Thermal power	250 MW$_{th}$[a]
Power density	1.0 MW/L
Maximum thermal neutron flux	1.0x10^{15} n/cm^2-sec[b]
Maximum fast flux	5.0x10^{14} n/cm^2-sec[b]
Number of flux traps	9
Number of experiment positions	62
Core	
Number of fuel assemblies	40
Active length of assemblies	1.2 m
Number of fuel plates per assembly	19
^{235}U content of an assembly[c]	1 075 g
Total core load[c]	43 kg
Coolant	
Design pressure	2.7 MPa
Design temperature	115°C
Reactor coolant	Light water
Maximum coolant flow rate	3.09 m^3/s
Coolant temperature (operating)	<52°C inlet, 71°C outlet

a) Maximum design power. ATR is seldom operated above 110 MWth. b) Parameters are based on the full 250 MWth power level and will be proportionally reduced for lower reactor power levels. c) Total ^{235}U is always less because of burn-up.

Table 8.2. Approximate peak flux values for ATR operating power of 110 MWth

Position	Diameter (cm [in])[a]	Thermal flux (n/cm^2-s)[b]	Fast flux (E>1 MeV) (n/cm^2-s)	Typical Gamma heating W/g (SS)[c]
Northeast and Northwest flux traps	13.3 [5.250]	4.4x10^{14}	2.2x10^{14}	
Other flux traps	7.62 [3.000][d]	4.4x10^{14}	9.7x10^{13}	
A-Positions				
(A-1-A-8)	1.59 [0.625]	1.9x10^{14}	1.7x10^{14}	8.8
(A-9-A-16)	1.59 [0.625]	2.0x10^{14}	2.3x10^{14}	
B-Positions				
(B-1-B-8)	2.22 [0.875]	1.2x10^{14}	8.1x10^{13}	6.4
(B-9-B-12)	3.81 [1.500]	1.1x10^{14}	1.6x10^{13}	5.5
H-Positions (14)	1.59 [0.625]	1.9x10^{14}	1.7x10^{14}	8.4
I-Positions				
Large (4)	12.7 [5.000]	1.7x10^{13}	1.3x10^{12}	0.66
Medium (16)	8.26 [3.500]	3.4x10^{13}	1.3x10^{12}	
Small (4)	3.81 [1.500]	8.4x10^{13}	3.2x10^{12}	
Outer tank positions				
ON-4	Var[e]	4.3x10^{12}	1.2x10^{11}	0.15
ON-5	Var[e]	3.8x10^{12}	1.1x10^{11}	0.18
ON-9	Var[e]	1.7x10^{12}	3.9x10^{10}	0.07
OS-5	Var[e]	3.5x10^{12}	1.0x10^{11}	0.14
OS-7	Var[e]	3.2x10^{12}	1.1x10^{11}	0.11
OS-10	Var[e]	1.3x10^{12}	3.4x10^{10}	0.05
OS-15	Var[e]	5.5x10^{11}	1.2x10^{10}	0.20
OS-20	Var[e]	2.5x10^{11}	3.5x10^9	0.01

a) Position diameter; capsule diameter must be smaller. b) Average speed 2 200 m/s. c) Configuration dependent. d) East, centre and south flux trap configurations contain seven guide tubes with inside diameters of 0.694 in. e) Variable; can be 0.875, 1.312, or 3.000 in.

Figure 8.1. ATR core layout showing irradiation positions
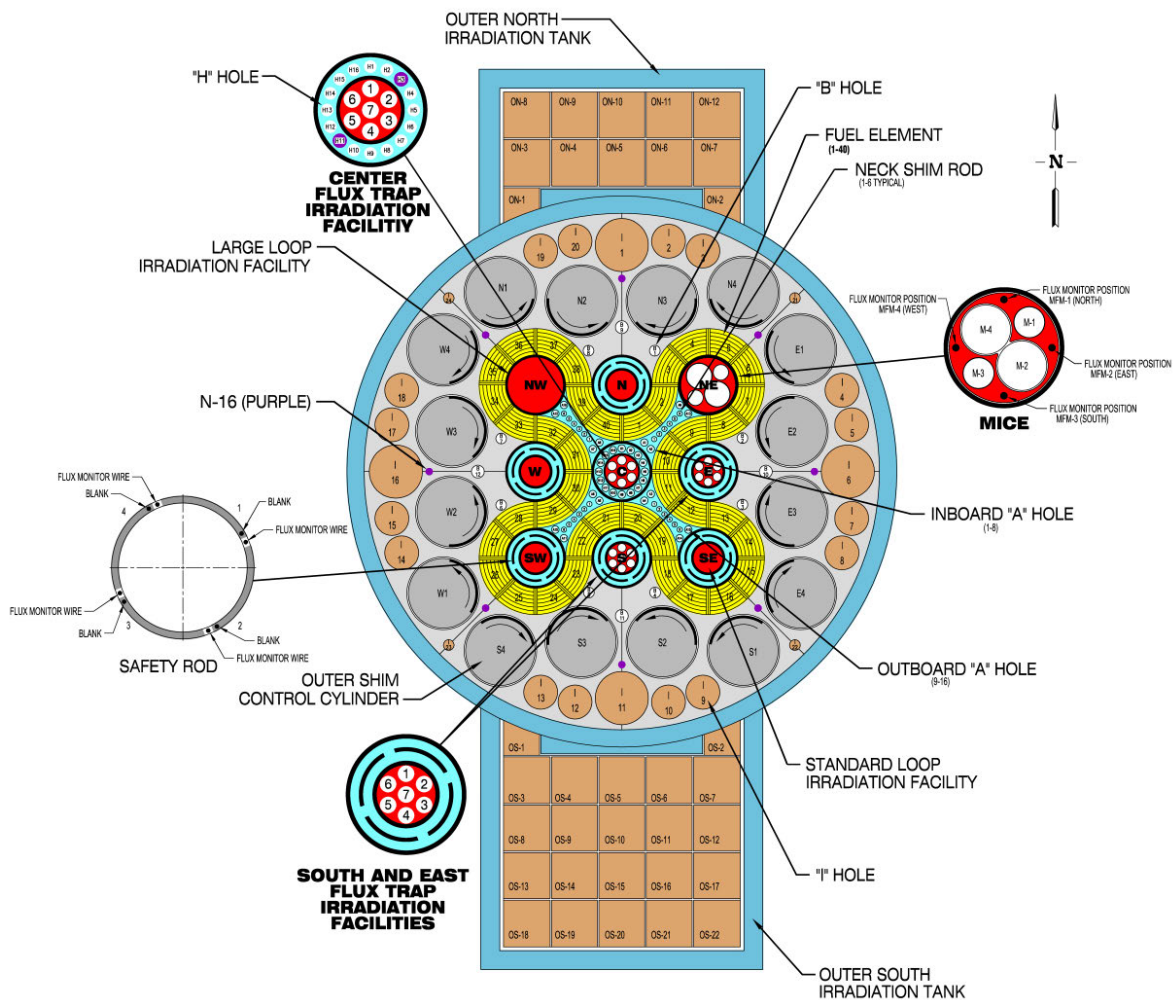
Source: INL, 2016.

Table 8.3. ATR primary coolant characteristics

	2-Pump operation	3-Pump operation
Coolant flow (m³/s [gpm])	3.26 [43 000]	3.71 [49 000]
Maximum inlet temperature (°C [°F])	51.6 [125]	51.6 [125]
Approximate temperature rise through core (°C [°F]) (varies with reactor power)	23 [41]	20 [36]
Coolant velocity through fuel assemblies (m/s [ft/s])	13.1 [43]	14.3 [47]
Minimum core inlet pressure (MPa [psig])	2.45 [355]	2.45 [355]
Pressure drop through core (MPa [psig], differential)	0.53 [77]	0.69 [100]
Primary pump flow rate (m³/s [gpm]) (each of 4 centrifugal pumps)	1.36 [18 000]	
Primary pump electric power (MW [hp]) (each of 4 pumps)	1.49 [2 000]	
Emergency pump flow rate (m³/s [gpm]) (each of 2 centrifugal pumps, one in stand-by)	0.356 [4 700]	
Heat exchanger capacity (MW [BTU/hr]) (total of 5 tube-and-shell)	241.8 [7.336 x 10⁸]	

Transient reactor test facility (TREAT) (INL, United States)

The transient reactor test facility (TREAT) at Idaho National Laboratory is currently being refurbished and is expected to resume operations in 2018.[9] Transient testing is an essential component in the development and validation of robust fuel designs and the fuel safety criteria that define their operational envelope. Transient testing involves the application of controlled, short-term bursts of intense neutrons directed towards a test specimen in order to study fuel and material performance under off-normal operational conditions and hypothetical accident scenarios. In TREAT, nuclear fuel or material test samples are placed into the reactor core centre and then subjected to quick, intense power bursts. After a transient test experiment is completed, the fuel or material is analysed at a post-irradiation examination facility utilising very high fidelity inspection equipment. A top view of the TREAT core is provided in Figure 8.2.

Figure 8.2. Top view of the TREAT core

Source: INL, https://factsheets.inl.gov/FactSheets/TransientReactorTestFacility.pdf.
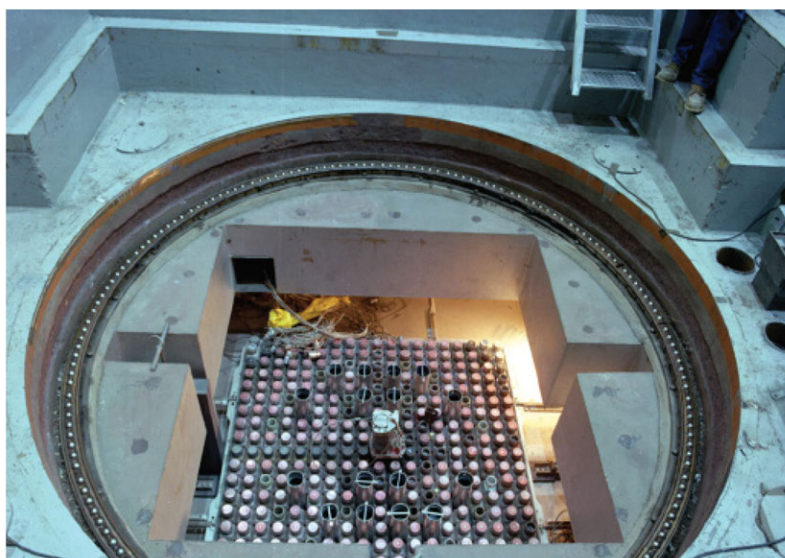
TREAT is a highly capable test reactor; its unique design offers real-time monitoring of the fuel or material's behaviour under postulated reactor accident conditions. TREAT's simple, self-limiting, air-cooled design can safely accommodate multi-pin test assemblies, enabling the study of fuel melting, metal-liquid reactions and overheated fuel and coolant interactions, as well as the transient behaviour of fuels for high-temperature (HT) system applications. It also allows for the detailed monitoring of the specimens during a test via the hodoscope, a system that detects fast neutrons and makes possible real-time evaluation of the fuel behaviour within a test sample.

TREAT's test region is flexible and can accommodate devices ranging from simple capsules for separate-effects studies through complex recirculating loops capable of simulating operating environment and accident conditions including a multi-stage LOCA simulation. The unique open core layout also enables easy access to the test region for real-time monitoring of the experiment during the test (see Figure 8.3 for examples of transients that may be applied).

---

9. For more information, see https://factsheets.inl.gov/FactSheets/TransientReactorTestFacility.pdf and https://factsheets.inl.gov/FactSheets/RTTP_Factsheet.pdf.

Figure 8.3. TREAT offers the ability to generate transients ranging from gradual power ramps through large, nearly instantaneous energy injection
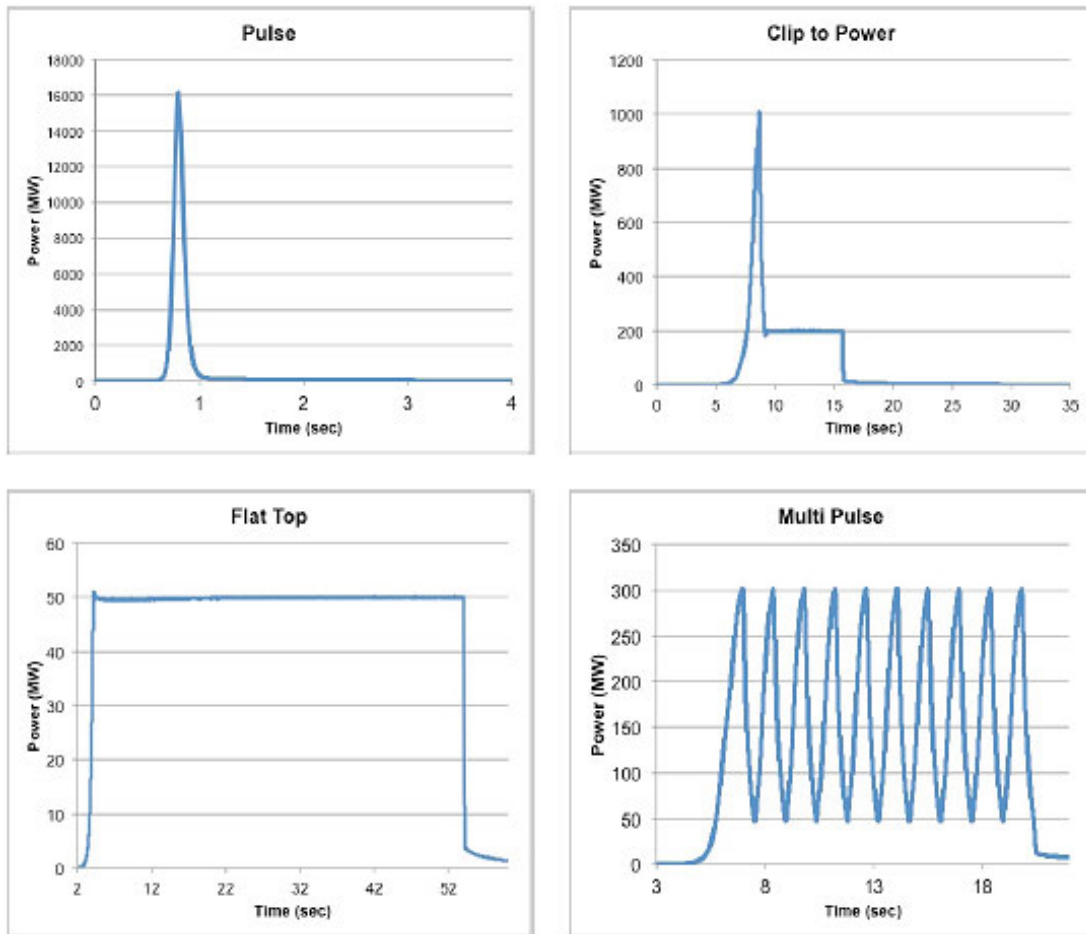
Source: J. Parry (INL), 2016.

High-flux isotope reactor (HFIR) (ORNL, United States)

The HFIR at ORNL in the United States is a beryllium-reflected, light water-cooled and -moderated, flux trap-type reactor that uses highly enriched ^{235}U as the fuel.[10] Figure 8.4 is a cutaway view of the reactor showing the pressure vessel, its location in the reactor pool and some of the experiment facilities.

The preliminary conceptual design of the reactor was based on the "flux trap" principle, in which the reactor core consists of four annular regions of fuel surrounding an unfuelled moderating region or "island" (see cross-section view). Such a configuration permits fast neutrons leaking from the fuel to be moderated in the island and thus produces a region of very high-thermal-neutron flux at the centre of the island. This reservoir of thermalised neutrons is "trapped" within the reactor, making it available for isotope production. The large flux of neutrons in the reflector outside the fuel of such a reactor may be tapped by extending empty "beam" tubes into the reflector, thus allowing neutrons to be beamed into experiments outside the reactor shielding. Finally, a variety of holes in the reflector may be provided in which to irradiate materials for later retrieval.

---

10. For more information, see https://neutrons.ornl.gov/hfir.

Figure 8.4. Cross-sections through HFIR (left) and the HFIR core (right)
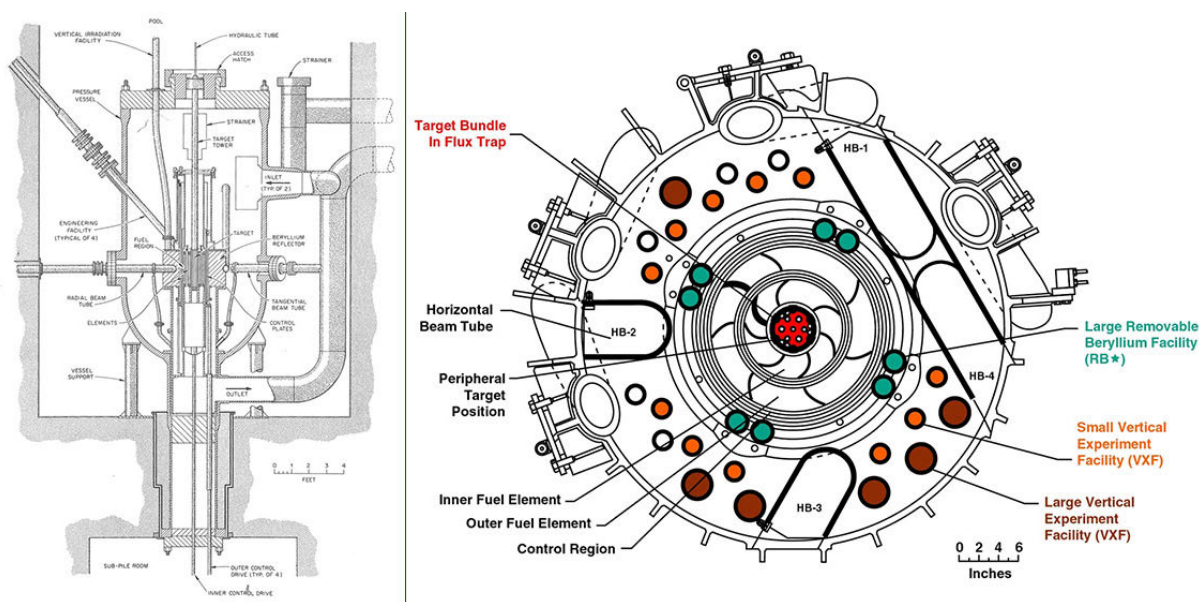
The original mission of HFIR was the production of transplutonium isotopes. However, the original designers included many other experiment facilities and several others have been added subsequently. Available experiment facilities include:

- Four horizontal beam tubes, which originate in the beryllium reflector.

- The hydraulic tube irradiation facility, located in the very high-flux region of the flux trap, which allows for insertion and removal of samples while the reactor is operating.

- Thirty target positions in the flux trap, which normally contain transplutonium production rods but can be used for the irradiation of other experiments (two of these positions can accommodate instrumented targets).

- Six peripheral target positions located at the outer edge of the flux trap.

- Numerous vertical irradiation facilities of various sizes located throughout the beryllium reflector.

- Two pneumatic tube facilities in the beryllium reflector, which allow for insertion and removal of samples while the reactor is operating for neutron activation analysis.

- Two slant access facilities, called "engineering facilities", located on the outer edge of the beryllium reflector. In addition, spent fuel assemblies are used to provide a gamma irradiation facility in the reactor pool.

The variety of in-core irradiation facilities at HFIR allows for a wide range of materials experiments and isotope production locations. Figure 8.5 shows the neutron flux values for each region.

Thirty-one target positions are provided in the flux trap (see Figure 8.6 for target positions). These positions were originally designed to be occupied by target rods used for the production of transplutonium elements; however, other experiments can be irradiated in any of these positions. A similar target capsule configuration can be used in

numerous applications. A third type of target is designed to house isotope or materials irradiation capsules that are similar to the rabbit facility capsules. The use of this type of irradiation capsule simplifies fabrication, shipping and post-irradiation processing.

Target irradiation capsules of each type must be designed such that they can be adequately cooled by the coolant flow available outside the target-rod shrouds. Excessive neutron poison loads in experiments in target positions are discouraged because of their adverse effects on both transplutonium isotope production rates and fuel cycle length. Such experiments require careful co-ordination to ensure minimal effects on adjacent experiments, fuel cycle length and neutron scattering beam brightness. Positions E3 and E6 are available for instrumented target experiments. Additional details on HFIR capabilities and experiment conditions can be found at https://neutrons.ornl.gov/hfir.

Figure 8.5. Neutron flux distributions at the core horizontal midplane with HFIR at 85 MW
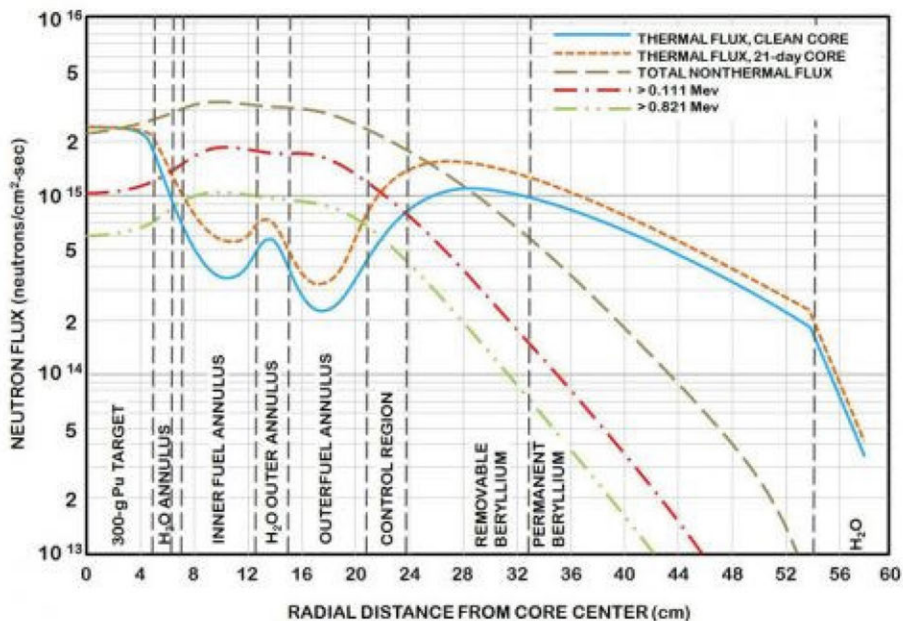
Source: ORNL, https://neutrons.ornl.gov/hfir/core-assembly, 2018.

Figure 8.6. HFIR reactor core assembly and target regions
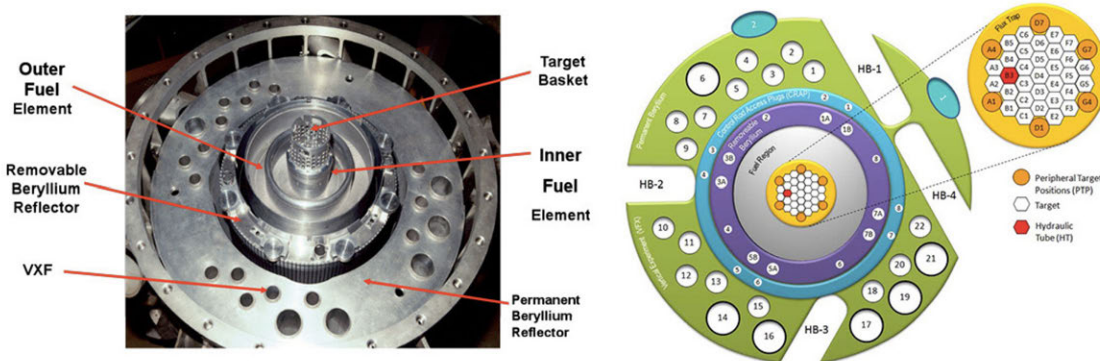
Source: McDuffee, J.L. et al., Design and Testing for a New Thermosyphon Irradiation Vehicle, 2017.

BR-2 Materials test reactor (Belgium)

The BR-2 in Belgium is a high-flux engineering test reactor that differs from comparable materials test reactors (MTRs) by its specific core array. The core is composed of hexagonal Be blocks with central channels (see Figure 8.7, left). These channels form a twisted hyperboloidal bundle and, hence, are close together at the midplane but more apart at the lower and upper ends. With this array, a high fuel density is achieved in the middle part of the vessel (reactor core with a fuelled height of 760 mm) while leaving enough space at the extremities for easy access to the channel openings.

In the BR-2 reactor, it is possible to irradiate fissile and structural materials intended for reactors of several types. For thermal reactor experiments, experimental irradiation devices were developed and used for LWRs and HT gas-cooled reactors. FR experience includes experimental irradiations for gas-cooled and liquid metal (sodium) cooled FRs. The irradiation conditions include and often focus on off-normal and transient conditions and on safety experiments.

Table 8.4 summarises the essential characteristics of the 100 different irradiation positions in BR-2 and Figure 8.7 (right) indicates a selection of neutron spectra available in the BR-2 reactor. In the same figure, an example is given of the flux spectra without (curve b) and with (curve c) cadmium screen located in the axis of a fuel element channel. The use in BR-2 of highly enriched fuel elements with high density and incorporated burnable poison allows the acceptance of a considerable amount of negative reactivity caused by strongly neutron-absorbing experiments. The current operating regime of the BR-2 reactor is based on 6 to 8 cycles of 21 to 28 days per year (i.e. approximately 120 to 180 effective full power days.

Table 8.4. Characteristic data for different irradiation positions in the reactor

Position (number of positions)	Useful diameter (mm)	Max neutron flux (n/cm²s)		Comment
		Thermal	E > 0.1 MeV	
Core region				
Within fuel elements (30-40)	17.4 to 51.6	$2.5\text{-}4\ 10^{14}$	$5\ 10^{14}$	(b)
Reflector region				
200 mm channel (1)	200	$1.0\ 10^{15}$	$2.5\ 10^{14}$	(*)
200 mm channels (4)	200	$3.5\ 10^{14}$	$8.0\ 10^{13}$	
84 mm channel (1)	29.5 to 80.6	$4.0\ 10^{14}$	$3\ 10^{14}$	
84 mm channels (2)	29.5 to 80.6	$3.5\ 10^{14}$	$1.6\ 10^{14}$	(a)
84 mm channels (20)	29.5 to 80.6	$2\text{-}3\ 10^{14}$	$<1.0\ 10^{14}$	
50 mm channels (10)	29.5 to 46	$1.5\ 10^{14}$	$3.0 10^{13}$	

The values indicated correspond to operation of BR-2 at the nominal power level of 58 MWth. The reactor power varies with its core configuration and may attain a maximum of 100-120 MW_{th}; the maximum power reached in the past was 106 MW_{th}.

(a), (b): See Figure 8.7 (right) for typical neutron spectra.

(*) For dedicated experiments, this central channel is loaded with a 200 mm driver fuel element to obtain a higher fast flux component.

Figure 8.7. Cross-section of the BR-2 core at the core midplane for a typical core configuration (left), neutron spectra for a selected number of positions (right): (a) in a reflector position; (b) inside a fuel element (c) and in a spectrum-tailored position
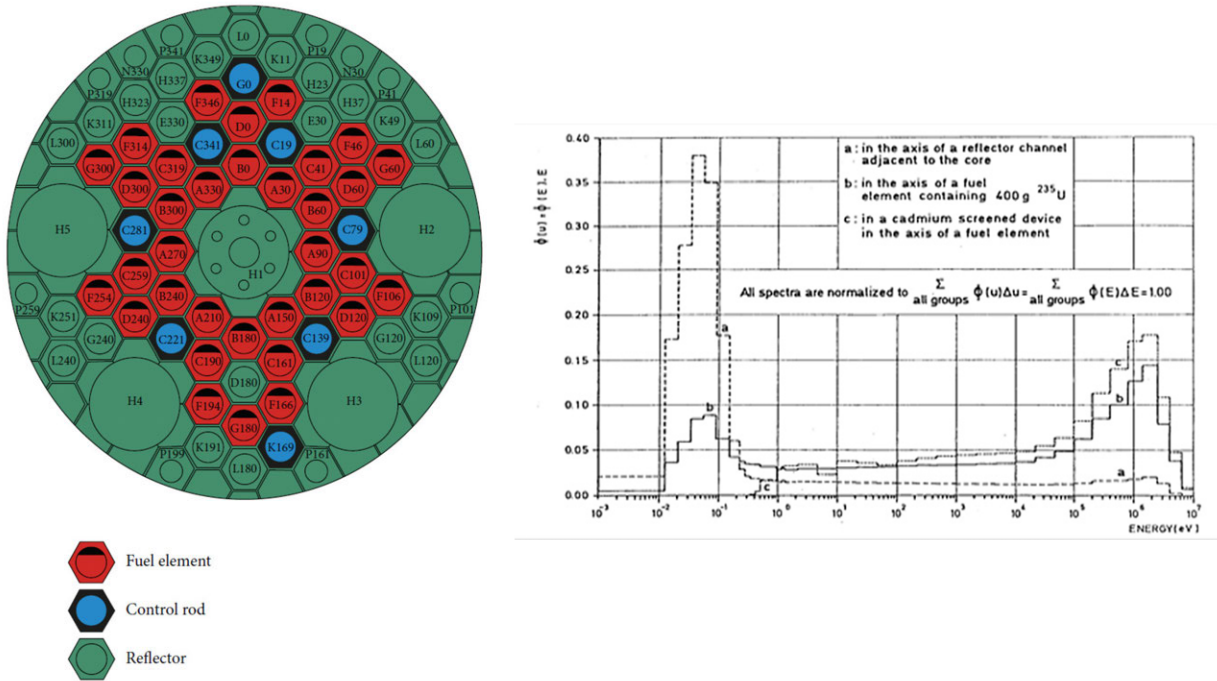
Source: SCK•CEN, 2018.

Halden Reactor Project (Norway)

The Halden BWR (HBWR)[11] is a natural circulation boiling heavy water reactor. The maximum power is 25 MW (thermal), and the water temperature is 240°C, corresponding to an operating pressure of 33.3 bar.[12] There are normally two to three main shutdowns per year, dictated primarily by the experimental programmes and a few additional cool downs for special tests. The flat reactor lid has individual penetrations for fuel assemblies, control stations and experimental equipment. A schematic drawing and the main characteristics are shown in Figure 8.8.

The Halden reactor has 11 loop systems to simulate PWR, BWR and CANDU conditions. Most irradiation experiments in the Halden reactor are heavily instrumented, allowing on-line measurements of various fuel or material properties (fission gas release, fuel swelling, fuel temperature, cladding diameter and elongation, crack growth, etc.). The Halden reactor is therefore ideally suited for studying various types of improved and ATFs. The irradiation conditions also include off-normal (such as LOCA) and transient conditions.

The Halden maximum thermal flux is 1.5 10^{14} n/cm²s and the maximum fast flux (E>0.1 MeV) is 0.8 10^{14} n/cm²s. About 1 dpa/year can be reached for materials tested in an instrumented fuel flask assembly (FFA), which is a pressure flask surrounded by booster fuel rods.

---

11. On the occasion of the IFE's Board of Directors meeting held on 27 June 2018, the Directors decided to not restart the Halden Reactor and to start the decommissioning procedure.
12. For more information, see www.ife.no/en/ife/halden/hrpfiles/halden-boiling-water-reactor.

Figure 8.8. Schematic drawing of the Halden reactor and summary of experimental positions

The Halden Boiling Water Reactor (HBWR) is a versatile tool for nuclear fuels and materials investigations:

- More than 300 positions individually accessible
- About 110 positions in central core
- About 30 positions for experimental purposes (any of 110/300)
- Height of active core 80 cm
- Usable length within moderator about 160 cm
- Experimental channel Ø:
  - 70 mm in HBWR moderator
  - 35-45 mm in pressure flask
- Loop systems for simulation of BWR/PWR conditions

Source: The Halden Reactor Project – IFE, 2018.

Cabri (France)

Cabri is an experimental pulsed reactor operated by the French Alternative Energies and Atomic Energy Commission (CEA) at the Cadarache research centre. Since 1978 the experimental programmes in Cabri have been aimed at studying the fuel behaviour under RIA conditions. The purpose of the transient tests performed as part of these programmes was to improve the safety of reactors in nominal and accidental operating situations. Since 2003, the Institut de Radioprotection et de Sûreté Nucléaire (IRSN, French TSO) has funded a complete refurbishment of the reactor together with the installation of a new experimental water loop capable of providing fully representative PWR conditions in terms of pressure, temperature and flow velocity. This new Cabri configuration is used to perform the Cabri International Programme (CIP), which gathers 14 organisations under the auspices of the NEA.

Cabri is a pool-type reactor (Hudelot et al., 2016) with a core made of 1 487 stainless steel clad fuel rods with 6% ^{235}U enrichment. The reactor is able to reach a steady-state power level of 25 MW. The reactivity is controlled via a system of 6 bundles of 23 hafnium control and safety rods (see Figure 8.9).

Figure 8.9. Cabri core
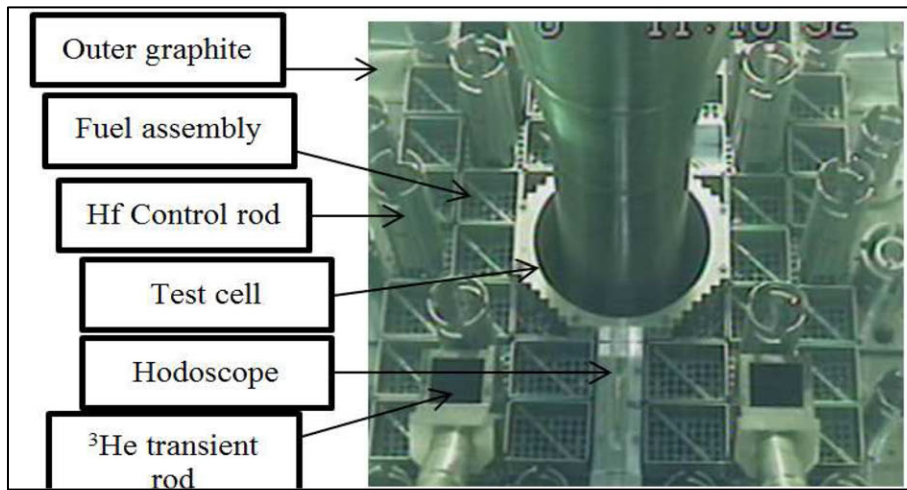

Source: IRSN, 2018.

Figure 8.10. Overall view of the Cabri facility
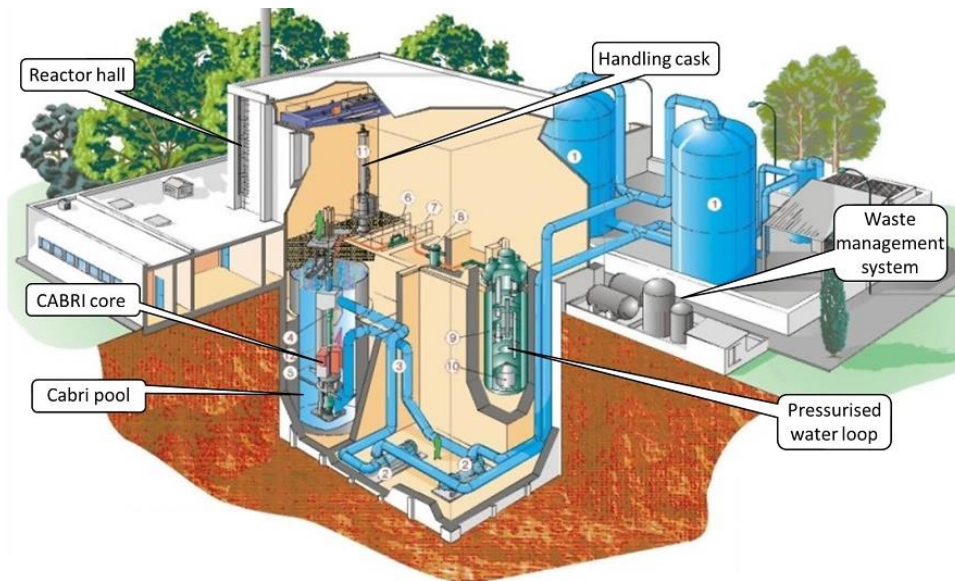
Source: IRSN, 2018.

Cabri has specific features that make it a uniquely capable advanced reactor for the transient testing of PWR fuel (Imholte and Aydogan, 2016). Those features are:

- reactivity injection system;
- pressurised water loop;
- hodoscope;
- IRIS imaging station.

The reactivity injection system

A key feature of the Cabri reactor is its reactivity injection system (Duc et al., 2014). This device allows the very fast depressurisation into a discharge tank of the ^{3}He (strong neutron absorber) previously introduced inside 96 tubes (so-called "transient rods") located among the Cabri fuel rods (see Figure 8.11).

The ^{3}He ejection leads to a reactivity injection (up to USD 4) in a short time, from a low initial power (100 kW). The transient characteristics (full width at half maximum [FWHM], energy, power) depend on the sequence applied to the two fast-opening valves:

- short FWHM (<10 ms) and high power (up to 30 GW) transients are obtained by opening a unique fast valve (high flow rate channel);

- 20 to 80 ms FWHM transients by successive and accurate opening of the two fast-opening valves.

The total energy deposit in the tested rod is adjusted by dropping the control and safety rods after the power transient.

Figure 8.11. Global view of the transient rod system (left) and of the typical Cabri ^{3}He Pressure and core power shapes during an RIA transient (right)
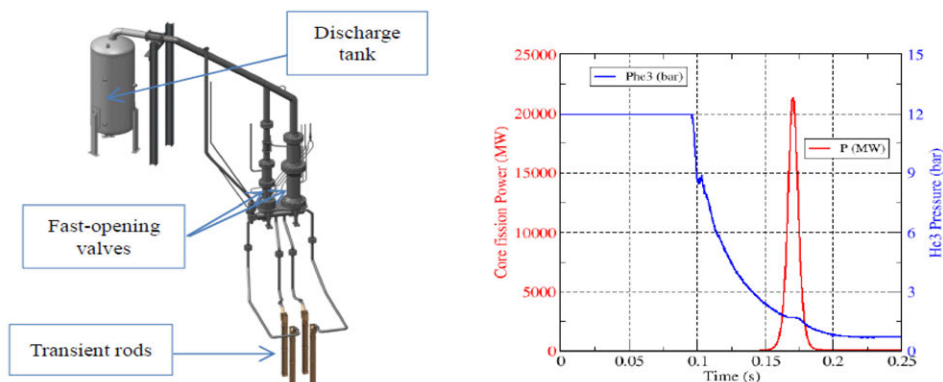
Source: IRSN, 2018.

The PWR water loop

The main function of the water loop is to ensure the typical thermal-hydraulic conditions of a PWR around the test rod (temperature of 300°C, pressure of 155 bar, velocity of 4 m/s; Bourguignon et al., 2010). It also has to remove the heat generated in the test rod, to filter the potential fuel debris issued from failure of the tested rod during the transient and to permit a safe and controlled discharge of gaseous and liquid radiological waste.

The hodoscope

The hodoscope is a multi-channel fuel motion detection system (Baumung et al., 1985) that operates in real-time during the transient. It is composed of 153 measurement channels (3 columns of 51 rows), each one being equipped with a fission chamber and a proton recoil counter. The 306 measurement signals issued may be monitored at a data acquisition rate up to 1 kHz. It is used for measuring the axial length of the test rod fissile column (hence its transitory and residual elongation), the axial power profile of the test rod, and the fuel movements (ejection, relocation). The hodoscope sensors detect fast neutrons emerging from the test rod and having passed along the 3 m-long channels of a massive steel collimator, motorised both in rotation and in verticality, which penetrates the core pool tank (see Figure 8.12).

Figure 8.12. Cross-section of the hodoscope
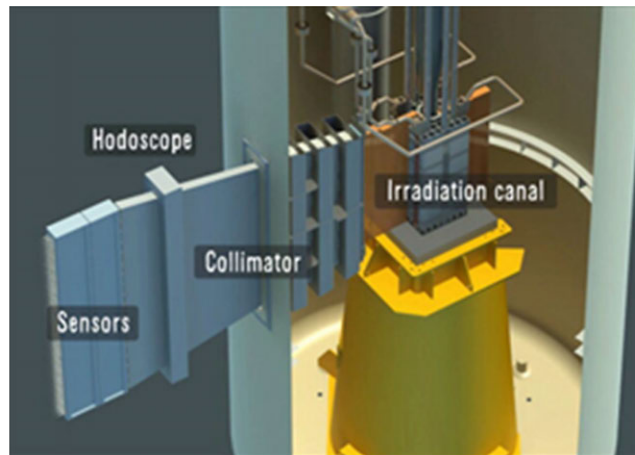
Source: IRSN, 2018.

The IRIS imaging station

IRIS is a non-destructive examination bench located inside the Cabri reactor building. It accommodates the test device vertically, such that it can be rotated or moved along a vertical translation, so as to scroll in front of two examination lines-of-sight.

The first line-of-sight is dedicated to gamma spectrometry. Gamma rays issued from the test rod are collimated through a 1 mm high slit to a low-efficiency hyper-pure Ge detector. The energy resolution is 1 keV at 121 keV and 1.7 keV at 1 408 keV. Scrolling the test device allows a quantitative gamma-scanning to be performed at an axial step of up to 1 mm.

The second line-of-sight is devoted to X-ray imaging. X-rays are generated using a linear electron accelerator, collimated through a 2 mm high slit and detected by a linear digital camera after being attenuated by the test device. The X-ray beam may be generated in a pulse mode (up to a 300 Hz frequency) with a maximum energy of 8 MeV and a mean energy of 2.5 MeV. Radiographs are acquired by translating the test device step by step. Steps of 100 μm may be performed. Tomographic images are acquired by rotating the test device step by step. 960 steps of 0.4° are performed. Examples of measurements carried out on dummy lead pellets are presented in Figure 8.13.

**Figure 8.13. Examples of IRIS calibrated pellets X-ray measurement
radiography (left) and tomography (right)**
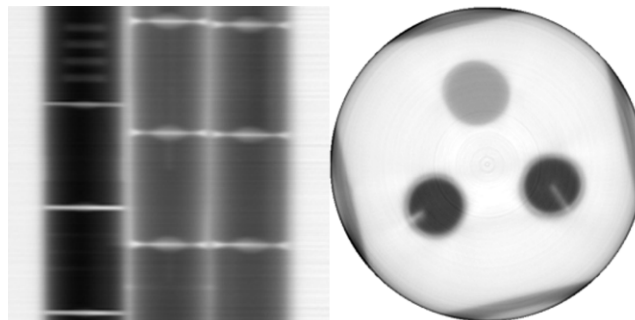
Source: IRSN, 2018.

Jules Horowitz (France)

The JHR is a materials test reactor under construction at the CEA Cadarache research centre. It is based on a 100 MWth pool reactor compact core cooled by a slightly pressurised primary circuit (about 10 bars). The core tank is located in the reactor pool. The fissile length is 60 cm, and the core diameter is 70 cm.

JHR will be a powerful reactor with numerous irradiation sites and irradiation conditions. The reactor design provides numerous irradiation locations. Locations situated inside the reactor core have the highest ageing rate, while locations situated in the beryllium reflector zone surrounding the reactor have the highest thermal flux (see Figure 8.14).

Numerous locations are implemented (up to 20 simultaneous experiments) with a large range of irradiation conditions (see Figure 8.15):

- seven in-core locations of small diameter (32 mm);

- three in-core locations of large diameter (80 mm – E103/211/301);

- ten fixed positions (100 mm of diameter and one location with 200 mm);

- six positions located on displacement devices located in water channels through the beryllium reflector. In the present configuration, a reflector block with two displacement devices is adapted and dedicated to molybdenum production (see Figure 8.14).

A typical reactor cycle is expected to last 25 days and CEA targets to operate the reactor 10 cycles per year.

The perturbed flux values at the core midplane (100 MW; 27% ^{235}U), i.e. calculated in the samples (stainless steel tubes), are given in Table 8.5. The fast neutron flux in the central part of the core allows experiments to reach about 16 dpa/y (in graphite). Regarding the locations in the reflector area, the perturbed flux values at the core midplane (100 MW; 27% ^{235}U), i.e. calculated in the samples (UO$_2$ fuel rod, 1 % of ^{235}U), are provided in Table 8.6. Examples of the neutron spectra are provided in Figures 8.16 and 8.17.

Figure 8.14. JHR experiment locations
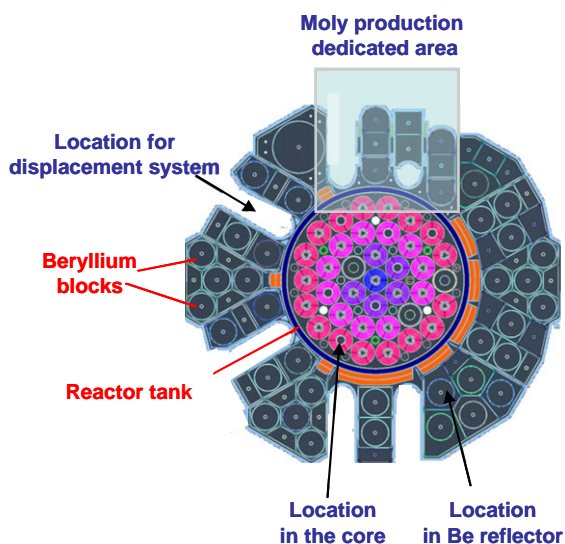
Source: www-rjh.cea.fr/_pdf/2014_%20EHPG_CEA%20Cadarache_SRJH%20paper.pdf – presented at the 38th Enlarged Halden Group Meeting – 2014 Røros, Norway, 7-12 September, 2014 – Fuel and Material Irradiation Hosting Systems in Jules Horowitz Reactor.

**Figure 8.15. Identification number of the experiment locations
in the JHR core and reflector**
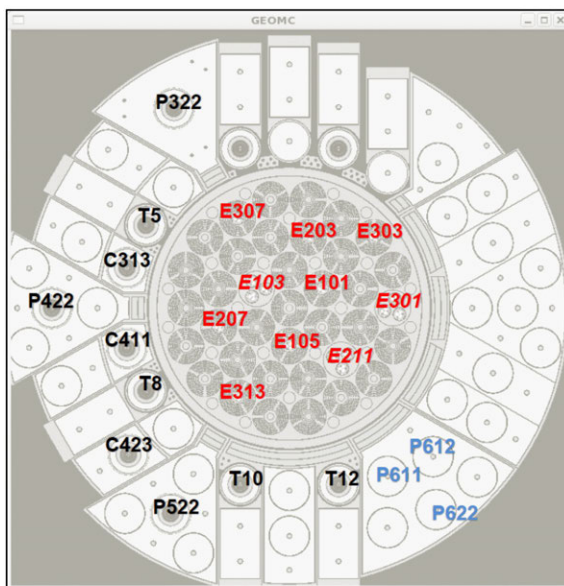
Source: CEA – partially presented at several events – www-rjh.cea.fr.

Table 8.5. Perturbed flux values at core midplane

Location	Thermal Flux – E < 0.625 eV (1.E14 n/cm².s) Value in stainless steel	Fast Flux – E > 0.907 MeV (1.E14 n/cm².s) Value in stainless steel	Nuclear heating (W/g) Value in aluminium
E101/105	3.01/3.03	5.01/5.14	21/20
E203/207	2.46/2.26	4.58/4.26	15/13
E303/307/313	1.57/1.83/1.79	3.27/3.48/3.68	11/10/11
E103	2.98	3.53	13
E211	2.46	3.05	11
E301	2.13	2.08	8

Table 8.6. Perturbed flux values in the reflector region

Location	Thermal Flux – E < 0.625 eV (1.E14 n/cm².s) Value in UO$_2$ fuel rod, 1 % of ^{235}U	Fast Flux – E > 0.907 MeV (1.E14 n/cm².s) Value in UO$_2$ fuel rod, 1 % of ^{235}U
P322	0.56	0.06
T5	2.56	0.49
C313	2.31	0.42
P422	0.39	0.04
C411	2.42	0.46
T8	2.73	0.52
C423	0.73	0.09
P522	0.45	0.05
T10	2.00	0.32
T12	1.91	0.31

Figure 8.16. JHR neutron flux
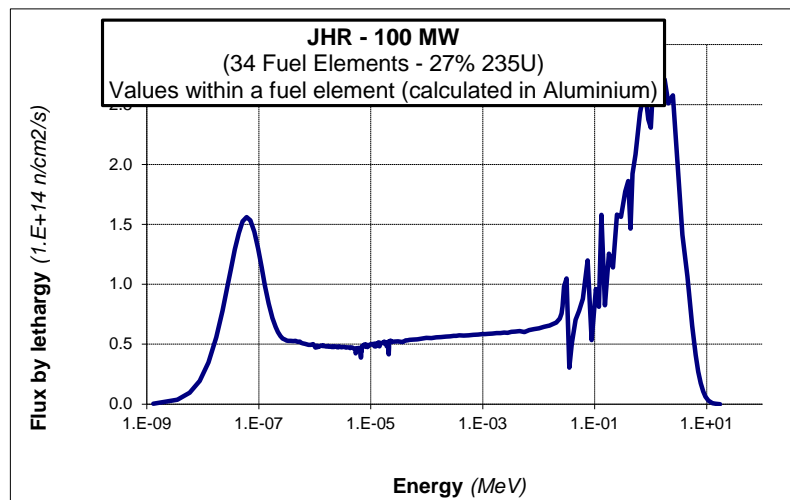
Source: CEA, 2018.

Figure 8.17. Example of neutron spectrum in the JHR core
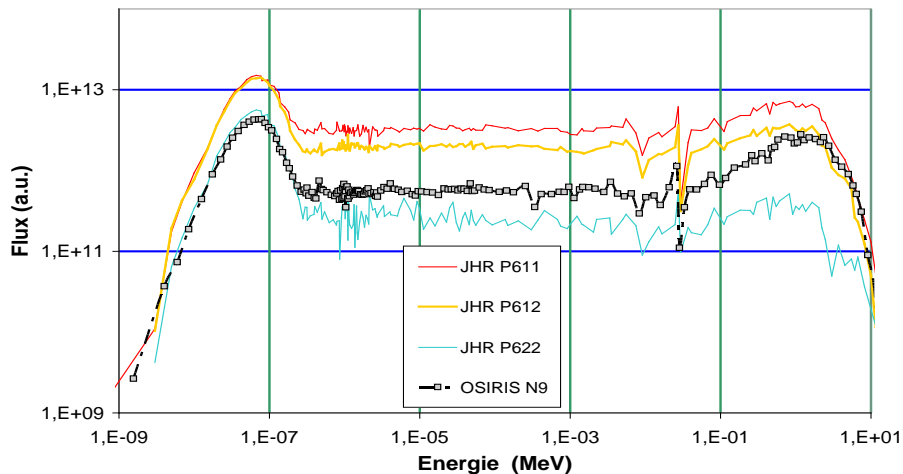
Source: CEA, 2018.

A set of test devices is currently under development for JHR. In order to meet the large range of experimental needs from the nuclear industry, CEA is developing a set of test devices that will be operational for the start-up of the reactor or a few years later. These experiment hosting systems will have to fulfil most experimental needs, particularly those concerning LWR technologies (PWR, BWR and VVER reactor technologies). The three first complementary fuel LWR experimental devices (located on displacement devices) are:

- the MADISON loop (Multi-rod Adaptable Device for Irradiation of experimental fuel Samples Operating in Normal conditions), which will allow testing the behaviour of several experimental fuel rods under normal operating conditions of power plants (no clad failure expected);

- the ADELINE loop (Advanced Device for Experimenting up to Limits Irradiated Nuclear fuel Elements), which will allow testing a single experimental rod up to its operating limits and during some incidental sequences;

- the LORELEI loop (Light water, One Rod Equipment for LOCA Experimental Investigations), which will allow testing a single rod under accidental situations that may lead to significant fuel damages.

Other test devices will allow determination of mechanical properties under irradiation for LWR materials (e.g. cladding materials, internal structures and pressure vessel steels). Some devices include: CALIPSO, MICA and OCCITANE are under development. The CLOE (Corrosion LOop Experiments) loop will allow researchers to understand corrosion mechanisms.

Nuclear Safety Research Reactor (NSRR, Japan)

The NSRR is a TRIGA® (Training, Research, Isotopes, General Atomics) reactor design. Located at the JAEA in Tokai, Japan (JAEA, Tokai), NSRR is the exclusive reactor for nuclear fuel safety research in Japan. Since its first criticality in June 1975, more than 3 000 pulse operations and more than 1 000 fuel irradiation experiments have been conducted. Modification of the experimental facilities in 1989 greatly improved the NSRR operational and experimental capabilities.

An RIA can be simulated by a pulse irradiation in the NSRR. The pulse operation is done by a quick withdrawal of three transient control rods, actuated by pressurised air. Because of the strong negative thermal feedback of TRIGA® fuel (uranium-zirconium-hydride fuel), the reactor power rapidly decreases after the quick withdrawal of the transient rods and an RIA-simulating power pulse can be produced safely.

Specifications of the NSRR are summarised in Table 8.7 and schematic illustrations of the NSRR are presented in Figure 8.18 (JAEA, 2017). To conduct a fuel irradiation experiment in NSRR, an experimental capsule containing the test fuel rod is loaded into the experimental cavity located at the centre of the reactor core. Schematic illustrations of experiment capsules used for the NSRR experiment are shown in Figure 8.18(c).

In the NSRR, pulse irradiation experiments have been conducted with both fresh fuels and fuels irradiated in commercial reactors. In the case of the experiment on irradiated fuel, the test rod is prepared in hot cells of the Reactor Fuel Examination Facility (RFEF) in JAEA, Tokai from a full-length fuel rod retrieved from a fuel assembly irradiated in a commercial reactor. The test fuel rod is transported to the NSRR and loaded into an experimental capsule after the necessary instruments are attached onto the test fuel rod in the NSRR hot cell. After the pulse irradiation, the test fuel rod is transported to the RFEF and post-test examinations are conducted.

Table 8.7. Specifications of the NSRR

Reactor core	
Effective height	~38 cm
Equivalent diameter	~63 cm
Moderator	Zirconium hydride and light water
Fuel rods	
Fuel	Uranium-zirconium-hydride
Enrichment	<20%
Cladding	Stainless steel (SUS 304)
Dimensions	3.75 cm diameter, 65 cm length
Number of rods in the core	157
Maximum inserted reactivity	USD 4.7
Maximum reactor power	23 GW
Maximum integrated power	130 MW·s

Figure 8.18. Schematic illustrations of the NSRR

(a) Vertical cross-section

(b) Horizontal cross-section

(c) Experimental capsule
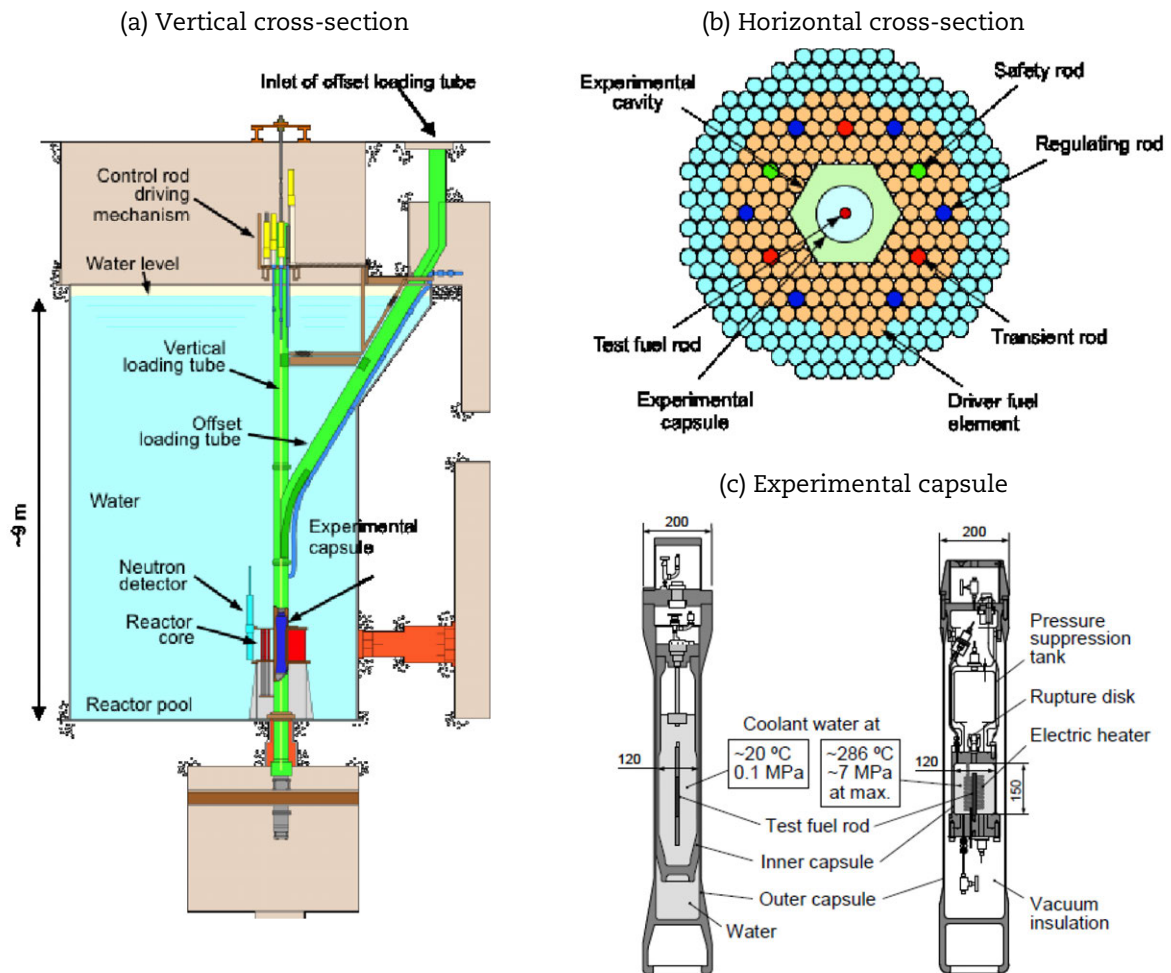
Source: a) and b) JAEA, 2017; c) Amaya et al., 2015.

HANARO (Korea)

The High-flux Advanced Neutron Application Reactor (HANARO) is a unique research reactor in Korea, which has been used for a material irradiation testing, radioactive isotopes and NTD (neutron transmutation doping) silicon production, neutron activation analysis and basic structural research for materials using a neutron beam. HANARO uses rod-type LEU silicide fuel and its active length is 700 mm. The heavy water in the zircaloy-4 tank is used as a reflector. Irradiation holes shown in Figure 8.19, such as CT, IRs, ORs and IPs, can be used for the material irradiation testing. The CT and IRs are hexagonal flux traps located in the core and the ORs and IPs are circular flux traps located in the reflector region outside the core as shown in Figure 8.19. Table 8.8 shows specifications of the irradiation holes in HANARO. The material specimen temperature can be controlled during irradiation by adjusting the system atmosphere and heater power. The fission power of the specimen is also adjusted by application of a hafnium or stainless steel shroud. The maximum neutron dose rate of the specimen is more than 0.4 dpa per cycle. HANARO is generally operated for seven cycles per year.

Figure 8.19. Cross-sectional schematic diagram of HANARO
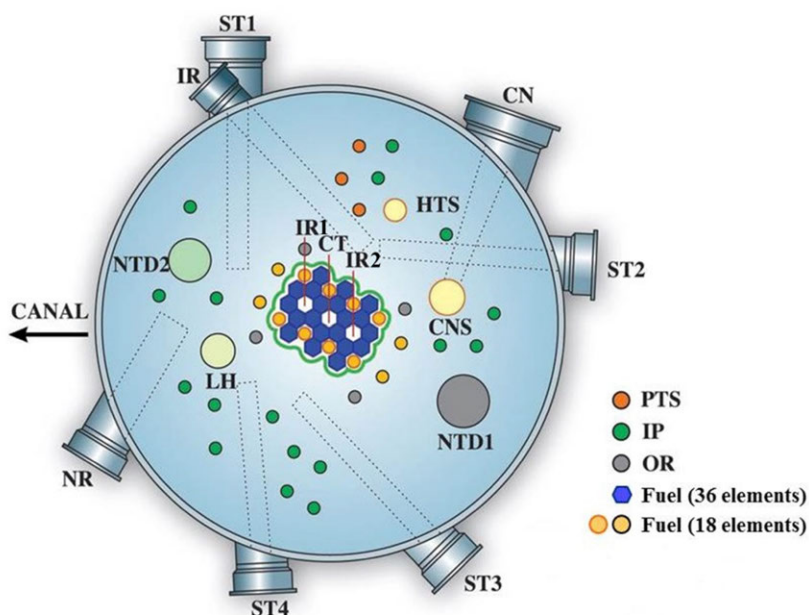
Source: KAERI, 2018.

Table 8.8. Specifications of the irradiation holes in HANARO

Hole		Inside Dia (cm)	Neutron flux (n/cm²·sec)	
Name	No.		Fast neutron (E>1.0 Mev)	Thermal neutron (<0.625 ev)
CT		7.44	1.54 x 1 014	4.39 x 1 014
IR		7.44	1.50 x 1 014	3.93 x 1 014
OR		6.0	2.07 x 1 013	3.36 x 1 014
IP		6.0	1.45 x 109 ˜ 2.20.x 1 012	2.40 x 1 013 ˜ 1.95 x 1 014

HANARO has contributed to the research and development of nuclear systems via material irradiation testing. Figure 8.20 shows the irradiated specimens at HANARO. The candidate core materials of the research reactor were irradiated for the production of the licensing database. The irradiation testing of coated particle fuel and metallic fuel were conducted to support the development of generation IV nuclear systems. The in-core performance of fuel and cladding material for a commercial reactor were also studied by irradiation testing in order to further enhance safety. The irradiation of materials for fusion systems and instrumentations is also planned.

**Figure 8.20. Irradiated specimens at HANARO: (a) plate-type fuel,
(b) coated particle fuel, (c) UO₂ fuel, (d) metallic fuel, (e) zirconium alloy**
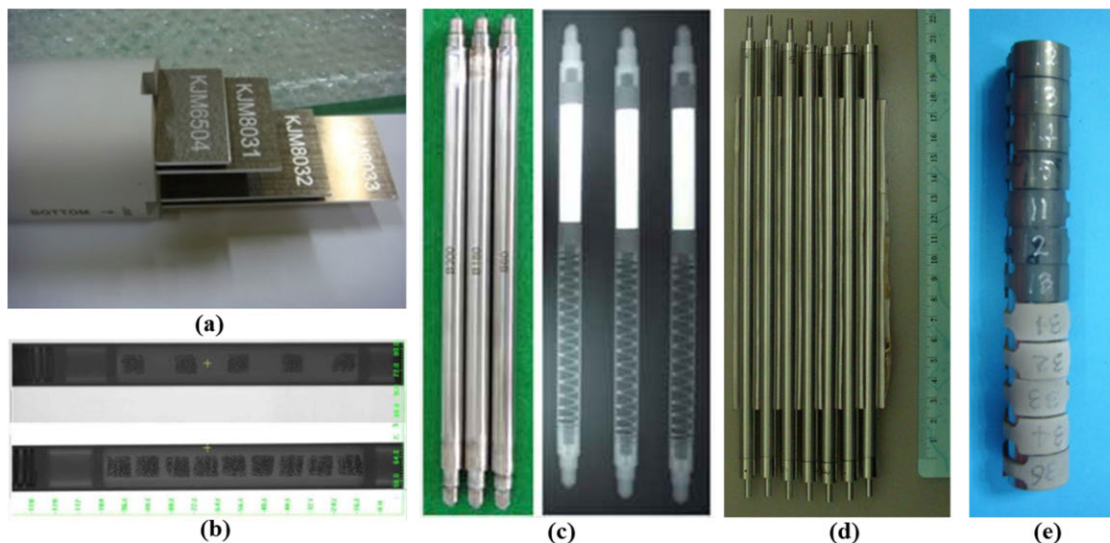
Source: KAERI, 2018.

HFR materials test reactor (the Netherlands)

The HFR Petten, located in the Netherlands, is a 45 MW$_{th}$ high-flux materials test reactor with a flexible square grid core layout (see Figure 8.21). The reactor is used for the production of ^{99}Mo and other medical and industrial isotopes, as well as for instrumented fuel and materials irradiations. More than 100 material and fuel tests have been performed in the past 15 years, including, for example, graphite qualification for long-term operation (LTO), ramp tests, irradiation creep tests, fuel qualification for HT reactors, FR fuel and functional materials for fusion.

The HFR is fuelled by aluminium-clad LEU silicide plates. Each position on the square grid is occupied by a fuel element, control rod, beryllium reflector element or one or more isotope targets or sample holders for material tests. The core is an under-moderated system. High-flux in-core positions (to the left within the core in Figure 8.21) possess a hard neutron spectrum suitable for material tests. Towards the right within the core in Figure 8.21 the thermal flux gradually decreases to values appropriate for LWR fuel. The stable and constant flux profile in each irradiation position allows for reliable and accurate control of experiment parameters (sample temperature, pressure, damage rate, power density) and is a unique HFR feature.

In addition to 17 in-core positions, the HFR has a poolside facility (PSF) with 12 experiment positions. PSF experiments can be moved to and from the reactor core using a trolley system. This allows for reliable and accurate ramp testing and power cycling, including high burn-up ramps beyond failure, without significantly affecting other operations in the HFR core.

The current operating regime is based on nine cycles of 31 days per year (i.e. approximately 280 effective full power days per year).

Figure 8.21. Schematic of the HFR core with indications of damage build up for materials and linear heat rate for fresh LWR fuel

| 0-3, location dependent | 5-8 | 3-5 | 1-3 | Material DPA rate (DPA/year) |
| 0-700, displacement controlled | n/a | 500-700 | 300-400 | Linear heat rate (W/cm fresh LWR fuel) |
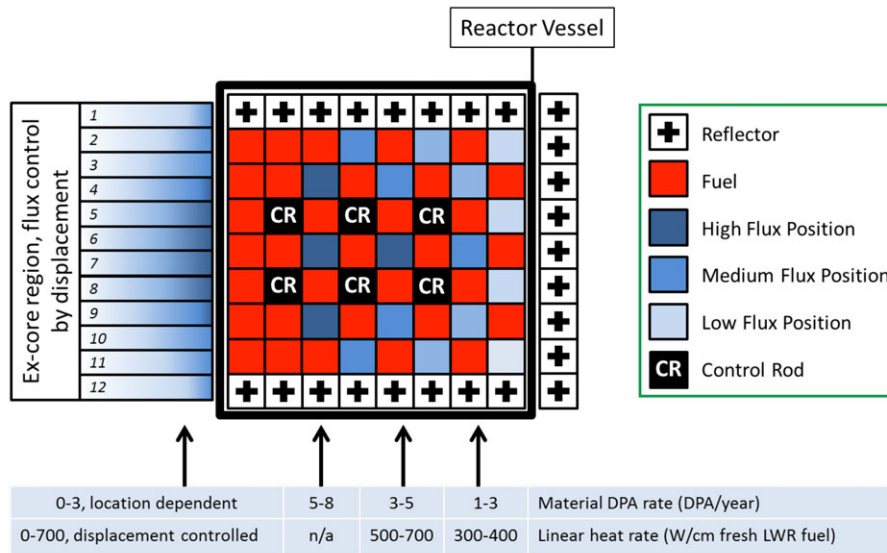
The poolside facility (to the left) allows for power ramp and power cycling operations.

Source: de Groot, 2014.

LVR-15 research reactor (Czech Republic)

The LVR-15 research reactor is a 10 MW multipurpose reactor utilised for basic and applied material research, isotope transmutation and production of medical and technical isotopes operated by CV Rez in the Czech Republic. LVR-15 is a light water tank-type research reactor placed in a stainless steel vessel under a shielding cover. Demineralised water is used as a moderator and an absorber. A reflector is composed of a water or beryllium block, depending on the operational configuration. The reactor core lattice has pitch of 71.5 mm and 80 cells. In the basic operation configuration, 28-32 cells contain fuel elements and 2-4 locations among the fuel cells are dedicated to channels for experimental devices. The fuel IRT-4M with uranium enrichment 19.75 % is used. The reactor is operated in 21-day irradiation cycles, with 9-10 cycles per year (i.e. approximately 200 effective full power days). LVT-15 operating parameters are summarised in Table 8.9.

Applied materials research is dedicated to material testing in a well-defined environment with parameters (temperature, pressure, coolant) as similar to fission and fusion reactors as possible with the presence of neutron and gamma radiation. The material testing can be performed either in loops with forced coolant media flow or in irradiation rigs with inner atmosphere. The variability of available neutron spectra is presented within Figure 8.22(b).

Fuel cladding corrosion testing and coolant chemistry studies related to the behaviour of activated corrosion products have been performed in the LVR, with 15 conducted in the PWR and VVER loops. The studies involved electrically heated cladding segments in the loop simulating the primary circuit exposed to the conditions defined by the research goals – e.g. pH effect, Zn addition, Crud formation, etc. Hot cells for loop and rig dismantling and basic PIE (visuals, dimension measurements) are available at the reactor. A new hot cell complex for detailed material analysis (mechanical testing, eddy current testing, LOM, SEM, nanoindentation, sample preparation, etc.) is being commissioned. For ATF cladding, the LVR-15 is unique in its ability to perform qualification experiments in simulated VVER conditions (chemistry and materials of the primary circuit).

In addition to the LWR cladding and corrosion studies, LVR-15 provides irradiation experiments focused on material behaviour research and the influence of radiation and chemical parameters (e.g. reactor pressure vessel studies, stress corrosion cracking studies). Several neutron beam tubes are used for basic research as well as neutron radiography.

Table 8.9. LVR-15 operation parameters

Parameter	Value
Moderator	Demineralised water
Reflector	Beryllium
Maximal thermal power	10 MW
Maximal thermal neutron flux	1.5×10^{14} n×cm^{-2}s^{-1}
Pressure	Atmospheric
Average moderator temperature	45°C

Figure 8.22. LVR-15 (a) reactor cross-section and (b) available neutron spectra
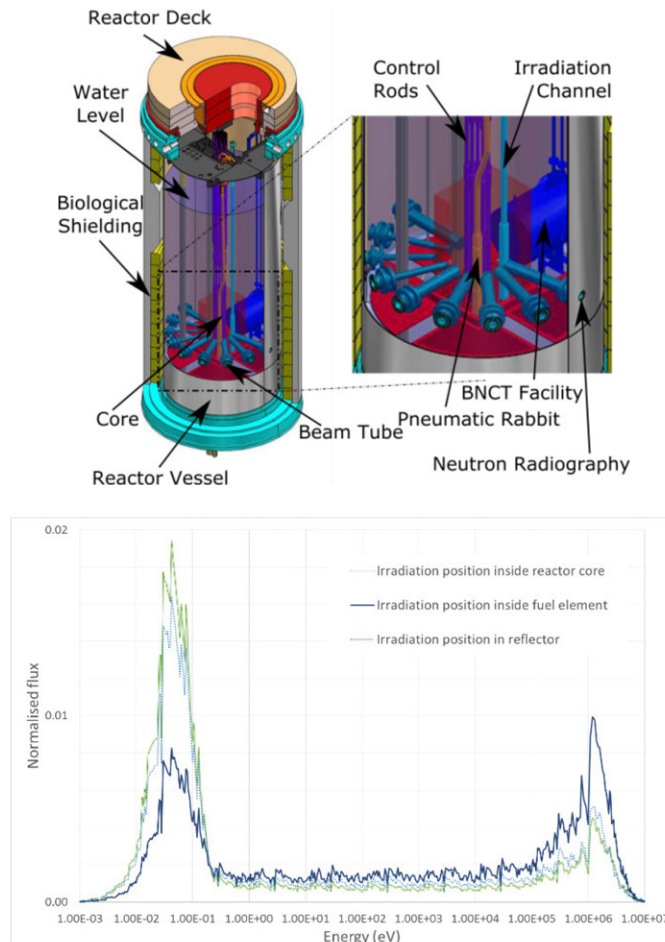
Source: a) reactor cross-section in *Measurement of Neutron Spectra in a Silicon Filtered Neutron Beam Using Stilbene Detectors at the LVR-15 Research Reactor; Applied Radiation and Isotopes*; https://doi.org/10.1016/j.apradiso.2017.06.026 and

b) available neutron spectra - [Internal document of Research Center Rez, not published]

Figure 8.23. LVR-15 (a) core and (b) fuel element cross-section

a   b

The China Mianyang research reactor (CMRR, China)

The CMRR (see Figure 8.24) is operated by the Institute of Nuclear Physics and Chemistry in the China Academy of Engineering Physics, located in Mianyang City, Sichuan Province. It is a multifunctional pool-type research reactor and has a liquid hydrogen cold neutron source.

Figure 8.24. Photograph of CMRR

Source: Wang, 2016.

Six neutron scattering instruments and two neutron radiography stations have been installed, including a high-resolution neutron diffractometer, residual stress neutron diffractometer, high-pressure neutron diffractometer, small-angle neutron spectrometer, time-of-flight and polarised neutron reflectometer, cold neutron triple-axis spectrometer thermal neutron radiography and cold neutron radiography.

The CMRR is able to reach a power level of 20 MW. The core is made of 6 061 aluminium alloy clad and fuel plates are comprised of U_3Si_2 particles dispersed in an aluminium matrix. The reactivity is controlled via a system of hafnium control and safety rods.

The reactor provides more than six irradiation locations inside the reactor core, with the highest fast flux of >2.8×10^{14} n/cm^{2}s. Additional irradiation locations are located in the heavy water reflector case surrounding the core, with the highest thermal flux >1.5×10^{14} n/cm^{2}s. The diameters of irradiation positions range from 50 mm to 120 mm.

The CMRR normally operates more than 150 days per year. In order to meet the experimental needs, a water loop with high temperature and high pressure will be developed in the very near future.

References

Amaya, M. et al. (2015), "Behavior of high burnup advanced fuels for LWR during design basis accidents", *Proceedings of Top Fuel 2015*, Zurich, 13-17 September 2015, pp.10-18.

Bauming, K. et al. (1985), "The Cabri fast neutron hodoscope", *Nuclear Technology*, volume 71.

Bourgignon, D. et al. (2010), "Design and construction of a zircaloy pressure vessel for the research reactor Cabri", *Proc. IGORR 13th Meeting,* Knoxville, Tennessee.

Duc, B. et al. (2014), "Renovation, improvement and experimental validation of the helium-3 transient rods system for the reactivity injection in the Cabri reactor", *International Group On Research Reactors*, 17-21 November 2014, Bariloche.

Hudelot, J.-P. et al. (2016), "Cabri Facility: Upgrade, refurbishment, recommissioning and experimental capacities", *Proceedings of PHYSOR 2016*, *American Nuclear Society*, 1-5 May 2016, ISBN:978-1-5108-2573-4, pp. 2286-2298, Sun Valley, Idaho.

Imholte, D. and F. Aydogan (2016), "Comparison of nuclear pulse reactor facilities with reactivity-initiated-accident testing capability", *Progress in Nuclear Energy*, Volume 91.

JAEA (2017), Nuclear Safety Research Reactor (NSRR) website, www.jaea.go.jp/english/04/ntokai/kasokuki/kasokuki_03.html, accessed 15 June 2017.

Wang, X. (2016), "Research progress in the field of advanced fuel system at CAEP", *ATF Workshop*, 23-24 June 2016, Shenzhen, China.

Part II: Cladding and core materials

9. Introduction

Within the Expert Group on Accident-tolerant Fuels for LWRs, the Task Force devoted to cladding and core materials gathered many contributors from different organisations (academia, national laboratories, fuel suppliers, regulators, experimental facilities, nuclear operators) spanning a broad variety of designs with very different characteristics.

Five different classes of cladding designs were the object of the review by this Task Force: coated and improved Zr-alloys, advanced steels, refractory metals, SiC and SiC/SiC-composite claddings and non-fuel components such as SiC/SiC channel boxes or accident-tolerant control rods (ATCR).

It became quickly obvious that depending on each contributors' background and the type of design they were more familiar with, their knowledge could be at the same time very valuable and very specific.

Thus, the main objective of the Task Force was to ensure a satisfying level of compilation of that knowledge without losing information in that process.

The work was organised in several steps:

- define an attribute guide as exhaustive as possible and covering the following fields already defined in (Bragg-Sitton et al., 2014): fabrication/manufacturability, normal operation and AOOs, design basis accidents, design extension conditions, fuel cycle-related issues (such as used fuel storage, transport, disposal, reprocessing);

- fill the attribute guide spreadsheet for each specific candidate design (not necessarily filling all the attributes) with a colour code added to explicit written comments and illustrating in a very visual way: challenging or not challenging lack of data, potential showstoppers, need for further optimisation, or demonstrated maturity for each single attribute; a selection of the filled attribute guides is shown in Appendix A;

- for each specific design, the key highlights are described relying, when available, on the filled attribute guide spreadsheet; 21 key highlights have been provided through that process by the contributing organisations shown in the following table:

Cladding designs				Core components	
SiC and SiC/SiC composites	Coated and improved Zr-alloys	Advanced steels	Refractory metals	SiC/SiC channel boxes	ATCR
KAERI	UIUC	ORNL	EPRI	Toshiba	CRIEPI
Muroran	FJP (*)	GE	CGN	EPRI	AREVA
FJP (*)	KAERI	NFD			
KIT	IFE				
ORNL	KIT				
PSI					
Westinghouse					

(*) French Joint Programme (CEA-AREVA-EDF).

- for each type of design, all the available information is summarised in the devoted chapter shown in this report.

That gradual process has been a rewarding one, enabling the Task Force to focus on a converged and structured way on the different designs.

The five subsequent chapters aim to present the most relevant summarised information on the covered designs, with more detail available in the Appendices with the attribute guides.

Reference

Bragg-Sitton, S. et al. (2014), "Advanced Fuels Campaign: Enhanced LWR Accident Tolerance Fuel Performance Metrics", Prepared for US Department Of Energy Advanced Fuel Campaign, February 2014, INL/EXT-13-29957, FCRD-FUEL-2013-000264.

10. Coated and improved Zr-alloys

Enhanced ATF concepts should either reduce fuel temperature and fission gas release (FGR) during normal operation by improved heat transport properties of the fuel or mitigate rapid waterside oxidation of the cladding during high-temperature transients in steam and/or steam/air mixture (Bragg-Sitton, 2014). In addition, ATF concepts should feature equivalent or superior performance during normal light water reactor (LWR) operational states compared to the UO_2/Zr-based alloys currently used in the worldwide nuclear fleet. Thus, the ideal ATF-cladding concept should have:

- reduced corrosion and stored hydrogen inventory during normal operation;

- equivalent or superior end-of-cycle radiation physical and mechanical properties (including creep and stress relaxation, resistance to pellet-clad mechanical interaction [PCMI] and stress corrosion cracking due to pellet-clad interaction [SCC-PCI], for example);

- negligible impact on the neutron economy within the core;

- significantly reduced HT steam oxidation kinetics leading to increased coping time relative to Zr-based alloys currently deployed in light water reactors (LWRs);

- higher mechanical strength at high temperature to maintain coolable geometry; for example, a cladding with reduced clad ballooning will limit sub-assembly flow blockage with localised hot spots, and will delay or even avoid burst occurrence.

This ideal cladding is difficult to find since many alternative options to the UO_2/Zr-based alloys feature advantages on some characteristics (or performances) and drawbacks on others; hence, the final choice will likely be led by a trade-off between advantages and drawbacks offered by alternative potential candidates. For the past 50 years, the nuclear fuel rod concept for LWRs with UO_2 pellets enclosed in zirconium cladding has been used and optimised aiming to improve its reliability and performance. Consequently it appears challenging to identify a better cladding material than zirconium alloys as far as normal operation is considered. One logical solution to improve the performance of the cladding in accident conditions while preserving the excellent behaviour under normal operating conditions is to slightly modify the current zirconium alloys through external surface treatments such as coatings deposition. This chapter will therefore discuss the various potential coatings and surface treatments developed to improve the accidental performance of the current zirconium alloy cladding, while keeping at least equivalent performances during normal operation.

Waterside and fuel side coatings both have potential safety advantages with respect to the materials' response of cladding during normal operational states and accident conditions. However, fuel side coatings are envisioned as protective permeation barriers to inhibit fission product (FP) attack at the onset of pellet-clad physical contact or to prevent tritium (created in ternary fission events) transport to the coolant. The latter process is generally not an issue for Zr-alloys since tritium is bound in the hydride phase within the matrix during normal operation and the zirconia layer formed on both the inner and outer surface of the cladding effectively acts as a tritium permeation barrier. This may not be the case for other monolithic cladding materials (for example FeCrAl) and the reader is advised to consult the relevant sections of this report for additional information. The use of fuel side coatings as a protective barrier for FP attack (iodine and Cd, in particular) and

associated stress corrosion cracking of the Zr-based cladding has been contemplated for decades (Lyon et al., 2009; Smith and Miller, 1979). This issue is not germane to the objective of this report since it is not linked to the improvement of the behaviour in accident conditions and especially high-temperature (HT) steam oxidation resistance and therefore coatings with respect to this functionality are not addressed here.

Waterside coatings on monolithic Zr-based alloys (or simply coatings in this chapter) have an important advantage compared to other enhanced accident-tolerant cladding concepts. Specifically, the benign mechanical and neutronic properties of Zr-alloys are conserved for coated fuel rods, provided the coating is not an appreciable fraction of the total wall thickness. Decades of research and development by industry, government national laboratories, academia and other research and development institutions throughout the world have generated an extensive amount of data, and most consider the response of monolithic Zr-alloy cladding to LWR environments during normal operation to be well understood. Surface coatings leverage this knowledge and potentially reduce the regulatory burden associated with the demonstration of safe use in LWRs. On the other hand, coatings have a critical disadvantage. The enhanced accident tolerance entirely relies on the coating itself; hence, any event or process that significantly damages or otherwise alters the physical integrity of the coating may partially or completely eliminate the protective role.

Therefore, it follows that coatings must maintain adhesion and be relatively unreactive to LWR coolant exposure during normal operation. In particular, coatings must be compatible with water chemistry control strategies and must not be influenced by (or affect) Crud formation (stability). Furthermore, coatings must promote protective oxide formation, remain adhered to the underlying cladding substrate and not undergo catastrophic morphological changes that expose significant amounts of unreacted Zr during transients. In addition, coating deposition will be required on an industrial scale along the entire fuel rod length with the necessary quality control and assurance.

This section reviews the current progress within those organisations contributing to the Expert Group on Accident-tolerant Fuels for LWRs (EGATFL) who are specifically engaged in evaluating the effectiveness of coatings to promote enhanced accident tolerance of LWRs and who have summarised their work in the form of key highlights provided to the corresponding Task Force. This section is thus a compilation of these highlights and represents efforts in North America, Europe and Asia and spans industrial, government national laboratory and academia research sectors. The chapter will be divided into four parts: fabrication, normal operation and AOOs, design-basis accidents (DBAs) and sesign extension conditions (DECs) and back-end issues (used fuel storage/transport/disposal/reprocessing).

Review of the various coating and surface modification concepts

Several organisations contributing to EGATFL have initiated studies of coatings on monolithic Zr-based alloys over the last five years with the goal of enhanced accident tolerance (Tang et al., 2017). The coatings studied thus far broadly fall within two categories:

- Metallic coatings:
  - Pure Cr (AREVA/CEA/EDF, the Korea Atomic Energy Research Institute [KAERI], and University of Illinois Urbana-Champaign [UIUC]);
  - Cr alloys: Cr-Al binary alloy (KAERI and UIUC);
  - FeCrAl and Cr/FeCrAl multi-layer (KAERI and UIUC). For FeCrAl or iron-based alloys, a barrier layer is needed at the coating/substrate interface to prevent the formation of Zr-Fe eutectic at around 900°C. In the KAERI concept, a barrier layer of Cr or Cr-Al alloy is considered.

- Ceramic coatings:

  – Nitrides: CrN, TiN, TiAlN, CrAlN or multi-layers of different nitrides (IFE/Halden, The Pennsylvania State University [PSU]);

  – MAX phases: Ti_2AlC, Cr_2AlC, Zr_2AlC, Zr_2SiC (KIT, AREVA).

Nitride ceramic coatings are used to harden materials and improve their wear behaviour, especially TiN and TiAlN. For example, they are commercialised for cutting tools and drill bits. Additionally, CrN is also used for corrosion protection. They are therefore commercially available on a large scale.

The $M_{n+1}AX_n$ (MAX) phases, where M is an early transition metal, A is a group 13 – 16 element and X is C and/or N, represent a family of layered ternary carbides and nitrides, which have attracted a great deal of attention in recent decades because of their unique combination of metallic and ceramic properties (Barsoum, 2000). Because of their good properties, MAX phases have been considered as both cladding materials and protective coatings for both current LWRs and broader applications in the future nuclear industry. Recent work has shown that some MAX phases, such as Ti_2AlC, are resistant to both heavy ion irradiation and neutron irradiation, maintaining phase stability and crystallinity up to high displacement per atom (dpa; Tallman et al., 2015). One of the key requirements for the manufacturing of MAX phase coatings is the control of the stoichiometry, an often challenging issue since it is a ternary compound with a multitude of other potential compounds possible with the same elements.

Additionally, surface treatments are also investigated at KAERI as a complement to coating deposition, with the objective of increasing the high-temperature strength of the zirconium substrate by the formation of an oxide dispersion strengthened (ODS) surface layer containing Y_2O_3 nano-particles (Kim et al., 2016). The KAERI concept is therefore more complex than other concepts (which feature only one external coating layer) because of the adoption of two surface treatments: an ODS surface layer in the zirconium substrate for HT strength and the deposition of a second coating on top for the HT steam oxidation behaviour. Figure 10.1 shows the schematic overview of the KAERI design.

**Figure 10.1. Schematic overview of KAERI's
modified zirconium alloy ATF concept**
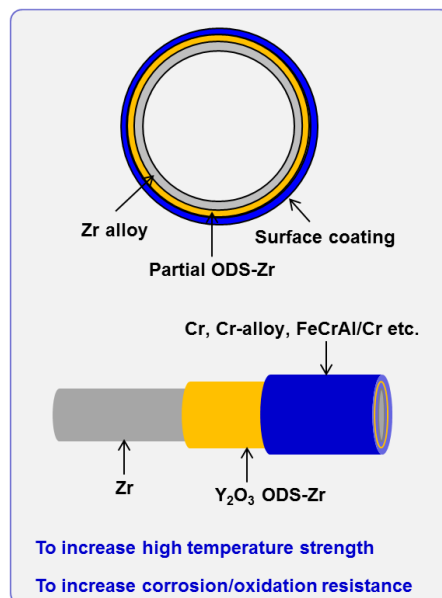
Source: Kim et al., 2016.

Fabrication/manoeuvrability

The properties and behaviour of coatings depend significantly on the fabrication technology used to deposit the coating. Four main categories of deposition technologies can be used:

- Physical vapour deposition (PVD): atomistic deposition of material, which is vaporised from a solid or liquid source in a vacuum or low-pressure chamber and condenses on the substrate. Subtechniques depend on the way the particles are evapourated and include:

  – sputter deposition;

  – arc vapour deposition;

  – ion plating.

- Chemical vapour deposition (CVD): deposition of atoms or molecules reduced or decomposed through chemical reactions from vapour precursors at relatively high temperatures.

- Thermal spray deposition (TSD): material droplets or powder are sprayed and accelerated to high speeds to impact and adhere to the substrate because of a transfer of kinetic energy. Several subtechniques exist mainly depending on the temperature of the particles that are sprayed and the technique used for accelerating these particles:

  – high velocity oxygen fuel spray: fuel-oxygen combustion provides the energy to accelerate particles;

  – cold spray: powders are accelerated to very high speeds by carrier gas going through a specific nozzle;

  – plasma spray.

- Three-dimensional laser coating: deposition of powder on the surface of the cladding with the powder melted by a laser to adhere on the surface.

Only PVD, thermal spraying and three-dimensional laser technologies are currently used to deposit coatings on zirconium alloys since temperatures needed for CVD are usually too high (above the 500°C Zr-alloy final annealing temperature), which would lead to a microstructural change in the substrate microstructure and degradation of the mechanical properties of the substrate. The PVD technique forms coatings atom by atom so very thin coatings can be obtained. It therefore produces very dense coatings with low surface roughness and where both the thickness and the microstructure can be modified as needed. Thermal spray, on the other hand, forms coatings by projecting particles (with different sizes) on the substrate, leading to more porous coatings with much higher surface roughness and significantly less control on the coating thickness or microstructure. Three-dimensional laser coating is a very recent technology and has not yet been well characterised. It is difficult to obtain coatings with a thickness smaller than 30 μm by spray methods but the deposition rate is significantly higher than for PVD.

Most groups working on coatings have in the end retained PVD as the fabrication method for coating deposition because it is the most industrially mature process providing high-quality coatings. As stated previously, it has been used for a while for the industrial production of cutting tools for example, so this process is technically feasible for large-scale production. Some examples also exist of PVD deposition on large substrates such as in the glass industry where coatings are deposited on 3 m × 6 m glass slabs and full cladding tube size PVD chambers are commercially available (van Nieuwenhove et al., 2016). Concerning three-dimensional laser coating and thermal spray, these techniques seem feasible on full-length tubes but have not yet been demonstrated at this scale and therefore need further developments.

The deposition of MAX phases (or alloys) on the cladding surface adds complexity to the industrialisation of the concept since the exact stoichiometry and elemental ratio of the elements to form the proper phase is needed but this can be challenging at large scale and for large production rates (Tang, 2017). Furthermore, once MAX phases are deposited on the surface, then in order to get crystallisation these have to be annealed in situ or ex situ at relatively high temperatures. This can modify the underlying zirconium substrate microstructure and it is sometimes difficult to fully sinter the MAX phase, leading to heterogeneity of the coating. Consequently, single-compound coatings (Cr, CrN for example) will be easier to implement on an industrial scale on a reasonably near term for full-length cladding tubes rather than alloys or multi-element compounds, such as FeCrAl or MAX phases for example.

Finally, security of supply is not an issue for all the coatings investigated worldwide, since the used elements are common and not too costly. The advantage of coating or surface treatment concepts in terms of fabrication is that the manufacturing infrastructure does not have to be replaced or significantly modified. This leads to relatively modest production overcosts, which places coatings on an economic advantage compared to some other ATF-cladding concepts.

Another significant advantage of coatings or surface treatments is that the majority of the cladding remains zirconium alloys, which have been used for the past 50 years. Consequently, cladding properties are modified only on its surface and therefore, licensing of these concepts may likely largely benefit from zirconium alloy behaviour and justification. As licensing of coated cladding concepts is likely greatly facilitated, a modest cost increase is anticipated. The impact of the coating on the global cladding properties and behaviour depends on the coating thickness, thus thinner coatings will likely less modify the cladding behaviour, which will ease the licensing.

Normal operation and AOOs

Influence of coating thickness

Coatings on zirconium substrates primarily modify the cladding surface properties rather than the behaviour of the cladding, but this is more the case for thin coatings below 20 µm; generally, the coating thickness plays a major role in maintaining the zirconium substrate properties and behaviour. For coatings below 20 µm, the neutronic impact on the fuel cycle cost or cycle length of all investigated coating types (Cr, Cr-Al, CrN, FeCrAl, MAX phase) is small and can be easily compensated by very slight design modifications. Since coating materials usually have a higher thermal neutron absorption cross-section than zirconium, a thick coating will negatively impact the fuel cycle cost and economics and therefore the coating thickness has to be taken into account in the normal operation assessment.

Also, if the coating has a low-thermal conductivity (especially for ceramic coatings) a thick coating will deteriorate the heat transfer from the pellet to the coolant, which may lead to increased fuel centreline temperature. For the coatings investigated here, this does not seem to be a major issue because the thicker coatings are metallic and the analysed ceramic coatings thicknesses were often on the order of 10 µm or less. Nevertheless, in the case of multi-layered coatings, the number of interfaces may impact the thermal conductivity since interfaces are often potential barriers. This will therefore have to be investigated for multi-layered coatings.

Mechanical behaviour

The advantage of using a coating rather than changing the bulk cladding is that the mechanical properties of the cladding are governed by the substrate and not by the coating, especially with thin coatings. In presence of material hardening under irradiation, the mechanical behaviour after irradiation is particularly significant. Some

irradiations are currently under way, but no specific analysis of the mechanical behaviour of coated and uncoated cladding after irradiation has been published to date. One of the goals of the irradiation of lead test fuel rods will be to verify the possible impact of the coating on creep, growth or bow under irradiation. This section will review the available out-of-pile results concerning the mechanical behaviour of various coatings.

All investigated coating materials (Cr, FeCrAl, Cr-Al, CrN, MAX phases) are harder than zirconium alloys so if the coating is sufficiently thick (> 30 µm), then mechanical properties will be modified with increased strength and reduced ductility. In the KAERI concept the combination of surface treated ODS zirconium alloy with a relatively thick coating leads to increased strength and reduced ductility (Kim et al., 2014; Kim et al., 2016). Furthermore, excessively thick coatings may potentially lead to even lower ductility under irradiation due to the irradiation hardening of the coating material.

The increased hardness of the coating materials has the benefit of potentially protecting the cladding against fretting and wear. For example, preliminary studies have shown that Cr-coating is very protective against cladding wear and therefore may significantly reduce the risk for cladding damages due to debris or grid-to-rod fretting. Additionally, CrN is known on an industrial scale to improve wear behaviour.

Metallic coatings

If the deposition technique does not modify the zirconium alloy microstructure and if the coating thickness is sufficiently thin, then mechanical properties and behaviour of the coated cladding should be similar to the uncoated cladding. For example, the AREVA/CEA/EDF Cr-coated M5® cladding showed similar mechanical behaviour than uncoated M5® on unirradiated material, as illustrated in Figure 10.2 (Bischoff et al., 2016). For the Cr-coatings, AREVA/CEA/EDF have studied the mechanical behaviour with experimental data on the tensile, burst and creep behaviour for typical in-service temperatures. In all cases, the mechanical behaviour of coated samples was similar to uncoated ones and always within the range of scatter from uncoated substrates. This is a significant advantage, which will facilitate the licensing process, as the mechanical integrity of the coated cladding is the same as that of the current zirconium alloy cladding.

Figure 10.2. Tensile tests at room temperature and 400°C of Cr-coated M5® compared to uncoated reference M5®
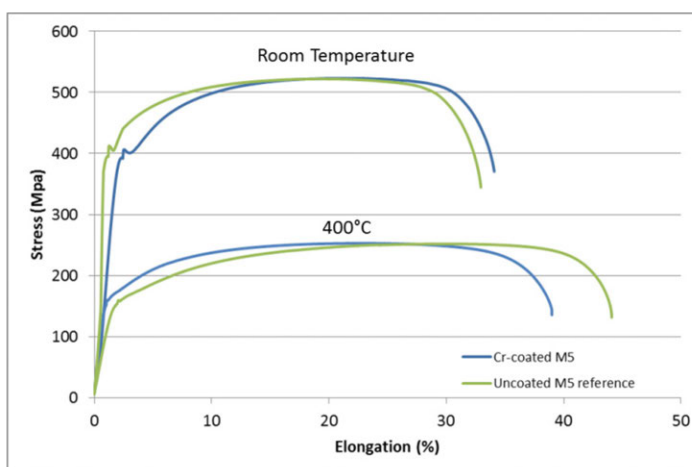
Source: Bischoff et al., 2016.

Ceramic coatings

No data, such as the tensile, creep or burst behaviour, exists concerning the mechanical behaviour of ceramic coatings on zirconium-based substrates. Ceramic coatings are much more brittle than metallic coatings and thus more likely to undergo cracking and damage. The CrN coating can however be stretched by about 1.5% (van Nieuwenhove, 2015) before narrow cracks appear, thereby satisfying the NEA safety criterium to cover the increase in diameter during the total fuel irradiation period in a commercial reactor (NEA Report No. 7072, *Nuclear Fuel Safety Criteria Technical Review*, Second Edition, 2012).

Concerning the wear behaviour, CrN and other ceramic nitride coatings were developed to improve wear behaviour so they will likely provide benefits in terms of fretting (Thamotharan et al., 2014).

Compatibility with the coolant (corrosion behaviour)

In order to investigate the compatibility of the coating with the coolant during normal operation, the standardised tests consist of corrosion tests in 360°C water with pressurised water reactor (PWR) chemistry ([Li]=2.2 ppm; [B]= 650-1 000 ppm) or oxidation in 415°C steam in order to accelerate the corrosion, so to simulate the increased corrosion due to irradiation. As the behaviour is highly dependent on the coating material, results will be presented separately for metallic and ceramic coatings.

Metallic coatings

The main results concern the Cr-coating developed by KAERI and AREVA/CEA/EDF, as well as some FeCrAl coating from UIUC. The Cr-coating in both cases exhibited a significantly reduced corrosion rate (at least ten times smaller) and, especially in the case of the AREVA/CEA/EDF coating, the weight gain remains stable for long exposure times suggesting very little evolution and growth of the Cr_2O_3 layer formed on the surface once it is formed, as shown in Figure 10.3. Consequently, the corrosion of Cr-coated zirconium alloys is reduced to close to zero, thus also decreasing the hydrogen uptake by the cladding. The cladding will therefore not exhibit hydrogen embrittlement, leading to increased operational margins and potentially longer fuel rod irradiations (very high burn-up). This behaviour will have to be verified under irradiation conditions representative of LWRs.

Concerning FeCrAl coatings, corrosion tests were performed in boiling water reactor (BWR) normal water chemistry at 288°C. Results were not as clear as for the Cr-coatings since Ni_2FeO_3 deposits were observed on the FeCrAl coated samples, which therefore exhibited increased weight gain compared to uncoated zircaloy-2 samples. No reliable data exist concerning the corrosion behaviour of FeCrAl coatings in representative LWR environments. Bulk FeCrAl exhibits very good corrosion resistance but sometimes weight loss, so if the coating is too thin, it may lose its protectiveness because of material loss. Consequently, additional data are needed to determine the behaviour of FeCrAl coatings in LWR environments.

Figure 10.3. Corrosion kinetics of Cr-coated samples exposed to (a) 360°C PWR water (KAERI), (b) AREVA/CEA/EDF), and (c) to 415°C steam (AREVA/CEA/EDF)
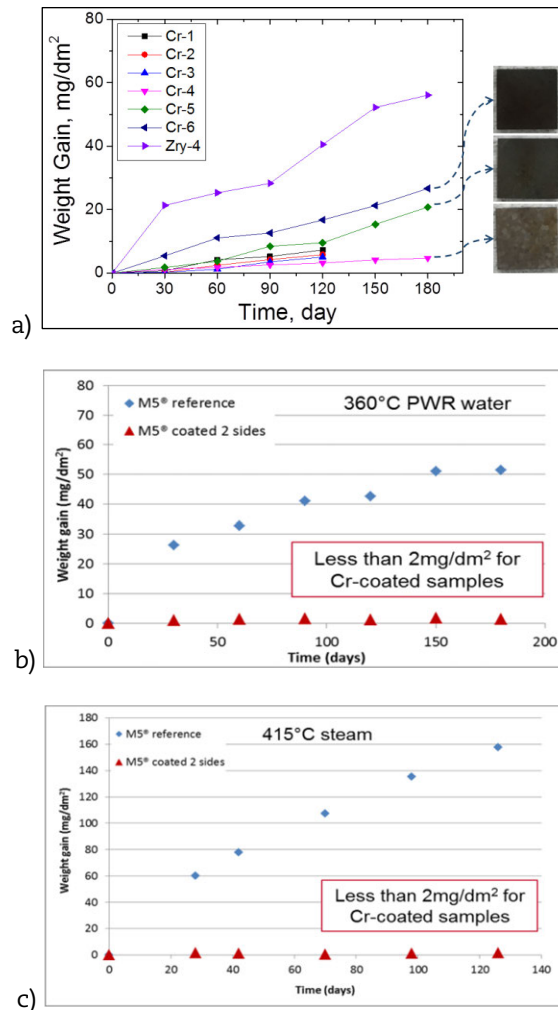
Source: Kim et al., 2017; Kim et al., 2013, 2015, 2016; Bischoff et al., 2016.

Ceramic coatings

No data was found concerning the corrosion of MAX phases in water around 280-360°C since most of the organisations who are developing these types of coatings started working on them for ATF purposes and therefore focused primarily on the HT steam behaviour (Tang et al., 2017). Consequently, there is a significant lack of data concerning the corrosion behaviour of MAX phases in normal LWR environments.

For other ceramic coatings such as nitrides, the behaviour is highly dependent on the Al content of the coating since Al_2O_3 is unstable in LWR environments and dissolves in the water. Thus TiAlN and CrAlN coatings have both shown poor corrosion behaviour, while TiN and CrN exhibit good corrosion behaviour (Alat et al., 2015 and 2016; Daub et al., 2015; van Nieuwenhove et al., 2014 and 2016). Concerning TiN, PSU observed that TiAlN dissolved in autoclave and therefore had to fabricate multi-layered TiAlN/TiN coatings with a final surface layer of TiN to have good corrosion behaviour after 30 days in 360°C PWR water (Alat et al., 2015 and 2016). Thus TiN seems compatible with the coolant but no long-term data exists to certify that the final TiN layer is thick enough to maintain this behaviour for a whole nuclear fuel rod life. Additionally, IFE/Halden in collaboration

with Canadian Nuclear Laboratories (CNL) has performed both out-of-pile autoclave tests and in-pile experiments to evaluate the behaviour of CrN, TiAlN and CrAlN in PWR or BWR environments. Tested coatings had thicknesses of 1-4 µm; in each case only CrN coating remained intact in both PWR and BWR conditions and formed a stable and uniform Cr_2O_3 oxide layer. Both TiAlN and CrAlN dissolved completely.

Consequently, TiN and CrN seem to be the only ceramic coatings tested to date compatible with the coolant and exhibiting significantly increased corrosion resistance compared to uncoated zirconium alloys. Additional data are needed concerning the behaviour of MAX phases in normal operating conditions.

First irradiation results

Metallic coatings

Preliminary ion irradiations were performed by the CEA on Cr-coated samples at 400°C with induced irradiation damage higher than 10 dpa (Wu et al., 2016).

The goal was to evaluate the stability of the Cr-Zr interface under irradiation and the first results showed no degradation of the Cr-Zr interface (the crystallinity of the interface bounding is preserved) and no irradiation-induced diffusion of Cr into the Zr substrate. Consequently, these results suggest that the Cr-coating is stable under irradiation and that the coating does not loose adherence to the bulk zircaloy. This indication needs further confirmation under more representative conditions, in particular under neutron irradiation.

Ceramic coatings

The only irradiation data in representative conditions to date concern the TiAlN, CrAlN and CrN coatings (2-3 µm thick) from IFE/Halden, which were irradiated in the Halden reactor. In a first irradiation campaign in 2012, small samples made of Inconel 600 and zircaloy-4, coated with TiAlN, ZrO_2 and CrN, were irradiated for 126 days under PWR conditions (van Nieuwenhove, 2014b). In a second irradiation campaing from 2011 to 2012, small samples made in Inconel 600, coated with TiAlN and CrN, were irradiated for 287 days under BWR conditions (van Nieuwenhove, 2014b). In a third irradiation campaign in 2014, the first in-pile tests of coated fuel rods with zircaloy-4 cladding were performed under PWR conditions for about 150 days (van Nieuwenhove, 2017). In the fourth irradiation campaign from 2015 to 2016, coated zircaloy-2 and Zr-2.5 Nb samples were irradiated under CANDU conditions for 120 days. A common observation in all these tests was that the CrN coating came out as superior. The coating thickness remained the same and no cracking or delamination occurred under normal conditions.

During the in-pile test of the coated fuel rods, the rods had insufficient cooling (caused by rod bowing), leading to overheating, and this was the only case in which some degree of cracking and delamination of the CrN coating occurred. However, approximately 80% of the coating remained intact.

Figure 10.4 shows the pictures of the fuel rods before and after irradiation. As stated previously, only the CrN coating survived the irradiation and both the TiAlN and CrAlN coatings disappeared from the fuel rod surface.

In the locations where the coating was cracked or removed, zirconium oxide grew below the coating, confirming the loss of protectiveness in these areas.

**Figure 10.4. Picture of the TiAlN, CrAlN, CrN and uncoated fuel rods prior
to irradiation and of the CrN fuel rod after irradiation**
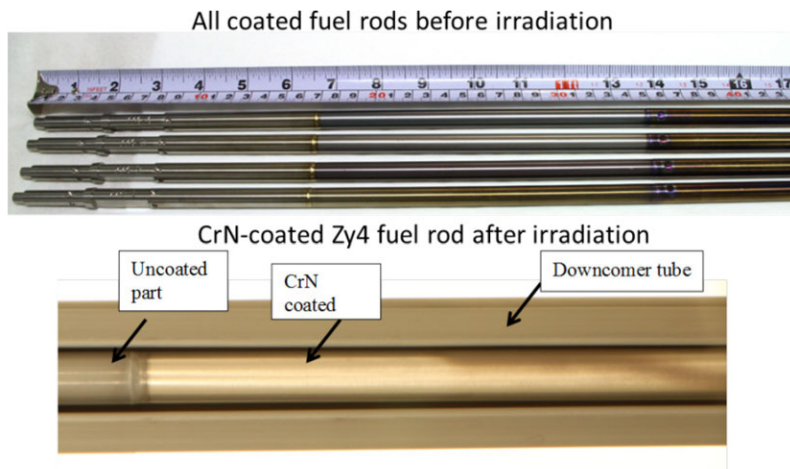
Source: van Nieuwenhoveet et al., 2016.

Summary of behaviour in normal operating conditions

Main advantages:

- low neutronic penalty if coating is sufficiently thin (<20 µm);

- similar mechanical behaviour as uncoated cladding if coating is sufficiently thin (<20 µm);

- significant reduction in corrosion kinetics for metallic coatings (Cr, Cr-Al, FeCrAl) and for some ceramic coatings (CrN and TiN) → increased margins and longer exposure times expected;

- significantly reduced hydrogen pickup and therefore hydrogen embrittlement for these same coatings → increased margins and longer exposure times expected;

- increased wear resistance → reduced fuel rod failures due to fretting are expected (but needs further assessment in representative irradiation conditions up to high burn-up).

Challenges to be monitored:

- coating thickness;

- dissolution of Al-containing coatings (TiAlN, CrAlN, and to a significantly lower extent FeCrAl);

- irradiation impact on coatings, which may lead to cracks or local removal of the coating;

- lack of out-of-pile data on the mechanical behaviour of ceramic coatings;

- lack of in-pile mechanical behaviour data in representative LWR conditions, especially at high burn-up;

- lack of out-of-pile corrosion behaviour of MAX phase coatings in normal operating conditions.

Design-basis accidents and design extension conditions

Most of the experimental work performed to evaluate the behaviour of coated cladding in accident conditions focused on the behaviour under high-temperature (HT) steam in LOCA-type conditions. This is due to the fact that the ATF developments were prompted by the Fukushima accident where the rapid oxidation of zirconium led to the production of an excess of H_2. Thus the main goal for implementing coatings on the surface of zirconium alloy cladding was to provide a barrier to HT steam oxidation to significantly reduce the produced heat and hydrogen compared to uncoated zirconium alloys.

LOCA – HT steam oxidation

Metallic coatings

Cr-coated cladding and other metallic-coated claddings significantly reduce the HT oxidation rates, as shown in Figures 10.5 and 10.6 for the KAERI and AREVA/CEA/EDF concepts, respectively. In both cases the weight gain measured for the coated samples was orders of magnitude lower and the coating served as an efficient barrier to oxygen. Additional tests were performed with Cr-Al and FeCrAl coatings at UIUC but did not show any significant decrease in HT steam oxidation behaviour, only a slight delay in the oxidation kinetic curve. This is likely due to the very thin (1 µm) coatings used by UIUC, where oxygen can diffuse easily through the coating thickness. No characterisations were performed after the oxidation tests to confirm that oxygen diffused and formed zirconium oxide. Consequently, it seems like a minimum coating thickness is necessary to provide significant benefits in terms of HT steam oxidation.

Figure 10.5. Weight gain results from HT steam oxidation tests at 1 200°C for the Cr, Cr-Al and FeCrAl for the KAERI coated concepts
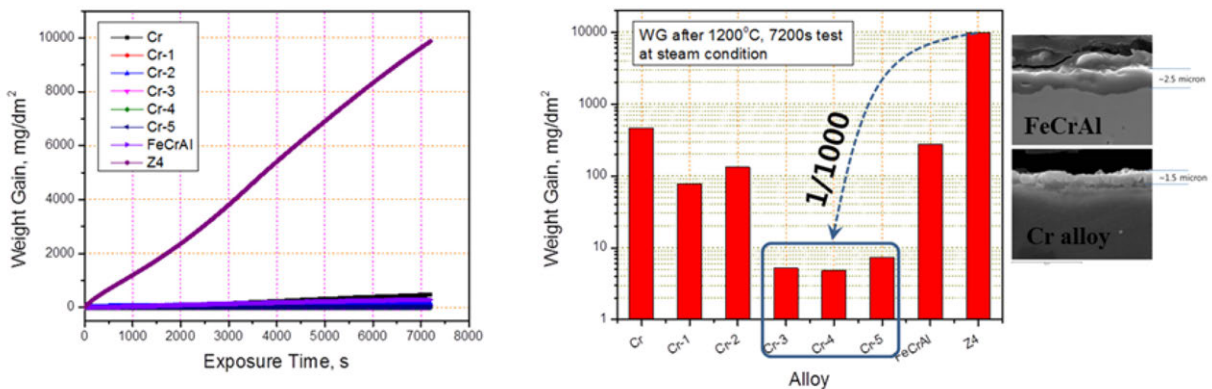
Source: Park et al., 2015.

Figure 10.6. Weight gain results from HT one-sided steam oxidation tests at 1 200°C for the AREVA/CEA/EDF Cr-coated concept with the corresponding oxygen concentration profile within the zirconium substrate of both uncoated and Cr-coated samples
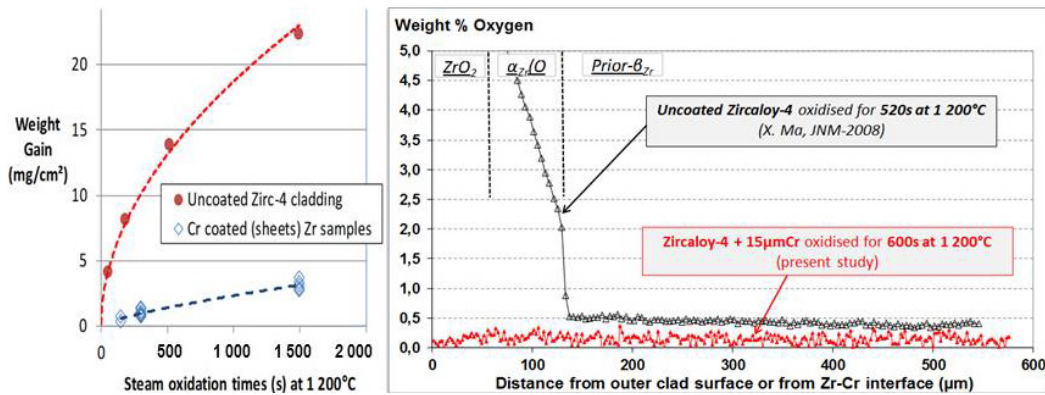

Source: Brachet et al., 2015.

As shown in Figure 10.6, after steam oxidation for 600 s at 1 200°C (which is close to the DBA-LOCA regulatory limit of $ECR_{Baker-Just}$=17% for one-sided oxidation of uncoated zirconium alloys) no diffusion of oxygen within the zirconium substrate was measured in the case of the Cr-coated sample compared to the uncoated one where oxygen ingress penetrated around 150 µm deep. This lack of oxygen diffusion in the substrate has a significant impact on the post-quench ductility since the Zr-α(O) phase formed by the solid solution of O in Zr is very brittle and the associated oxygen diffusion within the inner prior-βZr layer is well known to decrease the post-quenching clad ductility. Consequently, Cr-coated cladding exhibits significantly increased post-quench strength and residual ductility. KAERI has performed 4-point bend tests after HT steam oxidation to confirm that the coated cladding retained its mechanical behaviour (Figure 10.7). The CEA has verified the increased post-quench ductility through ring compression tests at 135°C (Figure 10.8). The consequence is that the coated cladding retains its integrity upon direct water quenching from the oxidation temperature after much longer oxidation times than uncoated samples as illustrated in Figure 10.9 after 6 000 s at 1 200°C steam.

Figure 10.7. KAERI's 4-point bend test after HT steam oxidation at 1 200°C for 2 000 s showing that the uncoated sample fractured while the coated cladding had retained ductility
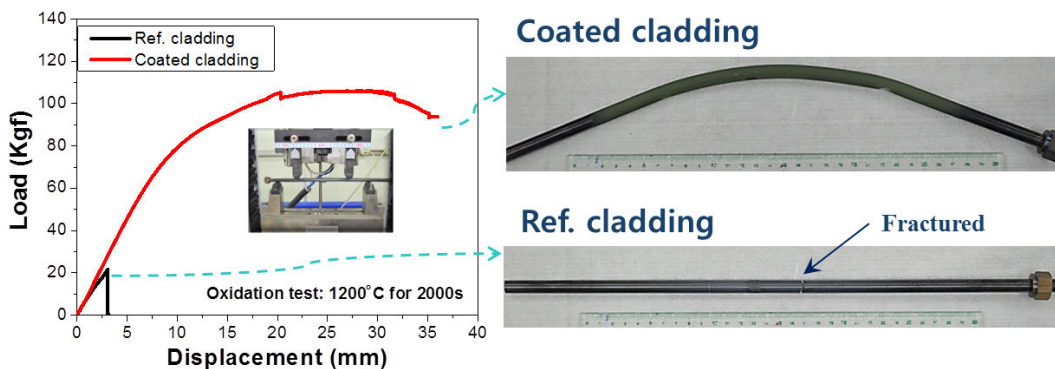
Source: Kim et al., 2013, 2015, 2016; Park et al., 2015.

Figure 10.8. Ring compression tests after 15 000 s HT one-sided steam oxidation tests at 1 000°C for the AREVA/CEA/EDF Cr-coated concept with the corresponding cross-sectional metallography showing the difference in oxide thickness
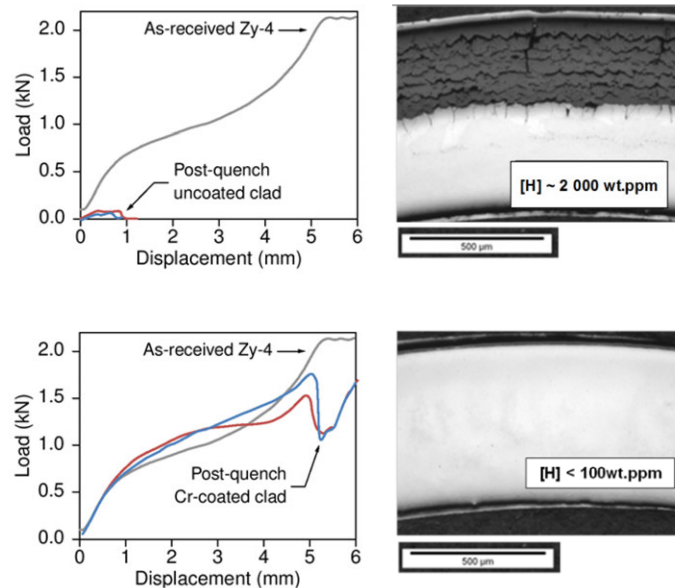
Source: Brachet et al., 2015.

Figure 10.9. Comparison of the visual aspect of Cr-coated and uncoated zircaloy-4 after HT one-sided steam oxidation at 1 200°C for 6 000 s
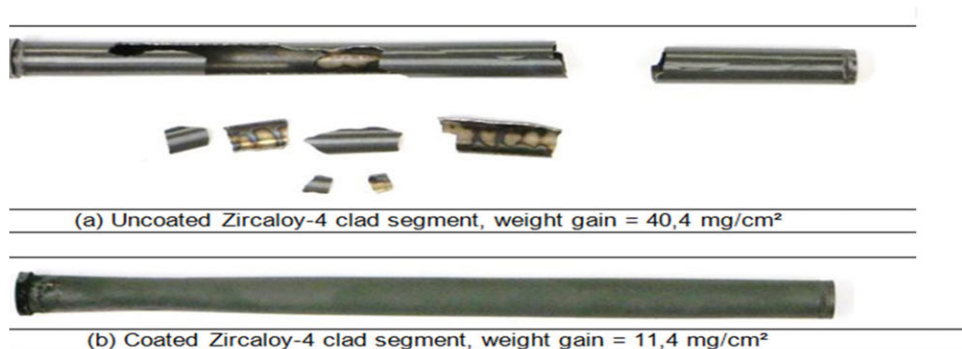
Source: Brachet et al., 2015.

Ceramic coatings

KIT has performed HT steam oxidation tests at various temperatures for different MAX phases. Ti_2AlC was used initially, but weight gain results were equivalent or slightly worse than uncoated samples as shown in Figure 10.10 (Tang et al., 2017). This result had also been obtained by AREVA with the same MAX phase, which led AREVA to abandon MAX phases as potential coatings for ATF applications (Kumar et al., 2016). The main reason is that TiO_2 is not stable beyond 800°C, which led to the degradation of the coating. This poor behaviour was improved at KIT by changing the type of MAX phase to Cr_2AlC, which showed some reduction in HT steam oxidation kinetics. Figure 10.11 shows the results for HT steam oxidation tests at 1 000°C and 1 200°C.

**Figure 10.10. Weight gain results from KIT for HT steam oxidation
at various temperatures for MAX phase Ti₂AlC coating**
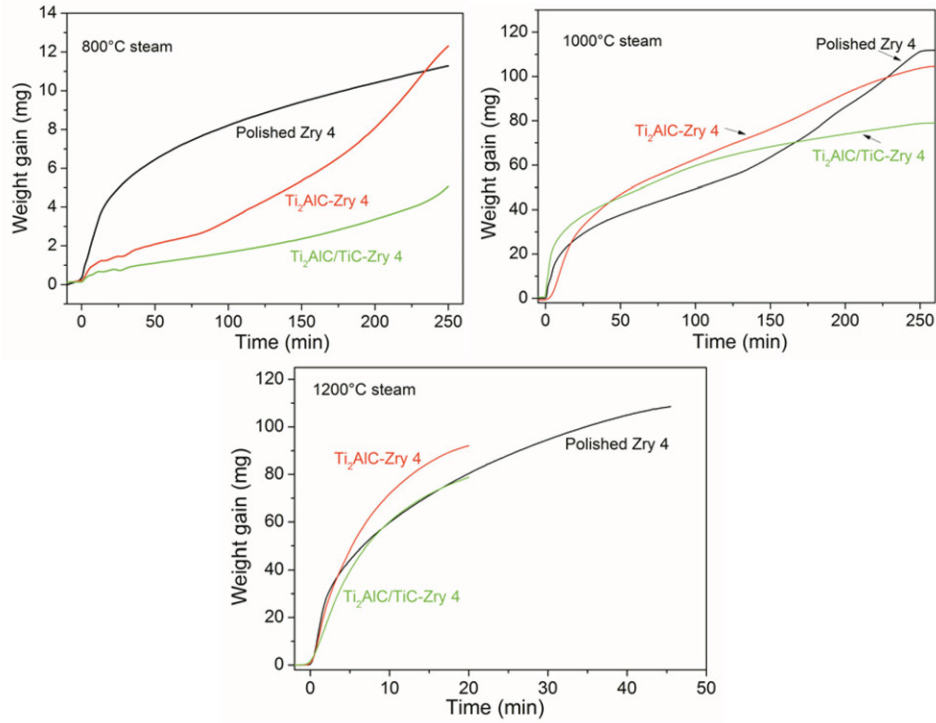
Source: Tang et al., 2017.

**Figure 10.11. Weight gain results from KIT for HT steam oxidation
at various temperatures for MAX phase Cr₂AlC coating**
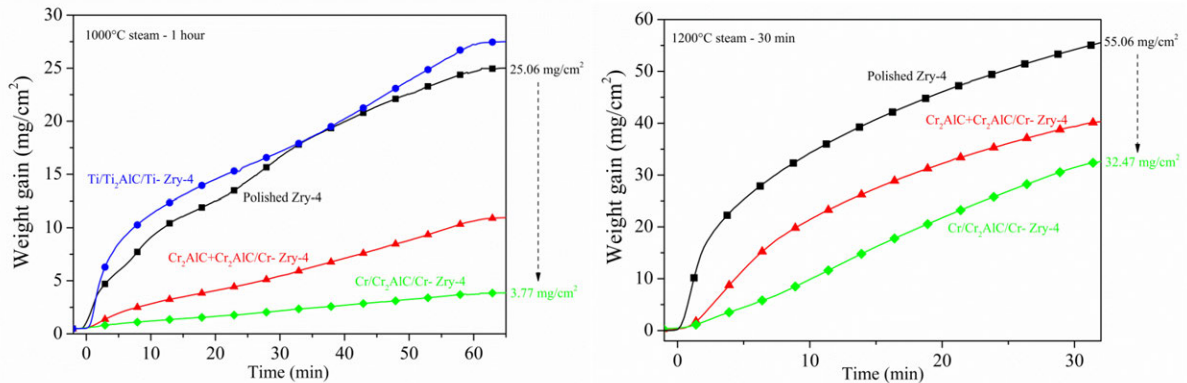
Source: Tang et al., 2017.

Very little HT steam oxidation results exist for other types of ceramic coatings. Some tests were performed at 1 000-1 100°C steam by CNL in collaboration with IFE/Halden on TiAlN, CrAlN and CrN coatings (Daub et al., 2015). Both TiAlN and CrAlN showed significant cracking and coating degradation, which led to poor oxidation performance due to the formation of zirconium oxide under the coating. CrN coating showed some cracking but was overall quite protective and reduced the HT steam oxidation kinetics, but it was not quantified in terms of weight gain.

LOCA – HT creep behaviour

Metallic coatings

Creep and ballooning tests have been performed by both KAERI and AREVA/CEA/EDF for Cr-type coatings and both groups showed similar behaviour:

- very good Cr-coating adhesion even after significant ballooning (no delamination);

- strengthening effect at high temperature (reduction of the creep rate, increase of the time to rupture), especially within the 600-800°C α-Zr temperature range;

- reduction of the balloon size (i.e. "uniform" and maximum hoop strains) and/or of the burst opening size, thus reducing the risk for fuel fragment relocation and/or dispersal in the coolant.

The strengthening effect of the Cr-coated cladding observed at high temperature is beneficial in that it delays the time to rupture (see Figure 10.12) and better preserves the coolable geometry of the nuclear fuel sub-assembly by mitigation of the flow blockage.

Figure 10.12. Time to rupture as a function of initial hoop stress for internal pressure isothermal creep tests performed at different temperatures
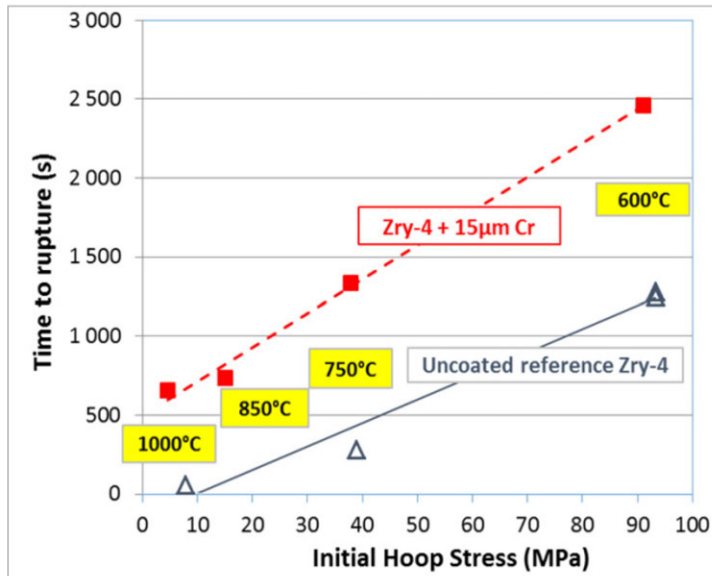
Source: Brachet et al., 2016.

Ceramic coatings

Very little data exist on the high-temperature creep behaviour of ceramic coatings. Only IFE/Halden in collaboration with CNL has performed an integral LOCA test with a ramp rate of 5°C/s at the ORNL Severe Accident Test Station. In this case, the coating did not influence the cladding burst behaviour. It remained adherent but significantly cracked in the vicinity of the balloon/burst location, as shown in Figure 10.13.

**Figure 10.13. Visual aspect of CrN-coated cladding after integral LOCA test
up to 1 200°C at a ramp speed of 5°C/s**
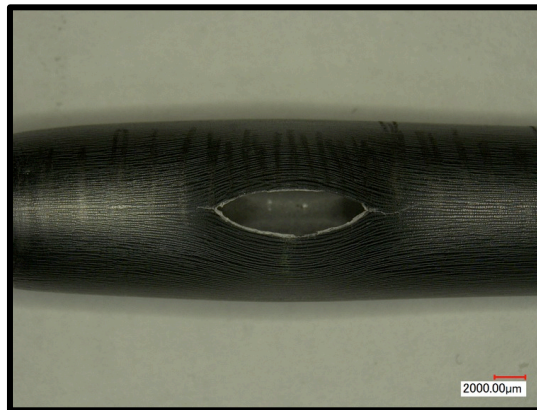
Source: Terrani K., 2018.

- Coating helps to significantly reduce ECR at burst location. Without coating (or with a brittle coating that cannot withstand the cladding straining), double sided oxidation has to be considered in the ballooned/burst location. If the coating is ductile enough to withstand the clad ballooning strains, one-sided oxidation can be considered. This will provide four times longer grace period before reaching the same ECR level. The same reasoning is applicable away from the ballooned/burst region.

- By reducing both the cladding balloon sizes and related clad thinning, coatings also help to reduce ECR levels in the ballooned/burst region.

**Figure 10.14. Schematic behaviour of the outer coating in the ballooned/burst location
during the high-temperature steam oxidation phase of a LOCA transient**
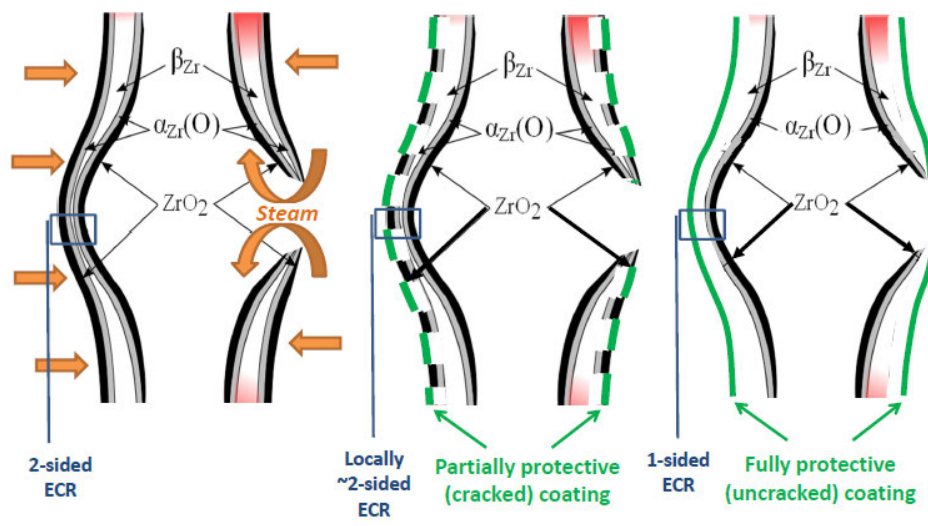
Note that the same reasoning applies away from the ballooned/burst location, in an area where cladding creep can be significant.

Source: Brachet, le Saux and CEA, 2017.

RIA

No specific tests have been performed for RIA behaviour. Since RIA behaviour is mainly affected by hydrogen (hydride density, morphology and orientation) in zircaloy fuel cladding, it can be assumed that RIA performance will be improved by application of coatings that significantly reduce corrosion and hydrogen pickup during normal operation. However, coating impact on RIA will still have to be assessed.

Design extension conditions

Behaviour during design extension conditions can be evaluated either by increasing the time of exposure at the same temperatures as LOCA tests or by increasing the temperature. In the first case, the tests concerning HT steam oxidation already answer to the behaviour at longer times.

One key issue for coated claddings that appears when evaluating their behaviour at temperatures beyond 1 200°C is the formation of an eutectic point between the coating material and the underlying zirconium substrate. For example, the Cr-Zr eutectic occurs at 1 330°C. KAERI has developed a Cr-Al coating that increases the eutectic temperature between the coating and the zirconium substrate. Another solution can be to incorporate a thin barrier layer between the coating and the substrate such as with molybdenum or other refractory metals to prevent the eutectic formation. Nonetheless, the behaviour of the coating beyond the eutectic point has to be investigated. To date, very little data exists concerning the eutectic behaviour for the different investigated coating materials. If the coating is too thick, the coating-substrate interaction will be much higher and might therefore lead to significant degradation of the cladding because of eutectic formation. Consequently, a compromise has to be determined between the minimum thickness necessary to provide significant benefits in HT steam oxidation and a maximum thickness allowing a reduction of the potential detrimental consequences of the eutectic.

Summary of behaviour in accident conditions

Main advantages:

- significantly reduced HT steam oxidation leading to reduced heat and hydrogen production;
- increased post-quench ductility;
- strengthening effect at high temperature leading to reduced creep and ballooning and to increased time to rupture.

Challenges to be monitored:

- coating has to be thick enough to provide significant reduction in HT steam oxidation;
- potential eutectic formation (especially for metallic coatings);
- coating has to be thin enough to limit the extent of potential eutectic formation for metallic coatings;
- few data exist for HT behaviour (mechanical and oxidation) of ceramic coatings.

Back end: Used fuel storage/transport/disposal/reprocessing

Low-hydrogen pickup during normal operation leads to a great benefit with respect to transport, intermediate storage in a spent fuel pool and reprocessing, as long as the coating remains efficient. Since the coating exhibits significantly reduced corrosion, it may also protect the cladding and thus the fuel, during long-term disposal or for certain spent fuel pool accident scenarios by increasing safety margins. This behaviour will nonetheless have to be evaluated through further studies.

Additionally, chromium apparently does not get dissolved in nitric acid, so it should not impact the quality of the vitrified waste conditioning during reprocessing for Cr based coatings. No data exists concerning the other types of coatings and their behaviour for reprocessing.

Table 10.1. Summary of coating systems properties

Institution	Coating system	Fabrication	Normal operation	Accidental behaviour
AREVA-CEA-EDF	Cr (5-20 μm)	PVD Full-length prototype ongoing	Extremely low corrosion + H pickup Similar mechanical behaviour as uncoated Very good adherence Cr-Zr interface stable under ion irradiation Increased wear resistance	Significantly reduced HT steam oxidation Increased post-quench ductility Strengthening effect of Cr – reduced HT creep, reduced ballooning Very adherent and no or very limited cracking after significand clad creep/balooning Zr-Cr eutectic (1 330°C) behaviour TBD
KAERI	Cr Cr-Al FeCrAl (40-80 μm)	PVD (ion plating) Three-dimensional laser coating	Extremely low corrosion + H pickup Increased strength and reduced ductility Very good adherence Increased wear resistance	Significantly reduced HT steam oxidation (up to 1 400°C) Increased post-quench ductility Strengthening effect of Cr – reduced HT creep, reduced ballooning Fe-Zr eutectic around 900°C (use of barrier layer)
IFE-Halden/ CNL	CrN (1-4 μm)	PVD Commercially available (full-length)	Extremely low corrosion + H pickup Good adherence Increased wear resistance Minor cracking of coating observed after irradiation	Reduced HT steam oxidation Some cracking of coating observed during HT steam oxidation Very adherent during HT bust test but significant cracking at burst/balloon location
	TiAlN CrAlN (1-4 μm)	PVD Commercially available (full-length)	Dissolves in water Poor adherence	Cracking and delamination observed after HT steam oxidation
KIT	MAX phases (Ti₂AlC; Cr₂AlC) (~5 μm)	PVD Difficult to obtain correct stoichiometry + microstructure	No data Potential dissolution of Ti₂AlC in water (Al₂O₃)	Similar HT steam oxidation resistance of Ti₂AlC to uncoated Zy4 Reduced HT steam oxidation of Cr₂AlC
UIUC	Cr-Al (~1 μm)	PVD	Difficult to interpret results (deposits) Reduced corrosion but weight loss for FeCrAl (dissolution of Al₂O₃)	Slight reduction in HT steam oxidation at 700°C Negligible effect at 1 200°C steam (too thin) Fe-Zr eutectic ~900°C
	FeCrAl (~1 μm)			
PSU	TiN / TiAlN (~10 μm)	PVD (multi-layer coating)	Low corrosion + H pickup if surface TiN	No data

References

Alat, E. et al. (2015), "Ceramic coating for corrosion (C3) resistance of nuclear fuel-cladding", *Surface and Coatings Technology,* Vol. 281, pp. 133-143.

Alat, E. et al. (2016), "Multi-layer (TiN, TiAlN) ceramic coatings for nuclear fuel-cladding", *J. Nucl. Mater.,* Vol. 478, pp. 236-244.

Barsoum, M.W. (2000), "The MN+1AXN phases: A new class of solids; thermodynamically stable nanolaminates", *Prog. Solid State Chem,* Vol. 28, pp. 201-281.

Bischoff, J. et al. (2016), "Development of Cr-coated zirconium alloy cladding for enhanced accident tolerance", *Proceeding of TopFuel 2016,* Boise, Idaho.

Bischoff, J. et al. (2015), "Development of fuels with enhanced accident tolerance", *Proceeding of TopFuel 2015,* 13-19 September 2015, Zurich.

Bischoff, J. et al. (2014), "Development of fuels with enhanced accident tolerance*", IAEA Technical meeting on ATF in LWRs,* ORNL.

Brachet, J.C. et al. (2016), "Behavior under LOCA conditions of enhanced accident tolerant chromium coated zircaloy-4 claddings", *Top Fuel 2016,* pp. 1173-1178, Boise, Idaho.

Brachet, J.C. et al. (2015), "On-going studies at CEA on chromium coated zirconium-based nuclear fuel claddings for enhanced accident tolerant LWRs fuel", *Proceedings of 2015 LWR Fuel Performance/TopFuel,* pp. 31-38, Zurich.

Bragg-Sitton, S. (2014), "Development of advanced accident-tolerant fuels for commercial LWRs", *Nuclear News,* Vol. 57(3), p. 83.

Cheng, B., P. Chou and Y.-J. Kim (2014), "Enhancing fuel resistance to severe loss-of-coolant accidents with molybdenum-alloy fuel cladding", *Proceedings of 2014 Water reactor fuel performance meeting/Top Fuel/LWR fuel performance meeting* (WRFPM 2014), p. 784.

Cheng, B., Y.J. Kim and P. Chou (2016), "Improving accident tolerance of nuclear fuel with coated mo-alloy cladding", *Nuclear Engineering and Technology,* Vol. 48(1), pp. 16-25.

Daub, K., R. van Nieuwenhove and H. Nordin (2015), "Investigation of the impact of coatings on corrosion and hydrogen uptake of zircaloy-4", *Journal of Nucl. Materials,* Vol. 467, pp. 260-270.

Kim, H.G. et al. (2016), "Development status of accident-tolerant fuel for LWRs in Korea", *Nuclear Engineering and Technology,* Vol. 48(1), pp. 1-15.

Kim, H.G. et al. (2015a), "Adhesion property and high-temperature oxidation behavior of Cr-coated zircaloy-4 cladding tube prepared by 3D laser coating", *Journal of Nuclear Materials,* Vol. 465, pp. 531-539.

Kim, H.G. et al. (2015b), "Application of coating technology on zirconium-based alloy to decrease high-temperature oxidation", *Zirconium in the Nuclear Industry: 17th Volume,* STP154320120161, B. Comstock and P. Barbéris, Ed., ASTM International, West Conshohocken, PA, pp. 346-369, https://doi.org/10.1520/STP154320120161.

Kim, H.G. et al. (2013), "High-temperature oxidation behavior of Cr-coated zirconium alloy", *Proceeding of LWR Fuel Performance Meeting/Top Fuel,* pp. 842-846.

Kim, J. et al. (2017), "Microstructure and oxidation behavior of CrAl laser-coated zircaloy-4 alloy", *Metals,* Vol. 7(2), p. 59.

Kumar, K.N.A.P. et al. (2016), "AREVA enhanced accident tolerant fuel program: Current results and future plans", *Proceeding of TopFuel 2016,* Boise, Idaho.

Lyon, W. et al. (2009), "PCI analysis and fuel rod failure prediction using FALCON", *Water Reactor Fuel Performance Meeting,* Paris.

Mandapaka, K.K. et al. (2017), *J. Nucl. Mater.*, forthcoming.

Park, D. et al. (2017), "TEM/STEM study of zircaloy-2 with protective FeCrAl layers under simulated BWR environment and high-temperature steam exposure", *J. Nucl. Mater.*, submitted.

Park, D.J. et al. (2016), "Behavior of an improved Zr fuel cladding with oxidation resistant coating under loss-of-coolant accident conditions", *J. Nucl. Mater.*, Vol. 482, pp. 75-82.

Park, J.H. et al. (2015), "High temperature steam-oxidation behavior of arc ion plated Cr-coatings for accident tolerant fuel claddings", *Surf. Coat. Technol.*, Vol. 280, pp. 256-259.

Smith, E. and A.K. Miller (1979), "Stress corrosion fracture of zircaloy cladding in fuel rods subjected to power increases: A model for crack propagation and the failure threshold stress". *J. Nucl. Mater.*, Vol. 80(2), pp. 291-302.

Tallman, D.J. et al. (2015), "Effect of neutron irradiation on select MAX phases", *Acta Mater*, Vol. 85, pp. 132-143.

Thamotharan, J. et al. (2014) "Characterization of CrN/TiN PVD coatings on 316L stainless steel", *Int.J. ChemTech Res.*, Vol. 6(6), pp. 3284-3286.

Tang, C., et al. (2017), "Protective coatings on zirconium-based alloys as accident tolerant fuel (ATF) claddings", *Corrosion Reviews*.

Terrani, K. (2018) "Accident tolerant fuel cladding development: Promise, status, and challenges", *Journal of Nuclear Materials*, doi: 10.1016/j.jnucmat.2017.12.043.

Terrani, K.A. et al. (2013), "Protection of zirconium by alumina-and chromia-forming iron alloys under high-temperature steam exposure", *J. Nucl. Mater.*, Vol. 438, pp. 64-71.

Van Nieuwenhove, R. et al. (2013), "Investigation of coatings, applied by PVD, for the corrosion protection of materials in supercritical water", *Sixth International Symposium on Supercritical Water-Cooled Reactors (ISSCWR-6),* Paper 13024, Shenzhen.

Van Nieuwenhove, R., K. Daub and H. Nordin (2014a), "Investigation of the impact on coatings on corrosion and hydrogen uptake of nuclear components", *Third meeting of the Nuclear Materials Conference,* Clearwater, Florida.

Van Nieuwenhove, R. (2014b), "IFA-774: The first in-pile test with coated fuel rods", *Enlarged Halden Program Group Meeting*, HWR-1106, Røros.

Van Nieuwenhove, R. (2015), *Investigation of Coatings for Nuclear Applications: Tensile Testing of Coated Specimens,* Report IFE/HR/F –1624, March 2015.

Van Nieuwenhove, R. et al. (2016), "In-pile testing of CrN, TiAlN, and AlCrN coatings on zircaloy cladding in the Halden Reactor", *Zirconium in the Nuclear Industry: 18th International Symposium*, ASTM STP1597, R.J. Comstock and A.T. Motta, EDS., ASTM International, West Conshohocken, PA, 2018, pp. 965-982, http://dx.doi.org/10.1520/STP159720160011 (ASTM 18th International Symposium on Zirconium in the Nuclear Industry 15-19 May 2016 in Hilton Head, SC.), Nuclear Industry, Hilton Head Island, South Carolina.

Wu, A. et al. (2016), "Behaviour of ion irradiated chromium coatings on zircaloy-4 substrate", *NuMat 2016*, Montpellier.

Wu, X., T. Kozlowski and J.D. Hales (2015), "Neutronics and fuel performance evaluation of accident tolerant FeCrAl cladding under normal operation conditions", *Annals of Nuclear Energy,* Vol. 85, pp. 763-775.

Zhong, W. et al. (2016), "Performance of iron-chromium-aluminum alloy surface coatings on zircaloy-2 under high-temperature steam and normal BWR operating conditions", *J. Nucl. Mater.*, Vol. 470, pp. 327-338.

11. Advanced steels: FeCrAl

The concept described here utilises an FeCrAl alloy material as fuel rod cladding in combination with uranium dioxide (UO_2) fuel pellets currently in use, resulting in a fuel assembly that leverages the performance of existing/current light water reactor (LWR) fuel assembly designs with enhanced accident tolerance.

By definition, the accident-tolerant fuel (ATF) technology should perform as well as the current zircaloy-UO_2 fuel system under operational states and better than the current system under accident conditions (Zinkle et al., 2014). FeCrAl alloy clad fuel rods (with UO_2 fuel) appear to exhibit properties that meet or exceed current fuel design technical requirements (with the exceptions noted below) while providing increased safety benefit during design-basis events and severe accident (SA) conditions.

There are two challenges for an FeCrAl alloy clad system. Neither is considered to be a high technical risk and both may be addressed and mitigated using well-developed strategies and technical methodologies. The first, a deployment challenge, is the increased parasitic neutron absorption of the FeCrAl alloy relative to the current zircaloy system. The second, a development challenge, is a potential increase in tritium release into the reactor coolant. Tritium is produced as a fission product (FP). FeCrAl does not react with hydrogen to form stable hydrides similarly to a zirconium-based alloy, resulting in higher permeability of tritium through the cladding to the reactor coolant. Mitigation technologies may be required to minimise this concern.

Other technical issues to be addressed include fabrication, regulatory and irradiated material performance. Fabrication is not identified as a key technical challenge because scoping studies indicate that traditional metal processing (such as pilgering, drawing, extruding and welding) are applicable to FeCrAl materials. Additional phases of the international ATF programmes will minimise this issue. Although regulatory changes will be required to implement FeCrAl alloy within a commercial product, the scope of potential changes is relatively minor and such changes will, in general, provide additional margin for safe nuclear fuel operations. Additional understanding of the performance of FeCrAl alloy will be required to access the areas impacted by potential regulatory changes. Lastly, the lack of some irradiated material properties and integral tests is a technical issue; however, it is anticipated that the irradiated materials will perform in a manner consistent with other ferrous alloys. Complete irradiated material properties and integral tests are expected to be obtained and performed in ongoing and future ATF development programmes.

Primary validation

The FeCrAl concept is compatible with existing fuel assembly mechanical/ neutronic/thermal-hydraulic requirements, regulatory requirements and Reactor Coolant System (RCS) chemistry requirements (normal operating regime). LTAs using FeCrAl as cladding material will be tested in existing commercial reactors (Hatch and Clinton) in the near term.

Table 11.1. Key properties of the cladding and fuel rod

Properties	Assessment for zircaloy	Assessment for FeCrAl
Thermal conductivity (beginning of life [BOL] and post-irradiation)	Good.	Good.
Mechanical		
PCMI	Good.	TBD, no issues anticipated.
Strength	Good.	Good.
Ductility, resistance to fragmentation upon re-flooding in a DBA and DEC	Good.	Superior in a DBA. TBD in DEC, no issues anticipated.
Hermeticity	Good.	Good.
Weldability	Good.	Good.
Fretting wear	Acceptable.	Superior.
Irradiation growth/swelling	Acceptable.	TBD, no issues anticipated.
Thermal cycling induced fatigue	Acceptable.	TBD, no issues anticipated.
Handling induced mechanical damage resistance	Good.	Good.
Fission product retention within cladding	Good.	TBD, no issues anticipated in current tests in Japan.
Pellet-clad chemical interaction (chemical compatibility with fuel)	Good.	TBD, no issues anticipated. Current tests at ATR.
Reactor coolant system compatibility	Good.	Excellent.
pH and lithium limitations	OK with current EPRI guidelines.	OK with current EPRI guidelines.
Crud/corrosion properties (i.e. oxidation, H pickup, etc.)	Acceptable with good practices.	TBD, no issues anticipated.
Neutron cross-sections	Excellent.	Fair.
Permeability (i.e. tritium)	Excellent.	Ten times higher than current zircaloy. Surface oxides suppresse tritium permeation.
Fuel rod		
Required fuel enrichment	4.95% ^{235}U.	4.95% ^{235}U.
Dimensional requirements	Current values.	Similar to current values.
Cladding	Current values.	Thinner wall (approximately half of current values for zircaloy)..
Fuel pellet	Current values.	Slightly larger diameter.
Reactivity vs. Burn-up (relative to a Zr-UO$_2$ rod)	Current values.	Some reduction anticipated for same enrichment.
Reactivity feedback coefficients for the fuel system	Current values.	Similar to current values.
Rod burn-up limits (MWD/MTU)	Current values.	Similar to current values.

The FeCrAl ATF concept for commercial LWRs involves the replacement of the zirconium alloy fuel cladding with an FeCrAl alloy (Terrani, Zinkle and Snead, 2014; Rebak et al., 2015; Yamashita et al., 2016), while retaining the existing UO_2 ceramic fuel pellets within a similar fuel rod design arrangement currently utilised in LWR fuel designs. That is, substitute one cladding material for another. It is noted that, prior to use of zirconium-based alloys, austenitic stainless steel (SS) materials were used for fuel rod cladding (Strasser et al., 1982). Preliminary studies on FeCrAl alloy materials indicate sufficient strength and ductility to perform acceptably as cladding alloy, similar to past use of SS cladding. However, compared to past experience with austenitic SS cladding, extensive crack propagation studies show that ferritic FeCrAl alloys provides orders of magnitude more resistant to environmentally assisted cracking than modern-type 304SS (Rebak, Brown and Terrani, 2015), which is more resistant to irradiation degradation than prior versions of SS cladding materials.

Proton irradiation studies performed at the University of Michigan showed that FeCrAl materials may be resistant to proton irradiation-induced cracking providing additional confirmation of the potential acceptability of FeCrAl materials for fuel rod cladding (Ahmedabadi, Was, 2016). Although there may be nominal changes in fuel rod geometry (e.g. clad thickness) for lead rod assembly designs and in fuel assembly designs (e.g. fuel channels) to accommodate differences in material performance in the future fuel designs, such changes are expected to be incremental to existing fuel rod and assembly designs, significantly leveraging the knowledge base for current fuel designs. Simulation studies performed at Brookhaven National Laboratory (BNL) showed that there is little or no impact on the thermal-hydraulic properties of the system by using a fuel rod clad with a FeCrAl alloy (Rebak, Brown and Terrani, 2015). It is expected that an FeCrAl alloy clad fuel rod can be considered with thermal-hydraulic design changes.

FeCrAl alloy cladding is completely compatible with the coolant chemistries used in either boiling water reactor (BWR) or pressurised water reactor (PWR) reactors; that is, significant coolant chemistry changes are not expected as a result of FeCrAl implementation. Extensive immersion studies with chemistries typically observed in both BWR and PWR reactors showed excellent corrosion resistance of the FeCrAl alloys (Terrani et al., 2016).

Electrochemical studies in high-temperature (HT) water showed that FeCrAl has behaviour similar to traditional reactor alloys such as type 304SS and nickel-based alloy X-750. Electrochemical studies performed at GE Global Research showed that FeCrAl rods in contact with a separator grid of alloy X-750 would not experience galvanic corrosion under irradiation conditions (Kim et al., 2015), allowing utilisation of existing grid/spacer designs.

Regulatory criteria affected by the change from a zirconium alloy system to an FeCrAl system include an increase in peak cladding temperature and strain capability of the cladding during normal and transient conditions. For design base conditions, affected regulatory requirements include the percentage of cladding reacted, fuel rod pressure containment behaviour and post-quench ductility behaviour during a loss-of-coolant accident, rewetting characteristics after dry-out and maximum fuel enthalpy for a reactivity insertion accident. For severe accidents, regulatory requirement intended to limit and manage hydrogen generation may be affected.

Use of FeCrAl cladding material is a promising ATF fuel concept and might be utilised in BWRs, PWRs and near term generation III+ reactor designs.

Issues to be resolved

The issues that need to be successfully resolved before full implementation of an FeCrAl alloy clad system relate to mitigation of increased parasitic neutron absorption of the FeCrAl compared to zirconium alloys (George et al., 2015). As a direct material substitution, (assuming some reduction in cladding thickness consistent with preliminary mechanical

performance and some increase in fuel pellet mass) application of FeCrAl alloy cladding will increase fuel cycle costs. It is estimated that an impact in the order of 20% increase in cost is expected (Terrani, Zinkle and Snead, 2014; George et al., 2015). Additional design changes (such as the water channel) may be required to meet bundle design requirements, further impacting fuel cycle economics. However, potential mitigation strategies that may partially or fully offset these penalties exist and may be further complemented by the overall fuel cycle cost impact. Such mitigation strategies include alternate fuel assembly materials (e.g. silicon carbide composite channel materials), higher allowable heat generation rates, as well as relaxation of regulatory requirements due to much improved fuel cladding performance under operational states and accident conditions, design basis and design extension conditions. Silicon carbide composite channel material development may be used with FeCrAl cladding for the fuel.

A second issue that requires resolution is the potential to increased release of tritium into the coolant. This is of particular concern for BWRs that do not benefit from a separate primary loop that exists in PWRs. One potential mitigation strategy, currently under investigation, is application or formation of an alumina layer (or other type of permeation barrier [Causey, Karnesky and Marchi, 2011]) in the inner diameter (ID) and/or outer diameter (OD) of the cladding (Levchuk et al., 2008). Preliminary results indicate that this strategy is promising. ORNL has calculated that the partial pressure of oxygen inside the fuel rod may be sufficient for the cladding to develop a protective oxide from the ID, which would minimise tritium diffusion into the coolant (Hu et al., 2015). Nippon Nuclear Fuel Development (NFD) has examined the barrier role of the surface oxide layer formed by the out-of-pile corrosion tests and has found a drastic suppression of tritium permeation, which would be an inherent barrier of FeCrAl alloy materials (Sakamoto et al., 2017).

As discussed in prior sections, there is insufficient irradiated material data available for FeCrAl alloy materials to allow for complete analysis of fuel rod design, thermal-mechanical modelling, resistance to pellet-cladding interaction failure mechanism (PCI and PCMI), efficacy of the tritium migration mitigation and performance during design-basis accident conditions (reactivity insertion enthalpy limits, LOCA blowdown and post-quench limits). Accordingly, the need for integral tests is highlighted here to further understand the behaviour of this fuel system. Currently, FeCrAl clad fuel is being exposed in the ATR at INL and the first PIE results may be available in 2018.

An FeCrAl alloy cladding system provides performance compatible with current zirconium alloy systems.

Benefit in off-normal operation conditions

The FeCrAl cladding design would increase reactor coping time, enhance the ability to maintain a coolable geometry, enhance FP retention, or improve reaction kinetics in accident conditions (regime: DBA, DEC). FeCrAl alloy cladding systems provide superior performance, as compared to current zirconium alloy clad systems, by providing improved coolant oxidation reaction kinetics (Pint et al., 2015) and an increase in the allowable peak cladding temperatures during operational states and accident conditions. Zirconium alloys rapidly oxidise with steam (water) at temperatures above 1 200°C in an exothermic reaction producing zirconium oxide and hydrogen (Moalem, Olander, 1991). The oxidation rate of FeCrAl is at least 1 000 times slower than that of zirconium (Pint et al., 2013), resulting in a significant reduction in heat generation and hydrogen generation during accident conditions (Robb, 2015). Reductions in released heat energy and hydrogen considerably reduce potential safety concerns for a reactor during an accident scenario. In Japan, as similar to the US DOE programmes, the alloy development of FeCrAl-ODS materials have been completed in the programme sponsored by MEXT (Ukai et al., 2016) and its applicability to BWRs is being conducted in the programme sponsored and organised in METI (Sakamoto et al., 2017). The excellent HT oxidation resistance of FeCrAl alloys relies on the formation of a protective alumina scale which may be an issue during fast transients (Tang et al., 2016).

Although the melting temperature of FeCrAl alloy is lower than a zirconium-based alloy (1 500°C vs. 1 850°C), zirconium-based alloys incur autocatalytic oxidation at temperatures above 1 200°C. As a consequence of the higher steam reaction kinetics and the resultant heat generated by oxidation, the zircaloy-cladding would be oxidised by steam and react with UO_2 pellet catastrophically before the melting of FeCrAl cladding. In addition, a zirconium alloy degraded at high temperatures results in a brittle material unlikely to retain a high level of integrity during the quenching. An FeCrAl alloy clad system is expected to provide increased coping time to cladding failure during design-basis LOCA for DBAs (Yan et al., 2014; Massey et al., 2016) and DECs (Ott, Robb and Wang, 2014). A semi-integral bundle test in the Quench Facility at KIT (Steinbrück et al., 2010) in co-operation with ORNL will be conducted at the end of 2017 with the aim to experimentally confirm the superior DEC behaviour of FeCrAl claddings. The experiment will be conducted with the same scenario as the test Quench-15 with ZIRLO™ claddings (Stuckert et al., 2011).

Additionally, FeCrAl alloys have mechanical strength similar or superior to that of zircaloy, with plastic yielding (ballooning) and perforation characteristics similar or better than zircaloy (Yamamoto et al., 2015; Kato et al., 2017). Without the autocatalytic heat-up experienced by zircaloy; however, the onset of deformation, yielding and perforation should occur later in the postulated event, contributing to a lengthened coping period for retaining FPs.

Calculations have been performed to show the increase of coping time by the use of FeCrAl cladding instead of zirconium alloy (Robb, 2015). In this analysis, coping time (more details on the definition of the fuel coping time are given in Part I of this state-of-the-art report) was defined as the allowed time before the fuel rod loses its coolable geometry (melts) or the time at which the reactor vessel may breach by the increase in its internal temperature and pressure. According to these calculations, the increase in the coping time for FeCrAl/UO_2 with respect to the current zircaloy/UO_2 system is shown in Figure 11.1.

Figure 11.1. Additional margin to onset of fuel failure for FeCrAl/UO_2 compared to zircaloy/UO_2 considering station blackout after loss of direct current (DC) power
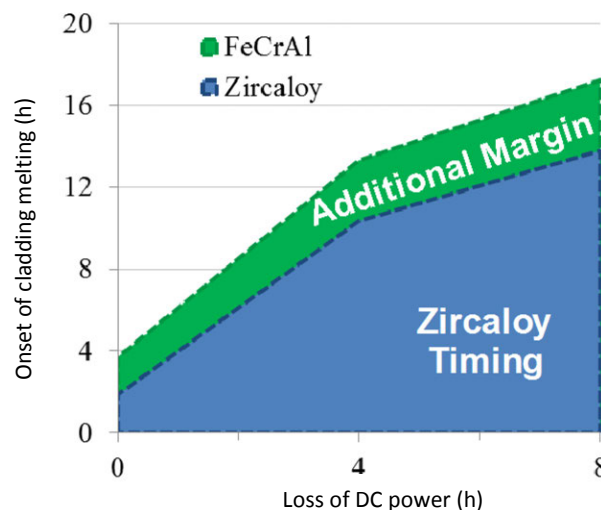
Source: Robb, 2015.

X-axis in Figure 11.1, is the time at which DC power is lost (not the duration of the loss). The margin increases for delayed accidents can be attributed to the decrease in the decay heat with time.

Additional evaluations should be considered in the future to further refine such estimates; however, this estimate identifies an incremental increase in coping time of two to four hours that improves the overall plant safety (Robb, 2015). It is important to note that the hydrogen released to the reactor environment is substantially reduced, significantly reducing the potential for catastrophic containment breaches.

A fuel rod assembly or component in a power reactor

The initial plan by the US Department of Energy was to have a design article or component fabricated using FeCrAl cladding into a power reactor by December 2022. However, current plans by GE/GNF and Southern Nuclear are to insert the first FeCrAl fuel prototype into a commercial reactor in the United States in 2018. The plant selected for the first effort is Southern Nuclears Plant Hatch, unit 1 during the Cycle 29 refuelling outage (1Q18). The plan is to insert 2-8 lead fuel rods (LFRs) into each of 2-4 GNF2 lead test assemblies (LTAs) as segmented rods. Two FeCrAl alloys are targeted for installation with approximate compositions as follows: APMT – Fe-21Cr-5Al-3Mo (Sandvik) and C26M – Fe-12Cr-6Al-2Mo-0.3Y (ORNL; Stachowski et al., 2017). APMT and C26M are the names of given alloys.

As stated previously, general corrosion and electrochemical studies (cladding-coolant compatibility) showed that FeCrAl alloys behave as well as known materials in the nuclear power industry such as 304SS and alloy X-750. On the other hand, FeCrAl is far superior to 304SS/X-750 regarding its resistance to environmentally-assisted cracking. In general, FeCrAl alloy cladding materials appear to be sufficiently compatible with existing fuel design basis that additional testing prior to LFR/LTA insertion is minimal. There will be useful information on irradiation performance from the ATF-1 that will be helpful in characterising the LFR design to apply to a commercial reactor. A few noteworthy but relatively straightforward additional tests include post-LOCA quench tests for ductility, crud deposition and wear tests. The testing and examinations necessary to support final fuel designs as a commercial product are expected to be significant. It is anticipated that tests that mitigate significant technical risks, such as those outlined in other sections, should be accelerated within future FeCrAl development programmes.

GE has engaged Exelon and Southern Nuclear utilities, which have shown interest in the FeCrAl cladding concept to work together towards the goal to insert lead fuel rod assemblies into operating commercial reactors. There are plans for insertion of segmented rods with FeCrAl cladding at the Hatch Plant operated by Southern Nuclear in Georgia (US) and in the Clinton Plant operated by Exelon. GE has deployed several test assemblies for material development (both cladding and fuel) in commercial reactors and will leverage that expertise and experience for these LFRs/LTAs, including techniques to facilitate sample retrieval and post-irradiation examination, such as segmented rod assemblies. This background has also provided knowledge of the required approach to take for licensing, in particular treatment of safety basis analyses for fuel systems with substantially increased uncertainties. GE is interacting with the US Nuclear Regulatory Commission to document the procedures and objectives for the insertion of the FeCrAl fuel components into Hatch and probably Clinton power plants.

Economic and plant impact of the proposed FeCrAl fuel system

The FeCrAl alloy concept is straightforward in the sense that one metal is being replaced by another. This is realistic since fuel-clad with type 304SS (FeCrNi) has been previously used in commercial power plants in the United States and elsewhere (Strasser et al., 1982). It is anticipated that the production cost of the FeCrAl cladding will be equal to or lower than the current zirconium alloy cladding once a mature supply chain is established. As mentioned previously, use of FeCrAl cladding results in a fuel cycle cost increase because of higher neutron absorption of the cladding material. However, it is anticipated that relaxation of regulatory requirements due to much improved fuel cladding performance under post critical heat flux or accident conditions may allow for

significant reduction in plant operating cost that may balance the fuel cycle cost impact of FeCrAl. The geometry of a fuel assembly using FeCrAl cladding will be the same as a fuel bundle using zirconium alloy cladding. Hence, no changes in-reactor equipment used to handle and store the fuel will be required. Fuel rods with FeCrAl cladding will maintain their geometry at the end of their useful life in the reactor; will be retrievable with current methods and will survive storage in spent fuel storage pools and subsequently in longer term dry storage.

Fabrication

The fuel pellets targeted for use with the FeCrAl alloy clad fuel assembly will be the same as used in current LWR fuel: UO_2, with a maximum of 5% enrichment of ^{235}U.

The FeCrAl/UO_2 fuel rod is compatible with current large-scale production technology. Pellet fabrication would remain the same as in the current process. The next phase of FeCrAl development will be fabrication of long (e.g. 4-5 m), thin-walled (e.g. 350 μm) tubes for lead fuel rod assemblies. Although the cladding fabrication process is yet untested for large-scale production, there does not appear to be a significant barrier for production quantities of the cladding. Current trials using both pilgering and drawing produced tubes of both APMT and C26M that are approximately 3 metres long and with a wall thickness of 0.4 mm. For the first insertion into a commercial reactor in 2018, the plan is to use segmented rods of FeCrAl of approximately 1 metre long each and with two wall thicknesses of 0.4 mm and 0.6 mm. Preliminary trials of the ATF programme demonstrated compatibility of FeCrAl with existing welding, manufacturing and quality practices used with current zircaloy-based rod assembly systems.

The fabrication processes for the FeCrAl/UO_2 system will be very similar to current LWR fuel fabrication processes (pilgering/extruding/drawing, heat treatments, welding, non-destructive evaluation [NDE] techniques, etc.), which are mature and well-understood. Issues complying with current nuclear industry quality and performance standards are not anticipated.

It is anticipated that the path to United States NRC licensing for an FeCrAl alloy fuel rod concept would be direct and achievable. It is understood that the US NRC fuel licensing process for cladding is currently zirconium centric, but this does not prevent adjustment for an FeCrAl alloy. The regulatory requirements governing safety limits for the core are well understood and FeCrAl/UO_2 fuel systems, in general, perform equivalent to or better than a zirconium/UO_2 fuel system with respect to plant safety. The licensing processes to be employed to support the insertion of LFR/LFAs are in place and can be used to meet the ATF programme objectives, with the caveat that a licensing exemption to 10CFR50.46 will be required.

FeCrAl/UO_2 fuel rod systems will have minimal or no impact in the handling of the fuel, shipping requirements and/or plant operations. It is expected that standard analyses techniques applied to zirconium alloy systems may be used substituting FeCrAl-specific properties to demonstrate acceptable performance under shipping and handling conditions, although licensing for shipping of the LFR/LFAs will need to be completed as well as in-core licensing. In particular, ensuring that unirradiated cladding exhibits acceptable ductility under possible very cold temperatures (below freezing) is necessary. However, this could likely be possible through a special letter of authorisation for limited shipments rather than through a change to the licence certificate.

Normal operation and AOOs

A significant population of the US BWR fleet is refuelled with reloads at a maximum practical enrichment. This maximum practical enrichment is defined by the allowable peak pellet enrichment (<5 w/o ^{235}U) and efficiency considerations associated with

peaking and axial blankets. This maximum practical enrichment results in variation in achievable batch average discharge exposures ranging from the low to high 40s (i.e. there is approximately 15% of burn-up variation) that depends upon power density and a variety of other core parameters. The higher thermal neutron absorption cross-section of FeCrAl results in a reduction in total exposure without some compensating measure. This is expected to materialise as a reduction in discharge exposure, a reduction in cycle length, or an increase in power coast down, or a combination of the three. Ultimately, this is simply one element of the overall economic assessment of a fuel system that includes FeCrAl as a cladding material that is expected to improve as it evolves. While some reduction in total exposure capability is expected in the first generation of an FeCrAl fuel system, it is expected that it can be considered adequate and part of the overall economic impact and optimisation.

Thermal-hydraulic interaction

Thermal-hydraulic interactions are primarily a function of the fuel assembly geometry (e.g. lattice spacing, tie plates and spacer/grids), which will remain unchanged for an LFA/LRA. There are some thermal-hydraulic effects of the material (e.g. emissivity, rewet temperature, etc.) but these effects are relatively minor and inconsequential for LFR/LFA applications. Figure 11.2 shows BNL modelling results for the relative heat flux, average fuel temperature and the coolant temperature as a function of the height of an average PWR fuel rod (Rebak, Brown and Terrani, 2015; Brown, Todosow and Cuadra, 2015). Little or no effect is seen when the zircaloy/UO_2 system is replaced by the FeCrAl/UO_2 system. Boiling and critical heat flux tests are planned and include testing with an alumina layer for tritium retention.

Mechanical strength, ductility (beginning of life and post-irradiation)

Under normal operational states, the mechanical strength of FeCrAl alloys is observed to be superior to the mechanical strength of zircaloy (at the beginning of life [BOL] – without irradiation). Figure 11.3 shows that the yield stress of APMT is approximately four times higher than for zircaloy-2, the UTS is approximately three times higher and the elongation to failure for the two metals is comparable (Yamamoto et al., 2015; Mehan, Wiesinger, 1961; Kanthal, n.d.).

Data is currently being generated to assess the mechanical strength of optimised FeCrAl at the end of life conditionsi.e. for an irradiation level of 15 dpa (Field et al., 2015; Gussev, Field and Yamamoto, 2016; Field et al., 2017). However, it is expected that mechanical properties, such as strength will increase and ductility will decrease, similarly to 304SS and other metallic alloys. This is primarily due to irradiation-induced defects such as dislocation loops (Field et al., 2017) and Cr-rich alpha precipitates (Briggs et al., 2017; Edmondson et al., 2016). Such changes in properties can be anticipated and BOL properties will conservatively bound LFA/LFR applications until characterisation is performed in future FeCrAl development tasks.

It is known that zirconium alloys absorb hydrogen during service and can react with hydrogen to form stable hydrides that tend to decrease the ductility of the cladding. FeCrAl alloys do not react with hydrogen to form stable hydrides; as a result, hydrogen has a higher mobility in FeCrAl alloys and will not accumulate in the alloy to reduce its mechanical properties by an embrittlement mechanism.

Creep of the FeCrAl cladding under irradiation is under investigation but no issues to prevent use are anticipated. Specifically, it is expected that both the thermal and irradiation creep of FeCrAl alloys is less than zirconium-based alloys. However, combined with pellet creep, stress accumulation during pellet-cladding mechanical interaction is not expected to go beyond the yield strength of these alloys.

A test was conducted in the OSIRIS reactor in which HT9 steel (12Cr1Mo0.5W) was exposed to PWR water (155 bars) with less than 10 ppb oxygen at 325°C for up to 361 days or 9.3 dpa (Brachet et al., 2002). Results show that after 3.5 dpa irradiation, the reduction of area decreased from 50% to 25%; however the elongation to failure was approximately 8% for the irradiated and non-irradiated conditions (Brachet et al., 2002).

Figure 11.2. Thermal-hydraulics for an average PWR rod shows no major impacts when replacing zircaloy-cladding with FeCrAl
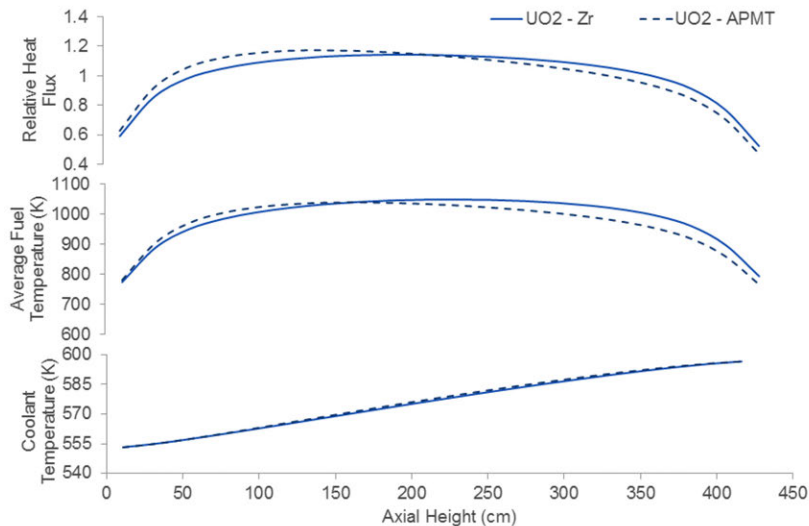
Source: Rebak, Brown and Terrani, 2015.

Figure 11.3. Yield strength of zircaloy-2 and APMT
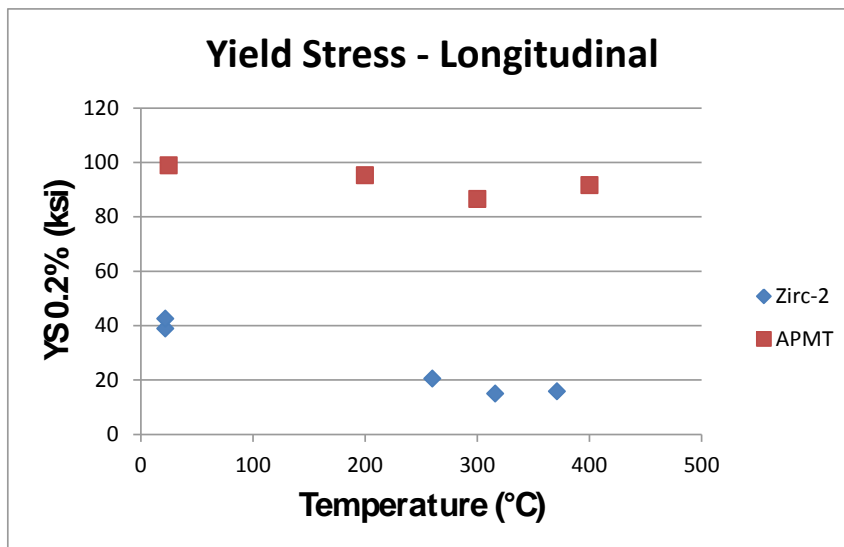
Source: Stachowski et al., 2017.

**Figure 11.4. Mechanical properties of zircaloy-2 and APMT
without irradiation (at the beginning of life)**
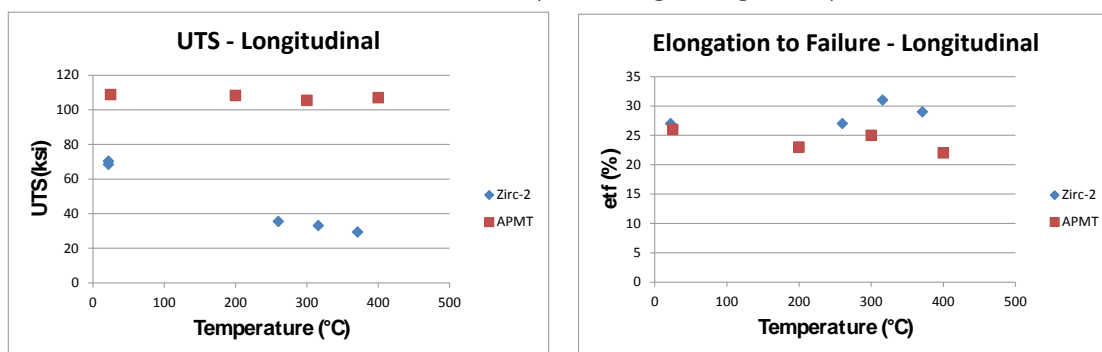
Source: Stachowski et al., 2017.

Thermal behaviour (conductivity, specific heat, melting)

Table 11.2 shows comparatively the thermal conductivities, the specific heats and the melting points for zircaloy-2 and APMT (Kanthal, n.d.; Whitmarsh, 1962). The thermal conductivities of the metals are comparable. APMT has a higher specific heat than zircaloy-2 that decreases the peak cladding temperature during a large-break LOCA scenario (more heat, stored energy in the fuel, is needed to push the cladding temperature up). The melting point of zircaloy-2 is approximately 350°C higher than the melting point of APMT, however, this increase in melting point has little impact on fuel design since zircaloy-cladding oxidises rapidly at high temperatures below the melting point of FeCrAl alloys such as APMT.

Table 11.2. Thermal properties of zircaloy-2 vs. commercial FeCrAl (APMT)

Alloy	Thermal conductivity (W/m.K)	Specific heat (kJ/kg.K)	Melting point (°C)
Zircaloy-2	14.5-14.2 (25°C to 425°C)	0.285-0.368 (25°C to 700°C)	1 849
APMT	11-21 (50°C to 600°C)	0.48-0.71 (20 to 600°C)	1 500

Neutronic behaviour (peaking factors, power levels)

Preliminary physics analyses indicate that lattice power distributions for an FeCrAl clad fuel bundle are similar to conventional fuels. As such, current nuclear design practices are considered applicable. It is noted, however, that the improved properties of FeCrAl may result in more favourable specified acceptable fuel design limits (SAFDLs) such that overall flexibility is improved.

Chemical compatibility, stability (e.g. oxidation behaviour)

FeCrAl alloys offer superior corrosion resistance in high-temperature water and in steam (Rebak, 2015). For comparison, an experiment was performed where coupons of zircaloy-2 and APMT were exposed to high-temperature water simulating conditions both of BWR and PWR coolant conditions for one year. Figure 11.5 shows a comparison of the oxides formed on the zircaloy-2 and APMT coupons after exposure to BWR simulated water chemistry (2 ppm O_2 at 288°C; Ellis, Rebak, n.d.). Similarly, Figure 11.6 shows the oxide formed on APMT coupons exposed to PWR simulated water chemistry (3.75 ppm hydrogen at 330°C). Both FeCrAl alloy coupons had a thin compact oxide on their surface that was approximately four to five times thinner than the oxide produced for zircaloy. Also, coupons of APMT and zircaloy-2 were exposed side by side in 100% steam at 800°C for 24 hours. The oxidation rate of APMT was approximately three orders of magnitude lower than that of zircaloy-2.

Figure 11.5. Cross-sections of coupons exposed to BWR
simulated conditions for one year (288°C + 2 ppm O$_2$)

Zr-2, Oxide thickness ~ 1.23 µm   APMT, Oxide thickness ~ 0.278 µm
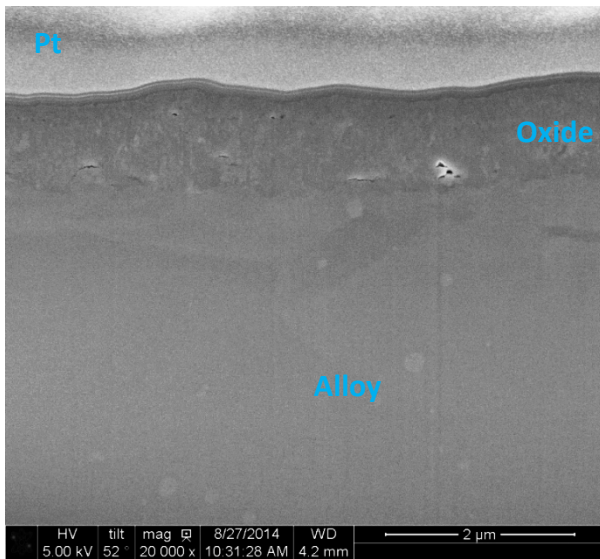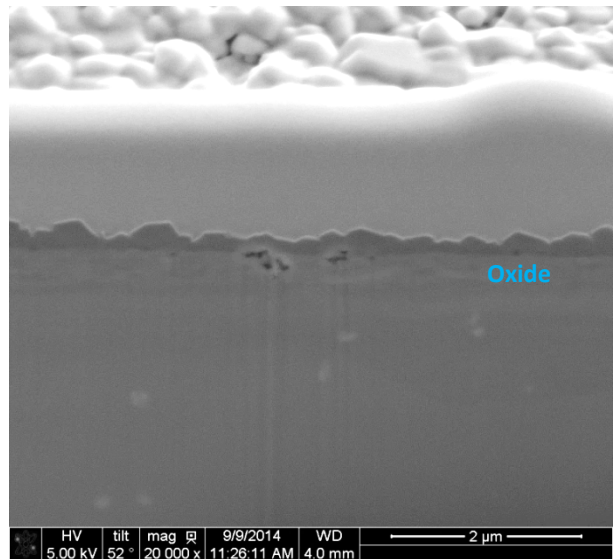
Source: Ellis, Rebak, n.d.

Figure 11.6. Cross-sections of APMT coupon exposed to PWR
simulated conditions for one year (330°C + 3.75 ppm H$_2$)
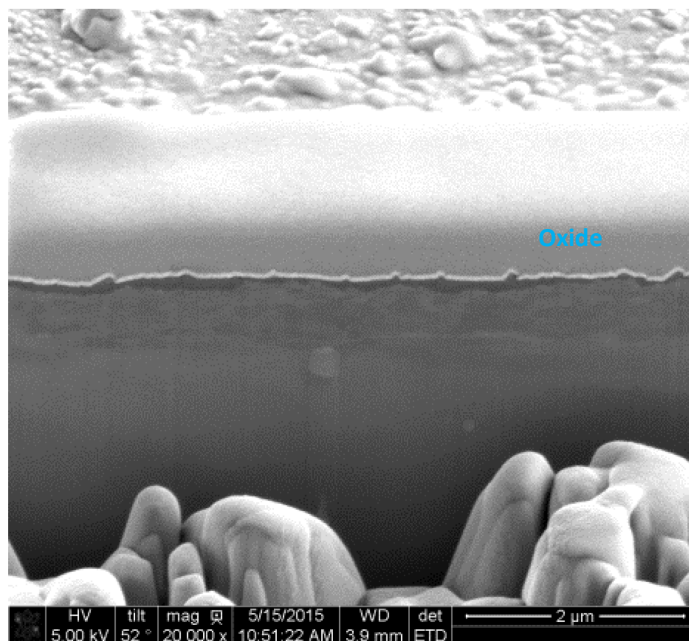
Source: Ellis, Rebak, n.d.

Chemical compatibility with an impact on coolant chemistry

There are no anticipated issues regarding chemical compatibility between the FeCrAl cladding and the coolant and no impacts on the coolant chemistry, i.e. no changes are anticipated for the coolant chemistry for either BWR or PWR LWRs. However, it was also reported in "Behavior of different austenitic stainless steels, conventional, reduced activation (RA) and ODS chromium-rich ferritic-martensitic steels under neutron irradiation at 325°C in PWR environment" (Brachet et al., 2002) that selective release of Mo and W into the coolant was observed for both in-pile and out-of-pile experiments (Brachet et al., 2002). Out-of-pile tests performed at GE at 288°C and 330°C found that FeCrAl (APMT) formed an oxide layer on the surface that was free from Mo and Al, suggesting that in exposure to water, these elements are selectively released into the coolant (Rebak, Larsen and Kim). Under hydrogen atmosphere the oxide film was only chrome oxide suggesting that iron is also selectively dissolved into the water, together with Mo and Al (Rebak, Larsen and Kim). It should be noted that the release of highly radioactive species in the coolant may have an impact on the filters' maintenance (dose consequences) and disposal.

Fission product behaviour

The production of fission gases and the fission gas pressure increase inside the cladding will be the same as for UO_2 fuelled rods operating at similar temperatures and irradiation conditions as there is no change in fuel pellet material.

Based on previous experience, it is likely that the use of FeCrAl cladding has a potential risk to result in a higher concentration of tritium in the coolant. The tritium release may be minimised by pre-oxidation of the cladding at 1 200°C for two hours, which will form a continuous layer of alpha alumina on the surface. An alumina layer may reduce the hydrogen permeation rate by more than three orders of magnitude (Levchuk et al., 2008). More studies are needed in this area. Figure 11.7 shows that when APMT is oxidised in steam at 1 200°C for 2 hours, a continuous and compact layer of alumina forms on its surface. This compact layer may minimise tritium diffusion through the cladding wall from the ID of the fuel rod to the coolant. Moreover, the oxide layer formed by corrosion with coolant water may act as an inherent barrier for tritium release to the coolant (Sakamoto et al., 2017). More studies are also needed in this area.

**Figure 11.7. Cross-sections of APMT coupon exposed to 100%
superheated steam at 1 200°C for 2 h**
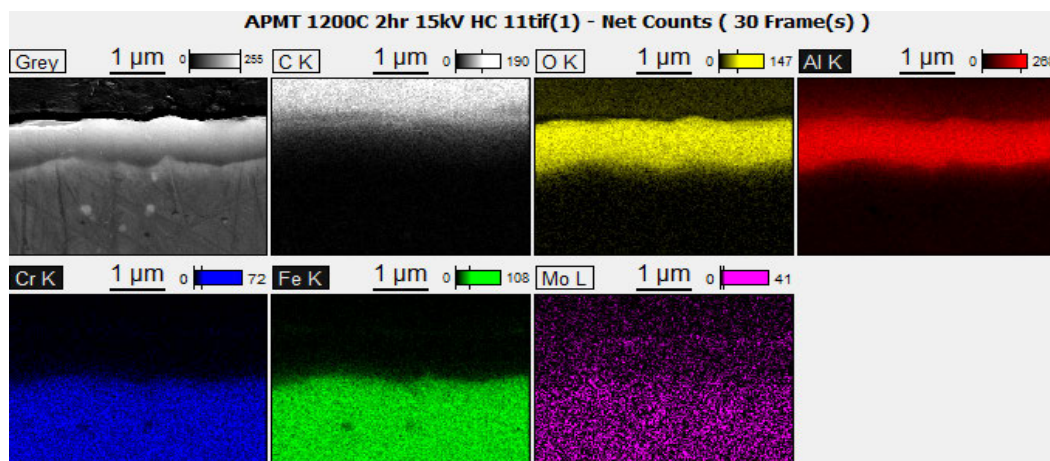
Note: A continuous 1 μm thick layer of alumina forms on its surface.

Source: Rebak et al., 2017.

Potential impacts on plant systems' margins and operational practices (such as manoeuvring restrictions)

Operational flexibility is largely influenced by the myriad limits placed upon the fuel (e.g. LHGR, MCPR, PCI risk reduction, etc.). Given the improved mechanical properties of FeCrAl, improved flexibility derived from more favourable thermal limits may be expected. It is noted that further investigation into the susceptibility of FeCrAl cladding to PCI failures is needed. One notable benefit that is anticipated is FeCrAl's resistance to debris fretting and grid-to-rod fretting compared to zirconium alloy cladding. While further study is needed in this regard, this cladding material may finally be able to provide the industry with a tool to use for its zero leaker initiative, driven by the Institute of Nuclear Power Operations (INPO).

Potential impacts on refuelling (e.g. twisting and bowing due to irradiation growth)

No impacts regarding refuelling since it is anticipated that the FeCrAl cladding will not suffer twisting and/or bowing or change in geometry during irradiation in the reactor.

Design-basis accidents

Reactivity control systems interaction

As noted above, a fuel system with FeCrAl alloy cladding behaves similarly to conventional fuel with respect to the control system SCRAM function. Faster pellet strain rates and similar final strain values have been calculated for FeCrAl clad UO_2 when compared with zirclaoy clad UO_2 (Brown et al., 2017). It is also expected that the core response to an SLCS (stand-by liquid control system) actuation is also normal.

Mechanical strength, ductility (as a function of when the DBA occurs, beginning of life and after irradiation), resistance to fuel rod fragmentation upon re-flooding (post-quench ductility)

Mechanical strength of the FeCrAl cladding after irradiation needs to be investigated, but no issues to prevent use are anticipated. Also, the effect of quenching on irradiated FeCrAl cladding needs to be investigated. Quench tests are ongoing.

Thermal behaviour (conductivity, specific heat, melting, swelling and PCI)

The FeCrAl cladding melts at 1 500°C, which is a temperature higher than the temperature limit for DBA. Data on thermal behaviour of several materials (including FeCrAl) have been published (Ott, Robb and Wang, 2014). Data of swelling and PCI for FeCrAl are not currently available; however, tests are being conducted at the ATR to determine the changes in geometry of FeCrAl rods and PCI effects.

Chemical compatibility, stability (including hydrogen pickup, corrosion, high-temperature steam interaction), chemical interactions for eutectics and defining the timing associated with the accident progression

FeCrAl alloys are resistant to attack by steam up to their melting point of 1 500°C. The elements in the alloy do not react with hydrogen to form stable hydride compounds. As temperature increases, the solubility of hydrogen in the alloy increases; however, the diffusion rate of hydrogen also increases since the hydrogen is not bound. At the temperatures of DBA conditions, there are no stable eutectics that would form by reaction of the FeCrAl cladding with the fuel or other components in the reactor (Sakamoto et al., 2016).

Fission product behaviour (including fission gas pressure and fission product retention)

The production of fission gases and the fission gas pressure increase inside the cladding will be the same as for UO_2 fuelled rods operating at similar temperatures and irradiation conditions as there is no change in fuel pellet material.

Combustible gas production

Reaction of FeCrAl with steam may result in the production of hydrogen gas, which is combustible. However, in the temperature regime of DBA, little hydrogen gas production is anticipated since FeCrAl is highly resistant to reaction with steam.

Potential impacts on plant systems margins and operational practices (such as ECCS capabilities)

Diminished concerns of exothermic oxidation reaction with steam associated with FeCrAl alloys may allow higher cladding temperatures during postulated design-basis events such as LOCA. Higher allowed accident temperatures translate to greater times for ECCS injection to affect core cooling, and system margins will be expanded. Use of FeCrAl alloys as cladding will not remove the need for engineered safety systems, but performance and maintenance requirements may change, along with longer time periods for limited conditions of operation, by leveraging the expanded margin. Cost savings for plant operators are possible when such requirement on system performance and surveillance are lowered.

Design extension conditions

Mechanical strength, ductility (as a function of when the DBA occurs, beginning of life and after irradiation), resistance to fuel rod fragmentation upon re-flooding (post-quench ductility)

The HT mechanical behaviour of FeCrAl for design extension conditions is excellent. The leading alloys (APMT, C26M and FeCrAl-ODS) were designed to offer superior mechanical properties at high temperatures. Figures 11.8 and 11.9 show the strength at high temperatures and the creep strength at 1 000°C of FeCrAl-ODS fuel claddings, respectively. It is demonstrated that the FeCrAl-ODS retains its strength even at high temperatures (Kato et al., 2017). Figure 11.10 shows the stress rupture at the BOL as a function of the Larson-Miller Parameter (LMP; LMP=T(C + log t), where t is the time in hours, T is the temperature in K and C is a constant), illustrating the two regimes where data are available.

Figure 11.8. Strength of FeCrAl-ODS fuel claddings at high temperatures
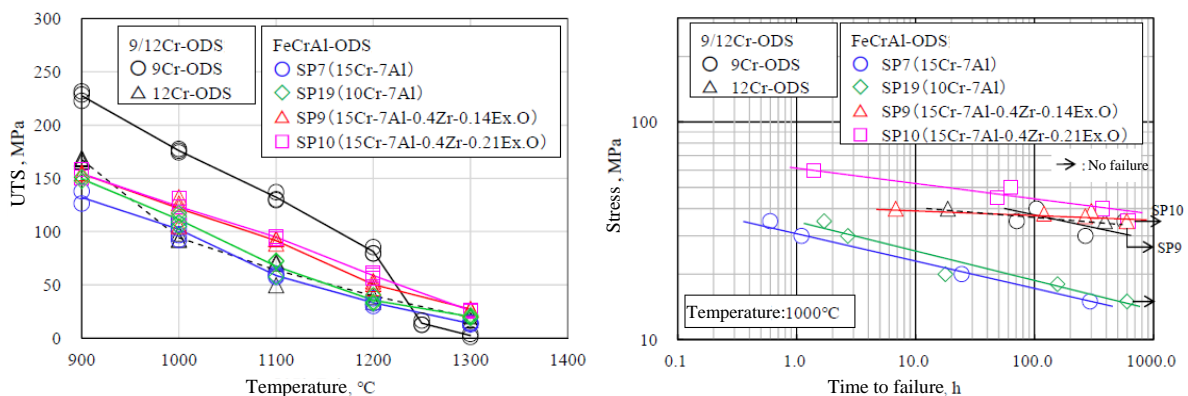
Source: Sakamoto et al., 2017.

Figure 11.9. Creep stress-rupture Larson-Miller Parameter for zircaloy-2 and APMT

LMP – temperature (K) and time (h)
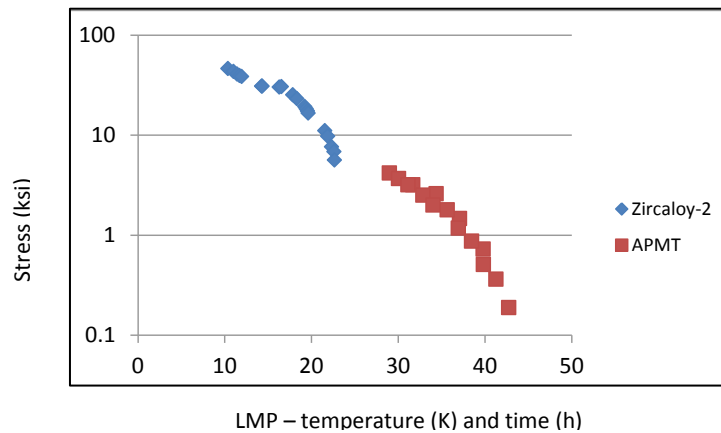
Source: Stachowski et al., 2017.

Mechanical data for APMT under irradiated conditions is not available, but there are no anticipated issues to prevent its use. Similarly, the resistance to fuel rod fragmentation (cladding burst) after flooding is not available for either at the BOL or under irradiated conditions.

Thermal behaviour (conductivity, specific heat, melting, swelling, PCI)

Adding to the data in Table 11.2, at 1 200°C the thermal conductivity of APMT is 29 W/m.K and the specific heat capacity at 1 200°C is 0.70 kJ/kg.K (Kanthal, n.d.). Data for zircaloy-2 in the 1 200°C temperature range are unavailable. Results for swelling and PCI for zircaloy-2 and APMT will be obtained following ATF planned tests at ATR/TREAT.

Chemical compatibility (fuel cladding), stability

Chemical compatibility between the fuel and the FeCrAl cladding under irradiation are currently unavailable. Out-of-pile tests showed that fuel and the cladding will be fully compatible at temperatures in the range of design extension conditions (Sakamoto et al., 2016).

Fission product behaviour (including fission gas pressure and fission product retention)

The production of fission gases and the fission gas pressure increase inside the cladding will be the same as for UO_2 fuelled rods operating at similar temperatures and irradiation conditions as there is no change in fuel pellet material.

Data is unavailable for FeCrAl-UO_2 on FP gas pressure and FP retention. Results from the planned ATF tests at ATR/TREAT may provide data in this regard, both for the FeCrAl cladding as well as the zircaloy-2 cladding for which data is also currently unavailable. LOCA heat-up tests for FeCrAl are also required to validate ballooning and perforation behaviour as like, or perhaps better than zircaloy.

Combustible gas production

When the metallic cladding reacts with superheated steam indesign extension conditions, the reaction produces the metal oxide and releases combustible hydrogen gas. One of the major advantages of FeCrAl compared to zircaloy alloys is the several orders of magnitude lower kinetics of oxidation with steam of the former, which will produce a much lower amount of hydrogen (Robb, 2015). Figure 11.10 shows the Arrhenius plots for the oxidation kinetics of zirconium alloy and APMT (FeCrAl) (Terrani, Zinkle and Snead, 2014). At 1 200°C, the oxidation rate of the FeCrAl alloys is approximately 1 000 times

lower than that for zirconium alloys. A slower reaction of FeCrAl with steam will therefore reduce the rate of hydrogen generation (Robb, 2015). This will decrease the rate of pressure build up inside the pressure vessel and increase the time for hydrogen release into the environment.

Figure 11.10. Arrhenius plots to show that the kinetics of oxidation of APMT is three orders of magnitude lower than the kinetics of oxidation of zirconium base alloys
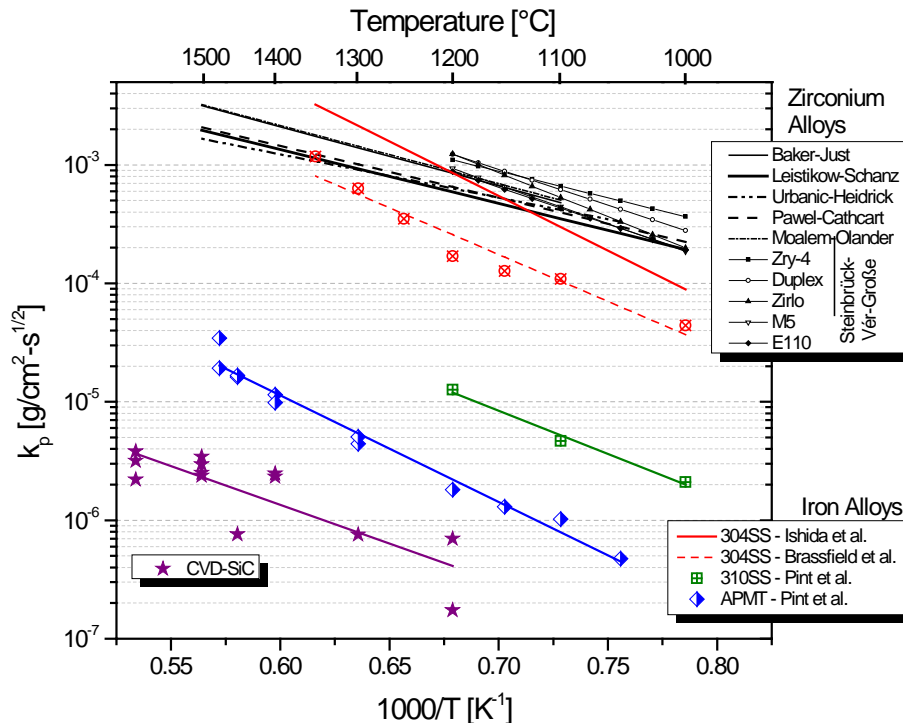
Source: Terrani, Zinkle and Snead, 2014.

Intensive HT oxidation tests of FeCrAl coupons in KIT demonstrated that the behaviour of the alloys was significantly influenced by the composition and the applied heating schedules (Tang et al., 2016). Critical amounts of chromium and aluminium were needed to establish a protective alumina scale at various temperatures during isothermal tests. Catastrophic oxidation, i.e. rapid and complete consumption of FeCrAl alloys without formation of protective alumina scale, was observed when as-received samples were isothermally oxidised above 1 300°C or during ramp tests with fast heating rates to high temperature in steam. Pre-oxidation at low temperature or during low heating rates during transient tests results in the formation of sufficiently thick alumina scale avoiding the catastrophic oxidation of the alloys and providing protective effect beyond the melting temperature. Addition of reactive elements (e.g. yttrium) can improve the steam compatibility of FeCrAl alloys, especially during ramp tests. Tube specimens of APMT which were pre-exposed to HT water for 73 days and then subjected to 4 h at 1 200°C in steam had the same oxidation resistance as non-pre-exposed tubes (Rebak, Jurewicz and Kim, 2017).

Figure 11.11 shows a typical hydrogen production rate during isothermal tests at different temperatures (left) and inserted post-test appearance of model alloy P14 (failure at 1 400°C) and commercial alloy Kanthal APM (protective at 1 500°C) (right).

Figure 11.11. Hydrogen production rate during the oxidation of FeCrAl alloys at T>1 200°C
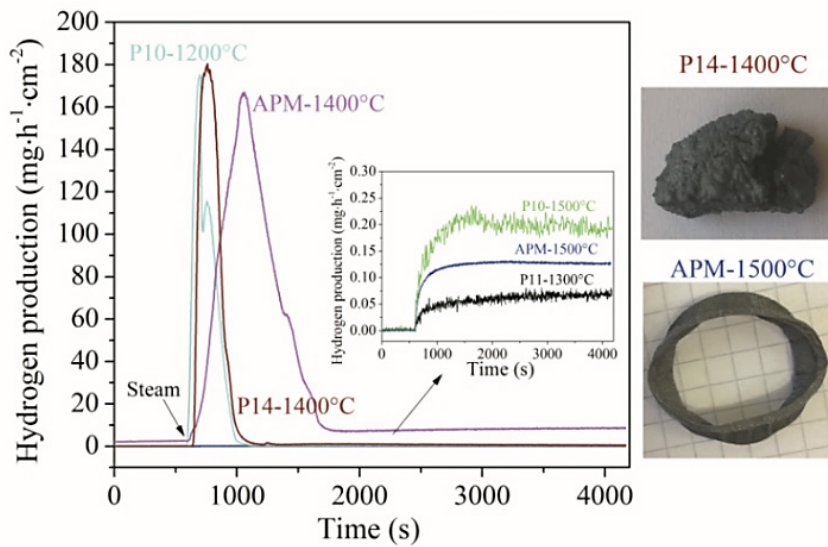
Note: P10-Fe12Cr5Al, P11-Fe12Cr8Al, P14-Fe16Cr8Al0.3Y, APM-Fe22Cr5.8Al (wt.%).

Source: Terrani, Zinkle and Snead, 2014.

Potential impacts on DEC protection equipment and strategy (e.g. FLEX)

Deployment of FeCrAl alloy cladding will substantially reduce combustible gas generation, as shown above, thereby reducing reliance on systems such as hydrogen igniters and passive autocatalytic recombiners placed throughout the containment and reactor building. Containment venting strategies could also become more flexible since containment pressures are reduced when the partial pressure of hydrogen is lowered and the need for a hardened vent back fit is lessened since the combustible gas loading is substantially reduced. A need remains, however, for alternate cooling sources (e.g. FLEX equipment) because sustained decay heat removal will be needed. Operational strategy, for example timing of injection and staging of additional FLEX equipment, would become more flexible with the higher cladding temperatures allowed with FeCrAl.

Used fuel storage, transport, disposal (include commentary on potential for reprocessing)

Mechanical strength and ductility

It is expected that spent fuel bundles with FeCrAl cladding will be easily removed from the reactor and transported first to cooling pools and later to dry cask storage. Their mechanical strength and ductility should be satisfactory for the transport and handling of used fuel rods and assemblies. There is confidence that fuel bundles will maintain their geometry and acceptable material conditions through operation and storage. It is anticipated that there will be no loss of mechanical properties for the FeCrAl fuel rods during >100 years of dry casket storage.

Thermal behaviour

FeCrAl alloys perform as well as or superior to existing zirconium-based alloy systems in terms of heat transfer and heat removal for spent fuel rods. There are no anticipated issues regarding the thermal behaviour for fuel rod designs using FeCrAl alloy cladding.

Chemical stability

Because of their chromium content, the FeCrAl alloy will remain passive in cooling pools. The considered FeCrAl alloys have enough chromium and molybdenum to provide protection against corrosion in the cooling pools. FeCrAl does not react with hydrogen to produce hydrides that may render the cladding brittle. That is, hydrogen does not accumulate chemically in the FeCrAl cladding. FeCrNi alloys have been used in the past as cladding for commercial fuel and they are currently under decades long safe storage in the United States (Cunningham et al., 1996; Rebak, Huang, 2015).

Fission product behaviour

There are no anticipated issues with chemical attack of the cladding due to fission by-products. However, because of the maturing nature of the FeCrAl composition, additional studies should be performed during future ATF programmes to evaluate the behaviour of FPs and the chemical interaction with the cladding.

Long-term stability under dry cask storage and transport conditions

FeCrAl clad fuel rods may be conventionally reprocessed. There are no major differences from the current zircaloy/UO_2 system.

References

Ahmedabadi, P.M. and G.S. Was (2016), "Stress corrosion cracking of ferritic-martensitic steels in simulated boiling water reactor environment", *Corrosion*, Vol. 72, January 2016, pp. 66-77

Brachet, J.-C. et al. (2002), "Behavior of different austenitic stainless steels, conventional, reduced activation (RA) and ODS chromium-rich ferritic-martensitic steels under neutron irradiation at 325°C in PWR environment", *Effects of Radiation on Materials: 20th International Symposium, ASTM STP* 1405, S.T. Rosinski, M.L. Grossbeck, T.R. Allen and A.S. Kumar, EDS., *American Society for Testing and Materials,* West Conshohocken, PA.

Briggs, S.A. et al. (2017), "A combined APT and SANS investigation of α phase precipitation in neutron-irradiated model FeCrAl alloys", *Acta Mater*., Vol. 129, pp. 217-228.

Brown, N.R. et al. (2017), "The potential impact of enhanced accident tolerant cladding materials on reactivity initiated accidents in LWRs", *Ann. Nucl. Energy.,* Vol. 99, pp. 353-365.

Brown, N.R., M. Todosow and A. Cuadra (2015), "Screening of advanced cladding materials and UN–U 3 Si 5 fuel", *J. Nucl. Mater.,* Vol. 462, pp. 26-42.

Causey, R.A., R.A. Karnesky and C.S. Marchi (2012), "Tritium barriers and tritium diffusion in fusion reactors", *Compr. Nucl. Mater*. Vol. 4, Elsevier, pp. 511-549.

Cunningham, M.E. et al. (1996), *Evaluation of Expected Behavior of LWR Stainless Steel-clad Fuel in Long-term Dry Storage,* Final report, Electric Power Research Inst., Palo Alto, CA, Pacific Northwest Lab., Richland, WA.

Edmondson, P.D. et al. (2016), "Irradiation-enhanced α precipitation in model FeCrAl alloys", *Scr. Mater.,* Vol. 116, pp. 112-116.

Ellis, D.D. and R.B. Rebak (n.d.), "Passivation characteristics of ferritic stainless materials in simulated reactor environments", Pap. C2016-7452, Corros. (NACE Int. Houston, TX).

Field, K.G. et al. (2017), "Mechanical properties of neutron-irradiated model and commercial FeCrAl alloys", *J. Nucl. Mater.*

Field, K.G. et al. (2017), "Heterogeneous dislocation loop formation near grain boundaries in a neutron-irradiated commercial FeCrAl alloy", *J. Nucl. Mater.* Vol. 483, pp. 54-61.

Field, K.G. et al. (2015), "Radiation tolerance of neutron-irradiated model Fe-Cr-Al alloys", *J. Nucl. Mater.*, Vol. 465, pp. 746-755.

George, N.M. et al. (2015), "Neutronic analysis of candidate accident-tolerant cladding concepts in pressurized water reactors", *Ann. Nucl. Energy,* Vol. 75, pp. 703-712.

Gussev, M.N., K.G. Field and Y. Yamamoto (2016), *Preliminary Analysis of the General Performance and Mechanical Behavior of Irradiated FeCrAl Base Alloys and Weldments*, ORNL, Oak Ridge, TN (United States). High-Flux Isotope Reactor (HFIR).

Hu, X. et al. (2015), "Hydrogen permeation in FeCrAl alloys for LWR cladding application", *J. Nucl. Mater.*, Vol. 461, pp. 282-291.

Kanthal APM and APMT (n.d.), "Tube Material Datasheet", AB Sandvik group, Sandviken, Sweden.

Kato, S. et al. (2017), "R&D of ODS ferritic steel cladding for maintaining fuel integrity at accident condition (3) – (2) Mechanical properties of FeCr- and FeCrAl-ODS steels at elevated temperature", *Proc. AESJ 2017 Spring Annu. Meet.*, p. 2J06.

Kim, Y.J. et al. (2015), "Environmental behavior of LWR accident tolerant candidate cladding materials under design conditions", Pap. C2015-5817, *Corros.* (NACE Int. Houston, TX).

Levchuk, D. et al. (2008), "Al-Cr–O thin films as an efficient hydrogen barrier", *Surf. Coatings Technol.,* Vol. 202, pp. 5043-5047.

Massey, C.P. et al. (2016), "Cladding burst behavior of Fe-based alloys under LOCA", *J. Nucl. Mater.*, Vol. 470, pp. 128-138.

Mehan, R.L. and F.W. Wiesinger (1961), *Mechanical Properties of Zircaloy-2,* KAPL-2110, Knolls Atomic Power Laboratory, Schenectady, NY, 1961.

Moalem, M. and D.R. Olander (1991), "Oxidation of zircaloy by steam", *J. Nucl. Mater.*, Vol. 182, pp. 170-194.

Ott, L.J., K.R. Robb and D. Wang (2014), "Preliminary assessment of accident-tolerant fuels on LWR performance during normal operation and under DB and BDB accident conditions", *J. Nucl. Mater.*, Vol. 448, pp. 520-533.

Pint, B.A. et al. (2013), "High temperature oxidation of fuel cladding candidate materials in steam-hydrogen environments", *J. Nucl. Mater.*, Vol. 440, pp. 420-427.

Pint, B.A. et al. (2015), "Material selection for accident tolerant fuel cladding", *Metall. Mater. Trans. E.*, Vol. 2(3), pp. 190-196.

Rebak, R.B. (2017), "Iron-chrome-aluminum alloy cladding for increasing safety in nuclear power plants", *EPJ Nuclear Sci. Technol.,* Vol. 3, DOI: 10.1051/epjn/2017029.

Rebak, R.B., M. Larsen and Y.-J. Kim (2017), "Characterization of oxides formed on iron-chromium-aluminum alloy in simulated light water reactor environments", published online: 28 June 2017, DOI: https://doi.org/10.1515/corrrev-2017-0011.

Rebak, R.B., N.R. Brown and K.A. Terrani (2015), "Assessment of advanced steels as accident tolerant fuel cladding for commercial LWRs", Paper 227, *17th International Conference on Environmental Degradation of Materials in Nuclear Power Systems – Water Reactors,* 9-12 August 2015, Ottawa, Ontario.

Rebak, R.B. and S. Huang (2015), "Anticipated improved performance of advanced steel cladding under long term dry storage of spent fuel", *ASME 2015 Press. Vessel. Pip. Conf.,* American Society of Mechanical Engineers, p. V007T07A042-V007T07A042.

Rebak, R.B., T.B. Jurewicz and Y.-J. Kim (2017), *Oxidation Resistance of FeCrAl in Simulated BWR and PWR Water Chemistries,* WRFPM 2017, Jeju Island.

Rebak, R.B. (2015), "Alloy selection for accident tolerant fuel cladding in commercial LWRs", *Metall. Mater. Trans*. E. 2, pp. 197-207.

Robb, K.R. (2015), "Analysis of the FeCrAl accident tolerant fuel concept benefits during BWR station blackout accidents", *Proc. 16th Int. Top. Meet. Nucl. React. Therm. Hydraul.*, pp. 1183-1195.

Sakamoto, K. et al. (2016), "Development of Ce-type FeCrAl-ODS ferritic steel to accident tolerant fuel for BWRs", *Proc. TopFuel2016*, pp. 673-680.

Sakamoto, K. et al. (2017), "Overview of Japanese development of accident tolerant FeCrAl-ODS fuel claddings for BWRs", *Proc. WRFPM2017*.

Stachowski, R.E. et al. (2017), *Progress of GE Development of Accident Tolerant Fuel FeCrAl Cladding,* WRFPM 2017, Jeju Island.

Steinbrück, M. et al. (2010), "Synopsis and outcome of the Quench experimental program", *Nuclear Engineering and Design,* Vol. 240 (7), pp. 1714-1727.

Strasser, A. et al. (1982), *An Evaluation of Stainless Steel Cladding for Use in Current Design LWRs*, NP-2642, Electric Power Research Institute, Palo Alto, CA, 1982.

Stuckert, J. et al. (2011), "Experimental and calculation results of the integral reflood test Quench-15 with ZIRLO™ cladding tubes in comparison with results of previous Quench tests", *Nuclear Engineering and Design,* Vol. 241 (8), pp. 3224-3233.

Tang, C. et al. (2016), "High-temperature oxidation behavior of kanthal APM and d alloys in steam", *International Congress on Advances in Nuclear Power Plants, ICAPP 2016,* 3, pp. 2112-2119.

Tang, C. et al. (2016), "High-temperature oxidation behavior of kanthal APM and d alloys in steam", *International Congress on Advances in Nuclear Power Plants,* ICAPP 2016, 3, pp. 2112-2119.

Terrani, K.A. et al. (2016), "Uniform corrosion of FeCrAl alloys in LWR coolant environments", *J. Nucl. Mater*., Vol. 479, pp. 36-47.

Terrani, K.A., S.J. Zinkle and L.L. Snead (2014), "Advanced oxidation-resistant iron-based alloys for LWR fuel cladding", *J. Nucl. Mater*., Vol. 448, pp. 420-435.

Ukai, S. et al. (2016), "Development of FeCrAl-ODS steels for ATF cladding", *Proc. TopFuel2016,* pp. 681-689.

Whitmarsh, C.L. (1962), *Review of Zircaloy-2 and Zircaloy-4 properties relevant to N.S. Savannah Reactor Design*, ORNL-3281, Oak Ridge National Laboratory, Oak Ridge, TN.

Yamamoto, Y. et al. (2015), "Development and property evaluation of nuclear grade wrought FeCrAl fuel cladding for LWRs", *J. Nucl. Mater*., Vol. 467, pp. 703-716.

Yamashita, S. et al. (2016), "Establishment of technical basis to implement accident tolerant fuels and components to existing LWRs", *Proc. TopFuel2016*, pp. 21-30.

Yan, Y. et al. (2014), "Post-quench ductility evaluation of Zircaloy-4 and select iron alloys under design basis and extended LOCA conditions", *J. Nucl. Mater*., Vol. 448, pp. 436-440.

Zinkle, S.J. et al. (2014), "Accident tolerant fuels for LWRs: A perspective", *J. Nucl. Mater.,* Vol. 448, pp. 374-379, doi:10.1016/j.jnucmat.2013.12.005.

12. Refractory metals: Lined Mo-alloy cladding

The design concept of lined Mo-alloy cladding utilises molybdenum's high strength at elevated temperatures to maintain fuel rod integrity and core coolability during accident conditions. The outer surface is lined with a metallurgically bonded Zr-alloy or Al-containing stainless steel (FeCrAl) layer to provide corrosion resistance in light water reactor (LWR) coolants for operational states and enhance steam oxidation resistance by forming a protective oxide layer of ZrO_2 or $(Al,Cr)_2O_3$ during accident conditions.

The fully metallic duplex Mo-Zr and Mo-FeCrAl cladding, where the outer layers were formed by physical vapour deposition, have been shown to maintain good integrity in high-temperature (HT) steam at 1 200°C for 12-24 hours and tests at higher temperatures will be performed to define its upper limit (Cheng et al., 2016). Molybdenum has a relatively high-neutron absorption cross-section, close to that of stainless steels and hence the thickness of the Mo-alloy layer will be limited to ~0.20-0.25 mm (0.008-0.010 inch), and the outer Zr-alloy or FeCrAl layer will be designed to add up to a total cladding wall thickness of 0.36-0.41 mm (0.014-0.016 inch) vs. the current 0.57 mm (0.0225 inch) for PWR cladding. A triplex cladding design with a thin intermediate layer of niobium to enhance the bonding strength has been fabricated by hot isostatic pressing (HIPing) and has been under evaluation (Cheng et al., 2016).

Duplex or triplex lined Mo-cladding tubes can be formed into the current LWR fuel cladding dimension, but with a thinner wall thickness to accommodate larger UO_2 fuel pellets to form fuel rods of the current design dimensions, e.g. 9.5 mm (0.374 inch) outer diameter for the PWR 17 × 17 fuel assembly design. Alternately, a smaller outer diameter of 9.1 mm (0.360 inch) may be considered to enhance fuel utilisation efficiency. The lined Mo-alloy cladding will have minimum impacts on fuel assembly thermal-hydraulic designs and hence, the effect on the assembly hardware design features, such as grids, mixing vanes and tie plates, will be minimum. Fuel assemblies using the lined Mo-cladding can be designed for about 18-month cycle length operation using 5% enriched UO_2. The larger UO_2 fuel pellets will have 15-20% more uranium loading than that required with the conventional Zr-alloy cladding to achieve similar neutron reactivity (Todosow, 2016).

Fabrication/manoeuvrability

For lined Mo-alloy to become a fuel cladding, long tubes in fuel rod length of ~5 metres will need to be fabricated via thermal-mechanical processes to achieve commercial-scale economics and quality requirements.

Fabrication of lined Zr-Mo-cladding is significantly more challenging than that of duplex or triplex Zr-alloy cladding with an inner or outer liner for boiling water reactor (BWR) and pressurised water reactor (PWR) fuel application, respectively, because of the large differences in the physical and mechanical properties of Mo and Zr-alloys. Although there are some property data available from research on Mo alloys for HT reactor applications (Cockeram et al., 2009) and its industrial applications at very high temperatures, thin-wall Mo-alloy tubes of <0.5 mm were not commercially available.

Under this study, the following step-wise approach has been undertaken on tube fabrication and endcap welding (Cheng et al., 2016; Cheng, Kim and Chou, 2016):

- Thin-wall Mo-alloy tubes of the LWR fuel cladding dimensions, 9.50-10.02 mm (0.374-0.400") OD, and wall thickness of 0.20-0.25 mm (0.008-0.010") have been fabricated in 1.5-metre (5 feet) length via warm drawing at a commercial fabricator in the United States under an EPRI project. Several batches of 1.5 metre tubes have been made of high-purity Mo and Mo-ODS with ~0.3% La_2O_3 from ~2.5-6 cm OD tubeshells fabricated using powder metallurgy (PM) and low carbon arc cast (LCAC) processes. Tube length is not a limitation via warm drawing. The axial and diametral ductility of Mo tubes can be improved through a partial recrystallisation annealing. The axial uniform and ultimate elongation of partially recrystallised Mo was measured to be 15-20% and 20-40%, respectively, at room temperature (RT) and at 320°C, as shown in Table 12.1. Examples of tested samples are shown in Figure 12.1.

**Table 12.1. Tensile properties of partially recrystallised Mo-alloy tubes
with 0.2 mm wall thickness**

Tensile property (1.5″ gauge length), room temperature			
Mo partial recrystallisation			
	PM	LCAC	ML-ODS
0.2% yield, (ksi/MPa)	73.5 (507)	82.4 (568)	90 (623)
UTS, (ksi/MPa)	80.1 (552)	85.4 (589)	92.2 (636)
Uniform elongation %	17	16	20
Total elongation %	52	39	43

Tensile property (1.5″ gauge length), 320°C			
PM Mo partial recrystallisation			
	1	2	3
0.2% yield, (ksi/MPa)	44.5 (307)	50.6 (349)	53.7 (370)
UTS, (ksi/MPa)	60.1 (415)	57.7 (398)	61 (421)
Uniform elongation %	17	18	15
Total elongation %	20	22	24

Figure 12.1. PM Mo tube after tensile test and local denting test at room temperature

Source: EPRI, 2016.

The diametral ductility of Mo is generally limited in as-drawn condition. Using an internally pressurised test with Ar gas until tube sample ruptures, the tube diameter is measured using laser beams. The diametral ductility of partially recrystallised Mo tubes was measured to be ~1.2-1.4% at a diametral strength of 380 MPa at 350°C, as shown in Figure 12.2. Expansion of the diametral ductility to ~15% can be achieved with a concomitant reduction in the diametral strength via an induction heat treatment of the tube samples to 1 300-1 700°C for 2-30 seconds, as shown in Figure 12.3. The very short heat treatment time is anticipated to reduce grain boundary contamination by species, such as oxygen, while allowing recrystallisation to take place.

**Figure 12.2. Failure strength as a function of diametral strain
of partially recrystallised LCAC Mo tubes**
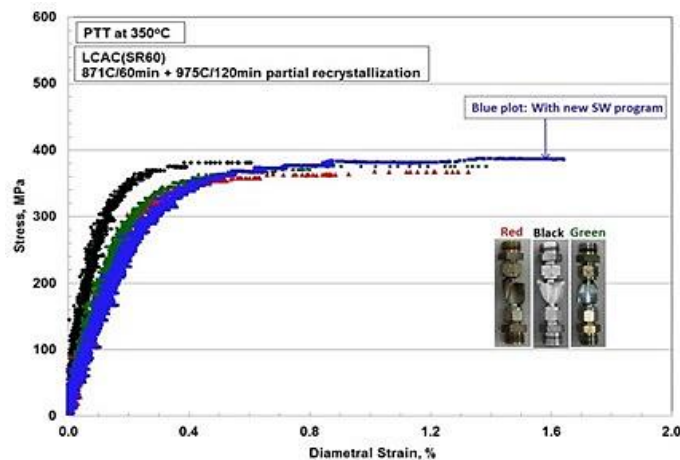
Source: EPRI, 2016.

Figure 12.3. Failure strength and diametral ductility of Mo-ODS tubes after receiving an induction heat treatment with temperature shown in the X-axis
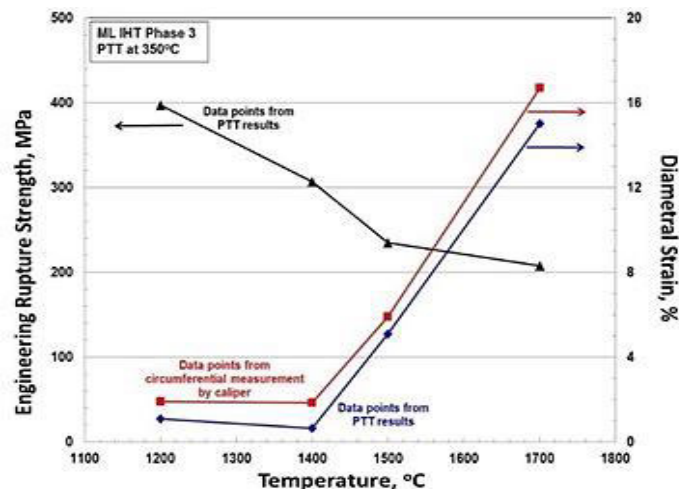
Source: EPRI, 2016.

In an independent development project led by China General Nuclear Power Corporation (CGN), thin-wall tubes of 0.3-0.5 mm wall thickness, 9.5 mm OD and 4.5-metre length have been successfully fabricated from Mo-ODS doped with nano-size

La₂O₃ and fabrication of even thinner wall tubes of 0.2 mm thickness is currently underway. The nano-size Mo-ODS (NS Mo-ODS) has been reported to possess superior strength and ductility (Liu et al., 2013). The tensile strength of the thin-wall tube has been determined to be 455 and 174 MPa at 400 and 1 200°C, respectively, and the total elongation is 25% at 400°C.

- Mo tube to Mo endcap welding via electron beam (EB) welding has been developed and used for fabricating sealed tube samples for testing, as shown in Figure 12.4 (A). Solid state welding using capacitive discharge welding (CDW) has been developed to fuse Mo endcap to Mo tube while preventing grain growth, as shown in Figure 12.4 (B). Development of a combination of CDW and final seal welding using tungsten inert gas (TIG) or EB welding to produce robust endcap welding is to be completed in 2017. Welding appears not to be a technical issue.

Figure 12.4. (A) EB and (B) CDW samples of 0.2 mm thin-wall Mo tube to Mo endcap
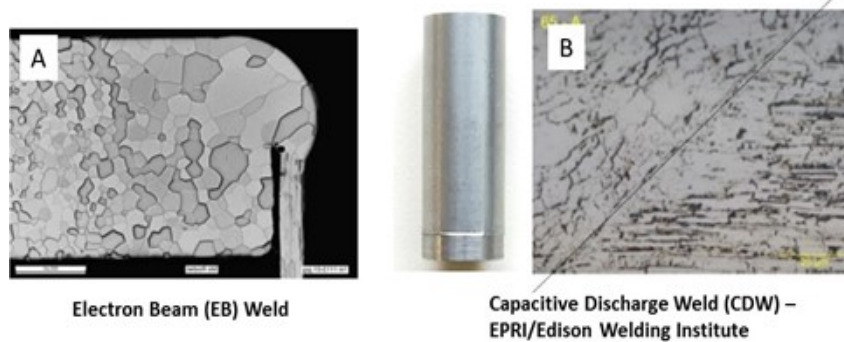
Source: EPRI, 2016.

The CGN project has been developing Mo tube to endcap welding using laser beam, EB and TIG welding. Preliminary success in laser beam welding has been demonstrated.

- Tubes with an outer layer of zircaloy or FeCrAl alloy in thickness of 50-75 μm (0.002-0.003") have been fabricated in 20 cm (~8") length via cathode arc physical vapour deposition (CA-PVD), as shown in Figure 12.5. The deposited outer layer and the Mo tube forms a metallurgical bonding with an inter-diffusion layer of <1 μm during the CA-PVD processing (Cheng et al., 2016). PVD coated samples have been used in feasibility studies to measure steam and corrosion resistance, inter-diffusion behaviour and diametral mechanical properties. The PVD coated samples have been shown to be capable of surviving in steam at 1 200°C for 12-24 hours.

Figure 12.5. Mo tubes coated with a zircaloy-4 or FeCrAl outer layer of ~50 μm vis CA-PVD
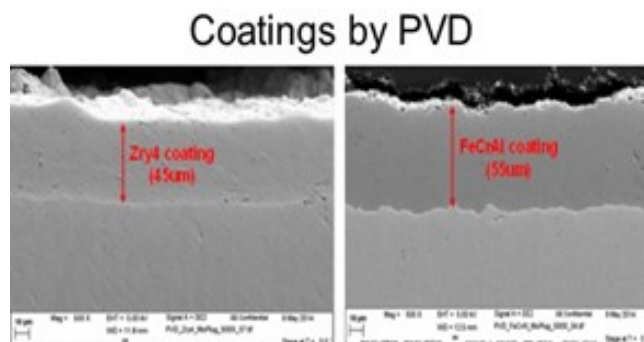
Source: EPRI, 2016.

Mo tubes of ~5-10 cm (2-4 inch) length were sealed with Mo endcaps using EB welding, followed by PVD coating of ~50 µm zircaloy-2 or -4 or FeCrAl (Kanthal) to form rodlets for steam oxidation tests. Figure 12.6 shows the rodlets tested in flowing steam at 1 200°C for 24 hours. The FeCrAl coated rodlet was intact after the test with formation of ~2-3 µm protective Al_2O_3. The zircaloy-2 and -4 coated rodlets lost the welded endcaps and had spalling ZrO_2, but ~50-70% of the Mo tube wall remained intact. Spallation of ZrO_2 is attributed to the loss of >50% of the alloying elements Fe, Cr (and Ni) and Sn in the coating during the PVD process. It has been known that ZrO_2 forms on high-purity Zr is susceptible to flaking and spallation. Similarly, more than 50% of Cr and Al in the Kanthal target material were lost in the coating.

Figure 12.6. Coated Mo rodlets tested in 1 200°C for 24 hours
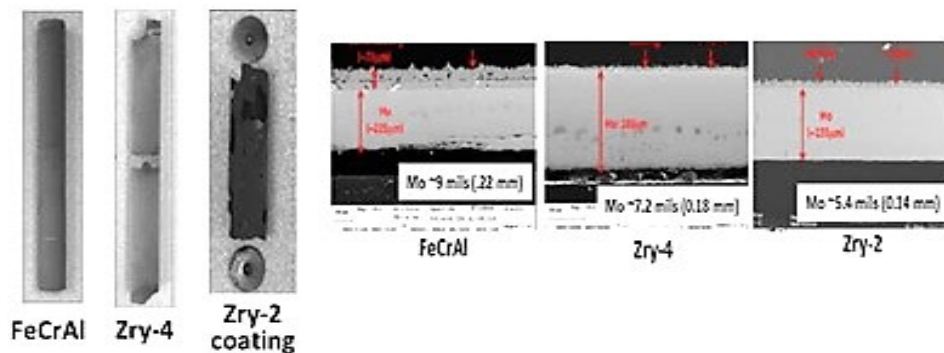
Source: EPRI, 2016.

In the CGN development effort, coating of a thin FeCrAl layer has been deposited on Mo tube by means of a magnetron sputtering technique. FeCrAl coated tube samples have been subjected to tests in a simulated PWR water loop for 72 hours and steam at 1 200°C for 8 hours both with satisfactory results.

The diametral failure strain of Mo tubes of 0.2 mm wall thickness with a ~0.050 mm PVD coating of either FeCrAl (Kanthal) or zircaloy-2 was measured using an internally pressurised test, as shown in Figure 12.7. The Mo tubes were stress relieved with a hoop strength of ~500 MPa at 350°C. An outer coating with a 0.050 mm Kanthal layer decreases the diametral failure strain from ~0.5% to ~0.3%, whereas a 0.050 mm layer increases the failure strain to ~1-2%. A similar trend in the effect of the two different coating types on the Mo tube failure strain was measured at 600 and 900°C.

- Mo tubes lined with a zircaloy or Zr-2.5Nb tube on the outer surface have been fabricated via hot isostatic pressing (HIPing) to produce metallurgically bonded tubes. A thin Nb intermediate layer can be added between the Zr-alloy and Mo tubes to allow inter-diffusion during HIPing to form metallurgical bonding and prevent formation of intermetallics. Without an intermediate Nb layer, a stable ZrMo2 has been observed at the Mo-Zr interface (Cheng et al., 2016). Tubes with wall thickness of 0.36-0.41 mm (0.014-0.016") have been fabricated. Tube samples have been delivered to the Halden Reactor Project for fabrication into fuelled rodlets for irradiation. Full characterisations of the lined Mo tubes were underway in 2017.

**Figure 12.7. The diametral stress and strain of 0.20 mm wall Mo tubes without or with an
outer coating of ~0.050 mm Kanthal or zircaloy-2 formed by CA-PVD**
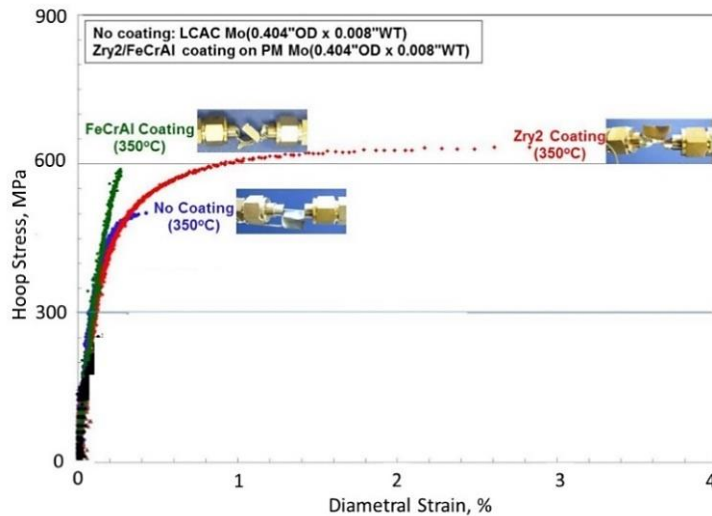
Source: EPRI, 2016.

The cross-section view of an 18 cm long Zr-2.5Nb lined Mo tube having a total wall thickness of 0.41 mm (0.016") is shown in Figure 12.8. The tube has an interfacial Nb layer that is ~0.035 mm thick. The interface structure and chemistry between the Zr-2.5Nb liner and Nb is shown in Figure 12.9. Mixing of Nb and Zr at the interface appears to result in the formation of new smaller grains at the interface, but with no evidence of new crystal phases. Also, there has been no observation of cracking at the interface.

**Figure 12.8. Cross-section view of a Zr-2.5Nb lined Mo tube
within intermediate Nb buffer layer**
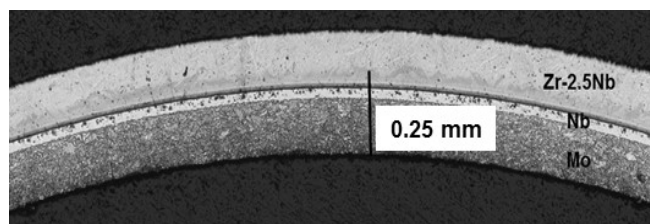
Source: EPRI, 2016.

Mo tubes with an FeCrAl (Kanthal) liner tube on the outer surface using HIPing has been fabricated, but with significant challenges. The challenges include: difficulty in fabricating Kanthal tubes of <0.5 mm wall thickness using cold or warm drawing due to the rapid rate of work hardening and susceptibility of thin-wall Kanthal tubes to crack when bonded to Mo tubes via HIPing. Further studies will be needed.

Welding of Zr-alloy lined Mo tubes to Zr-alloy endcap has been developed by the Halden Project using EB welding to join slotted endcap to the lined tube as illustrated in Figure 12.10. The outer zircaloy-4 liner is fused to the zircaloy-4 sleeve by the EB welding. One-end welded tube samples were tested with an He leak test at room temperature. Three samples were tested with an internally pressurised tube at 315°C. The welded tube samples passed the Ar gas pressure test at 207 bars (~3 000 psig) for 4 hours. One tube sample was pressurised to fail with an internal pressure of 300 bars (4 400 psig) or a tube hoop stress of 380 MPa.

Figure 12.9. TEM cross-section view of a 1.5 μm layer of inter-diffusion zone with mixed Zr and Nb as well as diffusion of Nb further into the Zr matrix on the right hand side
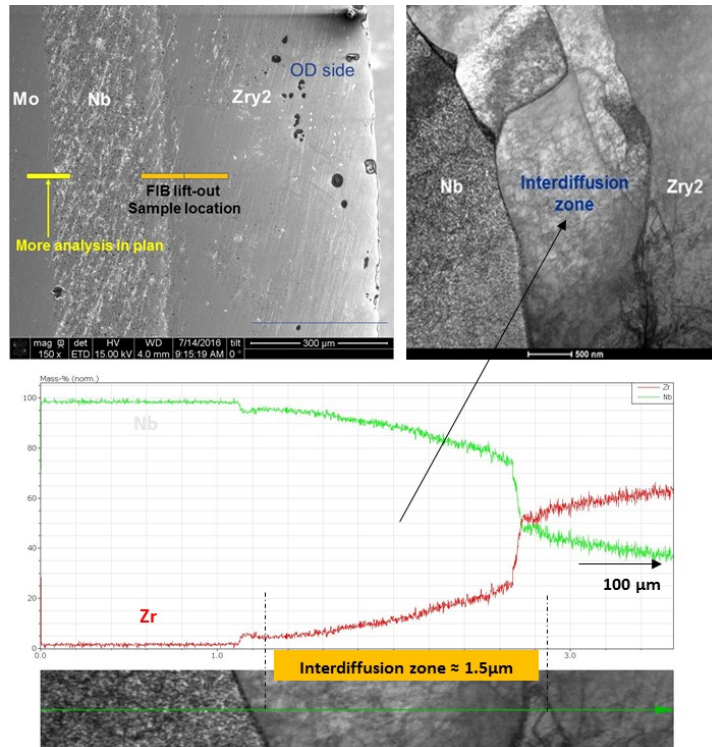
Source: EPRI, 2016.

Figure 12.10. Electron beam welding of zircaloy-4 lined tube to a zircaloy-4 endcap and subsequent internally pressurised test of a one-end welded tube
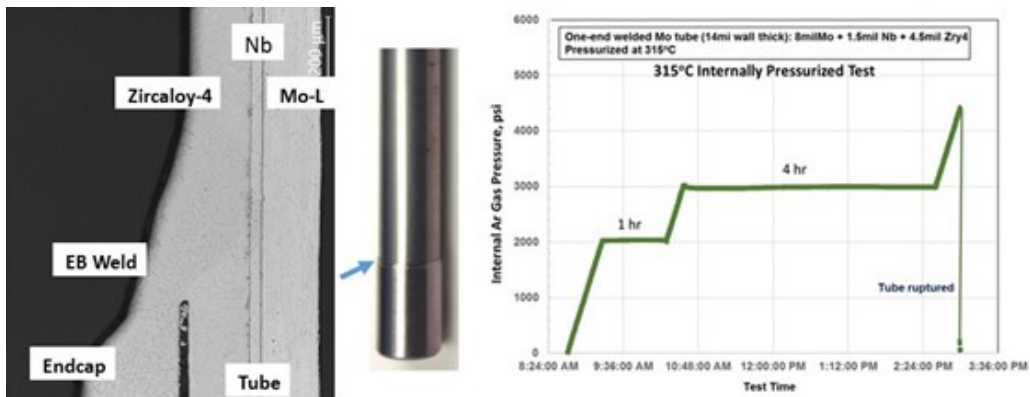
Source: EPRI, 2016.

Fabrication of long, lined Mo tubes via HIPing and drawing is in progress to demonstrate the feasibility for commercial-scale production of long-lined Mo fuel cladding. Composite tubes of greater than 2.5 cm or 1 inch are being prepared by HIPing or co-extrusion to achieve metallurgical bonding. The large OD tubes are then subjected to warm drawing to product smaller, thin-wall lined tubes. This challenging task is currently in progress with a plan to produce tubes of 1 meter or longer by the end of 2017.

Normal operation and AOOs

Corrosion resistance of lined Mo tubes

Compatibility of fuel cladding with the current LWR coolants is critically important for maintaining fuel cladding integrity as well as preventing distribution of radiative products to contaminate out-of-core components. With lined Mo-cladding, the outer liner of Zr-alloy or FeCrAl are anticipated to have high corrosion and hydriding resistance to burn-up exceeding the current limit of 62 GWd/MTU in PWRs. In PWRs, Zr-2.5 Nb has been shown to have excellent corrosion and hydriding resistance when irradiated as an outer liner of 0.10 mm on zircaloy-4 fuel cladding in a PWR to 80 GWd/MTU (Seibold, Garzarolli and Manzel, 2000) and similar good results have been reported as monolithic fuel cladding (Nishikawa et al., 2010). No corrosion data on Zr-2.5 Nb alloy has been reported in fuel cladding form for BWRs; coupon samples show performance similar to that of zircaloy in a test reactor irradiation (Cheng et al., 1983). For BWRs, alternate Zr-alloys such as a nickel-free, high chromium alloy may be considered for high corrosion and hydriding resistance at high burn-ups. An outer liner of FeCrAl alloy is anticipated to have excellent corrosion resistance with Cr concentration >18%, although additional irradiation test data will be required to validate its corrosion resistance because of lack of performance data of ferritic steels (no Ni) in LWRs.

Corrosion of bare molybdenum tubes

Molybdenum has been known to be susceptible to the formation of volatile MoO_3 in air at >~600°C because of interaction of Mo with free oxygen. At lower temperatures, a protective MoO_2 will form on Mo. Figure 12.11 shows a parabolic oxidation rate of Mo relative to zircaloy-2 in dry air at 400°C due to the formation of a stable black oxide of MoO_2. A bluish oxide will form on Mo when storing Mo in high moisture environments at room temperature. There is no such an issue with a well-cleaned Mo storing in a low humidity environment.

Figure 12.11. Oxidation rate (weight gain) of Mo and zircaloy-2 in heated dry air at 400°C
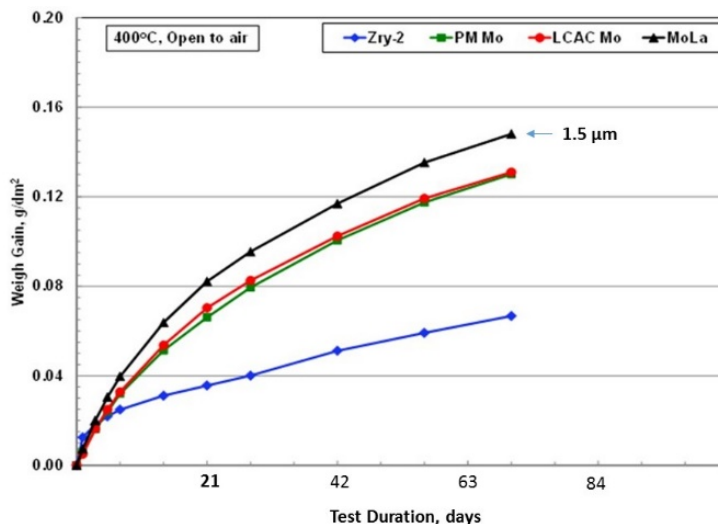
Source: EPRI, 2016.

In simulated LWR coolant conditions tested in autoclaves, bare Mo exhibits weight loss in all cases, as shown in Figure 12.12. The weight loss rate in water with 1 ppm dissolved oxygen at 290°C is quite excessive. With a dissolved hydrogen of 0.3 ppm,

which simulated a BWR-HWC condition, the linear weight loss is measured to be ~10 µm per month. With a dissolved hydrogen at 3.57 ppm at 330°C, which simulates a PWR condition, the weight loss was ~7 µm per month. The process of weight loss in hydrogenated water is believed to be due to the solubility of MoO_2, which decreases with increasing hydrogen and increases with increasing temperature. In oxygenated water, MoO_3 will likely form to accelerate the weight loss. The results illustrate the need to have a reliable protective outer layer. Figure 12.6 also shows results of two experimental Mo alloys that indicate the feasibility of enhancing the corrosion resistance of Mo by alloying, including adding Nb and Cr to Mo. Both alloys show the corrosion rate reduces to ~1 µm per month. Under irradiation in PWR coolant, it is anticipated that the corrosion rate shown in Figure 12.12, will be lower because typical hydrogenated PWR water under irradiation will have very little free oxygen (<5 ppb) because of radiolytic recombination of oxygen and hydrogen. In autoclave tests, low levels of oxygen will still be present even under hydrogen overpressure. Absence of oxygen in PWR water may also explain why most Zr-Nb binary alloys exhibit higher corrosion rates in autoclave tests than those measured in PWRs. There is an area where additional research will be necessary.

Figure 12.12. Corrosion weight loss of Mo, Mo-10%Nb and Mo-26%Nb-4%Cr in simulated BWR and PWR water tests
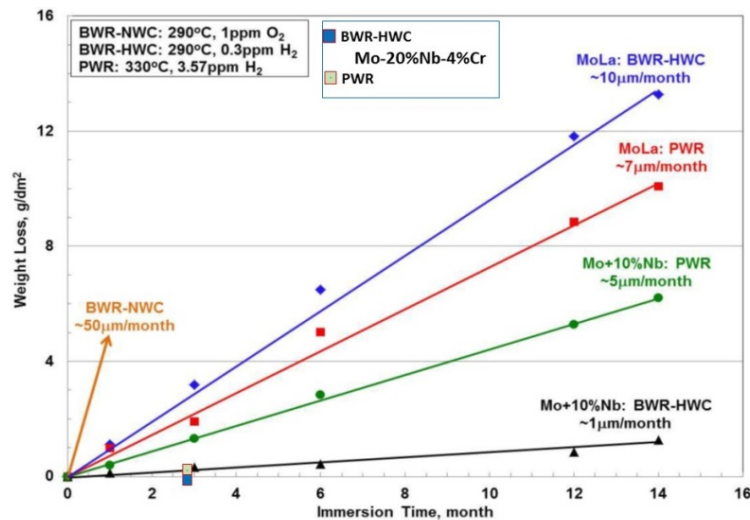
Source: EPRI, 2016.

Steam oxidation resistance of bare Mo

The steam oxidation resistance of bare Mo has been tested to support analysis of fuel rod degradation in the event of steam ingress after a fuel defect develops. Steam oxidation rate is also measured for analysis of the interaction of Mo with steam under a severe accident condition. Data in Table 12.2 show that Mo is highly resistant to oxidation in high-purity steam at the temperature range of 400-1 000°C. All samples tested in high-pressure steam at 415 and 500°C exhibit a shiny, black oxide surface. The very low oxidation rates indicate that the integrity of Mo-cladding in a failed rod will not be compromised, as water ingressing into the interior of a failed rod is anticipated to vaporise into steam and the environment should be rich in hydrogen, which can also reduce the oxidation rate. The relatively low oxidation rate of Mo relative to Zr-alloy in 1 000°C steam at atmospheric pressure further ensures that the lined Mo-cladding should easily survive in a design base accident.

Table 12.2. Oxidation rate (weight loss) of pure Mo and
Mo + 0.3% La$_2$O$_3$ in high-purity steam

Flowing steam	Test duration, days	Rate of Wt. loss, μm/day
415°C, 10.3 MPa	28,56	0.0036
500°C, 10.3 MPa	1,3	0.04
1 000°C, 0.1 MPa	1,3,7	20

Activation product and transport

Most materials will absorb neutrons and undergo transmutation leading to production of radioactive isotopes. Release of radioactive isotopes through corrosion of the fuel cladding to out-of-core components, like piping and turbines, may cause difficulty for plant operation and such an issue will need to be addressed. Current Zr-alloy cladding has a low rate of production of radioactive ^{95}Zr and ^{95}Nb due to the low neutron cross-sections of Zr and transport of these isotopes to out-of-core components has been very limited primarily because of the stability of ZrO$_2$, which is highly adherent to Zr-alloy cladding. The main core contamination issue of current reactor cores has been associated with release of radioactive crud from fuel rod surface during reactor shutdown. The source of crud is mainly from corrosion of out-of-core stainless steel and Ni-based alloy tube and piping and other components. With the Zr-lined Mo-cladding, no change in activation product release is anticipated, but the situation with FeCrAl-lined Mo-cladding is not clear and will need test or LWR operation data, as there has been little information available on the behaviour of ferritic steel (no Ni addition) in LWR coolants. Another potential issue with Mo is associated with the potential release of the radioactive isotope technetium-99 (^{99}Tc) if Mo is released into the LWR coolant. ^{99}Tc may be produced through activation of ^{98}Mo to ^{99}Mo by a (n, γ) reaction, which then transmutes to ^{99}Tc. ^{99}Tc is a β emitter and has a very long half-life of 211 000 years, thus it is in the same class as tritium (^{3}H) and ^{14}C isotopes under regulation to prevent contamination of drinking water. However, the production rate of ^{99}Tc is very slow because of the small neutron cross-sections of ^{98}Mo (at 0.06 barns, only ~1/3 that of Zr). Furthermore, ^{99}Tc is the most abundant fission product (FP) in spent fuel with a yield of 6.05%. Hence, the potential effect on release of ^{99}Tc is believed to be small, when high fuel reliability is maintained. Nevertheless, any additional release of radioisotopes due to use of new materials in the reactor is not desirable and must be evaluated.

Irradiation properties

Post-irradiation examinations of highly irradiated Mo-cladding rings and discs were recently conducted to evaluate the irradiation properties of molybdenum (Andersson, 2017). In research that took place starting in 2001, high-purity molybdenum in fuel cladding and disc forms were irradiated to an ultrahigh burn-up of ~112 GWd/MT at the Halden Reactor Project (HRP) under a project designed to study the thermal and other property behaviours of highly enriched (20% ^{235}U) fuel pellets in a thin wafer form. The test conditions and all photographic records of the test samples were analysed for their integrity. Five highly irradiated Mo-cladding rings and discs were selected for more detailed characterisations for integrity, fuel pellet interaction, dimensional stability and embrittlement. Examples of two such Mo rings are shown in Figure 12.13. The PIE results are summarised below.

- The Mo surfaces in tight contact with irradiated fuel discs during irradiation are essentially clean of measurable chemical interactions except for a few local spots. No oxide forms on the Mo surface.

- The Mo rings maintain relatively high integrity, with ~>70% of the cladding rings showing no evidence of through-wall cracking even under very severe operational conditions, including severe hoop tensile stresses due to ~10-15% volume expansion of the fuel pellets and average linear heat flux of ~130 to 50 kW/m (~40 to 15 kW/ft) for ~880 EFPD.

- Irradiation embrittlement of the Mo rings is evident, as a ring sample was broken by an impact force during defuelling.

- The Mo samples have high-dimensional stability with no evidence of irradiation-induced growth.

Figure 12.13. Mo rings irradiated with 20% enriched UO$_2$ to 112 GWd/MTU
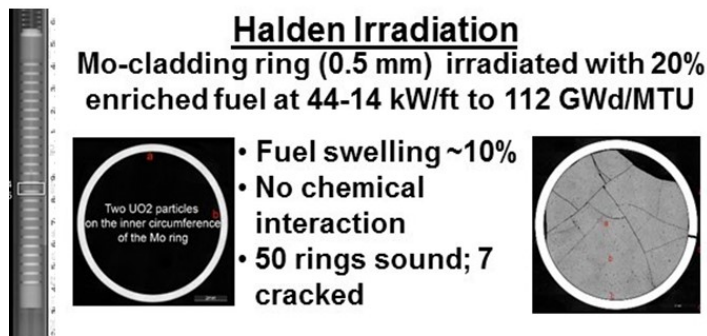
Source: EPRI, 2016.

Clearly, significantly more irradiation property data will be needed to support application of lined Mo-cladding in LWRs. In the CGN led development project, irradiation of the NS Mo-ODS samples has been scheduled to start in a Chinese research reactor.

Fuel reliability

Current Zr-alloy cladded fuel rods have reached rather low failure rates of <2-$5x10^{-6}$ in US LWRs. Fabrication methods to produce high-quality Zr or FeCrAl-lined Mo-cladding will need to achieve "perfect" status to match or exceed the current high fuel reliability. This will likely be very challenging, as the infrastructure available to support fabrication of refractory metals is at present limited.

Design-basis accidents and design extension conditions

RIA

During an RIA event, a rapid power transient in the order of ~20-50 ms will result in a fuel volume expansion of 1-2%, which will lead to rapid straining of the cladding due to PCMI. Zr-alloy cladding with high hydrogen concentrations may not survive an RIA if such an event occurs during a cold shutdown when the cladding temperature is low and the cladding is brittle. Mo exhibits ductile failure at ~300°C or higher, but will fail in a brittle fashion at lower temperatures. With an outer liner of high corrosion and hydriding resistant Zr-alloy as well as an intermediate ductile Nb, its behaviour under an RIA is difficult to assess and will need to be evaluated through a simulated transient test. As a result of the thermal conductivity of Mo being seven times higher, i.e. 138 vs. 22.6 W/m-K for Zr and the cladding wall being thinner, it is anticipated that the Mo temperature will be increased more rapidly by the heat generated in UO$_2$ pellet during an RIA. The higher cladding temperature will likely improve the cladding ductility, but such postulation requires to be validated through further tests and analysis.

LOCA

The lined Mo-cladding either with a Zr or FeCrAl alloy is anticipated to survive a design-basis LOCA, possibly with a tube burst due to its thin tube wall, but likely with no significant tube ballooning, at ~1 200°C, vs. bursting with large ballooning at ~800-900°C for Zr-alloy cladding. The fuel core should remain in a coolable geometry because of the remaining strength of the Mo-cladding at >1 200°C.

Design extension conditions

The main purpose of adopting Mo-alloy in this accident-tolerant fuel design is to evaluate the feasibility of maintaining the core in a coolable geometry during a design-basis accident and design extension conditions when the fuel cladding temperature exceeds 1 000°C, beyond which Zr-alloys will essentially lose all strength or be fully oxidised to ZrO_2. Mo has been reported as having tensile strength of ~60 MPa (or 10ksi) at 1 500°C. The Mo-cladding is anticipated to be protected by ZrO_2 or Al_2O_3 formed in situ from the outer liner during an accident (Cheng, Kim and Chou, 2016) as supported by two laboratory tests discussed below:

- ZrO_2 of ~75 μm is formed on a sealed Mo tube, through PVD deposition of zircaloy-4 and pre-oxidation in steam at 700°C. The Mo-ZrO_2 interface remains stable in a furnace at 1 500°C for 24 hours. With an FeCrAl deposit of 50 μm on an Mo tube, the FeCrAl remains covered by a thin protective layer of Al_2O_3 of ~2-3 μm at 1 350°C, but not 1 500°C. The results indicate that fuel rods with lined Mo-cladding may remain in their coolable state when protected by ZrO_2 formed by oxidation of the outer Zr-alloy liner to ~1 500°C or protected by a thin Al_2O_3 layer from oxidation of the FeCrAl liner to 1 300°C.

- Sealed Mo tubes with 50 μm coating of zircaloy-4 or FeCrAl by PVD were subjected to steam tests at 1 000 and 1 200°C and demonstrated that the coated tubes can survive in 1 200°C steam for 12-24 hours. Tests of tubes with liner by HIPing with much higher liner quality are planned to evaluate the upper temperatures that the lined Mo-cladding may survive. New data on the temperature boundaries for steam oxidation protection with the lined Mo tubes should be available by the end of 2017.

With the HT steam oxidation data, the additional safety margin or coping time to be gained in design extension conditions, such as a station blackout (SBO), can be analysed with a well benchmarked accident code. Our preliminary estimate for the lined Mo tube is in the order of hours. The produced hydrogen can be reduced by >80% if the outer Zr-liner is limited to <0.11 mm (20% of current PWR cladding wall thickness of 0.57 mm). The hydrogen reduction is anticipated to be even higher if FeCrAl is used as the outer liner.

Back end: Used fuel disposal

Activation of [98]Mo will lead to production of ^{99}Tc, which is a β emitter and is included in the list of long-lived isotopes, ^{14}C, ^{99}Tc, [129]I, [59]Ni, [94]Nb that are required to be reported in the nuclear waste burial requirements document under NRC regulation 10CFR61, even though the additional production of ^{99}Tc by use of Mo-cladding is likely small relative to its already large quantity in the spent fuel. Further evaluation of this issue is needed.

Summary

For lined Mo tubes to be successful as an alternate LWR fuel cladding to enhance accident tolerance, a reliable thermo-mechanical fabrication process will need to be developed to produce high-quality cladding. Processes for fabrication of short length Zr-alloy lined Mo tubes with an interfacial thin Nb layer to achieve good metallurgical bonding has been

successfully developed via hot isostatic hipping (HIPing). Fabrication of long-lined Mo tubes with an outer liner of Zr-alloy or FeCrAl (Kanthal) has been under development using HIPing to achieve metallurgical bonding, followed by extrusion and drawing. PVD coating can produce coated Mo tubes for testing, but it is questionable that it can be developed into a large-scale commercial process for producing long fuel cladding.

Solid state welding of thin-wall Mo tube to Mo endcap has been successfully developed using CDW. A combination of CDW welding of Mo endcap to lined Mo tube and followed by a seal weld of a Zr-alloy or FeCrAl endcap to the outer liner of Zr-alloy or FeCrAl using either EB or TIG welding will provide a tightly sealed fuel rod.

Zr-2.5 Nb is selected as the outer liner for PWRs and a new Zr-alloy such as a Ni-free, high Cr alloy may be considered for BWRs. The current design thickness for the outer Zr-alloy liner is 0.11 mm or a reduction of 80% from the current thickness of 0.56 mm for monolithic Zr-alloy cladding for PWR 17×17 cladding design. The Zr-alloy lined Mo-cladding is anticipated to possess sufficient corrosion and hydriding resistance for the current fuel burn-up limit and beyond. No inner protective liner is needed for Mo because Mo is highly resistant to oxidation in high-purity or reducing steam. Therefore, the lined Mo-cladding is anticipated to maintain good integrity in the event of steam ingress into a failed fuel rod, as well as under a design-basis LOCA. In the event the outer coating is locally removed, such as due to grid-to-rod fretting, localised corrosion of Mo may occur. Such an occurrence may be detected from monitoring of ^{99}Tc and ^{99m}Tc. However, grid-to-rod fretting has not been reported in BWR fuel and such an issue has been largely resolved for PWR fuel as well. Improvement in the corrosion resistance of Mo in LWR coolants may be achieved by adding alloying elements, such as Nb and Cr, to Mo. Further development efforts will be needed.

As test results show, PVD coated Mo tubes can survive in steam at 1 000°C for seven days or longer and 1 200°C for 12-24 hours. With FeCrAl coated Mo tube, oxidation protection from Al_2O_3 appears to be limited to ~1 350°C because of rapid diffusion of Mo into FeCrAl at elevated temperatures. With Zr-alloy coated by PVD, spallation of ZrO_2 leads to loss of protection of Mo tube. The cause of oxide spallation is attributed to the loss of alloying elements in the Zr-alloy coating during PVD. It is anticipated that the Zr-alloy liner produced by HIPing will form better quality ZrO_2. It is anticipated that the Zr-alloy liner produced by HIPing will form better quality ZrO2. However, test data is needed to demonstrate this possibility. Evaluation of such characteristics is planned to be completed in 2017.

The PIE results obtained on the Mo rings and discs constraining UO_2 fuel-water with 20% enrichment indicate that Mo-cladding can survive operation at very high heat fluxes with substantial fuel volume expansion to a burn-up of 112 GWd/MTU. Under such large hoop stress from fuel volume expansion and without an external compressive stress to support it, >70% of the ring samples were found intact, i.e. with no through-wall cracking and with very minimum chemical interaction with the spent fuel. PCMI and irradiation-induced embrittlement will need further study through irradiation tests.

References

Andersson, V. (2017), *Post Irradiation Examination of Mo Fuel Rings and Disks Containing Ultra-High Burnup Fuel Disks*, to be published by EPRI.

Cheng, B., P. Chou, C. Topbase, Y-J Kim, S. Armijo and D. Chuong, (2016), "Fabrication of rodlets with coated and lined Mo-alloy cladding for testing and irradiation", *Proceedings of TopFuel Meeting*, Paper #18054, Boise, Idaho.

Cheng, B., R. Adamson. W. Bell and R. Proebstle (1983), "Corrosion performance of some Zr-alloys irradiated in the steam generating heavy water reactor – Winfrith", *Proceedings of International Symposium on Environmental Degradation of Structural Materials in Nuclear Power Systems – Water Reactors*, Myrtle Beach, South Caroline, August 1983.

Cheng, B., Y.-J. Kim and P. Chou (2016), "Improving accident tolerance of nuclear fuel with coated Mo-alloy cladding", *Nuclear Engineering and Technology*, Vol. 48, pp. 16-25.

Cockeram, B.V. et al. (2009), "The change in the hardness of LCAC, TZM, and ODS molybdenum in the post-irradiated and annealed conditions", *J. Nucl. Mater.*, Vol. 393, p 12.

Liu, G., et al. (2013), "Nanostructured high strength molybdenum alloys with unprecedented tensile ductility", *Nature Materials*, Vol. 12, pp. 344-350.

Nishikawa, S. et. al. (2010), "J-alloy™, advanced PWR fuel cladding material; Program of J-alloy™ development", *TopFuel Meeting*, Florida.

Seibold, A., F. Garzarolli and R. Manzel (2000), "Material development for Siemens fuel elements", *Proceedings of TopFuel Meeting*, Park City, Utah.

Sato, D. et. al. (2010), "J-Alloy™, advanced PWR fuel cladding materials: In-pile performance of J-Alloy™", *Proceedings of 2010 LWR Fuel Performance/TopFuel/WRFPM*, Orlando, Florida, 26-29 September 2010.

Todosow, M. (2016), *Preliminary Scoping Analyses of Impacts of SS316, and Zr4 Coated Mo Cladding using TRITON code*, Brookhaven National Laboratory letter report, March 2016.

13. SiC/SiC-composite cladding

High-purity silicon carbide (SiC)-based ceramics and their composites (continuous SiC fibre-reinforced SiC matrix composites, SiC/SiC) have superior high-temperature (HT) properties, excellent irradiation resistance, inherent low activation and other superior physical/chemical properties. Through the development and demonstration of advanced SiC/SiC composites with a superior neutron irradiation tolerance, the composites have attracted interest for potential applications as in-core structures of fusion reactors and advanced fission energy systems, such as generation IV reactors (Katoh, 2012). Recently, there has also been intensive research on applying the SiC/SiC composites to accident-tolerant fuel claddings and core structures of LWRs after the Fukushima accident, while the initial concept utilising oxide composites was proposed in early 1990s (Feinroth, 1991).

Although technically proven design concepts are still being optimised, the SiC-composite claddings are based on multi-layered structures in all SiC/SiC-composite layer, combination with SiC/SiC-composite layer and monolithic CVD-SiC layer(s) or in some cases, metal layer. The high-density monolithic CVD-SiC or metallic liner renders a primary retention of fission products (FPs) because the CVI (chemical vapour infiltration)-processed SiC/SiC-composite does not have enough gas hermeticity. Another concept of all SiC/SiC-cladding, NITE (nano-infiltration and transient eutectic phase)-processed SiC/SiC, is reported to offer a better hermeticity to fission gas on the elastic deformation domain because of a higher density (Kohyama, 2016; Hayasaka, 2016). The SiC/SiC-composite layer is adopted to increase the tolerance to damage and prevent a catastrophic failure of the cladding tube.

The SiC-composite claddings and fuel components are expected to provide excellent passive safety features both in design-basis accidents and design extension conditions severe accidents (SAs). These are due to an excellent HT strength and an outstanding oxidation resistance to an HT steam. The SiC/SiC composites are anticipated to provide additional benefits over the Zr-alloys such as a reduced neutron absorption cross-section enabling a smaller uranium enrichment and that could also result in increasing the fuel cycle duration, a capability of higher fuel burn-ups and power uprates for a better economy, an exceptional inherent radiation resistance and a lack of progressive irradiation growth (Katoh, 2015). The combination of these attractive features makes the SiC composites one of the leading candidates for accident-tolerant LWR fuel cladding and core structures. In spite of these potential benefits of the composite cladding, however, there are some key issues that need to be addressed for the LWR application (Katoh, 2012; Bragg-Sitton, 2013). Among the various issues, the hydrothermal corrosion of SiC and the FPs retention capability of ceramic composites are identified as critical feasibility issues that need to be fully addressed in the relatively early stages in the course of the technology development (Katoh, 2015; Kim, 2013). In spite of the various technological hurdles, the SiC-composite cladding would significantly increase the fuel margin during LOCAs, eliminate DNB as a safety issue and provide added margin for design extension conditions.

Fabrication/manoeuvrability

Fabrication is feasible since the ability to shape tubular fibrous preforms from the third generation of SiC fibres (Hi-Nicalon Type S and Tyranno SA3) was demonstrated. The CVI process is also a mature technology to produce a silicon carbide matrix, perfectly crystallised and with high purity to ensure the neutron irradiation resistance. Fabrication of thin-walled CVI-processed SiC-composite tubes with a large length-to-diameter ratio has been demonstrated up to ~1 m (Deck, 2015; David, 2017). The NITE process is also increasing its maturity and a large-scale fabrication of thin-walled SiC-composite tubes with excellent hermeticity was demonstrated up to ~1 m (Kohyama, 2016). However, the structural design concept of SiC/SiC-composite claddings needs to be further optimised and a new devoted industrial network remains to be created for the production of full-length tubes.

Figure 13.1. (a) Examples of ~0.9 m-long SiC/SiC tubes, (b) cross-section of a tube structure with an outer monolithic-SiC coating, and (c) cross-section of a tube structure with an inner monolithic-SiC layer
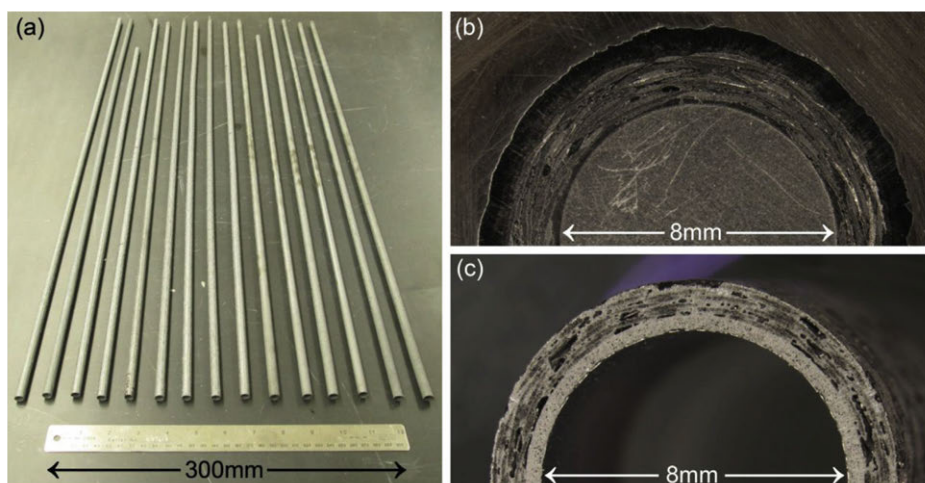
Source: Deck, 2015.

A technology for end-plug joining with gas tightness and adequate strength should be developed because the SiC ceramics cannot be welded. Although irradiation tolerant joining techniques for SiC/SiC-composite claddings are being developed, the joining of SiC to SiC is faced with both the hydrothermal corrosion resistance and the consequences of transient swelling under irradiation issues. In the recently developed technique, the SiC joint material exhibited excellent stability and strength retention following irradiation to 8.7 dpa at ~270°C and surpassed mechanical and permeability performance requirements (Khalifa, 2016). NITE-processed SiC/SiC claddings with zircaloy end-plugs have successfully completed HBWR irradiation three times, demonstrating sufficient hermeticity and strength under PWR and BWR conditions (Kohyama, 2016). A metal/ceramic hybrid clad concept such as the so-called "sandwich design", as illustrated in Figure 13.2 could significantly ease the seal by welding a plug on the metallic liner. The recent fabrication of prototypes has been demonstrated with a tantalum metal liner that was welded by a laser process fully compatible with the nuclear environment constraints. Full-scale tests under 200 bar pressure were successfully completed.

Figure 13.2. Segment of SiC/SiC fuel cladding including a metal liner

Source: Sauder, 2014.

New licensing guidelines will have to be issued to correspond with the specific failure modes of SiC/SiC-cladding. The licensing will therefore be difficult. In light of this, an important subject to be addressed early is the development of standard procedures for testing and evaluating composite materials and structures (defining a thermo-mechanical damage index for instance).

The issue of the relatively high current cost of the SiC fibres is to be balanced with both the large-scale production and the benefit of a potentially lower enrichment in UO_2.

Normal operation and AOOs

In normal operation, the main identified issues are:

- The chemical compatibility of SiC with the coolant at about 300°C leading to a recession in the water, at a rate depending on chemical environment characteristics (Park, 2013; Kim, 2015; Terrani, 2015), as exemplified in Figure 13.3. The hydrothermal corrosion of irradiated SiC and the effect of radiolysis need to be fully addressed.

- Mitigation solutions should be proposed; many of them such as coating, specific surface treatment or modification of water chemistry are currently the subject of intensive investigation within the scientific community.

- The low pseudo-ductility – leading to a potential PCI issue – must be assessed. There is a need for establishing the statistical failure properties of SiC/SiC-composite claddings, adequately defining design allowable stresses under a probabilistic design approach.

- The relatively poor thermal conductivity under neutron irradiation in the LWRs normal operating range, which could potentially cause significant mechanical stresses leading to early multi-cracking. High-temperature side of SiC/SiC fuel cladding is subjected to high tensile stress because of differential swelling of irradiated SiC. Irradiation-induced thermal conductivity decrease in SiC could worsen the situation (Katoh, 2015).

Furthermore, if the SiC/SiC composites thermal behaviour is deemed to be strongly dependent on the SiC matrix elaboration process and the nature of the SiC fibre as well as the fibrous arrangement, a multi-layered composite cladding design does not argue in favour of improving radial heat transfer. As reported in Table 13.1, the presence of monolithic ceramic or metallic liner for tightness purposes in multi-layered design induces interfacial thermal resistances that act as barriers to the heat conduction. This

could be exacerbated by interlaminar porosity and poor adhesion between some of the layers with significant issues in absence of careful interface (Fave, 2016).

- The irradiation-induced swelling and low-thermal conductivity of SiC-composite claddings under irradiation would increase the pellet-cladding gap and cause a large temperature drop across the cladding. This increase in the fuel temperature is considered a critical issue since it exacerbates fission gas release from the pellet. This issue calls for development of alternative fuels that offer higher thermal conductivity and modified fuel geometry such as annular pellets (Katoh, 2015; Yueh, 2010).

Figure 13.3. Corrosion behaviour of CVD-SiC depending on the LWR water chemistry
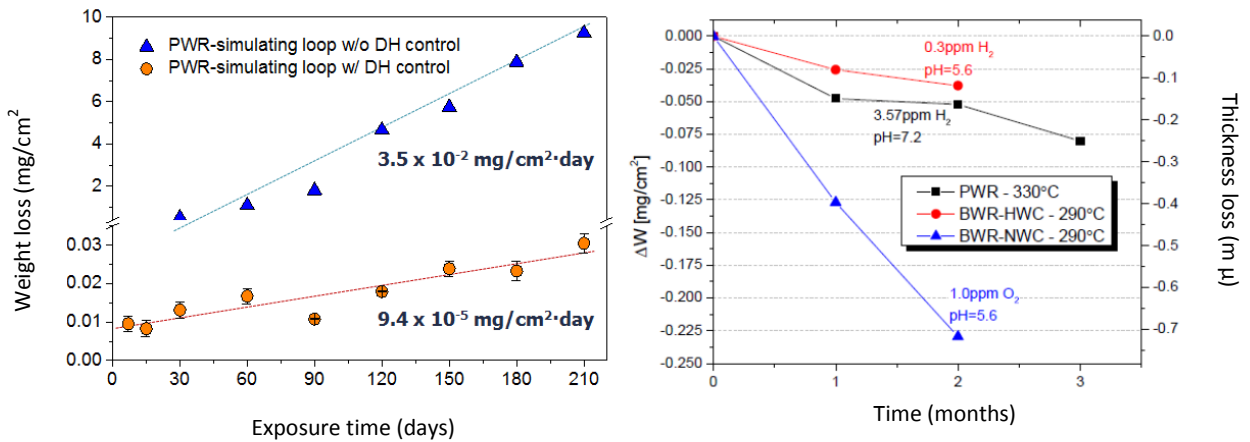
Source: Kim, 2015; Terrani, 2015.

Table 13.1. Radial thermal conductivity for nuclear grade SiC/SiC composites and SiC-based cladding in unirradiated condition

Material and design	Main characteristic	Radial thermal conductivity W.m-1. K-2	Method	Reference
CVI-SiC/SiC-composite	Filament winding 300 with HNS fibres (density 2.7)	10 (25°C)	Laser flash (from diffusivity)	Duquesne, 2016 Duquesne, 2016 Katoh, 2014 Katoh, 2014
	two-dimensional braiding 450 with HNS fibres (density 2.85)	28 (25°C)		
	HNS fibres	8.5 – 18.1 (25°C)		
	Tyranno SA3 fibres	15.2 – 23.7 (25°C)		
Sandwich cladding	CVI-SiC/SiC composites with Tantalum liner	0.2 to 1 (25-550°C) 30 (25°C) without metal/SiC decohesion 5 to 25 (25°C) with metal/SiC decohesion	Radial heat flow (steady-state) Numerical model Numerical model	Fave, 2016 Duquesne, 2015 Duquesne, 2015
Triplex cladding	CVI-SiC/SiC composites with SiC monolithic layer	0.2 to 4 (25-700°C)	Radial heat flow (steady-state)	Fave, 2017

By contrast, the SiC/SiC composites have the benefit of a number of undeniable advantages:

- They exhibit neutron transparency with a low cross-section. Higher neutron penalty could be expected for "sandwich" design because of the presence of the metal liner, depending on its nature and thickness (Sauder, 2014).

- Higher critical heat flux (CHF) than for conventional Zr-based alloys due to the improved surface wettability, depending on the surface roughness (Kim, 2015).

- High stiffness and competitive fatigue behaviour (good feedback from the aeronautic applications).

- Mechanical properties almost time independent during an HT transient.

It is important to underline that leak-tightness depends on the range of acceptable deformation as well as the cladding design. This can be seen as a critical issue since a fully ceramic SiC-cladding design cannot prevent the multi-cracking of the matrix beyond the elastic limit to the composite (i.e. at low loading). In case of a metal/ceramic clad concept, the presumably fair ductility of the metal ensures it to withstand any strain imposed by the deformation of the composite, so that the leak-tightness is guaranteed until the ultimate failure of the composite occurs, thus considerably extending the leak-tight domain.

Furthermore, it is now well-established that silicon carbide swells under neutron flux with irradiation temperature beyond 125°C up to a saturation dose (just a few dpa). For a nuclear grade silicon carbide, the volumetric swelling reaches a maximum value close to 2% at 300°C (see Figure 13.4).

Figure 13.4. Fluence-dependent evolutions of volumetric swelling and thermal conductivity of CVD-SiC
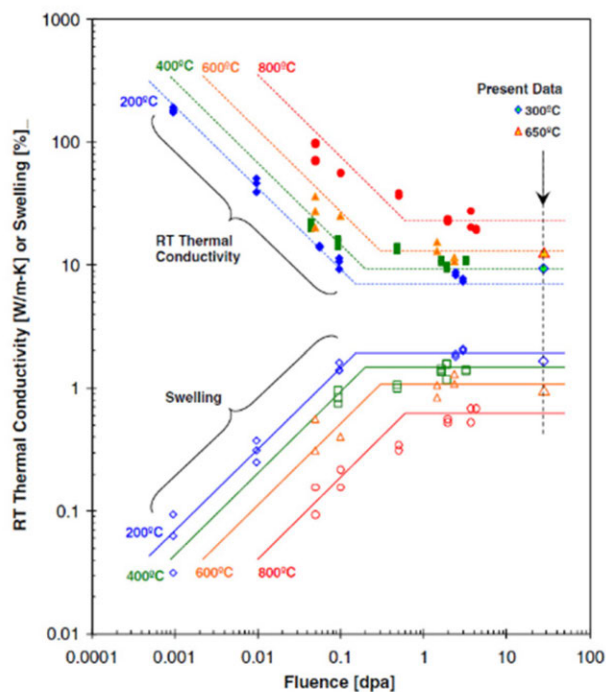
Source: (Katoh, 2011).

Design-basis accidents and design extension conditions

Several reports demonstrate that SiC composites have an outstanding oxidation resistance to HT steam compared to the current Zr-alloys (Terrani, 2014). Water quench tests from 1 000°C up to 1 500°C result in only a marginal decrease in mechanical properties (Kim, 2016; Lorrette, 2017) with a maintenance of impermeability to helium gas depending on the temperature quenching (Bacalski, 2016). These can also offer a significantly reduced hydrogen generation and an improved structural integrity under SA conditions.

A very interesting asset of SiC/SiC fuel is the fact that it will maintain a coolable geometry at high temperature, which is a very important improvement in accident conditions (see Figure 13.5).

Figure 13.5. Comparison of the 1 200°C air/steam oxidation between Zy-4 and SiC/SiC-composite tubes

Conditions: 1 bar, 1 200 C, Air/H2O (50/50)
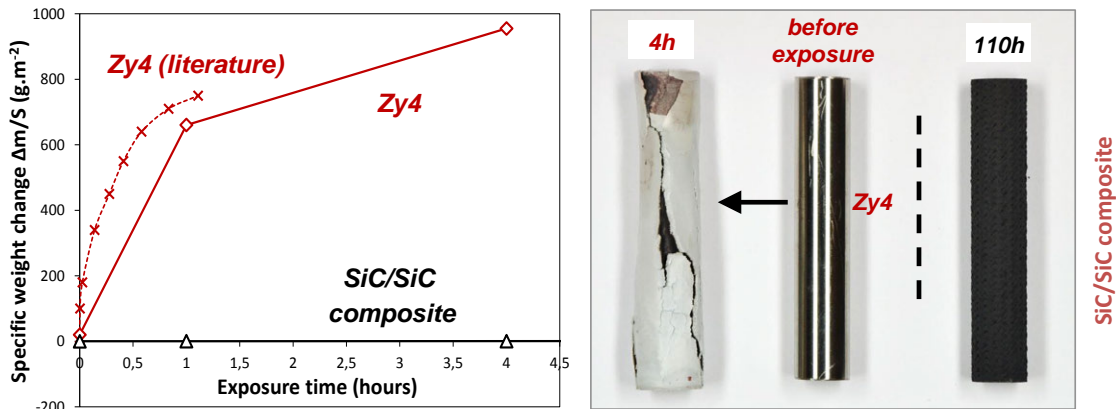
Source: Lorette, 2015.

Even if the potential hydrogen (and other gases) production and energy release is comparable or even higher compared to zirconium alloys, the extremely low oxidation kinetics in air and steam finally will cause a 2-3 orders of magnitude lower hydrogen and energy source terms up to approximately 1 800°C. From recent oxidation experiments (Avincola, 2015a), it can be concluded that SiC/SiC claddings can give an additional safety margin regarding the beyond LOCA margin, ensuring coolability in steam atmosphere for up to three days at 1 600°C and in the order of hours at 1 700°C and 1 800°C. The mechanism of SiC oxidation and volatilisation is well known, including active/passive oxidation, bubble formation of SiO_2 surface layer, paralinear kinetics and dependence on oxygen and steam partial pressure.

**Figure 13.6. Gas release during oxidation of SiC/SiC-cladding
in steam, and sample's post-test appearance**
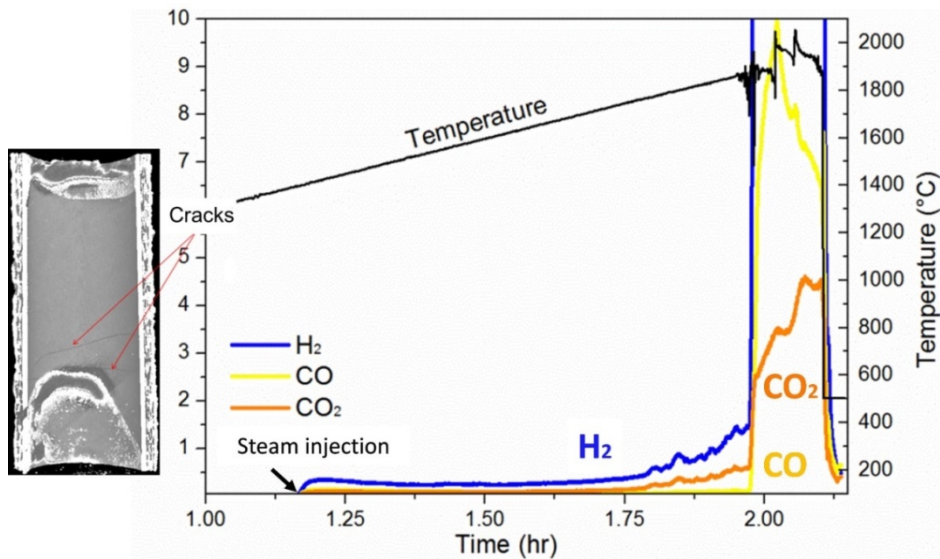
Source: Avincola, 2015a.

SiC-SiC-cladding samples survive quenching in water from up to 2 000°C, maintaining their coolable geometry. A thermodynamic database is available to predict volatilisation of silicon carbide components at very high temperature in steam-containing atmospheres (Avincola, 2015b).

**Figure 13.7. Formation of bubbles during oxidation of SiC/SiC in steam at temperatures
between 1 600°C and 2 000°C with final quench phase**
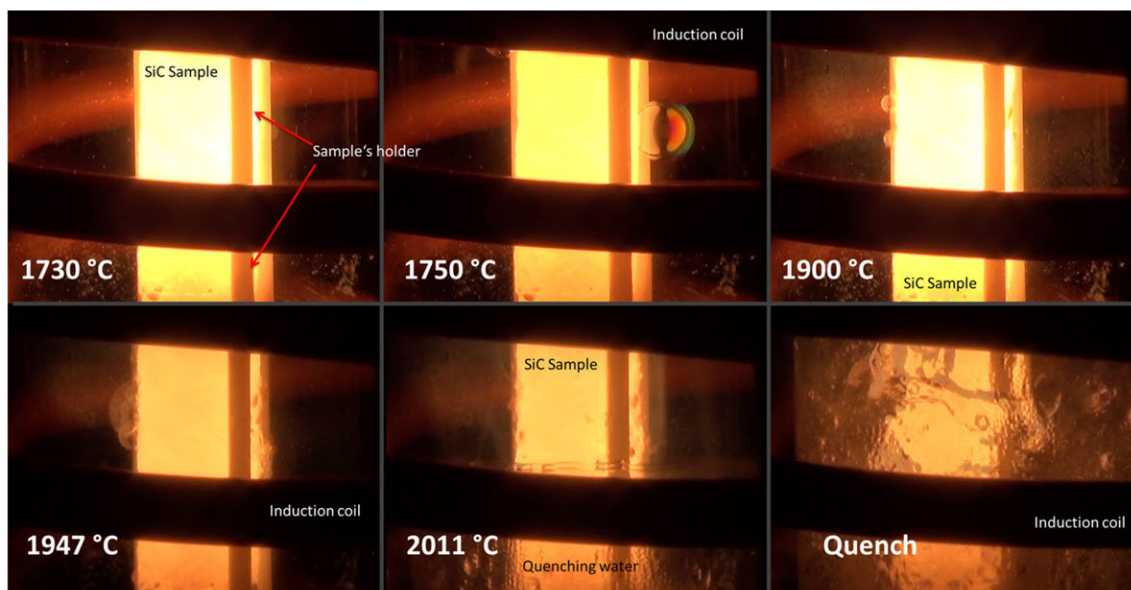
Source: Avincola, 2015b.

The low cladding pseudo-ductility raises some specific questions with respect to its thermo-mechanical behaviour (rapid mechanical pellet-cladding interaction) during an RIA transient.

Several solutions are under investigation such as the integration of a buffer layer able to accommodate the expansion/swelling of the fuel pellets to mitigate the PCMI risk.

Regarding the chemical compatibility of SiC with uranium dioxide, the margin to melting in case of a severe accident places the SiC/SiC composites in a more favourable position than the current zirconium-based alloys claddings. The first liquid phase is found to lie within the 1 850-1 950 K temperature range (Braun, 2017).

Used fuel storage/transport/disposal/reprocessing

Permeation to tritium release during normal operation, storage and reprocessing phases might be a key issue and needs to be investigated further. The choice of using a proper liner material could help mitigate this issue.

The fact that SiC does not react with any acid should be an asset with respect to current reprocessing techniques. Since the used fuel assembly are sheared during reprocessing, specific data on the SiC fuel rods bundles' behaviour need to be collected.

References

Avincola, V.A. et al. (2015a), "Oxidation at high temperatures in steam atmosphere and quench of silicon carbide composites for nuclear application", *Nuclear Engineering and Design*, Vol. 295, pp. 468-478.

Avincola, V., D. Cupid and H.J. Seifert. (2015b), "Thermodynamic modeling of the silica volatilization in steam related to silicon carbide oxidation", *Journal of the European Ceramic Society*, Vol. 35 (14), pp. 3809-3818.

Bacalski, C.F., G.M. Jacobsen and C.P. Deck (2016), "Characterization of SiC/SiC accident tolerant fuel cladding after stress application", *Top Fuel 2016*, Boise.

Bischoff, J. et al. (2015), "Development of fuels with enhanced accident tolerance", *Top Fuel 2015*, Zurich.

Brachet, J.C. et al. (2014), "CEA studies on advanced nuclear fuel claddings for enhanced accident tolerant LWRs Fuel (LOCA and beyond LOCA conditions)", SFEN Fontevraud 8 congress, Avignon.

Bragg-Sitton, S. et al. (2013), *Silicon Carbide Gap Analysis and Feasibility Study*, INL/EXT-13-29728, Idaho National Laboratory, Idaho Falls.

Braun, J., et al. (2017), "Chemical compatibility between UO_2 fuel and SiC cladding for LWRs: Application to ATF (Accident-Tolerant Fuels)", *Journal of Nuclear Materials*, Vol. 487, pp. 380-395.

David, P. et al. (2017), "Conception, manufacturing and characterization of SiC/SiC claddings for IV Generation Nuclear Reactors", *ICACC Conference,* Daytona Beach.

Deck, C.P. et al. (2015), "Characterization of SiC-SiC composites for accident tolerant fuel cladding", *Journal of Nuclear Materials*, Vol. 466, pp. 667-681.

Duquesne, L. et al. (2016), "A flash characterisation method for thin cylindrical multi-layered composites based on the combined front and rear faces thermograms", *Quantitative InfraRed Thermography Journal*.

Duquesne, L. (2015), *Thermal Characterization of Tubular SiC/SiC Composites for Nuclear Applications,* PhD, ENSAM PariTech, France.

Fave, L. and M.A. Pouchon (2016), "Effect of PyC interlayer amorphisation on the thermal conductivity of SiC/SiC composites", *HTR conference*, Las Vegas.

Fave, L. (2017), *Investigation of the Thermal Conductivity of SiC/SiC Cladding before and after Irradiation*, PhD, École polytechnique fédérale de Lausanne.

Feinroth, H. and E. Barringer (1991), "Filament wound oxide ceramic composites as water reactor cladding", *Proceedings of the Enlarged Halden Program Group Meeting on Fuels and Materials Performance*, Bolkesjo.

Hayasaka, D. et al. (2016), "Gas leak tightness of SiC/SiC composites at elevated temperature", *Fusion Engineering and Design*, Vol. 109-111, pp. 1498-1501.

Khalifa, H.E. et al. (2016), "Radiation tolerant joining for silicon carbide-based accident tolerant fuel cladding", *Top Fuel 2016*, Boise, Idaho.

Katoh, Y. and K.A. Terrani (2015), *Systematic Technology Evaluation Program for SiC/SiC Composite-based Accident-tolerant LWR Fuel Cladding and Structures: Revision 2015*, ORNL/TM-2015/454, Oak Ridge National Laboratory, Oak Ridge.

Katoh, Y. et al. (2014), "Continuous SiC fiber, CVI-SiC matrix composites for nuclear applications: Properties and irradiation effects", *Journal of Nuclear Materials*, Vol. 448, pp. 448-476.

Katoh, Y. et al. (2011), "Mechanical properties of advanced SiC fiber composites irradiated at very high temperatures", *Journal of Nuclear Materials*, Vol. 417, pp. 416-420.

Katoh, Y. et al. (2014), "Continuous SiC fiber, CVI-SiC matrix composites for nuclear applications: Properties and irradiation effects", *Journal of Nuclear Materials*, Vol. 448, pp. 448-476.

Katoh, Y. et al. (2012), "Radiation effects in SiC for nuclear structural applications", *Current Opinion in Solid State and Materials Science*, Vol. 16, pp. 143-152.

Katoh, Y. et al. (2011), "Stability of SiC and its composites at high neutron fluence", *Journal of Nuclear Materials*, Vol. 417, pp. 400-405.

Kim, D. et al. (2015), "Effect of dissolved hydrogen on the corrosion behavior of chemically vapor deposited SiC in a simulated pressurized water reactor environment", *Corrosion Science*, Vol. 98, pp. 304-309.

Kim, D.H. et al. (2015) "Critical heat flux for SiC- and Cr-coated plates under atmospheric condition", *Annals of Nuclear Energy*, Vol. 76, pp. 335-342.

Kim, W.-J. et al. (2016), "Development and property evaluation of SiC composite tubes for nuclear fuel cladding application", *ICACC 2016*, Daytona Beach, Florida.

Kim, W.-J., D. Kim and J.Y. Park (2013), "Fabrication and material issues for the application of SiC composites to LWR fuel cladding", *Nuclear Engineering and Technology*, Vol. 45, pp. 565-572.

Kohyama, A. et al. (2016), "Large scale production of high performance SiC/SiC fuel pins and the behavior under dynamic reactor water in Halden BWR", *2016 MRS Fall Meeting*, Boston, Massachusetts.

Lorrette, C. et al. (2017), *Quench behavior of SiC/SiC Cladding after High Temperature Rampe under Steam Conditions*, WRFPM 2017, Jeju Island.

Lorrette, C. et al. (2015), "SiC/SiC composite behavior in LWR conditions and under high temperature steam environment", *Top Fuel 2015*, Zurich.

Park, J.-Y. et al. (2013), "Long-term corrosion behavior of CVD-SiC in 360°C water and 400°C steam", *Journal of Nuclear Materials*, Vol. 443, pp. 603-607.

Rohmer, E., E. Martin and C. Lorrette (2014), "Mechanical properties of SiC/SiC braided tubes for fuel cladding", *Journal of Nuclear Materials*, Vol. 453, pp. 16-21.

Sauder, C. (2014) "Ceramic matrix composites: nuclear applications", Chapter 22 in *Ceramic Matrix Composite: Materials, Modeling and Technology*, edited by Wiley library.

Sauder, C. et al. (2013), "Assessment of SiC/SiC cladding for LWRs", *Top Fuel 2013*, Charlotte, NC.

Terrani, K.A. et al. (2015), "Hydrothermal corrosion of SiC in LWR coolant environments in the absence of irradiation", *Journal of Nuclear Materials*, Vol. 465, pp. 488-498.

Terrani, K.A. et al. (2014), "Silicon carbide oxidation in steam up to 2 MPa", *Journal of the American Ceramic Society*, Vol. 97, pp. 2331-2352.

Yueh, K., D. Carpenter and H. Feinroth (2010), "Clad in clay", *Nuclear Engineering International*, Vol. 55, pp. 14-16.

Yueh, K. and K.A. Terrani (2014), "Silicon carbide composite for LWR fuel assembly applications", *Journal of Nuclear Materials*, Vol. 448, pp. 380-388.

14. Non-fuel components

Accident-tolerant control rods

The neutron-absorbing materials such as Ag-In-Cd alloy and boron carbide (B_4C) loaded into stainless steel (S.S.) tubes are widely used for the reactivity control of current PWR and BWR. Nevertheless, the melting point of Ag-In-Cd alloy (~790°C), the eutectic temperature of boron carbide (B_4C) and Fe; (~1 150°C) and the eutectic temperature of Fe and Zr; (~950°C) are lower than the temperature (≥1 200-1 300°C) at which Zr-alloy fuel cladding begins to be intensively oxidised under severe accident (SA) conditions. This means that control rods (CRs) can be damaged and their neutronic worth is affected in the initial phase of a severe accident when the fuel rods still keep their integrity.

Additionally in the future, enhanced accident-tolerant fuel (EATF) implementation should offer an increase in the coping time before reaching limiting core temperatures. By tolerating loss of cooling in the reactor core for a considerably longer time period, control rod integrity may become more limiting than the fuel assembly.

When CRs are damaged in a PWR, molten Ag-In-Cd alloy will be ejected, which would result in the immediate volatilisation of Cd because of its high vapour pressure (boiling point at atmospheric pressure = 767°C). Moreover, when CRs are damaged in a BWR, the neutron-absorbing material, B_4C, comes in direct contact with high-temperature (HT) water vapour, possibly resulting in the formation of volatile boric acid (H_3BO_3). Since Ag-In-Cd alloy and B_4C will be removed from the core early in the severe accident, the disintegrated and molten fuel material is not expected to contain the neutron-absorbing materials. Thus, the injection of unborated or insufficiently borated water for emergency cooling of the reactor during a severe accident may lead to uncontrollable recriticality. The Central Research Institute of Electric Power Industry (CRIEPI, Japan) and AREVA NP (France) have proposed and started to develop a novel accident-tolerant control rod (ATCR) to improve the safety of light water reactors (LWRs) under all conditions including severe accidents (Ohta et al., 2014a, 214b; Ohta et al., 2016a, 2016b).

The following inherent characteristics are required in ATCR:

- The reactivity worth of ATCR should be comparable to or exceed that of conventional CR throughout the operation period of the reactor. A higher reactivity worth can be provided by ATCR, leading to a larger shutdown margin.

- The neutron-absorbing materials used in ATCR should have sufficiently high melting point and high eutectic temperature with SS cladding to prevent breakage of the CRs prior to extensive fuel rod failure in a severe accident, thus avoiding uncontrollable recriticality even if unborated water is injected for emergency cooling of the core.

- The neutron-absorbing materials must be stable even in water or steam so as not to disintegrate in case of CR cladding breakage.

Furthermore, provided that the neutron-absorbing materials melt at a temperature comparable to the melting point of the fuel material (UO_2) and are highly miscible with molten and solidified UO_2, uncontrollable recriticality can therefore be avoided even after core meltdown.

Retained candidates

For ATCR, the cladding is currently not the main concern. However, if EATF breakthrough solutions enable reaching much higher temperature than the melting point of S.S. ~1 450°C, then the change of the CR cladding might be studied as well.

The main idea is to replace the conventional neutron-absorbing materials with proper ceramic materials that satisfy the above requirements and do not impact the functional requirements of the CRs (Strasser, Yario, 1980). Theoretical density (TD), macroscopic neutron absorption cross-section and melting temperature of the ATCR candidate neutron-absorbing materials and conventional ones are summarised in Table 14.1. Sintered density and neutronic worth for the candidate mixture pellets are shown in Figure 14.1.

As new neutron-absorbing materials for ATCR, CRIEPI proposes a mixture of rare-earth sesquioxides (RE_2O_3, rare-earth elements [RE] = Sm, Eu, Gd, Dy or Er) and zirconium dioxide (ZrO_2) or RE_2O_3 and hafnium dioxide (HfO_2) for both of PWRs and BWRs (Ohta et al., 2014a, 214b; Ohta et al., 2016a, 2016b). It should be noted that ZrO_2 or HfO_2 is added to improve the chemical stability of RE_2O_3, even in water or steam.

AREVA NP proposes the substitution of the Ag-In-Cd rod by a combination of two pellet types: a hafnium carbide (HfC) pellet and a samarium hafnate (Sm_2HfO_5) pellet (see Figure 14.2). Regarding the replacement of B_4C, the europium hafnate (Eu_2HfO_5) has been retained as a non-alpha emitter presenting favourable properties towards swelling.

Table 14.1. Principal properties of ATCR candidate materials and conventional neutron absorbers

	ATCR Candidate materials								Conventional absorbers	
	Sm_2O_3	Eu_2O_3	Gd_2O_3	Dy_2O_3	Er_2O_3	ZrO_2	HfO_2	HfC	AIC [6]	B_4C
Theoretical density [g/cm³]	7.7 [4]	7.9 [4]	8.3 [4]	9.0 [4]	8.6 [5]	5.7	9.7	12.2	10.2	2.6
$\Sigma_{absorption}$ [1] [cm⁻¹] Thermal reactor [2] FR [3] (×10⁻³)	23.8 10	6.5 35	51.4 13	2.1 12	1.3 10	«0.01 0.5	1.2 8	1.6 11	4.6 19	6.9 41
Melting temperature [˚C]	2 270	2 290	2 340	2 230	2 340	2 700	2 800	3 900	800	2 350

[1] One group macroscopic neutron absorption cross-section, based on ORLIBJ40 (Okumura et al., 2012).

[2] PWR34J40.

[3] 600MMTOCJ40.

[4] Monoclinic crystal system.

[5] Cubic crystal system.

**Figure 14.1. Sintered density and neutronic worth
for representative neutron-absorbing materials**

$$RE_2MO_5 = RE_2O_3\text{-}MO_2 \text{ (Fluorite)}$$
$$RE_2M_7O_{17} = RE_2O_3\text{-}7MO_2 \text{ (Fluorite)}$$
$$(M = Zr \text{ or } Hf)$$
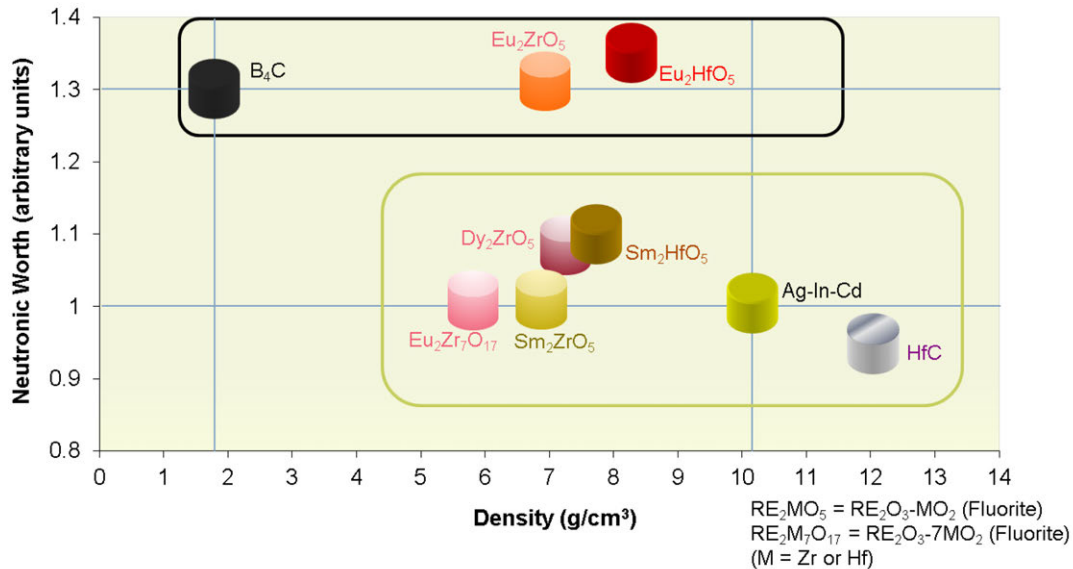
Source: Bischoff, 2018.

Figure 14.2. Combination of pellets to replace Ag-In-Cd
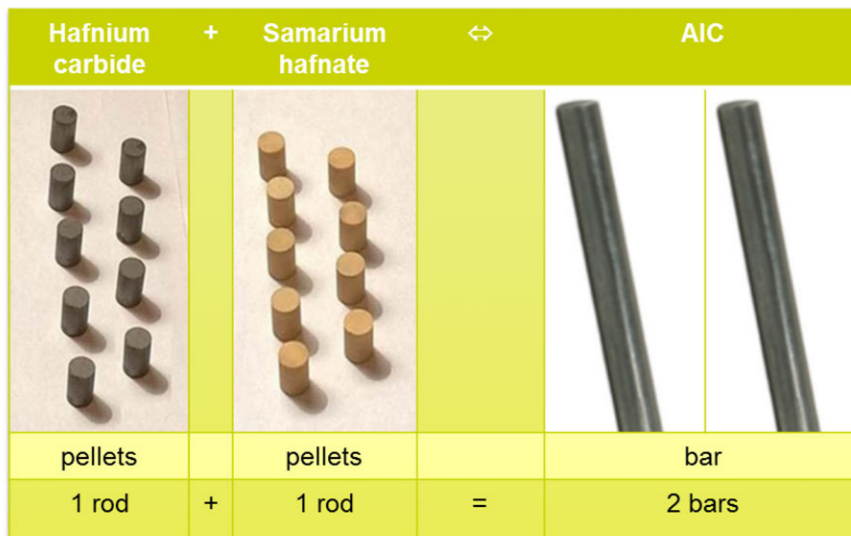
Source: Bischoff, 2018.

Fabrication

- Materials: Sm_2O_3, Eu_2O_3, Gd_2O_3, Dy_2O_3, Er_2O_3, ZrO_2, HfO_2 and HfC are available as raw materials and no risk is currently identified on large-scale quantities.

- Fabrication equipment: Current B_4C sintering furnaces are compatible with production needs of these materials.

- Fabrication processes: ATCR concept production processes are perfectly compatible with current fuel and control rod manufacturing plants.

- Inspection techniques: Existing standard techniques are appropriate for these materials.

HfC pellets and pellets of RE_2O_3 and HfO_2 or ZrO_2 mixtures were successfully fabricated (see Figure 14.3). The densities of the sintered pellets were high enough, >95%TD. First characterisations have been performed and are well in line with available data from literature (Risovany et al., 2006).

Figure 14.3. Sintered pellets of HfC, Sm_2O_3-HfO_2, Eu_2O_3-HfO_2 and Eu_2O_3-ZrO_2 mixtures

| HfC | Sm_2O_3-HfO_2 | Eu_2O_3-HfO_2 | Eu_2O_3-ZrO_2 |
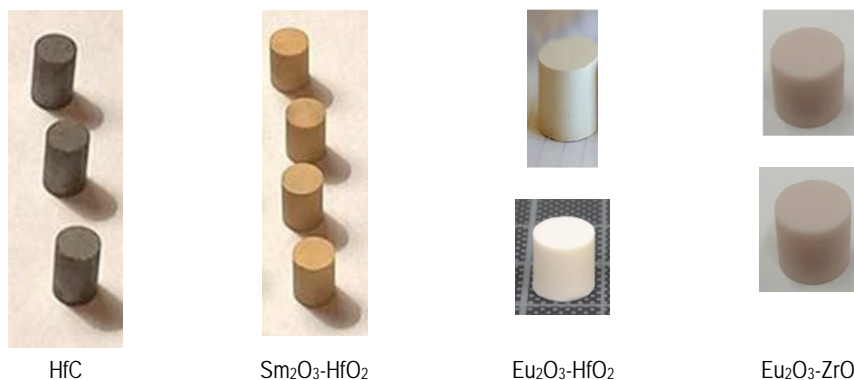
Source: Ohta, 2018; Bischoff, 2018.

Normal operation and anticipated operation occurences

- Utilisation and burn-up: ATCR can be designed to mimic standard CR for BWR or PWR with regard to normal operation performance (including reactivity worth) as illustrated in Figures 14.4 and 14.5, so no impacts on plant utilisation and burn-up are anticipated. Based on the anticipated improved irradiation behaviour with respect to swelling as described below, ATCR should enable extended lifetime and increased manoeuvrability.

- Swelling: Currently, the lifetime of CRs in LWRs is usually limited by swelling of the neutron-absorbing material (Ag-In-Cd alloy or B_4C). The new absorber materials used for ATCR are targeted to have a cubic (BCC, fluorite) structure known to feature low swelling under irradiation. Since a low transmutation level of the absorber isotopes and no phase change from the cubic phase are expected during the irradiation, the main swelling will be caused by irradiation damage. Such a mechanism leads to very low swelling for cubic structure. As the new absorber materials are (n, gamma) absorbers, no contribution to swelling is expected through outgassing (e.g. helium emission). This assessment is based on an extrapolation from data available in the open literature for similar materials (Spink et al., 1973; Risovany et al., 2000; Risovany et al., 1998). Therefore, ATCR would allow a considerable increase of the lifetime in comparison with current CRs, while providing additional flexibility regarding CR operation.

Further irradiation testing will be needed to quantify the swelling of the new absorber materials, in order to refine the design models and confirm and quantify the increase of the control rod lifetime.

- Thermal behaviour: The new absorber materials have a lower thermal conductivity than Ag-In-Cd (about 10 times lower for HfC and 50-100 times lower for RE_2O_3-HfO_2) and B_4C (about 10-25 times lower for RE_2O_3-HfO_2). However, the low power density within the CR absorber materials allows for a sufficient margin with respect to the melting temperature (see Table 14.1).

- Neutronic behaviour: The core neutronic behaviour does not change as long as the ATCR is designed to keep the same reactivity worth as the current CR. Even if the ATCRs have higher total reactivity worth in order to allow for a larger shutdown margin, the radial and axial power distributions during normal operation when the CRs are partially inserted are expected to be very similar to the reference design as illustrated in Figures 14.4 and 14.5. Therefore, no impact on the neutronic behaviour is anticipated.

- Chemical compatibility, stability: In normal and AOO conditions, control rod cladding is intact and no interaction with the coolant is expected. Additionally, the ATCR crack risk is further reduced by the absence of swelling and gas generation in the absorber material.

- Licensibility: For licensibility of ATCR, no data is available. However, it is expected that the licensing procedure for normal CRs will remain applicable.

Figure 14.4. Insertion depth dependence of CR reactivity worths in BWR for Eu_2O_3-HfO_2, Eu_2O_3-ZrO_2 and B_4C
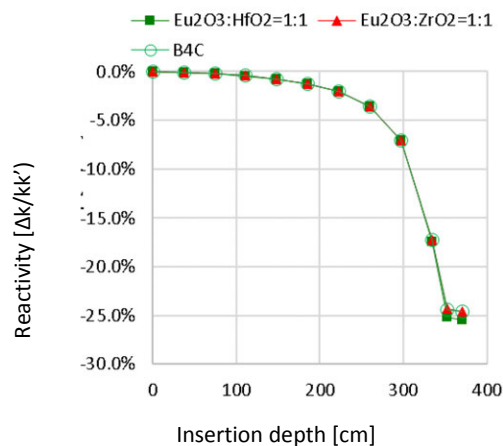
Source: Ohta et al., 2016a, 2016b.

Figure 14.5. Insertion depth dependence of CR reactivity worths in PWR for Eu_2O_3-HfO_2, Eu_2O_3-ZrO_2, Gd_2O_3-HfO_2, Sm_2O_3-ZrO_2 and Ag-In-Cd alloy
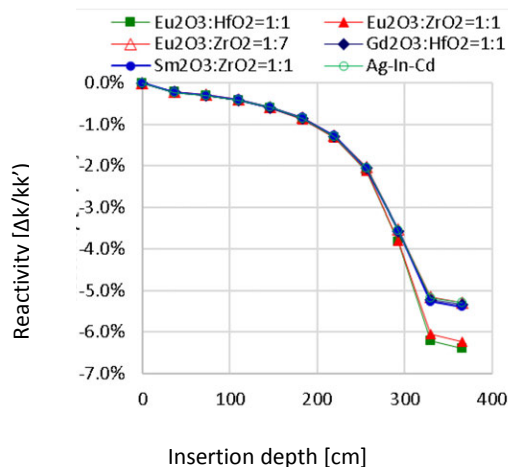
Source: Ohta et al., 2016a, 2016b.

Design-basis accidents and design extension conditions

Mechanical strength, ductility, resistance to fuel rod rupture upon reflood

The mechanical and geometric stability of the CRs is enhanced throughout the DBA as the absorber materials remain solid and experience neither melting (Ag-In-Cd) nor vapourisation (Cd) and as the eutectic reaction between B_4C and Fe (SS cladding) is excluded.

Thermal behaviour

The melting point of the ATCR absorber materials is significantly higher than that of SS cladding (~1 450°C), whereas melting point of Ag-In-Cd is 790°C and boiling point of Cd is 767°C at 1 atm.

An HT compatibility experiment of RE_2O_3/Fe, RE_2O_3/SS and RE_2O_3-HfO_2/Fe revealed that no significant reaction occurred at temperatures lower than the melting point of SS cladding, as shown in Figure 14.5. From the chemical similarities among REs or between Zr and Hf, the same behaviour is expected for RE_2O_3-ZrO_2 as well as other RE_2O_3-HfO_2. That is, new absorber materials do not cause eutectic with Fe like B_4C. Thus, even in case of eutectics at around 950°C between the CR cladding (SS) and guide tube thimble or channel box (Zr-alloy) no material expulsions are expected, allowing the absorber materials to remain in the solid phase.

These results indicate that ATCR is not expected to be damaged before serious failures of fuel rods in accident conditions take place.

Even after core meltdown, the neutron-absorbing materials, RE_2O_3-ZrO_2 and RE_2O_3-HfO_2, are expected to coexist with the molten and solidified fuel materials and prevent recriticality following the injection of possible unborated water. However, the benefits offered over the entire temperature range up to fuel melting ~2 800°C and performance advantages in SA conditions must be validated through further experiments.

Chemical compatibility, stability, oxidation behaviour

No known eutectics between ATCR absorber and cladding materials until the melting point of SS as described in 5b).

The oxidation reaction of the absorber materials is less exothermic than the oxidation of cladding materials (Zr-alloys, SS) and should contribute at a very low extent to the overall core system heating.

Although the RE_2O_3 is well known to be chemically unstable in water or moist air, it can be stabilised by mixing ZrO_2 and/or HfO_2.

These properties should be further checked and confirmed through experimental testing.

Figure 14.6. High-temperature compatibility of RE$_2$O$_3$(-HfO$_2$) and Fe or S.S.
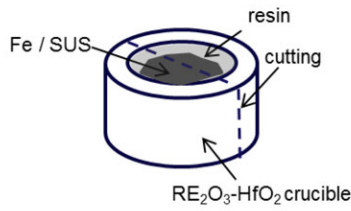
Experiment:

RE$_2$O$_3$(-HfO$_2$) crucibles containing Fe or S.S. (Fe-18Cr-8Ni-2Mn) were heated to 1 600°C under argon atmosphere and kept for 1 hour.
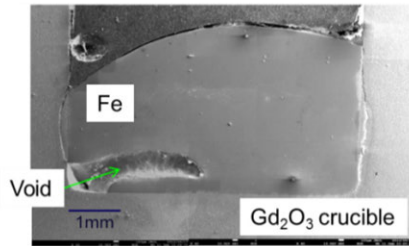
1) Gd$_2$O$_3$ / Fe
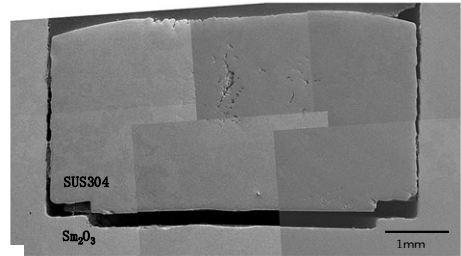
2) Sm$_2$O$_3$ / S.S.

Sm$_2$O$_3$ crucible
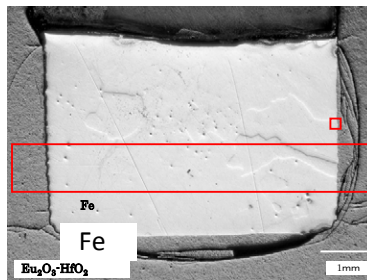
Eu$_2$O$_3$-HfO$_2$ crucible

3) RE$_2$O$_3$-HfO$_2$/Fe
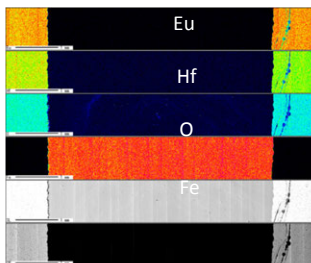
40μm

4) Radial distribution of each element

1mm
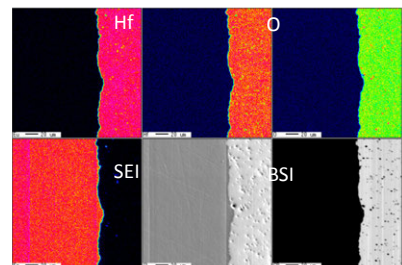
5) Microscopic element mapping

Source: Ohta et al., 2016.

Used ATCR storage/transport/disposition/reprocessing

As for storage, transport and disposition, the methodologies for current CRs are also available for ATCR, because the cladding materials are not changed. Still, a feature connected to long-term radioactivity of ATCR should be evaluated:

- The activation of the HfC and RE_2O_3-MO_2 (RE = Sm, Gd, Dy or Er, M = Zr or Hf) under irradiation is expected to be lower than the Ag-In-Cd mainly due to the absence of ^{110m}Ag.

- The activation of Eu_2O_3-MO_2 (M = Zr or Hf) is expected to be about ten times larger than Ag-In-Cd.

- Impacts of radioactivity of irradiated neutron absorbers need to be evaluated based on the amount of CR wastes taking the lifetime into account.

As with conventional CRs, ATCR is not designed to be reprocessed.

SiC-composite for BWR channel box

Silicon carbide (SiC) ceramic composite is a potential candidate as ATF-cladding materials and for BWR channel box applications. If most of the focus and attention has been brought on the possible application as fuel cladding instead of zircaloy, however, the channel box is also a major component, which makes up approximately 40% of zircaloy in a typical BWR core (Yueh et al., 2014).

SiC is used in the composite form for strength and fragmentation resistance (Kitano et al., 2013; Suyama et al., 2015). Its properties have been evaluated against BWR channel mechanical design requirements. The evaluation included fragmentation resistance, seismic loading, differential volumetric swelling and thermal shock resistance. The evaluation results indicate SiC-composite could meet BWR channel mechanical design requirements. However, SiC is not in its thermodynamic lowest energy state and may react with water under some conditions. Under HT steam accident conditions, SiC oxidises and forms a protective silica layer. Under operational conditions, a stable protective silica layer could not be formed because of high solubility of silica in water. Additional research is needed to address the operational oxidation issue under oxidising conditions. This chapter summarises the results provided by EPRI and Toshiba, which are both separately working on the development of a SiC channel box.

Fabrication

EPRI and Toshiba were individually successful in fabricating short length channel boxes and cladding tube by utilising CVD/CVI-SiC/SiC process. An example of a short channel piece fabricated by the Toshiba and Ibiden Co. Ltd is shown in Figure 14.7. The channel box has a width of ~140 mm and the length was scaled down to about 1 000 mm because of restriction of the furnace size (Toshiba, Ibiden, 2014; Toshiba, 2015; Yang, 2014; Kakiuchi et al., 2016). EPRI has fabricated two short channel pieces of similar dimensions. The SiC/SiC channel pieces were subjected to various characterisations as discussed below.

Figure 14.7. Trial fabrication of SiC/SiC composites by Toshiba and Ibiden
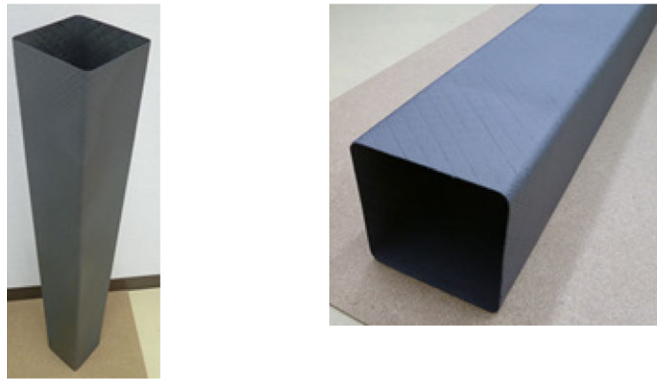
Source: Kakiuchi et al., 2016.

Normal operation and AOO

Smaller neutron absorption cross-section

SiC has a neutron absorption cross-section of approximately 60% that of zirconium. The lower neutron capture cross-section could support a slightly lower fuel enrichment requirement or higher discharged burn-up for the same enrichment. The lower neutron capture cross-section of SiC was verified through a SiC reactivity measurement test in the NCA (Toshiba Nuclear Critical Assembly) facility. The reactivity worth analyses were performed by a continuous-energy Monte Carlo code (core configurations with SiC sample and air reference). The value of the effective delayed neutron fraction (β_{eff}) was 0.696% as NCA empirical value. The calculated reactivity was in good agreement with the measured reactivity as shown in Figure 14.8. (Matsumiya et al., 2015). The actual neutronic economics to be gained by using SiC-composite channel will depend on the channel wall thickness in the final design.

Figure 14.8. Reactivity worth of SiC (reference air)
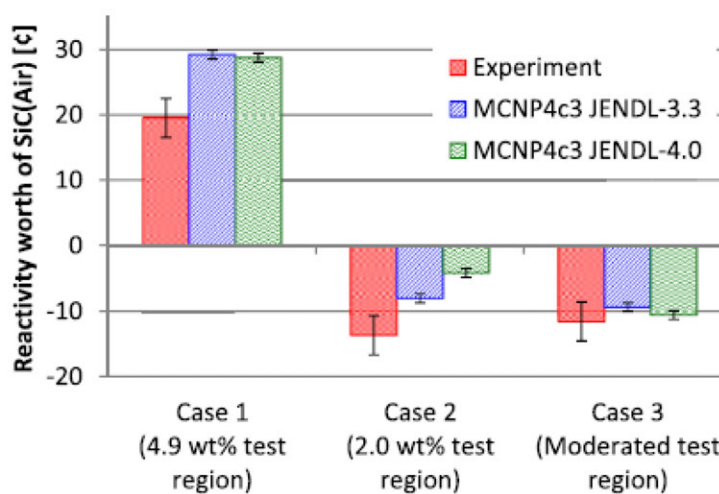
Source: Matsumiya et al., 2015.

Hydrothermal corrosion property

Hydrothermal corrosion reaction of SiC produces silica, which is soluble in HT water, leading to recession of the SiC-composite. The recession rate increases with the oxygen concentration in the water (Terrani et al., 2015; Lahoda et al., 2016). Therefore, the recession or corrosion property of SiC is one of its most important challenges for applications in LWRs, particularly in the oxidising condition of BWR-like water chemistry.

EPRI conducted a corrosion test of SiC-composite samples in a simulated BWR oxidising condition in the MIT test reactor. The coupon samples were prepared from a SiC-composite channel section. The coupon samples showed a high weight loss of nearly 15%. On the contrary, SiC tube samples showed no weight loss in simulated PWR water chemistry at the same reactor. This has verified the hypothesis that the oxidising condition of simulated BWR water chemistry is responsible for the observed high corrosion rate of the SiC-composite channel coupons. Currently, EPRI is working on surface modifications to stabilise the silica by forming a protective layer, e.g. zirconium silicate or titanium silicate, for the corrosion mitigation.

Concerning the mitigation of SiC corrosion, Toshiba has been confirming by the ongoing study that the hydrothermal corrosion property of CVD-SiC strongly depends on the fabrication process of SiC and the environment of the autoclave test simulating both BWR and PWR conditions. A consequence was that CVD-SiC samples fabricated with an optimised process has shown lower corrosion rates even in BWR condition as shown in Figure 14.9 (Uchihashi et al., 2017). More detailed studies are essential to clarify the corrosion mechanism through both out-of-pile and in-pile tests.

Figure 14.9. Autoclave test result for CVD-SiC with various fabrication processes

(290 deg C, 8 MPa, DO 8 ppm)
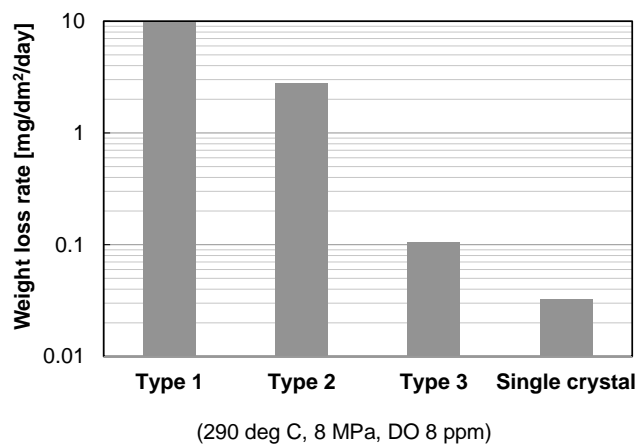
Source: Uchihashi et al., 2017.

Irradiation volumetric induced channel bow

Zr-alloy channels have experienced bow mainly caused by fast neutron flux gradient or differential hydriding of different sides of a channel or the combination of both factors. Significant channel bow can affect the channel gap, which influences fuel rod power and the control rod insertion function. SiC channel may provide a means for mitigation of channel bow. SiC will undergo irradiation-induced volume swelling of 1-2% at the beginning of life, but it saturates at around 1 dpa or after 6 months of irradiation in LWRs, and the dimension then become rather stable to very high-neutron fluence (Katoh et al., 2016). Irradiation tests of SiC channel should be conducted to demonstrate its potential for channel bow mitigation prior to the commercial utilisation.

Design-basis accidents and design extension conditions

High-temperature steam oxidation

The results of the HT steam oxidation tests are shown in Figures 14.10 and 14.11 (Okonogi et al., 2015). The oxidation rate of SiC in HT steam was confirmed to be less than 1/1 000 of Zry-2, which indicates that SiC has significant tolerance under SA conditions. As the current oxidation data are limited only to tests conducted in atmospheric or low steam pressure (Terrani et al., 2014), additional test data under high steam pressure conditions are needed for the future.

Figure 14.10. Visual appearance after high-temperature steam test
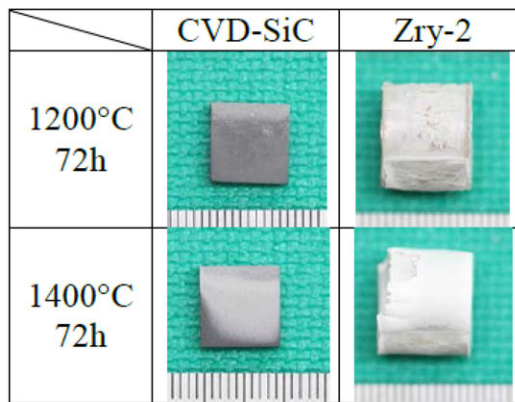
Source: Okonogi et al., 2015.

Figure 14.11. Corrosion rate as a function of the temperature
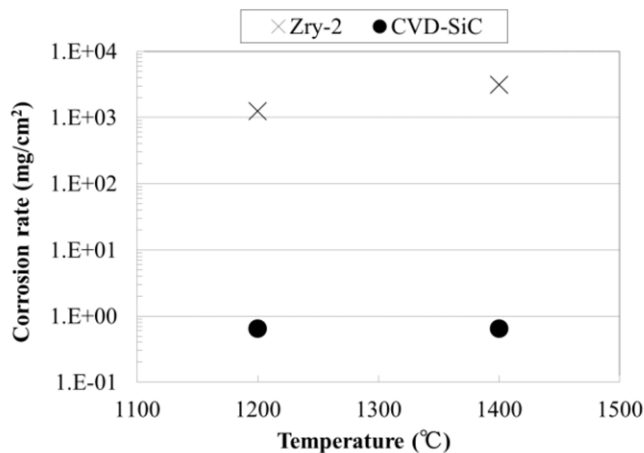
Source: Okonogi et al., 2015.

Thermal shock resistance and quench survivability

In order to confirm quench survivability during LOCA, a thermal shock test was performed by both Toshiba and EPRI, as shown in Figures 14.12 to 14.15 (Yueh et al., 2014; Kakiuchi et al., 2016). SiC/SiC channel box with shorter length was rapidly quenched from around 1 473 K to water at ambient temperature. No apparent damage was observed on the SiC test piece after quenching.

Figure 14.12. Surface temperature of channel box in thermal shock tests by EPRI
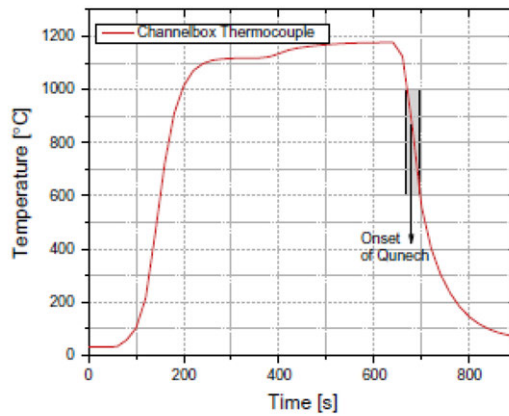
Source: Yueh et al., 2014.

Figure 14.13. Appearance after the thermal shock tests by EPRI
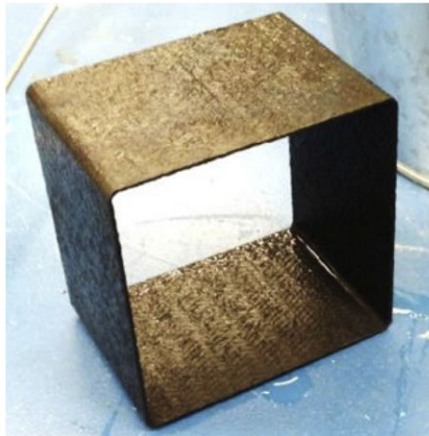
Source: Yueh et al., 2014.

Figure 14.14. Surface temperature of channel box in thermal shock tests by Toshiba
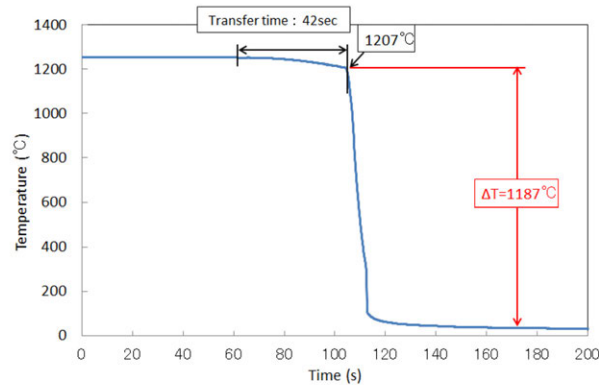
Source: Kakiuchi et al., 2016.

Figure 14.15. Appearance after the thermal shock tests by Toshiba

Source: Kakiuchi et al., 2016.

Used storage/transport/disposition/reprocessing

In terms of compatibility with back-end processes, the specific properties and the behaviour of SiC needs to be addressed in further studies.

References

Kakiuchi, K. et al. (2016), "Progress on ATF development of SiC for LWR", *TopFuel 2016,* Boise.

Katoh, Y. et al. (2016), "Irradiation – High heat flux synergism in silicon carbide-based fuel claddings for LWRs", *TopFuel 2016*, Boise.

Kitano, K. et al. (2013), "Development of innovative material for nuclear reactor core with enhanced safety", *TopFuel 2013*, Charlotte, North Carolina, 15-19 September 2013, pp.936-942.

Lahoda, E. et al. (2016), "SiC cladding corrosion and mitigation", *TopFuel 2016*, Boise.

Matsumiya, H. et al. (2015), "Reactivity measurements of SiC for accident-tolerant fuel", *Progress in Nuclear Energy*, Vol. 82, pp. 16-21.

Ohta, H. et al. (2016a), "Development of accident tolerant control rod for LWRs", *Proc. of Top Fuel 2016,* 17556.

Ohta, H. et al. (2016b), "Development of accident tolerant control rod – Reactivity analysis of innovative neutron-absorbing materials", *Proc. of AESJ 2016 autumn meeting,* in Japanese.

Ohta, H. et al. (2014a), *A Concept of Accident Tolerant Control Rod for LWRs*, CRIEPI Rep. L13005 (2014) in Japanese.

Ohta, H. et al. (2014b), "Development of accident tolerant control rod for LWR", *Proc. of AESJ 2014 annual meeting*, in Japanese.

Okonogi, K. et al. (2015), "Prognerr on the research and development of innovative material for nuclear reactor core with enhanced safety", *Top Fuel 2015*.

Okumura, K. et al. (2012), *A Set of ORIGEN2 Cross-Section Libraries Based on JENDL-4.0: ORLIBJ40*, JAEA-Data/Code 2012-032, in Japanese.

Risovany, V.D. et al. (2006), "Dysprosium hafnate as absorbing material for control rods", *Journal of Nuclear Materials*, Vol. 355, pp. 163-170.

Risovany, V.D. et al. (2000), "Dysprosium titanate as an absorber material for control rods", *Journal of Nuclear Materials,* Vol. 281, pp. 84-89.

Risovany, V.D. et al. (1998), *Dysprosium and Hafnium base Absorbers for Advanced WWER Control Rods,* IAEA-TECDOC 1132.

Spink, D.R. et al. (1973), "The development of rare-earth pyrohafnates for power reactor control rod materials", *Journal of Nuclear Materials*, Vol. 49, pp. 1-9.

Strasser, A. and W. Yario (1980), "Control Rod Materials and Burnable Poisons An evaluation of the state of the art and Needs for Technology Development", July 1980, EPRI, Table 6-1.

Suyama, S. et al. (2015), "Development of accident torlant core material for applying SiC/SiC composite", *FL ICACC'15 – 39th International Conference and Expo on Advanced Ceramics and Composites*, January 2015.

Toshiba (2015), "SiC reactor core material", *Toshiba review,* Vol.70, No.3.

Toshiba and Ibiden (2014), "Establish Manufacturing Technology for Reactor Core Material Using Silicon Carbide (SiC)", Press Releases, 3 July 2014, www.toshiba.co.jp/about/ press/2014_07/pr0301.htm

Terrani, K.A. et al. (2015), "Hydrothermal corrosion of SiC in LWR coolant environments in the absence of irradiation", *Journal of Nuclear Materials,* Vol. 465, pp. 488-498.

Terrani, K.A. et al. (2014), "Silicon carbide oxidation in steam up to 2 MPa", *Journal of American Ceramic Society,* Vol. 97, No. 8, pp. 2331-2352.

Uchihashi, M. et al. (2017), "Improvement of SiC corrosion property", *Atomic Energy Society of Japan 2017 Annual Meeting,* 27-29 March 2017.

Yang, J.H. (2014), "Summary presentation on SiC", *Second Meeting of the NEA Expert Group on Accident Tolerant Fuels for LWRs,* 23-25 September 2014, OECD, Paris.

Yueh, K. et al. (2014), "Silicon carbide composite for LWR fuel assembly applications", *Journal of Nuclear Materials,* Vol. 448, pp. 380-388.

Part III: Advanced fuel designs

15. Introduction

The fuel designs covered by the Task Force on Advanced Fuel Designs consisted of three different concepts: improved UO_2 fuel, high-density fuel and encapsulated fuel (TRISO-SiC-composite pellets). Regarding the improved UO_2 fuel, this particular design was divided into two sub-concepts, such as oxide-doped UO_2 and high-thermal conductivity UO_2 (designed by adding metallic or ceramic dopant).

The main objective of the Task Force on Advanced Fuel Designs, similarly as for the Task Force on Cladding and Core Materials, was to ensure a satisfying level of compilation of related knowledge without losing information in the course of that process.

As for the Task Force devoted to cladding and core materials, the work was organised in several steps:

- define an attribute guide (ABG) as exhaustive as possible and covering the following fields already defined in "Advanced Fuels Campaign: Enhanced LWR Accident Tolerance Fuel Performance Metrics" (Bragg-Sitton, 2014), fabrication/ manufacturability, normal operation and AOOs, DBA, DECs, fuel cycle-related issues (such as used fuel storage, transport, disposal, reprocessing);

- fill the ABG spreadsheet for each specific candidate design (not necessarily filling all the attributes) with a colour code added to explicit written comments and illustrating in a very visual way: challenging or not challenging lack of data, potential showstoppers, need for further optimisation or demonstrated maturity for each single attribute; a selection of the filled ABG after cross-reviewing is shown in a devoted Appendix;

- for each specific design, describe the *Key Highlights* (relying when available on the filled ABG spreadsheet), which have been provided through that process by the contributing organisations shown in the table below;

- for each type of design, summarise all the available information in the devoted chapter shown in this report.

Regarding high-density fuel, R&D works on silicide and nitride fuel concepts are ongoing in several institutes. For the purpose of comparing fundamental characteristics as applicable as an LWR fuel, the technical review was mainly based on a literature survey, performed for carbide and metal fuels.

Improved UO_2			
Doped UO_2		High-thermal conductivity UO_2	
		Metallic additive	Ceramic additive
Cr_2O_3 doped UO_2 Al_2O_3-Cr_2O_3 doped UO_2	Ceramic microcell UO_2	CERamic METal (CERMET), Mo-modified UO_2 Metallic microcell UO_2	BeO-modified UO_2 SiC/diamond modified UO_2
FJP (*) Westinghouse	KAERI	FJP (*) KAERI	CGN University of Florida

(*): French Joint Programme (CEA-AREVA-EDF).

High-density fuel				Encapsulated fuel
Silicide	Nitride	Carbide (**)	Metal (**)	
NRG Westinghouse	FJP (*)	TF3	TF3	CGN KAERI ORNL

(*): French Joint Programme (CEA-AREVA-EDF).

(**): Carbide and metal fuels were treated as reference concepts in TF3.

Reference

Bragg-Sitton, S. et al. (2014), "Advanced Fuels Campaign: Enhanced LWR Accident Tolerance Fuel Performance Metrics", prepared for US Department Of Energy Advanced Fuel Campaign, February 2014, INL/EXT-13-29957, FCRD-FUEL-2013-000264.

16. Improved UO₂

Doped UO₂

Desirable attributes for accident-tolerant fuel (ATF) pellets include enhancing the retention of fission products (FPs) and minimising pellet-cladding interaction. Various concepts are currently being suggested and evaluated worldwide to meet these requirements and ultimately to mitigate the consequences of an accident.

Among those concepts, the use of oxide additives in UO_2 is considered to be an attractive technical and economical solution. This technology might be able to reduce lengthy approval time frames for new fuel design because it uses existing infrastructure, experience and expertise, so that evolutionary concepts can be deployed in a shorter time frame.

According to the main role of additives and the amount of doping, oxide-doped UO_2 concepts can be categorised into two groups.

- doped UO_2 pellets, aiming at increasing grain size and enhancing the viscoplastic behaviour:

  - Cr_2O_3 doped UO_2 pellet (by French Joint Programme AREVA-CEA-EDF);

  - Al_2O_3-Cr_2O_3 doped UO_2 pellet (ADOPT pellet by Westinghouse).

- microcell UO_2 pellet, aiming at enhancing FP retention capability:

  - Si-based oxide-doped UO_2 pellet (ceramic microcell UO_2 by the Korea Atomic Energy Research Institute [KAERI]).

The overall key attributes of doped UO_2 fuel forms are summarised below.

Cr₂O₃ and Al₂O₃-Cr₂O₃ doped UO₂

In the early 90s, extensive programmes were launched to develop improved fuel pellets with the goal of increasing fuel robustness and efficiency with enhanced performance while ensuring improved safety margins. To that end, two main objectives were identified that would provide progress in reliability and operational flexibility of light water reactors (LWRs): improvement in fission gas retention and enhanced resistance to stress corrosion cracking due to pellet-clad interaction (SCC-PCI) (Delafoy, Arimescu, 2016; Delafoy et al., 2015; Teboul et al., 2012; Dewes, Delafoy, 2006; Delafoy et al., 2003). Indeed, this double goal can be achieved by an appropriate modification of UO_2 fuel. In particular, a large-grain fuel structure was sought to increase fission gas retention and to enhance fuel viscoplasticity, benefiting PCI and SCC-PCI resistance (Zemek et al., 2006). Pellet additives or "dopants" can provide the expected enhancement of key properties, adding value and reliability to nuclear fuel (Arborelius et al., 2005; Zhou et al., 2005; Kitano et al., 2005).

In the light of a tight selection process, AREVA NP chose chromia (Cr_2O_3) as the relevant dopant to obtain the desired fuel large-grain microstructure and enhanced viscoplastic behaviour (Delafoy, Arimescu, 2016). Based on the parametric studies, chromia content is specified at an optimum value of 0.16 wt% corresponding to the solubility limit of the dopant in UO_2 at the applicable sintering conditions (Riglet-Martial et

al., 2014; Cardinaels et al., 2012; Leenaers et al., 2003). For a given optimised chromia content level, large grains favourably increase Cr_2O_3-doped fuel viscoplasticity. These features confer a lower stress-resistance capability of Cr_2O_3-doped fuel as compared to reference UO_2 fuel, which might prove to be beneficial as far as PCI cladding stresses are concerned (Delafoy, Arimescu, 2016; Nonon et al., 2004; Nonon et al., 2003). This fuel is characterised by a homogenous large-grain microstructure, i.e. 50-60 µm (mean linear intercept value), providing beneficial features for the fuel performance: dimensional stability, improved behaviour in case of water/steam ingress, superior PCI and SCC-PCI resistance and a higher fission gas retention capability, which could lead to lower fission gas release (FGR) during accidental transients. Also, the crystalline growth enhances the fuel matrix densification. Therefore, a high-pellet density is easily obtained, and this offsets the slight reduction in fissile mass due to the addition of chromia in UO_2. The Cr_2O_3-doped UO_2 fuel qualification and licensing rely on an extensive global demonstration programme performed in commercial boiling water reactors (BWRs) and pressurised water reactors (PWRs). To date, a large database is available, allowing assessment of the performance of chromia-doped UO_2 fuel up to a maximum rod burn-up of approximately 75 GWd/tU. Thermal-mechanical models in existing qualified fuel performance codes are being refined to properly simulate the Cr_2O_3-doped UO_2 fuel behaviour and to take full benefit of the enhanced performance of that fuel (Garnier et al., 2004).

Westinghouse has developed UO_2 fuel containing Al_2O_3 and Cr_2O_3 (also referred to as ADOPT: Advanced DOped Pellet Technology). The additives facilitate densification and diffusion during sintering, which results in about 0.5% higher density within a shorter sintering time and about five times larger grains, compared with standard UO_2 fuel. While attaining the desired properties, the amount of chromium has been kept low in order to minimise the parasitic neutron absorption. Aluminium has a very small cross-section for thermal neutrons similar to that of Zr. Data show that Al_2O_3 enhances the grain size enlarging effect of Cr_2O_3, i.e. there is a synergy between the two additives. The properties of the Al_2O_3-Cr_2O_3-doped pellets are very similar to pellets with just Cr_2O_3 dopant and the Al_2O_3 can be viewed as a way to lower the total amount of dopant. In addition to the increased pellet density, which enables higher energy-density fuel – resulting in more energy production per fuel assembly –, poolside, hot cell and test reactor investigations have demonstrated significant performance advantages of Al_2O_3-Cr_2O_3-doped pellets. The benefits include reduced FGR during transients, increased margin to PCI and improved resistance against post failure secondary degradation. Reload volumes of fuel with Al_2O_3-Cr_2O_3-doped pellets have been irradiated to full discharge burn-up in many countries.

Fabrication/manufacturability

The manufacturing of both pellet variants is qualified for reload deliveries with no induced extra cost. The same production lines can be used as for standard UO_2 fuel, which is a major advantage in terms of infrastructure availability and economics. Once the oxide dopants have been blended into the UO_2 powder, the manufacturing process is exactly the same as for standard fuel. The specification differs mainly in grain size, dopant amounts and density, while the same quality control procedures used for standard fuel are applied. Finally, security of supply of the basic dopant materials (Cr_2O_3 and Al_2O_3) is not a concern.

Normal operation and AOOs

Cr_2O_3 and Al_2O_3-Cr_2O_3-doped fuels have been irradiated for a long time in many countries worldwide. Comprehensive databases are already available, including the outcomes from global demonstration programmes in commercial LWRs as well as separate-effect and integral analytical experiments. They enable the thorough investigation of the material properties and in-pile behaviour of that fuel.

The experience feedback highlights the following performance:

- Thermal behaviour: The dopant amounts in the Cr_2O_3-doped and Al_2O_3-Cr_2O_3-doped pellets are low enough not to induce significant change in the fuel thermal properties. The heat capacity, thermal expansion coefficient, melting temperature and thermal diffusivity of unirradiated UO_2 and doped pellet variants have been measured and compared (e.g. Arborelius et al., 2005). No measurable differences in these physical properties have been found. Consequently, the modelling of Cr_2O_3-doped and Al_2O_3-Cr_2O_3-doped fuels requires very little modification with respect to standard UO_2 fuel.

Fuel temperature measurements under irradiation up to high burn-ups have confirmed that Cr_2O_3-doped UO_2 thermal performances are fundamentally equivalent to that of reference UO_2 fuel (Muller et al., 2007; Valin et al., 2003). The well-known fuel thermal conductivity degradation with burn-up (related to the accumulation of solid FPs and of irradiation damages) is the main possible mechanism governing the evolution of the Cr_2O_3-doped UO_2 fuel thermal behaviour under irradiation.

- Thermal-mechanical, densification and swelling behaviours: Both fuel variants exhibit a very high-dimensional and microstructural stability up to high burn-up. In particular, a low in-reactor densification, in agreement with the measurements performed during the manufacturing process, after the standard 1 700°C – 24 hours resintering test is observed. For example, in the case of Al_2O_3-Cr_2O_3-doped fuel, densification is only about 20% than the one in the case of the standard pellets. This is also consistent with the OECD Halden Reactor Project experiment IFA-677, which shows almost no in-pile densification for the Al_2O_3-Cr_2O_3-doped pellets (Joseph, 2008). Poolside measurements of rod growth have shown that after the initial densification the swelling rates of the different pellet types are the same.

The diametral deformation of rods loaded with Cr_2O_3-doped UO_2 fuel pellets are well within the scatter of reference UO_2 fuel rods. Slight differences between the two fuels are observed at beginning of life because of the higher dimensional stability (less initial in-pile densification) of the doped fuel, which closes the pellet-clad gap earlier thus allowing fuel swelling to contribute to rod deformation (Delafoy et al., 2015; Delafoy et al., 2007). Afterwards, no additional bias with exposure is observed. Similarly, the axial deformation of Cr_2O_3-doped fuel rods is slightly above that of UO_2 rods (< ~30% rel.). However, these slight differences are such that the ability of the doped fuel to go to high burn-up exposures is not questioned.

- Fission gas release (FGR) behaviour: Chromia doping does not affect xenon release at low gas concentrations whereas it greatly affects gas trapping. Therefore, the benefits on FGR fractions and induced fuel rod internal pressure are better revealed at high burn-ups in baseload conditions and even more under power transient situations (Delafoy, Arimescu, 2016). Actually, a significant benefit, i.e. 50% at ~50 kW/m in the transient FGR kinetics is observed with the Cr_2O_3-doped UO_2 fuel as compared to standard UO_2 fuel (see Figure 16.1). The improved behaviour is due to the increased intragranular fission gas retention capability of Cr_2O_3-doped fuel.

**Figure 16.1. Comparison of fission gas release kinetics in UO₂ and
Cr₂O₃-doped UO₂ fuels in ramp testing conditions at medium burn-up**
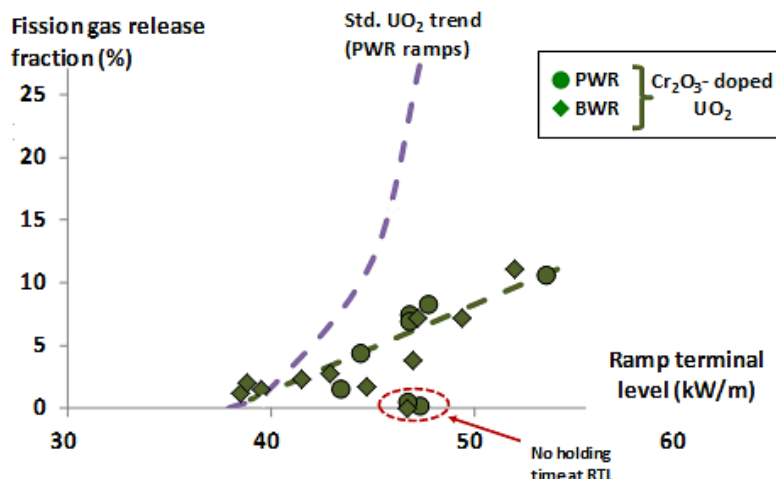
Source: Delafoy, Arimescu, 2016.

A side by side comparison of Al₂O₃-Cr₂O₃-doped and standard fuels was made in "bump" tests performed on fuel, which was base irradiated up to approximately 30 GWd/tU. The bump test consisted of a significant power increase followed by 17 days hold time. The FGR from the doped fuel rods was found to be 30% less than from standard fuel (Wright et al., 2005). For Al₂O₃-Cr₂O₃-doped pellets the majority of bubbles were found inside the grains, which is consistent with a lower rate of FGR.

- PCI and SCC-PCI behaviours: Ramp test programmes have been carried out to assess the PCI performance of the doped fuels.

The PCI performance of the Cr₂O₃-doped UO₂ fuel is established on a comprehensive database with test parameters that were selected such that the failure risk is maximised with respect to the PCI mechanism involved (Delafoy et al., 2015). Under both typical BWR and PWR transient conditions up to high burn-up, the Cr₂O₃-doped fuel pellets bring enhanced PCI resistance as compared to standard UO₂ fuel pellets (Delafoy, Arimescu, 2016; Julien et al., 2004). These pellets bring direct relief of peak cladding stress by virtue of enhanced creep deformation and the presence of more numerous and smaller outer pellet radial cracks, which reduce stress concentration at the cladding inner surface (Nonon et al., 2004; Nonon et al., 2003). In addition, the evolution of the chemical state of chromium during ramp test and the induced effect on oxygen potential may contribute to SCC mitigation (Delafoy, Arimescu, 2016; Delafoy et al., 2015).

Similarly, the Al₂O₃-Cr₂O₃-doped pellet has been shown to have significantly greater creep deformation at higher temperatures (see Figure 16.2; Wright et al., 2016). In ramp tests such creep deformation reduces the peak clad stress and can significantly increase the ramp test failure threshold. Oxygen release from the doped fuel may also be beneficial. A limited number of Al₂O₃-Cr₂O₃-doped fuel rods have been ramp tested and reported (Backman et al., 2009). Based on similarities in the creep performance with the above Cr₂O₃-doped pellet data, it is expected that a similar PCI benefit of Al₂O₃-Cr₂O₃-doped in the ramp test compared to standard fuel would be observed if ramped in similar circumstances without liner.

Figure 16.2. Ceramographies after ramp testing of (left) standard UO₂ and (right) ADOPT fuel showing enhanced creep evolution and peripheral cracking for the doped fuel
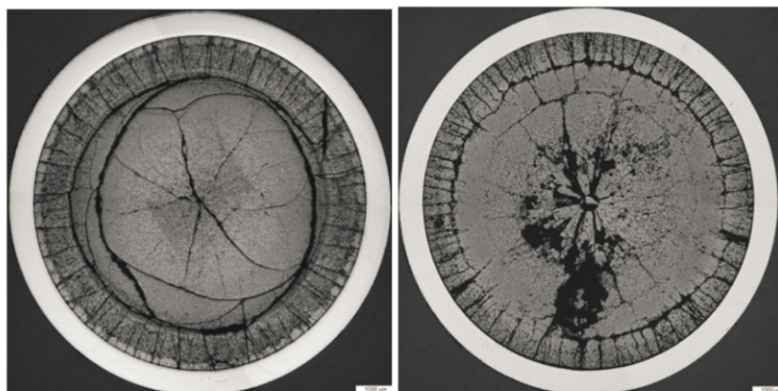
Source: Wright et al., 2016.

- Secondary degradation: In a fuel failure scenario, e.g. caused by debris fretting, uranium washout from the leaking rod can lead to contamination of the core, increased radiation doses to personnel and for BWRs, ultimately costly mid-cycle outages to remove the failed fuel.

The oxidation and washout behaviour of unirradiated non-doped and chromia-doped UO₂ fuel pellets has been analysed by thermogravimetry and by autoclave leaching tests simulating LWR conditions (Delafoy, Zemek, 2009). The entire testing programme demonstrates that chromia doping enhances the corrosion resistance of the fuel pellets. The oxidation resistance in water is distinctly increased with far less attack of the chromia-doped fuel surface as compared to UO₂ fuel. The fuel matrix grain size has a decisive impact here since oxidation proceeds by inter-granular mechanisms. Consequently, the washout rate of the chromia-doped pellets is reduced up to a factor of five in comparison to non-doped fuel types.

An oxidation test of fresh unirradiated pellets was performed and showed that the oxidation rate for Al_2O_3-Cr_2O_3-doped is about half that for standard fuel (Backman et al., 2009). In addition, a washout test was performed in the Studsvik R2 test reactor (Backman et al., 2009). The rodlets, which had open slots to the coolant, were irradiated for about 70 days at between 25 and 30 kW/m. The intention was to replicate an open primary failure and measure the amount of fuel washout. It was concluded that the fuel loss increases with power and decreases with density. Because of its higher density the Al_2O_3-Cr_2O_3-doped pellet had less washout.

Design-basis accidents (dbas) and DECs

Although no dedicated integral experiments have yet been performed in accidental conditions on Cr_2O_3- and Al_2O_3-Cr_2O_3-doped fuels, benefits are anticipated as a result of:

- A better intragranular gas retention capability, anticipated to decrease the rod internal pressure prior to the accident. This is beneficial in reducing the clad ballooning and the (burst) failure risk.

- A reduced amount of gas available for immediate release at the grain boundaries of the doped fuel pellets is likely favourable to limit the fuel fragmentation and dispersal in case of rod burst, since fuel fragmentation is likely generated by over pressurising inter-granular gas bubbles.

In the coming years, specific experiments will be performed under relevant accident conditions (such as LOCA and RIA) to provide valuable data to assess and to model the doped fuels behaviour under accidental situations.

Used fuel storage/transport/disposal/reprocessing

Because of the very low level of dopants and many properties being similar or better than standard UO₂ fuel, there are no anticipated particular fuel cycle implications for using the Cr₂O₃-doped or Al₂O₃-Cr₂O₃-doped pellets.

The dopant additions in UO₂ induce a slight reduction in the fissile mass, but the higher pellet density compensates that effect, hence preventing from increasing the initial fuel enrichment.

Because of lower FGR, improved back-end fuel cycle conditions are expected considering that a reduction of the fuel rod internal pressure induces a lower stress level on the cladding and therefore more flexibility in the management of storage casks.

Finally, the comprehensive scoping analyses done for the Cr₂O₃-doped UO₂ fuel confirmed the compatibility with the current French reprocessing process.

Microcell UO₂ pellets

The main purpose of the ceramic microcell UO₂ pellet is to minimise the FPs release contained in the pellet structure by providing a microcell structure with oxide additives (Koo et al., 2014; Kim et al., 2016). An improvement in FP retention capability leads to a reduction of the inner surface cladding corrosion caused by FPs as well as the internal pressure of the fuel rod. A soft thin wall facilitates the fast creep deformation of the pellets, thereby reducing the mechanical loading of the cladding under operational transients. A mesh-like rigid wall structure is also expected to prevent the massive fragmentation of pellets during a severe accident.

The chemical affinity of the wall to caesium may have a deep impact on the retention capability of FPs. The recent ramp test result for additive-doped UO₂ pellets demonstrated that the additive phases for both Al-Cr and Al-Si contain increased amounts of Cs in the hot region of the pellets (Jadernas et al., 2015). It was also shown that the Al-Si phase is better at retaining volatile elements, including iodine, within the fuel. This result suggests the chemical trapping of volatile FPs in an additive phase and a decreased possibility of the availability of aggressive species in the inside cladding. Based on the thermodynamic calculation results, SiO₂-based mixed oxides were selected as additive candidates for ceramic cell wall materials.

Ceramic microcell UO₂ fuel is characterised by a homogenous large-grain (~100 μm, mean linear intercept value) and cell structure, providing beneficial features for the fuel performance like dimensional stability, improved behaviour in case of water/steam ingress, superior PCI and SCC-PCI resistance and a higher FPs retention capability.

Fabrication/manufacturability

The fabrication feasibility of ceramic microcell UO₂ pellets has been demonstrated (Yang et al., 2014). The conventional liquid phase sintering technique has been applied. Less than 1 wt% of SiO₂-based oxide additives was blended into UO₂ powder and then the powder mixture was sintered at around 1 700°C for several hours in a dry hydrogen atmosphere. This manufacturing process is exactly the same as for standard fuel, which is an advantage in terms of infrastructure availability and economics. Figure 16.3 shows a microstructure of fabricated ceramic microcell UO₂ pellet. As it can be seen, the SiO₂-based mixed-oxide phase is homogeneously arranged in the grain boundary of UO₂ pellet.

**Figure 16.3. Optical micrography of Si-based oxide-doped
ceramic microcell UO$_2$ pellet**
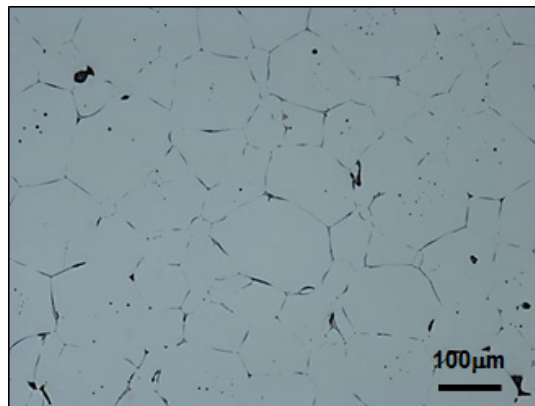
Source: Yang et al., 2014.

Normal operation and AOOs

The main benefit of ceramic microcell UO$_2$ pellets is an enhanced retention capability of the volatile FPs, such as Cs. A simple annealing test revealed the possibility that the Cs elements are preferentially segregated in the ceramic wall.

Thermal diffusivity and thermal expansion test results showed that the thermal properties of ceramic microcell UO$_2$ pellets are similar to those of a standard UO$_2$ pellet. By contrast, the compressive-creep deformation of ceramic microcell pellets at high temperature was faster than for standard UO$_2$ pellet. Fast creep deformation implies that the ceramic microcell pellets can reduce the cladding strain during a transient or accident, as well as during normal operation.

The ceramic wall is an oxide phase with inherent stability under a steam environment. Experimental results showed the enhanced resistance to steam oxidation in a ceramic microcell UO$_2$ pellet. Consequently, in a fuel failure scenario, it is expected that the washout rate of the ceramic microcell UO$_2$ is reduced in comparison to non-doped fuel types. This enhanced behaviour allows reducing on-site dose rates.

Microcell UO$_2$ pellets together with coated claddings are being tested in the Halden Research Reactor in Norway with the aim of assessing the fuel performance. Fuel temperatures, rod pressures and dimensional changes are being monitored online. Preliminary data show that fuel centreline temperatures can be lowered by incorporating Si-Ti-O as a microcell structure within the fuel. No abnormal behaviour has been noted during the first 100 days of irradiation.

Design-basis accidents (dbas) and DECs

Dedicated integral experiments have not been performed yet in accident conditions on ceramic microcell UO$_2$ pellet. However, benefits are expected since:

- Enhanced FPs retention capability will allow decreasing the rod internal pressure and minimising the degradation of clad robustness prior to the accident. This is beneficial in reducing the clad ballooning and the (burst) failure risk.

- A reduced amount of gas available for immediate release at the grain boundaries and mesh-like cell structure are likely favourable to limit the fuel fragmentation and dispersal in case of rod burst.

A LOCA simulating rapid heating test and a thermal transient test at a higher temperature than the melting point of ceramic wall also revealed that the structural integrity of pellets was well-preserved after the test.

Used fuel storage/transport/disposition/reprocessing

Neutronics calculations were performed to preliminarily evaluate the impact of microcell UO_2 pellet concepts on fuel cycle length and economy (Kim et al., 2016; Hwang, Hong and In, 2015). The impact on fuel cycle was found to be negligible because the neutron absorption due to ceramic wall is very small and higher pellet density compensates the reduction of fissile U induced by additives.

A higher robustness of cladding and a lower rod internal pressure are expected, inducing lower stress level on the spent fuel cladding and therefore more flexibility in the management of spent fuel storage.

High-thermal conductivity UO_2 fuel

Metallic additive fuel concept

The metal doped UO_2 fuel is generally called a CERMET fuel (CER for ceramic UO_2 and MET for metallic additive). When granules of UO_2 are surrounded by a thin metal wall, KAERI refers to this concept as metallic microcell fuels (Kim et al., 2016).

The first metal doped fuel that has been used in a commercial reactor was a stainless steel doped UO_2 fuel in the early 1960s. This fuel was the first fuel of the Vallecitos Boiling Water Reactor, the first commercial power reactor to be licensed in the United States (Holden, 1967).

For the last ten years, the international interest for the composite fuel and in particular for CERMET fuel has been confirmed in the framework of transmutation studies.

After the Fukushima Daiichi accident, CERMET fuel pellets are envisaged as having the potential to enhance the performance and safety of current LWR fuels for operational states as well as for accident conditions.

With a low volume fraction of highly conductive metallic additive, the CERMET fuel pellets present a higher conductivity than UO_2 standard pellets, lowering the fuel temperature in normal operating conditions and increasing the margins with respect to fuel melting in case of an accident. For a given amount of metal, the thermal conductivity of the pellet is higher when the metal forms a continuous structure around the UO_2 particle. Moreover, the metallic wall can provide multiple physical barriers against the movement of volatile FPs.

Low amounts of metals are added to UO_2 from 5 to 10% volume of the pellet in order to obtain a sufficient increase of the thermal conductivity, while at the same time limiting the increase of the ^{235}U pellet content. Some metal additives like Mo or Cr, slightly neutronically absorbant, may also induce a slight increase in the ^{235}U pellet content.

Fabrication/manufacturability

- Compatibility with large-scale production needs

UO_2-80vol% Molybdenum CERMET fuel pellets were produced by the French Alternative Energies and Atomic Energy Commission (CEA) by powder metallurgy process at a laboratory scale in the 90s. More representative fuels, i.e. pellets with lower Mo content (UO_2-10/20vol% Mo), were produced by KfK Karlsruhe in the 1970s. Those pellets (which exhibited a continuous Mo metal structure in the fuel) were fabricated by metallising small UO_2 spherical particles using a vapour deposition process. Then the metallised microspheres were vibrated into an Inconel cladding tube. After electron beam welding of the tubes, the pins were isostatically hot-pressed in He atmosphere.

Metallic microcell fuel pellets of UO$_2$-5vol% Cr and UO$_2$-5vol% Mo have been fabricated by KAERI (Kim et al., 2016; Yang et al., 2013; Kim et al., 2015; Lee et al., 2015; Yang et al., 2015; Hwang, Hong and In, 2015). These fuels present an optimised structure of the second metal phase with UO$_2$ granules surrounded by a wall of metal. The fabrication feasibility was demonstrated by KAERI at laboratory scale. However, specific quality control needs to be defined for a commercial-scale production. Metal powder coated UO$_2$ granules were compacted into green pellets, which were then sintered at high temperature under dry H$_2$ atmosphere (Kim et al., 2015). Figure 16.4 shows the shape and microstructure of fabricated metallic microcell UO$_2$ pellets.

Figure 16.4. Microstructures of (a) UO$_2$-5vol% Mo and (b) UO$_2$-5vol% Cr microcell fuel pellets, and (c) pellet shape of UO$_2$+5vol% Cr pellets
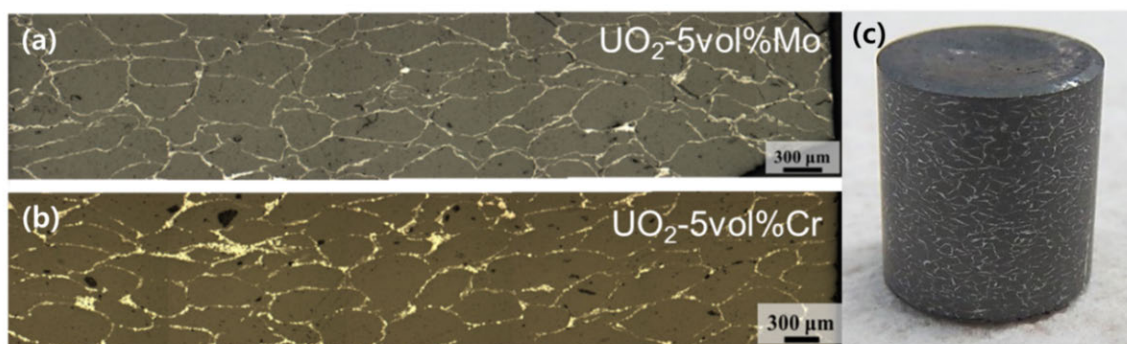
Source: Yang et al., 2015; Kim et al., 2017.

- Impact on the industrial network (suppliers and subcontractors)

Standard UO$_2$ and natural metallic Mo components can be easily supplied. As natural Mo cross-section is slightly neutron-absorbing (~2.65 barns), the use of light (^{95}Mo depleted) Mo, i.e. neutronically transparent because of enrichment in light Mo radioisotope, is preferred even if light Mo is more difficult and more expensive to supply. URENCO has studied the possibility of enriching/depleting molybdenum (Bakker et al., 2002). Molybdenum appears to be a suitable element for ultra-centrifuge enrichment/depletion using MoF$_6$ as a gaseous compound.

- Cost

Compared to UO$_2$ fuel manufacturing, higher costs are expected for UO$_2$-Mo fuel mainly because light molybdenum is used, higher ^{235}U/U enrichments are requested to compensate the lower uranium oxide content in the UO$_2$-Mo fuel and more complex fabrication line than for UO$_2$ standard pellets is needed.

Normal operation and AOOs

- Behaviour in normal operation

The main benefit of Mo or Cr containing granules of UO$_2$ is an enhanced thermal conductivity (Yang et al., 2015). A high-thermal conductivity can provide a low fuel temperature and a large thermal safety margin during transients. A cold pellet with a reduced temperature gradient is expected to be beneficial in mitigating the fuel relocation (cracking) and reducing the FPs release.

The UO$_2$-5vol% Cr microcell pellets are being irradiated in the Halden Research Reactor. The peak burn-up achieved to date is approximately 10.7 MWd/kgM. The UO$_2$-5vol% Cr rod showed a low centreline temperature, typically 15% lower than the

reference UO₂ fuel rod (see Figure 16.5). The temperature difference between the rods remains unchanged until now, indicating that the metallic network is intact.

Very low levels of FGR were measured (< 0.4%) in UO_2-80vol%. Mo fuel pellets irradiated by CEA in an MTR up to 125 GWd/t$_U$.

The second phase metal melting temperature is lower ($T_m(Mo)$= 2 623°C, $T_m(Cr)$= 1 907°C) than the UO₂ phase ($T_m(UO_2)$= 2 847°C) in the microcell fuel. However, the enhancement of thermal conductivity can compensate in some cases the reduction of temperature margin to metal melting in the fuel by reducing the fuel operating temperature.

Figure 16.5. Fuel centreline temperature and averaged linear heat rate as a function of operation time for UO₂+5vol% Cr
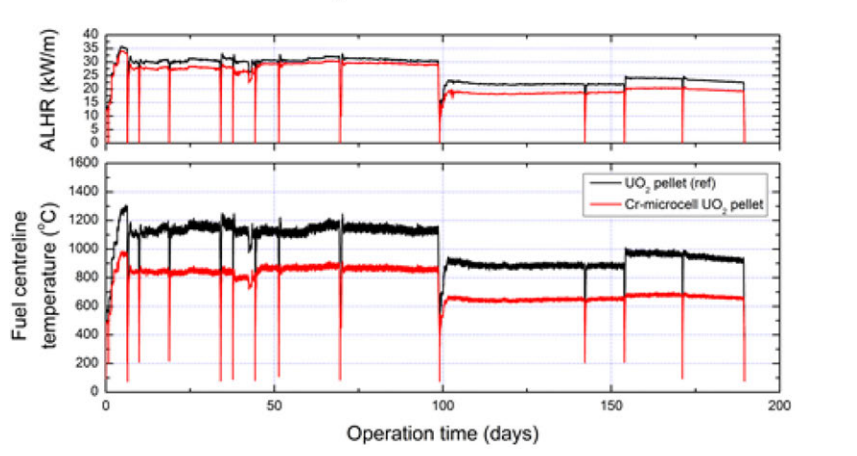
Source: Kim et al., 2017.

- Behaviour in AOOs

The benefit of microcell fuel with metal walls is to trap the corrosive FPs such as iodine, thus providing a better resistance to SCC/I.

Thus, CERMET fuels probably present a better resistance to PCI compared to a UO₂ standard pellet, but no experimental confirmation is available to date.

- Cladding/fuel interactions

The chemical compatibility between the composite fuel and stainless steel cladding is good as long as the fuel rod remains watertight. No data is available regarding a possible compatibility issue between UO₂-10%vol Mo and zirconium-based cladding.

The benefit of microcell fuel with metal walls is the reduced oxidation of the cladding due to direct contact with UO₂ and reduced contact between corrosive FPs and the cladding, resulting in a reduced cladding corrosion.

- Operating cycle length and neutrons penalty

Neutronic calculations were performed to preliminarily evaluate the impact of microcell UO₂ pellet concepts on fuel cycle lengths and economics. Because of the high-neutron absorption of Cr and Mo, a higher amount of ^{235}U in a Cr or Mo containing microcell UO₂ pellet is needed in order to keep the same fuel cycle duration (~0.5% of ^{235}U increase for a Cr containing pellet and ~1% of ^{235}U increase for an Mo containing pellet; Kim et al., 2016).

The reduction of fuel cycle length or enrichment of ^{235}U will increase the fuel cycle cost. The Mo^{95} isotope (~15.9% in molybdenum) is mostly responsible for the neutron absorption in molybdenum. Therefore, using molybdenum depleted in ^{95}Mo would mitigate the impact on the uranium enrichment.

- Specific behaviour of leakers during irradiation (further degradation with risk of fuel fragments dispersion)

Molybdenum metal is prone to a high oxidation rate in a steam environment. The MoO_3 oxide that is produced melts at only 795°C. Above this temperature, the MoO_3 forms eutectic mixtures with Fe, Ni and Cr oxides of the stainless steel cladding if this cladding is used.

But the steam oxidation tests (Yang et al., 2015; Kim et al., 2017) conducted by KAERI at 500°C and 800°C showed that the UO_2-5vol% Mo microcell pellets retained their structural integrity much longer compared with the standard UO_2 pellets. By contrast, a steam oxidation test at 1 100°C revealed a weight reduction and formation of tiny surface voids owing to a formation and evaporation of the volatile oxide phase. Nevertheless, the pellet maintained its sound cylindrical shape even after the 80h oxidation in steam at 1 100°C. Thus, UO_2-5vol% Mo microcell pellets present a better behaviour than the standard UO_2 pellet, at least until 1 100°C.

Figure 16.6. Comparison of pellet shape change of UO₂-5vol% Mo after the steam oxidation at various temperatures
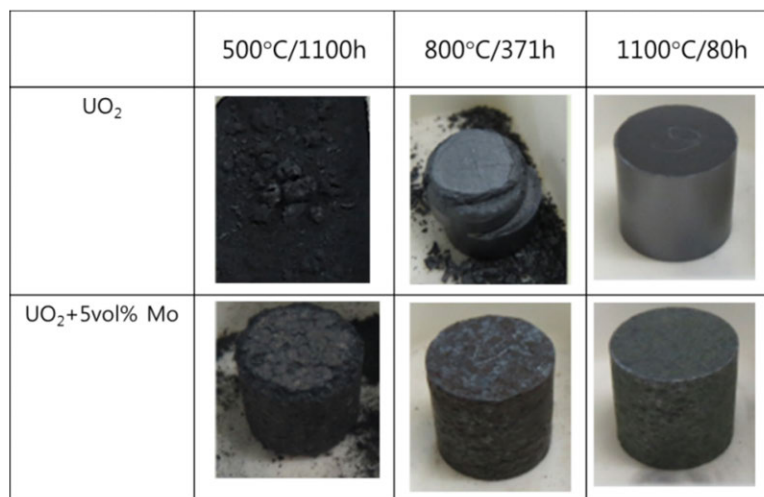
Source: Kim et al., 2017.

In the case of pellets containing Cr, the formation of the Cr_2O_3 phase, of a low density, resulted in the swelling and cracking of the pellets. The pellets containing Cr should be protected from coolant water steam ingress.

- Mechanical properties

Not investigated to date.

- Modelling

CERMET fuel has been modelled in the past with the CAST3M finite elements (FEs) calculation code in order to evaluate its thermal behaviour under irradiation in nominal conditions. The easiest way to model the CERMET geometry is to choose an octahedral shape, which represents the metal coated octahedral UO_2 particles. The UO_2 volume

fraction can reach very high values (close to 99 vol.% of UO$_2$) depending on the particles' size and the metal thickness around the UO$_2$ particles.

The equivalent homogeneous physical and thermo-mechanical behaviour laws of this heterogeneous fuel have been calculated with the same code on the bases of this design. Temperature calculations were performed with the EPR rod geometry for CERMETs fuels with the CEA thermal-mechanical METEOR V1.10 code modified with the properties of the composite fuels obtained with the CAST3M FE calculation code (Coulon-Picard et al., 2009).

The calculated CERMET or microcell metallic fuel temperature gain reaches several hundred degrees compared to a standard UO$_2$ fuel.

Design-basis accidents (dbas) and design extension conditions (DECs)

- LOCA

A recent impact assessment of the thermal conductivity of the fuel in a loss-of-coolant accident in a PWR showed that an increase in thermal conductivity reduces both the peak cladding temperature and the quench time of the fuel rod (Hwang, Hong and In, 2015).

Based on irradiated UO$_2$-80%Mo composite fuel up to 125 GWd/tU, then annealed at 1 350°C under vacuum for 3 hours in CEA hot laboratories, the UO$_2$-80%Mo composite fuel releases less fission gas in transient than a standard UO$_2$ fuel. This positive result should be confirmed for fuel with more representative lower Mo content.

Nevertheless, the pellet maintained its sound cylindrical shape even after the 80-hour oxidation in steam at 1 100°C. Thus, UO2-5vol% Mo microcell pellets is anticipated to feature a better behaviour than the standard UO2 pellet at least until 1 100°C.

When the rod cladding fails, the pellet is submitted to the water vapour. Out-of-pile vapour tests described in Figure 16.6, show that the pellet maintains its sound cylindrical shape even after the 80-hour oxidation in steam at 1 100°C. However, the reaction of metallic materials with HT steam would be a concern. The reaction kinetics for the formation of volatile or low density oxide phase will depend on the temperature profile of a pellet and ingression rate of steam.

- RIA

Microcell UO$_2$ rod is expected to feature a more benign behaviour during RIA because it has low stored energy. Reaction of metallic wall materials with HT steam is a concern.

- DECs

Metal phase reduces the CERMET fuel pellet temperatures thus increasing the "coping time".

For a UO$_2$-80%Mo composite fuel, out-of-pile thermal treatment tests performed in France at CEA at 1 750°C under vacuum for 3 hours have shown nearly the same level of FGR than for a standard UO$_2$ fuel.

In case of contact of the pellet with the coolant vapour, oxidation of metal phase will lead to degradation of pellets.

Used fuel storage/transport/disposal/reprocessing

High-thermal conductivity of pellets will provide a benefit with respect to used fuel storage in a spent fuel pool, dry storage and disposition.

Using higher [235]U/U fuel enrichment may generate specific issues (e.g. actual enrichment facilities are limited to about [235]U/U < 7% for UO$_2$).

The residual activity may be changed by the ^{99}Tc long-lived FP formed in reactor.

The UO$_2$-10% Mo reprocessing is not compatible with the current PUREX hydroprocess implemented at La Hague Facility, as Mo is soluble in nitric acid. Feedbacks from recent R&D performed within European Programmes on aqueous reprocessing Mo-CERMET fuel for ADS system ((Pu,Am)O$_2$-Mo fuels) may help to address that issue.

It is anticipated that reprocessing of UO$_2$-10%vol Mo fuel pellets will be likely more costly than for UO$_2$ standard fuel.

Ceramic additive fuel concept

In the early 1960s, UO$_2$-BeO fuel was studied by the US DOE and eventually abandoned for reasons which have not been retrieved in the framework of this review. Following the Fukusima Daiichi accident, the BeO-modified UO$_2$ concept fuel has been the object of a regain of interest.

Adding small fractions (e.g. 10% in volume) of a high conductivity solid phase such as BeO can produce a two-phase fuel, characterised by a continuous minor BeO phase at the grain boundaries in UO$_2$, for the purpose of increasing the thermal conductivity of UO$_2$ fuel, reducing the pellet centreline temperature, fission gas releasing rate and the risk of fuel melting, hence strongly improving its behaviour in accident conditions.

The choice of BeO among other high conductivity ceramics was motivated by several preferable characteristics. Besides being the oxide with the highest thermal conductivity, it is, first and foremost, compatible and insoluble with UO$_2$ up to 2 160°C, at which temperature it forms a eutectic. It is also compatible with zircaloy-cladding up to 1 200°C, does not react with water and very weakly with nitric acid (hence it would be compatible with spent nuclear fuel reprocessing). It also has a low neutron capture cross-section, good neutron moderation and an appreciable fast neutron multiplication via an (n, 2n) reaction with a threshold energy of 1.85 MeV.

BeO-doped UO₂ fuel

Fabrication/manufacturability

Current results from FE modelling calculations, and extrapolation of Ishimoto's results (Ishimoto, Hirai and Ito, 1996) suggested that additions of only 10 vol% of BeO could have a significant effect on thermal conductivity of the UO$_2$ fuel. The fabrication of the BeO-doped UO$_2$ fuel has been carried out at laboratory scale, in the aim of obtaining a few samples for out-of-pile or in-pile experiments (Zhou, Liu, 2015). The thermal conductivity of the BeO-doped UO$_2$ fuel pellets is increased by over 40%, with 10 vol.% of BeO-doped into UO$_2$. Two fabrication methods, i.e. slug bisque (SB) and green granule (GG), were employed to develop high-thermal conductivity UO$_2$-BeO oxide fuel pellets, namely SB-UO$_2$-BeO and GG-UO$_2$-BeO fuels, respectively. These two fabrication routes produced pellets presenting some differences, as detailed below:

- Grain size: The sintered SB-UO$_2$-BeO granules have an average grain size of ~170 µm, in contrast to 90 µm for the GG-UO$_2$-BeO granules.

- Density: The density of SB-UO$_2$-BeO pellets is 96.3%, while the sintered GG-UO$_2$-BeO pellets is 98.0%.

- Microstructure: The SB-UO$_2$-BeO pellets have an interface region, consisting of 12.2 vol% UO$_2$ particles, 72.7 vol% BeO and 15.1 vol% porosity, between the BeO phase and UO$_2$ granules. However, the contamination of the UO$_2$ in BeO phase is greater and much more dispersed in GG-UO$_2$-BeO.

- Thermal conductivity: The GG-UO$_2$-BeO thermal model shows better thermal conductivity than the SB-UO$_2$-BeO. Thermal conductivity of both the doped fuel pellets is greater than UO$_2$ (Bischoff et al., 2015). McGrath's test revealed a degradation of thermal conductivity of UO$_2$-BeO pellets during irradiation. Usually, thermal conductivity of UO$_2$-BeO is affected by the fraction of BeO, the distribution

mode of BeO, temperature and burn-up. However, the thermal conductivity of UO_2-BeO is always larger than UO_2, leading to a lower fuel temperature (Kim, Ko and Kim, 2010).

A sample of UO_2-BeO10 vol% is shown in Figure 16.7.

Figure 16.7. Sample of 10 vol% BeO-UO₂ fuel
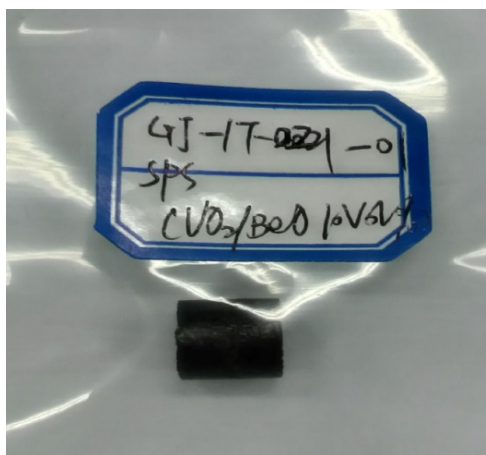
Source: Sun, Huang and Li, 2017.

- Cost

Cost-benefit analysis of the BeO-doped UO_2 nuclear fuel was investigated by Kim et al., showing that the optimum BeO content is about 4.8 wt%, assuming costs for BeO and uranium oxide of USD 317/kg and USD 64/kg, respectively (Kim, Ko and Kim, 2010). The BeO-doped UO_2 fuels require an increase in ^{235}U enrichment of 0.0073 wt%, in order to keep the cycle length unchanged. The increased thermal conductivity of BeO-doped UO_2 fuel could compensate the high expense of the BeO material, because the cost of nuclear fuel cycle could be lower than that of UO_2 fuel. The economic impact arisen from the expected longer fuel cycle possibly may extend beyond the fuel cost. The improved thermal performance of the fuel could support less restrictive peaking, operating and manoeuvering limits and less restrictive limits can contribute to the economic performance of a power plant (Kim, Ko and Kim, 2010).

Normal operation and AOOs

- Irradiation behaviour of BeO

Under fast neutron flux (E > 1.85 MeV), Be (Beryllium) undergoes an (n, 2n) reaction (Tulenko, 2016):

^{9}Be (n, 2n) ^{4}He   (1)
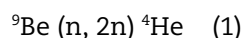
and an (n, α) reaction with a threshold neutron energy of 0.71 MeV and a cross-section of 25 mb, leading to ^{6}He production:

^{9}Be (n, α) ^{6}He.   (2)
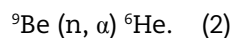
^{6}He decays very quickly to ^{6}Li with a half-life of 0.82s. Finally, tritium is produced by an (n, α) reaction on ^{6}Li with a very high cross-section of 950 barns. The net neutron production from Be depends on whether, ^{6}Li, ^{3}He or ^{3}H escape by diffusion, or are removed from the system by reprocessing or both.

In terms of radiation stability, fast neutron doses cause anisotropic crystal growth in BeO because of its hexagonal crystal structure. Keilholtz showed powdering of a specimen at a fast neutron dose of 1.5×10^{21} n/cm² (E > 1 MeV) at 100°C, but simple fractures at fast doses of 2×10^{21} n/cm² at temperature between 800 and 1 000°C. At a lower dose of 2×10^{20} n/cm² (E > 1MeV) microcracking began at ~100°C in BeO. Thus, very low temperature irradiations are problematic for BeO.

For introducing the longer fuel cycle concept, there is also the issue of fission-fragment damage, since the fragments may penetrate through the thickness of the BeO phase and produce damage as well as intense local heating. Hanna et al. examined fission-fragment damage in BeO by irradiating (U, Th)O₂ dispersed in a BeO matrix (Solomon, Revankar and McCoy, n.d.). The irradiation was done in thermal fluxes between 1.6 and 2.7×10^{13} n·cm⁻²·s⁻¹, and negligible fast fluxes at temperatures of 600 and 850°C . Fission densities were between 2×10^{19} and 1.8×10^{20} fissions per cm³. Samples were apparently unaffected by the thermal stresses that in some cases could exceed the modulus of rupture of the material. They concluded that fission-fragment damage produces volume increases of the specimen and strain in the BeO matrix. They observed that the strain appeared to be greater with fine (~1 µm) fuel particles, but this greater strain did not seem to affect the specimens with a small BeO grain size of 5 µm. Later, Hanna et al. even observed that the fission-fragment bombardment reduces the effect of the fast neutron damage (Solomon, Revankar and McCoy, n.d.). They argued that the fission-fragment local heating can either anneal the neutron-induced defects or simply enhance the creep process that relieves the growth strains.

Recent experiments compared thermal conductivity degradation with neutron irradiation of several high-thermal conductivity ceramics. BeO was the least affected by neutron damage for irradiation at temperatures below 300℃, and for low doses up to 0.1 dpa. Similar results were obtained for higher doses, but eventually, if microcracking occurs at high doses, the conductivity would likely be severely reduced (Solomon, Revankar and McCoy, n.d.).

- Visual observation

After irradiation, no swelling or cracking was detected at the claddings of the UO₂-20%vol-BeO fuel. Data are not yet available for the UO₂-10%vol-BeO, but this does not appear to be challenging because of expected very high-thermal conductivity of this type of fuel concept (Titus, Sailing, 1963).

- Fission gas release

In the analysis of the sample, krypton was found. The content of the BeO dopant has no significant influence on the FGR under the same range of burn-ups (Titus, Sailing, 1963). This may be because FGR is determined not only by the temperature but also by microstructure of the fuel. Compared to the standard UO₂ fuel pellets, UO₂-10%vol-BeO fuel pellets have an improved performance in FGR. A reduction of about 3.6% in values of gap pressure was observed in the cases of normal operation (Johnson, Mills, 1963; Chandramouli, Revankar, 2014). In addition, other irradiation experiments have shown the presence of tritium, which can increase the internal pressure. Additional data are expected from future experiments. Because of the lower temperature, McGrath's test did not find an FGR threshold in the BeO-doped UO₂ fuel pellets of burn-up or temperature like UO₂ fuel pellets and the FGR was also lower than UO₂ fuel (Johnson, Mills, 1963).

- Thermal-mechanical behaviour

The BeO-doped UO₂ fuel pellets exhibit a very high-dimensional and microstructural stability up to high burn-ups (Titus, Sailing, 1963; Johnson, Mills, 1963; Chandramouli, Revankar, 2014).

■ Fuel temperature

Compared to the standard UO_2 fuel pellets, the increased thermal conductivity leads to a remarkable average radial temperature reduction of the BeO-doped UO_2 fuel pellets (the prototypic BeO addivite is 10%vol) (Chandramouli, Revankar, 2014).

■ PCI behaviours

The internal pressure of 10%vol-BeO-doped UO_2 fuel pellets has a reduction of 9.1 MPa compared with UO_2 fuel pellets (McCoy, Mays, 2008), which has not been confirmed as beneficial to PCI resistance.

■ Densification and swelling

According to McGrath's test, pellets made of UO_2-BeO had more serious densification behaviour of 1% volume change than that of UO_2 pellets, with about 0.5% volume change. At higher burn-up, the swelling of two pellets both showed a linear relationship with the burn-up, and the swelling rate of UO_2 - BeO is lower than UO_2 (~94% rate of UO_2) (Johnson, Mills, 1963).

Figure 16.8. Fuel volume change of UO₂-BeO vs. UO₂ fuel
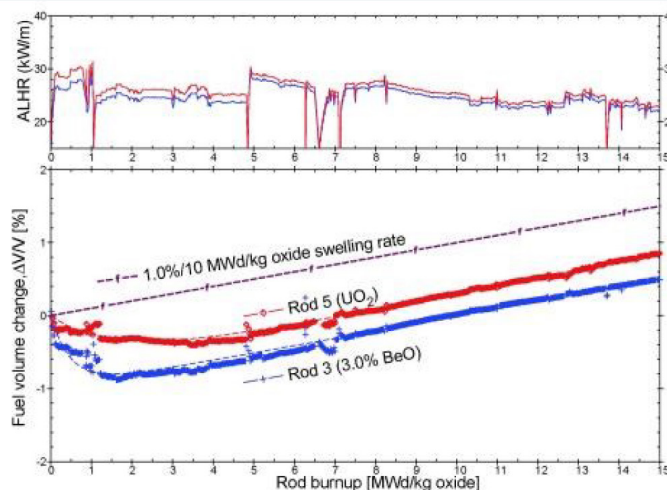
Source: Johnson, Mills, 1963.

DBAs and DECs

Although dedicated integral experiments have not yet been performed to study long-term phenomena like creep, stress-strain response of cladding and thermal ageing, the effects of BeO doping on overall performance of the fuel during transient conditions such as LOCA have been investigated. The results are presented below:

- A significant reduction in fuel centreline temperatures was observed under LOCA conditions, while not so significant under a rupture scenario (McCoy, Mays, 2008).

- Gas pressure in the gap between fuel and cladding was found to be reduced by approximately 3.6% in the BeO-doped UO_2 fuel pellets under LOCA condition. Energy in the fuel was also found to be reduced with the addition of BeO into UO_2.

- Cladding axial strain was found to be decreased with doping BeO (McCoy, Mays, 2008).

Specific experiments will be performed under simulated accident conditions to provide valuable data to assess and model the BeO-doped UO_2 fuel behaviour.

In the following section, results from simulation of the BeO-doped UO$_2$ fuel behaviour by FRAPCON/FRAPTRAN under steady-state and accident conditions will be provided. The thermal conductivity and thermal expansion of the BeO-doped UO$_2$ fuel are obtained from the out-of-pile experimental data (Sun, Huang and Li, 2017; DOE, 2006). Particularly, adjustment was done to the fuel thermal conductivity to account for the effects of dissolved FPs, precipitated FPs, porosity and irradiation damage, as for UO$_2$ fuel. The density of solid BeO recommended by the IAEA was used in the simulation (DOE, 2006). The correlations for the heat capacity and emissivity of the BeO-doped UO$_2$ fuel, as shown in "Sensitivity study for accident tolerant fuels: Property comparisons and behavior simulations in a simplified PWR to enable ATF development and design" (Spencer et al., 2016), were used in the simulation (Spencer et al., 2016).

- Steady-state

The engineering case of a typical CPR1000 power plant is used for the steady-state evaluation. Table 16.1 shows the comparison between standard UO$_2$ and 10 vol% BeO-doped UO$_2$ under steady-state conditions. It suggests that BeO-doped UO$_2$ improves the thermal conductivity, strength and deformation resistance of the fuel systems. The fuel system with the BeO-doped UO$_2$ pellets exhibits lower values of both the fuel centreline temperature and the plenum pressure.

**Table 16.1. Comparison between UO$_2$ fuel and BeO-doped UO$_2$ fuel
under steady-state conditions**

Fuel system	UO$_2$ + M5	UO$_2$-BeO + M5
Max fuel rod internal pressure, MPa	12.83	11.87
Max fuel centreline temperature, K	1 755.94	1 342.03
Max strain increment (elas + plas), %	0.419963	0.048377

Source: DOE, 2006; Spencer et al., 2016; Geelhood, Luscher, 2016.

Figure 16.9. Fuel rod internal pressure
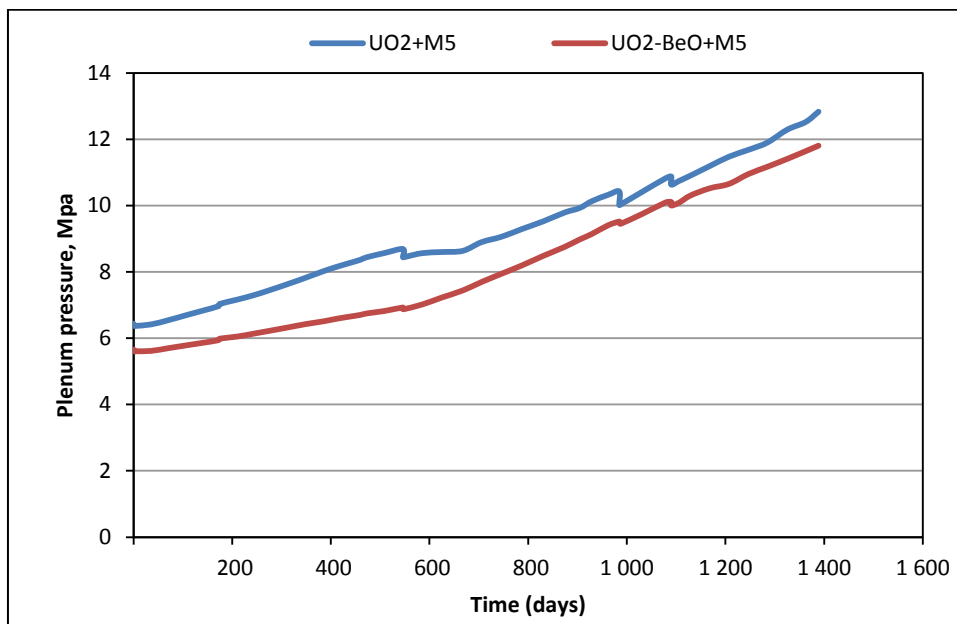
Source: DOE, 2006; Spencer et al., 2016; Geelhood, Luscher, 2016.

Figure 16.10. Maximum fuel pellet centreline temperature
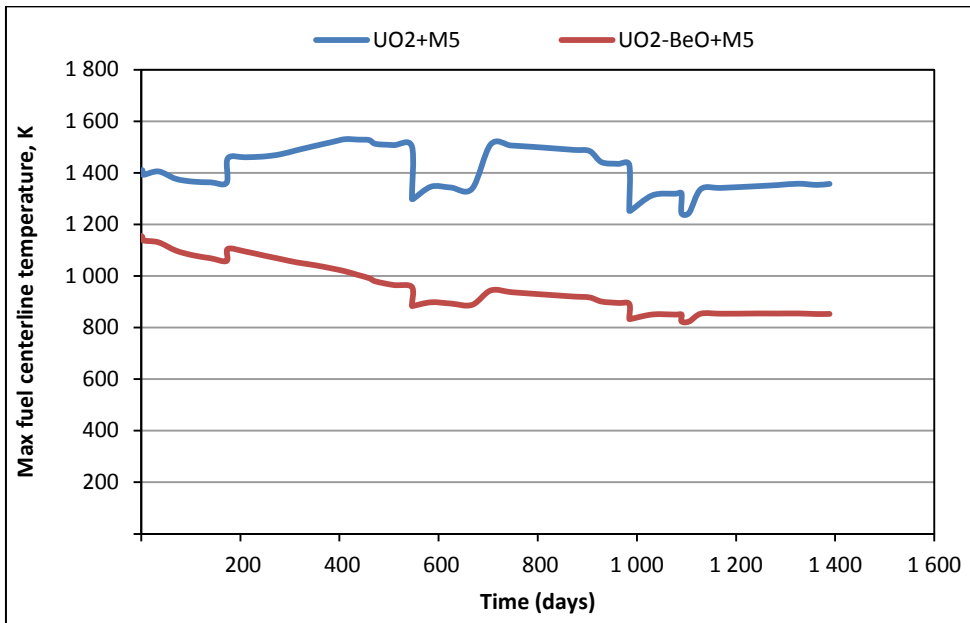
Source: DOE, 2006; Spencer et al., 2016; Geelhood, Luscher, 2016.

Figure 16.11. Maximum fuel thermal expansion
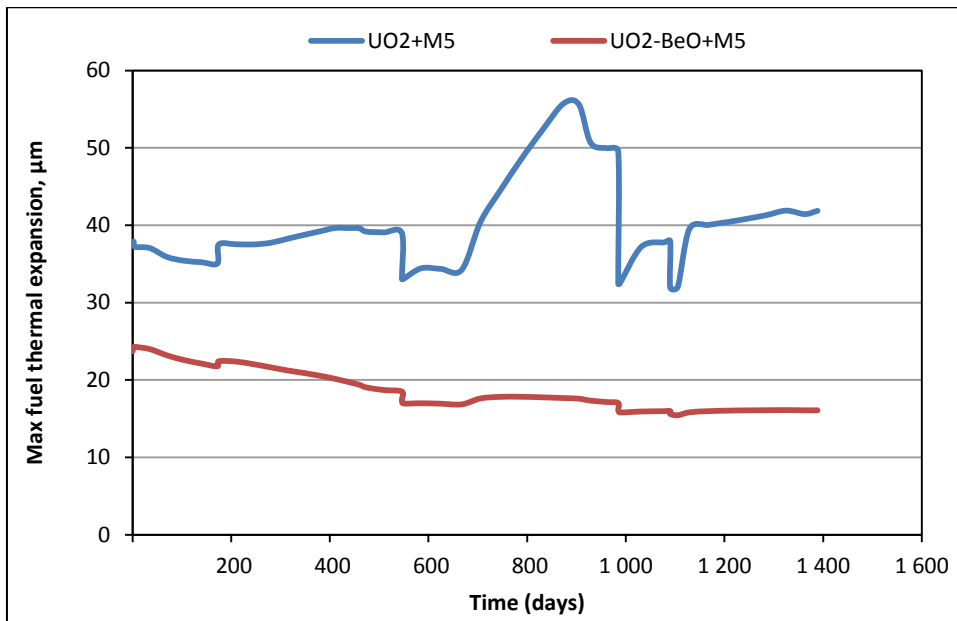
Source: DOE, 2006; Spencer et al., 2016; Geelhood, Luscher, 2016.

▪ Accident conditions

For the LOCA condition, the test case used is MT-1. This case (DOE, 2006) consists of 11 full-length PWR rods subjected to adiabatic heat-up followed by reflood for providing data for supporting LOCA analyses. The primary objective of the MT-1 test was to

determine the effects of fuel cladding dilatation and rupture on heat transfer within a full-length fuel bundle during a LOCA.

Under LOCA condition, the loss-of-coolant induces an increase of fuel temperature and high cladding temperature leading to high cladding stress/strain, until the instability strain rate is reached, with subsequent cladding ballooning and failure. Hence, for the fuel rod analysis of LOCA, temperature distribution of fuel rod and cladding hoop stress/strain are the important parameters.

Table 16.2 shows the results of the comparison between standard UO₂ fuel and 10 vol% BeO-doped UO₂ fuel under LOCA condition. It suggests that during LOCA, the BeO-doped UO₂ can generally reduce the system temperature and delay or avoid the fuel rod failure.

Table 16.2. Comparison between UO₂ and 10 vol% BeO-doped UO₂ under LOCA condition

Fuel system	UO₂ + Zry-4	BeO-doped UO₂ + Zry-4
Max plenum pressure, MPa	5.08	4.95
Max fuel temperature, K	1265.2	1196.0
Max cladding temperature, K	1140.7	1091.3
Rod failure time, s	61	68

Source: DOE, 2006; Spencer et al., 2016; Geelhood, Luscher, 2016.

Figure 16.12. Fuel rod internal pressure
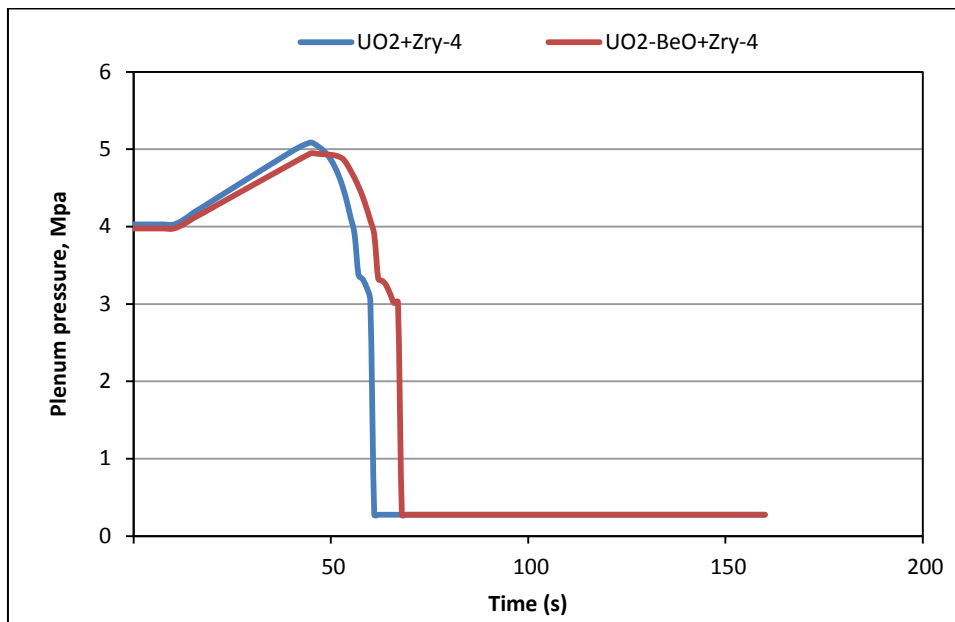
Source: DOE, 2006; Spencer et al., 2016; Geelhood, Luscher, 2016.

Figure 16.13. Maximum fuel surface hoop strain
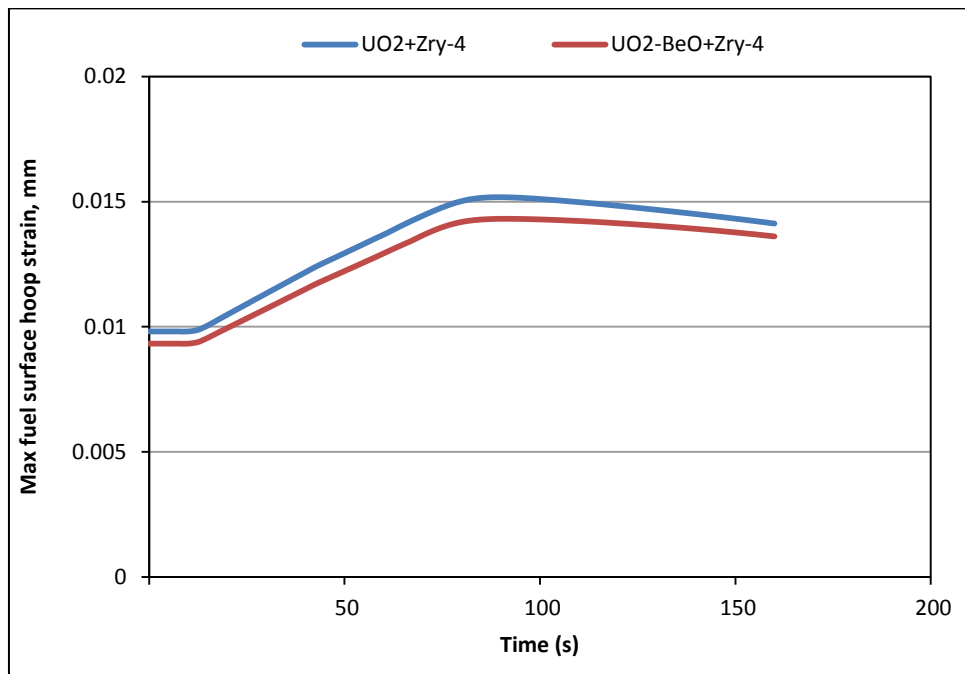
Source: DOE, 2006; Spencer et al., 2016; Geelhood, Luscher, 2016.

Figure 16.14. Maximum fuel pellet centreline temperature
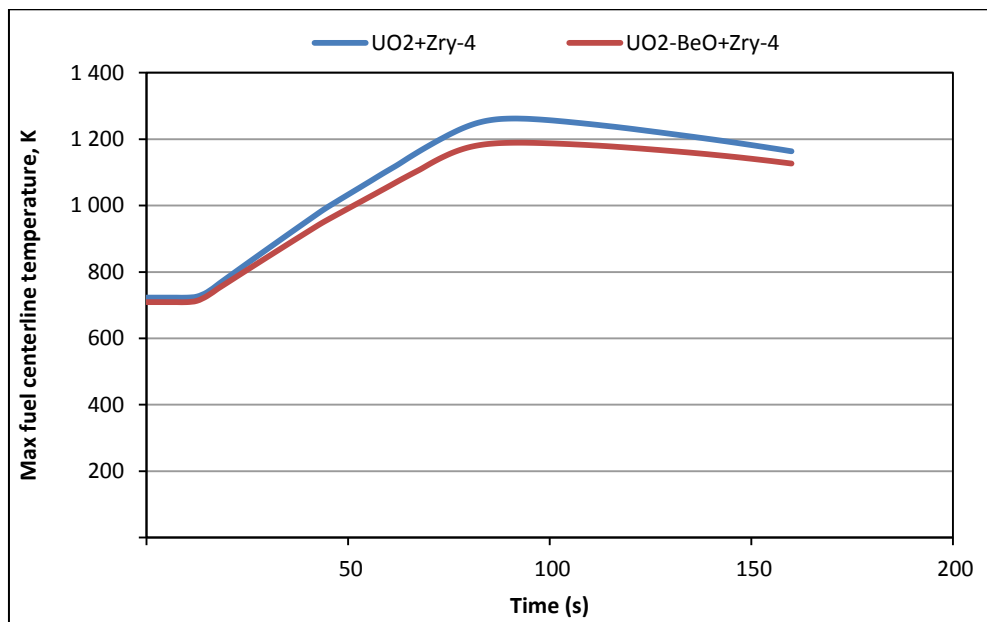
Source: DOE, 2006; Spencer et al., 2016; Geelhood, Luscher, 2016.

Figure 16.15. Maximum cladding average temperature
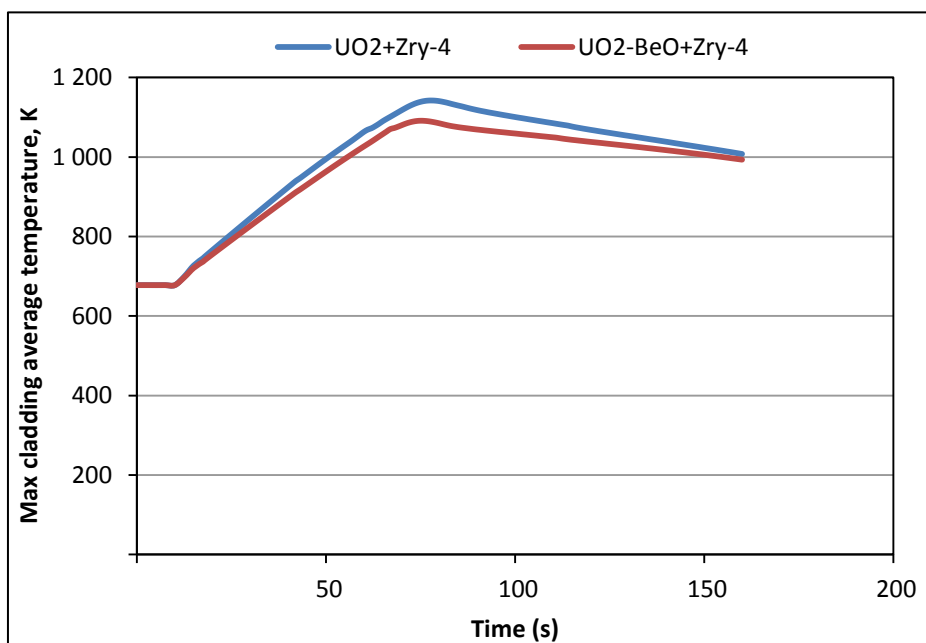
Source: DOE, 2006; Spencer et al., 2016; Geelhood, Luscher, 2016.

Spent fuel storage/transport/disposition/reprocessing

As already mentioned, a reduction of the fuel rod internal pressure is expected to decrease stresses acting on the cladding, thereby facilitating the management of storage casks. The adoption of BeO-doped UO_2 fuel pellets would require an enrichment increase of only 0.0073 wt% in order to maintain the cycle length unchanged. This slight increase is presumably related to the neutron multiplication reaction of [9]Be and the moderating effect of BeO. But the consumption of [9]Be through neutron multiplication reactions is small. It was found that only 0.15% of the initial [9]Be isotopic concentration was consumed.

Regarding reprocessing, potential issues should be further evaluated, but a likely higher cost for the BeO-doped UO_2 fuel pellets is expected (Kim, Ko and Kim, 2010).

SiC and diamond additive UO₂ fuel

As part of the DOE Enhanced Accident Tolerant Fuel Program, the University of Florida is developing with AREVA the following concepts for the fuel pellet: adding SiC and diamond to UO_2 pellets to increase the pellet thermal conductivity.

Fabrication/manufacturability

To control the chemical reactions between the uranium dioxide and the second phase, to achieve densification of the powders at significant lower temperatures and shorter processing time and also to increase the final bonding between the UO_2 and the additive, the spark plasma sintering (SPS) process has been used by the University of Florida (UF). That method involves pressing powders in a graphite die while simultaneously heating the die and powder with pulsed direct current. Additives include silicon carbide powder (SiC-p), silicon carbide whiskers (SiC-w) and diamond. These additives were selected because they have extremely high thermal conductivities, high melting points and small neutron capture cross-sections.

Figure 16.16 shows the microstructures of pellets with SiC-w and SiC-p. Densification was achieved either by oxidative sintering or SPS. SPS provides high density with a short processing time. SPS also forces the uranium dioxide matrix into intimate contact with the additive, ensuring good heat transfer between the phases and allowing the additive to serve as a thermal "short circuit".

The thermal conductivity of pellets with additives has been measured and typically exceeds that of plain uranium dioxide pellets by 50% for UO_2-10vol% SiC to 500% for UO_2-10vol% diamond (see Figure 16.17).

Sintering temperatures well below 1 500°C are recommended by UF for fabrication of UO_2-diamond composite pellets to avoid graphitisation process of the diamond (formation of graphite from diamond) and uranium carbide formation. Sintering temperatures applied by the UF varied from 1 400 to 1 600°C for the UO_2-SiC-composite fabrication.

It is clear from the results presented by UF that this SPS process not only offers a significantly shorter sintering time, but also provides a denser UO_2-SiC or UO_2-diamond composite with reduced formation of chemical products, better interfacial properties and above all, significantly better thermal conductivity than pellets obtained from oxidative sintering.

However, this SPS process is a laboratory scale fabrication process, not an industrial one.

Figure 16.16. Microstructures of uranium dioxide pellets with (a and b) SiC-w, (c and d) SiC-p (a and c), densified by conventional sintering or (b and d) SPS
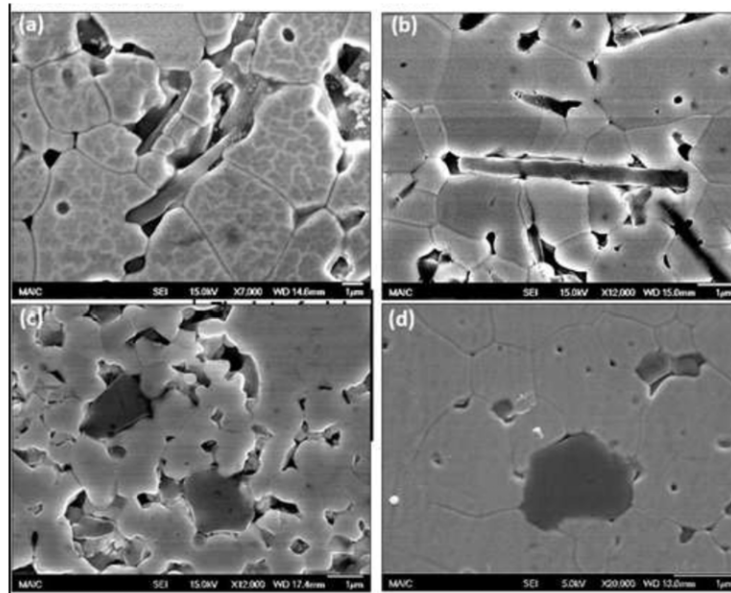
Source:Tulenko, 2016.

Figure 16.17. Thermal conductivity measurements of University of Florida on composite pellets of UO$_2$+10vol% SiC and UO$_2$-10vol% diamond fabricated by SPS
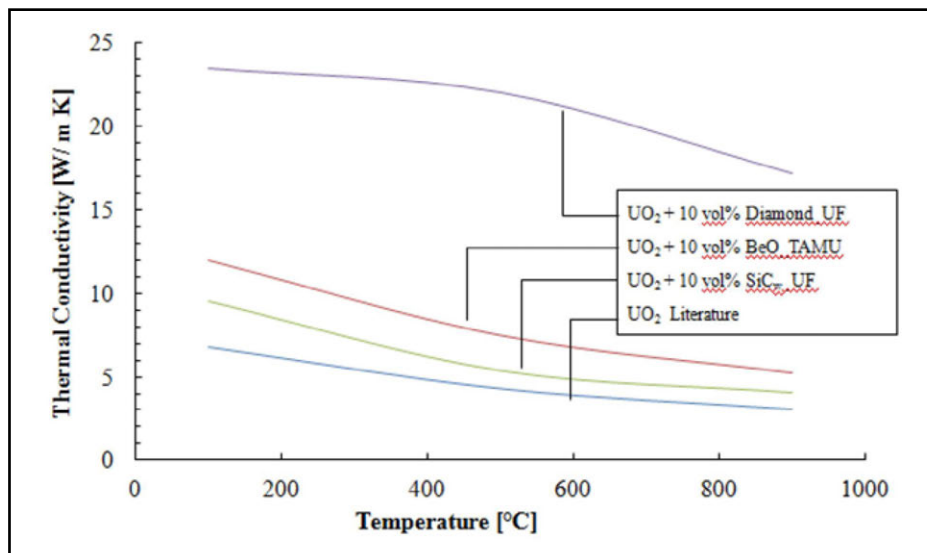
Source: Tulenko, 2016; Yeo et al., 2013.

Normal operation and AOOs

To assess the thermal behaviour of composite UO$_2$-diamond pellets, the fuel pellet temperature distribution was calculated for nominal reactor conditions (Yeo et al., 2013). Fuel thermal conductivity coefficients for UO$_2$ are literature-based, while the UO$_2$-diamond composite values were experimentally measured by Idaho National Laboratory. Table 16.3 and Figure 16.18 show the calculated radial temperature distribution of four pellets – pure UO$_2$ solid pellet (blue line), pure UO$_2$ annular pellet, diamond-doped solid pellet (grey line) and diamond-doped annular pellet. The diamond-doped pellet heat conductivity, as mentioned, was acquired experimentally. The benefits of diamond-doped fuel are clearly visible.

Table 16.3. Radial pellet temperature distribution for various pellet types

Temperatures	Solid UO$_2$ (°C)	Annular UO$_2$ (°C)	Solid UO$_2$-diamond (°C)	Annular UO$_2$-diamond (°C)
Average temperatures	959	864	744	685
Peak temperatures	1 519	1 226	1 089	908

Source: Kruszelnicki et al., 2016.

The ~600°C (430°C for solid pellets) decrease in maximum fuel temperature offers a greater operating factor of safety. The ~300°C (215°C for solid pellets) decrease in average fuel temperature leads to three main effects:

- lessened fuel expansion, and increased operating fuel density;
- lessened fuel cracking and decreased FGR.

Figure 16.18. Radial pellet temperature distribution for various pellet types
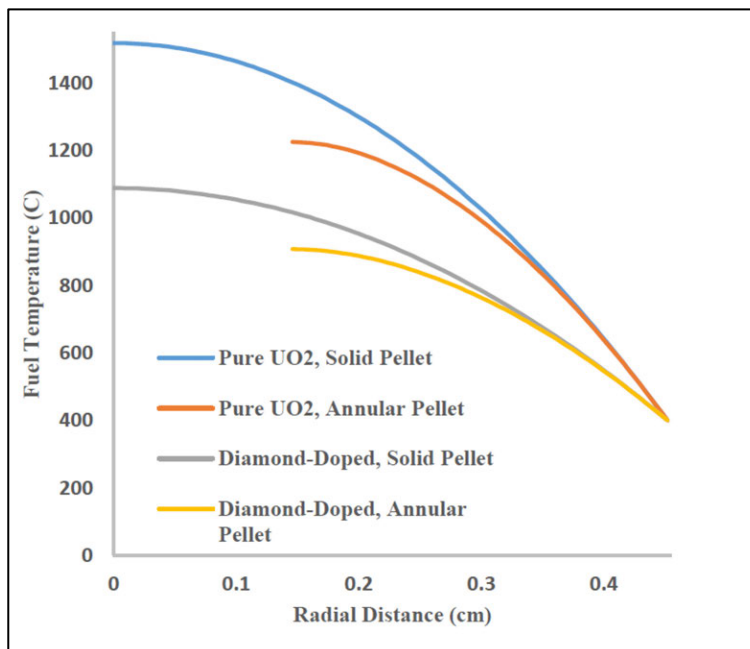
Source: Yeo et al., 2013.

The centreline temperatures of pure UO₂ and UO₂-10vol% SiC have been calculated with the fuel performance code FRAPCON 3.4 developed by The Pacific Northwest National Laboratory (PNNL) for the NRC (Yeo et al., 2013). The 60% increased thermal conductivity by 10vol% SiC addition leads to a nearly 150°C decrease in the maximum fuel centreline temperature.

A series of irradiation tests have been developed by the DOE/Fuel Cycle Research and Development to assess the performance of proposed ATF concepts under normal LWR operating conditions (the ATF series of irradiations). INL placed 6.5% enriched UO₂ with and without additives fuel capsules in the ATR.

The first group of three capsules: UO₂, UO₂-10vol% diamond and UO₂-10vol% SiC whiskers, fabricated by UF, has been taken out at ~8 000 to 10 000 MWD/MTU for an initial PIE.

Visual examination of these capsules did not reveal anything unusual. Capsule neutron radiography has also been performed on the three capsules. A thermal neutron radiography image from the 3 ATF-1 capsules is shown in Figure 16.19. There is some significant cracking present in the fuel for ATF-03 (UO₂-10vol% SiC whiskers). Also, there is some cracking in the other fuel pellets. The severity of this cracking relative to other fuel is not clear at this time. There does not appear to be any other significant breaches or deformations of the cladding, but more detailed radiographs will be taken after the rodlets are removed from the capsules.

UF and INL have fabricated another round of capsules which are waiting to go into the ATR reactor. INL will measure the thermal conductivity of the irradiated fuel as soon as INL procures a thermal conductivity measuring apparatus in the laboratory hot cells.

In case of leakers, the composite behaviour is not known.

**Figure 16.19. Capsule thermal neutron radiography of ATF-1
capsules ATF-00, ATF-03 and ATF-04 (from left to right)**
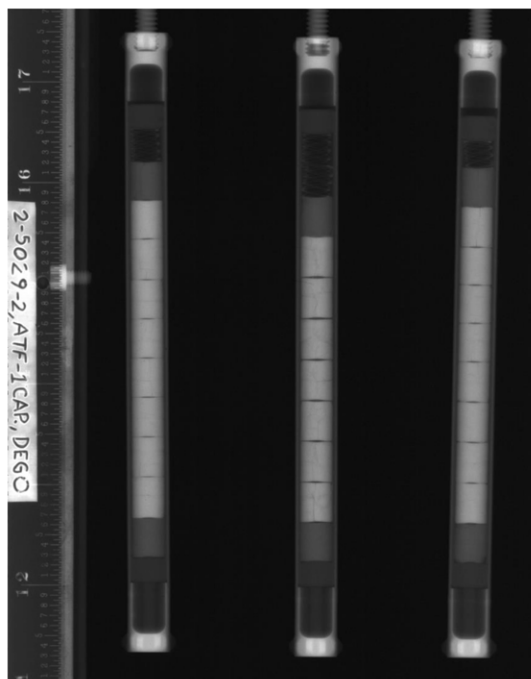
Source: Kruszelnicki et al., 2016.

DBAs and DECs

No calculations have been made on UO₂-diamond composite fuels. But, the performance of a UO₂/graphene composite fuel (highly conductive allotropic form of carbon) similar to a UO₂-diamond fuel but with a lower conductivity (conductivity of a UO₂-10vol% graphene is + 33% conductivity /UO₂ instead of about 500% more for UO₂-10vol% diamond) with different graphene additive volume (up to 10vol% graphene in UO₂) in Zy-4 cladding has been assessed in OPR-1000 during an LB-LOCA through the MARS-KS code.

The maximum peak cladding temperature during the LOCA was decreased by nearly 370°C (from 2 097 K to 1 727 K) with 10vol% graphene in UO₂ with a zircaloy-4 cladding. The benefits increased monotonically with increasing thermal conductivity in terms of reduced radial fuel rod temperature and PCT.

The melting temperatures of the examined additives are very high: 2 730°C for SiC and 3 546°C for diamond. The UO₂ melting temperature (i.e. 2 865 °C) is of the same order of magnitude. Thus, there is no limitation in temperature for the use of these additives.

The temperature limitation of the use of these composite fuels comes from the chemical reaction between the UO₂ and the additive: the chemical reaction between UO₂ and SiC occurs from about 1 427°C (reaction limited) and between UO₂ and diamond from about 1 500°C. Beyond these temperatures, chemical reactions between the UO₂ and the additive may occur, which consequences may be studied.

References

Arborelius, J. et al. (2005), "Advanced doped UO$_2$ pellets in LWR applications", *Water Reactor Fuel Performance Meeting*, Kyoto.

Backman, K. et al. (2009), *Westinghouse Advanced Doped Pellet – Characteristics and Irradiation Behaviour,* IAEA TechDoc-1654, Villingen.

Bakker, K. et al. (2002), "Using molybdenum depleted in 95 Mo in UMo fuel", *2002 International Meeting on Reduced Enrichment for Research and Test Reactors*, 3-8 November 2002, Bariloche.

Bischoff, J. et al. (2015), "Development of fuels with enhanced accident tolerance", *Proc. of Top Fuel 2015*.

Braun, J. et al. (2017), "Chemical compatibility between UO$_2$ fuel and SiC cladding for LWRs application to ATF (Accident-Tolerant Fuels)", *Journal of Nuclear Materials* (2017). (in print).

Cardinaels, T. et al. (2012), "Chromia doped UO$_2$ fuel: Investigation of the lattice parameter", *Journal of Nuclear Materials*, Volume 424, Issues 1-3, May 2012, pp. 252-260.

Chandramouli, D. and T. Shripad Revankar (2014), "Development of thermal models and analysis of uo$_2$-BeO fuel during a loss of coolant accident", *International Journal of Nuclear Energy*. Volume 2014, Article ID 751070, p.9.

Coulon-Picard, E. et al. (2009), "Assessment of cold composite fuels for PWRs", *Proceeding of Top Fuel 2009*, 6-10 September 2009, Paris.

Delafoy, C. and I. Arimescu (2016), "Developments in fuel design and manufacturing in order to enhance the PCI performance of AREVA NP's fuel", *Proceedings of the NEA Workshop on PCI in Water-Cooled Reactors. Lucca (Italy),* 22-24 June 2016.

Delafoy, C. et al. (2015), "AREVA Cr$_2$O$_3$-doped fuel: Increase in operational flexibility and licensing margins", *Proceedings of the Top Fuel 2015 – Reactor Fuel Performance meeting,* 13-17 September 2015, Zurich.

Delafoy, Ch. et al. (2007), "AREVA NP Cr$_2$O$_3$-doped fuel development for BWRs", *Proceedings of the 2007 International LWR Fuel Performance Meeting*, 30 September – 3 October 2007, San Francisco.

Delafoy, C. et al. (2003), "Advanced UO$_2$ fuel with improved PCI resistance and fission gas retention capability", *Proceedings of the 2003 Topfuel on LWR Fuel Performance,* 16-19 March 2003, Würzburg.

Delafoy, C. and M. Zemek (2009), "Washout behaviour of chromia-doped UO$_2$ and gadolinia fuels in LWR environments", *Proceeding of a Technical Committee Meeting on Advanced Fuel Pellet Materials and Fuel Rod design for Water Cooled Reactors,* 23-26 November 2009, Villigen.

Dewes, P. and C. Delafoy (2006), "FRAMATOME LWR UO$_2$ fuel development for challenging operating environments", *Proceedings of the Annual Meeting on Nuclear Technology,* 16-18 May, Aachen.

DOE (2006), *Thermophysical Properties Database of Materials for LWRs and Heavy Water Reactors*, Contract D.E.-AC05-76RL01830, IAEA-TECDOC-1496 IAEA, Vienna.

Garnier, C. et al. (2004), "The Copernic mechanical model and its application to doped fuel", *NEA International Seminar on Pellet-Clad Interaction in Water Reactor Fuels*, 9-11 March 2004, Aix en Provence.

Geelhood, K.J. and W.G. Luscher (2016), "FRAPTRAN-2.0: Integral Assessment", US Department of Energy.

Harp, J.M. (2016), "Current status of post irradiation examination for the ATF-1 irradiation", *Top Fuel 2016*, 11-15 September 2016, Boise.

Holden, A.N. (1967), *Dispersion Fuel Element, an AEC Monograph*, Gordon et Breach Science publishers, 1967.

Hwang, D.H., S.G. Hong and W.K. In (2015), "Evaluation of physical characteristics of PWR cores with accident tolerant fuels", *Autumn Meeting 2015, Korean Nuclear Society*, 29-30 October 2015, Gyeongju.

Ishimoto, J., M. Hirai and K. Ito (1996), "Thermal conductivity of UO_2-BeO pellet", *J. Nucl. Sci. Technol.*, Vol. 33 (1996), pp. 134-140.

Jadernas, D. et al. (2015), "PCI mitigation using fuel additives", *TopFuel 2015, American Nuclear Society*, 13-17 September 2015, Zurich.

Johnson, D.E. and R.G. Mills (1963), "Irradiation behavior of BeO-UO_2 fuel as a function of fuel particle size", *Unites States Atomic Energy Commission*, 16 April 1963.

Joseph, R. (2008), *The High Initial Rating Test IFA-677*, Final report on in-pile results, OECD Halden Reactor Project.

Julien, B. et al. (2004), "Performance of advanced fuel product under PCI conditions", *Proceedings of the 2004 International Meeting on LWR Fuel Performance*, 19-22 September 2004, Orlando.

Kim, D.J. et al. (2017), "Development status of micro-cell UO_2 pellet for accident tolerant fuel", *Water Reactor Fuel Performance Meeting 2017*, 10-14 September 2017, Jeju.

Kim, D.J. et al. (2015), "Fabrication of micro-cell UO_2-Mo pellet with enhanced thermal conductivity", *J. Nucl. Mater.*, Vol. 462, pp. 289-295.

Kim, H.G. et al. (2016), "Development status of accident-tolerant fuel for LWRs in Korea", *Nuclear Engineering and Technology*, Vol. 48, pp. 1-5.

Kim, S.K., W.I. Ko and H.D. Kim (2010), "Cost-benefit analysis of BeO-UO_2 nuclear fuel", *Progress In Nuclear Energy*, Vol. 52, pp. 813-821.

Kitano, K. et al. (2005), "Study on incipient cracks at inner surface of cladding after high power irradiation test", *Water Reactor Fuel Performance Meeting*, Kyoto.

Koo, Y.H. et al. (2014), "KAERI's development of LWR accident tolerant fuel", *Nucl. Technol.*, Vol. 186, pp. 295-304.

Kruszelnicki, J. et al. (2016), "Property analysis and advanced manufacturing technique development for LWR annular composite", *Top Fuel 2016*, 11-15 September 2016, Boise.

Lee, H.S. et al. (2015), "Thermal conductivity of metallic micro-cell fuel pellet with different unit cell geometry", *Spring Meeting 2015, Korean Nuclear Society*, 7-8 May 2015, Jeju.

Lee, S.W. et al. (2013), "Performance evaluation of UO_2/graphene composite fuel and SiC cladding during LB-LOCA using MARS-KS", *Nuclear Engineering and Design,* Vol. 257, pp. 139-145.

Leenaers, A. et al. (2003), "On the solubility of chromium sesquioxide in uranium dioxide fuel", *Journal of Nuclear Materials*, Vol. 317, pp. 62-68.

Nonon, C. et al. (2004), "PCI behaviour of chromium oxide doped fuel", *NEA International Seminar on Pellet-Clad Interaction in Water Reactor Fuels,* 9-11 March 2004, Aix en Provence.

Nonon, C. et al. (2003), "Impact of fuel microstructure on PCI behavior", *IAEA Technical Committee Meeting on Advanced Fuel Pellet Materials and Designs for Water Cooled Reactors*, 20-24 October 2003, Brussels.

McCoy, K. and C. Mays (2008), "Enhanced thermal conductivity oxide nuclear fuels by co-sintering with BeO: Fuel performance and neutronics", *Journal of Nuclear Materials,* Vol. 375, pp. 157-167.

Muller, E. et al. (2007), "Thermal behavior of advanced UO₂ fuel at high burnup", *Proceedings of the 2007 International LWR Fuel Performance Meeting*, 30 September – 3 October 2007, San Francisco.

Riglet-Martial, Ch. et al. (2014), "Thermodynamics of chromium in UO₂ fuel: A solubility model", *Journal of Nuclear Materials*, Volume 447, Issues 1-3, April 2014, pp. 63-72.

Solomon, A.A., T. Shripad Revankar, K. McCoy (n.d.), *Enhanced Thermal Conductivity Oxide Fuels,* School of Nuclear Engineering Purdue University.

Spencer, K.Y. et al. (2016), "Sensitivity study for accident tolerant fuels: Property comparisons and behavior simulations in a simplified PWR to enable ATF development and design", *Nuclear Engineering and Design,* Vol. 309, pp. 197-212.

Sun, M.Z., H.W. Huang and R. Li (2017), *Performance Analysis Report of Enhanced UO₂ Pellet*, CGN internal file, 29 March 2017, TF15AM-RL-TR-000068.

Teboul, N. et al. (2012), "AREVA optimized fuel rods for LWRs", *Proceeding of the Top Fuel 2012 – Reactor Fuel Performance meeting,* 2-6 September 2012, Manchester.

Titus, G.W. and J.H. Sailing (1963), "High-temperature irradiation of UO₂-BeO bodies", *University of Arizona Library Documents Collection*, 25 March 1963, M.A. McGrath, Yu. Volkov, Y. Russin, *In-reactor investigation of the composite UO₂-BeO fuel: background, results and perspectives*.

Tulenko, J. (2016), *Development of Innovative Accident Tolerant High Thermal Conductivity UO₂-diamond Composite Fuel Pellets*, Project No. 12-4037, NEUP Final Progress Report, January 2016.

Valin, S. et al. (2003), "Synthesis of the advanced UO₂ microstructures program in the TANOX device", *IAEA Technical Committee Meeting on Advanced Fuel Pellet Materials and Designs for Water Cooled Reactors*, 20-24 October 2003, Brussels.

Wright, J. et al. (2016), "Fuel hardware considerations for BWR PCI mitigation", *Top Fuel Meeting,* Boise Idaho.

Wright, J. et al. (2005), "Development of Westinghouse advanced doped pellet technology", *IAEA Technical Meeting on Fuel Behaviour Modelling under Normal, Transient and Accident Conditions and High Burnups*, 5-8 September, 2005.

Yang, J.H. et al. (2015), "Thermo-physical property of micro-cell UO₂ pellets and high density composite pellets for accident tolerant fuel", *IAEA Technical Meeting on Accident Tolerant Fuel Concepts for LWRs,* 13-14 October 2015, Oak Ridge National Lab.

Yang, J.H. et al. (2014), "Thermo-physical property of micro-cell UO₂ pellets and high density composite pellets for accident tolerant fuel", *IAEA Technical Meeting on Accident Tolerant Fuel Concepts for LWRs,* 13-14 October 2014, Oak Ridge National Lab.

Yang, J.H. et al. (2013), "Micro-cell UO₂ pellets for enhanced accident tolerant fuel", *TopFuel 2013, American Nuclear Society*, 15-19 September 2013, Charlotte.

Yeo, S. (2013), *UO₂-SiC Composite Reactor Fuels with Enhanced Thermal and Mechanical Poperties prepared by Spark Plasma Sintering*, A Dissertation presented to the Graduate School of the University of Florida in partial fulfillment of the requirements for the degree of doctor of philosophy, University of Florida.

Yeo, S. et al. (2013), "Enhanced thermal conductivity of uranium dioxide-silicon carbide composite fuel pellets prepared by Spark Plasma Sintering (SPS)", *Journal of Nuclear Materials*, Vol. 433, pp. 66-73.

Zemek, M. et al. (2006), "How oxidic additives Influence UO$_2$ fuel", *International Youth Nuclear Congress*, 18-23 June 2006, Stockholm.

Zhou, G. et al. (2005), "Westinghouse advanced UO$_2$ fuel behaviors during power transient", *Water Reactor Fuel Performance Meeting*, Kyoto.

Zhou, W.Z. and R Liu (2015), "Fabrication methods and thermal hydraulics analysis of enhanced thermal conductivity UO$_2$-BeO fuel in LWRs", *Annals of Nuclear Energy,* Vol. 81, pp. 240-248.

17. High-density fuel

The severe accidents in Fukushima Daiichi nuclear reactors strongly encouraged the enhancement of accident tolerances and a variety of fuel concepts have been proposed. These concepts are being developed worldwide.

At the initial stage of core degradation, the exothermic steam oxidation of metallic core components (such as fuel claddings and control rods) generates significant heat, which enhances the oxidation itself as well as the materials' interaction. This means that key approaches on the material development are suppression of steam oxidation at high temperatures and enhancement of resistance to the materials' interaction.

Most of the metallic materials suggested for use as cladding to reduce the steam oxidation present fairly large reactivity penalties compared to the traditional Zr-based claddings, resulting in an increase of the ^{235}U enrichment and/or a decrease in the cycle length. To compensate for this, the fissile density in the pellet has to be increased, while the in-pellet reactivity penalty should be kept low. The fissile density can be increased in several ways; one is to increase the density of the material, and another one is to increase the metal to non-metal ratio in the metal compound fuels, or to increase the ^{235}U enrichment. Increasing the ^{235}U enrichment is not covered in this chapter, which focuses on the other countermeasures. In case of cladding failure, the material behaviour with water or steam should be acceptable. None of the high-density fuel materials has as good a water and steam tolerance as the current UO_2. This may not disqualify the use of high-density fuels, as the water and steam sensitivity of a fuel concept has to be evaluated for the combination of cladding and fuel. Work is being made to increase the water tolerance for high-density fuels and the new accident-tolerant claddings are expected to have a much higher resistance to leakage.

The possible combinations of claddings and pellets have to be evaluated as a system, taking the cladding neutron penalty, the pellet neutron penalty and the pellet uranium density into account, as well as the thermal and chemical properties of both pellet and cladding, and finally the in-core behaviour of the full system (in particular fission gas release [FGR], in-pile swelling and pellet-clad interaction).

All the high-density fuels presented in this chapter are far from ready to be used as fuels in commercial light water reactors (LWR) reactors. The technology readiness levels for these fuels are low, in the TRL range of 3-4.

Nitride fuel

Fabrication/manufacturability (Matzke., 1986)

The fabrication experience of nitride fuel (especially (U,Pu)N fuels) has been carried out only on small batches (a few kilograms at the most) mainly to fabricate experimental specimens for out-of-pile or in-pile experiments.

A large variety of fabrication methods has been used to produce nitride fuels. The most common methods are:

- the nitridation of metallic U in N_2 or NH_3 at about 1 073 K to 1 173 K;

- the nitridation by arc melting of Pu and U metal in 3 to 5 bar of N_2;

- the hydride route from bulk metal U and Pu followed by nitridation;

- the sol-gel method: nitride precipitation at very low temperatures (liquid ammoniac: 240 K to 196 K), and this method leads to very pure nitride fuel but is limited to laboratory techniques and environment;

- the carbothermic reduction process: the nitride is obtained by reduction of UO_2 and PuO_2 fine powders with C, in nitrogen atmosphere.

The carbothermic reduction of oxide fuel is the most attractive process for a large production of nitride fuel pellets because the process is very similar to that of mixed-oxide fuels. However, a high level of micro homogeneity of the initial oxide-carbon blend is necessary to avoid formation of unwanted phases. In addition, the residual oxygen and carbon content is considered as a major drawback for this fabrication process. Minimising both residual C and O levels requires C/O levels close to the stoichiometric minimum followed by relatively long reaction times. Excess O (>1 000 ppm) results in poor pelleting performance and low resistance to water oxidation. Excess C (>500 ppm) results in excessive air and water oxidation. So the nitride compounds synthesis requires leak-tight gloveboxes maintained in an inert atmosphere containing less than 20 ppm of oxygen. The powder can be treated to provide minimal pre-oxidation that allows it to be taken out of the glovebox and handled in a normal containment for a short time.

^{15}N Enrichment

Natural nitrogen consists of 99.6% ^{14}N and 0.4% ^{15}N. Among the nuclear reactions concerning ^{14}N in a fast or thermal spectrum reactor, three products of transformation present major drawbacks:

- long life radiotoxic ^{14}C (which has to be managed in the wastes) from $^{14}N(n, p)$ reaction;

- He (which may lead to a larger fuel swelling and pin pressurisation) from $^{14}N(n,\alpha)$ reaction;

- a significant neutronic penalty of $U^{14}N$ in LWRs compared to UO_2.

These disadvantages can be avoided by ^{15}N enrichment. Several enrichment methods exist for a ^{15}N separation performance of 99.9% (which is equivalent to the most restricting ^{14}C release limitation for a reprocessing facility): NO/HNO_3 chemical exchange (nitrox process), cryogenic distillation of NO or NH_3, chromatographic process, adsorption on zeolite molecular sieves, dual colour laser technology and a combination of the gas centrifugation technique and NITROX process. While ^{15}N isotopic enrichment by the centrifugal method using N_2 is limited to 49%, the combination of the centrifugation technology with the nitrox process or cryogenic NH_3 process allows for an enrichment level of 99.9% to be attained.

Cost

Rough cost estimations were made more than ten years ago for the listed technologies (except for laser technology) based on an annual production of 165 tonnes: the results show that the most competitive process, which consists of combining centrifugation techniques and nitrox process, lead to an estimated cost of EUR 30 per gramme of ^{15}N (KTH, SSM, 2015). This price can be greatly reduced with ^{15}N recycling. When comparing to the current fabrication cost for UO_2 pellet (~a few euros per gramme), cost reduction is an important issue for nitride fuel.

In case of nitride fabrication with powder metallurgy (PM), an over cost may be anticipated as a result of the obligation to use a glovebox on account of nitride pyrophoricity and oxidation.

Normal operation and anticipated operational occurrences (AOOs)

Reactor operation

The experience of (U, Pu)N nitride fuel irradiation is limited to 150-200 pins, which have been irradiated in experimental FRs (RAPSODIE – France, DFR – UK, EBR-II – US, PHENIX – France, HFR – the Netherlands or JOYO – Japan). Two main fuel pin concepts exist to provide heat transfer between the fuel and cladding. The two concepts consist in filling the gap with a liquid metal (Na) or with a gas (He). In the context of thermal neutron reactors, the use of sodium is excluded on account of its strong chemical reaction with water. Only the results of the helium bonded pins irradiations are of interest here and will be presented.

FGR is significantly lower in nitride fuels compared to standard oxide fuels in normal operating conditions. This may be mainly attributed to the nitride fuels' higher conductivity. For instance, at 10 at% burn-up, the release rate for FR fuel nitride pins is of ~50% for nitride fuels and 80-85% for oxides fuels in the equivalent burn-up conditions. But if nitride fuels are fabricated with natural nitrogen, 16% of additional gases (He + H_2) are created and mostly released inside the fuel pin, this supplementary gas' creation being due to the nuclear reactions on ^{14}N.

Pellet-clad mechanical interaction (PCMI) requests specific attention for the nitride fuels because of their higher swelling rates, which are the dense fuels' main drawbacks. High swelling rates have been measured for FRs nitride fuel from 1%/at% to several 10%/at% at high temperatures, with the swelling rate depending on the burn-up and overall on the fuel temperature. In addition, fuel fragment relocation and clad mechanical properties degradation tend to increase PCMI.

To prevent large cladding deformations and/or cladding failures, a low fuel smear density, i.e. 70-80% depending on the targeted burn-up should be adopted by adjusting the pellets porosity and fuel-clad gap. Alternatively, a larger gap can be used; due to the much higher thermal conductivity of the UN fuel, this should not result in excessive centreline temperatures.

It seems that a maximum burn-up of 6.9 at% without failures has been reached by some (U, Pu)N fuel pins, He bonded, in stainless steel cladding irradiated in experimental FRs at 420 W/cm (KTH, SSM, 2015).

To our knowledge, no experience has been reported recently about UN irradiation in an LWR. Due to lower operating temperatures in LWR conditions compared to FR conditions, lower fuel swelling is expected in normal operating conditions. But, once the fuel cladding gap is closed, harder PCMI may occur, due to higher Young's modulus and lower irradiation creep at lower temperatures.

Cladding/fuel interactions

The cladding and fuel have to be considered as a system both to ascertain the synergisms as well as the incompatibilities. So, for instance, in fuel rods utilising SiC-composite cladding, a larger pellet-cladding gap could be designed, which would make the use of UO_2 questionable because of its low-thermal conductivity. However, the use of UN with its high-thermal conductivity along with SiC-cladding could be a viable option. The chemical compatibility of UN fuels with SiC and Zy claddings is not yet known. The chemical compatibility of (U,Pu)N fuel with stainless steel cladding is good in fast breeder reactor conditions.

For additional details on this issue, please refer to Part IV of this report (TRL evaluation).

Behaviour in AOOs

Off-normal behaviour of nitride fuel is not well known due to a lack of in-reactor experience. Based on the understanding of the root causes of the nitride fuel pins'

failures in fast breeder reactor normal irradiation conditions, once the fuel-clad gap is closed, PCMI may occur during AOO transients depending on fuel temperature and cladding ductility.

Cycle length

Longer operating cycle length could be envisioned based on possible higher ^{235}U/U content thanks to the higher nitride fuel density. But this benefit can be offset by a fuel design with a lower smear density to accommodate the in-pile fuel swelling and the nitride fuel neutronic absorption when using natural N.

Specific behaviour of leakers during irradiation (further degradation with risk of fuel fragments dispersion)

In case of cladding failure during irradiation, nitride fuel reacts with steam. This reaction occurs with an accelerated kinetic above ~523 K. Two reactions have been observed, leading to the production of explosive hydrogen:

$$UN + 2H_2O \rightarrow UO_2 + NH_3 + \tfrac{1}{2}H_2$$

$$3UN + 2H_2O \rightarrow UO_2 + U_2N_3 + 2H_2$$

Thus, nitride pellets fuel must be protected from coolant water steam ingress and any kind of loss of cladding leak-tightness must be avoided.

Research is underway to make the UN fuel waterproof: KTH and SSM have reported (KTH, SSM, 2015) that out-of-pile tests have shown that the water resistance of UN could be improved by minimising open porosity in conjunction with lowering the carbon content in the manufactured pellets. In addition, additives are being investigated such as U_3Si_2 to protect the UN grains from attack by water (KTH, SSM, 2015).

Neutron penalty

^{14}N neutron absorption in thermal neutrons is significant, producing radioactive ^{14}C and He and resulting in no increase in burn-up over a UO_2 fuel of the same theoretical density (TD) and ^{235}U enrichment. An economic means for ^{15}N enrichment of natural N_2 can be used (see Section on Nitride fuel, sub-section on fabrication/manufacturability) and is required for there to be any economic advantage for UN over UO_2.

Mechanical properties

- Nitride thermal and irradiation creep rates are much lower than for standard oxide fuel;
- Nitride Young's modulus is higher than oxide fuel;
- Nitride thermal expansion is the same as UO_2.

Fuel dissociation in (U, Pu)N fuel

The observations of Pu metallic phase on the inner side of the cladding for (U, Pu)N pellets irradiated at high linear power (Pl > 700 W/cm) in helium filled pins, have confirmed the dissociation of nitride fuel with Pu in He environment at high temperature (T>2 000 K) according to the reaction:

$$U_{1-x} Pu_xN(s) \rightarrow (1+x)U(l) + xPu(l) + 0.5 N_2(g) \text{ and the preferential evaporation of Pu.}$$
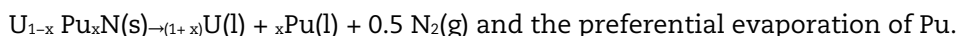
Thus, a maximum temperature of 2 000 K for normal operation conditions has then been suggested for (U, Pu)N fuels. Nevertheless, as the mobility of atomic species in nitride fuels is a slow process, this temperature limit could temporarily be overtaken without major consequences on fuel behaviour.

This dissociation needs to be further demonstrated for UN fuels without Pu.

Modelling

Up to now, the French Alternative Energies and Atomic Energy Commission (CEA) has used a version of the METEOR/TRANSURANUS fuel (U, Pu)N performance code initially devoted to PWR oxide fuel behaviour description, whose database has been modified to take into account the nitride fuel characteristics and behaviour laws.

DBAs and DECs

Accident conditions experienced by nitride fuel are very limited. Based on the understanding of the off-normal behaviour of carbide and oxide fuel systems in fast breeder reactors, it is expected that the off-normal behaviour of nitride fuel will mainly depend on the following issues:

- accelerated swelling of the nitride fuel at high temperature could rapidly lead to PCMI;

- the (U, Pu)N fuel decomposition at T> 2 000 K under He could lead to nitrogen release and thus to an over pressurisation of the rods and this is not an issue with UN fuels since sintering temperatures of up to 2 600 K have been used with no decomposition;

- in case of a cladding failure, nitride reaction with steam water will generate hydrogen; however, the water resistance of UN can be improved by minimising open porosity in conjunction with lowering the carbon content in the manufactured pellets (KTH, SSM, 2015; Lopes, Uygur and Johnson, 2017).

Experimental data on these items are sparse. As a result, the assessment of these issues is quite difficult and requires further studies.

Used fuel storage/transport/disposition/reprocessing

Nitride fuel is soluble in nitric acid. The reprocessing schemes for nitride will depend on whether or not ^{15}N will be used and recovered from the fuel, although ^{15}N enrichment of nitride may be not be conceivable without ^{15}N recycling for enrichment cost reasons.

The use of natural ^{14}N nitrogen in the nitride fuels composition, which shows significant cross-section for neutron capture, will produce significant amounts of ^{14}C. The long half-life of ^{14}C will create waste handling and environmental issues.

In case of a failure during long-term storage, nitride pellets can react with air and steam. The reaction kinetics, however, decreases with lowring temperature. No reaction has been observed at 353 K even after four days immersion in water. More studies should be performed to characterise the fuel behaviour in these conditions.

Silicide fuel

Of the series of compounds in the U-Si phase diagram, only U_3Si_2 is considered here following rejection of the higher density silicides based on unacceptable swelling and/or low melting point. Ideas exist to adopt either 2-phase UN-U_3Si_2 or 2-phase U_3Si-U_3Si_2 in order to further increase uranium density. The intermediate 2-phase silicide composition may also confer a reduction in swelling. A performance evaluation of high-density fuels including silicide fuel was recently performed in *Development of LWR Fuels with Enhanced Accident Tolerance* (Lahoda et al., 2015).

Fabrication

The starting materials for fabrication, i.e. uranium hexafluoride and silicon are readily available. For fabrication of specimens and test pellets for irradiation tests, uranium metal and silicon are arc melted, quenched, heat treated, pulverised, pressed and sintered to form pellets. Sufficient pellet density has been demonstrated but process

optimisation is ongoing (Harp, Lessing and Hoggan, 2015); no serious issues are foreseen in this area. Economic feasibility of silicide fuel could be improved by direct synthesis of U_3Si_2 from UF_6 (avoiding the metallic uranium intermediate), but no proven industrial process is currently available.

Normal operation and AOOs

The most important characteristics of silicide fuel with respect to normal operation are high-thermal conductivity and high uranium density. Testing up to a burn-up of 20 MWd/kgU has shown 0%+/-1% swelling and FGR of ~0.3% for linear heat generation rates (LHGRs) of 433 to 500 W/cm. This swelling rate and FGR is less than that for UO_2 at comparable LHGRs.

Due to the high-thermal conductivity of U_3Si_2 (5 to 10 times that of UO_2; White et al., 2014), fuel centreline temperatures will be significantly less affected by in-pile operations (control rod movement, fuel shuffling and power stepping) and fuel stored heat will be decreased. The improved thermal performance of U_3Si_2 compared to UO_2 fuel allows implementation of a more advanced cladding such as a SiC-SiC-composite, which besides the expected operational and safety benefits, also offers superior neutron economy and further fuel cycle cost savings relative to Zr-based claddings.

The neutronic characteristics of U_3Si_2 are similar to UO_2 fuel with some differences mainly related to the different cross-sections of the binding elements and the higher density of U_3Si_2.

- The higher density of U_3Si_2 compared to UO_2 results in a reduction in neutron moderation from the lower hydrogen to heavy metal (H/HM) ratios for the same size fuel pins and fuel arrangement. Therefore, the spectrum of U_3Si_2 is harder, meaning there is a higher neutron population at higher energies relative to the UO_2 fuel spectrum. The spectral ratio, defined as the ratio of the flux above and below 0.625 eV, is approximately 11 and 9, respectively for fresh U_3Si_2 and UO_2 in a typical 17 x 17 lattice. As the fuel is irradiated, the spectrum becomes harder for all fuels as a result of thermal captures in fission products (FPs) and in-bred Pu and the spectral differences among all fuels are reduced.

- The harder spectrum of U_3Si_2 has two reactivity effects. First, the fissile cross-sections and the instantaneous reactivity is decreased. Second, the ^{238}U to Pu conversion is increased due to the higher epithermal captures in ^{238}U, which slows down the reactivity loss as the fuel is burned. The net effect on reactivity depends on the fuel discharge burn-up. For instance, 5% ^{235}U-enriched U_3Si_2 fuel in a standard 17 x 17 lattice is initially less reactive than UO_2 fuel of the same enrichment and lattice conditions, but as the two fuels are burned the reactivity in U_3Si_2 fuel becomes larger than UO_2 fuel at burn-up greater than 50 MWd/kgU.

In case of a failed cladding tube, not enough is known about the U_3Si_2-pellet to water and steam behaviour to be able to completely assess the effects for the reactor operation, although fuel oxidation will be somewhat more exothermic than that of UO_2 (White et al., 2014).

DBAs and DECs

U_3Si_2 has a somewhat larger margin to melting compared to UO_2 despite the fact that U_3Si_2 melts at 1 665°C, whereas UO_2 melts at 2 878°C. Using 0.82 cm diameter pellets with a surface temperature of 673K, the maximum LHGR before centreline melting occurs in UO_2 is ~750 W/cm. A comparably sized U_3Si_2 pellet can have an LHGR of 2 300 W/cm before centreline melting occurs. This is due to the much higher thermal conductivity of this fuel compared to UO_2. Additionally, because the thermal conductivity of U_3Si_2 increases with temperature (dk/dT>0), the margin to melting of U_3Si_2 becomes even larger as peak linear power and fuel temperature increases. Generally, the thermal properties

and neutron economy properties for U_3Si_2 allows for a more advanced cladding to be used. Qualitatively, softer pellet-clad interactions (in relation to power ramps) and more exothermic fuel oxidation (in relation to clad failure) are expected compared to UO_2, but this is to be experimentally confirmed.

Figure 17.1. Fuel temperatures versus burn-up based on Westinghouse calculation
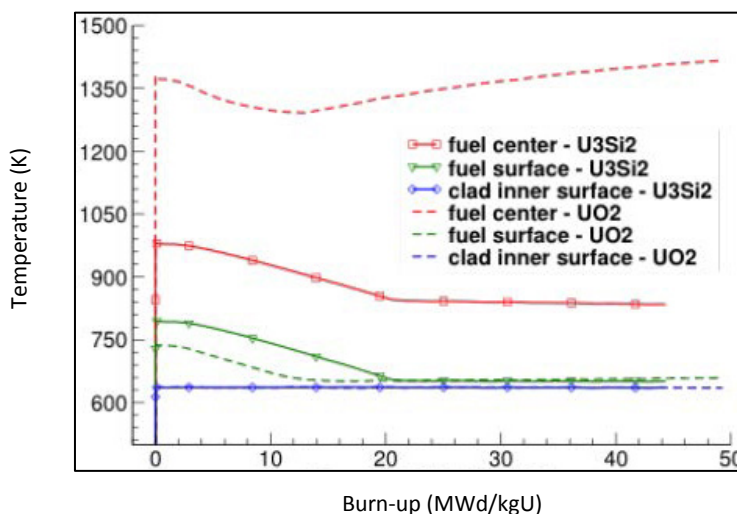
Source: Gamble et al, (INL) 2016.

Used fuel storage/transport/disposition/reprocessing

Insufficient data is available for thorough assessment of fuel storage options. However, within the context of materials test reactor (MTR) spent fuel it has been suggested that reprocessing is preferred over direct disposal; available data suggest the oxidation of U_3Si_2 in brine solutions and some sensitivity to leaching (Curtius, Brücher, 2005). AREVA recently completed industrial qualification and safety assessment of silicide fuel reprocessing at La Hague (Valery et al., 2015).

Technology readiness level

It is concluded that the R&Ds needed to achieve TRL-3 for the use of U_3Si_2 fuel pellets in the context of LWR accident-tolerant fuel concepts are ongoing. Several knowledge gaps will have to be filled in order to progress to the TRL4-5 stage (concept validation in lab and relevant environment), the most important ones being pellet swelling and creep, degradation of thermal conductivity, FGR and in-core and out-of-pile oxidation resistance.

Carbide fuel

In the framework of the development of fast breeder reactor (FBR) technologies, carbide fuels (UC and U(Pu)C) have been studied in France since the 1970s. This section highlights valuable elements resulting from French research, including results available in the open literature and discussion outcomes from the Task Force that delivered the current report.

In theory, carbide fuel is a good potential alternative to uranium and plutonium oxide fuels. Advantages for these alternative fuels are their higher TD (~+24% for UC compared to UO_2) and their higher thermal conductivity (>7 to 10 times than UO_2).

However, the higher swelling rate of carbide fuel under irradiation (roughly twice that of UO_2) was obsereved in previous tests. To compensate the large swelling, the design must decrease the pellet density by introducing a higher porosity. According to previous experiences, a carbide pellet with 95% of TD can be synthesised. Typically, 10 to 20% of porosity needs to be introduced. Consequently, it is potentially achievable to decrease the initial fuel enrichment because of the higher density of heavy atoms.

In normal operation, carbide fuels present lower temperature values than oxides. Moreover, (U,Pu)C has a high melting temperature greater than 2 470°C. Nevertheless, it has been observed that plutonium may vaporise under metallic form above 1 650°C. This feature can bring troubles mainly during the fabrication process. The risk of cladding carburation must also be accounted for, both during manufacturing and fuel design.

In this section, technical information has been compiled regarding in-pile behaviour of this fuel, in terms of advantages and disadvantages over the entire fuel cycle. Overall, significant development hurdles still exist and some remaining problems must be solved in the perspective of a large industrial scale deployment.

Fabrication/manufacturability

A potential large-scale production appears to be possible, and the manufacturing process can be qualified thanks to the carbothermic reduction of oxide powders mostly used for (U,Pu)C pellet fabrication. Moreover, the Los Alamos US facility fabricated (U,Pu)C pellets that have met or even exceeded the stringent internal quality insurance requirements. Indeed, manufacturing routine procedures have been established on a semi-industrial scale. Los Alamos laboratory production facility could produce up to 1 000 pellets a day in the 1980s with stringent quality insurance requirements. By 1983-1985, the Indian Facility for fuel production for the FBTR test reactor had a fabrication capacity of 1.2 kg of $(U,Pu_{0,3})C$ pellets/day. But, UC powder is pyrophoric and some incidents have been reported. Due to safety requirements, the fabrication process requires gloveboxes with controlled neutral atmosphere, which generates important extra costs.

Normal operation and AOOs

Behaviour in normal operation

In normal operation, specific PCMI can occur due to high swelling rate and to low irradiation/thermal creep rate of UC fuel pellets as compared to UO_2 fuel pellets (Dienst, Mueller-Lyda, Zimmermann, 1979). However, in the US irradiation test in the EBR-II reactor, (U,Pu)C fuel pins with 316 stainless steel cladding have reached burn-ups (BU) as high as ~20 at% without experiencing any cladding failure.

In terms of neutron economy and cycle length, UC high-density fuel allows for longer cycles since there is a higher [235]U/U content. Such fuel presents a higher density of heavy atoms compared to UO_2 fuel in spite of a necessary lower density of the UC fabricated pellets (using stainless steel cladding) in order to accommodate the UC swelling under irradiation.

Concerning irradiation properties of (U,Pu)C pellets, maximum reachable burn-up is around 150 GWd/t in normal operating conditions, using an "optimised" (U,Pu)C fuel rod design.

Even at high BU, measured FGRs of (U,Pu)C fuel pellet rods are much lower than those of oxide fuel pellets irradiated in the same operating conditions.

Very high microstructural and chemical stability was observed up to high BU (15 at %) at a temperature <~1 650°C (Chang, 1989). At temperatures > ~1 650°C Pu migrates and can even evaporate in (U,Pu)C fuel.

The UC swelling rates are not known in LWR conditions and have to be documented because (U,Pu)C fuel swelling rate is higher than $(U, Pu)O_2$ fuel in FBR conditions.

Behaviour in AOOs

In the situation of a closed gap between fuel and cladding, higher PCMI than for UO_2/Zr concept is expected since there is a higher Young's modulus and lower creep rate of UC fuel pellets (as compared to UO_2 fuel pellets).

Cladding carburisation and embrittlement can occur and might be a challenging problem in terms of PCMI failure risk. If the clad fails, the primary water ingress in the fuel rod will turn into steam and will interact with the UC pellets to form $UO_2 + CH_4$ or H_2 + carbon oxides gas. Most of these reaction products are explosive gas in air, which is a major drawback for plant outages and fuel handling. Significant works must be undertaken to develop waterproof UC pellets in the consideration of future LWR licensing.

DBAs and DECs

The major challenging problems expected during design-basis accidents and design extention conditions transients include: the Pu evaporates from (U, Pu)C fuel when temperatures exceed T~1 650°C; in case of high-temperature (HT) transients (i.e. resulting from "too much power transients" and "not enough cooling transients") the accelerated fuel swelling may be a design concern; the reactions of UC with steam could lead to reaction products such as $UO_2 + CH_4$ or H_2 + carbon oxides gas which, for the most part, are explosive gas in air.

In conclusion, UC pellets must be protected from steam at all time.

Used fuel storage/transport/disposition

In used fuel storage, transport and disposal conditions, uranium and/or plutonium carbide fuels exhibit three beneficial properties compared to UO_2 fuel. These are:

- higher density of UC fuel allows reducing $^{235}U/U$ enrichment as compared to UO_2 fuel;

- higher thermal conductivity of UC fuel leads to better thermal behaviour (lower T°C) than UO_2 fuel;

- less FGR in UC fuel as compared to UO_2 fuel will reduce rod internal pressure.

Reprocessing

Reprocessing is a potentially challenging issue on account of the poor solubility of the UC fuel in nitric acid. Specific reprocessing process or additional head-end process to make this fuel compatible with the PUREX process will have to be developed, which will increase the costs.

Metallic fuels

Metallic U-10Zr

Uranium-zirconium (U-Zr) alloy or uranium-plutonium-zirconium (U-Pu-Zr) alloy fuel was originally proposed by the US Argonne National Laboratory (ANL) in the 1980s (Chang, 1989; Hofman et al., 1994). This type of metal fuel is suitable for sodium (Na)-cooled FR because of its high heavy metal density and thermal conductivity. In recent years, the U(-Pu)-Zr metal fuel has been developed in India (Kumar, 2013), Japan (Nakamura et al., 2009), Korea (Kim, 2013), etc. as well as the United States for the purpose of improving reactor safety, economy, Pu breeding and nuclear proliferation resistance. Until now, however, the applicability of U(-Pu)-Zr fuel to LWR was hardly discussed in the literature.

Fabrication

The fuel fabrication technology has already reached a semi-industrial level. In the United States, more than 10 000 U-Zr fuel pins and about 600 U-Pu-Zr fuel pins have been fabricated thus far (Leggett et al., 1993) and these metal fuel assemblies were irradiated in the experimental breeder reactor–II (EBR-II) or the fast flux test facility (FFTF). In these irradiation experiments, a peak burn-up of ~20at.% was achieved (Pahl et al., 1990). This type of metal fuel fabrication technology has been established in other countries (see Figure 17.2).

Figure 17.2. U-20 Pu-10 Zr fuel slug fabricated by injection casting method in a collaboration project between CRIEPI and JAEA

Source: Nakamura et al., 2007.

Normal operation and AOOs

The smeared density of U(-Pu)-Zr fuel must not exceed 75%TD (Walter et al., 1980; Einzinger et al., 1980) because of the large irradiation swelling of the metal fuel (~40vol% at 1-2 at.% burn-up) and the resultant large gap between fuel slug and cladding inner wall is filled with a thermal bond material. In the case of Na-cooled FR fuel, metallic Na is applicable for the bond material, but alternative materials have to be investigated for LWR fuels.

The U(-Pu)-Zr-alloy, especially when it has been irradiated, reacts easily with water or steam and is oxidised (Papaioannou et al., 2012). As a result, the fuel alloy disintegrates into pieces (see Figure 17.3) and hydrogen (H_2) gas is generated. Additional measures to strictly prevent the contact between metal fuel and water/steam would be absolutely indispensable if the application to LWR is considered.

Figure 17.3. Metallographic image of irradiated U-Pu-Zr fuel cross-section
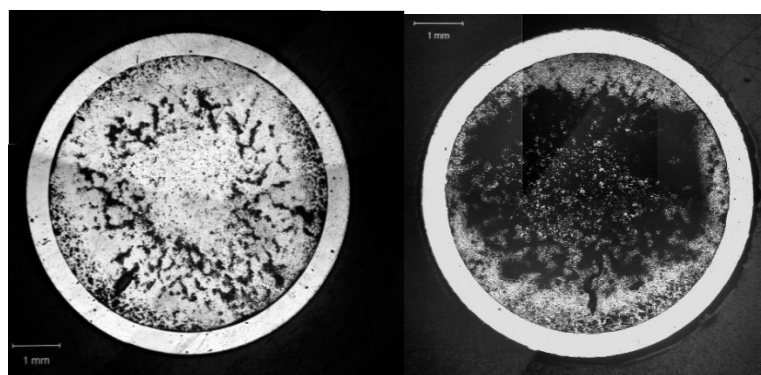
before oxidation   after oxidation

Source: Papaioannou et al., 2012.

DBAs and DECs

As mentioned above, the irradiated U(-Pu)-Zr-alloy is easily oxidised with H_2 gas generation and flows out when it comes in contact with water/steam. From the viewpoint of core safety including accident conditions, it is difficult to apply the U(-Pu)-Zr metal fuel developed for FR to LWR, irrespective of the cladding material such as zircaloy, stainless steel or alternative cladding materials, even if an alternative bond material to metallic Na was found.

Used fuel storage/transport/disposition/reprocessing

For the U(-Pu)-Zr metal fuel, technologies for used fuel storage, transport, disposure and a pyrometallurgical reprocessing (Chang, 1989), which have been developed for FR metal fuel cycle, are basically applicable.

Metallic U-50%Zr

U-Zr-alloy is a potential candidate for metallic fuels for nuclear reactors. The U-rich variants of the U-Zr system, i.e. alloys containing up to 10wt%Zr have been investigated for FBR (see previous section). On the other hand, the U-50wt%Zr system (UZr_2) is also used as fuel for Russian nuclear ships. In this context, large amounts of fuel assemblies, i.e. more than 3 000 are reported to be operating to an average burn-up level of 0.85 g-FP/cc (~25at%). However, there is no indication of the performance and behaviour of this metal fuel as the experience feedback of that programme is not openly documented. As a consequence, all data reported hereafter are issued from a literature survey.

Fabrication/manufacturability

In the past, injection casting was applied to prepare the U(Pu)-10wt%Zr fuels for FBRs; today, PM or arc melting practices are considered as well. The alloy preparation must be done in a chamber pressurised with argon or helium rather than under high vacuum to ensure that no gaseous impurity, especially oxygen, comes from the outside. Manufacturing capabilities exist at the laboratory scale; no mass production line is available in western countries.

Normal operation and AOOs

One of the major issues with metal alloy fuels is that they may undergo a large amount of swelling from low burn-up. This typical behaviour is primarily due to fission gas, neutrons flux irradiation damage, fuel composition and high operating temperatures. The anisotropic swelling behaviour of these fuels is a result of radial stresses caused by a difference in swelling behaviour between the inner and outer regions of the fuel and the response of the α phase that is inherently anisotropic (Matzke, 1986). Cavitational swelling results partly from anisotropic grain growth during irradiation of polycrystalline α-phase uranium wherein the growth of individual grains causes mismatched strain at grain boundaries resulting in plastic deformation. A lower amount of α-phase uranium or plutonium seem to be the cause of a lower swelling anisotoropy of U(Pu)-10wt%Zr-alloys under irradiation (Hofman et al., 1990). From the phase diagram shown in Figure 17.4 (Sheldon, Peterson, 1989), a particular alloy exists as the UZr_2 δ-phase structure below 600°C. The δ phase is not a line compound but has a composition range of 42.5-57.5 wt%Zr at 400°C. The δ phase is expected to be more stable and one experiment confirmed a lower volumetric swelling induced by irradiation at 1.2 at% burn-up in a capsule of (U-47wt%Zr) δ-phase metallic fuel microspheres on the order of 2.5% per atomic burn-up (Ogawa et al., 1998). This interesting result has to be confirmed for representative fuel pellets samples.

Figure 17.4. U-Zr diagram

Source: Sheldon, Peterson, 1989.

Both the thermal diffusivities and the thermal conductivities of the U-Zr-alloys exhibit minimum values in the δ-phase alloy (Ogata, 2012). Nonetheless, these values are much larger with respect to UO_2 fuel: ~15 W/m·K and 3 W/m·K respectively at 900 K for thermal conductivity. This higher thermal conductivity feature should allow operation at low temperature, typically around 370°C when the U-50wt%Zr-alloy is metallurgically bounded to the cladding (Malone et al., 2012). Under this condition, temperature-driven phenomena should be significantly reduced in the U-50wt%Zr fuel (e.g. diffusion and growth of fission gas bubbles or migration of gaseous FPs). As a result, FPs are anticipated to be primarily concentrated where they are generated and then leading to a reduction in the radioactive source term in case of cladding breach events if no water oxidation occurs. Degradation of the thermal conductivity under irradiation in the metallic fuel shall be quantified, but peak fuel temperatures are anticipated to remain below ~600°C up to very high burn-up levels.

The melting point of the metal alloy is to be related to the above low operating temperature conditions, with larger margins to melt being expected with respect to UO_2 fuel although the melting temperature of the U-50wt%Zr-alloy is of about 1 600°C (Ogata, 2012).

In general, metallic fuels are known for their poor behaviour in the event of contact with water (and/or vapour). In comparison to uranium metal, the addition of alloying elements results in improvements in corrosion resistance. In the high zirconium alloy content, the corrosion behaviour is largely governed by the zirconium, but weight gains are significantly higher than for cladding zirconium alloys. Matrix breakup is reported due to preferential attack along non-homogeneous secondary phases, such as hydrides for the alloys that resulted in cracks and an increased surface area (Polyakov et al., 1995). Experiments conducted in the 1950s on zircaloy bonded uranium fuels indicate that when the fuel cladding bond integrity is maintained, the exposed area for reaction is limited (Isserow, 1958).

Although there is no experience available, no PCI issue is anticipated especially when the U-50wt%Zr fuel is metallurgically bound to the cladding and that the integrity of the bond is maintained. The difference in swelling behaviour between fuel and cladding materials could result in bonding interface fuel cladding mechanical stresses.

DBAs and DECs

Accident conditions experienced by U-50wt%Zr are not reported. One major concern is related to the high amount of zirconium, with the risk of generating hydrogen during off-normal events.

The low operating temperature and improved heat transfer when the U-50wt%Zr fuel is metallurgically bounded to the cladding should facilitate the decay heat removal and prevent rapid temperature increase at the very beginning of an accidental transient. Therefore, increased time to restore cooling capability during DBA can be expected. However, according to Figure 17.4, a phase transition in the δ-phase alloy occurs from ~600°C what could result in swelling acceleration and detrimental PCMI. Therefore, in the absence of cooling over a long period, a worsening of the overall behaviour with respect to UO$_2$ is anticipated. As already mentioned, additional drawbacks of the the U-50wt%Zr fuel are its low melting temperature as well as its poor behaviour in the event of contact with vapour.

Used fuel storage/transport/disposition/reprocessing

The high Zr content reduces the uranium loading per unit volume to about one-half that of UO$_2$. Therefore, the metallic fuel requires increased enrichment to compensate for reductions in both the initial fissile loading and the fissile plutonium generated during reactor operation. A ^{235}U enrichment up to 19.7 wt% is anticipated. If this high enrichment remains within the internationally accepted limits for low-enriched uranium (LEU); however, such an enrichment would require considerable changes to existing enrichment and fuel fabrication facilities, amendments to plant licences and re-evaluation of transport and storage procedures. As a matter of fact, a negative impact on the fuel cost is anticipated.

As for other metal fuel concepts, spent U-50wt%Zr fuel is compatible with pyrometallurgical reprocessing technology.

References

Adorno Lopes, D. (2017), "Degradation of UN and UN–U$_3$Si$_2$ pellets in steam environment", *Journal of Nuclear Science and Technology*, Selim Uygur and Kyle Johnson DOI: 10.1080/00223131.2016.1274689.

Chang, Y.I. (1989), "The integral FBR", *Nucl. Technol.*, Vol. 88, p. 273.

Curtius, H. and H. Brücher (2005), "R&D for the final disposal of irradiated research reactor fuel elements, ENS RRFM Transactions", *9th International Topical Meeting on Research Reactor Fuel Management* (2005), pp. 164-168.

Dienst, W., I. Mueller-Lyda and H. Zimmermann (1979), "Swelling, densification and creep of oxide and carbide fuels under irradiation", *International Conference on FBR Fuel Performances,* Monterey, California.

Einzinger, R.E. et al. (1980), "Irradiation performance of metallic driver fuel in experimental breeder reactor–II to high burnup", *Nucl. Technol.*, 50, 25 (1980).

Finlay, M.R., G.L. Hofman and J.L. Snelgrove (2004), "Irradiation behavior of uranium silicide compounds", *JNM* 325 (2004), pp. 118-128; Kim, Y.S., G.L. Hofman, J. Rest, A.B. Robinson (2009), "Temperature and dose dependence of fission gas bubble swelling in U$_3$Si$_2$", *JNM* 389, pp. 443-449.

Gamble, K.A. et al. (2016), *Behavior of U$_3$Si$_2$ Fuel and FeCrAl Cladding under Normal Operating and Accident Reactor Conditions*, INL/EXT-16-40059 Rev. 0, September 2016, Idaho National Laboratory, Idaho Falls.

Harp, J.M., P.A. Lessing and R.E. Hoggan (2015), *Uranium Silicide Pellet Fabrication by Powder Metallurgy for Accident Tolerant Fuel Evaluation and Irradiation*, J. Nucl. Mater. Vol. 466, pp. 728-738.

Hofman, G.L. et al. (1994), "Metallic fast reactor fuels", *Materials Science and Technology*, A Comprehensive Treatment, R.W. Cain et al. EDS.; *Nuclear Materials*, 10A, Part 1, B.R.T. Frost, Ed., VCH Verlagsgesellschaft.

Hofman, G.L. et al. (1990), "Swelling of U-Pu-Zr fuel", *Metallurgical Trans*. A, 21A (1990).

Isserow, S. (1958), "Corrosion behavior of defected fuel elements with U-2wt% core clad Zircaloy-2", NMI-4364, *Nuclear Metals, Inc.*

Kim, Y. (2013), "Status of SFR development in Korea", *Int. Conf. on Fast Reactors and Related Fuel Cycles: Safe Technologies and Sustainable Scenarios (FR13)*, 4-7 March 2013, Paris.

KTH and SSM (2015), HRP Member White Paper (DRAFT 2015-10-14), ATUNE: Accident Tolerant Uranium Nitride Experiment, supported by NNL (UK), Westinghouse.

Kumar, A. (2013), "Development, fabrication and characterization of fuels for Indian fast reactor programme", *Int. Conf. on Fast Reactors and Related Fuel Cycles: Safe Technologies and Sustainable Scenarios (FR13)*, 4-7 March 2013, Paris.

Lahoda, E.J. et al. (2015), *Development of LWR Fuels with Enhanced Accident Tolerance* – Final Technical Report, Westinghouse RT-TR-15-34.

Leggett, R.D. et al. (1993), "Status of LMR fuel development in the United States of America", *J. Nucl. Mater*., Vol. 204, 23 (1993).

Malone, J. et al. (2012), "Lightbridge Corporation's advanced metallic fuel for LWRs", *Nuclear Technology*. Volume 180 (2012).

Matzke, H.J. (1986), *Science of Advanced LMFBR Fuels, Solid State of Physics, Chemistry and Technology of Carbides, Nitrides and Carbonitrides of Uranium and Plutonium*, North Holland, Elsevier Science Publishers B.V..

Nakamura, K. et al. (2009), "Fabrication of metal fuel slugs for an irradiation test in JOYO", *Proceedings of Global 2009*, 6-11 September 2009, Paris.

Nakamura, K. et al. (2007), *Development of Metal Fuel Fabrication Technology for Irradiation Test in JOYO: Injection Casting of Uranium-20wt% Plutonium-10wt% Zirconium Alloy,* CRIEPI Report L06005, in Japanese.

Ogata, T. (2012), *Metal Fuel in Comprehensive Nuclear Materials*, Editor-in-Chief: R.J.M. Konings. Elsevier Ltd. Edition (2012).

Ogawa, T. et al. (1998), "Irradiation behavior of microspheres of U-Zr-alloys", *Journal of Alloys and Compounds,* 271-273 (1998).

Pahl, R.G. et al. (1990), "Steady state irradiation testing of U-Pu-Zr fuel to >18at.% burnup", *Proc. of Int. Fast Reactor Safety Mtg.*, 12-16 August 1990, Snowbird, Session 2, Vol. IV, 129-137 (1990).

Papaioannou, D. et al. (2012), "Irradiation effects on actinide containing U-Pu-Zr metallic fuels at several burnups", *Presentation material at 2012 ANS Annual Meeting*, 24-28 June 2012, Chicago, Illinois.

Polyakov, V.N. et al. (1995), "High-temperature interaction of uranium and zirconium with water vapor", *Materials Science*, Vol. 31(3).

Sheldon, R. and D. Peterson (1989), "The U-Zr (uranium-zirconium) system", *Bulletin of Alloy Phase Diagrams,* Volume 10, Issue 2.

Valery, J.F. et al. (2015), "Status on silicide fuel reprocessing at AREVA La Hague (2015), Transactions of RERTR 2015", *36th International Meeting on Reduced Enrichment for Research and Test Reactors,* Seoul.

Walter, L.C. et al. (1980), "Development and performance of metal fuel elements for FBRs", *Nucl. Technol.*, Vol. 48, p. 273.

White, J.T. et al. (2015), "Thermophysical properties of U_3Si_2 to 1773 K", *JNM 464 (2015)*, 275-280; Nelson, A.T., J.T. White, D.D. Byler, J.T.Dunwoody, J.A. Valdez and K.J. McClellan (2014), "Overview of properties and performance of uranium-silicide compounds for LWR applications, transactions", *American Nuclear Society*, Vol. 110 (2014), 987-989.

18. TRISO-SiC-composite pellets

The tri-structural isotropic (TRISO) particle fuel, historically developed within various high-temperature gas-cooled reactor (HTGR) programmes, shows excellent performances in gaseous fission products (FPs) retention capability through the presence of multiple layers of ceramic coating, which are chemically stable and mechanically strong at very high temperature and very high burn-up.

TRISO fuel particles consist of fissile material-bearing kernels that are coated with multiple layers of porous or dense C and SiC (Nickel et al., 2002). These particles are embedded within a graphite matrix and constitute the fuel in HTGRs.

The TRISO-SiC-composite pellet concept aims at applying the TRISO particle fuel technology to light water reactors (LWRs). The philosophy of radionuclide containment during operational states and accident conditions is fundamentally different between HTGRs and LWRs. While the latter relies heavily on the fuel cladding, reactor pressure vessel and containment, the HTGR fuel is designed with inherent barriers to radionuclide release under normal and postulated accident conditions (Hanson, 2004). Each fuel particle relies on its own pressure vessel, in the form of a SiC coating layer, to retain FPs. Application of this reliable fuel form, the coated fuel particle, is the motivation for development and deployment of TRISO-SiC-composite fuel for LWRs or other advanced fission platforms (Snead et al., 2011; Terrani, Snead and Gehin, 2012). However, in the TRISO-SiC-composite fuel concept, TRISO particles are embedded inside a SiC matrix rather than a graphite matrix to provide dimensional and environmental stability necessary for the LWR operating conditions. SiC is considered as a promising material for nuclear application especially due to its high-temperature (HT) strength, high-thermal conductivity and stability under neutron irradiation. If utilised in an LWR, TRISO-SiC-composite pellets will be contained inside a metal or ceramic cladding. For an HTGR application, they can be directly stacked inside the graphite moderator (Powers et al., 2013).

Figure 18.1. TRISO-SiC-composite fuel concept
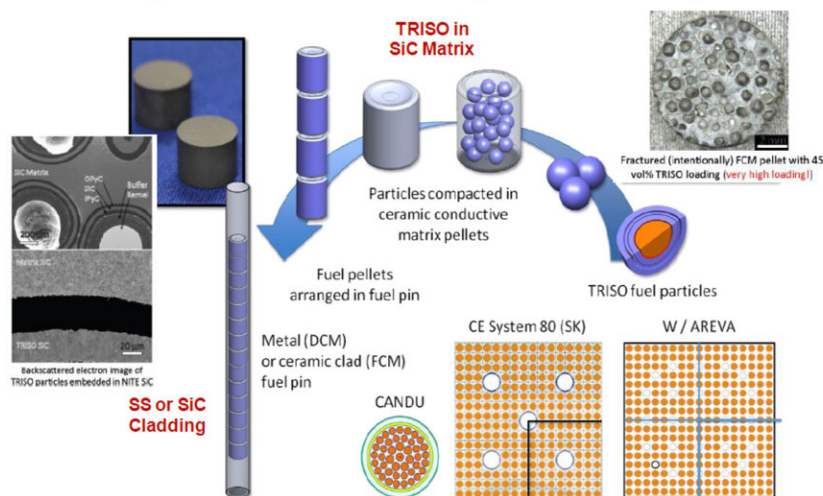
Source: Powers et al., 2013.

The TRISO-SiC-composite fuel is generally called a fully ceramic microencapsulated (FCM) fuel. This fuel is also called a particle-based accident tolerance (PBAT) fuel in Korea and an inert matrix dispersion pellets (IMDP) fuel in China.

The TRISO-SiC fuel is conceived as a promising medium-term concept to replace current UO_2 fuel pellets. It has potentially superior safety characteristics relative to other fuel forms as a result of its multiple barriers to FP dispersion, high mechanical stability and good thermal conductivity. However, the low fissile density caused by the presence of these barriers in the fuel needs to be compensated by appropriate fuel and core design. Additionally, the neutronic and thermal-hydraulic compatibility with existing LWR cores should be verified for practical application.

In the United States, this fuel concept has enjoyed nearly seven years of active R&D focused on development and fabrication (Terrani et al., 2012; Terrani et al., 2015), surrogate neutron irradiation testing (Snead et al., 2014) and system-level analysis (Gentry et al., 2014; George et al., 2014). Overall production steps and key attributes of this fuel form are summarised below.

Higher thermal conductivity and multiple barriers (TRISO and SiC matrix) for FPs release are the main benefits of TRISO-SiC pellet.

TRISO-SiC-composite fuel form is designed with multiple barriers to FPs release with the aim of near full retention during normal operation, postulated accidents, and even design extension conditions. Although a full irradiation testing of this fuel form is lacking to date, many separate-effects tests have been conducted to confirm the efficacy of this design. Some of these tests are summarised in the following sub-sections. Irradiation testing of FCM fuel under prototypical LWR conditions is planned under the US DOE programme in the upcoming years.

A low fissile material loading density is the major issue for this concept. In order to increase the fissile loading, the combination of uranium enrichment up to the practical upper limit of LEU (~19.7% of U^{235}), utilisation of high-density UN kernel, increasing kernel-to-particle volume fraction and TRISO-packing fraction, and enlarging fuel pin diameter was proposed.

International collaboration was carried out to assess the feasibility of replacing the current fuel of the existing fleet of LWRs with FCM fuel (Powers et al., 2013; Lee et al., 2014). Table 18.1 shows the TRISO-SiC fuel assembly design parameters for the Korean standard power reactor, OPR-1000. In order to compensate for the uranium loading reduction and to meet current fuel cycle requirements, this fuel assembly uses enriched UN kernels as fissile materials. The clad has larger diameter and thinner thickness than the reference rod in order to increase the uranium loading. FeCrAl is considered as fuel cladding because this alloy has higher mechanical strength than Zr tube. However, the FeCrAl clad design needs to compensate the neutron penalty in comparison to the Zry-based clad design.

Table 18.1. Optimised design parameters of TRISO-SiC fuel assembly for OPR-1000

	Item	Unit	16x16-Ref.	16x16-FCA
	Assembly Pitch	cm	20.78	←
	Cell Pitch	cm	1.285	1.285
TRISO Coated Particle	Fuel Material / Enrichment		UO₂ / < 5%	UN / < 20%
	Fuel Density	g/cc	10.176	14.32
	Fuel Kernel Diameter	μm	-	800
	Buffer Layer	μm	-	50
	Inner PyC Coating Layer	μm	-	35
	SiC Coating Layer	μm	-	35
	Outer PyC Coating Layer	μm	-	20
Fuel Rod	Pellet/Compact Material		UO₂	TRISO/SiC Matrix
	Pellet/Compact Density	g/cc	10.176	3.18
	Pellet/Compact Radius	cm	0.4095	0.4541
	TRISO Packing Fraction	%	-	45
	Clad Material		Zry-4	FeCrAl
	Clad Density	g/cc	6.55	7.10
	Clad Inner Radius	cm	0.4180	0.4626
	Clad Outer Radius	cm	0.4750	0.5000
	Clad Thickness	cm	0.0570	0.0374
	Gap Thickness	cm	0.0085	←
	Rod to Rod Spacing	cm	0.3350	0.2850
	Heavy Metal Loading, 1/4	g/cm	279.0	94.5

Source: Powers et al., 2013.

Fabrication/manoeuvrability

The advanced fuels campaign of the US DOE has been engaged in process development to produce FCM fuel in the past few years. FCM fuel production is carried out as a serial process, outlined in Figure 18.2. Kernel production, TRISO production and compact production constitute the three major steps during fuel fabrication.

Figure 18.2. Serial process for established FCM fuel production

Source: Terrani et al., 2012.
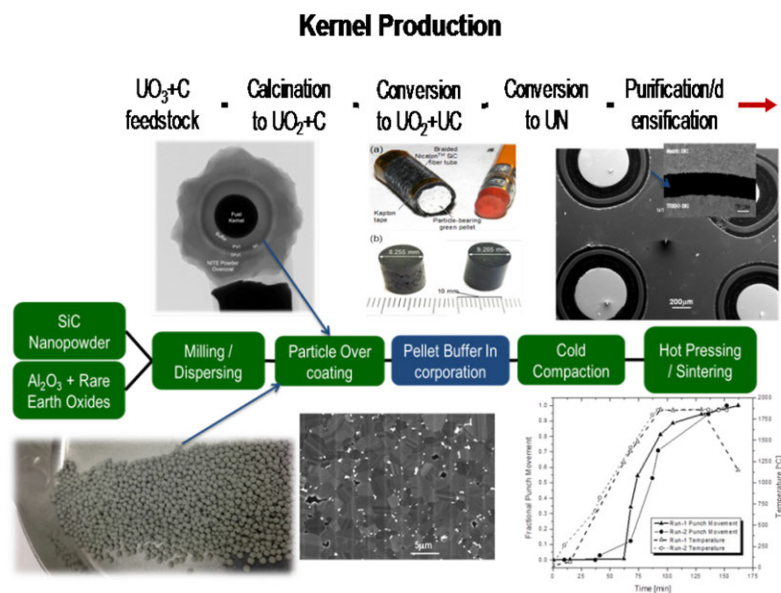
Fuel kernel production

For an efficient LWR core fuelled with FCM fuel bundles, significantly higher heavy metal (HM) densities are required compared to the fuel in a typical HTGR (George et al., 2014). This is also accompanied by an increase in required enrichment for LWR fuel; i.e. instead of ~5% for current oxide pellets in LWRs, ~15% ^{235}U is needed in LWR FCM pellets. High packing fractions of TRISO particles in the fuel matrix, large kernel-to-particle volume ratios and higher density kernels are all desired for the LWR application of FCM fuel. Pertaining to the latter, for the FCM fuel concept, the UO_2 or UO_2+UC_x kernels used in HTGRs are replaced with a uranium carbonitride U(C,N) kernel instead (Lindemer et al., 2017; Lindemer et al., 2014). This compound is essentially a solid solution of UC and UN with the latter being prevalent in the mixture. By utilising this compound instead of uranium dioxide, a ~40% increase in U density is obtained.

The UO_2+UC_x kernel production methodology is leveraged for production of U(C,N) kernels with a final step added at the end of the process. This step is carbothermic reduction to remove C and O and replace them with N and it takes place in a flowing nitrogen gas atmosphere to convert the two-phase mixture into U(C,N). This process occurs at temperatures >1 700°C and is sensitive to gas flow conditions (i.e. may be mass transport limited since CO product needs to be continuously removed from the system).

Figure 18.3. Optical micrograph of ~0.8 mm-diameter U(C,N) kernels with ~90% theoretical density after conversion
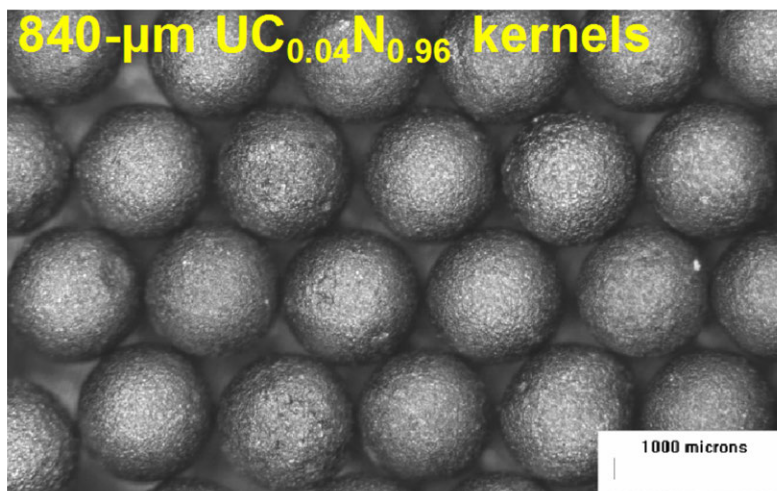
Source: Lindemer et al., 2017.

TRISO production

Once fuel kernels are produced, a fluidised bed chemical vapour deposition (FB-CVD) process is utilised to deposit the various coating layers and produce the TRISO fuel particles. This process uses propylene, acetylene and methyl trichlorosilane (MTS) as reactant gases to deposit the various coating layers yielding carbon buffer layer, dense pyrocarbon layers and the SiC coating layer. While the overall process is the same, once kernel size, kernel chemistry, or coating chamber size is varied, extensive changes in the process parameters may be necessary in order to produce the same quality coating layers.

TRISO-SiC pellet consolidation

Once TRISO fuel particles are available, they need to be encapsulated inside a dense SiC matrix to produce the FCM fuel form. The SiC matrix differs from the high-purity CVD-

SiC variant that forms the coating layer of the TRISO particles. It is formed via a liquid phase sintering (LPS) process that utilises the addition of oxides (alumina + rare-earth oxides) as sintering additives.

Once added in less than 10 wt%, these oxides undergo a eutectic reaction to form a liquid phase at temperatures below the onset of significant creep and grain growth in SiC (1 800°C) and facilitate the densification of SiC (Terrani et al., 2012). In this manner, the matrix is densified without damaging the SiC coating layer of the TRISO fuel particle. Once an appropriate mixture of SiC powder with oxide additives is prepared, it is used to overcoat the TRISO fuel particles. The specifics of the overcoating process are similar to the process used for graphite matrix fuel for HTGRs, as described in the literature (Pappano et al., 2008). In CGN, the TRISO particles were over coated by wet method, so each particle gets a powder shell with uniform thickness. The overcoated particles may then be pressed and densified via a hot pressing or direct current sintering process.

Figure 18.4. The over coated TRISO particles (by CGN)
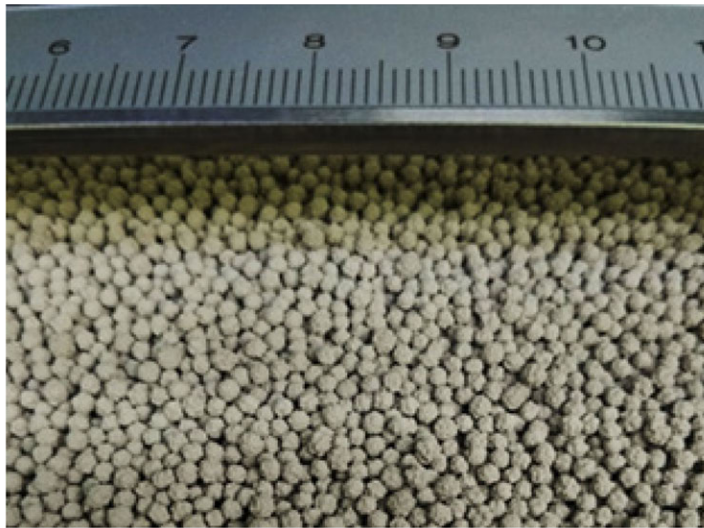
Source: Ma, Huang and Li, 2017.

Kepco Nuclear Fuel Company (KepcoNF) is developing advanced pellet manufacturing routes (Kim et al., 2016). The hot press technique is being applied to fabricate dense TRISO-SiC pellets (Terrani, Snead and Gehin, 2012). However, this technique may not be suitable for mass production. KepcoNF focused on the pressure-less sintering process to enable engineering-scale production of composite pellets. During the consolidation stage of the pressure-less sintering of TRISO embedded SiC pellets, the large difference of shrinkage rate between TRISO and SiC matrix leads to the formation of cracks at the interface between TRISO and SiC matrix. By adding newly developed additives that form liquid phase below the sintering temperature in matrix, and providing interlayer between TRISO and matrix, crack free pellets that have 25% of TRISO-packing fraction were successfully fabricated. The TRISO-SiC pellets with new additives show good oxidation behaviour under hydrothermal exposure condition. The fabrication process to increase the packing ratio of TRISO particles to the target value of 45 vol% is being studied in KepcoNF.

Figure 18.5. Optical photo and SEM microstructure of PBAT fuel pellet fabricated by pressure-less sintering process (by KepcoNF)

Source: Ma, Huang and Li, 2017.

China general nuclear power group (CGN) has developed its own technology to fabricate the IMDP, a mix of TRISO and inert materials. The over coated TRISO particles were pressed to be green pellets by one step forming technology and sintered in 1 800°C-1 900°C by hot pressing with 10 to 20 MPa. The IMDP has a fuel zone and a non-fuel buffer layer on the surface of these pellets, as shown in Figure 18.6.

Figure 18.6. SEM and CT photo of IMDP (by CGN)
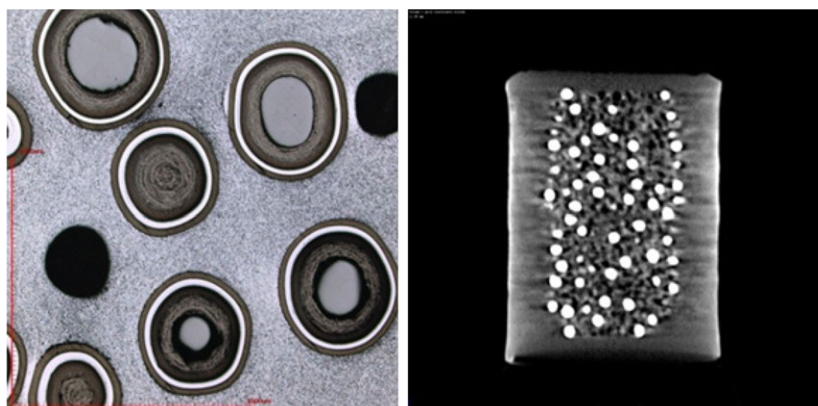
Source: Ma, Huang and Li, 2017.

Fabrication cost of TRISO-SiC fuel will be increased because of the chemical process for enriched UN kernel and TRISO and packing and hot press sintering process for composite pellet fabrication. Engineering-scale production should be demonstrated.

Normal operation and AOOs

FCM fuel form with surrogate TRISO fuel particles in a SiC matrix was neutron-irradiated to a dose of ~8 dpa (Snead et al., 2014). Surrogate particles (TRISO particles with a ZrO_2 kernel instead of a U-bearing material) facilitated out-of-cell post-irradiation examination.

The purpose of this test was to confirm the irradiation stability of the SiC matrix of this fuel form and to ensure no detrimental interaction occurred between the fuel particles and the matrix. As shown in Figure 18.7, no detrimental interaction between the matrix and the coating layers of the TRISO particle was observed. Furthermore, the coating layers did not debond from the matrix, ensuring that a robust path for heat transfer remains. The formation of gaps between coating layers will reduce the effective thermal conductivity of TRISO. Swelling of SiC matrix saturates at a few percent and it is much smaller than swelling for UO_2. SiC thermal conductivity degrades under neutron irradiation and saturates as a function of dose but is still better than UO_2 fuel.

Figure 18.7. X-ray tomography image of surrogate TRISO particle inside the SiC matrix of FCM fuel after neutron irradiation in the HFIR to ~8 dpa in the SiC matrix
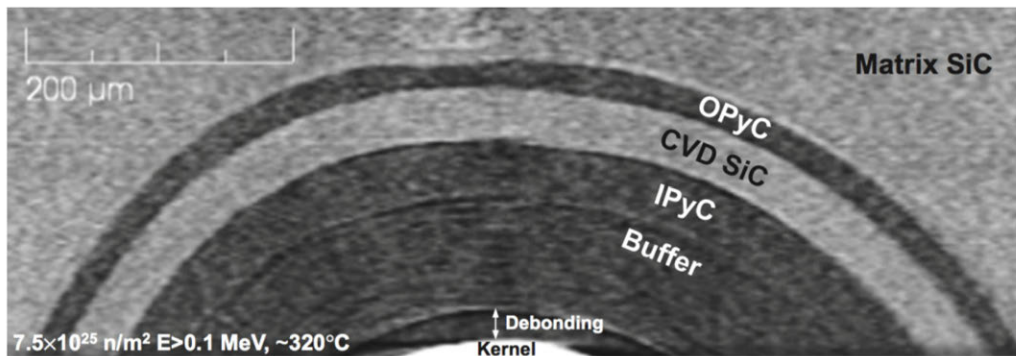
Source: Snead et al., 2014.

Corrosion of FCM fuel form in LWR coolant environments needs to be considered. In recent years, hydrothermal corrosion of high-purity SiC in these environments has received ample attention and is shown to be considerable if exposed continuously to water chemistry conditions with large dissolved oxygen contents (Ma, Huang and Li, 2017a; Ma, Huang and Li, 2017b; Carpenter, 2010). The corrosion rate of sintered SiC, constituting the matrix of the FCM fuel, is shown to be significantly (~100 x) higher than the high-purity CVD variants (Kondo et al., 2015). This implies that FCM fuel form should be clad in LWRs. The additives to enable low-pressure or pressure-less sintering can have negative effects on the steam corrosion of composite pellets.

Fuel failure (i.e. radionuclide release) mechanism is fundamentally different than the current UO_2–Zr-based cladding system. Release, if it is to occur, will take place from individual particles inside individual pellets. This is in contrast to the current fuel for which any breach in the cladding will expose the entire inventory of radionuclides in the rod to the potential for release.

The CVD-SiC matrix with high purity and density shows extremely high-thermal conductivity. Figure 18.8 shows the thermal conductivity of unirradiated IMDP with 36 vol% of TRISO and CVD-SiC matrix. In TRISO-SiC-composite pellet, however, thermal conductivity is reduced largely because of the nano-SiC structure with additives (Terrani et al., 2015). Irradiation forms defects in the matrix and causes further degradation of thermal conductivity. Nevertheless, it was estimated that thermal conductivity of composite pellets will be saturated to approximately 10 W/m K, still higher than commercial UO_2 pellets.

Figure 18.8. Thermal conductivity of IMDP with 36 vol% TRISO (by CGN)
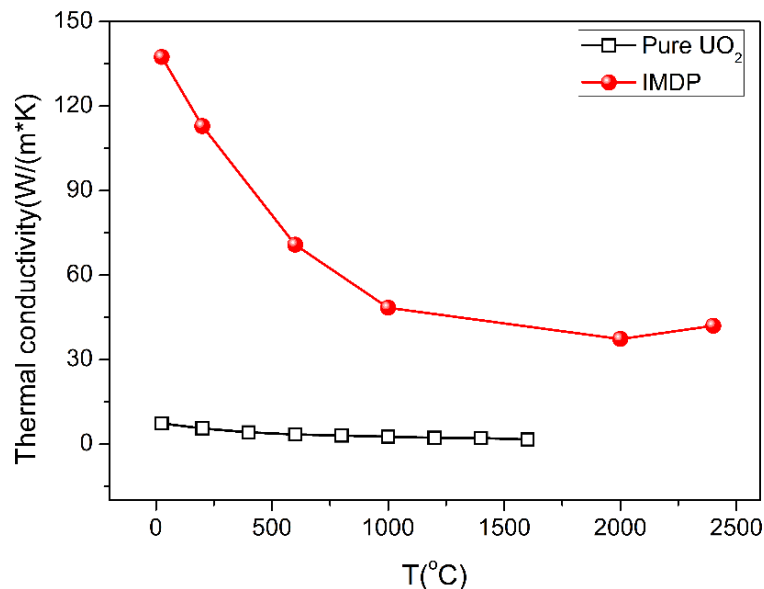
Source: Ma, Huang and Li, 2017.

The FCM fuel form involves higher uranium costs and fabrication costs. These costs are discussed (Terrani, Snead and Gehin, 2012) and can vary from at least 25% higher to over twice the cost of the current fuel system.

Neutronic calculation showed that FCM rods generally exhibit larger reactivity at the BOL and a faster rate of decrease in reactivity. Therefore, sophisticated neutronic design might be necessary. The addition of poison is necessary to manage reactivity swings in the fuel.

DBAs and DECs

The combination of multiple barriers to FP release and slow kinetic of the SiC reaction with high-temperature steam may provide larger margins of safety under DBAs and DECs.

CVD-SiC exhibits exceptional oxidation resistance in HT steam environments (Opila, Hann, 1997; Pint et al., 2012; Terrani et al., 2014). The SiC matrix of FCM fuel exhibits similar behaviour and is quite resistant to steam oxidation (Hinoki et al., 2016). Furthermore, the SiC coating layer in the TRISO particles, in addition to being a robust barrier to transport of most radionuclides, is also an effective layer to inhibit steam ingress into the coated fuel particles. This is shown in Figure 18.9, where after exposure to HT air and steam for a duration of many hours, only a small fraction of the SiC coating layer has been consumed to produce a protective silica layer. Exceptional steam oxidation resistance of SiC-based materials, coupled with the discrete nature of fuel particles and their inherent protective layer – the SiC coating shell – designates FCM fuel as a robust accident-tolerant fuel form.

The liquid phase sintered SiC matrix of PBAT fuel showed that HT oxidation resistance depends on the additive content and the chemistry of the additive composition. The grain boundary structure has a significant impact on the oxidation protection during hydrothermal exposure (Lim et al., 2016).

Figure 18.9. SiC coating layer of TRISO particle exposed to high-temperature oxidising environments representative of LWR severe accidents
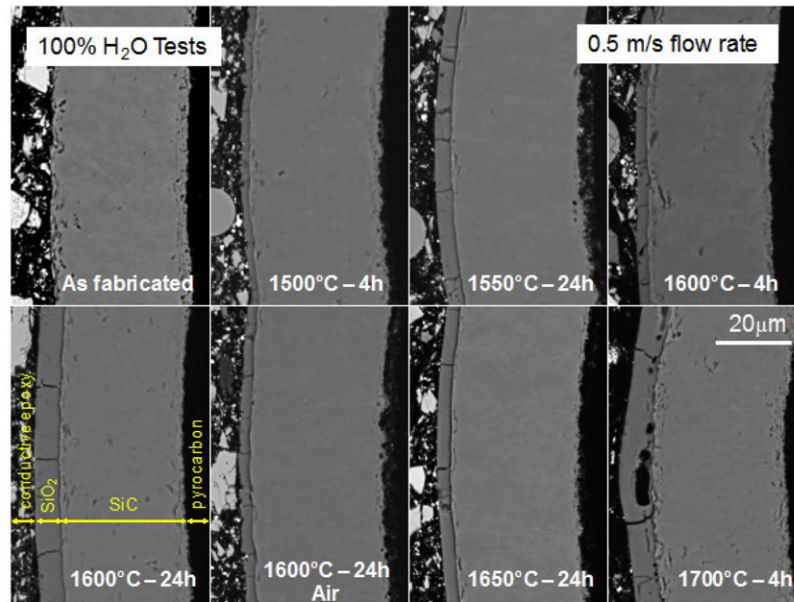
Source: Terrani, Silva, 2015.

By using the optimised TRISO-SiC fuel assembly design (FCM+FeCrAl rod, see Table 18.1) for OPR-1000, the safety margin has been assessed. In LB-LOCA, the optimised core reduces both the peak cladding temperature and the quench time of the fuel rod.

LB-LOCA is the main design-basis accident for CPR-1000 operated by CGN. A hypothetical double-ended guillotine break in a cold leg pipe was considered. The safety injection system of CPR-1000 consists of two trains of high-pressure safety injection (HPSI) and two trains of low-pressure safety injection (LPSI). In this study, a single failure of the diesel generator was considered. Thus, only one HPSI and one LPSI were activated. The major parameter of concern is the peak cladding temperature of the hottest fuel rod (see Figure 18.10). This picture is from the report of CGN (Ott, Robb and Wang, 2014; the source data is from [Liu, 2015]).

Very limited data exists with respect to the fuel behaviour and failure mechanism of TRISO-SiC fuel under postulated DEC conditions. Calculation results carried for OPR-1000 showed that FCM+FeCrAl core allows longer coping time under the SBO and LB-LOCA without safety injection when compared with those of a reference UO_2 core.

The SBO accident is an accident caused by the loss of all available electric power, including off-site power, emergency diesel power and alternative AC power. The reactor, turbine, reactor coolant pump and main feedwater are cut off because of the loss of off-site power. In an SBO accident, the loss of heat sink and coolant due to the opening of the pressuriser safety valve will rapidly increase the peak cladding temperature to failure levels (see Figure 18.11). This picture refers to (Sonat Sen, Broer, Bess, Pope and Ougouag, 2012; Xie, 2015).

Figure 18.10. Peak cladding temperature of ATFs during LB-LOCA (by CGN)
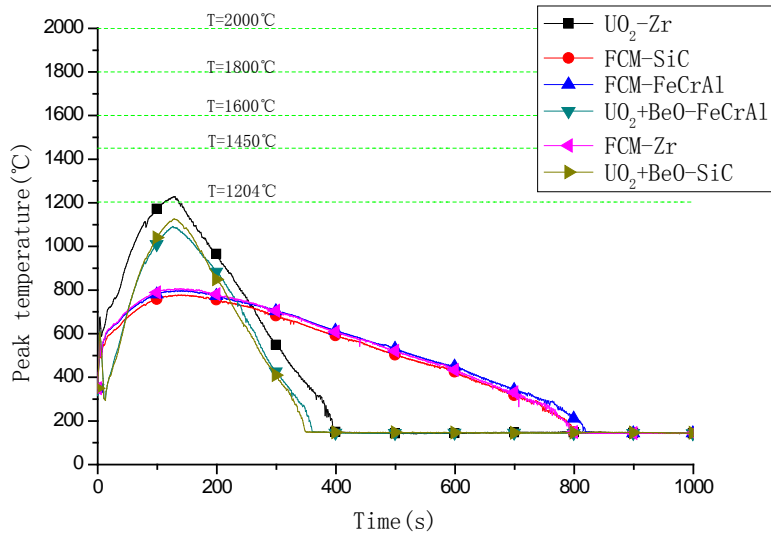
Source: Ott, Robb and Wang, 2014; Liu, 2015.

Figure 18.11. Peak cladding temperature of ATFs during SBO condition (by CGN)
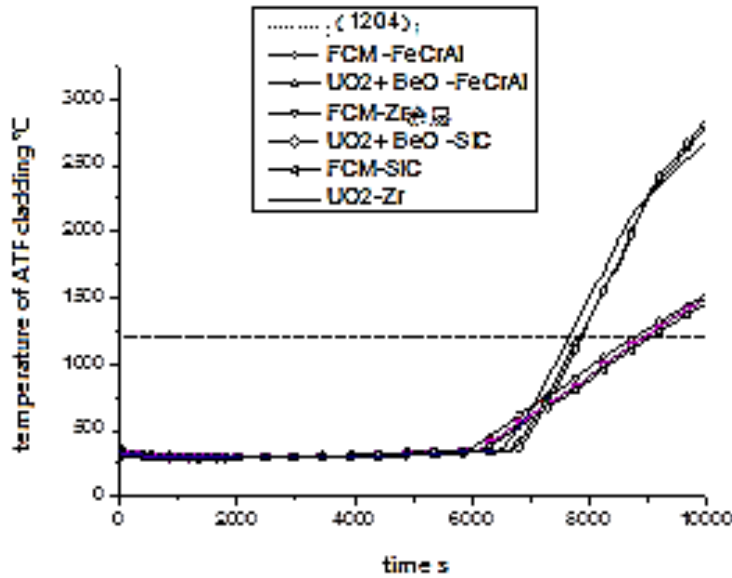
Source: Sonat Sen, Broer, Bess, Pope and Ougouag, 2012; Xie, 2015.

Used fuel storage/transport/disposition/reprocessing

No problem is anticipated for long-term storage of spent TRISO-SiC considering the very high-dimensional, microstructural and chemical stability.

TRISO-SiC is a repository ready fuel form and reprocessing would not be an option for this fuel cycle.

References

Carpenter, D.M. (2010), *An Assessment of Silicon Carbide as a Cladding Material for LWRs*, Massachusetts Institute of Technology.

Gentry, C. et al. (2014), "A neutronic investigation of the use of fully ceramic microencapsulated fuel for Pu/Np burning in PWRs", *Nucl. Technol.*, Vol. 186, doi:10.13182/nt13-75.

George, N.M. et al. (2014), "Neutronics studies of uranium-bearing fully ceramic microencapsulated fuel for pressurized water reactors", *Nucl. Technol.*, Vol. 188, doi:10.13182/NT14-3.

Hanson, D.L. (2004), *A Review of Radionuclide Release from HTGR Cores during Normal Operation*, Report 1009382, Electric Power Research Institute.

Hinoki, T. et al. (2016), *Effect of Constituents of Silicon Carbide Composites on Oxidation Behaviour*, IAEA-TECDOC Ser. (2016) 314.

Kim, Y.W. et al. (2016), *Low Temperature Pressure-less Sintering of Silicon Carbide Matrix for Fully Ceramic Microencapsulated Fuels*, ICAA, 26 January 2016.

Kondo, S. et al. (2015), "Effect of irradiation damage on hydrothermal corrosion of SiC", *J. Nucl. Mater.*, Vol. 464, pp. 36-42.

Lee, W.J. et al. (2014), "Feasibility of fully ceramic microencapsulated (FCM) replacement fuel assembly for OPR-1000 core", *19th Pacific Basin Nuclear Conference*, 24-28 August 2014, Vancouver.

Lim, K.-Y. et al. (2016), "Effect of additive composition on high temperature oxidation resistance of pressure-less sintered SiC ceramics for particle-based accident tolerance fuel", *KNS Spring Meeting*, 2016.

Lim, K.-Y. et al. (2015), "Effect of liquid phase content on thermal conductivity of hot-pressed silicon carbide ceramics", *KNS Spring Meeting*, 8 May 2015.

Lindemer, T.B. et al. (2017), "Quantification of process variables for carbothermic synthesis of UC1-xNx fuel microspheres", *J. Nucl. Mater.* Vol. 483, pp. 176-191.

Lindemer, T.B. et al. (2014), "Carbothermic synthesis of 820 µm uranium nitride kernels: Literature review, thermodynamics, analysis, and related experiments", *J. Nucl. Mater.* Vol. 448, pp. 404-411, doi:10.1016/j.jnucmat.2013.10.036.

Liu, P.P. (2015), *Preliminary Assessment of Accident-tolerant Fuels on LWR Performance during Station Blackout Severe Accident Condition*, Internal file of CGN, 17 December 2015, CNPRI-CM-F11-15REC003-005.

Ma, Z.D., H.W. Huang and R. Li (2017a), *Manufacturing Technique Report of Inert Matrix Dispersion Pellet*, Internal file of CGN, 29 March 2017, TF15AM-RL-TR-000070.

Ma, Z.D., H.W. Huang and R. Li (2017b), *Performance Analysis Report of Inert Matrix Dispersion Pellet*, Internal file of CGN, 29 March 2017, TF15AM-RL-TR-000069.

Nickel, H. et al. (2002), "Long time experience with the development of HTR fuel elements in Germany", *Nucl. Eng. Des.*, Vol. 217, pp. 141-151.

Opila, E.J. and R.E. Hann (1997), "Paralinear oxidation of CVD-SiC in water vapor", *J. Am. Ceram. Soc.*, Vol. 80, pp. 197-205.

Ott, L.J., K.R. Robb and D. Wang (2014), "Preliminary assessment of accident-tolerant fuels on LWR performance during normal operation and under DB and BDB accident conditions", *Journal of Nuclear Materials*, Vol. 448(1), pp. 520-533.

Pappano, P.J. et al. (2008), "A novel approach to fabricating fuel compacts for the next generation nuclear plant (NGNP)", *J. Nucl. Mater.,* Vol. 381, pp. 25-38, doi:10.1016/j.jnucmat.2008.07.032.

Parish, C.M. et al. (2017), "Microstructure and hydrothermal corrosion behavior of NITE-SiC with various sintering additives in LWR coolant environments", *J. Eur. Ceram. Soc.* Vol. 37, pp. 1261-1279.

Pint, B.A. et al. (2012), "High temperature oxidation of fuel cladding candidate materials in steam-hydrogen environments", *Proc. 8th Int. Symp. High Temp. Corros. Prot. Mater. Les Embiez.*

Powers, J.J. et al. (2013), *Fully Ceramic Microencapsulated (FCM) Replacement Fuel for LWRs,* KAERI/TR-5136/2013, ORNL/TM-2013/173.

Snead, L.L. et al. (2011), "Fully ceramic microencapsulated fuels: A transformational technology for present and next generation reactors – Properties and fabrication of FCM fuel, *Trans. Am. Nucl. Soc.,* Vol. 104.

Snead, L.L. et al. (2014), "Stability of SiC matrix microencapsulated fuel constituents at relevant LWR conditions", *J. Nucl. Mater.,* Vol. 448, pp. 389-398. doi:10.1016/ j.jnucmat. 2013.09. 056.

Sonat Sen, R. et al. (2012), *Advanced Fuels for LWRs: Fully-Ceramic Microencapsulated and Related Concepts,* Interim Report. 10.2172/1042368.

Terrani, K.A. et al. (2014), "Silicon carbide oxidation in steam up to 2 MPa", *J. Am. Ceram. Soc.* Vol. 97, pp. 2331-2352, doi:10.1111/jace.13094.

Terrani, K.A., C.M. Silva (2015), "High temperature steam oxidation of SiC coating layer of TRISO fuel particles", *J. Nucl. Mater.,* Vol. 460, pp. 160-165, doi:10.1016/j. jnucmat.2015.02.022.

Terrani, K.A. et al. (2012), "Fabrication and characterization of fully ceramic microencapsulated fuels", *J. Nucl. Mater.,* Vol. 426, pp. 268-276. doi:10.1016/j. jnucmat.2012.03.049.

Terrani, K.A. et al. (2015), "Progress on matrix SiC processing and properties for fully ceramic microencapsulated fuel form", *J. Nucl. Mater.,* Vol. 457, pp. 9-17. doi:10.1016/j.jnucmat.2014.10.034.

Terrani, K.A., L.L. Snead and J.C. Gehin (2012), "Microencapsulated fuel technology for commercial light water and advanced reactor application", *J. Nucl. Mater.,* Vol. 427, pp. 209-224. doi:10.1016/j.jnucmat.2012.05.021.

Terrani, K.A. et al. (2015), "Hydrothermal corrosion of SiC in LWR coolant environments in the absence of irradiation", *J. Nucl. Mater.,* Vol. 465, pp. 488-498. doi:10.1016/ j.jnucmat. 2015.06. 019.

Xie, X.F. (2015), *Preliminary Assessment of Accident-tolerant Fuels on LWR Performance during Large Break LOCA Condition,* Internal file of CGN, 17 December 2015, CNPRI- CM-F11-15REC003-004.

Part IV: Technology readiness level evaluation

19. Technology readiness level evaluation

The aim of this chapter is to evaluate the technology readiness level (TRL) of each accident-tolerant fuel (ATF) cladding, non-fuel component and advanced fuel concept presented in the previous chapters, referring to the general definition of TRLs provided in Chapter 5 of this report (recalled here in Table 19.1).

In the first step of this evaluation, specific definitions of TRLs for the following four categories have been carefully and collaboratively discussed in TF2 and TF3, as indicated in Table 19.2, also by referring to general references (Carmack, 2014; Kurata, 2016) on TRLs:

- irradiation;

- fabrication;

- safety for normal operation and anticipated operational occurrence (AOO);

- safety for off-normal conditions (design-basis accident [DBA] and design extension condition [DEC]).

In the discussion about the specific definitions, the following consensus has been reached on the relation between irradiation status and TRL:

- (TRL-3) sample/material irradiation, aiming at validation of the advanced concept, based on Labo-scale data, in a research reactor. "Proof-of-concept" stage is achieved after this level of irradiation;

- (TRL-4) prototype fuel irradiation, aiming at verification of the prototype fuel design, using a short length fuel rod or segment, in a research reactor;

- (TRL-5) lead test rod (LTR) irradiation, aiming at verification of a commercially used fuel design, using a full-length or enough length fuel rod manufactured by an industrial or equivalent process, in a commercial reactor;

- (TRL-6) LTA irradiation, aiming at verification of a commercially used fuel assembly manufactured by an industrial or equivalent process, in a commercial reactor. "Proof-of-principle" stage is achieved after this level of irradiation;

- (TRL-7) LUA irradiation, aiming at final confirmation of a commercially used fuel assembly manufactured in a commercial plant, in a commercial reactor.

Table 19.1. Summary of TRL definitions for advanced nuclear fuels and cladding technologies

TRL	Function	Definition
1	Proof-of-Concept	A new concept is proposed. Technical options for the concept are identified and relevant literature data reviewed. Criteria are developed.
2		Technical options are ranked. Performance range and fabrication process parametric ranges are defined based on analysis.
3		Concepts are verified through laboratory-scale experiments and characterisation. Fabrication process is verified using surrogates.
4	Proof-of-Principle	Fabrication of small samples (rodlets) at bench-scale. Irradiation testing of rodlets in a relevant environment. Design parameters and features are established. Basic properties are compiled.
5		Fabrication of full-length rods using prototypic materials at laboratory scale. Rod-scale irradiation testing in a relevant environment (test reactor). Primary performance parameters with representative compositions under normal operating conditions are quantified. Fuel compositions under normal operating conditions are quantified. Fuel behaviour models are developed for use in fuel performance code(s).
6		Fabrication of rods using prototypic materials at laboratory scale and using prototypic fabrication processes. Rod-scale irradiation testing at relevant (test reactor) and prototypic (commercial LWR) environment (steady-state and transient testing).[a] Predictive fuel performance code(s) and safety basis are established.
7	Proof-of-Performance	Fabrication of test assemblies using prototypic materials at engineering-scale and using prototypic fabrication processes. Assembly-scale irradiation testing in prototypic (commercial LWR) environment.[b] Predictive fuel performance code(s) are validated. Safety basis established for full-core operations.
8		Fabrication of a few core-loads of fuel and operation of a commercial reactor with such fuel.
9		Routine commercial-scale operations. Multiple reactors operating.

[a] Initial rods irradiated in a commercial LWR are referred to as "LFR".

[b] Initial assemblies irradiated in a commercial LWR are referred to as "LFA" or "LUA".

Table 19.2. Specific definition of TRL for advanced fuels and cladding technologies

TRL	Irradiation	Fabrication	Safety for normal operation and AOO	Safety for off-normal conditions (DBA and DEC)
1	Proposal of new fuel concept, literature survey, identification of attributes, evaluation of potential benefit.	Proposal of new fabrication process, literature survey, evaluation of potential benefit.	Literature survey, primary evaluation of safety.	Literature survey, primary evaluation of safety.
2	Databasing, extraction of R&D subjects, evaluation of upper limit of R&D target, survey of option technologies.	Databasing, extraction of R&D subjects, evaluation of upper limit of R&D target, survey of option technologies.	Databasing, extraction of R&D subjects.	Databasing, extraction of R&D subjects.
3	Sample irradiation test, establishment of database, improvement of fuel performance code.	Fabrication of samples, targeting of R&D objects for industrial scale fuel manufacturing.	Prioritisation of R&D subjects, targeting of R&D objects for commercial plant operation.	Prioritisation of R&D subjects, targeting of R&D objects for commercial plant safety analysis.
4	Irradiation test of prototype fuel cladding.	Fabrication of full (long) scale fuel rod, establishment of quality assurance technology.	Improvement of neutronics/core/hydro-thermic analysis code.	LOCA/RIA simulation test using non-irradiated specimens.
5	Irradiation of LTR, out-of-pile tests for prototype fuel.	Fabrication of LTR, industrial scale unit test.	Analysis of commercial plant characteristics.	Establishment of SA analysis method, LOCA/RIA simulation test using irradiated specimens.
6	Irradiation test of LTA, validation of fuel performance code, establishment of fuel design.	Fabrication of LTA, establishment of manufacturing process, control/monitoring technology.	Establishment of reactor physics and plant operation code.	Establishment of criteria on DBA and DEC for LTA.
7	Irradiation test of LUA.	Fabrication of LUA.	Establishment of static and dynamic characteristics of plant.	Establishment of safety analysis.
8	Full loading in commercial LWRs.	Mass production of commercial fuel assembly.	Validation of reactor physics & plant performance.	Establishment of safety analysis for commercial LWRs.
9	Commercial operation in LWRs.	Commercial operation of fuel manufacturing plant.	Commercial operation of LWRs.	Commercial operation of LWRs.

Evaluation results

Table 19.3(a) summarises the evaluation result of TRL for ATF claddings and non-fuel core components. In this table, for example, "3" means TRL-3 is achieved and "3-4" means TRL3 is achieved and TRL4 is ongoing. Tables 19.3(b), 19.3(c) and 19.3(d) summarise the evaluation results for advanced fuel concepts. Observing these tables, the following tendencies are clarified:

- Coated and improved Zry concepts for ATF cladding have mostly accomplished the "proof-of-concept" stage and the R&D for "proof-of-principle" stage is ongoing. Regarding fabrication, in particular, fabrication of LTRs and industrial scale unit tests (TRL-5) have started.

- Advanced steel concept for ATF cladding has also mostly accomplished the "proof-of-concept" stage and the R&D for "proof-of-principle" stage has started.

- Regarding revolutionary ATF-cladding concepts, such as refractory metal (use of Mo) and SiC/SiC composites, the R&D for TRL-3 is mostly ongoing.

- Non-fuel core components are mostly in TRL3.

- Some concepts of oxide-doped UO_2 are already mostly in commercial level, although data acquisition for accidental condition is still necessary.

- Microcell concept of SiO_2 oxide-doped UO_2 and metallic and BeO additive concepts of high-thermal conductivity UO_2 have mostly accomplished the "proof-of-concept" stage.

- Other revolutionary advanced fuel concepts, such as SiC/diamond additive, high-thermal conductivity UO_2, high-density fuels and encapsulated fuel, are still in the "proof-of-concept" stage.

Table 19.3(a). TRL evaluation result for ATF cladding and non-fuel core component

Category	Coated and Improved Zr alloys		Advanced steels: FeCrAl	Lined Mo alloy	SiC/SiC composite	SiC channel box	ATCR
	Cr-coated (semi-industrial PVD) – cold spray to be specified	CrN-coated (commercial PVD)					
Irradiation	3-4	4	3-4	2-3	2-3	3-4	3
Fabrication	4-5	4-5	3	3	3	3	3
Safety for normal operation and AOO	4	3-4	4	3-4	2-3	3	3
Safety for off-normal conditions (DBA, DEC)	4	3	4	3	3	3	3

Table 19.3(b). TRL evaluation result for oxide-doped UO₂ concepts

Category	Cr₂O₃-doped or Cr₂O₃-Al₂O₃-doped UO₂	SiO₂-based microcell UO₂ fuel
Irradiation	7-8 [#]	3-4
Fabrication	9 [#]	3
Safety for normal operation and AOO	9 [#]	3-4
Safety for off-normal conditions (DBA, DEC)	7-8 [#]	3-4

Although these fuels are considered on an industrial basis, some data under accidental conditions still need to be acquired when experimental means are operational (e.g. RIA testing).

Table 19.3(c). TRL evaluation result for high-thermal conductivity UO₂ concepts

Category	Metallic additive fuel Mo, Cr	Ceramic additive fuel BeO	Ceramic additive fuel Diamond or SiC wiskers
Irradiation	3-4	3-4	3
Fabrication	3	3	3
Safety for normal operation and AOO	3-4	3	2
Safety for off-normal conditions (DBA, DEC)	3-4	3 [#]	2

Some past experiences need to be performed again, taking into account current specifications, and need to be completed with integral tests.

**Table 19.3(d). TRL evaluation result for high-density fuel
and encapsulated fuel concepts**

Category	High density fuel					Encapsulated fuel
	Nitride	Silicide	Carbide	U-10Zr	U-50Zr[###]	TRISO-SiC
Irradiation [##]	3	2-3	3	2-3	2	2-3
Fabrication	3[#]	3	4	3	2	3
Safety for normal operation and AOO [##]	3	3	3	3	2	3
Safety for off-normal conditions (DBA, DEC) [##]	3	3	3	3	2	3

\# ^{15}N enrichment is an issue.

\#\# Irradiation data are available but not in LWR conditions.

\#\#\# These evaluations are based on publicly available data.

References

Carmack, J. (2014), *Technology Readiness Levels for Advanced Nuclear Fuels and Materials Development*, FCRD-FUEL-2014-000577, INL/EXT-14-31243, Idaho National Laboratory.

Kurata, M. (2016), "Research and development methodology for practical use of accident tolerant fuel in light water reactors", *Nucl. Eng. Technol.*, Vol. 48(1), pp. 26-32.

Part V: Cross-cutting issues between fuel and cladding

20. Allowed/not-allowed combinations of specific cladding and fuel technologies

Once the compilations on various cladding and various fuel designs became available, the next step was to consider the cross-cutting issues raised by the association of the different types of claddings with the different types of fuels. In the present report, the compatibility between claddings and fuels are discussed by comparing them to the ones involving conventional Zry-cladding and UO_2 fuel pellets.

Given the important number of potential combinations and the observation that data was lacking in many cases, using a colour code leaving room for qualitative assessments was the favoured option for synthetic information about the different combinations.

The same colour code as the one used for the attribute guides in Appendices A and B has been used, i.e.:

	properties not addressed; colour status not identified because of a lack of knowledge
	data available; results are good; concept is matured
	data available; results not good enough; further optimisation needed
	lack of data; not challenging
	lack of data and potentially challenging
	potential showstopper identified

The information is summarised in the following five tables, with Tables 20.1 to 20.4 each assessing the compatibility of a given type of cladding (coated and improved Zr, FeCrAl alloys, refractory metals, Sic-SiC/SiC) with all the different types of fuels. The compatibility of SiC channel boxes and accident-tolerant control rods (ATCRs) with conventional Zr-alloy claddings plus the four specific accident-tolerant fuel (ATF) cladding designs is also discussed in the last two sections of this chapter.

T stands for "temperature" in all the tables.

Four types of properties are represented in the tables (chemical, mechanical, neutronic, thermal).

Given that only green and orange colours express available data, the need for data gathering is one of the first very general conclusion illustrated by the tables, especially for cladding-fuel combinations involving fuel designs other than conventional UO_2 or oxide-doped UO_2.

Without detailing all the illustrated information, some general trends can be highlighted:

- high-density fuels lack data or need further optimisation, especially with regard to chemical and mechanical characteristics, whatever the cladding;

- neutronics is generally not an issue except that, compared to other cladding designs, FeCrAl alloys and refractory metals lead to a higher neutron absorption that calls for specific fuel adaptations except for high-density silicide, carbide and metal fuels;

- SiC/SiC&SiC claddings raise an important issue with respect to mechanical properties (PCMI) whatever the fuel design.

Table 20.1. Potential impacts of various fuel cladding combinations (chemical, mechanical, neutronics, thermal): Coated and improved Zr-alloys (coating on outer surface)

Properties	Conventional UO$_2$	Oxide-doped UO$_2$	High-thermal conductivity UO$_2$ (metal/ceramic dopant)	High-density fuel				Encapsulated fuel
				Silicide	Nitride	Carbide	Metal	
Chemical	Equivalent to conventional Zr/UO$_2$.		Some metal elements could be detrimental. No data for compatibility with Zr cladding.	Lack of data but potential risk of reaction with Zr should be mitigated.		Lack of data, might be challenging if cladding carburising occurs. Lower sesqui-carbides fuel content should reduce this risk.	Potential risk of reaction with Zr should be mitigated. A lining would be needed to prohibit the metal/Zr reaction.	Good compatibility. In case of a SiC matrix, possible reaction with the cladding above 700°C might be challenging.
Mechanical	Equivalent to conventional Zr/UO$_2$ (pellet-gap closure kinetics might be slightly different, with a potential impact on PCMI and SCC-PCI).		Lower temperature operation and possibly lower swelling and lower fission gas release compared to UO$_2$.	Lack of data but fuel design should be adapted to higher fuel swelling and lower expected cladding creep rate to address PCMI and SCC-PCI issue.			Lack of data but the specific fuel dimensional stability should be taken into account.	No issues identified so far.
Neutronics	Neutron absorption cross-section for coating might slightly impact pellet size or enrichment depending on the thickness.	The dopant might impact the pellet size/density or enrichment.	Lower fuel T due to higher conductivity (cladding + fuel) might modify the Doppler effect.					
Thermal	Equivalent to conventional Zry/UO2 but specific gap closure kinetics (depending on the dimension and the nature of the coating) may have an impact on fuel T.	Equivalent to Zry/UO$_2$ for most of the dopants, some might have slight effects and specific gap closure kinetics (depending on the dimension and the nature of the coating) and this may have an impact on fuel T.	Lower T anticipated, which might be partly offset depending on rod designing options.				Lower T anticipated, which might be partly offset depending on rod designing options. Margin to melt might be an issue if melting occurs before cladding degradation.	Lower T anticipated, which might be partly offset depending on rod designing options.

Table 20.2. Potential impacts of various fuel cladding combinations (chemical, mechanical, neutronics, thermal): FeCrAl alloy claddings

Properties	Conventional UO$_2$	Oxide-doped UO$_2$	High-thermal conductivity UO$_2$ (metal/ceramic dopant)	High-density fuel				Encapsulated fuel
				Silicide	Nitride	Carbide	Metal	
Chemical	Chemical compatibility between the fuel and the FeCrAl cladding under irradiation currently not available.		Mo and Cr additives are compatible with SS cladding. If MoO$_3$ is formed by oxidation with water, eutectic can be considered at 700°C with Fe and Cr oxides.	Potential risk of reaction with Fe should be mitigated. A lining would be needed to prohibit the fuel/cladding reaction.		Excess carbon may migrate into the FeCrAl cladding. Lower sesqui-carbides fuel content should reduce this risk.	Potential U/Fe and Pu/Fe eutectics at low T (<725°C) should be investigated under various levels of irradiation. A lining would be needed to prevent the phenomenon.	Good compatibility. In case of a SiC matrix, reaction with the inner coating or lining might be possible.
Mechanical	Resistance to SCC-PCI and PCMI needs to be characterised with irradiated material data.		Lower T operation and possibly lower swelling compared to UO$_2$ might mitigate possible PCMI related issues.	Lack of data but fuel design should be adapted to higher fuel swelling and lower expected cladding creep rate to address PCMI issue.			Lack of data but the specific fuel dimensional stability should be taken into account.	No issues identified so far.
Neutronics	High-neutron absorption cross-section for FeCrAl will impact pellet size or enrichment.							
				Higher density of fissile atoms in the fuel could compensate the expected increase of neutron absorption.				More challenging impact than for other fuel variants.
Thermal	Essentially the same as conventional Zr/UO2 but depending on gap closure kinetics (related to FeCrAl creep properties), gap conductance should be assessed under irradiation.		Lower T anticipated, which might be partly offset depending on rod designing options.				Lower T anticipated, which might be partly offset depending on rod designing options. Potential U/Fe and Pu/Fe eutectics at low T (<725°C) to investigate in terms of margin to melt.	Lower T anticipated.

Table 20.3. Potential impacts of various fuel cladding combinations (chemical, mechanical, neutronics, thermal): Refractory metal claddings (coating or lining potentially on both sides of the cladding)

Properties	Conventional UO$_2$	Oxide-doped UO$_2$	High-thermal conductivity UO$_2$ (metal/ceramic dopant)	High-density fuel				Encapsulated fuel
				Silicide	Nitride	Carbide	Metal	
Chemical	Lack of data, depends on internal liner which should be compatible with UO$_2$.		Potential eutectic formation with metallic part of the fuel.	Lack of data, but potential risk of reaction (nitridation, carburising,…) with metallic coating/lining should be mitigated.			A modified lining would be needed to prohibit the metal/metallic coating/lining reaction.	Good compatibility. In case of a SiC matrix, reaction with the inner coating or lining might be possible.
Mechanical	Specific PCMI behaviour needs further study.		Lack of data but lower T operation and possibly lower swelling compared to UO$_2$ might mitigate possible PCMI related issues.	Lack of data but fuel design should be adapted to higher fuel swelling and lower expected cladding creep rate to address PCMI issue.			Lack of data but the specific fuel dimensional stability should be taken into account.	Lack of data. No issues identified so far.
Neutronics	High-neutron absorption cross-section for Mo will impact pellet size or enrichment.							
				Higher density of fissile atoms in the fuel could compensate the expected increase of neutrons absorption.				More challenging impact than for other fuel variants.
Thermal	Essentially the same as for conventional Zr/UO$_2$ but depending on gap closure kinetics (related to Mo creep properties), gap conductance should be assessed under irradiation.						Lower T anticipated, which might be partly offset depending on rod designing options. Margins to melt might also be an issue.	Lower T anticipated, which might be partly offset depending on rod designing options.

Table 20.4. Potential impacts of various fuel cladding combinations (chemical, mechanical, neutronics, thermal): SiC-SiC/SiC-cladding

| Properties | Conventional UO$_2$ | Oxide-doped UO$_2$ | High-thermal conductivity UO$_2$ (metal/ceramic dopant) | High-density fuel | | | | Encapsulated fuel |
				Silicide	Nitride	Carbide	Metal	
Chemical	No reaction known below 1 600°C.		Lack of data. Should be sensibly the same as for UO$_2$.	Lack of data. Possible chemical interaction between U$_3$Si$_2$ and SiC but with low kinetics.	Lack of data.			Lack of data.
Mechanical	An optimised fuel design is required to avoid PCMI considering the low ductility of the SiC-cladding.							
Neutronics	Low neutron absorption cross-section for SiC is an asset for design optimisation.							
		Some dopants might lead to additional neutron penalty.						
Thermal	Irradiation-induced cladding swelling and thermal conductivity reduction cause higher fuel temperature and higher fission gas release.		Lower T with respect to UO$_2$.	Lower fuel T anticipated, which might be partly offset depending on rod design options to compensate higher swelling rate. Margins to melt might also be an issue.	Margins to fuel dissociation might also be an issue.	Lower fuel T anticipated, which might be partly offset depending on rod design options.	Lower T anticipated, which might be partly offset depending on rod design options. Margins to melt might also be an issue.	Lower T anticipated.

It seemed basically relevant to consider the same type of issue with regards to non-fuel components, such as control rod/blade and channel box, associated with the different types of cladding materials. The current candidate material for ATCR cladding is stainless steel and that for the advanced channel box is SiC. General tendency is discussed in the last part of the present chapter.

- The cladding material for ATCR is not fixed yet. Coating/improved Zry, advanced stainless steel, refractory metal and SiC are potential candidates for the ATCR cladding as well as conventional zircaloy and conventional stainless steel, although experimental data are insufficient. The compatibility between these ATCR cladding materials and fuel cladding materials is generally noted as the

interaction between these materials (currently, no challenging issue has been identified, neither on the chemical nor on the mechanical area).

- Better neutronic compatibility is potentially expected by the lower neutron cross-section of SiC than conventional zircaloy. However, channel box bow and pseudo-ductility of SiC are expected to influence the mechanical compatibility. Chemical compatibility between SiC and fuel cladding materials is necessary to be addressed in the near future, especially for high-temperature (HT) conditions.

Compatibility between accident-tolerant control rod and various cladding materials

A novel concept of ATCR, where the conventional neutron-absorbing material, B_4C or Ag-In-Cd, is replaced with RE_2O_3-MO_2 (RE = Sm, Eu, Gd, Dy or Er, M = Zr or Hf) and/or HfC, is developed by CRIEPI, Japan and AREVA NP, France (see previous chapter). For ATCR, the cladding material is currently not the main concern and the applicability of conventional steel is investigated in order to implement it to existing LWRs. However, if some enhanced accident-tolerant fuel claddings are put into practical use, the change of the CR cladding might be considered as well.

The candidates for ATCR neutron-absorbing materials have been experimentally confirmed to have high chemical compatibility with Fe, Zr, Cr and a conventional steel, and no liquid phase is formed up to >1 200°C. Such results indicate that conventional steel, conventional zircaloy and Cr-coated zircaloy are promising as ATCR cladding materials. In addition, an advanced steel (FeCrAl) is also expected to be applicable to ATCR cladding and is planned to be experimentally verified. On the other hand, available data and knowledge on chemical compatibility with Mo-alloy and SiC are still insufficient.

The new neutron-absorbing materials used for ATCR are targeted to have a fluorite structure known to feature low swelling under neutron irradiation. Since no phase change and gas generation are expected during the irradiation, the main swelling will be caused by irradiation damage. Such properties of the neutron-absorbing materials lead to the mechanical stability of ATCR, regardless of the cladding materials. Further irradiation experiments are necessary for the engineering demonstration of the ATCR concept with various cladding materials.

Compatibility between SiC channel box and various cladding materials

SiC channel box properties include a smaller neutron capture cross-section, the saturation of swelling during the initial irradiation and a lower pseudo-ductility. These properties are independent of the cladding materials.

- SiC neutron absorption cross-section is approximately 60% of the zirconium absorption cross-section. That lower neutron capture cross-section could support a slightly lower fuel enrichment requirement or a higher discharged burn-up for the same enrichment.

- SiC channel box may have the potential of channel bow mitigation since the initial irradiation.

Regarding compatibility issues during severe accidents, the chemical reaction between SiC channel box and the cladding depends on the cladding material. A lack of detailed data is observed. Reaction tests with a high-temperature steam environment will be necessary.

Summary and conclusions

The present report is the product of work that was conducted between April 2014 and June 2017 by the NEA Expert Group on Accident-tolerant Fuels for Light Water Reactors (EGATFL). The experts who participated in the group represented 35 organisations from 14 countries, including R&D institutions, fuel vendors, utilities, and safety and regulatory organisations.

It is important to emphasise that the objective of the report is to provide an overview of the state of the art for various technologies currently being pursued by many organisations. While expert opinions are provided on technology readiness levels of the different options, data gaps and potential difficulties for different technologies, the objective is not to favour or dismiss any given technology. The evaluation criteria are provided as a guide to decision makers.

Part I provides a strong basis for the remainder of the report by establishing a common vernacular for the anticipated benefits and performance attributes associated with accident tolerant fuels, including clarification of the definition of "fuel coping time" under off-normal conditions. The work outlines a proposed approach for the evaluation of candidate accident-tolerant fuel (ATF) concepts to characterise their performance relative to current design, operational, economic and safety requirements for light water reactor (LWR) fuels, and provides a framework for evaluation of cladding and fuel concepts presented in Parts II and III of this report. Chapters 1 through 8 thus propose a set of international metrics, related standardised tests and illustrative severe accident scenarios for the evaluation of ATF concepts that would be used in pressurised water reactors (PWRs), boiling water reactors (BWRs) and water-water energetic reactors (VVERs). While this set of tests and postulated accident scenarios cannot be expected to be comprehensive adjacent to the analyses that will be conducted by developers of specific ATF concepts, they nevertheless provide a common set that can be used across various companies, organisations and countries to allow for comparison of results – particularly with regard to performance trends – that are observed for similar materials under investigation by multiple entities. A common definition of the technology readiness level (TRL), which includes assessment of fabrication process maturity, fuel performance maturity and performance code maturity, was also provided to help understand the development status and performance of materials being developed by multiple organisations. This set of TRL definitions and maturity levels thus informed the assessment of fuel, cladding and system maturity provided in Parts II and III of the report.

To conduct an evaluation of proposed fuel and cladding systems, it is necessary to review fuel performance and severe accident analysis codes that have been updated to include properties and behaviours of fuel and cladding materials being considered for ATF application. A summary of the current development status and plans for future code enhancements were therefore provided by the participating organisations. Each organisation is expected to use modelling and analysis tools that have been developed by and/or approved by that organisation. While there is no expectation that analysis tools will be compared directly, tools that have been updated to include properties and behaviours of ATF concepts would be expected to provide the same trends (e.g. improved

or reduced performance) when used to assess the same or similar concepts under a specified operational or accident regime.

A summary of applicable research reactor facilities around the world, which may be used for irradiation testing of ATF cladding and fuel materials for either steady-state or transient testing, is provided in Part I of the report. The summary is not intended to be a comprehensive review of all potential testing facilities, but instead includes facilities that are currently operating in NEA member and observer countries that are part of the EGATFL. Because of the limited availability of irradiation facilities and the unique capabilities at some facilities, it is expected that some organisations may want to use foreign facilities to obtain the performance data necessary to inform analysis of ATF concepts and to gain regulatory approval for use of ATF materials in commercial facilities.

The state of the art of claddings and core materials covered within the context of work by EGATFL are discussed in Chapters 9 to 14, and the TRL levels are evaluated in Chapter 19. Four types of cladding designs, as well as non-fuel components such as SiC/SiC channel boxes or ATCRs, were reviewed based on their attributes, covering the different fields: fabrication, normal operation and anticipated operational occurrences, accident conditions, design extension conditions and fuel-cycle-related issues.

The first group, "coated and improved zirconium alloys", encompasses different types of coatings: metallic (Cr, Cr-Al, multi-layer including FeCrAl), ceramic (nitrides, including multi-layer concepts, MAX phases); and oxide dispersed strengthened (ODS) surface treatments, which are also investigated as a complement to coating deposition. For this first group, security of supply is not an issue, and the manufacturing infrastructure does not need to be replaced or significantly modified. If the coating is sufficiently thin (less than 20 µm), a similar mechanical behaviour to that of uncoated cladding is observed, and the neutronic penalty is low; increased resistance to debris fretting and wear is expected, but further assessment is needed in representative irradiation conditions up to high burn-ups. Under normal operation, very low corrosion and hydrogen pick-up are observed with metallic coatings and some ceramic coatings; some concepts show very promising results for accident conditions, with significantly reduced high-temperature (HT) steam oxidation. One strengthening effect is observed, in particular with some Cr coated concepts where there is reduced HT creep and reduced ballooning. Potential eutectic formation might be an issue, especially for metallic coatings. Most concepts in this group have accomplished the "proof-of-concept" stage, and some concepts have already undergone prototype fuel irradiation.

The second type of cladding design is "advanced steels" (FeCrAl). As in the case of coated and improved zirconium alloys, security of supply is not an issue, and manufacturing infrastructure does not need to be replaced or significantly modified. For normal operating conditions, the main assets are improved mechanical properties compared to zircaloy, increased resistance to debris fretting and wear, and lower oxidation rates. However, the following issues need to be taken into account: high neutron absorption, tritium release into the coolant, and Mo and Al release in the coolant. For accident conditions, the oxidation rate at high temperature is significantly slower than for Zircaloy. FeCrAl has reached "proof-of-concept" stage.

The third type of cladding design is lined molybdenum alloy (Mo-alloy) cladding. Fabrication of Mo-alloy is still a challenge, and some issues were identified with respect to normal operating conditions: high neutron absorption and high corrosion in air requiring an outer liner such as Zr or FeCrAl. The release of radioactive isotopes could also be an issue. For accident conditions, high strength at elevated temperatures leads to coolable geometry maintenance; no significant ballooning is expected up to 1 500°C with Zr liner and 1 300°C with FeCrAl, whereas bursting with large ballooning appears at 800-900°C for

Zr-alloy cladding. The "proof-of-concept" stage is on the verge of being reached, once a sample/material irradiation is successfully irradiated in a research reactor.

The fourth type of cladding design is SiC/SiC cladding. SiC/SiC tubes represent a significant fabrication challenge, which will require the creation of a new devoted industrial network. For normal operating conditions, the main asset is the reduced neutron absorption compared to Zr-alloy, but some specific concerns are raised by recession in the water, fission products retention capability, low ductility leading to potential PCI issues, irradiation induced swelling and low thermal conductivity. For accident conditions, outstanding oxidation resistance in high temperatures and coolable geometry maintained at high temperatures are very important assets. "Proof-of-concept" has not yet been reached.

The "core materials" group includes ATCRs and SiC/SiC channel boxes. ATCRs do not raise a specific industrial challenge and no security of supply issue has been identified with the new rod materials being considered; reduced swelling is expected compared to AIC rods and this reduced swelling could lead to an increase in the duration of operating life. The considerably higher melting temperature than that of SS cladding is a significant asset. ATCRs are not expected to fail before failure of fuel rods in accident conditions. ATCRs are judged to have reached the "proof-of-concept" stage.

SiC/SiC channel boxes are envisioned for BWRs, with the main asset of having reduced neutron absorption and potential mitigation for channel bow. However, the issue of recession in the water, already identified for SiC/SiC cladding, must be addressed. Outstanding oxidation resistance in high-temperature steam and quench survivability are expected given available test results. The SiC/SiC channel box is judged to have reached the "proof-of-concept" stage.

The state of the art of advanced fuel concepts is discussed in Chapters 15 to 18 and the TRL levels are evaluated in Chapter 19. Advanced fuel concepts are divided into four groups, based on their attributes and their targeted properties or behaviours to be improved. The first group, "oxide doped UO_2", is a typical evolutionary concept. With the addition of Cr_2O_3, Al_2O_3-Cr_2O_3 dopants and other candidates to current UO_2 pellets, the grain size is increased and viscoplastic behaviour is enhanced. These additions contribute to the enhancement of the retention of fission products and the minimisation of pellet-cladding interaction. Some "oxide doped UO_2" concepts are almost at the commercial level.

The second group is "high thermal conductivity fuel". By adding a ceramic (SiO_2, BeO, SiC, diamond, etc.) or metallic (Mo, Cr, etc.) material into UO_2 pellets, the thermal conductivity may be enhanced. Although this concept is based on the improvement of UO_2 pellets, it is categorised as revolutionary. Most concepts in this group have accomplished the "proof-of-concept" stage.

The third group, "high-density fuels", is a typical revolutionary concept. The most important objective of this concept is to increase the fissile density in order to compensate for the neutronic penalty of several ATF-cladding concepts. The current R&D status and the technology gap to practical use are evaluated for silicide, nitride, carbide and metal fuels. Carbide and metal fuels react particularly easily with water or steam, which represents specific challenges. All candidate concepts are still in the "proof-of-concept" stage.

The fourth group is "encapsulated fuel", which was originally developed for gas-cooled reactor fuel. This concept has many benefits with respect to safety enhancement, but raises many issues to be solved, including fuel cost.

Different combinations of ATF claddings and advanced fuels are discussed in Chapter 20, based on chemical, mechanical, neutronic and thermal compatibility. General tendencies are also identified. For an efficient and fair discussion among the fuel and cladding task forces, several attribute guide tables were introduced (see Appendix A). While the evaluation results given in these tables were not fully reviewed by all the experts, these results were included in the report so as to maintain a proper trace of the evaluation process and as a guide for subsequent development of these technologies.

The report provides a set of evaluation criteria as a guide to decision makers and a systems-level discussion for the development of accident tolerant fuels. It also demonstrates that there are a number of technology options being pursued by various institutions. Options exist with potentially large performance benefits under different operational and off-normal conditions. Many of these concepts are at the "proof-of-concept" stage, requiring additional data and analyses. It is important to emphasise that the purpose of the report is to provide an objective overview of the state of the art for various technologies being pursued by many organisations. While expert opinions are provided in terms of the technology readiness levels of different options, data gaps and potential difficulties for the different technologies, the objective is not to favour or dismiss any given technology.

Appendix A. Attribute guides for cladding and core materials

The following colour code was used for the qualitative assessment of the status of the attributes, which were evaluated for the cladding and core materials:

	properties not addressed; colour status not identified because of a lack of knowledge
	data available; results are good; concept is matured
	data available; results not good enough; further optimisation needed
	lack of data; not challenging
	lack of data and potentially challenging
	potential showstopper identified

Attribute evaluation for the SiC/SiC-cladding

Table A.1. SiC/SiC: Fabrication/manufacturability

		Design: Sic/Sic-cladding
Compatibility with large-scale production needs	Qualification of product and associated process	Considering the probabilistic properties of the SiC material, and the challenge raised by reproductibility issues, a new type of process (standards, code) is needed to qualify the fabrication of SiC/SiC claddings.
	Security of supply for each component (material)	Manufacture of nuclear grade SiC fibres is concentrated in Japan.
	Fabrication receipt criteria (technical file)	
	Long-tube fabrication	Production of 1 m-long CVI-SiC/SiC tubes without metallic liner already demonstrated by CEA in collaboration with industrial partners. Validation of the process to manufacture "sandwich" cladding design with length greater than 20 cm has not been demonstrated so far but no issue identified. It will also depend on the type of metal used in the metallic liner.
	Large-scale pellet fabrication	N/A
	Seal/welding	Sandwich design offers welding possibility with the liner.
		New technologies required for SiC/SiC composites (brazing has demonstrated positive results under neutron irradiation).
	Fuel assembly manufacturing	Demonstration remains to be done.
Compatibility with quality and uniformity standards	Quality control/inspectability	Need to implement specific quality control features and standards adapted to the SiC/SiC composites. For inspectability, critical flaws of the final product have to be identified and specific instrumentation needs to be developed.
	Reject ratio	
Cost		Must be related to the expected gain in terms of performance. A large-scale production of nuclear grade SiC fibres will inevitably reduce the cost.
Impact on the industrial network (suppliers and subcontractors)		A whole new industrial network needs to be implemented for nuclear application.

Table A.2. SiC/SiC: Normal operation and anticipated operational occurrencess (AOOs)

		Design: Sic/Sic-cladding
Reactor operation	Behaviour in normal operation	For the "sandwich" SiC/SiC-cladding design with embedded metal liner.
	Behaviour in AOOs	Potentially challenging PCI issue is addressed below (see ramp behaviour).
	Operating cycle length (12, 18, 24 months ?...)	
	Reactivity control systems interaction	Not yet studied for LWR but no issue expected.
	Impact of load following on the overall cladding behaviour/properties	Potentially challenging PCI issue is addressed below (see ramp behaviour).
	Specific behaviour of leakers during irradiation (further degradation with risk of fuel fragment dispersion)	A failed SiC/SiC rod is expected to show a good behaviour (no secondary defect, given the fact that the cladding does not show hydriding).
	Impact of specific fabrication defects (e.g. scratches on the cladding OD, localised delamination)	SiC does not have a high-thermal conductivity (between 20 and 30 W.m-1.K-1 at room temperature according to the manufacturing parameters (fibres, architectures,…), decrease with temperature and under irradiation up to saturation dose, which can be of concern if the defect affects an already not so good conductivity. Tests needed on pre-damaged samples to assess the efficiency of pyrocarbone interphase to deviate cracks.
	Neutron penalty	SiC/SiC shows very good properties with respect to neutronics, to be adjusted however depending on the material chosen for the metallic liner. A thin thickness (< 100 µm) of such a metal liner reduces the penalty.
Mechanical properties	Creep	No creep under 1 400°C.
	Ductility	SiC/SiC can be deformed by inherent damageable mechanism. Maximum strain level is about 1% according to the fabrication parameters, and enabled thanks to the pyrocarbon interphase.
	Toughness	Crack propagation is better than for a monolithic ceramic material, but worse than for a metallic material.
	Strength	Not as good as zircaloy in normal conditions
	Fatigue	Good feedback from the aeronautics field, lack of data in the nuclear area.
	Ramp behaviour	PCI issue
	Adhesion of coatings	N/A for sandwich SiC/SiC design with embedded metal liner.
	Resistance to debris	More resistant than a metal cladding that can be stamped.
	Resistance to fretting/wear	Lack of data, good behaviour expected – SiC material is very hard.
	Circumferential buckling	No ovalisation permitted.
	Rod bow	

Table A.2. SiC/SiC: Normal operation and AOOs (continued)

		Design: Sic/Sic-cladding
	Assembly bow	
Thermal behaviour	Conductivity	Between 20 and 30 $W.m^{-1}.K^{-1}$ depending on the manufacturing parameters (fibres, architectures,...), decreases with temperature and under irradiation up to saturation dose. Multi-layer character of SiC-cladding may affect conduction properties.
	Specific heat	600/700 $J.Kg^{-1}.K^{-1}$, increases with temperature ; independent of the SiC grade.
	Melting	SiC does no melt, cristallinity is stable from RT to normal operating temperature.
Fuel/cladding interaction	Chemical compatibility (fuel/cladding)/stability	Stable in normal conditions, long duration experiments is ongoing at CEA.
	Resistance to PCMI	Includes potential cumulative damage.
	resistance to SCC/I	Not an issue with embedded metal liner (no stress).
	Tritium permeation	Would be black without a metal liner. Cladding design could accommodate.
	Permeability (hydrogen, fission products)	See leak-tightness.
	Leak-tightness	Gas tightness can not be ensured beyong elastic limit of SiC/SiC-composite due to matrix microcracking – "Sandwich" design with a metal liner has demonstrated leak-tighness up to ultimate failure. Demonstration of leaktightness in temperature (600/1000°C) and under high pressure (>200 bar) is ongoing at CEA.
Impact of irradiation	Irradiation limit	Irradiation stability after saturation dose for nuclear grade SiC – Liner could be weakened depending on its material.
	Fission product behaviour	
	Embrittlement	Good resistance for nuclear grade (high purity), amorphisation under 125°C.
	Irradiation-induced microstructural /chemical composition evolution	Liner-dependant. Green in case there is no interaction between SiC and the liner material.
	Dimensional stability (growth/swelling)	Swelling of SiC under irradiation up to saturation level but limited for nuclear grade material (2% in the range 200-400°C).
Coolant interaction	Chemical compatibility with and impact on coolant chemistry	Issue of SiC recession in water, with residual Si in the coolant; to be considered in connection with the existing criteria, and temperature dependance of the solubility of silica.
	Oxidation behaviour	Mechanism implies recession/weight loss of SiC but it stays limited (0.5 μm lost after 3 500 h in pressurised water 360°C/180bar/PWR chemistry in autoclave). Positive behaviour even if the mechanism is not clearly understood yet.
	Shadow corrosion (eg: compatibility with spacer grids)	SiC-cladding can not be implemented in the current infrastructures, it requires specific fixtures.
	Hydriding behaviour	Liner dependent.

Table A.2. SiC/SiC: Normal operation and AOOs (continued)

		Design: Sic/Sic-cladding
	Erosion	Recession of SiC in hydrothermal oxydation regime, exacerbated by the dynamic conditions (loop with filtration).
	Crud deposition	Risk of silica deposit in cold parts of the reactor.
	Thermal-hydraulic interaction (DNB issue)	Higher critical heat flux (CHF) for SiC/SiC than Zy4 and sustainable structural integrity after CHF that can be advantageous in securing a high safety margin. Recent paper by Korean universities on that topic.
Licensibility	Capability of codes to simulate the behaviour	Major issue but not technically challenging.
	Reproductibility and robustness of experiments in support to licensing	Not easy to reconcile with the SiC/SiC probabilistic behaviour.
	Methodology issues	Licensing could represent a big challenge.

Table A.3. SiC/SiC: Design-basis accidents

		Design: Sic/Sic-cladding
Reactor operation	Behaviour in accidental transients	LOCA: green (HT steam oxidation behaviour leading to a significantly longer "grace time period" than for Zy4).
		Orange (need for post-quench tests and data on ballooning/burst tests).
		RIA: black because of PCMI and swelling behaviour.
	Impact of load following on the overall cladding behaviour /properties	Potentially challenging PCI issue is addressed in "ramp behaviour".
	Specific behaviour of leakers that appeared during normal operation (lower resistance during a DBA)	A failed SiC/SiC rod is expected to show a good behaviour (no secondary defect, given the fact that the cladding does not show hydriding).
High-temperature mechanical properties	Creep	No creep under 1 400°C.
	Ductility	Low ductility if pyracarbon interphase is affected.
	Toughness	Crack propagation is better than for a monolithic ceramic material, but worse than for a metallic material.
	Strength	Good performance in accident conditions.
	Fatigue	Good feedback from the aeronautics field, lack of data in the nuclear area.

Table A. 3. SiC/SiC: Design-basis accidents (continued)

		Design: Sic/Sic-cladding
	adhesion of coating	Not relevant for the sandwich SiC/SiC design
Thermal behaviour	Conductivity	Between 20 and 30 $W.m^{-1}.K^{-1}$ depending on the manufacturing parameters (fibres, architectures,…), decreases with temperature and under irradiation up to saturation dose. Multi-layer character of SiC-cladding may affect conduction properties. depending on the manufacturing parameters (fibres, architectures,…), decreases with temperature and under irradiation up to saturation dose. Multi-layer character of SiC-cladding may affect conduction properties and generate specific thermal gradient.
	Specific heat	
	Melting	SiC does no melt but sublimates beyond 2 400°C.
Fuel/cladding interaction	Chemical compatibility/stability (e.g. oxidation behaviour)	Liquid phase appearance in the SiC/UO_2 system in the same range of temperature as in the Zr/UO_2 system.
	Fission product behaviour	
	Fission gas generation	Release of hydrogen, CO, CO_2 but very low kinetics in comparison to Zy4.
	Resistance to PCI	PCMI issue.
	Environment interaction of the inner cladding layer	N/A for the sandwich SiC/SiC design.
LOCA	High-temperature steam oxidation (1 200°C)	Integrity and geometry of specimen fully preserved after 110h exposure at 1400°C in steam environment, retention of the non-linear elastic damageable behaviour. See CEA and ORNL studies on subject/silica oxide scale formation protects SiC at high temperature /mechanism result from competition between simultaneous growth and volatilisation of silica.
	HT breakaway oxidation	
	Quench tolerance / Post-Quench Mechanical behaviour	Does not seem to be an issue. "SiC article remains structurally sound after quench that eliminates the quench survavibility concern", Yueh et al. 2014, confirmed this year by CEA and the community.
	Degradation mode of the cladding	Potentially almost no degradation during LOCA scenarios.
	Phase transformation, H and O, diffusion and distribution	Not an issue for SiC, but may vary depending on the type of liner.
RIA	Degradation mode of the cladding	
	Mechanical behaviour (PCMI high speed ramp/tensile test at high temperatures)	
	Steam oxidation at 1 480°C /1 500°C	

Table A. 3. SiC/SiC: Design-basis accidents (continued)

		Design: Sic/Sic-cladding
Seismic behaviour	Fuel assembly mechanical behaviour	
Thermal-hydraulic interaction		Steam environment; given the thermal exchanges and thermal conductivity, different axial gradients for metal liner.
Licensibility	Capability of codes to simulate the behaviour	Major issue but not technically challenging.
	Reproductibility and robustness of experiments in support to licensing	Not easy to reconcile with the SiC/SiC probabilistic behaviour.
	Methodology issues	Licensing could represent a big challenge.

Table A.4. SiC/SiC: Design extension conditions

	Design: Sic/Sic-cladding
Mechanical strength and ductility	Green: high strength.
	Orange: low ductility if pyrocarbon interphase is affected.
Thermal behaviour (melting)	No melting before 2 000°C.
Chemical compatibility/stability (including high-temperature steam interaction)	Oxidation kinetics accelerates with high temperature but stay limited below 1 600°C.
Fission product behaviour	
Combustible gas production	Release of hydrogen, CO, CO_2 but very low kinetics in comparison to Zy4.
Oxidation acceleration due to the exothermic HT reaction	Low oxidation kinetics.
Physical interaction of the molten material	Corium cooling capacity may be an issue: even if SiC sublimates beyond 2 400°C, how does it behave when mixed with the reactor vessel?

Table A.5. SiC/SiC: Fuel cycle issues

		Design: Sic/Sic-cladding
Enrichment limit		
Mechanical strength and ductility		
Thermal behaviour		
Chemical stability		
Fission product behaviour		
Transport	Mechanical behaviour (ductility)	If long claddings, flexion sollicitations might be an issue with transport vibrations.
	Behaviour in fire	
	Impact of specific fabrication defects (e.g. scratches on the OD cladding, localised delamination)	
	Behaviour under accident conditions (punch test)	
Long-term storage	Hydride reorientation	Liner dependent.
	Corrosion behaviour	
	Impact of specific fabrication defects (e.g. scratches on the OD cladding, localised delamination)	
	Residual radioactivity	SiC does not get activated.
	Long-term microstructural/chemical composition evolution	Liner dependent.
Reprocessing	Tritium	
	Shearing	Lack of data.
	Chemical compatibility with reprocessing reaction (nitric acid)	SiC does not react with any acid.
	Reprocessibility	Not explored.
Cost		

Attribute evaluation for the Cr-coated zirconium cladding

Table A.6. Cr-coated zirconium: Fabrication/manufacturability

		Design: Cr-coated zirconium
Compatibility with large-scale production needs	Qualification of product and associated process	Qualification process needs to be adapted.
	Security of supply for each component (material)	
	Fabrication receipt criteria (technical file)	First fabrication criteria have been defined for IMAGO irradiation (Gösgen).
	Long-tube fabrication	Not yet demonstrated but achievable. KAERI and CEA have manufactured a few dm long Cr-coated tubes. Prototypical full-length tubes manufacturing is underway in France.
	Large-scale pellet fabrication	N/A
	Seal/welding	Tests confirmed welding strength is OK.
	Fuel assembly manufacturing	
Compatibility with quality and uniformity standards	Quality control/inspectability	Type of acceptable/non-acceptable flaws to be defined. Cr-coating might need to develop specific intrsumentation.
	Reject ratio	
Cost		If the coating manufacturing process is reliable and robust, the additional cost should be reasonable.
Impact on the industrial network (suppliers and subcontractors)		Will use the same manufacturing plants as today. No specific challenge.

Table A.7. Cr-coated zirconium: Normal operation and AOOs

		Design: Cr-coated zirconium
Reactor operation	Behaviour in normal operation	In the worse case scenario (assuming the coating would be affected and would disappear under irradiation) remaining characteristics of the tube would be those of the cladding.
	Behaviour during AOOs	
	Operating cycle length (12, 18, 24 months ?...)	
	Reactivity control systems interaction	
	Impact of load following on the overall cladding behaviour/properties	
	Specific behaviour of leakers during irradiation (further degradation with risk of fuel fragments dispersion)	
	Impact of specific fabrication defects (e.g. scratches on the cladding OD, localised delamination)	No impact identified in out-of-pile tests. To be investigated under irradiation.
	Neutron penalty	OK for thin enough Cr-coatings (up to at least 20 µm).
Mechanical properties	Creep	Mechanical properties not affected by thin Cr-coating (0-15 µm). Zr substrate not affected by the coating manufacturing process (CEA-AREVA-EDF).
	Ductility	Mechanical properties not affected by thin Cr-coating and orange (need for post-quench tests and data on ballooning / burst tests [0-15 µm]). Zr substrate not affected by the coating manufacturing process (CEA-AREVA-EDF).
	Toughness	Mechanical properties not affected by thin Cr-coating (0-15 µm). Zr substrate not affected by the coating manufacturing process (CEA-AREVA-EDF).
	Strength	Mechanical properties not affected by thin Cr-coating (0-15 µm). Zr substrate not affected by the coating manufacturing process (CEA-AREVA-EDF).
	Fatigue	Not tested yet.
	Ramp behaviour	With respect to SCC-PCI, similar behaviour as for the non-coated cladding is expected.
	Adhesion of coatings	Good results in as-received conditions (out-of-pile) and after ion irradiation or first neutron irradiations (low fluence). Needs to be confirmed under higher fluences.
	Resistance to debris	Not assessed yet. Should be improved as compared to current Zirconium claddings.
	Resistance to fretting/wear	Good results in as-received conditions. Need further data under irradiation. Wear of grid springs and dimples to be checked.
	Circumferential buckling	
	Rod bow	Lack of data but should be comparable to the current fuel rods w/o coating.
	Assembly bow	Lack of data but should be comparable to the current fuel rod bundles w/o coating.

Table A.7. Cr-coated zirconium: Normal operation and AOOs (continued)

		Design: Cr-coated zirconium
Thermal behaviour	Conductivity	Cr conductivity (93 W/m/K) higher than that of the cladding thus good conductivity expected.
	Specific heat	Not affected by the coating.
	Melting	Zr-Cr eutectic at 1 330°C in accident conditions needs further investigations.
Fuel/cladding interaction	Chemical compatibility (fuel/cladding)/stability	
	Resistance to PCMI	Not modified.
	Resistance to SCC/I	Not modified.
	Tritium permeation	TBD because the lower OD ZrO_2 barrier will be less effective.
	Permeability (hydrogen, fission products)	Not modified.
	Leak-tightness	Not modified.
Impact of irradiation	Irradiation limit	
	Fission product behaviour	N/A.
	Embrittlement	Embrittlement is reduced thanks to reduced H uptake. Possible damage/embrittlement of the OD coating under irradiation needs to be investigated.
	Irradiation-induced microstructural/chemical composition evolution	Good stability of coating/Zr interface under ion irradiation. To be confirmed under neutron irradiation.
	Dimensional stability (growth/swelling)	Similar to Zr (TBD). NB: Cr doesn't swell under irradiation.
Coolant interaction	Chemical compatibility with and impact on coolant chemistry	Good.
	Oxidation behaviour	Significantly improved. Extremely low corrosion kinetics in autoclave tests in 360°C wtaer and 415°C steam, with little variation with time.
	Shadow corrosion (e.g. compatibility with spacer grids)	Cr-coating should be an improvement compared to the Zy cladding alone.
	Hydriding behaviour	Lower H intake could is benficial but need to be confirmed in specific coolant chemistries (i.e. high H chemistry).
	Erosion	Probably improved as compared to Zy (to be confirmed under irradiation).
	Crud deposition	Unknown and TBD (Cr exhibits specific surface characteristics, with greater outer surface roughness).
	Thermal-hydraulic interaction (DNB issue)	The coating surface might affect the CHF correlation. According to a Korean paper (KAIST): might not be as performant as uncoated Zy.
Licensibility	Capability of codes to simulate the behaviour	Similar to Zy with additional issues previously mentionned to be addressed.
	Reproductibility and robustness of experiments in support to licensing	Similar to Zy with additional issues previously mentionned to be addressed.
	Methodology issues	Similar to Zy with additional issues previously mentionned to be addressed.

Table A.8. Cr-coated zirconium: Design-basis accidents

		Design: Cr-coated zirconium
Reactor operation	Behaviour in accident transients	Not modified.
		Improved HT oxidation.
	Impact of load following on the overall cladding behaviour /properties	No an issue regarding SCC-PCI cladding behaviour (i.e. similar to Zy cladding w/o coating). Potential for load following related cracks initiation in the OD coating needs to be investigated but it should not be an issue: cladding surface remains protected by the coating.
	Specific behaviour of leakers that appeared during normal operation (lower resistance during a DBA)	Not modified.
High-temperature mechanical properties	Creep	Strengthening effect of the OD coating has been observed.
	Ductility	Enhanced post-quench behaviour (due to lower H uptake of coated Zy and to the coating strengthening effect).
	Toughness	
	Strength	Strengthening effect of the OD coating has been observed.
	Fatigue	N/A
	Adhesion of coating	Very good adherence up to high deformation. To be confirmed inder irradiation.
Thermal behaviour	Conductivity	
	Specific heat	
	Melting	
Fuel/cladding interaction	Chemical compatibility/stability (e.g. oxidation behaviour)	Not a concern.
	Fission product behaviour	Not a concern.
	Fission gas generation	
	Resistance to PCI	SCC-PCI behaviour of OD coated tubes is similar to cladding w/o OD coating.
	Environment interaction of the inner cladding layer	N/A.
LOCA	High-temperature steam oxidation (1 200°C)	Much higher oxidation resistance than Zy4. KAERI: Cr-coated Zy4: no severe oxidation after 2 000 s at 1 200°C. CEA data: Cr-coatings developed so far have shown good high-temperature oxidation resistance , i.e. at least 10 times lower weight gains as compared to uncoated Zr4 (in addition, OD coating seems to reduce (critical) oxygen ingress into the Zr substrates up to ~1-2h at 1 200-1 300°C).
	HT breakaway oxidation	CEA tests confirmed Cr-coated Zr claddings do not exhibit any oxidation breakaway or significant H uptake at 1000°C for up to at least 4h.
	Quench tolerance/Post-Quench Mechanical behaviour	Improved as compared to Zr-alloys w/o OD coating (less H diffusion in the base metal).
	Degradation mode of the cladding	To be determined.
	Phase transformation, H and O, diffusion and distribution	No secondary hydriding ; also, chromium gets dissolved in the Zr cladding, which is a positive characteristic. (ex. from CEA data: at 1 000°C, Cr-coated claddings did not experience breakaway, nor significant hydrogen uptake up to at least 4h).

Table A.8. Cr-coated zirconium: Design-basis accidents (continued)

		Design: Cr-coated zirconium
RIA	Degradation mode of the cladding	To be determined.
	Mechanical behaviour (PCMI high speed ramp/tensile test at high temperatures)	To be determined for RIA conditions including on irradiated samples.
	Steam oxidation at 1480°C / 1500°C	Improved but possible Cr-Zy eutectic at 1 330°C should be further investigated.
Seismic behaviour	Fuel assembly mechanical behaviour	Rather improved (no hydriding).
Thermal-hydraulic interaction		The coating surface might affect the CHF correlation. According to a Korean paper (KAIST): might not be as performant as uncoated Zy.
Licensibility	Capability of codes to simulate the behaviour	Not a concern as long as the OD coating is thin.
	Reproductibility and robustness of experiments in support to licensing	Very similar to Zr cladding w/o OD coating.
	Methodology issues	To be determined, no concern anticipated with thin OD coating.

Table A.9. Cr-coated zirconium: Design extension conditions

		Design: Cr-coated zirconium
Mechanical strength and ductility	at temperature <1 300°C	CEA (Cr-coating on Zr-alloy base metal): 15 000 s at 1000°C tests show significantly improved post-quench ductility and strength.
	at temperature >1 300°C	Need to generate additional experimental data.
Thermal behaviour (melting)		Need to investigate the Cr-Zr eutectic issue.
Chemical compatibility/stability (including high-temperature steam interaction)		HT oxidation is significantly reduced.
Fission product behaviour		N/A.
Combustible gas production		Delayed (for instance during a LOCA in a spent fuel pool).
Oxidation acceleration due to the exothermic HT reaction		Delayed (for instance during a LOCA in a spent fuel pool).
Physical interaction of the molten material		No specific impact of thin Cr-coating is expected.

Table A.10. Cr-coated zirconium: Fuel cycle issues

		Design: Cr-coated zirconium
Enrichment limit		N/A for thin coating.
Mechanical strength and ductility		Similar to Zr-alloy base metal or improved (less H diffusion into the base metal thanks to the coating).
Thermal behaviour		N/A.
Chemical stability		Coating behaviour on the long term should be investigated.
Fission product behaviour		N/A.
Transport	Mechanical behaviour (ductility)	Provided long-term adhesion of the coating is confirmed, there will be less H uptake in the base metal.
	Behaviour in fire	
	Impact of specific fabrication defects (e.g. scratches on the OD cladding, localised delamination)	Should be investigated (adhesion of the coating and H diffusion on the long term).
	Behaviour under accident conditions (punch test)	
Long-term storage	Hydride reorientation	Not a concern due to low in-service hydriding (protective effect of OD coating).
	Corrosion behaviour	Significant advantage for dry storage or in case of spent fuel pool LOCA. CEA preliminary tests results show no detrimental impact of air on coated cladding HT oxidation.
	Impact of specific fabrication defects (e.g. scratches on the OD cladding, localised delamination)	Potential delamination of coating.
	Residual radioactivity	For fusion reactors application, chromium has been considered as reduced-activation materials.
	Long-term microstructural/chemical composition evolution	Similar to Zr cladding.
Reprocessing	Tritium	
	Shearing	Similar to Zr cladding.
	Chemical compatibility with reprocessing reaction (nitric acid)	Unknown TBD.
	Reprocessibility	Unknown TBD.
Cost		Unknown TBD.

Attribute evaluation for the CrN-coated zirconium alloy cladding

Table A.11. CrN-coated zirconium alloy: Fabrication/manufacturability

		CrN commercial coating (PVD), investigated by Halden
Compatibility with large-scale production needs	Qualification of product and associated process	Qualified.
	Security of supply for each component (material)	No shortage.
	Fabrication receipt criteria (technical file)	
	Long-tube fabrication	4 m-long tubes can be coated.
	Large-scale pellet fabrication	Not relevant.
	Seal/welding	Not relevant.
	Fuel assembly manufacturing	No impact.
Compatibility with quality and uniformity standards	Quality control/inspectability	Quality guaranteed by manufacturer.
	Reject ratio	0.
Cost		Industrial PVD coatings are very cheap and will only slightly influence the total cost.
Impact on the industrial network (suppliers and subcontractors)		Not relevant.

Table A.12. CrN-coated zirconium alloy: Normal operation and AOOs

		CrN commercial coating (PVD)
Reactor operation	Behaviour in Normal Operations	
	Behaviour in AOOs	
	Operating cycle length (12, 18, 24 months ?...)	9 months tested.
	Reactivity control systems interaction	Not relevant.
	Impact of load following on the overall cladding behaviour /properties	Not relevant.
	Specific behaviour of leakers during irradiation (further degradation with risk of fuel fragments dispersion)	Not relevant.
	Impact of specific fabrication defects (e.g. scratches on the cladding OD, localised delamination)	Not yet investigated.
	Neutron penalty	None.

**Table A.12. CrN-coated zirconium alloy: Normal operation and
AOOs (continued)**

		CrN commercial coating (PVD)
Mechanical properties	Creep	Not relevant.
	Ductility	Not relevant.
	Toughness	Very good.
	Fatigue	Not relevant.
	Ramp behaviour	Not relevant.
	Adhesion of coatings	Very good, never spalled off.
	Resistance to debris	Very good.
	Resistance to fretting/wear	Very good.
	Circumferential buckling	Not relevant.
	Rod bow	Not relevant.
	Assembly bow	Not relevant.
Thermal behaviour	Conductivity	No impact; thin and 10-20 W/mK.
	Specific heat	Not relevant.
	Melting	1 770°C (coating).
Fuel/cladding interaction	Chemical compatibility (fuel/cladding)/stability	Not relevant.
	Resistance to PCMI	Not relevant.
	resistance to SCC/I	Not relevant.
	Tritium permeation	Reduced tritium permeability.
	Permeability (hydrogen, fission products)	Reduced tritium permeability.
	Leak-tightness	Not relevant.
Impact of irradiation	Fission product behaviour	Not relevant.
	Embrittlement	No embrittlement up to 287 days.
	Irradiation-induced microstructural/chemical composition evolution	Stable.
	Dimensional stability (growth/swelling)	No swelling.

Table A.12. CrN-coated zirconium alloy: Normal operation and AOOs (continued)

		CrN commercial coating (PVD)
Coolant interaction	Chemical compatibility with and impact on coolant chemistry	No degradation BWR and PWR.
	Oxidation behaviour	Protective oxide.
	Hydriding behaviour	Likely reduced hydriding of underlying zircaloy.
	Erosion	Improved.
	Crud deposition	Not investigated.
	Thermal-hydraulic interaction (DNB issue)	Not relevant.
Licensibility	Capability of codes to simulate the behaviour	Not relevant.
	Reproducibility and robustness of experiments in support to licensing	Reproducible.
	Methodology issues	

Table A.13. CrN-coated zirconium alloy: Design-basis accidents

		CrN commercial coating (PVD)
Reactor operation	Behaviour in accident transients	
	Behaviour in accident transients	
	Impact of load following on the overall cladding behaviour /properties	Not relevant.
	Specific behaviour of leakers that appeared during normal operation (lower resistance during a DBA)	Not relevant.
High-temperature mechanical properties	Creep	The coating can be deformed up to 1.5%. Beyond that, small narrow cracks occur.
	Ductility	
	Toughness	
	Fatigue	
	Adhesion of coating	Tested 1 000°C.
Thermal behaviour	Conductivity	Not relevant (very thin, 10-20 W/mK).
	Specific heat	Not relevant.
	Melting	1 770°C.

Table A.13. CrN-coated zirconium alloy: Design-basis accidents (continued)

Fuel/cladding interaction	Chemical compatibility/stability (e.g. oxidation behaviour)	Tested up to 1 000°C.
	Fission product behaviour	Not relevant.
	Fission gas generation	Not relevant.
	Resistance to PCI	Not relevant.
	Environment interaction of the inner cladding layer	Not relevant.
LOCA	High-temperature steam oxidation (1 200°C)	Not yet tested.
	Quench tolerance/Post-Quench mechanical behaviour	Not yet tested.
	Degradation mode of the cladding	Ballooning, followed by burst, uncoated cladding exposed.
	Phase transformation, H and O, diffusion and distribution	
RIA	Degradation mode of the cladding	As for standard zircaloy-cladding.
	Mechanical behaviour (PCMI high speed ramp/tensile test at high temperatures)	As for standard zircaloy-cladding.
	Steam oxidation at 1480°C/1500°C	Not investigated.
Seismic behaviour	Fuel assembly mechanical behaviour	As for standard zircaloy-cladding.
Thermal-hydraulic interaction		None.
Licensibility	Capability of codes to simulate the behaviour	As for standard zircaloy-cladding.
	Reproductibility and robustness of experiments in support to licensing	Easy to license.
	Methodology issues	

CrN-coated zirconium alloy: Design extension conditions

The attributes of the CrN-coated zirconium alloy in design extension conditions were evaluated as being equivalent to those of the zircaloy-cladding.

CrN-coated zirconium alloy: Fuel cycle issues

The CrN coating was evaluated as having no impact on the fuel cycle issues.

Attribute evaluation for the Cr$_2$AlC-coated zirconium cladding

Table A.14. Cr$_2$AlC-coated zirconium: Fabrication/manufacturability

		Cr$_2$AlC-coated Zry
Compatibility with large-scale production needs	Qualification of product and associated process	Composition and quality control of the coatings might be challenge.
	Security of supply for each component (material)	Easy access and cheap materials.
	Fabrication receipt criteria (technical file)	Unkown.
	Long-tube fabrication	Coating technology upscaling to long tubes needed.
	Large-scale pellet fabrication	Standard pelletets used.
	Seal/welding	Lack of data and welding issue generally challenging. Welding the end caps on a coated tube might be a concern.
	Fuel assembly manufacturing	Lack of data and insertion of the fuel rods into the assembly might be a concern.
Compatibility with quality and uniformity standards	Quality control/inspectability	Special quality control for adherence of coating, scratches.
	Reject ratio	
Cost		Higher than classical Zry claddings.
Impact on the industrial network (suppliers and subcontractors)		No specific challenge is expected.

Table A.15. Cr$_2$AlC-coated zirconium: Normal operation and AOOs

		Cr$_2$AlC-coated Zry
Reactor operation	Behaviour in normal operation	
	Behaviour in AOOs	
	Operating cycle length (12,18,24 months ?...)	Comparable to Zry.
	Reactivity control systems interaction	Comparable to Zry.
	Impact of load following on the overall cladding behaviour/properties	Brittle nature of MAX phase and possible cracking and spllation during high load.
	Specific behaviour of leakers during irradiation (further degradation with risk of fuel fragments dispersion)	
	Impact of specific fabrication defects (e.g. scratches on the cladding OD, localised delamination)	Strong impact on surface coating.
	Neutron penalty	Thin coating with no obvious neutron penalty.

Table A.15. Cr$_2$AlC-coated zirconium: Normal operation and AOOs (continued)

		Cr$_2$AlC-coated Zry
Mechanical properties	Creep	Comparable to Zry.
	Ductility	
	Toughness	
	Fatigue	
	Ramp behaviour	Possibly spallation of coating.
	Adhesion of coatings	Most important!
	Resistance to debris	Possibly damage of coating.
	Resistance to fretting / wear	Could be improved compared to Zry.
	Circumferential buckling	
	Rod bow	Comparable to Zry.
	Assembly bow	Comparable to Zry.
Thermal behaviour	Conductivity	
	Specific heat	
	Melting	High melting point of Cr2AlC MAX phase.
Fuel/cladding interaction	Chemical compatibility (fuel/cladding)/stability	Like Zry (only external coating).
	Resistance to PCMI	Like Zry (only external coating).
	Resistance to SCC/I	
	Tritium permeation	Similar to Zry or better.
	Permeability (hydrogen, fission products)	Like Zry or better.
	Leak-tightness	Like Zry or better.
Impact of irradiation	Fission product behaviour	Like Zry or better.
	Embrittlement	Like Zry or better (lower O/H absorption).
	Irradiation-induced microstructural/chemical composition evolution	
	Dimensional stability (growth/swelling)	Like Zry.

Table A.15. Cr$_2$AlC-coated zirconium: Normal operation and AOOs (continued)

		Cr$_2$AlC-coated Zry
Coolant interaction	Chemical compatibility with and impact on coolant chemistry	
	Oxidation behaviour	
	Hydriding behaviour	
	Erosion	
	Crud deposition	
	Thermal-hydraulic interaction (DNB issue)	Like Zry or better.
Licensibility	Capability of codes to simulate the behaviour	Possible.
	Reproductibility and robustness of experiments in support to licensing	Depending on type (composition) and thickness of coating.
	Methodology issues	

Table A.16. Cr$_2$AlC-coated zirconium: Design-basis accidents

		Cr$_2$AlC-coated Zry
Reactor operation	Behaviour in accident transients	
	Impact of load following on the overall cladding behaviour/properties	
	Specific behaviour of leakers that appeared during normal operation (lower resistance during a DBA)	
High-temperature mechanical properties	Creep	Similar to Zry with loss of mechanical strength at temperatures above 600°C dur to thin coatings.
	Ductility	
	Toughness	
	Fatigue	
	Adhesion of coating	Most important issue.
Thermal behaviour	Conductivity	Good thermal behaviour of MAX phase.
	Specific heat	
	Melting	

Table A.16. Cr₂AlC-coated zirconium: Design-basis accidents (continued)

		Cr$_2$AlC-coated Zry
Fuel/cladding interaction	Chemical compatibility/stability (e.g. oxidation behaviour)	Like Zry (without internal coating of Zry).
	Fission product behaviour	
	Fission gas generation	
	Resistance to PCI	
	Environment interaction of the inner cladding layer	Like Zry, inner oxidation after ballooning and burst.
LOCA	High-temperature steam oxidation (1 200°C)	Good oxidation performeance for short time and signficant improved compared to Zry. Thermal runaway after failure of coating possible.
	Quench tolerance/Post-Quench mechanical behaviour	Good.
	Degradation mode of the cladding	Spall-off of coating, oxidation, ballooning and burst, inner oxidation and secondary hydrogen uptake.
	Phase transformation, H and O, diffusion and distribution	Good H and O barrier up to at least 1 200°C.
RIA	Degradation mode of the cladding	
	Mechanical behaviour (PCMI high speed ramp/tensile test at high temperatures)	
	Steam oxidation at 1480°C/1500°C	Most like failure due to thin coatings.
Seismic behaviour	Fuel assembly mechanical behaviour	Like Zry due to thin coatings.
Thermal-hydraulic interaction		
Licensibility	Capability of codes to simulate the behaviour	
	Reproductibility and robustness of experiments in support to licensing	
	Methodology issues	

Table A.17. Cr₂AlC-coated zirconium: Design extension conditions

	Cr₂AlC-coated Zry
Mechanical strength and ductility	Given as long as beta-phase (with low oxygen content) is existing mechanical stability given by oxide scale to a certain extent.
Thermal behaviour (melting)	Melting of residual (non-oxidised) metal at around 2 200 K.
Chemical compatibility/stability (including high-temperature steam interaction)	Limited interaction with steam and air at high temperatures up to 1 200°C as long as coating is intact; thermal runaway after failure of coating above ca. 1 300°C.
Fission product behaviour	Good barrier as long as intact.
Combustible gas production	Significant hydrogen production after failure of the coating, main hydrogen source term.
Physical interaction of the molten material	

Table A.18. Cr₂AlC-coated zirconium: Fuel cycle issues

		Cr₂AlC-coated Zry
Enrichment limit		Unchanged or slightly improved.
Mechanical strength and ductility		
Thermal behaviour		
Chemical stability		
Fission product behaviour		
Transport	Mechanical behaviour (ductility)	
	Behaviour in fire	
	Impact of specific fabrication defects (e.g. scratches on the OD cladding, localised delamination)	
	Behaviour under accident conditions (punch test)	
Long-term storage	Hydride reorientation	
	Corrosion behaviour	
	Impact of specific fabrication defects (e.g. scratches on the OD cladding, localised delamination)	
	Long-term microstructural/chemical composition evolution	
Reprocessing	Tritium	
	Shearing	
	Chemical compatibility with reprocessing reaction (nitric acid)	
Cost		

Attribute evaluation for the advanced steels cladding

Table A.19. Advanced steels: Fabrication/manufacturability

	Advanced steels
Compatibility with large-scale production needs	Main area of GE focus in 2015-2016. Longstanding industry experience with processing ferritic steels into seamless tubing. Being studied at GE/Sandvik, ORNL, LANL.
Compatibility with quality and uniformity standards	Define quality standards and conform. No issues anticipated.
Licensibility	Achievable, steels have been licensed in the past as commercial nuclear fuel.
Seal	Can be welded. Practicle technique needs to be developed for commercial fabrication.
Inspectability	No inspection issues anticipated. Define criteria and conform.
Cost	Need to quantify cost impact with steels although initial estimates by GE/ORNL are on order of 15-25% increase in fuel cost.

Table A.20. Advanced steels: Normal operation and AOOs

		Advanced steels
Operating cycle length (12, 18, 24 months ?...)		Important to maintain current fuel cycles for BWRs and PWRs.
Thermal-hydraulic interaction (DNB issue)		Assumed to be a function of geometry which will remain unchanged.
Reactivity control systems interaction		Needs to be evaluated.
Mechanical properties (creep, ductility, strength, toughness, fatigue)		Improved strength and creep under normal operating temperatures and under accident scenarios. Ductility should be better or comparable to Zr (when considering irradiation effects and hydrogen pickup by Zr-alloys).
Thermal behaviour	Conductivity	Very similar to Zr (17-20 W/m-K).
	Specific heat	Volumetric heat capacity is higher that is a positive aspect for transients.
	Melting	Metal melts at 1 500°C and oxide at ~1 750°C.
Chemical compatibility (fuel/cladding)/stability		Will be less severe than Zr (no significant O pickup by the inner clad surface).
Chemical compatibility with and impact on coolant chemistry		Positive test results from GE in BWR and PWR water chemistries. Resistant to general corrosion and SCC ; less susceptible than Zr-alloys to galvanic corrosion with other reactor materials under irradiation.
Fission product behaviour		Tritium release could be higher. Develop method to minimise tritium release.
Resistance to fretting		To be evaluated. Results available??
Resistance to PCI		To be evaluated.
Resistance to debris		To be evaluated. Similar to fretting resistance.

Table A.20. Advanced steels: Normal operation and AOOs (continued)

		Advanced steels
Oxidation behaviour		Much superior to Zr under normal and accident conditions.
Hydriding behaviour		H and O do not dissolve (insignificant) in ferritic grains. No pickup.
IASCC		BCC structure should not be susceptible. SCC testing on irradiated HT-9 at GE-GRC shows no SCC under conditions tested.
Irradiation limit, embrittlement, growth, swelling		Being evaluated.ORNL HFIR data up to 16 dpa show good results. GE-GRC testing in ATR.
Erosion		To be evaluated.
Dimensional stability		Being evaluated. ATR testing. Negligible swelling anticipated.
Permeability (hydrogen, fission products)		To be evaluated. This may be an issue to mitigate.
Leak-tightness		Need to develop reliable welding methodology.
Crud deposition		To be evaluated.
Impact of specific fabrication defects (e.g. scratches on the cladding OD, localised delamination)		To be evaluated.
Specific behaviour of leakers during irradiation (further degradation with risk of fuel fragments dispersion)		No secondary hydriding like Zr-alloys will be present.
Impact of load following on the overall cladding behaviour/properties		To be evaluated.
Neutron penalty		To be evaluated. Depends on wall thickness, pellet diameter, etc. 0.5% enrichment penalty at maximum.

Table A.21. Advanced steels: Design-basis accidents

		Advanced steels
Thermal-hydraulic interaction		To be evaluated.
Mechanical strength and ductility		
Thermal behaviour	Conductivity	Very similar to Zr (17-20 W/m-K).
	Specific heat	Volumetric heat capacity is higher that is a positive aspect for transients.
	Melting	Metal melts at 1 500°C and oxide at ~1 750°C.
Phase transformation		None expected.
Chemical compatibility/stability (e.g. oxidation behaviour)		Positive test results from GE in BWR and PWR water chemistries. Resistant to general corrosion and SCC ; less susceptible than Zr-alloys to galvanic corrosion with other reactor materials under irradiation.
High-temperature steam oxidation		Several hundred times more resistant than current Zr-alloys.

Table A.21. Advanced steels: Design-basis accidents (continued)

		Advanced steels
Fission product behaviour		TBE.
Combustible gas production		TBE.
Quench tolerance		ORNL LOCA tests show no issue. O does not dissolve in the iron matrix, so there is no PQD issues. To be evaluated at GE-GRC.
Environment interaction of the inner cladding layer		TBE.
Specific behaviour of leakers appeared during normal operation (lower resistance during a DBA)		TBE.
Impact of load following on the overall cladding behaviour/properties		TBE.
Degradation mode of the cladding		TBE.

Table A.22. Advanced steels: Design extension conditions

	Advanced steels
Mechanical strength and ductility	Expected to be improved compared to Zr-alloys. Still being evaluated.
Thermal behaviour (melting)	Lower melting temperature compared to Zr.
Chemical compatibility/stability (including high-temperature steam interaction)	Excellent chemical compatibility and steam oxidation resistance.
Fission product behaviour	To be evaluated.
Combustible gas production	To be evaluated.
Physical interaction of the molten material	To be evaluated.

Table A.23. Advanced steels: Fuel cycle issues

	Advanced steels
Enrichment limit	Small enrichment penalty <0.5%.
Mechanical strength and ductility	Enables thin cladding to offset neutron penalty.
Thermal behaviour	To be evaluated.
Chemical stability	Excellent chemical stability and steam oxidation resistance.
Fission product behaviour	Potential implications of tritium release to plant.
Impact of specific fabrication defects (e.g. scratches on the OD cladding, localised delamination)	To be evaluated.
Cost	15-25% increase in fuel cost possible.

Attribute evaluation for the SiC channel box

Table A.24. SiC channel box: Fabrication/manufacturability

		SiC channel box
Compatibility with large-scale production needs	Qualification of product and associated process	Because SiC channnel fabrication process is different from Zry, the ivestigation is needed.
	Security of supply for each component (material)	Multi-vendors are needed.
	Fabrication receipt criteria (technical file)	The investigation is needed.
	Long-tube fabrication	Equipment and process that enable manufacturing 4m long tube are needed to establish.
	Large-scale pellet fabrication	—
	Seal/welding	—
	Fuel assembly manufacturing	—
Compatibility with quality and uniformity standards	Quality control/inspectability	The inspection method is needed to establish.
	Reject ratio	Undecided.
Cost		Undecided.
Impact on the industrial network (suppliers and subcontractors)		The investigation is needed.

Table A.25. SiC channel box: Normal operation and AOOs

		SiC channel box
Reactor operation	Behaviour in normal operations	—
	Behaviour in AOOs	—
	Operating cycle length (12, 18, 24 months ?...)	It is necessary to evaluate comprehensively based on each characteristic.
	Reactivity control systems interaction	—
	Impact of load following on the overall cladding behaviour/properties	It is necessary to evaluate comprehensively based on each characteristic.
	Specific behaviour of leakers during irradiation (further degradation with risk of fuel fragments dispersion)	—
	Impact of specific fabrication defects (e.g. scratches on the cladding OD, localised delamination)	It is necessary to evaluate comprehensively based on each characteristic.
	Neutron penalty	The neutron economy of SiC is superior to Zry.
Mechanical properties	Creep	SiC is considered to have almost no creep deformation. The experimental data is needed.
	Ductility	Since the ductility of SiC is inferior to Zry, it is necessary to take into account of the mechanical design. The experimental data is needed.
	Toughness	Since the toughness of SiC is inferior to Zry, it is necessary to take into account of the mechanical design. The experimental data is needed.
	Strength	It is necessary to take into account of the mechanical design. The experimental data is needed.
	Fatigue	—
	Ramp behaviour	—
	Adhesion of coatings	—
	Resistance to debris	—
	Resistance to fretting/wear	—
	Circumferential buckling	—
	Channel bow	SiC channel may provide a means for mitigation of channel bow. The experimental data is needed.
	Assembly bow	—
Thermal behaviour	Conductivity	—
	Specific heat	—
	Melting	It is advatageous that the melting point of SiC is higher than Zry.

Table A.25. SiC channel box: Normal operation and AOOs (continued)

		SiC channel box
Fuel/cladding interaction	Chemical compatibility (fuel/cladding)/stability	—
	Resistance to PCMI	—
	Resistance to SCC/I	—
	Tritium permeation	—
	Permeability (hydrogen, fission products)	—
	Leak-tightness	—
Impact of irradiation	Irradiation limit	—
	Fission product behaviour	—
	Embrittlement	It is necessary to take into account of SiC brittle property.
	Irradiation-induced microstructural/chemical composition evolution	SiC is considered to be no problem. The experimental data is needed.
	Dimensional stability (growth/swelling)	The experimental data is needed.
Coolant interaction	Chemical compatibility with and impact on coolant chemistry	The experimental data is needed.
	Oxidation behaviour	The experimental data is needed.
	Shadow corrosion (eg: compatibility with spacer grids)	Shadow corrosion is considered to be no problem in case of SiC.
	Hydriding behaviour	Hydride is considered to be no problem in case of SiC.
	Erosion	—
	Crud deposition	—
	Thermal-hydraulic interaction (DNB issue)	The basic experimental data regarding the pressure drop is needed.
Licensibility	Capability of codes to simulate the behaviour	The investigation is needed.
	Reproductibility and robustness of experiments in support to licensing	The investigation is needed.
	Methodology issues	The investigation is needed.

Table A.26. SiC channel box: Design-basis accidents

		SiC channel box
Reactor operation	Behaviour in accident transients	
	Behaviour in accident transients	
	Impact of load following on the overall cladding behaviour/properties	It is necessary to evaluate comprehensively based on each characteristic.
	Specific behaviour of leakers that appeared during normal operation (lower resistance during a DBA)	It is necessary to evaluate comprehensively based on each characteristic.

Table A.26. SiC channel box: Design-basis accidents (continued)

		SiC channel box
High-temperature mechanical properties	Creep	—
	Ductility	The experimental data simulating DBA is needed.
	Toughness	—
	Strength	The experimental data simulating DBA is needed.
	Fatigue	—
	Adhesion of coating	—
Thermal behaviour	Conductivity	—
	Specific heat	—
	Melting	It is advatageous that the melting point of SiC is higher than Zry.
Fuel/cladding interaction	Chemical compatibility /stability (e.g. oxidation behaviour)	—
	Fission product behaviour	—
	Fission gas generation	—
	Resistance to PCI	—
	Environment interaction of the inner cladding layer	—
LOCA	High-temperature steam oxidation (1 200°C)	It is considered that the corrosion resistance is superior to Zry at 1 200°C. The accumulation of the experimental data is needed.
	HT breakaway oxidation	It is considered that the corrosion resistance is superior to Zry at 1 200°C. The accumulation of the experimental data is needed.
	Quench tolerance/Post-Quench mechanical behaviour	It is considered that the qunchproperty is superior to Zry. The accumulation of the experimental data is needed.
	Degradation mode of the cladding	The investigation is needed.
	Phase transformation, H and O, diffusion and distribution	It is no phase transformation in DBA temperature region.
RIA	Degradation mode of the cladding	—
	Mechanical behaviour (PCMI high speed ramp/tensile test at high temperatures)	—
	steam oxidation at 1 480°C/1 500°C	—
Seismic behaviour	Fuel assembly mechanical behaviour	The investigation is needed.
Thermal-hydraulic interaction		—
Licensibility	Capability of codes to simulate the behaviour	The investigation is needed.
	Reproductibility and robustness of experiments in support to licensing	The investigation is needed.
	Methodology issues	The investigation is needed.

Table A.27. SiC channel box: Design extension conditions

	SiC channel box
Mechanical strength and ductility	The experimental data simulating BDBA is needed.
Thermal behaviour (melting)	The experimental data simulating BDBA is needed.
Chemical compatibility/stability (including high-temperature steam interaction)	The experimental data simulating BDBA is needed.
Fission product behaviour	—
Combustible gas production	The investigation is needed.
Oxidation acceleration due to the exothermic HT reaction	The experimental data simulating BDBA is needed.
Physical interaction of the molten material	The investigation is needed.

Table A.28. SiC channel box: Fuel cycle issues

		ATCR	SiC channel box
Enrichment limit			—
Mechanical strength and ductility		The change in CR stiffness due to the replacement of the neutron-absorbing materials should be confirmed. Cladding material is unchanged.	The investigation and the experimental data is needed.
Thermal behaviour		Cladding material is unchanged.	The investigation and the experimental data is needed.
Chemical stability			The investigation and the experimental data is needed.
Fission product behaviour		The investigation is needed.	
Transport	Mechanical behaviour (ductility)	The investigation is needed.	
	Behaviour in fire		
	Impact of specific fabrication defects (e.g. scratches on the OD cladding, localised delamination)		
	Behaviour under accident conditions (punch test)		

Table A.28. SiC channel box: Fuel cycle issues (continued)

		ATCR	SiC channel box
Long-term storage	Hydride reorientation	—	
	Corrosion behaviour	The investigation and the experimental data is needed.	
	Impact of specific fabrication defects (e.g. scratches on the OD cladding, localised delamination)	The investigation and the experimental data is needed.	
	Residual radioactivity	It is considered to be no problem. The investigation is needed.	
	Long-term microstructural /chemical composition evolution	It is considered to be no problem. The investigation is needed.	
Reprocessing	Tritium	The investigation is needed.	
	Shearing		
	Chemical compatibility with reprocessing reaction (nitric acid)		
	Reprocessibility		
Cost		The investigation is needed.	

Attribute evaluation for the accident-tolerant control rods

Table A.29. ATCR: Fabrication/manufacturability

		ATCR CRIEPI	ATCR AREVA
Compatibility with large-scale production needs	Qualification of product and associated process		
	Security of supply for each component (material)	Enough amounts of RE: Sm, Eu, Gd, Dy and Er), Zr and Hf resources have been confirmed, though currently most REs are supplied by only a few countries.	No risk identified.
	Fabrication receipt criteria (technical file)	Achievable. Current technologies for CR fabrication are available.	Preliminary assesment: no show stopper identified.
	Long-tube fabrication	Achievable. Cladding material is unchanged.	N/A.
	Large-scale pellet fabrication	Achievable. Current B4C sintering furnaces are compatible with large-scale production needs of ATCR absorber pellts of RE2O3 – MO2 (M = Zr or Hf).	Feasibility demonstrated with current manufacturing technologies at lab scale.
	Seal/welding	Achievable. Current technologies are available.	N/A.
	Fuel assembly manufacturing		N/A.

Table A.29. ATCR: Fabrication/manufacturability (continued)

		ATCR CRIEPI	ATCR AREVA
Compatibility with quality and uniformity standards	Quality control/inspectability	Existing inspection techniques for B4C or UO2 pellet are also appropriate for RE2O3 – MO2 pellet.	Preliminary assessment: no show stopper identified.
	Reject ratio		
Cost		Impact on cost increase is limited. CR life extension is effective to cost decreae.	Cost increase for B4C replacement candidate. Impact on cost should be beneficial for AIC replacement. Global impact on cost is design dependent.
Impact on the industrial network (suppliers and subcontractors)			

Table A.30. ATCR: Normal operation and AOOs

		ATCR CRIEPI	ATCR AREVA
Reactor operation	Behaviour in normal operations	Equivalent to the current CR.	
	Behaviour in AOOs	It is expected to be equivalent to the current CR. (Further evaluation is needed).	
	Operating cycle length (12, 18, 24 months ?...)	Equivalent to or better than the current CR.	N/A.
	Reactivity control systems interaction	Equivalent to the current CR.	When RCCA mass and neutronic efficiency is kept no impact. If change in one of this parameter then to be assessed (design dependent).
	Impact of load following on the overall cladding behaviour /properties		Equivalent to the current CR, better irradiation behaviour could drive to higher flexibility.
	Specific behaviour of leakers during irradiation (further degradation with risk of fuel fragments dispersion)		No impact for fuel rods, impact for control rods to be further studied.
	Impact of specific fabrication defects (e.g. scratches on the cladding OD, localised delamination)	Equivalent to the current CR cladding material is unchanged.	N/A.
	Neutron penalty	Equivalent to current CR no significant influence on normal operation condition.	Equivalent to current CR (no residual penalty).

Table A.30. ATCR: Normal operation and AOOs (continued)

		ATCR CRIEPI	ATCR AREVA
Mechanical properties	Creep	Equivalent to the current CR cladding material is unchanged.	No creep expected for absorber materials.
	Ductility		N/A.
	Toughness		N/A.
	Strength		N/A.
	Fatigue		N/A.
	Ramp behaviour		N/A.
	Adhesion of coatings		
	Resistance to debris	Cladding material is unchanged.	
	Resistance to fretting / wear	The flow-induced vibration properties of ATCR should be confirmed. Cladding material is unchanged.	N/A.
	Circumferential buckling	The stiffness of ATCR should be measured.	N/A.
	Rod bow	Although cladding material is unchanged, the gap width between neutron absorber pellets and cladding inner wall is not same as current ones.	N/A.
	Assembly bow		N/A.
Thermal behaviour	Conductivity	Although the thermal conductivity of RE2O3-MO2 pellet is lower than that of B4C and AIC, the integrity of ATCR is not affected because the CR is not strong heat generator as well as the melting point of RE2O3 – MO2 is fairly high.	Thermal conductivity are lower than B4C and AIC leading to a temperature increase within the absorber. However this should not be critical because the CR itself is not heat generator and high margins to melting are available.
	Specific heat	No available data for the specific heat of RE2O3 – MO2.	See remark on conductivity.
	Melting	No liquid phase is formed between RE2O3 – MO2 and cladding material (Fe) up to > 1 200℃.	No known eutectics below SS melting + high melting temperature.

Table A.30. ATCR: Normal operation and AOOs (continued)

		ATCR CRIEPI	ATCR AREVA
Fuel/cladding interaction	Chemical compatibility (fuel/cladding)/stability	No liquid phase is formed between RE2O3 – MO2 and cladding material (Fe) up to > 1 200°C.	No known eutectics below SS melting + high melting temperature.
	Resistance to PCMI	Need to experimentally obtain thermal and irradiation-induced swelling data of RE2O3 – MO2 pellet. It is expected that the PCMI does not significantly occur in the ATCR because of the excellent swelling property of materials with fluorite structure such as RE2O3 – MO2.	Lower swelling (from literature) + improved thermal expansion.
	Resistance to SCC/I	Equivalent to the current CR cladding material is unchanged.	N/A.
	Tritium permeation		
	Permeability (hydrogen, fission products)		N/A.
	Leak-tightness		N/A.
Impact of irradiation	Irradiation limit	The irradiation limit of ATCR is expected to be equivalent or improve to that of current CRs.	Improved dimensional stability should enable increased lifetime.
	Fission product behaviour	No FP generation	
	Embrittlement	No available data on embrittlement of irradiated RE2O3 – MO2 pellet. Cladding material is unchanged.	N/A.
	Irradiation-induced microstructural/chemical composition evolution	It is expected that the microstructural change and the composition evolution of RE2O3 – MO2 are not significant because the elemental composition of RE does not basically change by neutron capture reactions.	Expected materials stability under irradiation.
	Dimensional stability (growth/swelling)	High-dimensional stability is expected in ATCR, because RE2O3 – MO2 has a stable fluorite structure.	No creep expected. Lower swelling expected.
Coolant interaction	Chemical compatibility with and impact on coolant chemistry	Equivalent to the current CR cladding material is unchanged.	Limited oxidation of absorber materials expected. To be confirmed by tests.
	Oxidation behaviour		Limited oxidation of absorber materials expected. To be confirmed by tests.
	Shadow corrosion (eg: compatibility with spacer grids)		N/A.
	Hydriding behaviour		N/A.
	Erosion		N/A.
	Crud deposition		N/A.
	Thermal-hydraulic interaction (DNB issue)		
Licensibility	Capability of codes to simulate the behaviour		No issues identified.
	Reproductibility and robustness of experiments in support to licensing		
	Methodology issues		

Table A.31. ATCR: Design-basis accidents

		ATCR CRIEPI	ATCR AREVA
Reactor operation	Behaviour in accident transients		
	Behaviour in accident transients		
	Impact of load following on the overall cladding behaviour/properties		N/A.
	Specific behaviour of leakers that appeared during normal operation (lower resistance during a DBA)		No impact for fuel rods, impact for control rods to be further studied.
High-temperature mechanical properties	Creep	Equivalent to the current CR cladding material is unchanged.	No creep expected for absorber materials.
	Ductility		N/A.
	Toughness		N/A.
	Strength		N/A.
	Fatigue		N/A.
	Adhesion of coating		N/A.
Thermal behaviour	Conductivity	Although the thermal conductivity of RE2O3 – MO2 pellet is lower than that of B4C and AIC, the integrity of ATCR is not affected because the CR is not strong heat generator as well as the melting point of RE2O3 – MO2 is fairly high.	Thermal conductivity are lower than B4C and AIC leading to a temperature increase within the absorber. However this should not be critical because the CR itself is not heat generator and high margins to melting.
	Specific heat	No available data for the specific heat of RE2O3 – MO2.	See remark on conductivity.
	Melting	No liquid phase is formed between RE2O3 – MO2 and cladding material (Fe) within the range of DBA conditions (up to ~1 200°C).	No known eutectics below SS melting + high melting temperature.
Fuel/cladding interaction	Chemical compatibility/stability (e.g. oxidation behaviour)	No chemical reaction occurs between RE2O3 – MO2 and cladding material (Fe) within the range of DBA conditions (up to ~1 200°C).	No known eutectics below SS melting + high melting temperature.
	Fission product behaviour	No FP generation.	N/A.
	Fission gas generation	No gas generation.	No vapourisation of elements is expected.
	Resistance to PCI	Need to experimentally obtain thermal and irradiation-induced swelling data of RE2O3 – MO2 pellet. It is expected that the PCMI does not significantly occur in the ATCR because of the excellent swelling property of materials with fluorite structure such as RE2O3 – MO2.	Lower swelling (from literature) + improved thermal expansion.
	Environment interaction of the inner cladding layer	Equivalent to the current CR cladding material is unchanged.	

Table A.31. ATCR: Design-basis accidents (continued)

		ATCR CRIEPI	ATCR AREVA
LOCA	High-temperature steam oxidation (1 200°C)		N/A.
	HT breakaway oxidation		N/A.
	Quench tolerance/Post-Quench Mechanical behaviour		N/A.
	Degradation mode of the cladding		N/A.
	Phase transformation, H and O, diffusion and distribution		N/A.
RIA	Degradation mode of the cladding		N/A.
	Mechanical behaviour (PCMI high speed ramp/tensile test at high temperatures)		
	steam oxidation at 1 480°C/1 500°C	Equivalent to the current CR cladding material is unchanged.	N/A.
Seismic behaviour	Fuel assembly mechanical behaviour	Need to evaluate mechanical behaviour in consideration of ATCR weight. Density of RE2O3 – MO2 is ~3 times larger than B4C and equivalent to AIC.	Need to evaluate mechanical behaviour in consideration of ATCR weight if modified (depending on design).
Thermal-hydraulic interaction		Equivalent to the current CR. Cladding material is unchanged and the CRs are not strong heat generator.	Equivalent to the current CR. Cladding material is unchanged and the CR itself is not heat generator.
Licensibility	Capability of codes to simulate the behaviour	No data is available. However, it is expected that a licensing procedure for normal CRs is applicable.	
	Reproductibility and robustness of experiments in support to licensing		
	Methodology issues		

Table A.32. ATCR: Design extension conditions

	ATCR CRIEPI	ATCR AREVA
Mechanical strength and ductility	Cladding material is unchanged. The liquid phase formation temperature of cladding is higher than that in current CR.	The mechanical and geometric stability of the control rods are enhanced as the absorber materials do not experiencing either melting (Ag-In-Cd) or vapourisation (Cd) until much higher temperatures are achieved.
Thermal behaviour (melting)	Cladding material is unchanged. The melting point of SS is ～1 400°C.	Higher melting point of the material absorber candidates.
Chemical compatibility/stability (including high-temperature steam interaction)	Cladding material is unchanged. RE2O3 – MO2 is chemically stable even in water or moist air. High-temperature compatibility between RE2O3 – MO2 and SS in the steam atomsphere should be experimentally confirmed.	Not data available for oxidation reaction.
Fission product behaviour	No FP generation.	N/A.
Combustible gas production	Cladding material is unchanged. No gas produces from RE2O3 – MO2.	N/A.
Oxidation acceleration due to the exothermic HT reaction	Cladding material is unchanged. Oxidation reaction of RE2O3 – MO2 is less exothermic than that of SS cladding.	N/A.
Physical interaction of the molten material	The molten control materials are mixed and stabilised with the molten fuel (UO_2).	Need to be further evaluated.

Table A.33. ATCR: Fuel cycle issues

		ATCR CRIEPI	ATCR AREVA
Enrichment limit			
Mechanical strength and ductility		The change in CR stiffness due to the replacement of the neutron-absorbing materials should be confirmed. Cladding material is unchanged.	N/A.
Thermal behaviour		Cladding material is unchanged.	N/A.
Chemical stability			N/A.
Fission product behaviour		No FP generation.	N/A.
Transport	Mechanical behaviour (ductility)	Cladding material is unchanged.	N/A.
	Behaviour in fire		N/A.
	Impact of specific fabrication defects (e.g. scratches on the OD cladding, localised delamination)		N/A.
	Behaviour under accident conditions (punch test)		N/A.
Long-term storage	Hydride reorientation	N/A.	N/A.
	Corrosion behaviour	Lack of data on long-period storagecondition.	Lack of data on long-period storage condition.
	Impact of specific fabrication defects (e.g. scratches on the OD cladding, localised delamination)	Cladding material is unchanged.	N/A.
	Residual radioactivity	Need to evaluate radioactivation level of ATCR.	Need to evaluate radioactivation level of ATCR.
	Long-term microstructural/chemical composition evolution	Lack of data on long-period storagecondition.	Lack of data on long-period storagecondition.
Reprocessing	Tritium	N/A.	N/A.
	Shearing		N/A.
	Chemical compatibility with reprocessing reaction (nitric acid)		N/A.
	Reprocessibility		N/A.
Cost			

Appendix B. Attribute guides for advanced fuel designs

The following colour code was used for the qualitative assessment of the status of the attributes, which were evaluated for advanced fuel designs:

	properties not addressed; colour status not identified because of a lack of knowledge
	data available; results are good; concept is matured
	data available; results not good enough; further optimisation needed
	lack of data; not challenging
	lack of data and potentially challenging
	potential showstopper identified

Attribute evaluation for the Doped UO$_2$ fuel

Table B.1. Doped UO$_2$: Fabrication/manufacturability

		Cr$_2$O$_3$-doped UO$_2$ (AREVA)	Al$_2$O$_3$-Cr$_2$O$_3$-doped UO$_2$ (WH)	Ceramic microcell UO$_2$ dopant: SiO$_2$-TiO$_2$ (KAERI)	BeO-modified UO$_2$ up to 10 vol% (CGN)
Compatibility with large-scale production needs	Qualification of product and associated process	AREVA manufacturing lines are currently qualified to produce Cr$_2$O$_3$-doped UO$_2$ fuel.	Production lines qualified to produce reload quantities.	No qualified manufacturing line.	High-temperature hydrogen furnace and SPS are not licensed by NRC.
	Security of supply for each component (material)	No problem to supply Cr$_2$O$_3$ and UO$_2$ powders.	No problem.	No problem to supply component materials.	Beryllium is toxic and must be handled with care. Otherwise no trouble.
	Fabrication receipt criteria (technical file)	The technical file for Cr$_2$O$_3$-doped UO$_2$ fuel pellet exists.	The technical file exists.	Feasibility has been demonstrated at a laboratory scale.	—
	Long-tube fabrication	—	—	—	same as conventional process.
	Large-scale pellet fabrication	Several tonnes of Cr$_2$O$_3$-doped UO$_2$ fuel have been already produced on AREVA fuel manufacturing lines.		—	Traditional sintering methods can be used.
	Seal/welding			-	same as conventional process
	Fuel assembly manufacturing			-	same as conventional process
Compatibility with quality and uniformity standards	Quality control/inspectability	The lab methodologies to control Cr$_2$O$_3$-doped UO$_2$ fuel pellet exist.	Method exist.	Lack of data.	Toxic, otherwise same as conventional process.
	Reject ratio	Cr$_2$O$_3$-doped UO$_2$ fuel has a lower propensity to the formation of pellet flaws (e.g. missing pellet surface) during manufacturing.	Lack of data.	Lack of data.	Lack of data.

Table B.1. Doped UO₂: Fabrication/manufacturability (continued)

		Cr_2O_3-doped UO_2 (AREVA)	Al_2O_3-Cr_2O_3-doped UO_2 (WH)	Ceramic microcell UO_2 dopant: SiO_2-TiO_2 (KAERI)	BeO-modified UO_2 up to 10 vol% (CGN)
Cost		The manufacturing throughput for Cr_2O_3-doped UO_2 fuel is the same as for UO_2 fuel.	Lack of data.	Fabrication cost is estimated to be same with that of standard UO_2.	Traditional sintering methods are used. Minimal cost.
Impact on the industrial network (suppliers and subcontractors)		Same production lines as for UO_2.	Same production lines as for UO_2.	This concept uses existing infrastructure, experience and expertise to the maximum extent possible.	same as conventional process.

Table B.2. Doped UO₂: Normal operation and AOOs

		Cr_2O_3-doped UO_2 (AREVA)	Al_2O_3-Cr_2O_3-doped UO_2 (WH)	Ceramic microcell UO_2 dopant: SiO_2-TiO_2 (KAERI)	BeO-modified UO_2 up to 10 vol% (CGN)
Reactor operation	Behaviour in normal operation	At least equal to UO_2 fuel pellet with fission gas release and internal pressure benefit at end of life.		Enhanced FPs Retention. Irradiation test programme is ongoing.	Bue to higher conductivity of UO_2-10%vol. BeO,better fission gas behaviour and thermal-mechanical were found.(According to investigation from Purdue).
	Behaviour in AOOs	The ramp testing programme demonstrates that the Cr_2O_3-doped fuel PCI failure threshold brings benefits in comparison to standard UO_2 fuel. No adverse rod deformation observed with that ramp programme.	Ramp test programme show enhanced behaviour wrt UO_2 due to significantly greater creep deformation at high temperatures.	Enhaced performance is expected. Irradiation test programme is ongoing.	Behaviour in ramp conditions and PCI are expected to be better than for UO_2 standard fuel due to higher conductivity of UO_2-10%vol. Be.(According to investigation from Purdue and AREVA).
	Operating cycle length (12, 18, 24 months ?...)			Irradiation test programme is ongoing.	
	Reactivity control systems interaction			It will be same with that of standard UO_2. Irradiation test programme is ongoing.	

Table B.2. Doped UO$_2$: Normal operation and AOOs (continued)

		Cr$_2$O$_3$-doped UO$_2$ (AREVA)	Al$_2$O$_3$-Cr$_2$O$_3$-doped UO$_2$ (WH)	Ceramic microcell UO$_2$ dopant: SiO$_2$-TiO$_2$ (KAERI)	BeO-modified UO$_2$ up to 10 vol% (CGN)
Reactor operation	Impact of load following on the overall cladding behaviour/properties	No detrimental impact anticipated.		Enhaced performance is expected. Irradiation test programme is ongoing.	
	Specific behaviour of leakers during irradiation (further degradation with risk of fuel fragments dispersion)	A dedicated testing program highlighted enhanced post-primary defect pellet behaviour of the Cr$_2$O$_3$-doped UO$_2$ fuel: the washout rate of the Cr$_2$O$_3$-doped pellets has been shown to be reduced up to a factor of 5 in comparison to non-doped fuel types.	Specific experiment show the Cr$_2$O$_3$-Al$_2$O$_3$-doped pellet had less washout that standard UO$_2$.	Irradiation test programme is ongoing.	
	Impact of specific fabrication defects (e.g. scratches on the cladding OD, localised delamination)			Enhaced performance is expected. Irradiation test programme is ongoing.	
	Neutron penalty	Slight reduction in fissile mass due to the addition of Cr$_2$O$_3$ in UO$_2$ but high-pellet density is easily reached to offset that effect.	The dopant additions induce a slight reduction in the fissile mass which is compensated by higher pellet density.	Negligible Neutron penalty Irradiation test programme is ongoing.	Having more Berylium in the fuel will decrease the Uranium density. Si and C both have negligible absorption cross-sections.

Table B.2. Doped UO$_2$: Normal operation and AOOs (continued)

		Cr$_2$O$_3$-doped UO$_2$ (AREVA)	Al$_2$O$_3$-Cr$_2$O$_3$-doped UO$_2$ (WH)	Ceramic microcell UO$_2$ dopant: SiO$_2$-TiO$_2$ (KAERI)	BeO-modified UO$_2$ up to 10 vol% (CGN)
Mechanical properties	Creep	Improved viscoplastic properties.	Greater creep deformation at high temperatures.	Enhaced performance is expected.	
	Elastic properties				Better than regular UO$_2$.
	Thermal expansion				Better than regular UO$_2$ (According to CGN work).
	Ductility				
	Toughness				
	Strength				
	Fatigue				
	Ramp behaviour				Better than regular UO$_2$ (According to investigation of Purdue University).
	Adhesion of coatings				
	Resistance to debris				
	Resistance to fretting/wear				
	Circumferential buckling				
	Rod bow				
	Assembly bow				

Table B.2. Doped UO$_2$: Normal operation and AOOs (continued)

		Cr$_2$O$_3$-doped UO$_2$ (AREVA)	Al$_2$O$_3$-Cr$_2$O$_3$-doped UO$_2$ (WH)	Ceramic microcell UO$_2$ dopant: SiO$_2$-TiO$_2$ (KAERI)	BeO-modified UO$_2$ up to 10 vol% (CGN)
Thermal behaviour	Conductivity	Cr$_2$O$_3$-doped UO$_2$ fuel thermal conductivity equivalent to UO$_2$ fuel from 1 200K, below a slight degradation is measured.	No measurable differences wrt UO$_2$.	Almost same with that of standard UO$_2$.	About 50% higher than UO$_2$ at room temperature.(According to CGN work and results from Purdue university).
	Specific heat	The Cr$_2$O$_3$ addition has insignificant effect on reference UO$_2$ specific heat.	No measurable differences wrt UO$_2$.	Almost same with that of standard UO$_2$.	
	Melting	Cr$_2$O$_3$ addition has an insignificant effect on non-doped UO$_2$ fuel melting temperature.	No measurable differences wrt UO$_2$.	Ceramic addition has an insignificant effect on non-doped UO$_2$ fuel melting temperature.	Above 2 400°C – according to investigation and prepare work of CGN.
Fuel/cladding interaction	Chemical compatibility (fuel/cladding) / stability			Enhanced performance is expected. Irradiation test programme is ongoing.	Toxic and volatise at high temperature.
	Resistance to PCMI	The ramp testing programme shows no exacerbated gaseous swelling effect with Cr$_2$O$_3$-doped fuel that could lead to detrimental fuel rod deformation.		Enhanced performance is expected. Low-thermal expansion. Low FG release.	internal pressure decrease, specific result is not definited.
	Resistance to SCC/I	The ramp testing programme demonstrates that the Cr$_2$O$_3$-doped fuel PCI failure threshold brings benefits in comparison to standard UO$_2$ fuel.	Higher resistance wrt UO$_2$.	Enhanced performance is expected. Reduce the mobility of FPs. Low pellet temperature & Physical protection.	
	Tritium permeation				May be existed, will be considered later.
	Permeability (hydrogen, fission products)				Krypton may be found.
	Leak-tightness				

Table B.2. Doped UO₂: Normal operation and AOOs (continued)

		Cr_2O_3-doped UO_2 (AREVA)	Al_2O_3-Cr_2O_3-doped UO_2 (WH)	Ceramic microcell UO_2 dopant: SiO_2-TiO_2 (KAERI)	BeO-modified UO_2 up to 10 vol% (CGN)
Impact of irradiation	Irradiation limit			Reduced FG release. Irradiation test programme is ongoing.	
	Fission product behaviour	In baseload conditions and high BU, FGR measurements of Cr_2O_3-doped UO_2 are in the lower bound of the UO_2 fuel data. Under power transient conditions, FGR with Cr_2O_3-doped UO_2 fuel is significantly reduced due to significant intragranular fission gasesous precipitation.	Under bump test, the majority of bubbles were found inside the grains of the Cr_2O_3-Al_2O_3-doped pellets which is consistent with a lower rate of fission gas release.	Enhanced FPs Retention. Irradiation test programme is ongoing.	Lower FGR release expected due to lower fuel temperatures.
	Embrittlement	NA.		Connected metal network. Irradiation test programme is ongoing.	
	Irradiation-induced microstructural /chemical composition evolution	Very high microstructural and chemical stability observed up to high BU.		Maintaining a cell structure is a main concern. Irradiation test programme is ongoing.	
	Dimensional stability (growth/swelling)	Very high-dimensional stability up to high BU: low in-reactor densification and the fuel solid swelling kinetic of the Cr_2O_3-doped UO_2 fuel is similar to that for the reference UO_2 fuel.	Low in-reactor densification and similar swelling rate incomparison to UO_2.	Irradiation test programme is ongoing.	

Table B.2. Doped UO$_2$: Normal operation and AOOs (continued)

		Cr$_2$O$_3$-doped UO$_2$ (AREVA)	Al$_2$O$_3$-Cr$_2$O$_3$-doped UO$_2$ (WH)	Ceramic microcell UO$_2$ dopant: SiO$_2$-TiO$_2$ (KAERI)	BeO-modified UO$_2$ up to 10 vol% (CGN)
Coolant interaction	Chemical compatibility with and impact on coolant chemistry	A dedicated testing program highlighted enhanced post-primary defect pellet behaviour of the Cr$_2$O$_3$-doped UO$_2$ fuel: the washout rate of the Cr$_2$O$_3$-doped pellets has been shown to be reduced up to a factor of 5 in comparison to non-doped fuel types.	Specific experiment show the Cr$_2$O$_3$-Al$_2$O$_3$-doped pellet had less washout that standard UO$_2$.	No chemical reaction with coolant water.	
	Oxidation behaviour				Same as UO$_2$.
	Shadow corrosion (e.g. compatibility with spacer grids)				
	Hydriding behaviour				
	Erosion				
	Crud deposition				
	Thermal-hydraulic interaction (DNB issue)				
Licensibility	Capability of codes to simulate the behaviour	Thermal-mechanical models are being refined to properly simulate Cr$_2$O$_3$-doped fuel and to allow taking full benefit of the enhanced behaviour of that fuel in-service.	the modelling of Cr$_2$O$_3$-Al$_2$O$_3$-doped fuel requires very little modification to that used for standard UO$_2$ fuel.		
	Reproductibility and robustness of experiments in support to licensing	The qualification programme under BWR and PWR irradiation is completed. Results show a robust behaviour and clear improvements for fuel reliability and performance.			
	Methodology issues	Nothing to report.			

Table B.3. Doped UO₂: Design-basis accidents

		Cr_2O_3-doped UO_2 (AREVA)	Al_2O_3-Cr_2O_3-doped UO_2 (WH)	Ceramic microcell UO_2 dopant: SiO_2-TiO_2 (KAERI)	BeO-modified UO_2 up to 10 vol% (CGN)
Reactor operation	Behaviour in accident transients	No data available (LOCA – RIA).	No data available (LOCA – RIA).	No data available (LOCA – RIA).	Compare with UO_2, UO_2-BeO shows lower system temperature under LOCA condition and delay the fuel rod failure.
	Impact of load following on the overall cladding behaviour /properties				
	Specific behaviour of leakers that appeared during normal operation (lower resistance during a DBA)				
High-temperature mechanical properties	Creep	Improved viscoplastic properties, more plastic.	Greater creep deformation at high temperatures.	Enhaced performance is expected.	
	Ductility				
	Toughness				
	Strength				
	Fatigue				
	Adhesion of coating				
Thermal behaviour	Conductivity	At high temperature (up to 3 000 K) the thermal conductivity of unirradiated Cr_2O_3-doped UO_2 fuel is similar to that for UO_2 fuel.	No measurable differences wrt UO_2.	Almost same with that of standard UO_2	The results of testing in high temperature show that the conductivity is 40% more than UO_2.
	Specific heat	No data available above 1 500 K	No data available above 1 500 K.	Almost same with that of standard UO_2	
	Melting	Cr_2O_3 addition has an insignificant effect on non-doped UO_2 fuel melting temperature.	No measurable differences wrt UO_2.	Lack of data	above 2 400°C – according to investigation and prepare work of CGN.

Table B.3. Doped UO₂: Design-basis accidents (continued)

		Cr₂O₃-doped UO₂ (AREVA)	Al₂O₃-Cr₂O₃-doped UO₂ (WH)	Ceramic microcell UO₂ dopant: SiO₂-TiO₂ (KAERI)	BeO-modified UO₂ up to 10 vol% (CGN)
Fuel/cladding interaction	Chemical compatibility/stability (e.g. oxidation behaviour)	Very high-dimensional, microstructural and chemical stability.		Enhanced FPs Retention. Irradiation test programme is ongoing.	
	Fission product behaviour			Enhanced FPs Retention. Irradiation test programme is ongoing.	The results of simulation show that the plenum pressure of UO₂-BeO fuel system is lower than UO₂.
	Fission gas generation	The same as UO₂.	The same as UO₂.	Basically UO₂. Irradiation test programme is ongoing.	
	Resistance to PCI			Enhaced performance is expected.	PCI behaves probably better than UO₂.
	Environment interaction of the inner cladding layer				
LOCA	High-temperature steam oxidation (1200°C)				BeO and UO₂ have good chemical compatibility with steam.
	HT breakaway oxidation				
	Quench tolerance/Post-Quench mechanical behaviour				
	Degradation mode of the cladding				
	Phase transformation, H and O, diffusion and distribution				

Table B.3. Doped UO₂: Design-basis accidents (continued)

		Cr₂O₃-doped UO₂ (AREVA)	Al₂O₃-Cr₂O₃-doped UO₂ (WH)	Ceramic microcell UO₂ dopant: SiO₂-TiO₂ (KAERI)	BeO-modified UO₂ up to 10 vol% (CGN)
RIA	Degradation mode of the cladding				
	Mechanical behaviour (PCMI high speed ramp/tensile test at high temperatures)				
	Steam oxidation at 1 480°C/ 1 500°C			Enhaced performance is expected.	BeO and UO₂ have good chemical compatibility with steam, and CGN will operate a steam oxidation test in 1 500°C.
Seismic behaviour	Fuel assembly mechanical behaviour				
Thermal-hydraulic interaction					
Licensibility	Capability of codes to simulate the behaviour	No dedicated modelling available for accident conditions – no problem anticipated.	No dedicated modelling available for accident conditions – no problem anticipated.		CGN is developing the code that is suitable to BeO-UO₂ pellets.
	Reproductibility and robustness of experiments in support to licensing				Lack of data.
	Methodology issues				CGN is developing the code that is suitable to BeO-UO₂ pellets.

Table B.4. Doped UO$_2$: Design extension conditions

	Cr$_2$O$_3$-doped UO$_2$ (AREVA)	Al$_2$O$_3$-Cr$_2$O$_3$-doped UO$_2$ (WH)	Ceramic microcell UO$_2$ dopant: SiO$_2$-TiO$_2$ (KAERI)	BeO-modified UO$_2$ up to 10 vol% (CGN)
Mechanical strength and ductility	-	-		-
Thermal behaviour (melting)	Cr$_2$O$_3$ addition has an insignificant effect on non-doped UO$_2$ fuel melting temperature.	No measurable differences wrt UO$_2$.	Ceramic addition has an insignificant effect on non-doped UO$_2$ fuel melting behaviour.	Above 2 400°C (according to investigation and prepare work of CGN).
Chemical compatibility/stability (including high-temperature steam interaction)	-	-	-	BeO and UO$_2$ have good chemical compatibility.
Fission product behaviour				The results of simulation show that the plenum pressure of UO$_2$-BeO fuel system is lower than UO$_2$.
Combustible gas production	The same as UO$_2$.		The same as UO$_2$.	BeO and UO$_2$ have good chemical compatibility with steam.
Oxidation acceleration due to the exothermic HT reaction	-	-	-	
Physical interaction of the molten material	-	-	-	

Table B.5. Doped UO$_2$: Fuel cycle issues

		Cr$_2$O$_3$-doped UO$_2$ (AREVA)	Al$_2$O$_3$-Cr$_2$O$_3$-doped UO$_2$ (WH)	Ceramic microcell UO$_2$ dopant: SiO$_2$-TiO$_2$ (KAERI)	BeO-modified UO$_2$ up to 10 vol% (CGN)
Enrichment limit		The same as for UO$_2$.	The same as for UO$_2$.	The same limit.	Higher ^{235}U/U enrichment is needed due to lower uranium content, ^{235}U/U < 5% for UO$_2$.
Mechanical strength and ductility					
Thermal behaviour		The same as UO$_2$.	No measurable differences wrt UO$_2$.	The same as UO$_2$.	
Chemical stability		The same as UO$_2$.		The same as UO$_2$.	Toxic.

Table B.5. Doped UO₂: Fuel cycle issues (continued)

		Cr₂O₃-doped UO₂ (AREVA)	Al₂O₃-Cr₂O₃-doped UO₂ (WH)	Ceramic microcell UO₂ dopant: SiO₂-TiO₂ (KAERI)	BeO-modified UO₂ up to 10 vol% (CGN)
Fission product behaviour		In baseload conditions and high BU, FGR measurements of Cr₂O₃-doped UO₂ are in the lower bound of the UO₂ fuel data.		Reduced FG release is expected.	
Transport	Mechanical behaviour (ductility)				
	Behaviour in fire				
	Impact of specific fabrication defects (e.g. scratches on the OD cladding, localised delamination)				
	Behaviour under accident conditions (punch test)				
Long-term storage	Hydride reorientation				
	Corrosion behaviour				
	Impact of specific fabrication defects (e.g. scratches on the OD cladding, localised delamination)				
	Residual radioactivity				
	Long-term microstructural/chemical composition evolution	No problem anticipated considering the very high-dimensional, microstructural and chemical stability observed in baseload conditions.	No problem anticipated.	Lack of data, but not challenging.	

Table B.5. Doped UO₂: Fuel cycle issues (continued)

		Cr₂O₃-doped UO₂ (AREVA)	Al₂O₃-Cr₂O₃-doped UO₂ (WH)	Ceramic microcell UO₂ dopant: SiO₂-TiO₂ (KAERI)	BeO-modified UO₂ up to 10 vol% (CGN)
Reprocessing	Tritium				
	Shearing				
	Chemical compatibility with reprocessing reaction (nitric acid)	Scoping studies do not highlight incompatibility issues.	No problem anticipated.		BeO is not soluble in nitric acid.
	Reprocessibility	Scoping studies do not highligh incompatibility issues.	No problem anticipated.		
Cost		The same as for UO₂.			BeO-UO₂ may be expensive than UO₂.

Attribute evaluation for the high-thermal conductivity fuels

Table B.6. High-thermal conductivity fuels: Fabrication/manufacturability

		CERMET UO₂-10vol% Mo (CEA)	SiC/diamond modified UO₂ up to 10 vol% (UFL)	Mo-modified UO₂ up to 10 vol% (UFL)	Metalic microcell UO₂ 5 vol% Mo or -Cr (KAERI)
Compatibility with large-scale production needs	Qualification of product and associated process	Powder metallurgy process only in laboratory facility has been used to fabricate UO₂-80%vol Mo pellets. But with lower 10%vol. content of Mo, it could be another type of fabrication.	SPS is not licensed by NRC.	Traditional sintering is licensed by the NRC.	No qualified manufacturing line.

Table B.6. High-thermal conductivity fuels: Fabrication/manufacturability (continued)

		CERMET UO$_2$-10vol% Mo (CEA)	SiC/diamond modified UO$_2$ up to 10 vol% (UFL)	Mo-modified UO$_2$ up to 10 vol% (UFL)	Metalic microcell UO$_2$ 5 vol% Mo or -Cr (KAERI)
	Security of supply for each component (material)	UO$_2$ and natural Mo are available. Natural Mo is neutronically absorbant ~2.65 barns. To avoid this absorption, the use of Mo "light", ie. neutronically transparent, could be used but may be more difficult to provide.	Silicon Carbide whiskers are not a secured material. No trouble.	Molybdenum is not a secured material. No Trouble.	No problem to supply component materials.
	Fabrication receipt criteria (technical file)				Feasibility has been demonstrated at a laboratory scale.
	Long-tube fabrication	-	The same as conventional process.	The same as conventional process.	-
	Large-scale pellet fabrication	Lack of data.	Spark plasma sintering yields the best results for this type of fuel. Very few facilities with large-scale SPS capabilities.	Traditional sintering methods are used.	
	Seal/welding		The same as conventional process.	The same as conventional process.	-
	Fuel assembly manufacturing		The same as conventional process.	The same as conventional process.	-
Compatibility with quality and uniformity standards	Quality control/inspectability		The same as conventional process.	The same as conventional process.	
	Reject ratio				
Cost		Higher cost due to ^{235}U/U higher enrichment and Mo supplying (depending on Mo "light" or not using, and more complex fabrication lines.	Implementation of mass production SPS facilities.	Traditional sintering methods are used. Minimal cost.	Lack of data. Fabrication cost is estimated to be increased about 10% including the enrichment cost.
Impact on the industrial network (suppliers and subcontractors)		Supply UO$_2$ with higher ^{235}U/U content, supply of natural Mo (or Mo light).		The same as conventional process.	This concept uses existing infrastructure, experience and expertise to the maximum extent possible.

Table B.7. High-thermal conductivity fuels: Normal operation and AOOs

		CERMET UO_2-10vol% Mo (CEA)	SiC/diamond modified UO_2 up to 10 vol% (UFL)	Mo-modified UO_2 up to 10 vol% (UFL)	Metalic microcell UO_2 5 vol% Mo or Cr (KAERI)
Reactor operation	Behaviour in normal operation	Lack of data but not challenging. Due to higher conductivity of UO_2-10%vol. Mo, lower operating temperatures are expected, enabling to have also lower FGR.			Enhaced thermal conductivity. Irradiation test programme is ongoing.
	Behaviour in AOOs	Lack of data but not challenging. Behaviour in ramp conditions is expected to be better than for UO_2 standard fuel due to higher conductivity of UO_2-10%vol. Mo.			Enhaced performance is expected. Irradiation test programme is ongoing.
	Operating cycle length (12,18,24 months ?...)	The cycle length will depend on the UO_2 particules $^{235}U/U$ enrichment (use or not of Mo light) and burnable poison content.			Slightely higher enrichment is required to keep the fuel cycle length of standard UO_2. Irradiation test programme is ongoing.
	Reactivity control systems interaction	Natural Mo presents neutronic absorption: Mo = 2.65 barn (neutronic absorption should be lower with "light" Mo).			It will be same with that of standard UO_2. Irradiation test programme is ongoing.
	Impact of load following on the overall cladding behaviour /properties				Enhaced performance is expected. Irradiation test programme is ongoing.
	Specific behaviour of leakers during irradiation (further degradation with risk of fuel fragments dispersion)	Mo is prone to catastrophic oxidation under water vapour as temperature exceeds about 700°C, the point above which MoO_3 forms eutectic mixtures with Fe, Ni and Cr oxides. The oxide MoO3 melts at 795°C. Catastrophic oxidation rapidly renders a metal into a useless powdery oxide.			Reaction with high-temperature steam is a concern. Additives is being modified and optimised. Irradiation test programme is ongoing.
	Impact of specific fabrication defects (e.g. scratches on the cladding OD, localised delamination)				Enhaced performance is expected. Irradiation test programme is ongoing.

Table B.7. High-thermal conductivity fuels: Normal operation and AOOs (continued)

		CERMET UO$_2$-10vol% Mo (CEA)	SiC/diamond modified UO$_2$ up to 10 vol% (UFL)	Mo-modified UO$_2$ up to 10 vol% (UFL)	Metalic microcell UO$_2$ 5 vol% Mo or Cr (KAERI)
	Neutron penalty	Reduction in fissile mass due to the addition of Mo in UO$_2$ and neutron penalty due to the neutronic absorption of natural Mo = 2.65 barn (not the case for "light Mo").	Having more SiC in the fuel will decrease the uranium density. Si and C both have negligible absorption cross-sections.	Having more molybdenum in the fuel will decrease the uranium density. Si and C both have negligible absorption cross-sections.	Slightely higher enrichment is required to compensate the neutron penalty from additives. Irradiation test programme is ongoing.
Mechanical properties	Creep				Enhaced performance is expected.
	Elastic properties		Better than regular UO$_2$.	Better than regular UO$_2$.	
	Thermal expansion				
	Ductility				
	Toughness				
	Strength				
	Fatigue				
	Ramp behaviour				
	Adhesion of coatings				
	Resistance to debris				
	Resistance to fretting/wear				
	Circumferential buckling				
	Rod bow				
	Assembly bow				

Table B.7. High-thermal conductivity fuels: Normal operation and AOOs (continued)

		CERMET UO$_2$-10vol% Mo (CEA)	SiC/diamond modified UO$_2$ up to 10 vol% (UFL)	Mo-modified UO$_2$ up to 10 vol% (UFL)	Metalic microcell UO$_2$ 5 vol% Mo or Cr (KAERI)
Thermal behaviour	Conductivity		With 10%vol SiC the results were as follows: At 100°C 54.9% increase. At 500°C 57.4% increase. At 900°C 62.1% increase.	At 5 wt% and 1 000 K there is a 32.2% increase.	Enhanced thermal conductivity.
	Specific heat				Almost same with that of standard UO$_2$.
	Melting	Mo addition to UO$_2$ leads to a slight reduction of the compsite fuel melting temperatures (TmMo = 2623°C, TmUO$_2$= 2847°C).			Metal addition has an insignificant effect on non-doped UO$_2$ fuel melting temperature.
Fuel/cladding interaction	Chemical compatibility (fuel/cladding) / stability	Mo is compatible with stainless steel cladding. No data for compatibility with Zr cladding.			Enhaced performance is expected. Irradiation test programme is ongoing.
	Resistance to PCMI	Probably better than UO$_2$ due to lower temperature operation and probably lower swelling compared to UO$_2$.			Enhaced performance is expected. Low-thermal expansion. Low FG release.
	Resistance to SCC/I	If Mo surrounds physically the UO$_2$, the Mo could hold back the corrosive FP as iodine and prevent them to reach the cladding and prevent to corrode it.			Enhaced performance is expected. Reduce the mobility of FPs. Low pellet temperature and physical protection.
	Tritium permeation				
	Permeability (hydrogen, fission products)				
	Leak-tightness				

Table B.7. High-thermal conductivity fuels: Normal operation and AOOs (continued)

		CERMET UO$_2$-10vol% Mo (CEA)	SiC/diamond modified UO$_2$ up to 10 vol% (UFL)	Mo-modified UO$_2$ up to 10 vol% (UFL)	Metalic microcell UO$_2$ 5 vol% Mo or Cr (KAERI)
Impact of irradiation	Irradiation limit				Reduced FG release and pellet operating temperature. Irradiation test programme is ongoing.
	Fission product behaviour	Lower FGR release expected due to lower fuel temperatures.			Enhanced FPs retention. Irradiation test programme is ongoing.
	Embrittlement				Connected metal network. Irradiation test programme is ongoing.
	Irradiation-induced microstructural / chemical composition evolution				Maintaining a cell structure is a main concern. Irradiation test programme is ongoing.
	Dimensional stability (growth/swelling)				Irradiation test programme is ongoing.
Coolant interaction	Chemical compatibility with and impact on coolant chemistry	The same as reactor operation, specific behaviour of leakers during irradiation (further degradation with risk of fuel fragments dispersion).			No chemical reaction with coolant water.
	Oxidation behaviour	The same as reactor operation, specific behaviour of leakers during irradiation (further degradation with risk of fuel fragments dispersion).			Reaction with high-temperature steam is a concern. Additives is being modified and optimised.
	Shadow corrosion (eg: compatibility with spacer grids)				
	Hydriding behaviour				
	Erosion				
	Crud deposition				
	Thermal-hydraulic interaction (DNB issue)				

Table B.7. High-thermal conductivity fuels: Normal operation and AOOs (continued)

		CERMET UO$_2$-10vol% Mo (CEA)	SiC/diamond modified UO$_2$ up to 10 vol% (UFL)	Mo-modified UO$_2$ up to 10 vol% (UFL)	Metalic microcell UO$_2$ 5 vol% Mo or Cr (KAERI)
Licensibility	Capability of codes to simulate the behaviour				
	Reproductibility and robustness of experiments in support to licensing				
	Methodology issues	Nothing to report.			

Table B.8. High-thermal conductivity fuels: Design-basis accidents

		CERMET UO$_2$-10vol% Mo (CEA)	SiC/diamond modified UO$_2$ up to 10 vol% (UFL)	Mo-modified UO$_2$ up to 10 vol% (UFL)	Metalic microcell UO$_2$ 5vol% Mo or Cr (KAERI)
Reactor operation	Behaviour in accident transients				No data available (LOCA – RIA).
	Impact of load following on the overall cladding behaviour /properties				
	Specific behaviour of leakers that appeared during normal operation (lower resistance during a DBA)				
High-temperature mechanical properties	Creep	No data.			Enhaced performance is expected.
	Ductility				
	Toughness				
	Strength				
	Fatigue				
	Adhesion of coating				

Table B.8. High-thermal conductivity fuels: Design-basis accidents (continued)

		CERMET UO$_2$-10vol% Mo (CEA)	SiC/diamond modified UO$_2$ up to 10 vol% (UFL)	Mo-modified UO$_2$ up to 10 vol% (UFL)	Metalic microcell UO$_2$ 5vol% Mo or Cr (KAERI)
Thermal behaviour	Conductivity	Remains better than UO$_2$ except if there is a contact with the water coolant: then MoO$_3$ is formed with a thermal conductivity probably less than the UO$_2$ one.			Remains better than UO$_2$.
	Specific heat				Lack of data.
	Melting	T melting Mo= 2 623°C, T melting UO$_2$= 2 865°C. But if MoO$_3$ is formed by oxidation (see hereafter "LOCA" table), it melts at 795°C.			Lack of data.
Fuel/cladding interaction	Chemical compatibility /stability (e.g. oxidation behaviour)	Above 700°C, if MoO3 is formed by oxidation (see hereafter "LOCA table"), it forms then eutectic mixtures with Fe, Ni and Cr oxides.			Lack of data.
	Fission product behaviour	UO$_2$-80%Mo FGR is lower than UO$_2$ at 1 350 °C (out-of-pile tests). But results may be not similar with lower 10%vol Mo content.			Enhanced FPs Retention. Irradiation test programme is ongoing.
	Fission gas generation				Basically UO$_2$. Irradiation test programme is ongoing.
	Resistance to PCI	UO$_2$-10%vol. Mo behaves probably better than UO$_2$.			Enhaced performance is expected.
	Environment interaction of the inner cladding layer				

Table B.8. High-thermal conductivity fuels: Design-basis accidents (continued)

		CERMET UO$_2$-10vol% Mo (CEA)	SiC/diamond modified UO$_2$ up to 10 vol% (UFL)	Mo-modified UO$_2$ up to 10 vol% (UFL)	Metalic microcell UO$_2$ 5vol% Mo or Cr (KAERI)
LOCA	High-temperature steam oxidation (1 200°C)	Molybdenum is prone to catastrophic oxidation under water vapour when temperature exceed ~700°C, the point above which MoO$_3$ forms eutectic mixtures with Fe, Ni and Cr oxides. The oxide MoO$_3$ melts at 795°C. Catastrophic oxidation rapidly renders a metal into a useless powdery oxide.			Reaction of metallic wall with high-temperature steam is a concern. Additives is being modified and optimised.
	HT breakaway oxidation				
	Quench tolerance/Post-Quench mechanical behaviour				
	Degradation mode of the cladding				
	Phase transformation, H and O, diffusion and distribution				
RIA	Degradation mode of the cladding				
	Mechanical behaviour (PCMI high speed ramp/tensile test at high temperatures)				
	Steam oxidation at 1 480°C/1 500°C	Molybdenum is prone to catastrophic oxidation as temperature exceed about 700°C. See above the "LOCA table".			Reaction of metallic wall with high-temperature steam is a concern. Additives is being modified and optimised.
Seismic behaviour	Fuel assembly mechanical behaviour				
Thermal-hydraulic interaction					
Licensibility	Capability of codes to simulate the behaviour				
	Reproductibility and robustness of experiments in support to licensing				
	Methodology issues				

Table B.9. High-thermal conductivity fuels: Design extension conditions

	CERMET UO₂-10vol% Mo (CEA)	SiC/diamond modified UO₂ up to 10 vol% (UFL)	Mo-modified UO₂ up to 10 vol% (UFL)	Metalic microcell UO₂ 5 vol% Mo or Cr (KAERI)
Mechanical strength and ductility	-	-	-	
Thermal behaviour (melting)	T melting Mo= 2 623°C, T melting UO₂= 2 865°C. But if MoO₃ is formed by oxidation (see under LOCA table), it melts at 795°C.			Metal addition has an insignificant effect on non-doped UO₂ fuel melting behaviour.
Chemical compatibility/stability (including high-temperature steam interaction)	Molybdenum is prone to catastrophic oxidation when temperature exceeds about 700°C. See Normal operating conditions. See Design Basic Accident.	-	-	-
Fission product behaviour	No data with UO₂-10% vol. Mo. But with UO₂ -80%vol Mo, FGR is nearly the same as UO₂ at 1 750°C (out-of-pile tests).			
Combustible gas production	Steam oxidation of Mo may lead the production of hydrogen.			Steam oxidation of metal additive may lead the production of hydrogen.
Oxidation acceleration due to the exothermic HT reaction	-			
Physical interaction of the molten material	At above 700°C, MoO₃ forms eutectic mixtures with Fe, Ni and Cr oxides. The oxide MoO₃ melts at 795°C.			

Table B.10. High-thermal conductivity fuels: Fuel cycle issues

		CERMET UO$_2$-10vol% Mo (CEA)	SiC/diamond modified UO$_2$ up to 10 vol% (UFL)	Mo-modified UO$_2$ up to 10 vol% (UFL)	Metalic microcell UO$_2$ 5vol% Mo or Cr (KAERI)
Enrichment limit		Higher ^{235}U/U enrichment is needed due to lower uranium content and natural molydenum absorption – less with Mo "light" (Actual enrichment facilities are limited to about ^{235}U/U < 7% for UO$_2$).			Higher ^{235}U/U enrichment is needed due to lower uranium content and natural molydenum absorption – less with Mo "light" (actual enrichment facilities are limited to about ^{235}U/U < 7% for UO$_2$).
Mechanical strength and ductility					
Thermal behaviour		Lack of data, but not challenging.			Lack of data, but not challenging.
Chemical stability		Lack of data, but not challenging.			Lack of data, but not challenging.
Fission product behaviour		Long-lived fission product technetium ^{99}Tc is formed (less with Mo "light").			Reduced FPs release is expected.
Transport	Mechanical behaviour (ductility)				
	Behaviour in fire				
	Impact of specific fabrication defects (e.g. scratches on the OD cladding, localised delamination)				
	Behaviour under accident conditions (punch test)				

Table B.10. High-thermal conductivity fuels: Fuel cycle issues (continued)

		CERMET UO$_2$-10vol% Mo (CEA)	SiC/diamond modified UO$_2$ up to 10 vol% (UFL)	Mo-modified UO$_2$ up to 10 vol% (UFL)	Metalic microcell UO$_2$ 5vol% Mo or Cr (KAERI)
Long-term storage	Hydride reorientation				
	Corrosion behaviour				
	Impact of specific fabrication defects (e.g. scratches on the OD cladding, localised delamination)				
	Residual radioactivity	Long-lived fission product technetium ^{99}Tc is formed (less with Mo "light").			
	Long-term microstructural / chemical composition evolution	Lack of data, but not challenging.			Lack of data, but not challenging.
Reprocessing	Tritium				
	Shearing				
	Chemical compatibility with reprocessing reaction (nitric acid)	Mo is soluble in nitric acid.			
	Reprocessibility	Reprocessing of UO$_2$-Mo is not compatible with actual facilities and needs R&D on representative objects: the process must be adapted to separate UO$_2$ from metal Mo.			
Cost		UO$_2$-10%vol. Mo may be more expansive to reprocess than UO$_2$.			

Table B.11. High-density fuels: Fabrication/manufacturability

		Uranium nitride and/or (U, Pu)-nitride (France, WH)	Uranium silicide (WH, NRG)	Metal, U-10wt%Zr (Japan, based on knowledge as FBR fuel)	Metal, U-50wt%Zr (AREVA NP, based on literature survey)	Carbide, (U,Pu)C (CEA)
Compatibility with large-scale production needs	Qualification of product and associated process	Today none manufacturing line is qualified to produce uranium and/or plutonium nitride fuel in France.	Today no manufacturing is qualified to produce uranium silicide pellets in large quantities. Production of pellets that meet or exceed 95% TD with acceptable impurity levels has been successful. Alternative production routes for making the U_3Si_2 powder from UF6 or UF4 are under development.	Today, there is no engineering-scale manufacturing facility for U-Zr fuel. However, the fabrication technology has been basically proven.	Fabrication technologies exist.	Carbothermic reduction of oxide powders is mostly used for (U, Pu)C pellet fabrication.
	Security of supply for each component (material)	The security of N15 supply may be a problem.	No problem in sourcing raw materials either from metal route or from possible UF6/UF4 routes.	No problem in sourcing raw materials.	No problem in sourcing raw materials.	No identified problem.
	Fabrication receipt criteria (technical file)	The technical file for uranium and/or plutonium nitride fuel pellet already exist at a laboratory scale.	Specifications for U_3Si_2 powder and pellets have been developed by Westinghouse.	Enough experiences are accumulated for U-Zr fuel slug fabrication in ANL (INL), US, CRIEPI, Japan, KAERI, Korea, etc.	Not an issue considering past experiences on U-10wt%Zr.	The Los Alamos US facility has fabricated (U, Pu)C pellets that met or even exceeded the stringent internal quality insurance requirements. Today no manufacturing line is qualified to produce uranium and/or plutonium carbide fuel in France.
	Long-tube fabrication		Long-tube fabrication should not be an issue.	NA		

Table B.11. High-density fuels: Fabrication/manufacturability (continued)

		Uranium nitride and/or (U, Pu)-nitride (France, WH)	Uranium silicide (WH, NRG)	Metal, U-10wt%Zr (Japan, based on knowledge as FBR fuel)	Metal, U-50wt%Zr (AREVA NP, based on literature survey)	Carbide, (U,Pu)C (CEA)
Compatibility with large-scale production needs	Large-scale pellet fabrication	May be challenging due to N15 enrichment and UN powder pyrophoricity.	May be challenging due to lack of industrial manufacturing process other than arc melting. Other methods are being explored. Room temperature resistance to oxidation of fine U_3Si_2 powder in air is a possible issue, although U_3Si_2 is reported by Shimizu as RT stable.	For U-Zr fuel slug, routine procedures have been established on a semi-industrial scale.	No large-scale production available , might be challenging due to high ^{235}U enrichment.	For (U, Pu)C pellet, routine procedures have been established on a semi-industrial scale. Los Alamos laboatory production facility could produce up to 1 000 pellets a day in the 1980s with stringent quality insurance requirements. By 1983-1985, the Indian Facility for fuel production for FBTR test reactor had a fabrication capacity of 1,2 kg of (U, Pu0,3)C pellets /day. UC powder is pyrophoric and some incidents have been reported. Fabrication needs glovebox with controlled neutral atmosphere.
	Seal/welding		Seal/welding not an issue.	NA		
	Fuel assembly manufacturing		Fuel assembly manufacture is not an issue.	NA		
Compatibility with quality and uniformity standards	Quality control/inspectability	Lack of data.	Pellets manufactured to date have demonstrated acceptable quality and consistency. Controls on powders and final product expected to be similar to UO_2. No issues foreseen regarding U_3Si_2 powder controls (impurity measurements,stoichiometry, morphology etc.).	No problem.		No problem.
	Reject ratio			Lack of disclosed data.		

Table B.11. High-density fuels: Fabrication/manufacturability (continued)

		Uranium nitride and/or (U, Pu)-nitride (France, WH)	Uranium silicide (WH, NRG)	Metal, U-10wt% Zr (Japan, based on knowledge as FBR fuel)	Metal, U-50wt% Zr (AREVA NP, based on literature survey)	Carbide, (U,Pu)C (CEA)
Cost		Over cost due to N15 enrichment and UN pyrophoricity which requires glovebox with neutral atmosphere.	Lack of data. Depends mostly on final powder manufacturing method/route. If done with U and Si metals, some additional cost though well within commercially acceptable levels. If done directly from UF6 or UF4, little increase in manufacturing cost.	Reduction of UF6 to metallic U is expected to add to cost.	No data available but likely higher depending on the final production route selected and due to side regulation constraints linked to the use of very high ^{235}U enrichment.	Over cost due to fabrication with glove box due to UC pyrophoricity.
Impact on the industrial network (suppliers and subcontractors)			Lack of data. Depends mostly on final powder manufacturing method/route. If done with U and Si metals, there will be a requirement for ~1 500 metric tonnes per year of U metal. Si metal should not be an issue. If done directly from UF6 or UF4, no issue with supply.	Significant changes in fuel fabrication are expected.	Significant changes in fuel fabrication with respect to oxide fuels.	

Table B.12. High-density fuels: Normal operation and AOOs

		Uranium nitride and/or (U, Pu)-nitride (France, WH)	Uranium silicide (WH, NRG)	Metal, U-10wt% Zr (Japan, based on knowledge as FBR fuel)	Metal, U-50wt% Zr (AREVA NP, based on literature survey)	Carbide, (U,Pu)C (CEA)
Reactor operation	Behaviour in normal operation	PCMI possible problems due to high swelling rate, low irradiation and thermal creep rate of UN fuel pellet compared to UO_2 fuel pellet. However, no failure and low FGR were observed for (U, Pu0,2) N fuel pins with low smear density ~75/80% irradiated in FBR up to 7 at% b.u. (Depending on the system, no experience on UN fuel in LWR conditions).	Lack of data. Tests in ATR underway Start May 2015. First data expected by end of 2017.	The fuel smear density must reduce to less than 75% because of the large irradiation swelling of metal fuel, and the resultant large gap between fuel slug and cladding is filled by a thermal bond material. Metallic sodium is applicable to FR fuel as the bond material, but alternative materials have to be investigated for LWR fuels.	No data available in LWR conditions. The composition corresponds to the UZr_2 δ-phase structure below 600°C. The δ is phase is known to be stable and to exhibit low volumetric swelling in comparison to U-rich variants. Also due to operation at low temperature, temperature-driven phenomena are expected to be significantly reduced in the U-50wt%Zr fuel (e.g. diffusion and growth of fission gas bubbles or migration of gaseous fission products).	PCMI possible problems due to UC fuel pellet high swelling rate, low irradiation and thermal creep rate compared to UO_2 fuel pellet. However, in the US irradiation test EBR-II reactor, He -bonded (U, Pu)C fuel pins with 316 stainless steel claddings have achieved peak burn-ups of ~ 20 at% without failure.
	Behaviour in AOOs	When the fuel-clad gap is closed, PCMI is possible due to higher Young's modulus and lower creep rate of UN fuel.	Info needed; tests in ATR underway. Stronger swelling and softer PCMI suspected compared to UO_2.	When the fuel-clad gap is closed, FCMI is possible due to low creep rate of U-Zr in the range of LWR operation temperature. However it is not expected to be significant.	FCMI might be an issue but expected to be mitigate when the U-50wt%Zr fuel is metallurgically bounded to the cladding allowing to keep en enhanced heat transfer with respect to UO_2-Zr fuel systems.	When the fuel-clad gap is closed, PCMI is possible due to higher Young's modulus and lower creep rate of UC fuel pellets compared to UO_2 fuel pellets.
	Operating cycle length (12,18,24 months ?...)	Possibly longer cycle due to higher $^{235}U/U$ content.	Possibly longer cycle due to higher $^{235}U/U$ content.	Longer cycles possible through higher U density.	Longer cycles might be possible.	Possibly longer cycle due to higher $^{235}U/U$ content due to higher fuel density.
	Reactivity control systems interaction			-	-	-

Table B.12. High-density fuels: Normal operation and AOOs (continued)

		Uranium nitride and/or (U, Pu)-nitride (France, WH)	Uranium silicide (WH, NRG)	Metal, U-10wt% Zr (Japan, based on knowledge as FBR fuel)	Metal, U-50wt% Zr (AREVA NP, based on literature survey)	Carbide, (U,Pu)C (CEA)
Reactor operation	Impact of load following on the overall cladding behaviour /properties	Stronger mechanical interaction is expected between UN fuel pellets and the cladding compared to UO_2 and generates higher stresses in the cladding than UO_2.	Tests in ATR underway.	-	-	Stronger mechanical interaction is anticipated between UC fuel and a cladding compared to UO_2 fuel and generates higher stresses in the cladding than UO_2, according to the experience with stainless steel cladding.
	Specific behaviour of leakers during irradiation (further degradation with risk of fuel fragments dispersion)	UN reacts with steam above ~250°C: UN + 2 H_2O --> UO_2+ NH_3 + 1/2H_2 or UO_2+ U_2N_3 + 2H_2 with fuel fragmentation. UN pellets must be protected from steam.	Probably, oxidation by and dissolution in water.	U-Zr reacts with water/steam. U-Zr-alloy must be protected from water/steam.	Past experiences on zircaloy bonded uranium fuels indicate that when the fuel cladding bond integrity is maintained, the exposed area for reaction is limited.	UC reacts with steam from 350 °C to 2 500°C. Most observed reactions of UC with steam, depending on temperature, conducts to reaction products as UO_2 + CH_4 or H_2 + carbon oxide gas.
	Impact of specific fabrication defects (e.g. scratches on the cladding OD, localised delamination)			-	-	-
	Neutron penalty	^{14}N neutron absorption in thermal neutrons is very significant, producing radioactive ^{14}C and conducting to higher ^{235}U enrichment to reach the same power. ^{15}N enrichment of ^{14}N can be used.	Some penalty due to higher cross-section for thermal neutrons than UO_2 and $U^{15}N$, but significantly lower than $U^{14}N$. Initially harder neutron spectrum.	U-Zr-alloy presents a higher density of heavy atoms than UO_2 fuel in spite of a necessary lower smear density.		UC fuel presents a higher density of heavy atoms compared to UO_2 fuel in spite of a necessary lower smear density of the UC fabricated pellets (in a stainless steel cladding) to accomodate the UC swelling under irradiation.

Table B.12. High-density fuels: Normal operation and AOOs (continued)

		Uranium nitride and/or (U, Pu)-nitride (France, WH)	Uranium silicide (WH, NRG)	Metal, U-10wt% Zr (Japan, based on knowledge as FBR fuel)	Metal, U-50wt% Zr (AREVA NP, based on literature survey)	Carbide, (U,Pu)C (CEA)
Mechanical properties	Creep	UN thermal and irradiation creep rates are much lower than UO_2 fuel. The PCMI may be higher.	Info needed; Tests at Los Alamos National Laboratory underway. Expected to be high compared to UO_2.	U-Zr thermal and irradiation creep rates are much higher than UO_2 fuel.	Expected to be high compared to UO_2.	UC thermal and irradiation creep rates are much lower than UO_2 fuel. The PCMI may be higher.
	Elastic properties	UN Young 's modulus higher than UO_2 fuel: PCMI higher with UN fuel.	Info needed; Tests at Los Alamos National Laboratory underway	Young 's modulus of irradiated U-Zr is lower than that of UO_2 fuel.	Young 's modulus of irradiated U-Zr is lower than that of UO_2 fuel.	UC Young 's modulus higher than UO_2 fuel: FCMI higher with UC compared to UO_2 fuel.
	Thermal expansion	Nearly the same as UO_2.	Information is needed; tests at Los Alamos National Laboratory underway.	Thermal expansion of irradiated U-Zr is higher than that of UO_2 fuel.		Nearly the same as UO_2.
	Ductility					
	Toughness					
	Strength					
	Fatigue					
	Ramp behaviour				No data available but expected not to be an issue due to low operating temperature and fuel-clad metallurgical bond.	
	Adhesion of coatings					

Table B.12. High-density fuels: Normal operation and AOOs (continued)

		Uranium nitride and/or (U, Pu)-nitride (France, WH)	Uranium silicide (WH, NRG)	Metal, U-10wt% Zr (Japan, based on knowledge as FBR fuel)	Metal, U-50wt% Zr (AREVA NP, based on literature survey)	Carbide, (U,Pu)C (CEA)
Mechanical properties	Resistance to debris		Fresh U_3Si_2 is ductile above 800°C; significantly lower thermal stresses expected from high conductivity, similar thermal expansion. Shimizu observed cracking not worse than UO_2 at <1% BU.			
	Resistance to fretting/wear					
	Circumferential buckling					
	Rod bow					
	Assembly bow					
Thermal behaviour	Conductivity	UN fuel thermal conductivity is better than UO_2 fuel: factor # 13 without porosity and # 6 with 25% porosity for fresh fuel. NB: the aim of this porosity is to accomodate the UN fuel swelling.	Very high-thermal conductivity (factor 4-5 above UO_2 for fresh fuel; 15-20% reduction under irradiation estimated based only on Shimizu); High dk/dT (positive for temperature profile in pellet).	U-Zr fuel thermal conductivity is better than UO_2 fuel.	Unirradiated fuel thermal conductivity better than UO_2 fuel but data needed to assess the evolution under irradiation up to high burn-up level.	UC fuel thermal conductivity is better than UO_2 fuel: factor # 6 with 25% porosity for fresh fuel. NB: the aim of this porosity is to accomodate the UC fuel swelling under irradiation.

Table B.12. High-density fuels: Normal operation and AOOs (continued)

		Uranium nitride and/or (U, Pu)-nitride (France, WH)	Uranium silicide (WH, NRG)	Metal, U-10wt% Zr (Japan, based on knowledge as FBR fuel)	Metal, U-50wt% Zr (AREVA NP, based on literature survey)	Carbide, (U,Pu)C (CEA)
Thermal behaviour	Specific heat	The uranium and/or plutonium nitride specific heat is lower than Oxide fuel. Above 1 500°K lack of data.	Good data available.	Data are avairable.	Lack of data above ~1 100 K.	The uranium and/or plutonium carbide fuel specific heat is lower than the oxide fuel one. Above 1 500°K lack of data.
	Melting	The uranium and/or plutonium nitride fuel melting temperature is equivalent to Oxide fuel but chemical dissociation of UPuN fuel under He atmosphere (not under N$_2$ atmosphere) occurs at ~1 730°C .	Significantly lower melting temperature than UO$_2$ and UN, Tm= 1 665 °C, Thermal conductivity compensates when cooling is present.	Significantly lower melting temperature than UO$_2$, Thermal conductivity compensates when cooling is present.	Significantly lower melting temperature than UO$_2$, i.e 1 600°C but the margins to melting should be much larger as a result of higher thermal conductivity and enhanced heat transfer in case of fuel-clad metallurgical bond.	The uranium and/or plutonium carbide fuel melting temperature T melting= 2 480°C is lower than oxide fuel one (Tmelting= 2 780°C). Metal plutonium evaporation/migration occurs from ~1 650°C in (U, Pu)C fuels.
Fuel/cladding interaction	Chemical compatibility (fuel/cladding)/stability	Cladding properties and mechanical behaviour might be lowered and challenged by nitriding.	Interaction with metals Cr, Fe, Zr have been reported. These interactions may be avoided with a passivating (ceramic or metallic) layer between pellet and cladding. Establishing such a layer may be difficult. (red). The compatibility with SiC/SiC-cladding is good (green).	Diffusion couple experiment of U-Pu-Zr / Zr exhibited slight chemical interaction at 700°C for 75 hrs. Further experiments on the compatibility of U(-Pu)-Zr / zircaloy at 300-1 200°C are needed.	Might be an issue considering feedback experience on U-Pu-Zr/Zr fuel systems; experimental testing needed.	Potentially challenging if cladding carburisation occurs.
	Resistance to PCMI	Lack of data in LWR conditions but higher swelling rate and lower irradiation creep rate could conduct to higher PCMI.	Good compatibility with SiC/SiC-cladding.	Lack of data in LWR conditions. Compensation of higher swelling rate and higher irradiation creep rate is expected.	Lack of data in LWR conditions but expected not to be an issue due to low operating temperature and fuel-clad metallurgical bond.	Potentially challenging if cladding carburisation occurs.

Table B.12. High-density fuels: Normal operation and AOOs (continued)

		Uranium nitride and/or (U, Pu)-nitride (France, WH)	Uranium silicide (WH, NRG)	Metal, U-10wt% Zr (Japan, based on knowledge as FBR fuel)	Metal, U-50wt% Zr (AREVA NP, based on literature survey)	Carbide, (U,Pu)C (CEA)
Fuel/cladding interaction	Resistance to SCC/I					
	Tritium permeation					
	Permeability (hydrogen, fission products)					
	Leak-tightness					
Impact of irradiation	Irradiation limit	Limits have been estimated to 150 GWj/t for UPuN in normal operation for optimised designed UN fuel rod.	Tests at ATR underway.	Limits have been estimated to 200 GWd/t for U-Zr in normal operation.	Expected to be compatible with discharge burn-up of about 270 MWd/tHM.	The burn-up limits have been estimated to 150 GWj/t for (U,Pu)C in normal operating conditions for "optimised" designed UPuC fuel rod.
	Fission product behaviour	He production by (n,α) reaction on ^{14}N, which makes about 10% more gas. However, for FBR fuels, UPuN FGR is much lower than UPuO₂ FGR.	Tests at ATR underway.	Fission gas release 70-80% at <1% burn-up in FR condition. (T>500°C) No available data in LWR condition.	Lack of data in LWR conditions but expected to be low due to operation at temperature around 400°C.	Up to high BU, measurements of (U, Pu)C fuel pellets fission gas release are much lower than Oxide fuel pellets irradiated at the same linear power.
	Embrittlement					
	Irradiation-induced microstructural/chemical composition evolution	Very high microstructure and chemical stability observed up to high BU (7 at %) and under ~ 1 730°C for UPuN fuel under FBR conditions.	Available data mostly limited to low temperatures/ high burn-ups. No amorphisation occurs above 250 Celsius. Significant grain growth occurs starting below 1000 Celsius. tests at ATR underway.	Very highchemical stability observed up to high BU (~20 at %) for U-Pu-Zr fuel under FBR conditions.	Lack of data in LWR conditions but U-Zr δ-phase expected to be stable due to low operating conditions and according to data acquired in test reactors.	Very high microstructural and chemical stability observed up to high BU (15 at %) and under T°C ~1 650°C. At T°C > ~ 1 650°C, beginning of metal Pu evaporation/migration occurs in (U, Pu)C fuel.

Table B.12. High-density fuels: Normal operation and AOOs (continued)

		Uranium nitride and/or (U, Pu)-nitride (France, WH)	Uranium silicide (WH, NRG)	Metal, U-10wt% Zr (Japan, based on knowledge as FBR fuel)	Metal, U-50wt% Zr (AREVA NP, based on literature survey)	Carbide, (U,Pu)C (CEA)
Impact of irradiation	Dimensional stability (growth/swelling)	UN swelling rate is not known in LWR conditions. UPuN fuel swelling rate is higher than UPuO$_2$ fuel in FBR conditions.	U$_3$Si$_2$ swelling rate is not known in LWR conditions. Tests at ATR underway.	Significant swelling is expected even in LWR conditions.	Lack of data in LWR conditions but U-Zr δ-phase expected to be stable due to low operating conditions and to exhibit low volumetric swelling in comparison to U-rich variants.	UC swelling rate is not known in LWR conditions. (U, Pu)C fuel swelling rate is higher than (U, Pu)O$_2$ fuel in FBR conditions.
Coolant interaction	Chemical compatibility with and impact on coolant chemistry	UN reacts with steam above ~250°C: UN + 2 H$_2$O --> UO$_2$+ NH$_3$ + 1/2H$_2$ or UO$_2$+ U2N$_3$ + 2H$_2$ with fuel fragmentation. UN pellets must be protected from steam.	U$_2$Si$_3$ may react with steam at high temperatures	Irradiated U-Zr reacts with water/steam with fuel fragmentation, and the reaction product of H2 gas is generated. U-Zr-alloy must be protected from steam.	Past experiences on zircaloy bonded uranium fuels indicate that when the fuel cladding bond integrity is maintained, the exposed area for reaction is limited.	UC reacts with steam from 350°C to 2 500°C. Reactions of UC with steam, depending on temperature, conducts to reaction products as UO$_2$ + CH$_4$ or H$_2$ + carbon oxide gas which for most of them are explosive gas in air. UC pellets must be protected from steam.
	Oxidation behaviour					
	Shadow corrosion (eg: compatibility with spacer grids)					
	Hydriding behaviour					
	Erosion					
	Crud deposition					
	Thermal-hydraulic interaction (DNB issue)					

Table B.12. High-density fuels: Normal operation and AOOs (continued)

		Uranium nitride and/or (U, Pu)-nitride (France, WH)	Uranium silicide (WH, NRG)	Metal, U-10wt% Zr (Japan, based on knowledge as FBR fuel)	Metal, U-50wt% Zr (AREVA NP, based on literature survey)	Carbide, (U,Pu)C (CEA)
Licensibility	Capability of codes to simulate the behaviour	Thermal-mechanical models are already implemented in French code. Modelling specific UN behaviours in PWR conditions (fuel swelling, fuel behaviour above 1 700°C or UN reaction with steam in case of a leaking fuel) might be challenging . No code in LWRs pellets conditions.		Thermal-mechanical models are already implemented in FBR models . No models in LWRs conditions.	No models in LWRs conditions.	Thermal-mechanical models are already implemented in FBR models. No models in LWRs conditions.
	Reproductibility and robustness of experiments in support to licensing					
	Methodology issues	Nothing to report.		Nothing to report.		Nothing to report.

Table B.13. High-density fuels: Design-basis accidents

		Uranium nitride and/or (U, Pu)-nitride (France, WH)	Uranium silicide (WH, NRG)	Metal, U-10wt% Zr (Japan, based on knowledge as FBR fuel)	Metal, U-50wt% Zr (AREVA NP, based on literature survey)	Carbide, (U,Pu)C (CEA)
Reactor operation	Behaviour in accidental transients	No data for UN fuel in LWR accident conditions. Maximum UN fuel temperatures may be lower than UO$_2$ fuel due to higher conductivity of UN fuel. But UPuN fuel dissociates into Pu and U metal and N$_2$ under He atmosphere when temperature exceeds T~1730°C. RIA is also potentially challenging. In case of cladding burst in LOCA, at high temperature, accelerated fuel swelling may be challenging.	No data for U$_2$Si$_3$ fuel in LWR accident conditions. Maximum U3Si2 fuel temperatures may be lower than UO$_2$ fuel due to higher conductivity of U$_3$Si$_2$ fuel. Tm of 1 665 °C may be an issue.	No data for U-Zr fuel in LWR accident conditions. Maximum U-Zr fuel temperatures may be lower than UO$_2$ fuel due to higher conductivity. Low melting temperature of 1 200°C may be an issue.	No data in LWR accident conditions. Peak fuel temperatures may be lower than UO$_2$ fuel due to higher conductivity. Low fuel melting temperature of 1600°C may be an issue if the absence of cooling for a long period.	No data for UC fuel in LWR accident conditions. Maximum UC fuel temperatures may be lower than UO$_2$ fuel at the same linear power due to the higher conductivity of UC fuel. But Pu evaporates from (U, Pu)C fuel when temperature exceeds T~ 1 650°C. RIA is also potentially challenging. In case of cladding burst in LOCA, at high temperature, accelerated fuel swelling may be challenging.
	Impact of load following on the overall cladding behaviour /properties					
	Specific behaviour of leakers that appeared during normal operation (lower resistance during a DBA)					
High-temperature mechanical properties	Creep	UN thermal and irradiation creep rates are much lower than UO$_2$ fuel. The PCMI may be higher.	Tests in ATR underway.	Creep rates expected to be higher compared to UO$_2$.	Creep rates expected to be higher compared to UO$_2$.	UC thermal and irradiation creep rates are much lower than UO$_2$ fuel. PCMI may be higher.
	Ductility					
	Toughness					
	Strength					
	Fatigue					
	Adhesion of coating					

Table B.13. High-density fuels: Design-basis accidents (continued)

		Uranium nitride and/or (U, Pu)-nitride (France, WH)	Uranium silicide (WH, NRG)	Metal, U-10wt% Zr (Japan, based on knowledge as FBR fuel)	Metal, U-50wt% Zr (AREVA NP, based on literature survey)	Carbide, (U,Pu)C (CEA)
Thermal behaviour	Conductivity	Higher conductivity than UO$_2$ fuel.	4X Higher conductivity than UO$_2$ fuel and increasing with temperature.	Higher conductivity than UO$_2$ fuel.	Higher conductivity than UO$_2$ fuel.	Higher conductivity than UO$_2$ fuel.
	Specific heat	No data available above 1 500 K. We assume that the specific heat should be better than oxide fuel.	Good data available.	Data available.	Lack of data above ~1 100 K.	No data available above 1 500 K. We assume that the specific heat should be better than oxide fuel.
	Melting	UN temperature reached during accident is not known and can be lower than for UO$_2$ fuel. But if temperature is higher than ~ 1 730°C, chemical dissociation of UPuN fuel occurs under He (not under N$_2$ atmosphere).	U$_3$Si$_2$ temperature reached during accident is not known and can be lower than for UO$_2$ fuel. But Tm of 1 665°C may be an issue.	Low margin to melt.	Low margin to melt.	UC temperature reached during accident is not known and can be lower than for UO$_2$ fuel. But if temperature is higher than T°C ~ 1 650°C, Pu evaporates from UPuC fuel.
Fuel/cladding interaction	Chemical compatibility/stability (e.g. oxidation behaviour)	Cladding properties and mechanical behaviour might be lowered and challenged by nitriding.	Interaction with metals Cr, Fe, Zr have been reported. These interactions may be avoided with a passivating (ceramic or metallic) layer between pellet and cladding. Establishing such a layer may be difficult. (red).The compatibility with SiC/SiC-cladding is being tested at Los Alamos National Laboratory and Westinghouse.	Diffusion couple experiment of U-Pu-Zr /Zr exhibited slight chemical interaction at 700°C for 75 hrs. Further experiments on the compatibility of U(-Pu)-Zr /zircaloy at 300-1 200°C are needed.	Might be an issue considering feedback experience on U-Pu-Zr /Zr fuel systems; experimental testing needed.	Cladding properties and mechanical behaviour might be lowered and challenged by carburisation.
	Fission product behaviour		Tests with ceramic SiC/SiC-cladding in ATR underway.	FP mobility in U-Zr-alloy is higher than that in UO$_2$ pellet, and FP chemical stability is expected to be low.	Lack of data – FP mobility might be significantly activated with fuel temperature increase not allowing to remain in the UZr$_2$ δ-phase.	

Table B.13. High-density fuels: Design-basis accidents (continued)

		Uranium nitride and/or (U, Pu)-nitride (France, WH)	Uranium silicide (WH, NRG)	Metal, U-10wt% Zr (Japan, based on knowledge as FBR fuel)	Metal, U-50wt% Zr (AREVA NP, based on literature survey)	Carbide, (U,Pu)C (CEA)
Fuel/cladding interaction	Fission gas generation	He production by (n,α) reaction on ^{14}N, which makes about 10% more gas.	Tests with ceramic SiC/SiC-cladding in ATR underway.	Fission gas release from U-Zr is higher than that from UO_2.	Lack of data – FGR might be significantly activated with fuel temperature increase not allowing to remain in the UZr_2 δ-phase.	
	Resistance to PCI		Expected high creep and swelling. Performance depending on cladding material and fuel design.		Performance depending on cladding material and fuel design.	
	Environment interaction of the inner cladding layer					
LOCA	High-temperature steam oxidation (1200°C)		Exothermic fuel oxidation/hydrogen generation in case of clad failure suspected, mitigation needed.	Irradiated U-Zr reacts with water/steam with fracmentation. U-Zr-alloy must be protected from steam.	Poor behaviour in the event of contact with water and/or vapour.	UC reacts with steam from 350°C to 2 500°C. Reactions of UC with steam, depending on temperature, conducts to reaction products as UO_2 + CH_4 or H_2 + carbon oxide gas which, for most of them, are explosive gas in air. UC pellets must be protected from steam.
	HT breakaway oxidation					
	Quench tolerance / Post-Quench mechanical behaviour					
	Degradation mode of the cladding					
	Phase transformation, H and O, diffusion and distribution					

Table B.13. High-density fuels: Design-basis accidents (continued)

		Uranium nitride and/or (U, Pu)-nitride (France, WH)	Uranium silicide (WH, NRG)	Metal, U-10wt% Zr (Japan, based on knowledge as FBR fuel)	Metal, U-50wt% Zr (AREVA NP, based on literature survey)	Carbide, (U,Pu)C (CEA)
RIA	Degradation mode of the cladding					
	Mechanical behaviour (PCMI high speed ramp/tensile test at high temperatures)					
	Steam oxidation at 1480°C/1 500°C		Exothermic fuel oxidation/hydrogen generation in case of clad failure suspected, mitigation needed.	Irradiated U-Zr reacts with water/steam with fracmentation. U-Zr-alloy must be protected from steam.	Poor behaviour in the event of contact with water and/or vapour.	
Seismic behaviour	Fuel assembly mechanical behaviour					
Thermal-hydraulic interaction						
Licensibility	Capability of codes to simulate the behaviour	No dedicated modelling available for accident conditions LOCA/RIA.	No dedicated modelling available for accident conditions LOCA/RIA.	No dedicated modelling available for accident conditions LOCA/RIA in LWRs.	No dedicated modelling available for accident conditions LOCA/RIA.	No dedicated modelling available for accident conditions LOCA/RIA.
	Reproductibility and robustness of experiments in support to licensing	There are no dedicated tests available for accident conditions as LOCA/RIA. Interaction of the fuel with steam is likely an issue.	There are no dedicated tests available for accident conditions as LOCA/RIA. Interaction of the fuel with steam may be an issue.	There are no dedicated tests available for accident conditions as LOCA/RIA in LWRs. Interaction of the fuel with water/steam is likely an issue.	There are no dedicated tests available for accident conditions as LOCA/RIA. Interaction of the fuel with steam is likely an issue.	There are no dedicated tests available for accident conditions as LOCA/RIA. Interaction of the fuel with steam is likely an issue.
	Methodology issues					

Table B.14. High-density fuels: Design extension conditions

	Uranium nitride and/or (U, Pu)-nitride (France, WH)	Uranium silicide (WH, NRG)	Metal, U-10wt% Zr (Japan, based on knowledge as FBR fuel)	Metal, U-50wt% Zr (AREVA NP, based on literature survey)	Carbide, (U,Pu)C (CEA)
Mechanical strength and ductility					
Thermal behaviour (melting)	Dissociation of uranium and/or plutonium nitride fuel above ~ 1 730°C under He atmosphere (not under N_2 atmosphere).	Tm of 1 665°C may be an issue. However, U_3Si_2 will be paired with more accident-tolerant cladding (SiC composites or coated Zr) that will protect U_3Si_2 from environment longer.	The U-Zr fuel melting temperature is lower than UO_2. Melting temperature is 1 200°C.	Low fuel melting temperature of 1 600°C.	The uranium and/or plutonium carbide fuel melting temperature is lower than oxide fuel and evaporation of plutonium occurs from T°C ~ 1 650°C. The carbide reacts with water with reaction product H_2, perhaps explosive.
Chemical compatibility/stability (including high-temperature steam interaction)		Fuel oxidation/hydrogen generation.	Irradiated U-Zr reacts with water/steam with fracmentation. U-Zr-alloy must be protected from steam.	Poor behaviour in the event of contact with water and/or vapour.	UC reacts with steam from 350°C to 2 500°C. Reactions of UC with steam, depending on temperature, conducts to reaction products as $UO_2 + CH_4$ or H_2 + carbon oxides gas which, for most of them, are explosive gas in air.
Fission product behaviour	Potential release of C14 when ^{14}N is used (not ^{15}N used).	Tests in ATR underway.		Generally higher HT FP mobility expected.	
Combustible gas production				Fuel oxidation/hydrogen generation.	
Oxidation acceleration due to the exothermic HT reaction	-	Fuel oxidation /hydrogen generation.		Fuel oxidation/hydrogen generation.	
Physical interaction of the molten material			-		-

Table B.15. High-density fuels: Fuel cycle issues

		Uranium nitride and/or (U, Pu)-nitride (France, WH)	Uranium silicide (WH, NRG)	Metal, U-10wt% Zr (Japan, based on knowledge as FBR fuel)	Metal, U-50wt% Zr (AREVA NP, based on literature survey)	Carbide, (U,Pu)C (CEA)
Enrichment limit		If ^{14}N used, then ^{235}U must be increased. But higher UN density allows to reduce this enrichment compared to UO_2 fuel. Neutronic calculations have to be done.	Higher density will likely compensate for higher thermal cross-section of U_3Si_2. Neutronic calculations have been done.	Higher U-Zr density allows to reduce the ^{235}U enrichment compared to UO_2 fuel. Neutronic calculations have to be performed.	High ^{235}U enrichment (up to 19.7%) to be considered to overcome the high Zr content reducing the uranium loading.	Higher UC density allows to reduce the $^{235}U/U$ enrichment compared to UO_2 fuel. Neutronic calculations have to be performed.
Mechanical strength and ductility						
Thermal behaviour		Lack of data but we can assume that the uranium and/or plutonium nitride fuel will have a better thermal behaviour than Oxide fuel since its thermal conductivity is better. Lower temperatures are expected.	Lack of reactor based data but U_3Si_2 has ~4x better thermal behaviour than Oxide fuel since its thermal conductivity is better. Lower temperatures are expected. Strong (positive) temperature dependence of dk/dT.	U-Zr fuel have better thermal behaviour than UO_2 since its thermal conductivity is better. Lower temperature expected.	Lower temperature expected due to imporved heat transfer capability.	Lack of data but we can assume that the carbide of uranium and/or plutonium fuel will have a better themal behaviour than Oxide fuel since its thermal conductivity is better. Lower temperature expected.
Chemical stability		Less good than UO_2 pellet because of UN pellet potential reaction with water or air.	Less good than UO_2 pellet because of U_3Si_2 pellet potential reaction with steam; corrosion in brine solutions reported.	Less good than UO_2 pellet because of U-Zr-alloy potential reaction with water or air.	Lack of data – No issue expected especially in design with fuel-clad metallurgical bond.	
Fission product behaviour		He is produced with (n,α) reaction on ^{14}N, which makes about 10% more FG. ^{14}C is produced due to reaction on ^{14}N with environnemental problems and waste storage.	Tests in ATR underway. FP leaching suspected based on corrosion in brine solutions.	FP mobility in U-Zr-alloy is higher than that in UO_2 pellet, and FP chemical stability is expected to be low. Fission gas release from U-Zr is higher than that from UO_2.	Lack of data – No issue expected due to operation at low temperature.	In baseload conditions and high BU, FGR measurements of carbide of uranium and/or plutonium fuel pellet are lower than the oxide fuel data. Lower pressure expected.

Table B.15. High-density fuels: Fuel cycle issues (continued)

		Uranium nitride and/or (U, Pu)-nitride (France, WH)	Uranium silicide (WH, NRG)	Metal, U-10wt% Zr (Japan, based on knowledge as FBR fuel)	Metal, U-50wt% Zr (AREVA NP, based on literature survey)	Carbide, (U,Pu)C (CEA)
Transport	Mechanical behaviour (ductility)					
	Behaviour in fire		Sensitive to exothermic oxidation.			
	Impact of specific fabrication defects (e.g. scratches on the OD cladding, localised delamination)					
	Behaviour under accident conditions (punch test)					
Long-term storage	Hydride reorientation					
	Corrosion behaviour					
	Impact of specific fabrication defects (e.g. scratches on the OD cladding, localised delamination)					
	Residual radioactivity					
	Long-term microstructural /chemical composition evolution					

Table B.15. High-density fuels: Fuel cycle issues (continued)

		Uranium nitride and/or (U, Pu)-nitride (France, WH)	Uranium silicide (WH, NRG)	Metal, U-10wt% Zr (Japan, based on knowledge as FBR fuel)	Metal, U-50wt% Zr (AREVA NP, based on literature survey)	Carbide, (U,Pu)C (CEA)
Reprocessing	Tritium					
	Shearing					
	Chemical compatibility with reprocessing reaction (nitric acid)	Nitride fuel is soluble in nitric acid.	Dissolution in Hg catalysed HNO_3, of both irradiated and unirradiated fuels was demonstrated in the 1980s.	U(-Pu)-Zr-alloy is soluble in hydrofluoric acid. In pyro-reprocessing of U-Zr fuel, molten salt is used as solvent.	Should not be an issue considering U(-Pu)-Zr-alloy experience.	Not soluble in nitric acid.
	Reprocessibility	UN is compatible with PUREX process.	Qualified; AREVA awaiting ASN approval. (earlier report of slowing down of TBP-acid separation after mixing).	A lot of pyro-reprocessing data for (irradiated) U-Zr fuel are available.	Should not be an issue considering U(-Pu)-Zr-alloy experience.	Difficult due to the lack of solubility with nitric acid.
Cost		Over cost due to ^{15}N enrichment and probably storage UN fuel rods in neutral atmosphere because of UN reactivity with water.	Existing infrastructure used, relatively small deviations from PUREX, additional silica waste stream will add somewhat to cost (centrigugation of silica gel).			Slightly more expensive due to the lack of reprocessing process.

Attribute evaluation for the encapsulated fuels

Table B.16. Encapsulated fuels: Fabrication/manufacturability

		Encapsulated fuel/SiC-cladding (US)	Encapsulated fuel (China)	Encapsulated fuel (Korea)
Compatibility with large-scale production needs	Qualification of product and associated process	Rapid sintering techniques such as DCS/SPS should be explored. Preliminary data shows promise.	Pellets may be produced by SPS.	Pressure-less sintering process by using additives is under developing.
	Security of supply for each component (material)	TRISO is mature technology and SiC powder supply is well established.	No problem to supply SiC and TRISO powders.	Lab-scale supply system for UO_2-TRISO. International and domestic supply system for SiC powder.
	Fabrication receipt criteria (technical file)	Fuel processing and spec is well-defined in US DOE programme.	The technical file for FCM fuel pellet does not exist.	Hot press sintering process and feasibility of pressure-less sintering process has been demonstrated at a laboratory scale.
	Long-tube fabrication			
	Large-scale pellet fabrication	Rapid sintering techniques such as DCS/SPS should be explored. Preliminary data shows promise.	No FCM fuel have been already produced.	Engineering-scale fuel production in conformance with the fuel specification should be demonstrated.
	Seal/welding			
	Fuel assembly manufacturing	Rapid sintering techniques such as DCS/SPS should be explored. Preliminary data shows promise.		
Compatibility with quality and uniformity standards	Quality control/inspectability	Unknown.	The lab methodologies to control FCM fuel pellet do not exist.	
	Reject ratio	Unknown.	Lack of knowledge.	
Cost		At least 25% higher and likely twice the cost of current fuel.	The manufacturing throughput for FCM is expensive than UO_2 fuel.	Over cost is anticipated. 20% enriched ^{235}U, UN kernel.
Impact on the industrial network (suppliers and subcontractors)		The fuel production process differs widely from the current system.	The pellets may be sintered by SPS, the cost may raise up a lot.	The fuel production process is quite different to the current UO_2 pellet system.

Table B.17. Encapsulated fuels: Normal operation and AOOs

		Encapsulated fuel/SiC-cladding (US)	Encapsulated fuel (China)	Encapsulated fuel (Korea)
Reactor operation	Behaviour in normal operation	No integral test to date. Separate-effects tests show promise.	Better than UO$_2$ fuel pellet with fission gas release and internal pressure benefit at end of life.	Lake of experimental data but enhanced performance is expected.
	Behaviour in AOOs	No data, but behaviour should be robust.	Nothing to report.	Prelimanary safety analysis for UN-TRISO FCM predicted prosmissing behaviour.
	Operating cycle length (12, 18, 24 months ?...)	If enough heavy metal loading is achieved by using large TRISO and high enrichment (~15-19% ^{235}U), current operational cycles may be preserved.		To meet current fuel cycle, UN kernel with higher enriched ^{235}U(~19%) is required.
	Reactivity control systems interaction	Japanese RIA tests on loose TRISO show promise.		A specific fuel design is required to control the large reactivity at the BOL.
	Impact of load following on the overall cladding behaviour /properties	Unknown but should be robust.	No detrimental impact anticipated.	
	Specific behaviour of leakers during irradiation (further degradation with risk of fuel fragments dispersion)	Acceptable corrosion resistance and no radionuclide release.	Nothing to report.	Lake of data. Long-term steam reaction is under studing.
	Impact of specific fabrication defects (e.g. scratches on the cladding OD, localised delamination)	Unknown but should be robust.		
	Neutron penalty	Heavy metal loading is too low.	SiC has very low neutron penalty.	Lake of data. For UN-TRISO, thermal neutron absorption of ^{14}N would be significant. ^{15}N enrichment might be required.

Table B.17. Encapsulated fuels: Normal operation and AOOs (continued)

		Encapsulated fuel/SiC-cladding (US)	Encapsulated fuel (China)	Encapsulated fuel (Korea)
Mechanical properties	Creep	Negligible.	ORNL has reported the creep of SiC is good.	Lake of data. More experimental confirmation needed for UN-TRISO fuel and irradiated fuel.
	Elastic properties	Well known.	ORNL has reported the creep of SiC is good.	Lake of data. More experimental confirmation needed for UN-TRISO fuel and irradiated fuel.
	Thermal expansion	Well known.	ORNL has reported the creep of SiC is good.	Lake of data. More experimental confirmation needed for UN-TRISO fuel and irradiated fuel.
	Ductility			
	Toughness			
	Strength			
	Fatigue			
	Ramp behaviour			
	Adhesion of coatings			
	Resistance to debris			
	Resistance to fretting/wear			
	Circumferential buckling			
	Rod bow			
	Assembly bow			

Table B.17. Encapsulated fuels: Normal operation and AOOs (continued)

		Encapsulated fuel/SiC-cladding (US)	Encapsulated fuel (China)	Encapsulated fuel (Korea)
Thermal behaviour	Conductivity	Higher than UO₂.	Thermal conductivity is enhanced.	Lake of data. More experimental confirmation needed for UN-TRISO fuel and irradiated fuel.
	Specific heat	Well known.	Considering the same as SiC.	Lake of data. More experimental confirmation needed for UN-TRISO fuel and irradiated fuel.
	Melting	Dissociates, does not melt.	SiC matrix has 2 500°C melting temperature.	Lake of data. More experimental confirmation needed for UN-TRISO fuel and irradiated fuel.
Fuel/cladding interaction	Chemical compatibility (fuel/cladding)/stability	No interaction.	SiC has potential risk to react with metal cladding.	Limited chemical interaction between fuel and cladding is expected.
	Resistance to PCMI		Nothing to report.	Experimental data is required.
	Resistance to SCC/I		Nothing to report.	Lack of data. Superior FPs retention and delayed gap closure will mitigate SCC/I.
	Tritium permeation	SiC is a good barrier to T permeation.		
	Permeability (hydrogen, fission products)	SiC is a good barrier to radionuclides.		
	Leak-tightness	Microcracking may compromise leak-tightness.		
Impact of irradiation	Irradiation limit		Nothing to report.	Fission-fragment radiation damages will be confined to the TRISO particle.
	Fission product behaviour	SiC is a good barrier to radionuclides.	TRISO particle has good ability.	FP-gas retained inside in particles at <1 800°C for UO₂-TRISO fuel.
	Embrittlement	SiC does not degrade in mechanical properties after irradiation.	N/A.	
	Irradiation-induced microstructural/chemical composition evolution	None expected.	Nothing to report.	More experimental confirmation needed for UN-TRISO fuel.
	Dimensional stability (growth/swelling)	Well-known and manageable swelling.	ORNL has reported.	Good dimensional stability is expected under LWR condition.

Table B.17. Encapsulated fuels: Normal operation and AOOs (continued)

		Encapsulated fuel/SiC-cladding (US)	Encapsulated fuel (China)	Encapsulated fuel (Korea)
Coolant interaction	Chemical compatibility with and impact on coolant chemistry	Coating layer may be needed.	Considering the same as SiC-cladding.	More experimental confirmation needed for irradiated fuel.
	Oxidation behaviour	Slow oxidation in steam.		More experimental confirmation needed for irradiated fuel.
	Shadow corrosion (eg: compatibility with spacer grids)	Dissolves in water.		
	Hydriding behaviour			
	Erosion			
	Crud deposition			
	Thermal-hydraulic interaction (DNB issue)			
Licensibility	Capability of codes to simulate the behaviour	Robust codes are being developed.	Nothing to report.	Lack of data. Major issue but not technically challenging.
	Reproductibility and robustness of experiments in support to licensing	Probabilistic design approach is needed.	Nothing to report.	Lack of data. For utilsation/licensing, further investigations and obtainment of experimental data is needed.
	Methodology issues	Probabilistic design approach is needed.	Nothing to report.	Licensing would be a challenge and associated with cladding candidates.

Table B.18. Encapsulated fuels: Design-basis accidents

		Encapsulated fuel/SiC-cladding (US)	Encapsulated fuel (China)	Encapsulated fuel (Korea)
Reactor operation	Behaviour in accidental transients	Investigating applicability of codes.	No data available (LOCA – RIA).	
	Impact of load following on the overall cladding behaviour/properties	The same as property for SiC-cladding.		
	Specific behaviour of leakers that appeared during normal operation (lower resistance during a DBA)	Evaluated FP-gas release behaviour versus operating temperature for high-temperature gas reactor.		
High-temperature mechanical properties	Creep	The same as property for SiC-cladding.	ORNL has reported the creep of SiC is good.	
	Ductility	The same as property for SiC-cladding.		
	Toughness	Data obtained for high-temperature gas reactor.		
	Strength	Data obtained for high-temperature gas reactor.		
	Fatigue	The same as property for SiC-cladding.		
	Adhesion of coating	Data obtained for high-temperature gas reactor.		
Thermal behaviour	Conductivity	Data obtained for high-temperature gas reactor.	At high temperature (up to 3 000 K) the thermal conductivity is higher than UO_2 fuel.	
	Specific heat		No data available above 1 500 K.	
	Melting		SiC matrix has 2 500°C melting temperature.	

Table B.18. Encapsulated fuels: Design-basis accidents (continued)

		Encapsulated fuel/SiC-cladding (US)	Encapsulated fuel (China)	Encapsulated fuel (Korea)
Fuel/cladding interaction	Chemical compatibility/stability (e.g. oxidation behaviour)		Nothing to report.	
	Fission product behaviour	Data obtained for high-temperature gas reactor.	TRISO particle has good ability.	
	Fission gas generation	Data obtained for high-temperature gas reactor.	The same as UO$_2$.	
	Resistance to PCI		For SiC has better thermal conductivtiy and expansion property, we consider the performance will good.	
	Environment interaction of the inner cladding layer		No data.	
LOCA	High-temperature steam oxidation (1 200°C)	High-temperature corrosion data to be obtained.	Has been reported by ANL and ORNL, the result is quite good.	
	HT breakaway oxidation	High-temperature corrosion data to be obtained.		
	Quench tolerance/Post-Quench mechanical behaviour	The same as property for SiC-cladding.		For cladding.
	Degradation mode of the cladding	The same as property for SiC-cladding.		For cladding.
	Phase transformation, H and O, diffusion and distribution	The same as property for SiC-cladding.		For cladding.
RIA	Degradation mode of the cladding	The same as property for SiC-cladding.		For cladding.
	Mechanical behaviour (PCMI high speed ramp/tensile test at high temperatures)	Pulse irradiation data obtained for high-temperature gas reactor.	The thermal expansion rate of SiC is very low, and the high-temperature strength of SiC is good.	
	Steam oxidation at 1480°C/1500°C		No data.	
Seismic behaviour	Fuel assembly mechanical behaviour			
Thermal-hydraulic interaction				
Licensibility	Capability of codes to simulate the behaviour	Investigating applicability of codes.	No dedicated modelling available for accident conditions – no problem anticipated.	
	Reproductibility and robustness of experiments in support to licensing		Nothing to report.	
	Methodology issues	Investigating applicability of codes.	Nothing to report.	

Table B.19. Encapsulated fuels: Design extension conditions

	Encapsulated fuel/SiC-cladding (US)	Encapsulated fuel (China)	Encapsulated fuel (Korea)
Mechanical strength and ductility		The high-temperature strength of SiC is good.	
Thermal behaviour (melting)		The reaction between SiC and UO$_2$ addition has some effect on melting temperature.	
Chemical compatibility/stability (including high-temperature steam interaction)		Lots of good experiment results have been achieved.	
Fission product behaviour	Most resistant to release.	TRISO particle has good ability.	
Combustible gas production		The same as high temperater gas cooling reactor fuel.	
Oxidation acceleration due to the exothermic HT reaction		The exthermic HT reaction of SiC can be ignored.	
Physical interaction of the molten material		No data.	

Table B.20. Encapsulated fuels: Fuel cycle issues

		Encapsulated fuel/SiC-cladding (US)	Encapsulated fuel (China)	Encapsulated fuel (Korea)
Enrichment limit			Higher than UO$_2$.	Higher ^{235}U enrichments are necessary.
Mechanical strength and ductility				
Thermal behaviour			Higher than UO$_2$.	
Chemical stability			SiC reatcs with UO$_2$ at high temperature.	
Fission product behaviour			No data available.	
Transport	Mechanical behaviour (ductility)		No data available.	
	Behaviour in fire			
	Impact of specific fabrication defects (e.g. scratches on the OD cladding, localised delamination)			
	Behaviour under accident conditions (punch test)			

Table B.20. Encapsulated fuels: Fuel cycle issues (continued)

|		Encapsulated fuel/SiC-cladding (US)	Encapsulated fuel (China)	Encapsulated fuel (Korea)
Long-term storage	Hydride reorientation			For cladding.
	Corrosion behaviour			
	Impact of specific fabrication defects (e.g. scratches on the OD cladding, localised delamination)			
	Residual radioactivity			
	Long-term microstructural/chemical composition evolution		No problem anticipated considering the very high-dimensional, microstructural and chemical stability observed in baseload conditions.	
Reprocessing	Tritium			Repository ready fuel form. Reprocess would not be an option.
	Shearing			Repository ready fuel form. Reprocess would not be an option.
	Chemical compatibility with reprocessing reaction (nitric acid)		SiC of FCM fuel is not soluble in nitric acid.	Repository ready fuel form. Reprocess would not be an option.
	Reprocessibility	Very difficult to reprocess (proliferation resistant).	No data available.	Repository ready fuel form. Reprocess would not be an option.
Cost			Much more expensive than UO_2.	

NEA PUBLICATIONS AND INFORMATION

The **full catalogue of publications** is available online at www.oecd-nea.org/pub.

In addition to basic information on the Agency and its work programme, the NEA website offers free downloads of hundreds of technical and policy-oriented reports. The professional journal of the Agency, **NEA News** – featuring articles on the latest nuclear energy issues – is available online at www.oecd-nea.org/nea-news.

An **NEA monthly electronic bulletin** is also distributed free of charge to subscribers, providing updates of new results, events and publications. Sign up at www.oecd-nea.org/bulletin.

Visit us on **Facebook** at www.facebook.com/OECDNuclearEnergyAgency or follow us on **Twitter** @OECD_NEA.

State-of-the-Art Report on Light Water Reactor Accident-Tolerant Fuels

As part of a broader spectrum of collaborative activities underpinning nuclear materials research, the Nuclear Energy Agency is supporting worldwide efforts towards the development of advanced materials, including fuels for partitioning and transmutation purposes and accident-tolerant fuels (ATFs). This state-of-the-art report on ATFs results from the collective work of experts from 35 institutions in 14 NEA member countries, alongside invited technical experts from the People's Republic of China. It represents a shared and consensual position, based on expert judgment, concerning the scientific and technological knowledge related to ATFs. The report reviews available information on the most promising fuels and cladding concepts in terms of properties, experimental data and modelling results, as well as ongoing research and development activities. It also includes a description of illustrative accident scenarios that may be adopted to assess the potential performance enhancement of ATFs relative to the current standard fuel systems in accident conditions, a definition of the technology readiness levels applicable to ATFs, a survey of available modelling and simulation tools (fuel performance and severe accident analysis codes), and the experimental facilities available to support the development of ATF concepts. The information included in this report will be useful for national programmes and industrial stakeholders as an input to setting priorities, and helping them to choose the most appropriate technology based on their specific strategy, business case and deployment schedules.